



**HAL**  
open science

# Design of amphiphilic copolymers incorporating vinyl alcohol units and their use as stabilizers for the emulsion copolymerization of vinyl acetate

Marie Raffin

► **To cite this version:**

Marie Raffin. Design of amphiphilic copolymers incorporating vinyl alcohol units and their use as stabilizers for the emulsion copolymerization of vinyl acetate. *Polymers*. Université Claude Bernard - Lyon I, 2022. English. NNT : 2022LYO10122 . tel-04860598

**HAL Id: tel-04860598**

**<https://theses.hal.science/tel-04860598v1>**

Submitted on 1 Jan 2025

**HAL** is a multi-disciplinary open access archive for the deposit and dissemination of scientific research documents, whether they are published or not. The documents may come from teaching and research institutions in France or abroad, or from public or private research centers.

L'archive ouverte pluridisciplinaire **HAL**, est destinée au dépôt et à la diffusion de documents scientifiques de niveau recherche, publiés ou non, émanant des établissements d'enseignement et de recherche français ou étrangers, des laboratoires publics ou privés.



**THESE de DOCTORAT DE  
L'UNIVERSITE CLAUDE BERNARD LYON 1**

**Ecole Doctorale N° 206  
Chimie, Procédés, Environnement**

**Discipline : Chimie**

Soutenue publiquement le 21/11/2022, par :

**Marie RAFFIN**

---

**Design of amphiphilic copolymers  
incorporating vinyl alcohol units and  
their use as stabilizers for the  
emulsion copolymerization of vinyl  
acetate**

---

Devant le jury composé de :

DELAITE Christelle	Professeure, Université de Haute Alsace	Rapportrice
BALLARD Nicholas	Professeur associé, University of the Basque Country	Rapporteur
BEYOU Emmanuel	Professeur, Université Lyon 1	Président du jury
DESTARAC Mathias	Professeur, Université de Toulouse	Examineur
D'AGOSTO Franck	Directeur de recherche, CNRS	Directeur de thèse
LANSALOT Muriel	Directrice de recherche, CNRS	Co-directrice de thèse
MELCHIN Timo	Responsable industriel, Wacker	Invité



## **Université Claude Bernard – LYON 1**

Président de l'Université	M. Frédéric FLEURY
Président du Conseil Académique	M. Hamda BEN HADID
Vice-Président du Conseil d'Administration	M. Didier REVEL
Vice-Président du Conseil des Etudes et de la Vie Universitaire	M. Philippe CHEVALLIER
Vice-Président de la Commission de Recherche	M. Petru MIRONESCU
Directeur Général des Services	M. Pierre ROLLAND

### **COMPOSANTES SANTE**

Département de Formation et Centre de Recherche en Biologie Humaine	Directrice : Mme Anne-Marie SCHOTT
Faculté d'Odontologie	Doyenne : Mme Dominique SEUX
Faculté de Médecine et Maïeutique Lyon Sud - Charles Mérieux	Doyenne : Mme Carole BURILLON
Faculté de Médecine Lyon-Est	Doyen : M. Gilles RODE
Institut des Sciences et Techniques de la Réadaptation (ISTR)	Directeur : M. Xavier PERROT
Institut des Sciences Pharmaceutiques et Biologiques (ISBP)	Directrice : Mme Christine VINCIGUERRA

### **COMPOSANTES & DEPARTEMENTS DE SCIENCES & TECHNOLOGIE**

Département Génie Electrique et des Procédés (GEP)	Directrice : Mme Rosaria FERRIGNO
Département Informatique	Directeur : M. Behzad SHARIAT
Département Mécanique	Directeur : M. Marc BUFFAT
Ecole Supérieure de Chimie, Physique, Electronique (CPE Lyon)	Directeur : Gérard PIGNAULT
Institut de Science Financière et d'Assurances (ISFA)	Directeur : M. Nicolas LEBOISNE
Institut National du Professorat et de l'Éducation	Administrateur Provisoire : M. Pierre CHAREYRON
Institut Universitaire de Technologie de Lyon 1	Directeur : M. Christophe VITON
Observatoire de Lyon	Directrice : Mme Isabelle DANIEL
Polytechnique Lyon	Directeur : Emmanuel PERRIN
UFR Biosciences	Administratrice provisoire : Mme Kathrin GIESELER
UFR des Sciences et Techniques des Activités Physiques et Sportives (STAPS)	Directeur : M. Yannick VANPOULLE
UFR Faculté des Sciences	Directeur : M. Bruno ANDRIOLETTI





## Acknowledgments

First of all, I would like to express my sincere gratitude to Dr. Timothy McKenna for giving me the opportunity to conduct my doctoral work at the CP2M laboratory.

I express my gratitude to Dr. Christelle Delaite and Dr. Nicholas Ballard for having accepted to judge my research work. Thank you for the time you devoted to read this manuscript and for the interest you have shown in this work. I sincerely thank Dr. Emmanuel Beyou for having presided over the thesis jury. Finally, I express all my gratitude to Dr. Mathias Destarac, who made me the great honor to participate in my jury.

Now I would like to warmly thank Dr. Franck D'Agosto and Dr. Muriel Lansalot for all the supervision, supports and valuable discussions you provided throughout my thesis, as well as the confidence you placed on my work. Thank you for your rigorous and deep approach of science and for the patience you showed with proof reading the drafts. Thank you also for encouraging me when I felt a little bit lost in all this research and for providing good advice in the research of my future work (which I did not really follow, but I sincerely valued your advice and still hope we will see each other's on conferences). I am a bit sad that we will not be able to make a partnership on future topics...

I also owe my gratitude to my third supervisor Dr. Timo Melchin from Wacker Chemie AG, for your unreserved pass of knowledge. Many parts of the thesis would not have been possible without your support and guidance. I benefit a lot from your supervisions and experienced considerable progress on how to conduct scientific work. Many thanks for all the things and support you provided me with. I only had to ask. I know how busy you are with all the different projects you lead, but you always took the time to answer my questions and organize regular meetings during my stay at Wacker. Thank you very much for organizing this visit during this troublesome covid time. I know it was much work.

I would also like to take this opportunity to express my thanks to the following people at Wacker, when I carried out my experiments there: Dr. Sebastian Krickl, Dr. Ulf Dietrich, Dr. Laura Arschel and Dr. Jesica Rodríguez-Fernández for your help in the lab and the fruitful discussions. And a more special thanks to Dr. Markus Bannwarth for your encouragements and support at work, for bringing me to the climbing wall of Burghausen and for introducing me to new people. You contributed a lot to my social well-being during my time at Burghausen. Many thanks also for putting so much effort in trying to find a position for me at Wacker. You know I liked the city and I could see myself living there (I already had improvement projects at the climbing wall 😊), but you know, French cheese was calling me back too hard.

Many thanks to Markus Grandl, my climbing partner during my time at Burghausen and the only person I could talk French with (it made my weeks). I promise I will work on my French accent to improve my “German skills”.

A special thanks also to Katrin Brandstätter. It was a real pleasure to talk about nothing and everything during the breaks, to go hiking with you and Andy in the Bavarian Alps, and share beers and Kaiserschmarrn (whatever the number of consonants, I will never get used to it 😊). I was happy to make you discover the pepper salami and Comté cheese from France! Thank you for always making the effort to talk English with me and being such a nice lab mate. More than that, thank you for making me discover the Chemsee! I couldn't come to Germany and not see the Bavarian Sea 😊 (Ja Quenau).

Thank you to Angelika Sendlmeier for providing me all the equipment I needed in the lab and for introducing me to the lab mates. We had a brief time together but I could see you were a kind person. All the best for your recovery. I hope you got many nice words on your cast.

I would like to thank Julia Hautz also for all the efforts you put in asking the analytical departments to make my analysis fast. Thank you for the nice discussions we had together. I hope your garden house is still holding tight against the wind and that the fish are doing well for the next bbq!

Many thanks to the most French-German person I had the chance to meet during the last week at Burghausen, Pierre-Valery Chassagnon. I is a pity we only met during my last week because I did not have the chance to defeat you at Badminton! I hope the transmission from the Bavarian radio to Lyon radio will still work for a bit of a time and that we will keep in touch. Our mortar is the best anyway! I am still looking for the best honey from Jura to send you 😊

Finally, many thanks to all the persons I shared the lab with, who were always kind and helpful to me, and many thanks to the technicians who analyzed my samples.

Back to CP2M lab, many thanks to Pierre-Yves Dugas, Edgar Espinoza and Nathalie Jouglard for your technical and even more important, for your human support. Your kindness goes beyond what I was expecting when I started my PhD. PY, I owe you a special thanks for the patience you showed for the analysis of ALL the samples at the CryoTEM!

Thank you to the permanent staff, trainees, PhD students and post doc... who made my life in the lab so appreciable. I will miss the coffee breaks, Tupperware meetings and afterwork parties.

More personally, I would like to thank my office mates: Flo, little angle who left too early this office, thank you for passing me your technical knowledge at the beginning of my PhD and for your mental support in the moments of doubts. I liked you so much I followed you in my new job, because I missed your permanent (but funny) complaints! :P

To Alice, my English girl! Our friendship goes way beyond the boarder, Brexit or not! Thank you for your uncountable advice, proof reeding of drafts, mental support, and for teaching me how to make a circular pizza crust (I still have to improve on that, but I am working on it). I can't wait to go skiing with you again!

A special thanks to my best office mate, Mistinguette Laura Sinnnnniniigier. I will miss our breaks in front of the wall, where we talked about all and nothing. Thank you for listening to my complaints (and hell they were numerous 😊). I am looking forward for another ski-croziflette week-end with you, and I promise I won't bring you off-piste on the first descent next time! I hope you will appreciate the best desk from this office and that my ghost will not come to haunt you :P

To Paul, office and lab mate since the beginning (le sang de la veine). At least but not last, Nedjma, thank you for bringing some tidiness in this office! Your happiness and smile were always a pleasure to meet.

Thank you, Cam, sunshine of the lab, for the deep discussions we had whatever the hour (especially at night). I was happy to share more personal moments with you at the PJ parties, climbing, skitouring week-end and so on. I am also happy that I taught you the conversion at skitouring but please, don't try to kill your sister next time you show her!

Many thanks, Mag for all the best tricks and plans and for being my 1<sup>st</sup> (and only) fan with the firefighter calendar 😊. To Thibs, BruBru (co-coffee addict), Stan, Johan, Juju de la street, Tiffaine (alias la marseillaise, for the good music and atmosphere you brought to the lab since you started your PhD) and many others, for sharing many good moments of life together inside and outside the lab. I will miss our holidays all around the world. Thibs and Stan, we still have to find a techno party that we couldn't find in Berlin... in the only pub of Dole maybe héhé? 😄

Fanny and Laura, my French grimpeuses de choc! You made my last weeks in Lyon so appreciable. I will deeply miss the grimperos, sushi training session, croziflette traquenard and week end saucisson. These moments were like bubbles of heaven in the troublesome moments of the redaction. Laura, I wish you the best to find the ideal position you are seeking, either in Switzerland or in the south (because Lyon is already North for you ;P) and don't forget, Il reste une minute, ce serait con d'abandonner maintenant hein!

Fanny, I admire your courage and abnegation. You were a strong model of tête de mule to me. Many many thanks for your countless support you showed during the worst moments (and probably also some of the bests). You helped me in my periods of doubts to focus on what

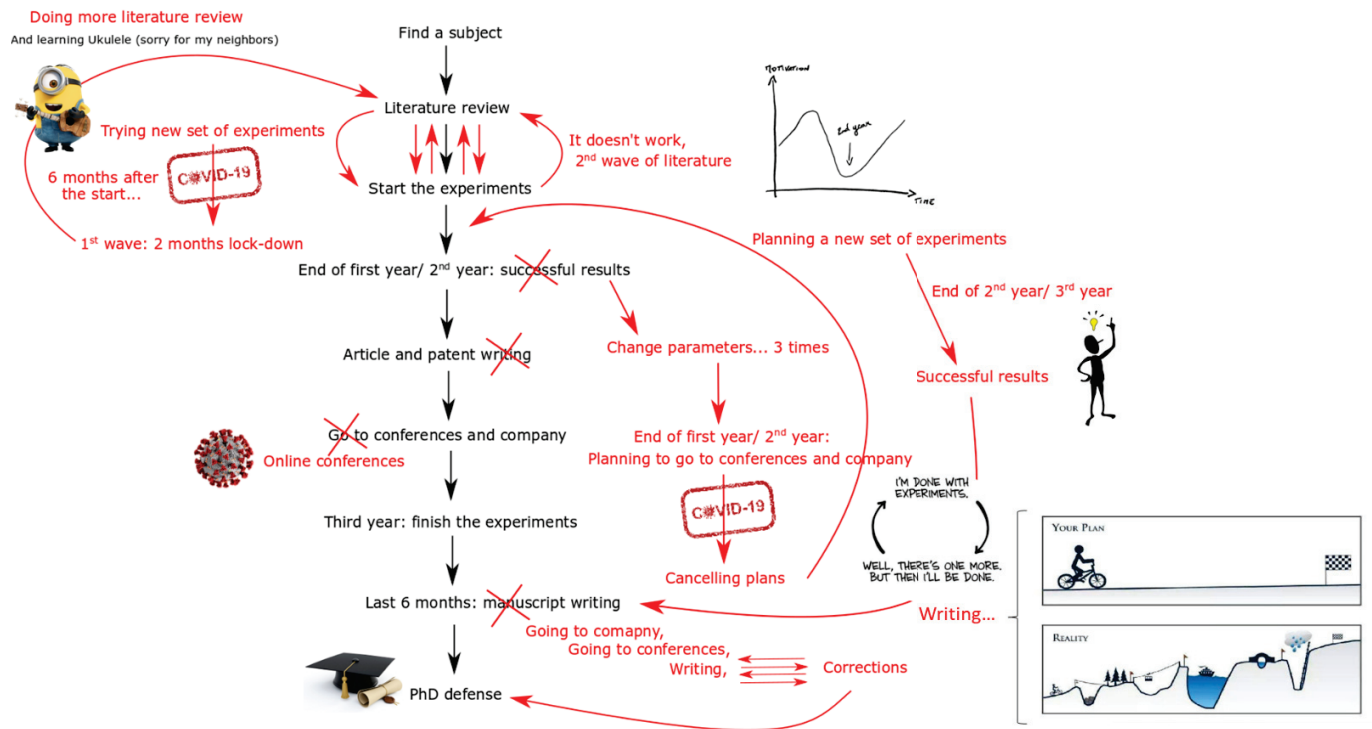
was truly important, and helped me to change my view on many things. I am happy that you made me discover the best brioche from Vence (ouch, should I say craquelin), and that we learnt together that kitten were elastic 😊.

Many thanks to my best friends, Lud and Marion, for their tireless support. Life has taken us away physically, but our friendship remains unchanged every time we see each other's. Many thanks Lud, for crossing two borders and driving 10 h to come and visit in Burghausen. We have now new anecdotes to add to our circular loop of jokes 😊. There was no other friend I wanted to spend my last redaction week with but you! You are strong persons and personalities which I admire deeply.

I would like to thank my parents for their understanding and everlasting support. I go to a far distance where I am not able to pay my due services to you. This sentence is rather short because I do not even have the words to express how much I owe you and love you, and to tell you what you represent for me. My parents, grand-parents, my brother (when he does not annoy me :P), and more generally speaking the whole family ("les pièces rapportées", la tribu and the like) made me who I am today with all the moral values that I respect and hold dear. But also, let's be honest, all the marvelous moments we spend together and make the strong unity of our family (usually around a few bottles of champagne, and a lot of good food!).

Lastly, many many thanks to the most important person in my life (actually second after our cat). Guillaume alias M. Mock, thank you for your tireless support. I have no word to describe how important you are to me, but I wouldn't be here today without you. Thank you for your supportiveness in all the fields of life, for your patience, for the everlasting and deep discussions we had and have, for the supportive pasta you cooked when I came home late, for the organization of the surprise week ends (that never were surprises because you couldn't keep a secret :P) and many many other countless things that make my life so sweet. I owe you much and I love you more than I could ever tell you.

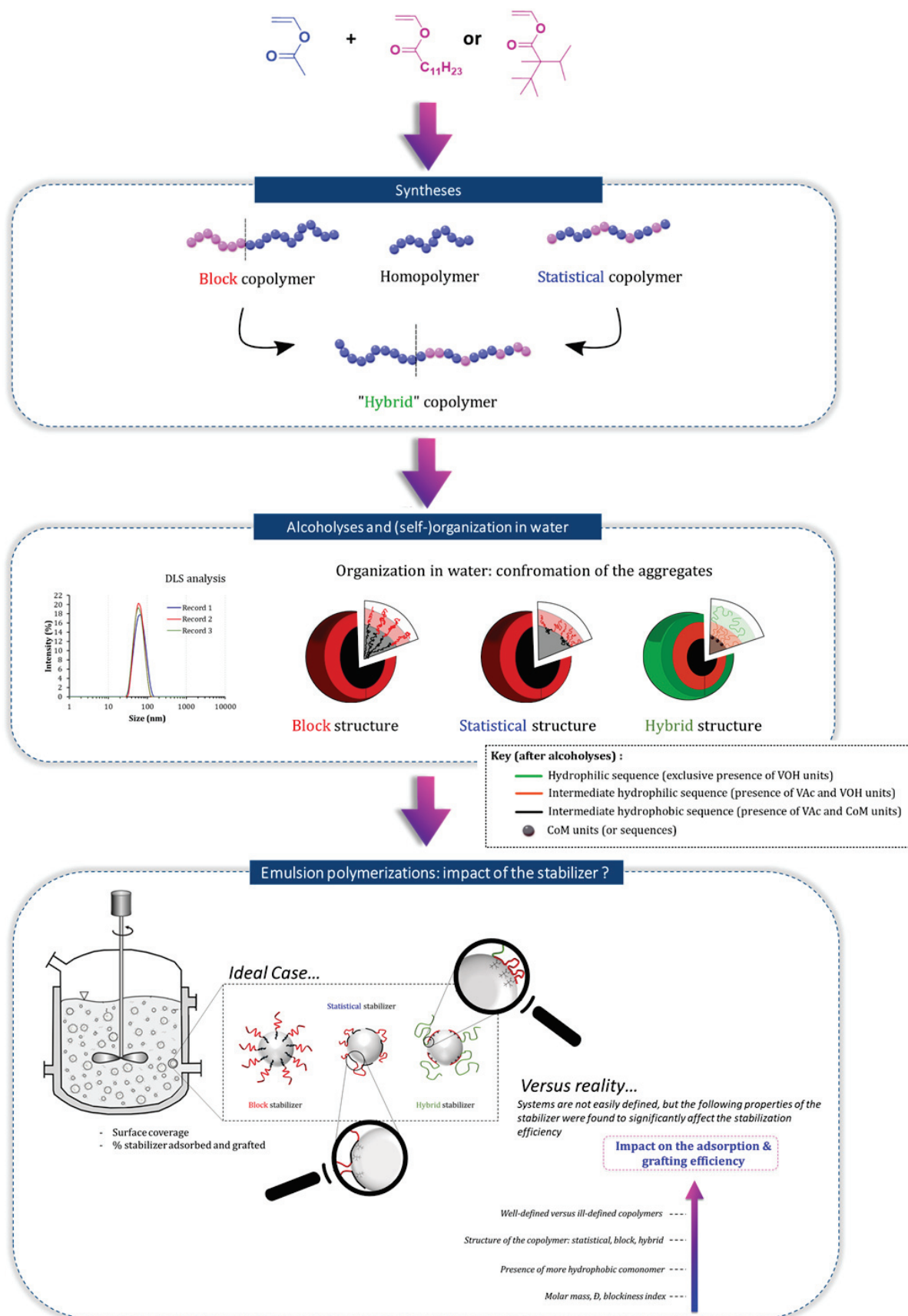
## How I imagined my PhD vs Reality











## Title

Design of amphiphilic copolymers incorporating vinyl alcohol units and their use as stabilizers for the emulsion copolymerization of vinyl acetate

## Abstract

Poly(vinyl alcohol-*co*-vinyl acetate) ((PVOH-*s*-VAc)) copolymers obtained by partial alcoholysis of poly(vinyl acetate) (PVAc) are of practical importance for many applications, including as stabilizers for emulsion copolymerization of vinyl acetate (VAc). In the latter case, the obtained products can be used either as a latex or as a re-dispersible powder after spray drying and find applications in various fields such as *e.g.*, adhesives, binders, medical applications or paints. However, during the emulsion process, all the P(VOH-*s*-VAc) chains are not involved in the stabilization of the particles. Indeed, free P(VOH-*s*-VAc) chains can be found in the aqueous phase, which can impact the properties of the end-products. The aim of the present project is to synthesize new amphiphilic copolymers incorporating VOH units, that are able (i) to stabilize VAc-based latexes with a better involvement in the stabilization of the particles, and (ii) to circumvent the potential problems resulting from remaining water-soluble chains encountered when the final polymer product is processed.

The synthesis of the targeted amphiphilic copolymers relies on reversible addition-fragmentation chain transfer (RAFT) polymerization, that allows the formation of well-defined polymer architectures. A careful design of copolymers of VAc and vinylic ester comonomers (CoM) was first performed to access a range of copolymer structures, including block copolymers. As CoM, vinyl neodecanoate (Veova, brand name Versa®10) and vinyl laurate (VL, brand name Versa®12) were chosen and hydrolysis conditions that could be selective of the VAc units were identified. After hydrolysis, the resulting well-defined amphiphilic copolymer structures were evaluated as stabilizers in the emulsion copolymerization of VAc and Veova.

The structures presenting the best results in terms of latex stability and of adsorption efficiency and grafting onto the particles were then synthesized on a larger scale at Wacker to be tested in various fields of applications.

## Keywords

Poly(vinyl acetate), Poly(vinyl alcohol-*co*-vinyl acetate), RAFT, copolymers, alcoholysis, statistical copolymers, block copolymers, vinyl acetate, vinyl alcohol, emulsion polymerization, latex, stabilizer.

## Titre

Synthèse et utilisation de copolymères amphiphiles incorporant des unités alcool vinylique en tant que stabilisant pour la copolymérisation en émulsion de l'acétate de vinyle

## Résumé

Les copolymères de type poly[(alcool vinylique)-*co*-(acétate de vinyle)] P(VOH-*s*-VAc) sont obtenus par alcoolyse partielle du poly(acétate de vinyle) (PAcV). Ces macromolécules trouvent des applications dans des domaines variés, et sont en particulier très utilisées comme stabilisants dans la (co)polymérisation en émulsion de l'acétate de vinyle (AcV). Cependant, au cours du procédé de polymérisation en émulsion, toutes les chaînes de P(VOH-*s*-VAc) ne sont pas impliquées dans la stabilisation des particules. Celles-ci se retrouvent dans la phase aqueuse en fin de polymérisation et ont un impact négatif sur les propriétés finales du produit. Le but de ce projet de recherche est donc de synthétiser de nouvelles structures de copolymères amphiphiles incorporant des unités VOH, qui soient capables de répondre aux problèmes associés à l'utilisation de P(VOH-*s*-VAc) conventionnels dans la synthèse de latex à base d'acétate de vinyle (AcV).

La polymérisation radicalaire contrôlée par transfert de chaîne réversible par addition-fragmentation (RAFT) a largement été utilisée dans la littérature pour accéder à des architectures contrôlées, bien définies et diverses telles que des copolymères à blocs. Après avoir sélectionné le néodécanoate de vinyle (Veova) et le laurate de vinyle (VL) comme comonomères de l'AcV, et réalisé les copolymérisations correspondantes à l'aide du procédé RAFT, l'hydrolyse sélective des unités AcV dans les copolymères bien définis obtenus a été évaluée. Le pouvoir stabilisant des copolymères amphiphiles résultant de l'hydrolyse a été testé dans un système de copolymérisation en émulsion de l'AcV et du Veova.

Les structures présentant les meilleurs résultats en termes de stabilité des latexes et en termes d'adsorption et greffage sur les particules, ont ensuite été synthétisées à plus grande échelle pour y être testées dans des domaines d'applications variés.

## Mots-clés

Poly(acétate de vinyle), poly[(alcool vinylique)-*co*-(acétate de vinyle)], RAFT, copolymère, copolymères statistiques, copolymères à blocs, acétate de vinyle, alcool vinylique, alcoolyse, polymérisation en émulsion, latex .





## Table of content

<b>Résumé .....</b>	<b>22</b>
<b>Abbreviations.....</b>	<b>26</b>
<b>General Introduction .....</b>	<b>30</b>

---

### Chapter I - State of the Art

---

I. INTRODUCTION .....	36
II. VINYL ACETATE-BASED EMULSION POLYMERIZATION .....	38
II.1 General introduction to emulsion polymerization.....	38
II.2 Overview of the mechanism and kinetics .....	42
II.3 Specificities of the emulsion polymerization of VAc.....	47
II.4 Emulsion copolymerization of VAc with VeoVa .....	50
III. POLY(VINYL ALCOHOL-S-VINYL ACETATE) (P(VOH-s-VAc)).....	54
III.1 Synthesis of P(VOH-s-VAc).....	54
III.2 The role of P(VOH-s-VAc) as stabilizer for the emulsion (co)polymerization of VAc.....	60
IV. CONTROLLED RADICAL POLYMERIZATION TECHNIQUES: THE EXAMPLE OF RAFT.....	67
IV.1 Generalities on reversible-deactivation radical polymerization (RDRP) .....	67
IV.2 Reversible addition fragmentation chain transfer (RAFT) .....	69
V. APPLICATION OF THE RDRP TECHNIQUES TO THE SYNTHESIS OF WELL-DEFINED VOH-BASED MACROMOLECULES. ....	76
V.1 VOH-based statistical copolymers.....	76
V.2 VOH-based block copolymers.....	76
V.3 Other structures of VOH-based copolymer .....	80
VI. MOTIVATION AND OBJECTIVES OF THIS WORK.....	83

---

### Chapter II

#### Synthesis of well-defined P(VOH-s-VAc) by alcoholysis of RAFT/MADIX synthesized poly(vinyl acetate).

#### Evaluation as stabilizers for the emulsion copolymerization of VAc and VeoVa

---

I. INTRODUCTION .....	92
II. RAFT/MADIX POLYMERIZATION OF VAc .....	93
III. ALCOHOLYSIS OF THE WELL-DEFINED PVAc .....	102
III.1 General introduction on the alcoholysis of PVAc and the associated method of characterization ...	102
III.2 Alcoholysis of the library of PVAc obtained by RAFT/MADIX polymerization .....	109
III.3 Influence of the DP of the PVAc on the kinetics of alcoholysis .....	113
III.4 Study of the microstructure of the well-defined P(VOH-s-VAc) by NMR, and chain-end analysis .....	115
IV. (SELF-)ORGANIZATION IN WATER.....	118
IV.1 Organization in water.....	119

IV.2	Surface tension.....	124
IV.3	Conclusion on the (self-)organization of P(VOH-s-VAc) in water.....	126
V.	EMULSION COPOLYMERIZATION OF VAc AND VEOVA STABILIZED WITH MOWIOL 4-88 AND THE RAFT/MADIX-SYNTHESIZED P(VOH-s-VAc). ....	127
V.1	Set up of the experimental parameters for the emulsion copolymerization of VAc and VeoVa .....	130
V.2	Influence of the hydrolysis degree at fixed DP = 75 and fixed amount of stabilizer (10 wt.% based on monomers).....	134
V.3	Influence of the polymerization degree at fixed HD = 88% and fixed amount of stabilizer (10 wt.% based on monomers).....	135
V.4	Influence of the amount of stabilizer at fixed DP = 75 and HD = 88%.....	146
VI.	CONCLUSION.....	149

---

### Chapter III

#### Synthesis and evaluation as stabilizer of P(VAc-s-CoM-s-VAc) statistical copolymers

---

I.	INTRODUCTION .....	158
II.	RAFT/MADIX COPOLYMERIZATION OF VAc WITH VEOVA OR VL .....	160
II.1	General procedure .....	160
II.2	Characterization of P(VAc-s-VL) copolymers.....	161
II.3	Characterization of P(VAc-s-VeoVa) copolymers.....	164
III.	ALCOHOLYSIS OF P(VAc-s-VL) AND P(VAc-s-VEOVA) COPOLYMERS.....	169
III.1	Alcoholysis of P(VAc <sub>0.90</sub> -s-VL <sub>0.10</sub> ) .....	169
III.2	Alcoholysis of P(VAc-s-VeoVa).....	173
III.3	Conclusion on the alcoholysis of the statistical copolymers.....	176
IV.	(SELF-)ORGANIZATION OF THE COPOLYMERS IN WATER.....	177
IV.1	Dispersibility of the statistical copolymers in water.....	177
IV.2	Organization of the copolymer in water: DLS study .....	179
IV.3	Surface tension.....	184
IV.4	Conclusion.....	185
V.	EMULSION COPOLYMERIZATION OF VAc AND VEOVA WITH P(VOH-s-CoM-s-VAc) COPOLYMERS .....	187
V.1	Screening with KPS .....	187
V.2	Emulsion copolymerization of VAc and VeoVa initiated by a redox couple. ....	188
VI.	CONCLUSION.....	204

---

### Chapter IV

#### Synthesis and evaluation as stabilizer of PCoM-b-P(VOH-s-VAc) (or reverse order P(VOH-s-VAc)-b-PCoM) block copolymers

---

I.	INTRODUCTION .....	210
II.	SYNTHESIS OF THE BLOCK COPOLYMERS.....	213
II.1	RAFT/MADIX polymerization of VeoVa or VL .....	213

II.2	<i>Synthesis and characterizations of low molar mass PVL homopolymers for further block copolymerization synthesis</i> .....	220
II.3	<i>Chain extension of PVeOVA and PVL with VAc</i> .....	223
II.4	<i>Conclusion on the synthesis of block copolymers</i> .....	226
III.	ALCOHOLYSIS OF THE BLOCK COPOLYMERS.....	228
III.1	<i>Alcoholysis of the VeOVA-based block copolymers</i> .....	228
III.2	<i>Alcoholysis of the VL-based block copolymers</i> .....	230
IV.	(SELF-) ORGANIZATION OF THE BLOCK COPOLYMERS IN WATER.....	234
IV.1	<i>Dispersibility of the block copolymers in water</i> .....	234
IV.2	<i>Organization of the block copolymers in water: DLS study</i> .....	235
IV.3	<i>Surface tension</i> .....	237
IV.4	<i>Conclusion</i> .....	238
V.	EMULSION COPOLYMERIZATION OF VAc AND VEOVA WITH THE SELECTED BLOCK COPOLYMER CANDIDATES 239	
V.1	<i>Kinetics of the polymerizations and colloidal features of the latexes</i> .....	239
V.2	<i>Adsorbed and grafted stabilizer</i> .....	245
V.3	<i>Evaluation of the alkali resistance of the latexes at different pH</i> .....	246
VI.	CONCLUSION.....	247

---

## Chapter V

### Synthesis and evaluation as stabilizer of P(VOH-s-VAc)-b-P(VOH-s-CoM-s-VAc) “hybrid” block copolymers

---

I.	INTRODUCTION.....	252
II.	SYNTHESIS AND CHARACTERIZATIONS OF THE “HYBRID” PVAc-B-P(VAc-S-CoM) STRUCTURES.....	253
II.1	<i>Variation of the molar fraction of VeOVA in 75_PVAc-b-P(VAc-s-VeOVA)<sub>y/z</sub></i> .....	254
II.2	<i>Variation of the DP of PVAc (DP1) in PVAc-b-P(VAc-s-VeOVA)<sub>y/z</sub></i> .....	257
II.3	<i>Synthesis of PVAc-b-P(VAc-s-VL)<sub>y/z</sub></i> .....	261
II.4	<i>Conclusion on the synthesis of the hybrid structures</i> .....	262
III.	ALCOHOLYSIS OF THE HYBRID COPOLYMERS.....	263
IV.	(SELF-)ORGANIZATION OF THE HYBRID COPOLYMERS IN WATER.....	265
V.	EMULSION COPOLYMERIZATION OF VAc AND VEOVA STABILIZED WITH THE SELECTED HYBRID COPOLYMERS 271	
V.1	<i>Emulsion copolymerization of VAc and VeOVA stabilized with the CoM-based hybrid stabilizers</i> ....	271
VI.	CONCLUSION.....	281

---

## Chapter VI

### Selection of the most promising stabilizer candidates for the scale-up experiments and applications

---

I.	INTRODUCTION.....	288
II.	SCALE-UP OF THE (CO)POLYMER SYNTHESSES.....	289



II.1	Materials .....	289
II.2	Polymerizations.....	289
II.3	Alcoholysis of the (co)polymers.....	290
II.4	Evaluation of the biodegradability of the stabilizers .....	292
III.	SCALE-UP OF THE EMULSION COPOLYMERIZATIONS OF VAc AND VEOVA.....	296
III.1	Set up of the experimental parameters in a 1 L scale reactor .....	296
III.2	Influence of the amount of stabilizer on the stabilization of the particles .....	299
IV.	EVALUATION OF THE PERFORMANCES OF THE LATEXES IN DIFFERENT APPLICATIONS .....	301
IV.1	Evaluation of the alkali resistance of the latexes at different pH.....	301
IV.2	Mortar application.....	303
IV.3	Spray drying.....	318
V.	CONCLUSION.....	322

---

## General Conclusion

---



---

## Experimental procedures and characterization techniques

---

I.	MATERIALS.....	334
II.	SYNTHESIS OF THE RAFT AGENT .....	334
III.	POLYMERIZATION PROCEDURES .....	336
III.1	Homopolymerization of VAc (Chapter II).....	336
III.2	Homopolymerization of VeoVa and VL (Chapter IV).....	336
III.3	Statistical copolymerization of VAc and VeoVa or VL (Chapter III).....	337
III.4	Block copolymerization of VAc and either VeoVa or VL (CoM) (Chapters IV and V) .....	338
IV.	ALCOHOLYSIS PROCEDURES.....	340
IV.1	Alcoholysis of PVAc.....	340
IV.2	Alcoholysis of statistical and block copolymers .....	340
V.	EMULSION COPOLYMERIZATION OF VAc AND VEOVA.....	342
V.1	Screening with KPS (Chapters II and III).....	342
V.2	Emulsion copolymerization of VAc and VeoVa initiated by a redox couple .....	342
V.3	Scale up of the emulsion polymerization to a 1000 mL reactor.....	343
VI.	CHARACTERIZATION TECHNIQUES .....	345
VI.1	Nuclear magnetic resonance (NMR).....	345
VI.2	Size exclusion chromatography (SEC).....	345
VI.3	UV-visible spectroscopy.....	346
VI.4	Fourier-transform infrared (FTIR) spectroscopy.....	346
VI.5	Gravimetric analysis.....	347
VI.6	Dynamic light scattering (DLS).....	347
VI.7	Cryogenic electron transmission microscopy (Cryo-TEM) .....	348
VI.8	Determination of the amount of adsorbed & grafted stabilizer.....	348
VI.9	Surface tension.....	350
VII.	PROCEDURES FOR THE USE OF THE LATEXES IN VARIOUS FIELD OF APPLICATION .....	351
VII.1	pH stability.....	351

VII.2	<i>pH stability for latexes stored in the fridge .....</i>	<i>351</i>
VII.3	<i>Aging tests: pH stability for latexes stored at 40 °C .....</i>	<i>351</i>
VII.4	<i>Mortar calorimetry .....</i>	<i>351</i>
VII.5	<i>Spray drying.....</i>	<i>354</i>
<b>Appendix .....</b>		<b>356</b>



## Résumé

Les travaux de recherche décrits dans ce manuscrit s'inscrivent dans le cadre d'une collaboration entre le laboratoire CP2M et Wacker Chemie. Wacker est un leader mondial dans la synthèse de polymères. Un des axes majeurs de recherche de cet industriel est la synthèse et le développement du poly(acétate de vinyle) (PACV). Wacker produit des homopolymères, mais également des copolymères à base d'acétate de vinyle (AcV) et d'éthylène ou de néodécanoate de vinyle (VeoVa). Ces copolymères sont synthétisés par le procédé de polymérisation en émulsion qui conduit à la formation de particules de polymère dispersées dans l'eau. La dispersion résultante est également appelée latex. Ces latex sont utilisés dans de nombreux domaines d'applications tels que la construction, la peinture, les adhésifs ou encore les emballages. Afin d'assurer la stabilité de ces latex, Wacker utilise des stabilisants macromoléculaires : le poly(alcool vinylique) (P(VOH-*s*-AcV)). Ce copolymère, constitué d'unités alcool vinylique et acétate de vinyle, est produit industriellement par alcoololyse du PACV, lui-même obtenu par polymérisation radicalaire. Afin de stabiliser efficacement les particules de polymère constituant le latex, un degré d'hydrolyse de 84 à 89% est préférable.

Les unimères de P(VOH-*s*-AcV) s'organisent dans l'eau (avec un cœur riche en unités AcV et des boucles riches en unités VOH). Lorsque le P(VOH-*s*-AcV) est utilisé comme stabilisant pour la polymérisation en émulsion de l'AcV, il existe une synergie entre plusieurs mécanismes de stabilisation. L'AcV possède une solubilité dans l'eau élevée (2.5 wt.% à 25 °C, 4.2 wt.% à 60 °C)<sup>[1-3]</sup> par rapport à la plupart des autres monomères usuellement utilisés en émulsion, et aussi une constante de propagation élevée ( $k_p = 3.6 \times 10^3 \text{ L mol}^{-1} \text{ s}^{-1}$  à 25 °C),<sup>[4]</sup> qui favorisent tous deux la nucléation homogène. A l'image de la plupart des systèmes de polymérisation en émulsion, les oligoradicaux issus de l'amorçage, qui a lieu dans l'eau, vont croître jusqu'à atteindre une taille critique à partir de laquelle ils ne sont plus solubles dans l'eau, et vont précipiter pour former une particule. Cette particule sera stabilisée par migration de chaînes de P(VOH-*s*-AcV) à sa surface. Cette nucléation homogène contribue majoritairement à la formation des particules.<sup>[5]</sup>

Du fait de la constante de transfert élevée des chaînes de PACV en croissance, ces oligoradicaux peuvent également subir des réactions de transfert et arracher un atome d'hydrogène du groupement acétate des unités AcV (-CH<sub>3</sub>) du P(VOH-*s*-AcV), ou du squelette du polymère (-CH<sub>2</sub>- des unités AcV et VOH). Cela génère un radical sur la chaîne de P(VOH-*s*-AcV), qui est capable de réagir avec de l'AcV présent dans la phase aqueuse, et entraîne la formation de greffons PACV sur le P(VOH-*s*-AcV). Lorsque ces greffons atteignent une certaine taille, la structure globale du P(VOH-*s*-AcV) greffé devient tensio-active. Cette structure est alors exclue de la phase aqueuse et peut migrer vers la surface d'une particule

existante. Elle peut aussi conduire à la formation d'une nouvelle particule par agrégation avec d'autres chaînes greffées, suivie par l'entrée de radicaux.

Enfin, il n'est pas exclu qu'une partie des oligoradicaux migrent dans les unimères initiaux de P(VOH-*s*-AcV), conduisant ainsi à la formation d'une particule. Dans les deux derniers cas, la formation de particules peut s'assimiler à une nucléation de type micellaire.

La stabilité d'une particule de PAcV obtenue par polymérisation en émulsion conduite en présence de P(VOH-*s*-AcV) est ainsi assurée à la fois par du P(VOH-*s*-AcV) fortement adsorbé à sa surface, mais également par du P(VOH-*s*-AcV) physiquement greffé (ou ancré) dans la particule par les greffons de PAcV.

Toutefois, la totalité du P(VOH-*s*-AcV) engagé dans la polymérisation ne participe pas à la stabilisation des particules, et une partie reste en phase aqueuse. Ces chaînes peuvent avoir des impacts négatifs sur les propriétés du latex lorsqu'il est utilisé dans certaines applications précédemment citées, et Wacker cherche à réduire cette fraction libre.

Le but de ces travaux de thèse est donc de synthétiser de nouveaux stabilisants macromoléculaires mimant le P(VOH-*s*-AcV), mais avec une meilleure implication dans la stabilisation des particules de polymère. Dans un premier temps nous avons comparé la capacité d'un P(VOH-*s*-VAc) de faible masse molaire et faible dispersité à stabiliser les particules de polymères d'un latex, par rapport à un P(VOH-*s*-VAc) commercial (Mowiol 4-88) de haute masse molaire et dispersité élevée. Par la suite, nous avons émis l'hypothèse que l'introduction de comonomères plus hydrophobes que l'AcV (CoM) dans la structure du P(VOH-*s*-AcV) permettrait d'améliorer l'affinité du stabilisant avec les particules de polymère et ainsi de diminuer la fraction de polymère résiduelle dans l'eau. La synthèse de P(VOH-*s*-AcV-*s*-CoM) a donc été envisagée par alcoololyse de chaînes de P(AcV-*s*-CoM) préformées. Ainsi, le CoM doit donc également ne pas être sensible (ou moins sensible que l'AcV) à l'alcoololyse.

Diverses architectures macromoléculaires (copolymères statistiques, à blocs et leurs dérivés) incorporant des unités AcV, VOH et CoM ont ainsi été synthétisées par une polymérisation radicalaire par désactivation réversible (longtemps dénommée polymérisation radicalaire contrôlée). Parmi les diverses techniques existantes, la polymérisation radicalaire contrôlée par transfert de chaîne réversible par addition fragmentation (RAFT en anglais), (ou « macromolecular design *via* interchange of xanthate (MADIX) dans le cas où l'agent de transfert est un xanthate) est l'une des plus performantes pour la synthèse de PAcV. La RAFT a donc été privilégiée dans ce projet de recherche.

Le **Chapitre I** dresse une revue non exhaustive introduisant les principaux concepts et techniques utilisés dans ces travaux, à savoir, la polymérisation en émulsion, la RAFT, et différents exemples de copolymères contenant des unités VOH synthétisés par RAFT/MADIX.

Le **Chapitre II** est dédié à la synthèse d'une gamme de P(VOH-*s*-AcV)s obtenus par alcoolysé de PAcVs, eux-mêmes obtenus par RAFT/MADIX, avec différents degrés de polymérisation (DP) et degrés d'hydrolyse (DH). L'objectif est d'évaluer la capacité de tels copolymères à stabiliser un latex et de comparer l'efficacité de stabilisation à un P(VOH-*s*-AcV) commercial fourni par Wacker (Mowiol 4-88) et utilisé comme référence au cours de ces travaux lors de la copolymérisation en émulsion de l'AcV et du néodécanoate de vinyle (Veova). Dans une première approximation, la détermination de la fraction de stabilisant adsorbée et greffée sur les particules de polymère permet d'évaluer l'affinité du copolymère avec ces dernières.

Dans le **Chapitre III**, nous étudions l'incorporation de comonomères plus hydrophobes (CoM), tels que le laurate de vinyle (VL) ou le Veova au sein de la structure statistique bien définie de P(VOH-*s*-AcV). Le but est d'essayer d'augmenter l'affinité du stabilisant avec les chaînes de polymères qui composent les particules finales, et ainsi essayer de diminuer la fraction de stabilisant libre dans l'eau. Cette performance est à nouveau évaluée par la détermination de la fraction de stabilisant adsorbé et greffé.

Les **Chapitres IV** et **V** sont consacrés à la synthèse d'architectures de copolymères à blocs. Ces structures incorporent toujours des unités AcV, VOH et CoM, mais l'objectif est de déterminer l'influence de l'architecture de ces nouveaux copolymères sur leur capacité à stabiliser le latex. Les copolymères à blocs sont étudiés dans le **Chapitre IV**. Dans le **Chapitre V**, une combinaison des deux structures des **Chapitres III** et **IV** est étudiée : une série de copolymères à blocs statistiques (désignés hybrides), et composés d'un bloc de PAcV et d'un bloc de P(AcV-*s*-CoM) est synthétisée, alcoolysée, et les copolymères hybrides résultants sont évalués comme stabilisants pour la copolymérisation en émulsion de l'AcV et du Veova.

Enfin, dans le **Chapitre VI**, les nouvelles structures développées au cours de ce travail de recherche ayant donné les résultats les plus prometteurs sont sélectionnées pour être synthétisées à plus grande échelle et leur biodégradabilité est évaluée. Ces copolymères sont ensuite testés en tant que stabilisants dans le procédé de copolymérisation en émulsion de l'AcV et du Veova à plus grande échelle (1 L) que celle testée au laboratoire (75 mL). Les propriétés mécaniques des latex résultants sont évaluées dans diverses applications à visées industrielles telles que la formulation de mortiers et le séchage par pulvérisation.

## Références

- [1] Y. H. Erbil, *Vinyl Acetate Emulsion Polymerization and Copolymerization with Acrylic Monomers*, CRC Press, **2000**.
- [2] X. S. Chai, F. J. Schork, A. DeCinque, K. Wilson, *Ind. Eng. Chem. Res.* **2005**, *44*, 5256–5258.
- [3] *Polymerization of Vinyl Acetate in Emulsion. US2694052A*, **1954**.
- [4] S. Beuermann, S. Harrisson, R. A. Hutchinson, T. Junkers, G. T. Russell, *Polym. Chem.* **2022**, *13*, 1891–1900.
- [5] B. M. Budhlall, E.D.Sudol, V.L.Dimonie, A.Klein, M. S.El-Asser, *J. Polym. Sci. Part A Polym. Chem.* **2001**, *39*, 3633 - 3654..

## Abbreviations

$\rho$	Density
AIBN	Azobisisobutyronitrile
$A_s$	Specific surface area
AsAc	Ascorbic acid
$\beta$	Blockiness index
BOD	Biochemical oxygen demand
$CDCl_3$	Deuterated chloroform
COD	Chemical oxygen demand
CoM	Comonomer
Cryo-TEM	Cryogenic electron transmission microscopy
CTA	Chain transfer agent
$C_{tr}$	Chain transfer constant
$\bar{D}$	Dispersity
DLS	Dynamic light scattering
DMSO	<i>N,N</i> -dimethyl sulfoxide
DOC	Dissolved organic carbon
DP	Degree of polymerization
$D_n$	Number-average particle diameter
$D_v$	Volume-average particle diameter
$D_w$	Weight-average particle diameter
$D_w/D_n$	Dispersity of the particle diameter
EVA	Poly(vinyl acetate- <i>co</i> -ethylene) statistical copolymer
$f_{CoM,0}$	Molar fraction of CoM in the monomer mixture
$f_{VAc,0}$	Molar fraction of VAc in the monomer mixture
$F_{monomer}$	Molar fraction of the monomer (either VAc, VOH or CoM) in the copolymer
FRP	Free radical polymerization
FTIR	Fourier-transform infrared spectroscopy
HD	Hydrolysis degree
HSQC	Heteronuclear single-quantum correlation spectroscopy
ITP	Iodine transfer polymerization
KPS	Potassium persulfate
LALS	Low angle light scattering
LAM	Less activated monomer
LCB	Long chain branching
macroCTA	Macromolecular chain transfer agent
MADIX	Macromolecular design by interchange of xanthate



MeOH	Methanol
$M_n$	Number-average molar mass
$M_w$	Weight-average molar mass
mol.%	Molar content
$N_{agg}$	Number of aggregation
$n_0^{VOH}$	Average number of VOH units in a PVOH sequence of P(VOH- <i>s</i> -VAc)
$n_0^{VAc}$	Average number of VAc units in a PVAc sequence of P(VOH- <i>s</i> -VAc)
$\bar{n}$	Average number of radicals per particle
NaOH	Sodium hydroxide
NMP	Nitroxide-mediated polymerization
NMR	Nuclear magnetic resonance
$N_p$	Number of particles
PdI	Polydispersity index
PE	Polyethylene
PEO	Poly(ethylene oxide)
PPO	Poly(propylene oxide)
PS	Polystyrene
PSD	Particle size distribution
PVAc	Poly(vinyl acetate)
PVAc- <i>b</i> -PCoM	Poly(vinyl acetate)- <i>b</i> -poly(vinyl ester comonomer) block copolymer
P(VAc- <i>s</i> -CoM)	Poly(vinyl acetate- <i>s</i> -vinyl ester comonomer) statistical copolymer
PVOH	Poly(vinyl alcohol)
PVOH- <i>b</i> -PCoM	Poly(vinyl alcohol)- <i>b</i> -poly(vinyl ester comonomer) block copolymer
P(VOH- <i>s</i> -VAc)	Poly(vinyl alcohol- <i>s</i> -vinyl acetate) statistical copolymer
P(VOH- <i>s</i> -CoM)	Poly(vinyl alcohol- <i>s</i> -vinyl ester comonomer) statistical copolymer
RAFT	Reversible addition-fragmentation chain transfer
RDRP	Reversible-deactivation radical polymerization
$R_h$	Hydrodynamic radius
RI	Refractive index
REM	Reflection electron microscopy
SEC	Size exclusion chromatography
Sc	Solid content
T	Temperature
TBHP	<i>Tert</i> -butyl hydroperoxide
TEM	Transmission electron microscopy
$T_g$	Glass transition temperature
THF	Tetrahydrofuran
ThOD	Theoretical oxygen demand
UV	Ultra violet
VAc	Vinyl acetate

VeoVa	Vinyl neodecanoate
VL	Vinyl laurate
VOH	Vinyl alcohol
wt.%	Weight content
$X_{\text{mol}}$	Overall molar conversion of the monomers
$X_{\text{VAc}}$	Individual conversion of VAc
$X_{\text{CoM}}$	Individual conversion of CoM
$Z_{\text{av}}$	Intensity-weighted mean diameter measured by DLS



## General Introduction

This research work is part of a collaboration between the CP2M laboratory and Wacker Chemie. Wacker is a world leader in polymer synthesis. One of the major research fields of this company is the synthesis and development of poly(vinyl acetate) (PVAc). Wacker produces homopolymers, but also copolymers based on vinyl acetate (VAc) and ethylene or vinyl neodecanoate (Versa10® or VeoVa). These copolymers are synthesized *via* emulsion polymerization which leads to the formation of polymer particles dispersed in water. The resulting dispersion is also called a latex. These latexes are used in many fields of application such as construction, paints, adhesives or packaging.

To ensure the stability of these latexes, Wacker uses a macromolecular stabilizer produced industrially *via* alcoholysis of PVAc (itself obtained by radical polymerization) resulting in a statistical copolymer containing vinyl alcohol and vinyl acetate units P(VOH-*s*-VAc), generally though abusively called poly(vinyl alcohol). In order to stabilize the latex efficiently, a hydrolysis degree of 84 to 89% is preferable.

P(VOH-*s*-VAc) unimers organize in water (with a core rich in VAc units and loops rich in VOH units). When P(VOH-*s*-VAc) is used as a stabilizer for the emulsion (co)polymerization of VAc, the mechanism of generation of the particles is rather complex and involves different modes of particle nucleation. VAc has a high solubility in water (2.5 wt.% at 25 °C, 4.2 wt.% at 60 °C)<sup>[1-3]</sup> compared to most of the monomers commonly used in emulsion and also a high propagation rate constant ( $k_p = 3.6 \times 10^3 \text{ L mol}^{-1} \text{ s}^{-1}$  at 25 °C),<sup>[4]</sup> which both favor homogeneous nucleation. Like in other emulsion systems, oligoradicals are formed in water after initiation and a few propagation steps. These oligoradicals will grow until they reach a certain size above which they are no longer soluble in water, and will precipitate to form a particle. This particle will be stabilized by migration of P(VOH-*s*-VAc) chains at its interface. This homogeneous nucleation is the main route contributing to particle formation.<sup>[5]</sup>

Due to the high transfer constant of the growing PVAc chains, the oligoradicals can also abstract a hydrogen atom from the acetate group of the VAc units (-CH<sub>3</sub>) of P(VOH-*s*-VAc), or a hydrogen atom from the polymer backbone (-CH<sub>2</sub>- of the VAc and VOH units). This generates a radical on the P(VOH-*s*-VAc) chain, which is able to react with VAc present in the aqueous phase, and leads to the formation of PVAc grafts on the P(VOH-*s*-VAc). When these grafts reach a certain size, the overall structure of the grafted P(VOH-*s*-VAc) becomes "surface active". This structure is then excluded from the aqueous phase and migrates towards an existing particle. It can also form a new particle by aggregation with other grafted chains and radical entry. In addition, it is not excluded that radical entry could occur into the initial organized unimers of P(VOH-*s*-VAc). In the two latter cases, particle formation would occur according to a micellar type of nucleation.

A particle of PVAc obtained by emulsion polymerization carried out in the presence of P(VOH-*s*-VAc) is thus ensured by strongly adsorbed P(VOH-*s*-VAc) on its surface, or by physically grafted (or anchored) P(VOH-*s*-VAc) in the particle *via* the PVAc grafts, or by a combination of both.

However, not all the P(VOH-*s*-VAc) chains involved in the polymerization participate in the stabilization of the particles, and a portion remains in the aqueous phase. These chains can have negative impacts on the properties of the latex when used in some of the applications mentioned above, and Wacker is looking for ways to reduce this free fraction.

The aim of this research work is therefore to synthesize new macromolecular stabilizers mimicking P(VOH-*s*-VAc), but with a higher efficiency in the stabilization of the polymer particles. At first, we evaluated the ability of a low-molecular-weight and low-dispersity P(VOH-*s*-VAc) to stabilize polymer particles in a latex compared to a high-molecular-weight, high-dispersity commercial P(VOH-*s*-VAc) (Mowiol 4-88). Then, we hypothesized that the introduction of more hydrophobic comonomers (CoM), compared to VAc, into the P(VOH-*s*-VAc) structure would improve the affinity of the stabilizer with the polymer particles and thus decrease the fraction of free polymer in water. The synthesis of P(VOH-*s*-VAc-*s*-CoM) was therefore considered by alcoholysis of preformed P(VAc-*s*-CoM) chains. To keep CoM units in the final alcoholized structure, the CoM must be chosen in a way that it is not sensitive or at least less sensitive than VAc to alcoholysis.

Various macromolecular architectures (statistical copolymers, block copolymers and their derivatives) incorporating VAc, VOH and CoM units have been synthesized by a reversible deactivation radical polymerization (RDRP), and more precisely by reversible addition-fragmentation chain transfer (RAFT) / macromolecular design via interchange of xanthate (MADIX) in the present work. Indeed, among the various existing RDRP techniques, RAFT/MADIX is one of the most versatile for the synthesis of PVAc.

**Chapter I** provides a non-exhaustive review introducing the main concepts and techniques used in this work, namely, emulsion polymerization, RAFT, and different examples of copolymers containing VOH units synthesized by RDRP.

**Chapter II** is dedicated to the synthesis of a library of well-defined P(VOH-*s*-VAc)s obtained by alcoholysis (or more abusively hydrolysis) of PVAc obtained by RAFT/MADIX polymerization. Copolymers with different degrees of polymerization (DP) and degrees of hydrolysis (HD) are targeted. The aim is to evaluate the ability of such copolymers to stabilize a latex and compare the stabilization efficiency to a commercial P(VOH-*s*-VAc) named Mowiol 4-88 (Kuraray) and used as a benchmark.

In **Chapter III** we investigate the incorporation of more hydrophobic comonomer units (CoM), either vinyl laurate (VL) or VeoVa, inside the well-defined statistical structure of P(VOH-*s*-VAc). The aim is to determine whether this CoM improves the stabilization efficiency of the copolymer by a better affinity of the stabilizer with the polymer particles, enhancing the amount of adsorbed and grafted stabilizer.

**Chapter IV and V** are devoted to the synthesis of well-defined block copolymers architectures. These structures still incorporate VAc, VOH and CoM units, but the aim is to determine the influence of the architecture of the copolymers on the stabilizing efficiency of the latex. Block structures of PVeoVa-*b*-P(VOH-*s*-VAc) and PVL-*b*-P(VOH-*s*-VAc) are studied in **Chapter IV**. **Chapter V** combines the best attributes of statistical and block copolymer structures identified in **Chapters III and IV** in the same chains of well-defined statistical block copolymers. Thus, well-defined block-statistical copolymers (shortened as hybrids copolymers), composed of a PVAc block and a statistical block containing VAc and CoM units are synthesized, alcoholized, and the resulting hybrid copolymers are evaluated as stabilizer candidates for the emulsion copolymerization of VAc and VeoVa.

Finally, in **Chapter VI**, the most promising stabilizer structures developed during this thesis are selected and their synthesis is scaled up for them to be used in large scale emulsion copolymerization of VAc and VeoVa. The mechanical properties of the resulting latexes are tested in various industrial applications such as in mortar formulation, film formation (for adhesive or paints) and spray drying.

## References

- [1] Y. H. Erbil, *Vinyl Acetate Emulsion Polymerization and Copolymerization with Acrylic Monomers*, CRC Press, **2000**.
- [2] X. S. Chai, F. J. Schork, A. DeCinque, K. Wilson, *Ind. Eng. Chem. Res.* **2005**, *44*, 5256–5258.
- [3] *Polymerization of Vinyl Acetate in Emulsion. US2694052A*, **1954**.
- [4] S. Beuermann, S. Harrisson, R. A. Hutchinson, T. Junkers, G. T. Russell, *Polym. Chem.* **2022**, *13*, 1891–1900.
- [5] B. M. Budhlall, E.D.Sudol, V.L.Dimonie, A.Klein, M. S.El-Asser, *J. Polym. Sci. Part A Polym. Chem.* **2001**, *39*, 3633 - 3654.



---

# Chapter I

## State of the Art

---



## Table of content

I. INTRODUCTION.....	36
II. VINYL ACETATE-BASED EMULSION POLYMERIZATION .....	38
II.1 General introduction to emulsion polymerization.....	38
II.2 Overview of the mechanism and kinetics.....	42
II.2.1 Interval I: nucleation .....	43
II.2.2 Interval II: particle growth.....	46
II.2.3 Interval III: final stage of the polymerization .....	47
II.3 Specificities of the emulsion polymerization of VAc.....	47
II.4 Emulsion copolymerization of VAc with VeoVa.....	50
III. POLY(VINYL ALCOHOL-S-VINYL ACETATE) (P(VOH-s-VAc)).....	54
III.1 Synthesis of P(VOH-s-VAc).....	54
III.2 The role of P(VOH-s-VAc) as stabilizer for the emulsion (co)polymerization of VAc.....	60
IV. CONTROLLED RADICAL POLYMERIZATION TECHNIQUES: THE EXAMPLE OF RAFT.....	67
IV.1 Generalities on reversible-deactivation radical polymerization (RDRP).....	67
IV.2 Reversible addition fragmentation chain transfer (RAFT).....	69
IV.2.1 Choice of the RAFT/MADIX agent .....	71
IV.2.2 Livingness in RAFT/MADIX .....	73
IV.2.3 Introduction on the limitations encountered in RAFT/MADIX polymerization of LAM .....	74
V. APPLICATION OF THE RDRP TECHNIQUES TO THE SYNTHESIS OF WELL-DEFINED VOH-BASED MACROMOLECULES. ....	76
V.1 VOH-based statistical copolymers.....	76
V.2 VOH-based block copolymers.....	76
V.2.1 VOH-based block copolymer obtained by extension of RAFT-synthesized PVAc (route 1).....	77
V.2.2 VOH-based block copolymer obtained via combination of preformed well-defined homopolymers (route 2).....	79
V.3 Other structures of VOH-based copolymer.....	80
VI. MOTIVATION AND OBJECTIVES OF THIS WORK.....	83

## I. Introduction

Emulsion polymerization is widely used industrially to produce synthetic latexes, (*i.e.*, colloidal dispersion of polymer chains in water). This technique relies on a free radical process, and is carried out in water (continuous phase). At the end of the polymerization, the polymer particles are dispersed in the continuous phase, and the stabilization of the polymer particles is ensured by the surfactant, which allows to decrease the surface tension of the polymer/water interface and to avoid phase separation. The latex particle size usually ranges between 50 – 1000 nm.<sup>[1]</sup>

Poly(vinyl alcohol-*s*-vinyl acetate) (P(VOH-*s*-VAc)), most of the time referred to as poly(vinyl alcohol)) is the most commercially important water-soluble polymer produced. Different types of P(VOH-*s*-VAc) can be formed under different conditions by hydrolysis of preformed poly(vinyl acetate) (PVAc) chains, obtained by radical polymerization. It is of practical importance for many applications, including as a stabilizer for the emulsion polymerization of highly reactive monomers such as vinyl acetate (VAc) and vinyl chloride (VC).<sup>[2-4]</sup> The final product is used either as a latex or as a re-dispersible powder after spray drying,<sup>[5]</sup> and finds applications in various fields such as adhesives, carpet backing, medical applications, paints and barrier coating additives for construction materials in Portland cement, mortar and concrete for examples.<sup>[3],[6-8]</sup>

When it is used as a stabilizer, P(VOH-*s*-VAc) participates to the stabilization of VAc-based latexes in different ways: by direct adsorption at the surface of the particles *via* hydrogen bonding, but also by the formation of physical PVAc grafts *via* transfer reactions occurring along the P(VOH-*s*-VAc) chains. Both fractions were found to be present onto the polymer particles at the end of the polymerization.<sup>[9]</sup> Due to this capacity to adsorb at the surface, P(VOH-*s*-VAc) is designed as a “surface-active” copolymer. However, not all the P(VOH-*s*-VAc) chains are involved in particle stabilization, and free P(VOH-*s*-VAc) can also be found in the aqueous phase,<sup>[9]</sup> which can have a negative influence on the final properties of the latex. The present project aims to synthesize new amphiphilic copolymers incorporating VOH units, that are able (i) to stabilize VAc-based latexes with a better involvement of the copolymers in particle stabilization. The focus of the work can be split into four main topic areas: (i) the synthesis of well-defined PVAc homo and copolymers with more hydrophobic comonomers (CoM) such as vinyl neodecanoate (VeoVa) and vinyl laurate (VL) by controlled radical polymerization, (ii) the alcoholysis of these copolymers to incorporate vinyl alcohol (VOH) (iii) the emulsion copolymerization of VAc and VeoVa, in the presence of the aforementioned copolymer that will hopefully act as stabilizers; and (iv) the scale-up of the best emulsion polymerization systems at a pre-industrial level, for advanced

characterizations of the properties of the latexes resulting from the most promising macromolecular stabilizers developed over the course of the PhD.

This first chapter aims to provide the reader with a general background on the fundamental concepts used throughout this thesis. In the first part, the general characteristics and features of emulsion polymerization, in the particular context of VAc polymerization using P(VOH-*s*-VAc) macromolecular stabilizers, will be depicted. In a second part, the concept of controlled radical polymerization and the potentiality of the technique to design original and well-defined macromolecular architectures will be discussed, again with a particular emphasis on VAc as well-defined VOH-based stabilizers targets.

## II. Vinyl acetate-based emulsion polymerization

In this section, a general overview of the classical mechanism of emulsion polymerization is first described, before focusing on the special case of the emulsion polymerization of VAc and copolymerization of VAc with vinyl neodecanoate (VeoVa), using P(VOH-s-VAc) as macromolecular stabilizer (shorten stabilizer).

### II.1 General introduction to emulsion polymerization

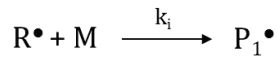
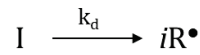
Emulsion polymerization development mostly took off during the Second World War, to produce synthetic rubber latexes and overcome the natural rubber latex shortage, intensively used for war needs (essentially for tires). Subsequently, the versatility of the technique led to the development of a wide range of polymers produced *via* this method and for diverse applications such as textiles, adhesives, paints or even in the biomedical and pharmaceutical fields. Emulsion polymerization is now widely used industrially as it presents many economic and environmental attractive features:<sup>[10]</sup>

- High molar mass polymers can be synthesized at high polymerization rates (higher than in bulk or suspension polymerization),
- No organic solvent is required, which is a considerable advantage in an era of ever more stringent pollution controls,
- The continuous phase (water) has a high heat capacity, which allows for easy heat dissipation and temperature control,
- The viscosity control is much less problematic than in bulk polymerization and allow to reach high solid content.

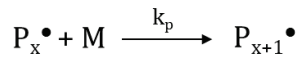
Emulsion polymerization usually proceeds *via* free radical polymerization (FRP). This technique is based on a chain growth-process, where the polymer is formed by successive addition of the propagating (macro)radical onto a vinylic monomer. This radical has a very short lifetime in comparison to the total duration of the polymerization process. In about one second, the different steps of the polymerization occur, namely initiation, propagation, transfer and/or termination (**Figure I-1**). This polymerization method inevitably leads to a large disparity, not only in terms of degree of polymerization (DP) of the different chains in a sample, but also in the nature of the chain-ends.

---

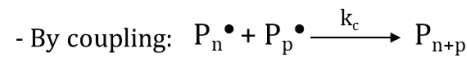
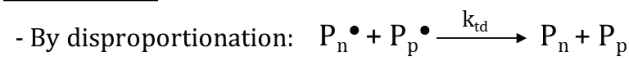
(a) **Initiation**



(b) **Propagation**



(c) **Termination**



(d) **Chain transfer**

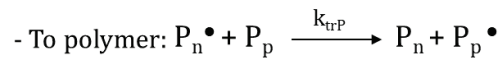
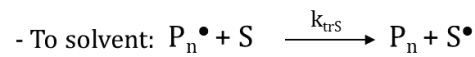
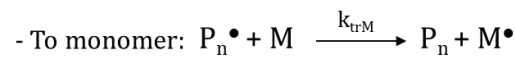
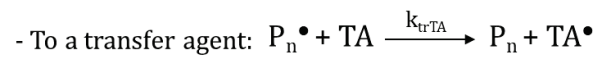


**Figure I-1: General mechanism of free radical polymerization.** Where I is the initiator, i is the number of radicals R<sup>•</sup> produced from the initiator, M is the monomer, P<sub>z</sub><sup>•</sup> is a propagating radical with degree of polymerization z, P<sub>z</sub> is a polymer chain with degree of polymerization z, S is the solvent, TA is a transfer agent, M<sup>•</sup> and TA<sup>•</sup> are radicals produced by chain transfer to monomer and transfer agent, respectively, and k<sub>y</sub> represents the rate coefficient for the reaction y. Adapted from ref [11], with permission from the publisher.

---

The first step of the mechanism is *initiation*. Initiation of the reaction requires a radical center to start chain growth, which is typically supplied by the decomposition of an initiator molecule (I). This is most commonly achieved by thermal decomposition. However, redox or photochemical activations also exist. The decomposition of (I) gives i (usually 2) radical species (R<sup>•</sup>) with a decomposition rate constant *k<sub>d</sub>* (**Figure I-1 (a)**). These species (R<sup>•</sup>) are capable of reacting with the double bond of a first monomer unit (M) to create the active center (P<sub>1</sub><sup>•</sup>), with a rate constant *k<sub>i</sub>* (**Figure I-1 (a)**). The second step is *propagation*. The polymer chain grows by successive addition of the active center (P<sub>n</sub><sup>•</sup>) onto monomeric units with a propagation rate constant *k<sub>p</sub>* (**Figure I-1 (b)**). In an ideal system, propagation is only governed by the consumption of all monomer units available in the medium. In reality, it is not. Indeed, radicals are highly reactive species, which induce side reactions that disrupt the propagation process: termination and transfer reactions. *Termination* occurs when two active radical species react together and the growth of the polymer chain ceases. Two types

of termination reactions exist: combination or disproportionation (**Figure I-1 (c)**). Combination occurs when two propagating chains ( $P_n^\bullet$  and  $P_p^\bullet$ ) react together to form one dead chain. Disproportionation is the abstraction by a growing polymer chain ( $P_n^\bullet$ ) of an H atom on a  $C_\beta$  of another growing polymer chain ( $P_p^\bullet$ ), leading to two dead chains, one with a terminal saturated group and one with an unsaturated group. Transfer reactions (**Figure I-1 (e)**) occur when the  $P_n^\bullet$  active center reacts with another species present in the reaction medium, such as the solvent (S), a transfer agent (TA), the polymer ( $P_p$ ), to which the radical can be transferred to. The growth of the  $P_n^\bullet$  chain is then stopped, and the new active center ( $S^\bullet$ ,  $TA^\bullet$ ,  $P_p^\bullet$ ) eventually propagates to grow a new polymer chain, depending on its ability to reinitiate.<sup>[12]</sup> FRP can be carried out in bulk, solvent, or in the case of emulsion polymerization, in water.

A classical emulsion polymerization system is composed of a continuous phase (water), a water-soluble initiator, organosoluble monomer(s) and surfactant(s) (or stabilizer). A surfactant is an amphiphilic molecule that is composed of a hydrophilic head and a hydrophobic tail. A surfactant can be molecular or macromolecular (polymeric material). In the latter case, it will be called stabilizer, and the organization of the hydrophilic and hydrophobic parts can differ from that of a classical surfactant. This will be developed elsewhere. In the initial stage of the emulsion polymerization, monomer droplets of 1-10  $\mu\text{m}$  in diameter (also called monomer reservoirs) are formed under stirring and the surfactant is located at the interface water/droplets. If the concentration of the surfactant is high enough (above the critical micelle concentration (CMC), defined as the critical surfactant concentration at which micelles start to form), both monomer-swollen micelles and free surfactant in the aqueous phase (also called unimer) are also present (**Figure I-2**).<sup>[11]</sup>

---

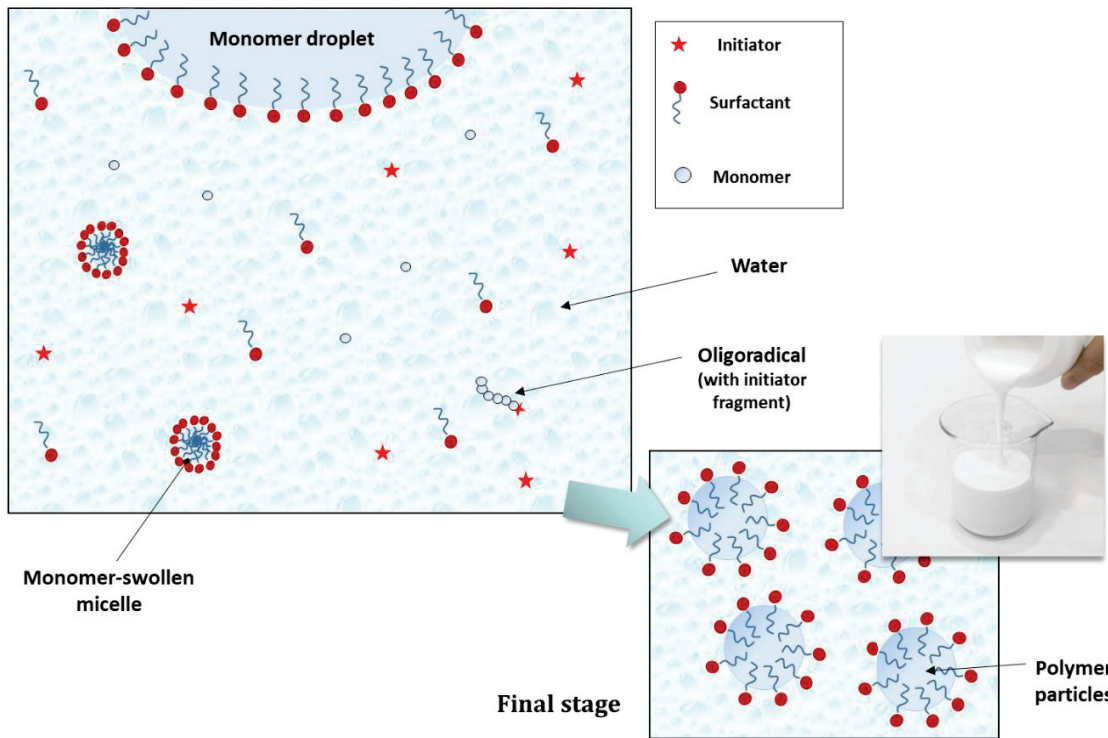
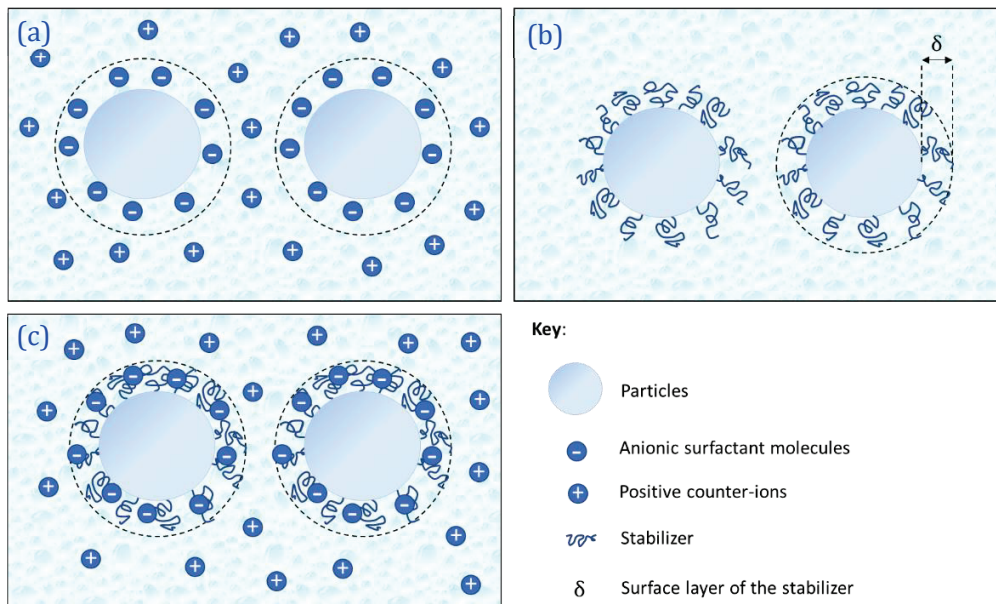
**Initial stage**

Figure I-2: Initial and final stages of the emulsion polymerization.

---

In a typical emulsion polymerization process, ionic surfactants are used. They adsorb at the surface of the particles with their charged head group, and provide *electrostatic stabilization* (**Figure I-3, (a)**). The counterions are free in the aqueous phase. When the latex is stabilized with a polymer, the stabilization is ensured by *steric hindrance* provided by the stabilizer, which is chemically or physically attached (by adsorption or grafting) to the surface of the particles (**Figure I-3, (b)**)<sup>[11]</sup> or a combination of both: *electrosteric stabilization* if the stabilizer is charged (**Figure I-3, (c)**).<sup>[6], [11],[13], [14]</sup>





**Figure I-3: Scheme of the modes of colloidal stability for particle dispersions in water: (a): electrostatic stabilization due to adsorbed ionic surfactant molecules (anionic shown); (b): steric stabilization due to strongly adsorbed or grafted water-soluble polymer chains; (c): electrosteric stabilization provided by a negatively charged water-soluble polymer (anionic shown).**

## II.2 Overview of the mechanism and kinetics

The first qualitative mechanism for emulsion polymerization was suggested by Harkins.<sup>[15],[16]</sup> He postulated that the main locus of chain growth was in the stabilized polymer particles rather than in the large monomer droplets. This assumption was further developed by the Smith and Ewart model in the late 40s'.<sup>[17]</sup> The initiation of the polymerization inside the monomer droplets is generally considered an insignificant route in conventional emulsion polymerization systems, due to the small surface area provided for radical entry into these large droplets (1 - 10  $\mu\text{m}$ ). According to this theory, in the case where micelles are present in the polymerization medium, the emulsion polymerization process can be divided into three intervals which correspond to nucleation (interval I), particle growth (interval II) and the final stage of the polymerization (interval III). During these three stages, the conversion and polymerization rate evolve specifically as depicted in **Figure I-4**.



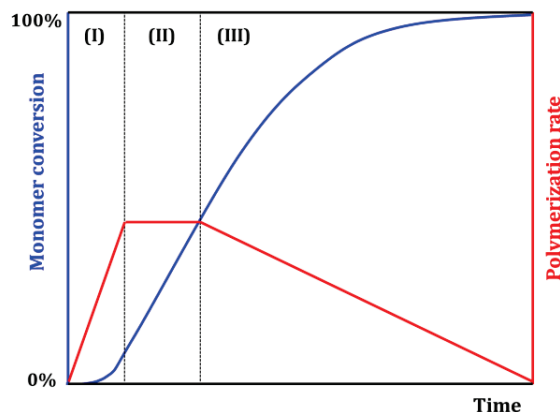


Figure I-4: Classical steps of emulsion polymerization with Interval (I): nucleation; Interval (II): particle growth and Interval (III): end of the polymerization.

### II.2.1 Interval I: nucleation

Interval I corresponds to particle nucleation. This period is usually short and allows to reach a conversion of about 10 to 20%. This step plays a key role in the control of the final characteristics of the latex, such as particle sizes and particle size distribution (PSD). The polymerization starts in water where radicals are formed by decomposition of the initiator. These radicals add on the monomer units present in water to form oligoradicals, which grow until they reach a critical size for which they are not soluble in water anymore. Particles are generated *via* two main mechanisms, depending on the concentration of surfactant and the solubility of the monomer:

- Micellar nucleation
- Homogeneous nucleation
- **Micellar nucleation**

When the concentration of surfactant is above the CMC, the insoluble oligoradical which has reached a critical degree of polymerization to become surface active (defined as  $z$ ) migrates inside a micelle to form a polymer particle. As monomer is also present inside the micelles, the oligoradical keeps growing inside the particle (**Figure I-5**). Part of the micelles will become particles. The others will contribute to stabilize the growing particles by migration of unimers at their surface. The nucleation step ends when there are no more micelles in the medium.<sup>[6],[11],[18-20]</sup>

- **Homogeneous nucleation**

Homogeneous nucleation is observed when the concentration of surfactant is below the CMC, and/or when the monomer has a significant solubility in water (*e.g.*, VAc) (even above the CMC value). In this case, the oligoradicals keep growing by propagation with the monomer present in the aqueous phase. This growth increases the hydrophobic character of the oligoradicals until they reach a critical length (referred to as  $j_{crit}$ ), corresponding to the limit of their solubility in water ( $j_{crit} > z$ ), and precipitate to form primary particles (**Figure I-5**). These particles are stabilized by the migration at their surface of the surfactant present in the reaction medium.<sup>[11]</sup> Then, the particles will grow or merge (limited coalescence) with other particles to form stable aggregates, depending on the efficiency and the availability of the surfactant in the polymerization medium.

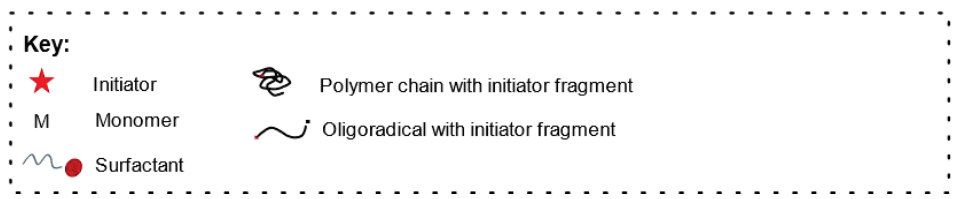
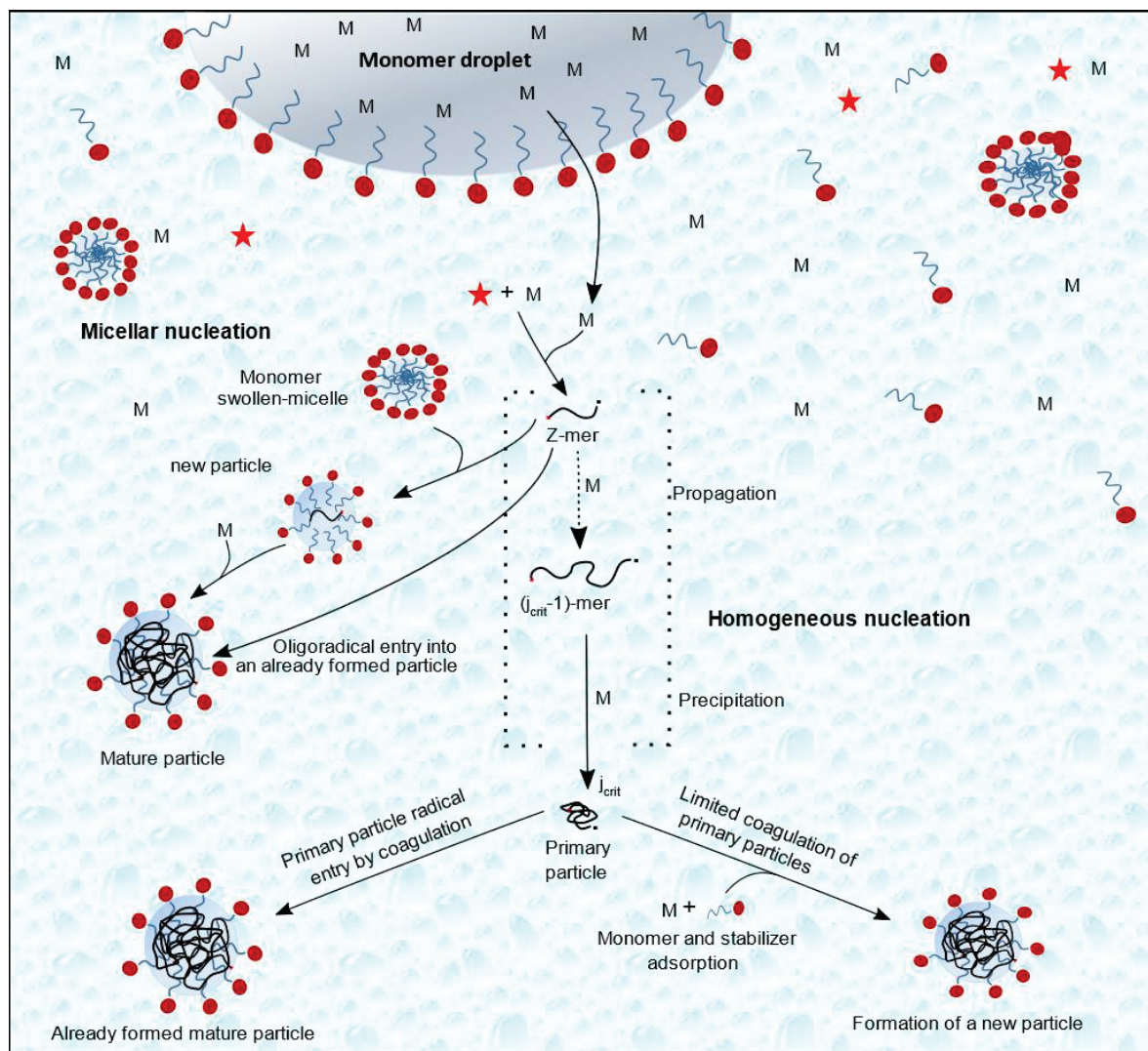


**Figure I-5: Fate of aqueous phase oligomeric radicals in emulsion polymerization.** Arrows with dashed lines indicate multiple aqueous phase propagation reactions of a growing oligoradical with monomer. Dotted lines indicate that all oligoradicals with degrees of polymerization in the range  $z$  to  $j_{crit} - 1$  are capable of entry by diffusion into monomer-swollen micelles and already-existing particles. Adapted from ref [11] with permission from the publisher.

After nucleation, if there is no continuous or secondary nucleation, the number of particles ( $N_p$ ) will remain constant through the polymerization.  $N_p$  is given by **Equation 1**.

$$N_p = \frac{6 \times [M]_0}{\Pi D_v \rho} \quad (1)$$

With  $N_p$  the number of particles per volume of latex ( $\text{cm}^{-3}$ ),  $x$  the conversion (%),  $[M]_0$  the initial monomer concentration ( $\text{g L}^{-1}$ ),  $D_v$  the average diameter of the particles ( $\text{cm}$ ), and  $\rho$  the density of the polymer ( $\text{g cm}^{-3}$ ).

## II.2.2 Interval II: particle growth

After particle nucleation, the particles created during interval I become the main locus for polymerization during Intervals II and III (**Figure I-4**). During interval II, if there is no secondary nucleation, the polymerization proceeds at a steady rate inside the particle as monomer diffuses from the monomer droplets to the polymer particles, and the size of the particles increases. Monomer concentration inside the particles remains thus constant. The rate of polymerization is given by **Equation 2**.

$$R_p = \frac{d[M]}{dt} = k_p [M]_p [M^\bullet] = k_p \frac{N_p \bar{n}}{N_A} [M]_p \quad (2)$$

With  $R_p$  the rate of polymerization ( $\text{mol L}_{\text{latex}}^{-1} \text{s}^{-1}$ );  $k_p$  the propagation rate constant ( $L_p \text{ mol}^{-1} \text{s}^{-1}$ );  $[M]_p$  the concentration of monomer inside the particle ( $\text{mol L}_p^{-1}$ );  $[M^\bullet]$  the radical concentration in the latex ( $\text{mol L}_{\text{latex}}^{-1}$ );  $\bar{n}$  the average number of radicals per particle and  $N_A$  the Avogadro's constant ( $6.022 \times 10^{23} \text{ mol}^{-1}$ ).

Smith and Ewart<sup>[17]</sup> demonstrated that the main factor which governed the rate of polymerization during this interval was the average number of radicals per particle ( $\bar{n}$ ). They predicted three possible values for  $\bar{n}$ :

- **Case 1,  $\bar{n} \ll 1$ .** This scenario occurs if the radical can exit a particle, and in the case where the rate of radical exit from the particle is much greater than the rate of radical entry into a particle, which in turn is much greater than the rate of radical termination in a particle. Case 1 conditions with  $\bar{n} < 0.5$  is common and can happen for instance when (i) the particles are small; (ii) the transfer constant (to monomer, polymer, transfer agent or surfactant) is high, which leads to the formation of a small and highly mobile monomeric radical that has sufficient water solubility to exit the particle.
- **Case 2,  $\bar{n} = 0.5$ .** A new radical enters inside an active particle (which already contains a radical), leading to termination reaction. The number of radical per particle is thus either one (active particle) or zero (after termination). In the case of the emulsion polymerization of styrene, the authors determined that this phenomenon occurs every 10 seconds on average.

- **Case 1,  $\bar{n} > 1$ :** the rate of radical entry is greater than the rate of termination. This situation can occur when the particles are large enough, or when the viscosity is high enough to accommodate more than one propagating macroradical per particle.

When the monomer has little solubility in water, the emulsion polymerization system generally follows the Smith-Ewart kinetic model case 2, developed in 1948 for the emulsion polymerization of styrene in the presence of sodium dodecyl sulfate (SDS) micelles. If  $\bar{n}$  is constant, and in the case where there is no secondary nucleation ( $N_p$  constant), then the rate of polymerization (given by **Equation 1**) is constant. Interval II lasts until the disappearance of the monomer reservoirs and allows to reach 40 - 60% conversion in batch.<sup>[11],[20]</sup>

### II.2.3 Interval III: final stage of the polymerization

Eventually, interval III begins when the monomer reservoirs disappear, after they are completely depleted by supplying monomer to the growing polymer particles. As the concentration of the monomer decreases, a proportionate reduction of the polymerization rate occurs, until it reaches zero at complete conversion.<sup>[11],[20]</sup>

## II.3 Specificities of the emulsion polymerization of VAc

The emulsion polymerization of VAc was first patented in 1940.<sup>[21]</sup> Despite the practical importance of VAc-based latexes, relatively few patents are available. Most of them were written between 1940 and 1950, and mostly concern process optimization.<sup>[22,23]</sup> From the open literature however, it is now well established that what was described in the previous section about emulsion polymerization concerned the classical mechanism of this technique, where hydrophobic monomers (*e.g.*, styrene) are used. This mechanism is significantly different with VAc, because of its peculiar behavior in water. Indeed, the emulsion polymerization of VAc differs from the classical case 2 of the Smith and Ewart theory, because of the relatively high solubility of this monomer in water (2.5 wt.% at 25 °C, 4.2 wt.% at 60 °C)<sup>[19],[24],[25]</sup> and high chain transfer constant to monomer and polymer ( $C_{M,PVAc} = 1 - 5 \times 10^{-4}$ )<sup>[26]</sup> compared to most of the other conventional monomers used in emulsion polymerization (**Table I-1**).<sup>[19],[27],[28]</sup> A different mechanism was therefore proposed by Jacobi<sup>[29]</sup> and Priest.<sup>[30]</sup> It is based on homogeneous nucleation, and the authors supported the concept of an equilibrium distribution of radicals, brought by a high rate of interchange of radicals between polymer particles. The rapid escape of radicals from the particles is possible because of the relatively high rate of chain transfer to monomer (due to the high reactivity of the propagating radical) and the relative water solubility of monomeric and oligomeric radicals. These two combined effects can lead to the formation of “small” mobile oligoradicals which can diffuse out of a particle.

**Table I-1: Chain transfer constants ( $C_M$ ) and transfer rate constant ( $k_{tr}$ ) of some common monomers at 50 °C.  $C_M = k_{tr}/k_p$ .**

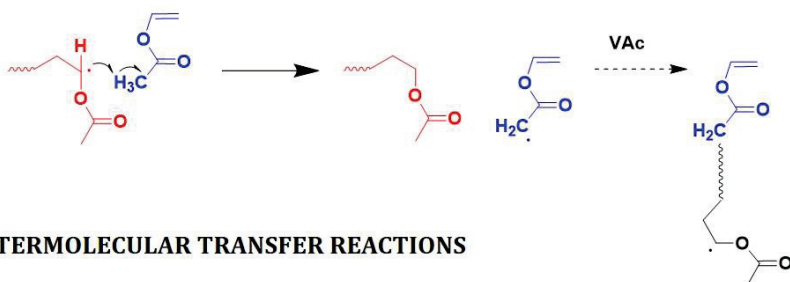
Monomer	$C_M \times 10^4$	$k_{tr} \times 10^3$ (L mol <sup>-1</sup> s <sup>-1</sup> )	REF
Styrene	0.35 – 0.78	9.1 -20.2	[31]
Methyl acrylate	0.8	N/A	[31]
Methyl methacrylate	0.1 – 0.85	6.5	[31]
Vinyl neodecanoate	4	2120	[32]
Vinyl acetate	1.28	859	[32]

$\bar{n}$  values ranging from 0.02 to 60 have been reported in the literature.<sup>[33]</sup> It is difficult to establish a more precise value of  $\bar{n}$  as no group of researchers used exactly the same experimental conditions. Nevertheless, the low values of  $\bar{n}$  are consistent with Priest and Jacobi's propositions where low molar mass radicals can diffuse out of the particles. The high chain transfer to monomer can provide a source of such radicals (**Figure I-6** route 1 (blue)). Noteworthy, the case where  $\bar{n} \ll 1$  is more often depicted in the literature.<sup>[28],[34]</sup> On the other hand, high values of  $\bar{n}$  would be consistent with case 3, where several macroradicals migrate inside a particle at the same time. This would require that the particles were large enough to allow the presence of more than one radical at a time.

Other transfer reactions were identified in the case of the emulsion polymerization of VAc: Primary radicals or macroradicals also have a strong tendency to abstract hydrogen atoms from the polymer chains. This abstraction can occur not only onto the PVAc chains formed during the polymerization but also onto the stabilizer, in the case where a stabilizer such as P(VOH-*s*-VAc) is used, leading to the formation of PVAc grafts along these chains.<sup>[28]</sup> The latter case, and the specific grafting sites onto P(VOH-*s*-VAc) stabilizer will be described later in **Section III.2**. As for transfer reactions onto PVAc, the two main possibilities are intermolecular and intramolecular chain transfer reactions (**Figure I-6**, routes 2 and 3, respectively).<sup>[35],[36]</sup> Intermolecular chain transfer to polymer was found to be more significant in emulsion polymerization than in homogeneous free radical polymerizations (see below). It can occur either by H-abstraction from the methyl group of the ester function, or from the methine of the polymer backbone. Mechanism (b) (**Figure I-6**, route 2) was found to be dominant because the produced radical is more efficiently stabilized by resonance with the C=O function of the ester group than in case (a)<sup>[11],[37]</sup> and leads to branching. These branches disrupt the local polymer chain conformation and can alter the properties of copolymers that crystallize (*e.g.*, P(VOH-*co*-ethylene) or P(VOH-*s*-VAc) copolymers). Intramolecular transfer occurs exclusively onto a hydrogen from the polymer backbone of the same polymer chain (backbiting, **Figure I-6**, route 3) and results in a branched and dead polymer chain.

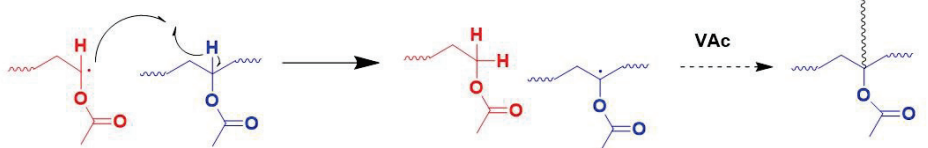


### 1. TRANSFER TO MONOMER

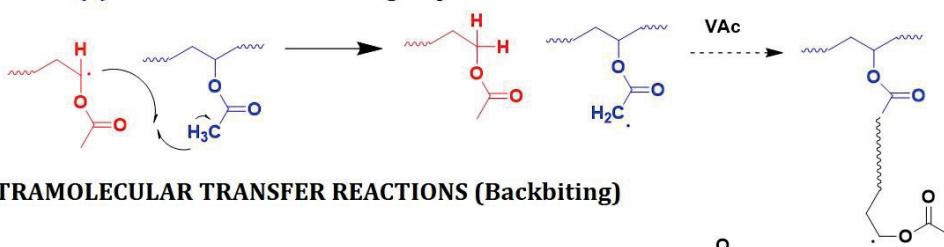


### 2. INTERMOLECULAR TRANSFER REACTIONS

(a): H abstraction from the backbone



(b): H abstraction from side group



### 3. INTRAMOLECULAR TRANSFER REACTIONS (Backbiting)

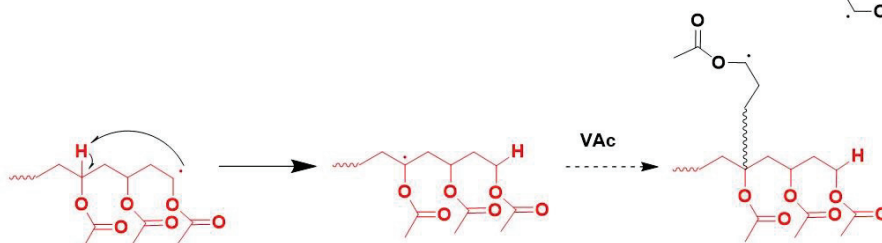


Figure I-6: Main chain transfer reactions in the polymerization of VAc. Dashed lines for arrows indicate multiple processes of the same kind.

Lovell and coworkers<sup>[37]</sup> compared the occurrence of chain transfer reactions to polymer in bulk and emulsion polymerization of VAc. The authors found that in both cases the percentage of branches increased with conversion, and that the levels of branching in the PVAc synthesized by emulsion polymerization were higher than in the PVAc synthesized in bulk (0.6 - 0.75 mol.% vs 0.13 - 0.23 mol.% respectively). The authors attributed these results to the fact that in emulsion polymerization, the polymerization is more compartmentalized as it almost exclusively takes place inside the latex particles and at high conversion.

The mechanism and kinetics of the emulsion polymerization of VAc is quite complex and still debated. Nevertheless, there is some agreement that the reaction is influenced by the stabilizer type and concentration, the initiator type and concentration, the temperature, the mode or rate of monomer addition, and the presence of comonomers.

#### II.4 Emulsion copolymerization of VAc with VeoVa

In 1938, Wacker started manufacturing polymer dispersions on an industrial scale and has developed its production process ever since. Using VAc as the major raw material, Wacker produces a variety of polymer dispersions including PVAc homopolymers and copolymers of VAc and ethylene, under the trade names VINNAPAS® and ETONIS®.<sup>[38]</sup> This class of copolymers is often referred to as vinyl acetate-ethylene copolymers (VAE or EVA depending on their VAc content). According to their properties (viscosity, particle size etc.) VAc-based latexes can be used in a variety of applications such as in adhesives, coatings, paints, construction. The glass transition temperature ( $T_g$ ) of PVAc is around 32 °C. The minimum film formation temperature (MFFT), which is the minimum temperature at which the particles will coalesce and provide a homogeneous film, of PVAc dispersions is around 20 °C, because the water present in the films acts as a plasticizer. A plasticizer is a substance (typically a solvent or an additive) added to a synthetic resin to produce or promote plasticity and flexibility, and reduce brittleness. Indeed, PVAc alone is a rigid polymer. The pendant acetate groups restrict the rotation around the carbon-carbon bonds, and in addition, the interaction of these pendant acetate groups restricts the flow of the polymer chains with each other. The result is a hard, brittle material, which is suitable for the applications previously mentioned, but which renders VAc-based latex unsuitable for many other applications. A solution is to incorporate external plasticizing species into the material. However, they have a tendency to migrate over time and can be released from the polymer film, resulting again in a brittle material. A more suitable strategy is to incorporate the plasticizing species into the PVAc chains *via* copolymerization. This strategy leads to a lower  $T_g$  for the resulting material, in comparison to PVAc homopolymer. In addition, copolymerization also prevents the plasticizer from migrating out of the film once it is formed. For this approach to be successful, the reactivity of the comonomer must be approximately the same as that of VAc. Several suitable candidates can be found in the literature,<sup>[10],[19]</sup> but only VeoVa (**Figure I-7** was of interest for this PhD. VeoVa (which is composed of a mixture of isomeric vinyl esters of neodecanoic acid) derives its plasticizing effect from its ability to separate the polymer chains. By contrast, ethylene imparts its plasticizing effect from its ability to render the individual macromolecules more flexible by increasing the freedom of rotation of the carbon-carbon bonds.



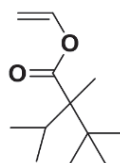


Figure I-7: Simplified chemical structure of VeoVa.

The reactivity ratios of VAc and VeoVa are respectively 0.99 and 0.92.<sup>[39]</sup> The water solubility of VeoVa is 0.005 g L<sup>-1</sup> at 20 °C. The  $T_g$  of PVeova is -3 °C.<sup>[40]</sup> The most distinguishing feature of these bulky vinyl esters is their resistance to hydrolysis, both as monomers and in polymers. Bulky vinyl esters offer excellent hydrophobic properties. These esters are strongly resistant to saponification, water absorption, and UV degradation. Indeed, the properties of PVAc polymers, such as water and alkali resistance and exterior durability, improve with these esters. All these advantages make the copolymers of VAc and bulky vinyl ester suitable for many applications such as architectural paints, interior and exterior applications for example.<sup>[10],[19]</sup>

Despite the practical importance of P(VAc-co-VeoVa) copolymers, the open literature dealing with the emulsion copolymerization of VAc and VeoVa is not so extensive. Asua *et al.* studied the kinetics of this copolymerization and reported that high conversions could be reached by conducting the process at low temperature and/or low initiator concentrations and/or under starved conditions, temperature being the most important factor. Unfortunately, these conditions produce long process times, resulting in low production rates.<sup>[41]</sup> Redox systems can be employed as an alternative to thermal initiators and limit the temperature dependence. In 2019 and 2022, recent papers investigated the influence of a specific redox system onto the efficiency of the emulsion copolymerization of VAc and VeoVa.<sup>[42],[43]</sup> The redox system was composed of L-ascorbic acid (AsAc), *tert*-butyl hydroperoxide (TBHP) and ammonium iron(III) sulfate dodecahydrate (Fe-cat) as a catalyst (AsAc/TBHP/Fe-cat). This redox system is widely used for the emulsion copolymerization of VAc and VeoVa,<sup>[44],[45]</sup> as it allows to work in mild temperature conditions (compared to thermal initiator). It provides the double advantage of reducing the cost of production and lowering the rate of chain transfer to polymer, (thus reducing the possibility of side reactions which may impact the final properties of the latex) while reaching high conversion rate in short time scales.<sup>[46]</sup> Even though the exact mechanism of the AsAc/TBHP/Fe-cat system has not been clarified yet, Werner Pauer *et al.*<sup>[42]</sup> investigated for this redox system the decomposition rate of AsAc in a broad range of temperatures (from 10 to 70 °C), and used statistical modeling to identify the most appropriate kinetic model. They also highlighted the importance of the Fe-cat, by showing that high conversions in short reaction times could be achieved in the 10 – 70 °C temperature range by increasing the Fe-cat content. Jacob *et al.*<sup>[43]</sup> investigated the influence of the AsAc/TBHP/Fe-cat ratios at temperatures ranging from -1 to 87 °C onto the properties

of the latex. They obtained high conversions (90 – 99%) in variable and fast reaction times (2 – 240 min), and found that the reaction rate was adjustable by varying the catalyst amount without changing the product properties (molar mass, particle size,  $T_g$ ). In contrast, variation of the TBHP content resulted in changes of the molar mass, but not in PSD nor in the particle size. The results provided in both papers confirmed the high flexibility of the redox initiator system, allowing for specific adjustment of component ratios to customize the system and covering a broad range of process conditions.

Bohorquez and Asua<sup>[47]</sup> showed that high-solids P(VAc-co-VeoVa) latexes stabilized with P(VOH-s-VAc) could be produced *via* batch miniemulsion polymerization, whereas batch emulsion polymerization resulted in massive coagulation. The authors studied the influence of different initiators (thermal water- and oil-soluble and redox water-soluble) and the influence of the concentration of P(VOH-s-VAc) onto the properties of the miniemulsions. They demonstrated that the extent of grafting of P(VOH-s-VAc) in batch process was strongly related to the type of initiator, and it has been reported that grafting increased in the following order: benzoyl peroxide  $\approx$  lauryl peroxide  $\ll$  TBHP/AsAc  $<$  potassium persulfate (KPS). This was attributed to the fact that grafting occurs predominantly in the aqueous phase, and to the nature of the more hydrophilic initiator combined: it was demonstrated that the difference between KPS and TBHP/AsAc was due to the higher solubility of KPS in water compared to TBHP/ASAC, and thus, to the longer time that the sulfate ion radicals and the resulting oligomeric radicals spent in the aqueous phase where they have the opportunity to abstract hydrogens from the free and adsorbed P(VOH-s-VAc). Grafting of the stabilizer plays a major role in the stabilization mechanism of PVAc latexes and will be further described in **Section III.2**. Additionally, the authors pointed out that that optimal P(VOH-s-VAc) concentration to maximize droplet nucleation was 2 to 4 wt.%. Higher stabilizer concentration led to particle formation by secondary micellar nucleation and lower concentrations led to coagulum formation. Additionally, the fraction of grafting was found to be higher in miniemulsion than in emulsion polymerization.<sup>[48]</sup>

To overcome the batch emulsion polymerization process limitation, optimal polymerization strategies to maximize the production rate of high solid content ( $S_c = 51$  wt.%) VAc–VeoVa latexes, stabilized by an anionic surfactant and produced in tank reactors with a limited heat removal capacity, were reported by Unzué *et al.*<sup>[41]</sup> The emulsion polymerizations were thermally initiated by KPS and performed in semi-continuous reactors. The feed was divided in three streams. The first was an aqueous solution of sodium dithionite, potassium carbonate, and a nonionic emulsifier (Descofix 202). The second was an aqueous solution of KPS, and the third a mixture of monomers (VAc, VeoVa and acrylic acid). By varying the different feed parameters, they found that a 40% reduction in the process time could be achieved, maintaining the final product quality.

Several other papers deal with the successful emulsion copolymerization of VAc and VeoVa at high solid content (up to 57 wt.%) *via* a continuous process.<sup>[45],[44]</sup> Agirre *et al.* investigated

the semi-continuous emulsion copolymerization of VAc and VeoVa, stabilized with P(VOH-*s*-VAc) or a non-ionic stabilizer, and carried out with different initiators, under industrial-like conditions ( $Sc = 57$  wt.%). It was found that P(VOH-*s*-VAc) reduced the rate of radical entry into the polymer particles and thus, affected the kinetics of the polymerization. This effect was attributed to the chain transfer of the entering radicals to P(VOH-*s*-VAc) and depended on the initiator system used. It was more pronounced for KPS/sodium metabisulfite (NaMS) than for TBHP/AsAc (due to different rate of radical generation). A consequence of the chain transfer to P(VOH-*s*-VAc) was the formation of P(VOH-*s*-VAc)-*graft*-P(VAc-*s*-VeoVa) copolymer, which strongly affected the resulting polymer microstructure.

Asua and coworkers <sup>[49]</sup> also investigated the differences between the emulsion copolymerization of VAc and VeoVa, initiated by a redox system, either in a CSTR or in a continuous loop reactor for high solid content latex. The experimental set ups (hydroxy cellulose as stabilizer, mixing, feed composition, reaction time) were maintained similar from one experiment to the other. It was found that when the heat-removal capacity of the reactor exceeded the heat generation, there was no difference between the two reactors in terms of conversion, particle size, number of particles and molar mass distributions. However, when the heat generation rate was high, a thermal runaway occurred in the CSTR, whereas the temperature was more easily controlled with the loop reactor.

P(VOH-*s*-VAc) is one of the most widely used stabilizers for the industrial emulsion copolymerization of VAc with VeoVa, and its use provides specific stability to the latex and imparts desirable properties such as high water and heat resistance.

As discussed in **Section II.3**, the mechanism of particle formation for VAc emulsion polymerization carried out with P(VOH-*s*-VAc) is more complex than what is usually described for more conventional emulsions systems (see **Section II.1**). It is ensured by both homogeneous nucleation and chain transfer reactions occurring along the P(VOH-*s*-VAc) chains during the polymerization, which leads to the formation of PVAc grafts along the stabilizer.<sup>[3],[50]</sup> The second part of this chapter is thus dedicated to this peculiar stabilizer and aims to describe how P(VOH-*s*-VAc) brings stabilization to the particles formed during emulsion polymerization of VAc.

### III. Poly(vinyl alcohol-*s*-vinyl acetate) (P(VOH-*s*-VAc))

#### III.1 Synthesis of P(VOH-*s*-VAc)

Before we discuss the specific mechanism of stabilization provided by P(VOH-*s*-VAc) in the emulsion polymerization of VAc, the synthetic routes leading to P(VOH-*s*-VAc) and the influence of these routes on the characteristics of the resulting polymers are discussed.

The only way to prepare P(VOH-*s*-VAc) is by hydrolysis of poly(vinyl esters) (usually PVAc), but several experimental conditions exist and will be described below. This polymer was first synthesized by Hermann and Haehnel in 1924 by hydrolysis of PVAc in ethanol with potassium hydroxide.<sup>[51],[52],[53]</sup> This copolymer cannot be prepared by copolymerization of VAc with vinyl alcohol (VOH), as the latter is thermodynamically unstable with respect to its tautomer acetaldehyde (**Figure I-8**).<sup>[35],[19]</sup> Thus, before reviewing the different methods to obtain P(VOH-*s*-VAc), it is important to have some knowledge about the synthesis of the initial PVAc, as its structure and the way it is synthesized can influence the properties of the resulting P(VOH-*s*-VAc) after hydrolysis.

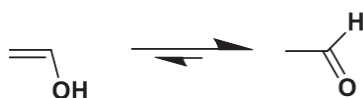


Figure I-8: Tautomerization reaction of vinyl alcohol (left) to acetaldehyde (right).

---

Fritz Klatter reported the first official synthesis of PVAc in 1912.<sup>[32]</sup> He left vinylic ester monomers in round bottom flasks exposed to sunlight and noticed a solidification occurring. Thereafter, no further advancements were made until the late 20's. In 1928, Wacker started the industrial production of PVAc in Burghausen.<sup>[54]</sup>

Since then, poly(vinyl ester)s have a rich history in polymer research and industrial production. As mentioned above, PVAc is a hydrophobic polymer, used in many applications, such as in adhesives for porous substrates (*e.g.*, wood, paper and cloth), emulsion paints and as powder additives for construction materials.<sup>[55]</sup>

The only way to polymerize VAc is by radical means. Free radical polymerization is one of the most widely used chain-growth polymerization techniques, both industrially and academically.<sup>[56]</sup> The general mechanism of FRP was already described in **Section II.1**. FRP is useful for the industry as it presents valuable advantages, such as (i) it can be used with a large variety of monomers; (ii) it is tolerant towards a wide range of functional groups and

reaction conditions, unlike the ionic polymerizations; (iii) it is simple to implement and inexpensive compared to other polymerization methods.

However, the FRP (and in this particular context, that of VAc) exhibits some limits, with the most notable being the high reactivity of the carbon radicals, resulting in many undesirable side termination or transfer reactions (to monomer, solvent, polymer) as mentioned in **Section II.3** for VAc emulsion polymerization.

The initiating radicals are continuously formed throughout the reaction, and the very short lifetime of the propagating radicals ( $< 1$  s) does not allow for control of the architecture or molar mass distribution of the polymer produced. The very different reactivities of the growing radicals (high) and the monomer (low) result in a high level of chain transfer reactions, which result in branching along the polymer backbone, as previously mentioned. In addition to transfer reactions, many chain irregularities due to head-to-head addition of a monomer unit onto the growing macroradical are keen to occur (**Figure I-9**), and makes the production of uniform polymers rather difficult. [12],[37]

---

#### HEAD-to-HEAD ADDITION

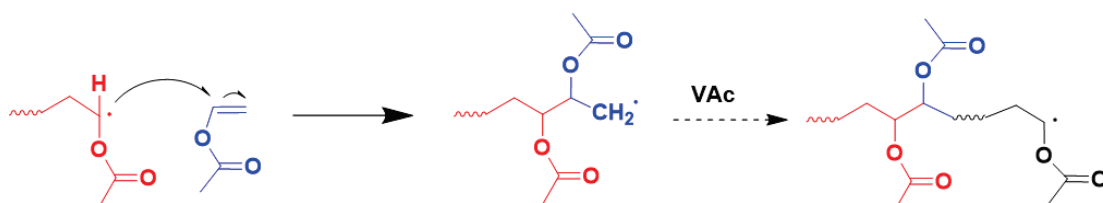
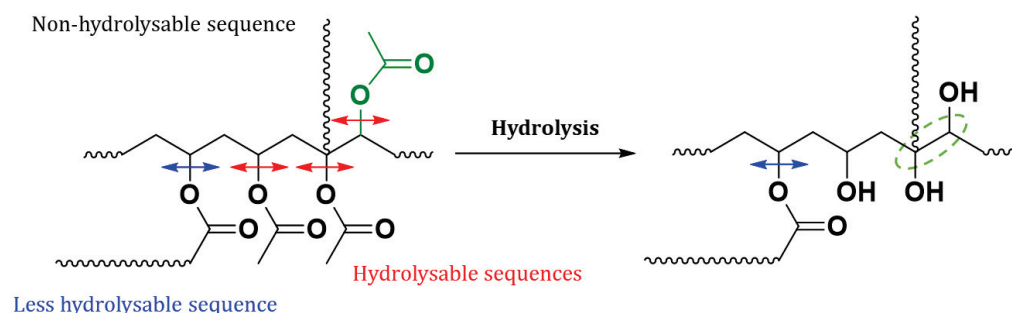


Figure I-9: Irregular head-to-head addition of VAc on a growing macroradical.

---

These regio-irregularities along the polymer backbone were accounted for 1 – 2 mol.% in the final PVAc.<sup>[36]</sup> As a consequence, the polymer composition and architecture (stereochemistry, star, block, etc.) cannot be controlled precisely *via* this technique, and these irregularities and branchings will remain present in the resulting P(VOH-s-VAc) after hydrolysis: the regio-irregularities coming from the head-to-head addition will provide 1,2-glycol sequences, and the branchings will result in non-hydrolysable sequences (**Figure I-10**).<sup>[57]</sup>



**Figure I-10:** Simplified scheme of the structure of the P(VOH-s-VAc) after hydrolysis resulting from the PVAc irregularities (branchings and head-to-head addition (**green unit**) leading to 1,2-glycol sequences (**dashed green circle**). The **red** and **blue** arrows highlight the more easily and less easily hydrolysable sites, respectively. Depending on the length of the branches resulting from H-abstraction from the side group of the PVAc, this branch can remain on the resulting P(VOH-s-VAc), whereas the branch resulting from H-abstraction from the polymer backbone provides a non-hydrolysable sequence.

Noteworthy, it has been well documented that the content of 1,2-glycol sequences and carbonyl groups as well as the presence of hydrolysable and non-hydrolysable branches influence the stabilizing properties of P(VOH-s-VAc), and that the structure of the copolymer defines its physical properties. For instance, the solubility of P(VOH-s-VAc) in water depends on its degree of polymerization, its rate of hydrolysis, and the tacticity of the polymer.<sup>[55]</sup> These aspects will be developed further later.

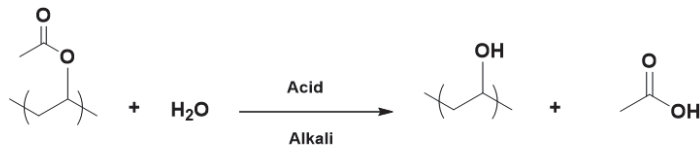
P(VOH-s-VAc) can be obtained by several methods schematized in **Figure I-11**.<sup>[57-59]</sup>

1. Acid and alkaline hydrolysis.<sup>[60]</sup>
2. Reacetylation of PVOH (from fully alcoholized or hydrolyzed PVAc).<sup>[61]</sup>
3. PVAc alcoholysis catalyzed by a base or an acid in methanol or ethanol (also called alkali transesterification).<sup>[59],[62]</sup>

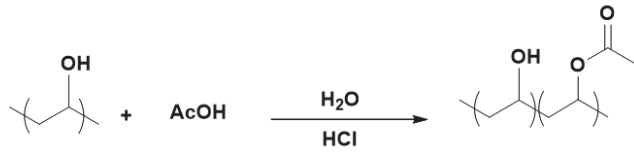
In any case, it is possible to stop the reaction at the desired hydrolysis degree (HD), which is defined as the molar fraction of hydroxyl groups in the final P(VOH-s-VAc) copolymer.

---

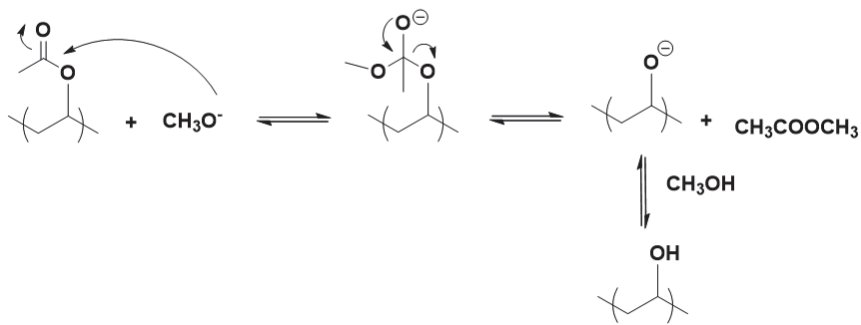
### 1. Hydrolysis



### 2. Recetylation



### 3.1 Alcoholysis: base catalysis



### 3.2 Alcoholysis: acid catalysis

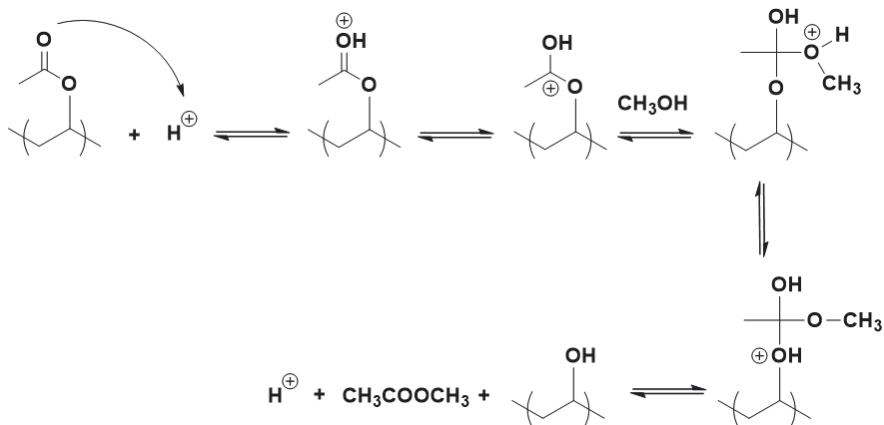


Figure I-11: General scheme of 1. Hydrolysis of PVAc; 2. Recetylation of PVOH [61] and 3. Base and Acid catalyzed alcoholysis of PVAc.[62]

---



During alcoholysis, when the polymer reaches approximately HD = 70%, it is no longer soluble in the solvent (alcohol) and precipitates. The most widely used catalysts for preparing P(VOH-*s*-VAc) *via* alcoholysis in methanol are sodium or potassium hydroxide (NaOH and KOH, respectively). Noteworthy, although the chemical mechanisms are different, the terms hydrolysis and alcoholysis have been intensively used interchangeably in the literature to describe the reaction wherein PVAc is converted to P(VOH-*s*-VAc).

The main parameters which define the characteristics of P(VOH-*s*-VAc) are the hydrolysis degree (HD), the blockiness index ( $\beta$ ) and the degree of polymerization (DP):

*Degree of hydrolysis:* The HD is usually controlled by the hydrolysis reaction time, the concentration of catalyst, and the temperature of the reaction medium.<sup>[63]</sup> For example, Fabini *et al.*<sup>[64]</sup> observed that the amount of NaOH has a considerable impact on the rate of hydrolysis. It also impacts the HD from one chain to another, leading to a composition dispersity when the concentration of NaOH increases.

Different grades of P(VOH-*s*-VAc) exist, depending on their HD:

- Fully hydrolyzed PVAc (PVOH): HD higher than 97%,
- Partially hydrolyzed PVAc (P(VOH-*s*-VAc)): HD from 84 to 89%,
- Moderately hydrolyzed PVAc (P(VOH-*s*-VAc): HD from 90 to 96%.

The water solubility of a P(VOH-*s*-VAc) polymer depends on both its DP and HD, but usually, P(VOH-*s*-VAc) becomes water-soluble for a HD of 65 - 70%. Experimentally, it was observed that partially hydrolyzed PVAc (HD = 84 – 89%) improves the stability of the emulsion<sup>[3]</sup> and that for similar molar masses, the less hydrolyzed PVAc generates smaller average particle size.<sup>[11],[65],[66]</sup>

*Blockiness index:* Industrially, the alcoholysis of PVAc is preferably performed *via* alcoholysis with NaOH and methanol (methanolysis), as it favors blockier distribution of the acetate units along the polymer, and ensures better stability of the particles.<sup>[67]</sup> The blockiness-like structure, first defined by Moritani and Fujiwara,<sup>[58],[68]</sup> characterizes the distribution of the residual acetate groups along the polymer after alcoholysis. The authors defined the blockiness index ( $\beta$ ) *via* <sup>13</sup>C NMR analysis:

$$\beta = \frac{F_{\text{VOH,VAc}}}{2 \cdot F_{\text{VOH}} \cdot F_{\text{VAc}}} \quad (3)$$

With  $F_{\text{VOH}}$  the molar fraction of the alcohol units,  $F_{\text{VAc}}$  the molar fraction of acetate units and  $F_{\text{VOH,VAc}}$  the diads fraction of alcohol and acetate, respectively. If  $0 < \beta < 1$ , the polymer has a blocky structure. If  $\beta = 1$ , the P(VOH-*s*-VAc) has a random distribution and if  $1 < \beta < 2$ , it has



a statistical distribution (**Figure I-12**).

The same authors found that P(VOH-s-VAc) prepared by complete hydrolysis of PVAc followed by reacetylation resulted in a random distribution of the acetyl groups.

Finally, the use of acid catalyst to partially hydrolyze PVAc into P(VOH-s-VAc) leads to a more random distribution of the acetate groups along the chain than when alkali is used.<sup>[57],[69],[70]</sup> Later, Carrà *et al.*<sup>[9]</sup> provided some evidence that the sequence distribution of the residual acetate units (*i.e.*,  $\beta$  value) influenced the auto-association of the P(VOH-s-VAc) chains in water, and thus, their stabilizing efficiency. This study will be developed further in the following section.

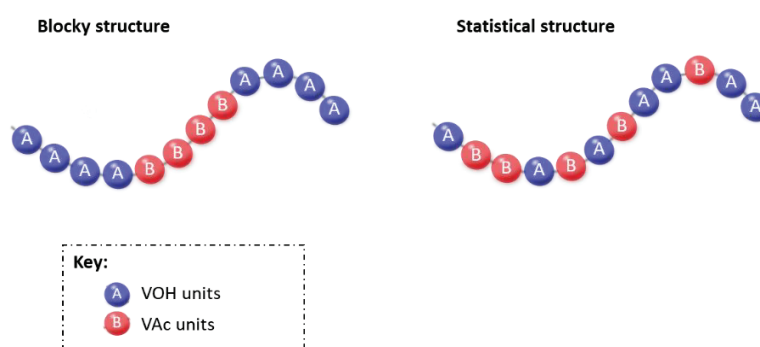


**Figure I-12: Schematic representation of the different P(VOH-s-VAc) structures depending on the experimental conditions.**

Experimentally, it has been observed that partially alcoholized (from 84 to 88 mol.%) and blocky P(VOH-s-VAc) stabilized PVAc latexes most efficiently.<sup>[28],[71]</sup>

*Degree of polymerization:* The DP of P(VOH-s-VAc) is defined by **Equation 4**

$$DP = m + p \quad (4)$$

Where  $m$  is the average number of VAc units and  $p$  the average number of VOH units.

It is important to highlight that the DP of P(VOH-s-VAc) post-hydrolysis may differ from that of the original PVAc. This is due to possible cuts of the branched sequences which are formed during the polymerization of VAc as previously mentioned (**Figure I-10**).

This section reviewed the different routes to obtain a P(VOH-s-VAc) copolymer, starting from the alcoholysis or hydrolysis of a PVAc homopolymer. This copolymer can be used as stabilizer and ensures the stability of the latex *via* a particular mechanism, which is slightly more complicated than the classical mechanisms depicted in **Section II.2**. The following

section aims to provide a better understanding of the involvement of P(VOH-s-VAc) in the emulsion (co)polymerization of VAc-based latexes.

### III.2 The role of P(VOH-s-VAc) as stabilizer for the emulsion (co)polymerization of VAc

As previously highlighted, these stabilizers are usually characterized by their molar mass, their degree of hydrolysis, and their blockiness index. The structure of the polymer plays a major role in the final properties of the latex and its use is desirable because of its advantageous performance properties compared to conventional stabilizers. For instance, P(VOH-s-VAc) contributes to an increase in the mechanical strength of application products such as adhesives for paper, packaging or in their use as binder powder in adhesives or mortar, and imparts stability against freezing and thawing of the latex.<sup>[72]</sup> The chemical properties of P(VOH-s-VAc) were also found to impact the final properties of the latex: for instance, the blockier the structure, the smaller the particle size of the latex. Additionally, this kind of stabilizer does not migrate out of the final latex product, resulting in the retention of its properties during its entire life cycle (unlike conventional stabilizers).

When P(VOH-s-VAc) is used as stabilizer, it plays a dual role in the stabilization process. First, it provides colloidal stability to the growing particles by adsorption at the particle-water interface and decreases the surface tension of the system.<sup>[9],[72]</sup> Indeed, due to its amphiphilic character, the stabilizer adsorbs at the surface of the particles with the PVAc sequences (trains) oriented inside the particle, and the PVOH sequences (loops) oriented towards the aqueous phase as schematically represented in **Figure I-13**.

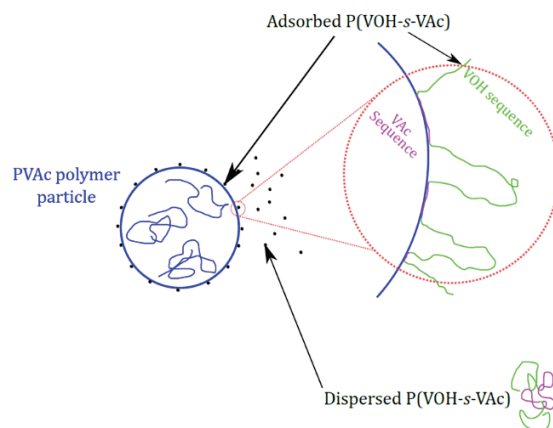


**Figure I-13: Scheme of the stabilization of the emulsion polymerization of VAc by adsorption of P(VOH-s-VAc) stabilizer.**

Second, P(VOH-*s*-VAc) provides sites for particle nucleation. Indeed, it has been shown that the other mechanism by which P(VOH-*s*-VAc) stabilizes a latex of PVAc was by formation of grafts of PVAc *via* transfer reactions of the oligoradicals to the stabilizer. The specific sites of transfer and further on the grafting onto P(VOH-*s*-VAc) are akin to those described in the previous section for intermolecular branching on PVAc (**Section II.3, Figure I-6, route 2 (a) and (b)**), and involve chain transfer to the stabilizer, as shown schematically in **Figure I-14**. Noteworthy, in the presence of both P(VOH-*s*-VAc) and PVAc<sup>•</sup> oligoradicals in the polymerization medium, Okamura and Motoyama reported that chain transfer to P(VOH-*s*-VAc) was more likely to occur than chain transfer to PVAc, according to the measured transfer constant of vinyl acetate to these species:<sup>[57]</sup>

- Transfer constant to PVAc:  $1.5 \times 10^{-4}$
- Transfer constant to P(VOH-*s*-VAc):  $35 \times 10^{-4}$

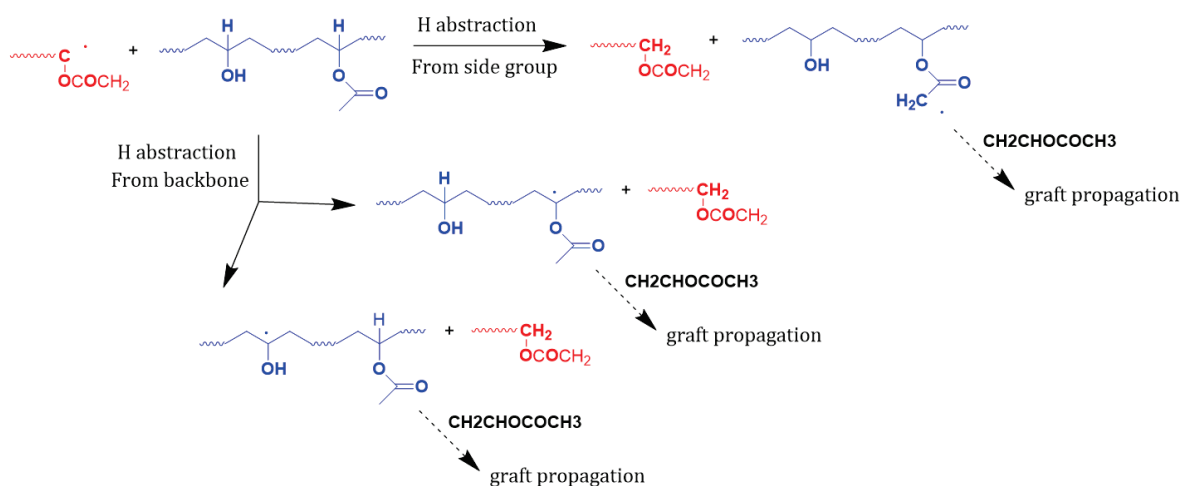


**Figure I-14: Mechanisms of grafting of P(VOH-*s*-VAc) in emulsion polymerization of vinyl acetate. Adapted from ref <sup>[11]</sup>, with permission from the publisher. Dashed lines for arrows indicate multiple processes of the same kind.**

Grafting occurs in the aqueous phase by abstraction of a hydrogen from the stabilizer side group or backbone (**Figure I-14**). This abstraction is induced either by a radical from the initiator, or an oligoradical. Then, monomer units add to the radical produced on P(VOH-*s*-VAc), resulting in the growth of a grafted chain. The propagation continues until the grafted polymer reaches a critical size where the overall structure of the grafted polymer is not soluble in water anymore. It becomes surface active and can either enter into an existing particle (or into a micelle if present), or it can separate to form a primary particle (see **Figure I-16, route 2**).<sup>[3],[11],[57]</sup>

Although only present at relatively low levels, the methyl ester C–H bonds are a major site for grafting, in part because of the amplification factor of having three labile C–H bonds per

repeat unit, but also because of resonance stabilization of the produced radical by the ester C=O group.

Even though the probability of abstraction of the methine on VAc or VOH units is difficult to predict, one can imagine that both phenomena coexist. Indeed, in the early stages of the emulsion polymerization of VAc, P(VOH-s-VAc) is dissolved in the aqueous phase. Therefore, more hydroxyl groups and fewer acetyl groups may be available for radical attack, owing to clustering of the acetyl groups of P(VOH-s-VAc) in the aqueous solution, favoring the methine abstraction on VOH units. Later in the process, when the stabilizer is adsorbed onto the surface of PVAc particles, the VAc units may be nearer to the locus of polymerization at the surface of the particle, thus resulting in higher grafting onto the P(VOH-s-VAc) having higher acetyl content (**Figure I-13**).<sup>[19]</sup>

Additionally, Markley<sup>[57]</sup> showed that the abstraction efficiency of the methine from a primary radical was dependent on the configuration of the repetitive units. He highlighted that in a statistical P(VOH-s-VAc), hydrophilic sulfate ion-radical may be hindered from passing through the bulky hydrophobic acetate groups to the P(VOH-s-VAc) methine carbons (**Figure I-15**).

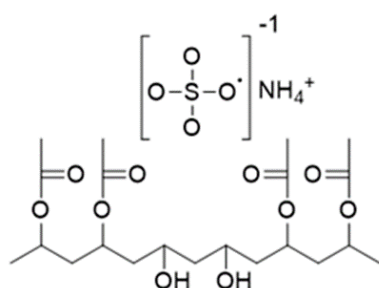


**Figure I-15: Illustration of steric hindrance to methine abstraction. Reprinted from ref <sup>[57]</sup>.**

The amount and type of initiator also proved to play an important role in the grafting reactions.<sup>[57]</sup> It was found that increasing the concentration of initiator usually resulted in increasing the extent of grafting. This has been observed when KPS was used as the initiator. Adversely, when azobisisobutyronitrile (AIBN) or a redox system (*e.g.*, hydrogen peroxide with Fe<sup>2+</sup> and a reducer) were used, a lower graft proportion was formed in comparison with KPS initiator. In good agreement with Markley's work, Okamura and Motoyama reported that 14% of the AIBN reacted with the stabilizer, while 97% of the KPS did so. This was attributed to an easier H-abstraction of the persulfate free radicals (which has lower activation energy).<sup>[73]</sup>

In any case, a synergy exists between adsorption and grafting of P(VOH-*s*-VAc) onto the polymer particles during the emulsion polymerization of VAc,<sup>[28],[74],[75]</sup> and extensive studies support that the structure and properties of the P(VOH-*s*-VAc) may favor one or the other mode of stabilization. Budhlall *et al.*<sup>[50]</sup> investigated the influence of three different P(VOH-*s*-VAc) with similar molar masses but different  $\beta$ , on the extent of grafting during the batch emulsion polymerization of VAc initiated by KPS ( $S_c = 10\%$ ). The polymerizations were carried out at 60 °C in a 1 L reactor equipped with a baffle and turbine impeller. The authors reported that the amount of grafting on P(VOH-*s*-VAc) was significantly higher for the more random structure than for the blockier one (10% vs 30%, respectively). They attributed this to the fact that grafting occurs predominantly in water. Thus, the P(VOH-*s*-VAc) with a higher degree of blockiness adsorbed faster and more strongly at the surface of the nucleated particles. As a consequence, it spent a shorter time in the aqueous phase where the grafting reactions occur, compared to the less blocky P(VOH-*s*-VAc) and was then less grafted. The authors also highlighted that no constant rate of polymerization was observed in interval II, and that a nonlinear relationship was obtained between the rate of polymerization and the number of particles ( $N_p$ ). The final  $N_p$  was independent of the degree of blockiness of the stabilizer, and the authors obtained broad and bimodal particle size distribution, which led them to conclude to the occurrence of continuous nucleation over the course of the polymerization.

More recently, Carrà *et al.*<sup>[9]</sup> performed similar investigations with the same grades of stabilizers. They carried out batch emulsion polymerizations of VAc at 60 °C, initiated by KPS, in 3.5 L reactors equipped with a mechanic anchor and targeted a solid content of 15%. Adversely, no significant difference was observed from one system to another in terms of kinetics, and they obtained isometric latexes of approximately 150 nm, regardless of the blockiness index of the stabilizer. The authors then applied a selective solubilization procedure onto the latexes, based on Magallanes's work<sup>[76]</sup> to separate the different fractions of P(VOH-*s*-VAc) in the final latexes. These three fractions are free P(VOH-*s*-VAc) in the aqueous phase, physically adsorbed and chemically grafted stabilizer onto the polymer particles. Contrarily to Budhlall's findings, they claimed that grafted fraction remained relatively constant (approximately 20%) regardless of the blockiness index of the stabilizer, and that this fraction was lower than the physically adsorbed fraction. These results were confirmed by P(VOH-*s*-VAc) adsorption measurements (determined by adsorption isotherms), which led them to conclude that the structure of P(VOH-*s*-VAc) did not seem to have a great effect on the chemistry of the grafting process. Nevertheless, both research groups agreed that there was a clear dependence of the amount of adsorbed stabilizer onto the particles which correlated well with its blockiness index. This can be explained in terms of the better stabilizing properties of the highly blocky P(VOH-*s*-VAc) types, and greater affinity towards the particle surface.

Additionally, the extent of adsorption and grafting reactions has been shown to be dependent on the hydrolysis degree of the P(VOH-*s*-VAc). El-Aasser's group<sup>[77]</sup> performed the emulsion copolymerization of VAc and butyl acrylate carried out in the presence of P(VOH-*s*-VAc) of different HD, and found that the grafting reactions of the stabilizer with VAc in the aqueous phase affected the rates of individual monomer consumption, and the overall polymerization kinetics. The authors found that the rate of polymerization was faster, and the conversion higher, when partially alcoholized PVAc was used, compared to when fully alcoholized stabilizer was used ( $R_p = 5.8$  vs  $2.3 \text{ g L}^{-1} \text{ min}^{-1}$ , respectively). The authors also highlighted the existence of a limit value of acetate content on the P(VOH-*s*-VAc) to keep its water solubility, and calculated it to be 18 mol.%. This suggests that the stabilizer becomes insoluble when it reaches a HD of 82 mol.%. The partially alcoholized PVAc (HD = 88 mol.%) can then graft with VAc until an average HD of 82 mol.% is reached (to become surface active), which represents an increase of 6 mol.% of the acetate character on the copolymer chain. Fully hydrolyzed PVAc (PVOH with HD = 98 mol.%) can also graft with VAc until an overall HD of 82 mol.% is reached, and this represents an increase of 16 mol.% of the acetate character before the stabilizer becomes surface active. These findings explain why the higher the HD, the lower the effectiveness of the stabilizer. Similarly, Okamura and Yamashita<sup>[78]</sup> found a greater degree of grafting on fully hydrolyzed PVAc than on the partially hydrolyzed PVAc.

In light of the competitive modes of stabilization (either adsorption or grafting) provided by P(VOH-*s*-VAc) when used as a stabilizer in the emulsion polymerization of VAc, Magallanes proposed a general mechanism for particle nucleation (**Figure I-16**).<sup>[79]</sup>

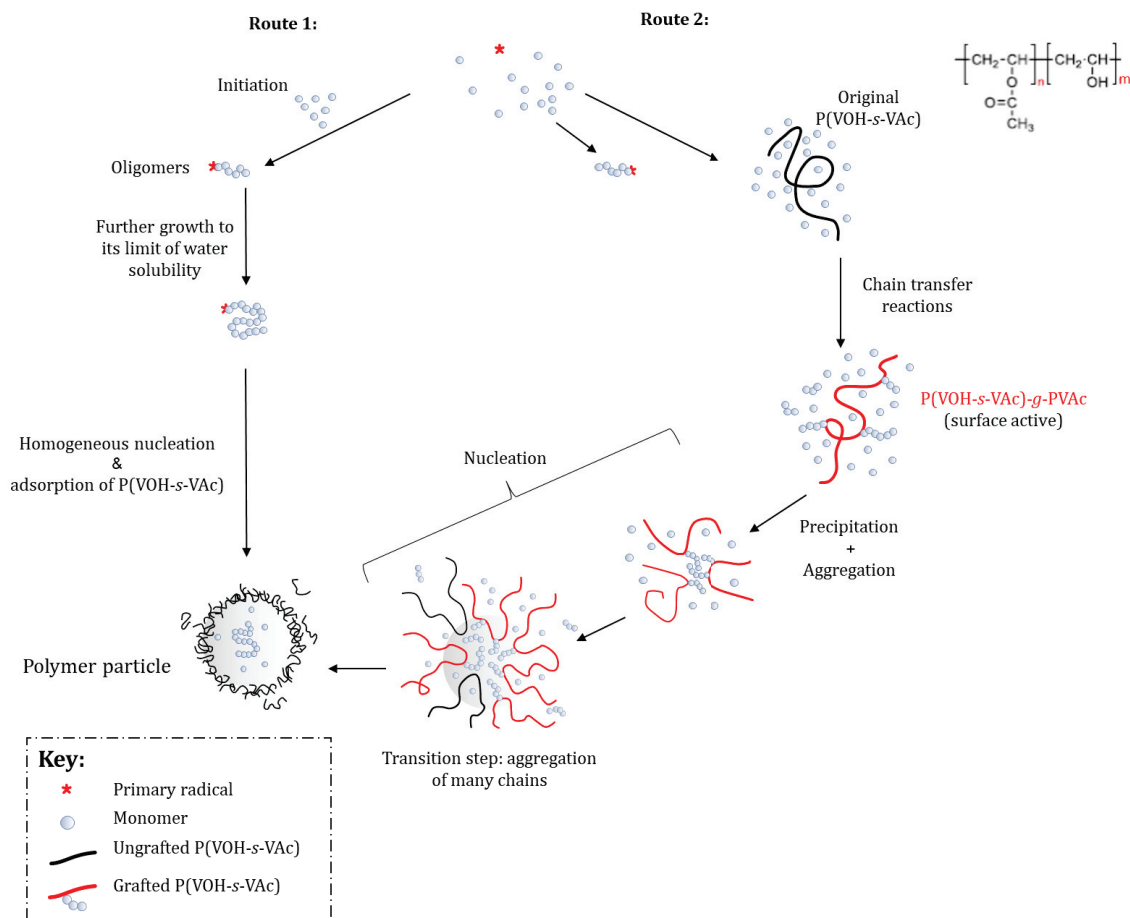


**Figure I-16: Scheme of the different modes of particle nucleation during the emulsion polymerization of VAc stabilized with P(VOH-s-VAc). Adapted from ref [79].**

The first route is similar to homogeneous nucleation described in **Section II.2**: after initiation in water, oligomeric radicals grow until they reach a critical chain length, at which point they will no longer be soluble in water. At this point, the oligoradicals precipitate to form primary particles. These primary particles will be stabilized by adsorption of P(VOH-s-VAc) (with a contribution of ionic end groups in case the initiator is charged, *e.g.*, KPS). The resulting particles become the primary loci of the polymerization and they grow with increasing monomer conversion. Because of the presence of P(VOH-s-VAc) as stabilizer, primary particles formation may also take place *via* aggregation of grafted P(VOH-s-VAc) (**Figure I-16**, route 2). At the end of the polymerization, the polymer particles will then be stabilized by the presence of both adsorbed and grafted P(VOH-s-VAc) at their surface.



*In summary*, it is all the molecular characteristics of a P(VOH-*s*-VAc), including the DP, the dispersity  $\mathcal{D}$  ( $M_w/M_n$ ), the HD with the corresponding distribution, as well as the average length of the PVAc sequences, that determine the characteristics of a P(VOH-*s*-VAc) material and therefore, its application. The use of P(VOH-*s*-VAc) as stabilizer complicates the picture of phenomena occurring in emulsion polymerization for several reasons: (i) depending on the polymerization conditions, the conformation of the stabilizer in solution will radically change and, hence, accordingly also its stabilizing properties; (ii) the radical transfer processes entail the formation of graft polymers, which also greatly affect the stabilizing properties, and thus the characteristics of the latex; (iii) the synthesis of P(VOH-*s*-VAc) is never perfectly reproducible from one batch to another, due to the aforementioned 1,2-glycol repetitive units and to the presence of hydrolysable and non-hydrolysable segments resulting from branching reactions occurring during the synthesis of the PVAc precursor. It is thus difficult to obtain a reproducible and well-defined structure of the resulting stabilizer, and it has been proved that this also led to variations in its stabilization of the latex. <sup>[67],[72]</sup> In this context, research studies have evolved towards the techniques of reversible-deactivation radical polymerization (RDRP).<sup>[80]</sup>

This PhD aims to synthesize new structures of stabilizers for the emulsion copolymerization of VAc and VeoVa, which include VOH and more hydrophobic units. In the attempt to compare the stabilizing efficiency of these new polymers, correlated to their structure, it is essential to synthesize well-defined and reproducible polymers (from one batch to another). Additionally, original structures which cannot be accessed by FRP (*e.g.*, block copolymers) will be synthesized. This is why the synthesis of the targeted copolymers relied on reversible addition-fragmentation chain transfer (RAFT) polymerization, one of the most used controlled radical polymerization techniques, as it allows the formation of well-defined polymer architectures and for the formation of block copolymers among other architectures.<sup>[81]</sup> The general concept of controlled radical polymerization is described in the following section, with a more detailed section dedicated to the RAFT technique, before the specific application to the synthesis of well-defined P(VOH-*s*-VAc) structures is discussed in the last section of this chapter.



## IV. Controlled radical polymerization techniques: the example of RAFT

### IV.1 Generalities on reversible-deactivation radical polymerization (RDRP)

As previously mentioned, FRP suffers from irreversible termination reactions, transfer to monomer, polymer or solvent, and lack of control on the molar mass, the architecture and the composition of the polymer chains. Adversely, controlled polymerization (or RDRP) techniques rely on a dynamic equilibrium between growing (active) radicals and dormant species to minimize the proportion of terminated chains by degenerative transfer reactions, which in turn allows for control of molar mass and dispersity. Therefore, RDRP provides a new set of tools that affords very precise control over the polymerization process, while retaining much of the versatility of FRP.<sup>[56]</sup> The techniques used in RDRP give the possibility to produce polymers with well-defined architectures and compositions, that can be used for a wide range of applications from novel surfactants, dispersants, coatings and adhesives, to biomaterials and drug delivery media.

The different techniques of RDRP are all based on the same principle: the reversible-deactivation equilibrium established between the dormant and active propagating species. Depending on the chain controlling agent (CTA) used, they are classified mechanistically into two categories, which are a reversible termination process (such as Nitroxide Mediated Polymerization (NMP)<sup>[82]</sup> and Atom Transfer Radical Polymerization (ATRP)<sup>[83]</sup>), (**Figure I-17 (a)**) or a reversible transfer process (as iodine transfer polymerization (ITP),<sup>[84]</sup> cobalt-mediated radical polymerization (CMRP),<sup>[85]</sup> tellurium-mediated radical polymerization (TERP)<sup>[86]</sup> and reversible addition-fragmentation chain transfer (RAFT),<sup>[87]</sup> (**Figure I-17 (b)**),<sup>[12],[88]</sup>

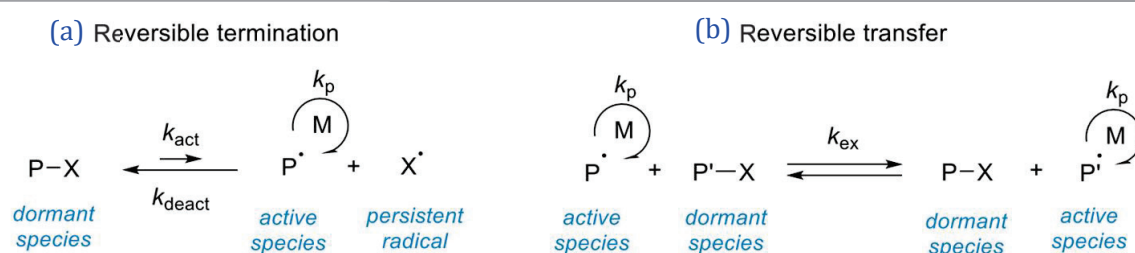


Figure I-17: Schematic mechanism of reversible termination (a) and reversible transfer (b) for RDRP.

In an ideal RDRP, the creation of chains should be fast to allow all chains to grow simultaneously and ensure a high concentration of growing chains. Meanwhile, the propagating radical concentration at any given time should be kept low. This apparent paradox is fulfilled by the controlling agent, which creates a dynamic exchange between dormant chains and propagating radicals. As a result, the polymer chains can grow

simultaneously throughout the reaction with very low concentrations of radicals present thorough the polymerization process, thus minimizing secondary reactions of irreversible termination and/or transfer (even though not completely avoided).<sup>[88],[12]</sup> The minimization of transfer and termination events comes from the reduction of the radical lifetime from 1 to  $\approx 10^{-4}$  seconds. This is achieved by the use of an appropriate agent that provides reversible capping of the active center.

A controlled polymerization process should display the following features:<sup>[89],[90]</sup>

- First-order kinetic behavior,
- Linear evolution of molar mass ( $M_n$ ) with conversion. This comes from maintaining a constant number of chains throughout the polymerization,
- Narrow molar mass distribution (or low dispersity:  $\mathcal{D} = M_w/M_n$ ),
- Long-lived polymer chains with preserved end-functionalities.

This involves the following requirements and depends on the choice of the CTA, adapted to the specified system (*e.g.*, the monomer):

1. The rate of initiation must be fast in comparison to the rate of propagation, allowing simultaneous growth of all the polymer chains.
2. The exchange between species involved in the equilibrium must be fast in comparison with the rate of propagation. This condition ensures that all the active chain termini are equally susceptible to react with monomer, allowing uniform chain growth.
3. The extent of irreversible chain transfer or termination reactions should be negligible.
4. The rate of depropagation must be substantially lower than propagation, which guarantees that the polymerization is essentially irreversible.

In RDRP, the lifetime of a growing chain may exceed several hours, in contrast to less than one second for the propagating radicals in FRP. Generally, less than 10 % of the chains are terminated in an irreversible manner. Therefore, the minimization of transfer and termination events enables the chains to retain their active center after the full consumption of the monomer. This allows for the preparation of various structures such as block copolymers for instance, by sequential monomer addition. It will be shown in **Chapter 4** and **5** that this characteristic was a major advantage for the synthesis of new macromolecular stabilizers which enhanced the properties of the resulting latex.

To date, RAFT polymerization has proven to be the most versatile technique for controlling the polymerization of vinyl esters. ITP, OMRP and CoMRP also provided interesting results, but presented some limitations of different kinds. For instance, PVAc derived from ITP undergoes decomposition of the iodide chain-end to form an aldehyde.<sup>[91]</sup> OMRP based on

methyl telluride (TeMe) compounds only allowed to access low molecular weight PVAc because of the accumulation of low-activity inverted VAc-TeMe adducts during polymerization.<sup>[92]</sup> Finally, while high molar mass PVAc samples with low dispersities were successfully synthesized by CoMRP, this technique is applicable only to a narrow range of monomers, which hampered its development. Consequently, the RAFT technology was of particular interest for this PhD, and was chosen among the other RDRP techniques for the synthesis of well-defined new stabilizer architectures, incorporating VOH units derived from the alcoholysis of well-defined PVAc polymers. The specificities of this technique will be further presented in the following.

## IV.2 Reversible addition fragmentation chain transfer (RAFT)

RAFT polymerization was discovered by the CSIRO group in the late 90's.<sup>[93][94]</sup> In parallel, a similar polymerization technique, macromolecular design by interchange of xanthate (MADIX) was invented and patented in France.<sup>[95],[96]</sup> Both RAFT and MADIX are based on an addition-fragmentation chain transfer mechanism. The difference lies in the nature of the controlling agent (CTA): MADIX refers to polymerizations mediated by xanthates while RAFT is usually mediated by dithioesters or di- and trithiocarbonates (**Figure I-18**). The choice of the RAFT agent is explained below.

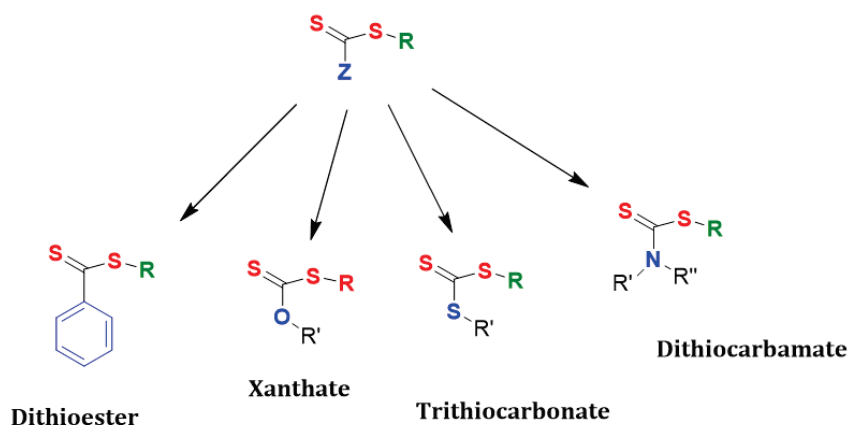


Figure I-18: RAFT/MADIX agent structures.

The RAFT/MADIX mechanism is depicted in **Figure I-19**. As in FRP, the first step consists of the initiation: the decomposition of the initiator leads to the formation of two radicals, (**Figure I-19**, step 1). This process forms the propagating polymer chain  $P_n^\bullet$  (**Figure I-19**, step 1). Subsequently, the radical species  $P_n^\bullet$  adds to the RAFT/MADIX agent (Z-C(S)-S-R, chain transfer agent, CTA) **1**, to enter a pre-equilibrium between the active and the dormant

species (**Figure I-19**, step 2). Addition of the propagating radical onto a thiocarbonyl compound **1** results in the formation of a non-propagating radical intermediate **2**. Then, there are two possible pathways:

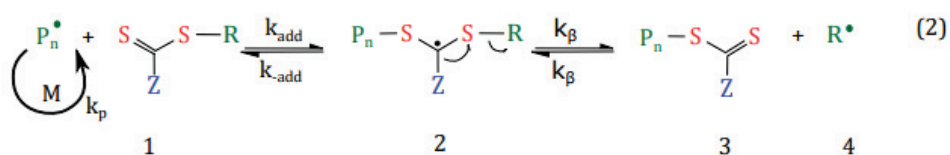
- Either the reverse of the addition, releasing the same propagating radical  $P_n^\bullet$  and the same Z-C(S)-S-R species **1**.
- Or fragmentation of **2**, thus creating a new dormant species Z-C(S)-S- $P_n$  **3** and releasing the radical  $R^\bullet$  **4**, capable of re-initiating the polymerization (step 3).

After all the CTA **1** is consumed (pre-equilibrium), the polymerization shifts to the main equilibrium (step 4), where propagating macro-radicals **5** and dormant species **3** are the main species present in the polymerization medium. The equilibrium between dormant species **3** and active species **5** ensures the simultaneous growth of all polymer chains in a controlled fashion.

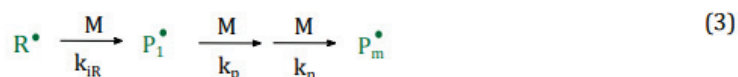
#### Initiation



#### Initialization



#### Reinitiation



#### Main equilibrium

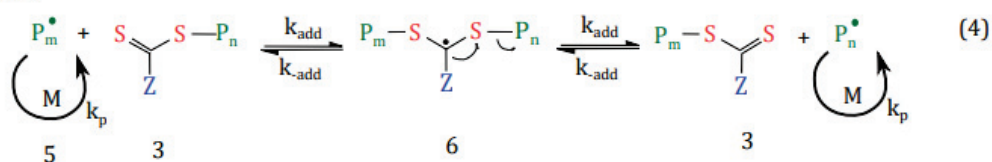


**Figure I-19: General RAFT/MADIX polymerization scheme. Redrawn from ref [81] with permission from the publisher.**

In an effective process, the rate of the addition/fragmentation equilibrium is higher than that of the propagation, so there should be less than one monomer unit added per activation cycle in average. This process is determined by the chain transfer constant value  $C_{tr}$  ( $C_{tr} = k_{tr}/k_p$ ).

As a general rule, the higher the  $C_{tr}$  value, the better the control of the polymerization. Therefore, all chains will have a similar DP at a given time, resulting in low dispersity.

#### IV.2.1 Choice of the RAFT/MADIX agent

Successful RAFT polymerization depends on the design of the RAFT/MADIX agent. To date many different RAFT/MADIX agents have been reported.<sup>[81],[93],[94],[97]</sup> R and Z groups are found to be monomer specific. Monomers can be considered as belonging to one of two broad classes. The “more activated” monomers (MAMs) are those where the double bond is conjugated to an aromatic ring. The “less activated” monomers (LAMs) are those where the double bond is adjacent to a saturated carbon, an oxygen or nitrogen lone pair, or the heteroatom of a hetero- aromatic ring. VAc is a LAM. Typical examples of MAMs and LAMs are provided in **Figure I-20**. Ethylene does not belong to these groups as it is even less reactive than the LAMs. In this context, it can be considered as a non-activated monomer.

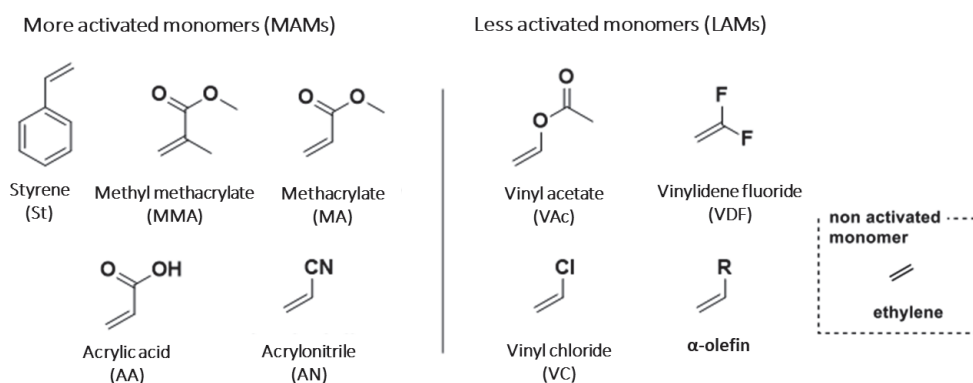


**Figure I-20: Examples of more and less activated monomers (MAMs, and LAMs, respectively).**

MAMs produce more-stabilized and less reactive radicals (the electron resulting from radical addition is stabilized by resonance and steric factors) than LAMs. Therefore, in free radical polymerization, MAMs react more readily than LAMs. To ensure a high livingness, Z and R groups must be chosen wisely and depend on which monomer is polymerized (MAMs or LAMs).

*The Z group* influences both the rate of addition of the propagating radicals ( $P_n^\bullet$ ) to the thiocarbonyl group of **1** and **3** and the rate of fragmentation of the intermediate radicals **2** and **6** in **Figure I-19**. For MAMs, propagating radicals are relatively stable. Therefore, the Z group must help with the stabilization of the intermediate radical to favor radical addition on the C=S. Trithiocarbonate ( $Z = S\text{-alkyl}$ ) or dithiobenzoate ( $Z = Ph$ ) CTAs are typically

suitable to control MAMs polymerization. By contrast, the high reactivity of LAMs (higher  $k_p$ , higher  $k_{add}$ ) makes them poor homolytic groups. Thus, they require less stable intermediate radicals, such as xanthates ( $Z = O\text{-alkyl}$ ) or dithiocarbamate ( $Z = N\text{-alkyl}$ ), in order to favor fragmentation of the propagating radical. A more stable intermediate is not desired, as it would act as radical sink and limit polymerization.<sup>[97],[81]</sup>

General guidelines for the selection of the Z group are shown in **Figure I-21**.

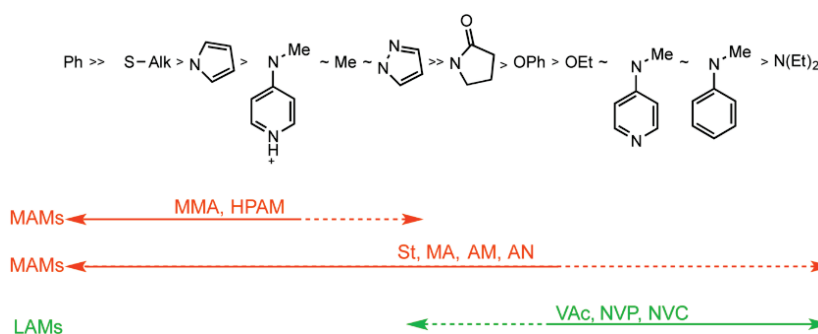


**Figure I-21:** Guidelines for selection of the Z group of RAFT/MADIX agents Z-C(S)-SR. Addition rate decreases and fragmentation rates increases from left to right. A dashed line indicates a partial control (*i.e.*, good control of  $M_n$  but poor control of  $\bar{D}$ ). Abbreviations: MMA = methyl methacrylate, HPAM = N-(2-hydroxypropyl)methacrylamide, St = styrene, MA = methyl acrylate, AM = acrylamide, AN = acrylonitrile, VAc = vinyl acetate, NVP = N-vinylpyrrolidone and NVC = N-vinylcarbazole. Reprinted from ref <sup>[81]</sup> with permission from the publisher.

The R group must be a good leaving group compared to that of the propagating radical  $P_n^\bullet$ , to ensure fragmentation of **2** and favor formation of **3** and R. It must also be able to reinitiate the polymerization.<sup>[81],[98]</sup> General guidelines for the selection of the R-group are shown in **Figure I-22**.

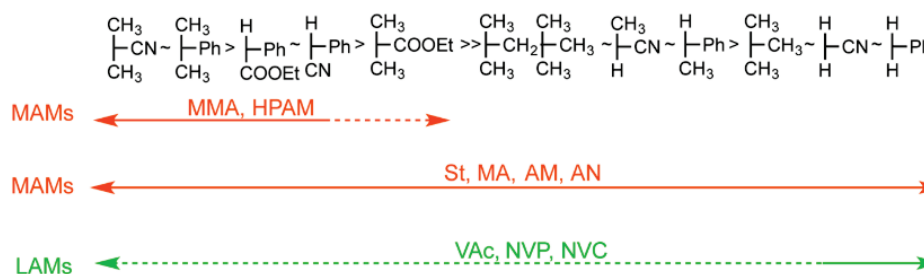


**Figure I-22:** General guidelines for the selection of the R group of RAFT/MADIX agents Z-C(S)-SR. Partition coefficients decrease from left to right. A dashed line indicates a partial control (*i.e.*, good control of  $M_n$  but poor control of  $\bar{D}$ , or substantial retardation). Reprinted from ref <sup>[81]</sup> with permission from the publisher.

## IV.2.2 Livingness in RAFT/MADIX

Another key requirement in RAFT/MADIX polymerization is the use of radical initiators. As in any RDRP, RAFT/MADIX polymerization cannot prevent undesired irreversible termination reactions that lead to the formation of dead chains. These reactions are directly related to the quantity of initiator used and thus a minimum amount is preferable. This seems to contradict most of the other RDRP systems, where the radical source allows tuning of the system in terms of polymerization rate and number fraction of living chains. Indeed, in these systems the number of chains that undergo irreversible bimolecular termination directly corresponds to the number of radicals initially produced in the system. However, in RAFT/MADIX polymerization, a bimolecular termination does not lead to the loss of a living chain-end, and the number of chains with the thiocarbonylthio end-group remains the same throughout the polymerization regardless of the extent of termination.<sup>[81]</sup> Therefore, the number of dead chains can be predicted and controlled by controlling the amount of radicals introduced in the system. Reducing the initiator concentration is key to optimizing the livingness of the system (**Figure I-23**).

The livingness of the polymerization medium is defined as:

$$L = \frac{[\text{CTA}]_0}{[\text{CTA}]_0 + 2f[\text{I}]_0(1 - e^{-k_d t})\left(1 - \frac{f_c}{2}\right)} \quad (5)$$

With  $[\text{CTA}]_0$  and  $[\text{I}]_0$  the initial concentration of RAFT/MADIX agent and initiator, respectively. The factor 2 comes from the fact that one molecule of initiator gives two primary radicals with a certain efficiency  $f$  (typically 0.5 for diazo-initiators).  $1 - f_c/2$  represents the number of chains produced by termination with  $f_c$  the coupling factor ( $f_c = 1$  corresponds to 100% bimolecular termination by combination;  $f_c = 0$  means 100% bimolecular termination by disproportionation).  $k_d$  is the decomposition rate.



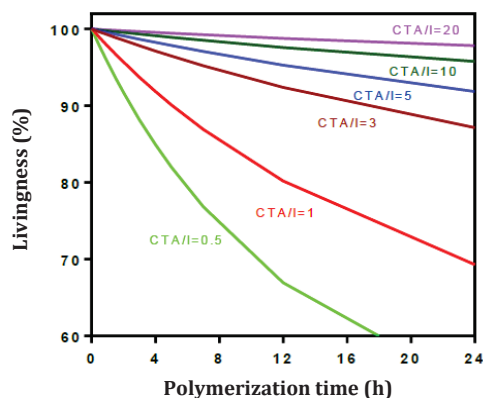


Figure I-23: Illustration of the influence of the [CTA]:[Initiator] ratio on livingness and polymerization kinetics. Reprinted from ref [99].

### IV.2.3 Introduction on the limitations encountered in RAFT/MADIX polymerization of LAM

One limitation encountered during the RAFT/MADIX polymerization of LAM (illustrated here with VAc), is the occurrence of head-to-head addition. When this reverse addition is immediately followed by addition/fragmentation reaction with the CTA, it forms less reactive primary carbon (**Figure I-24 (a)**), which renders the chains less reactivable by affecting their ability to fragment. The RDRP of VAc is thus not trivial due to the gradual accumulation of these less active  $\text{CH}(\text{OAc})\text{CH}_2\text{-X}$  (noted  $\text{PVAc}_T\text{-X}$  for brevity, X being the xanthate extremity) chains, resulting in a significant loss of control over the polymerization.<sup>[100],[101]</sup>

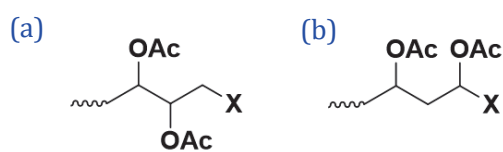


Figure I-24: Dormant chains resulting from (a): head-to-head and (b): head-to-tail propagation of VAc followed by addition to CTA (X) during RDRP polymerization by reversible transfer reaction.

In the case of the present research work, a careful design of amphiphilic copolymers of VAc and vinylic ester comonomers (CoM) was first performed in order to access a range of copolymers structures including block copolymers. In order to finely tune the amphiphilicity of the resulting hydrolysed copolymers, hydrophobic CoM were chosen and hydrolysis conditions that could be selective of the VAc units were sought. Vinyl laurate (VL) and VeoVa were the most promising CoM candidates.



The idea of using RDRP techniques for the synthesis of well-defined VOH-based polymer is not new. It is well documented in the literature (see below), and is still a subject of dynamic research. Kuraray company, one of the main producers of P(VOH-*s*-VAc) patented a process for the preparation PVOH-*b*-PVAc in 1987.<sup>[102]</sup> More recent examples are the preparation of well-defined P(VOH-*s*-VAc) by hydrolysis of RAFT-synthesized PVAc, published in 2012 and 2022.<sup>[103],[104]</sup> The following section provides a non-exhaustive review on the use of CRP techniques (mostly RAFT), to synthesize VOH-based copolymers which could be used for the emulsion or suspension polymerization. But to the best of our knowledge, none of them were effectively tested as stabilizers for the emulsion polymerization of VAc.

## V. Application of the RDRP techniques to the synthesis of well-defined VOH-based macromolecules

### V.1 VOH-based statistical copolymers

The first paper that claimed the synthesis of well-defined statistical P(VOH-*s*-VAc) obtained by RAFT polymerization was published in 2012.<sup>[104]</sup> More recently Ballard and coworkers<sup>[105]</sup> showed that it was possible to adapt the process of polymerization to reduce the number of inactive chains, and prepare well-defined P(VOH-*s*-VAc) by hydrolysis of PVAc synthesized by RAFT polymerization in suspension. The authors showed that the use of RAFT polymerization allowed to obtain very similar DP after hydrolysis of the PVAc when compared to the one obtained by FRP, because the amount of long-chain branching was significantly reduced. RAFT suspension polymerization proved to be an efficient strategy for the synthesis of a well-defined and uniform structure of P(VOH-*s*-VAc).

Finally, Congdom *et al.*<sup>[61]</sup> studied the effect of more hydrophobic side chains (acetyl, propanoyl and butanoyl) onto the thermal properties of P(VOH-*s*-VAc). The authors synthesized a library of well-defined PVAc with different DP (ranging from 80 to 350) *via* RAFT, using *O*-Ethyl-*S*-1-phenyl carbonodithioate. Then, they fully hydrolyzed their PVAc, and partially reacylated the chains with vinyl butanoate and vinyl propionate. They showed that at fixed DP, the higher the more hydrophobic comonomer (CoM) content, the lower the phase transition temperature (from dispersed state to insoluble one). Adversely, they highlighted that longer P(VOH-*s*-CoM) had an inverse relationship between phase transition temperature and chain length.

### V.2 VOH-based block copolymers

The synthesis of amphiphilic block copolymers is of practical use in many applications, such as drug delivery<sup>[106],[107],[108]</sup>, rheological modifiers for personal care products<sup>[108]</sup> and microelectronics.<sup>[109]</sup> The literature is well furnished with examples and the most extensively studied non-ionic block copolymer stabilizers are comprised of a hydrophobic block (*e.g.*, poly(propylene oxide),<sup>[108]</sup> polybutadiene<sup>[110]</sup>) and a hydrophilic poly(ethylene oxide) (PEO) block.

V. Ladmiral *et al.*<sup>[100]</sup> studied the RAFT (co)polymerization of vinylidene fluoride (VDF) followed by chain extension with several other monomers (including VAc), to form block copolymers. They noticed the occurrence of head-to-head configuration of the last inserted monomer unit, connected to the CTA (noted PVDF<sub>T</sub>-X for brevity, X being thiocarbonylthio function) during VDF polymerization, resulting in less reactivable chains. Indeed, these chains were not reactivated when *N*-vinylpyrrolidone (NVP), *n*-butyl acrylate (BA) or *N,N*-

dimethyl-acrylamide (DMA) monomers were used for extension. Only VAc allowed the reactivation of both PVDF<sub>H</sub>-X (issued from the regular head-to-tail addition) and PVDF<sub>T</sub>-X chains, but the latter was slower. Nevertheless, they claimed the obtention of well-defined PVDF-*b*-PVAc block copolymers with relatively high end-group fidelity and low dispersity. After hydrolysis, this work also opened access to new PVDF-*b*-P(VOH-*s*-VAc) amphiphilic block copolymers.

The RAFT copolymerization of vinyl boronic acid pinacol ester (VBpin) (used as VOH-precursor monomer) and the successive extension with styrene (St) allowed for the synthesis of well-defined PVBpin-*b*-PSt.<sup>[111]</sup> The commercially available boron-attaching vinyl compound exhibited better copolymerization behaviors with conjugated monomers (such as St) than VAc, and PVOH-*b*-PSt block copolymers were obtained *via* oxidation of the boron pendant group. The synthetic approach is valuable for functional materials, because the copolymers made of well-known hydrophilic/hydrophobic materials are inaccessible with the combination of VAc and St due to the respective duality of the LAM and MAM nature of the monomers.

Well-defined PVAc-*b*-PVOH amphiphilic block copolymers can be obtained *via two main pathways* allowing a good control over the block sizes. *The first one* consists of the preparation of the first block of the copolymer with a chain-end group allowing for the re-initialization of the polymerization in the presence of a second monomer. *The second pathway* consist in a combination of two preformed well-defined homopolymers carrying a functionality that allows for the coupling (*e.g.*, “click chemistry”).

### **V.2.1 PVAc-*b*-PVOH block copolymer obtained by extension of RAFT-synthesized PVAc (*first pathway*)**

So far, a limited number of studies are available on PVAc-*b*-PVOH, due to the complexity of synthesizing this block copolymer. Mahanthappa and coworkers<sup>[112]</sup> described a straightforward synthesis pathway of PVAc-*b*-PVOH amphiphilic block copolymers with variable compositions and narrow dispersities, and demonstrated *via* cryo-TEM that this kind of copolymer forms micelles in aqueous media. The authors sequentially copolymerized, by RAFT VAc, and the electron-deficient vinyl chloroacetate (VClAc), as a VOH-precursor monomer. The rate of chloroacetate ester cleavage being seven hundred sixty times faster than acetate ester ones, they obtained well-defined PVAc-*b*-PVOH upon hydrolysis of the block copolymer precursor. They also used this strategy to synthesize well-defined PVAc-*b*-PVOH-*b*-PVAc triblock copolymer hydrogels.<sup>[113]</sup> Another example is the statistical or block copolymerization of VAc with vinyl trifluoroacetate (VTFAc).<sup>[103]</sup> Controlled poly(vinyl esters) with tunable thermal properties and tacticity were obtained, and well-defined PVAc-

*b*-PVOH diblock copolymers were produced by selective methanolysis of the VTFAc units of the starting copolymer.

Another original approach to obtain well-defined VOH-based block copolymers was described by Kamigaito *et al.*<sup>[114]</sup> The authors used cationic RAFT polymerization combined with a Lewis acid to manage the stereoselectivity of the first block of bulky vinyl ether monomers (such as *tert*-butyl, benzyl, trimethylsilyl, and *tert*-butyldimethylsilyl vinyl ether) using dithiocarbamates and BF<sub>3</sub>•OEt<sub>2</sub> or EtAlCl<sub>2</sub>. The control of the molar mass of the first block was achieved by the thioester-mediated reversible chain-transfer reaction, while isospecific propagation was ascertained by the steric hindrance of bulky substituents of the vinyl ethers and appropriate counter anions derived from the Lewis acids. One of the most interesting features of cationic RAFT polymerization is the possibility to synthesize block copolymers composed of both cationically and radically polymerizable monomers. Thus, in a second time, the first block was successfully extended with VAc. After hydrolysis, isotactic-P(VOH-*s*-VAc)-*b*-atactic-P(VOH-*s*-VAc) was obtained.

In a different approach, Atanase *et al.*<sup>[59]</sup> used acidic hydrolysis on a RAFT-synthesized PVAc to keep the xanthate extremity undamaged and tried to chain-extend the resulting PVOH-X with additional VAc monomer. However, they faced several limitations:

- The hydrolysis temperature damaged the xanthate extremity. This reaction had to be performed at low temperature (35 - 40 °C) to limit the loss of chain-end functionality, but in counterpart, it took several days to hydrolyze the polymer.
- After hydrolysis, low chain extension efficiency and high dispersity were obtained.

They explained this last result by the possibility that the terminal xanthate group had lost its effectiveness. Indeed, if the xanthate group attached to a VAc unit was effective to control the polymerization, it did not seem to be the same if the penultimate unit is of VOH type. These two possibilities are schematically represented in **Figure I-25**. The difference in reactivity of these two structures can be attributed to the fragmentation of the xanthate group and/or the stability of the PVOH• macroradical.

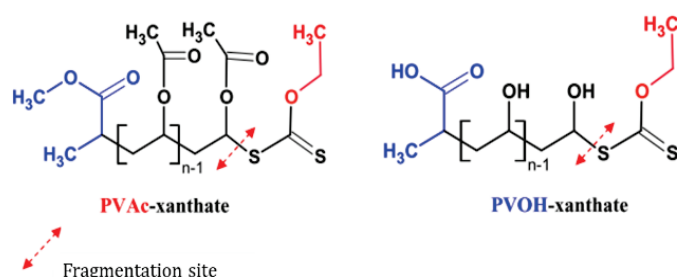


**Figure I-25: Fragmentation site of a terminal xanthate group in the case of a penultimate unit vinyl acetate (left) and vinyl alcohol (right). Adapted from ref [59].**

## V.2.2 PVAc-*b*-PVOH block copolymer obtained via combination of preformed well-defined homopolymers (*second pathway*)

The *second pathway* to synthesize well defined VOH-based block copolymers involves the synthesis of each block separately, which are then coupled by functional end groups, by “click” chemistry. For instance, Atanase *et al.* tried to combine click chemistry together with RAFT techniques. They used Tong *et al.*<sup>[115]</sup> route to synthesize a PVAc-N<sub>3</sub> precursor by using a xanthate functionalized with a non-hydrolysable azide function, allowing them to obtain well-defined PVAc-N<sub>3</sub>. In parallel, they developed the synthesis of a PVAc alkyne (PVAc≡), with a non-hydrolysable alkyne function using a new CTA (Figure I-26, blue square), which provided a PVOH≡ after alcoholysis.

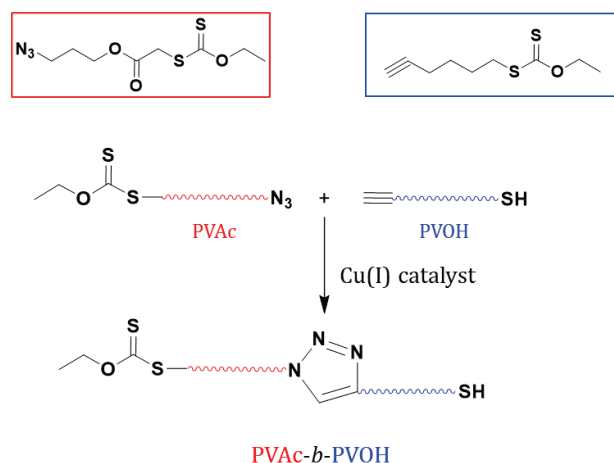


Figure I-26: Scheme of the 1,3-dipolar cycloaddition between an azide functionalized PVAc and an alkyne functionalized PVOH for the synthesis of well-defined PVOH-*b*-PVAc. Adapted from ref <sup>[59]</sup>.

In 2015, Monge *et al.*<sup>[116]</sup> also claimed the synthesis of well-defined PVAc-*b*-PVOH *via* the MADIX polymerization and Cu(I)-catalyzed azide–alkyne cycloaddition (CuAAC) techniques (also reported as an example of click reaction). In their work, PVAc chains were prepared using xanthate CTAs that contained either a non-hydrolysable azide or an alkyne-Si terminated functions. Good control over the molar masses and linear evolution of  $M_n$  as a function of the conversion were obtained for both polymers, regardless of the targeted molar masses. In a second step, PVAc-N<sub>3</sub> was hydrolyzed to provide PVOH-N<sub>3</sub> polymer, while removal of the trimethylsilyl function by the deprotection of the alkyne end group of PVAc-alkyne-Si was performed onto the second polymer, to provide PVAc-alkyne. In a third step, CuAAC of both homopolymers was carried out and led to successful formation of copolymers. These copolymers self-organized in water and formed aggregates observed by DLS. The  $R_h$  of these objects ranged from 52 to 75 nm and CAC ranged from 11 to 44 mg L<sup>-1</sup>, depending on

the hydrophilic block length. If both Atanase and Monge provided an efficient synthesis route for well-defined PVAc-*b*-PVOH, this multistep click chemistry process is not likely to be suitable at an industrial level.

### V.3 Other structures of VOH-based copolymer

In addition to statistical and block structures, original studies present the synthesis of PVAc comb- or star-like architectures *via* MADIX polymerization and the resulting P(VOH-*s*-VAc) combs after their subsequent hydrolysis.<sup>[117-119]</sup> The interest in developing synthetic methods for such complex architectures P(VOH-*s*-VAc) stems from some of the unique properties exhibited by hyperbranched polymers and stars (for example, low bulk and solution viscosity and high functionality).<sup>[118]</sup> In the case of combs, the backbones were prepared by RAFT to obtain well-defined P(VOH-*s*-VAc) polymers with different DP. Subsequent functionalization with xanthates *via* a R-group or a Z-group approach resulted in the formation of a macromolecular controlling agent (macroCTA). In the Z-group approach, the growing macroradical remains permanently tethered to the scaffold structure. The polymerization exclusively takes place in the solution surrounding the main polymer backbone. Adversely, in the R-group approach, the xanthate moiety leaves the core of the structure, mediates the polymerization in solution and exchanges with the fixed Z-moiety. The introduction of xanthate groups (R or Z) had drastic consequences on the solubility and control of the polymers. Z-designed xanthate functionalized polymer backbone were not soluble in VAc and consequently not suitable for the bulk polymerization of VAc. The authors hypothesized that the presence of impurities and remaining xanthic acid salt which could explain this behavior. Steric congestion around the xanthate functionality, restricting the access of macroradicals to the C=S bonds was also suggested as a limitation (**Figure I-27 (a)**).

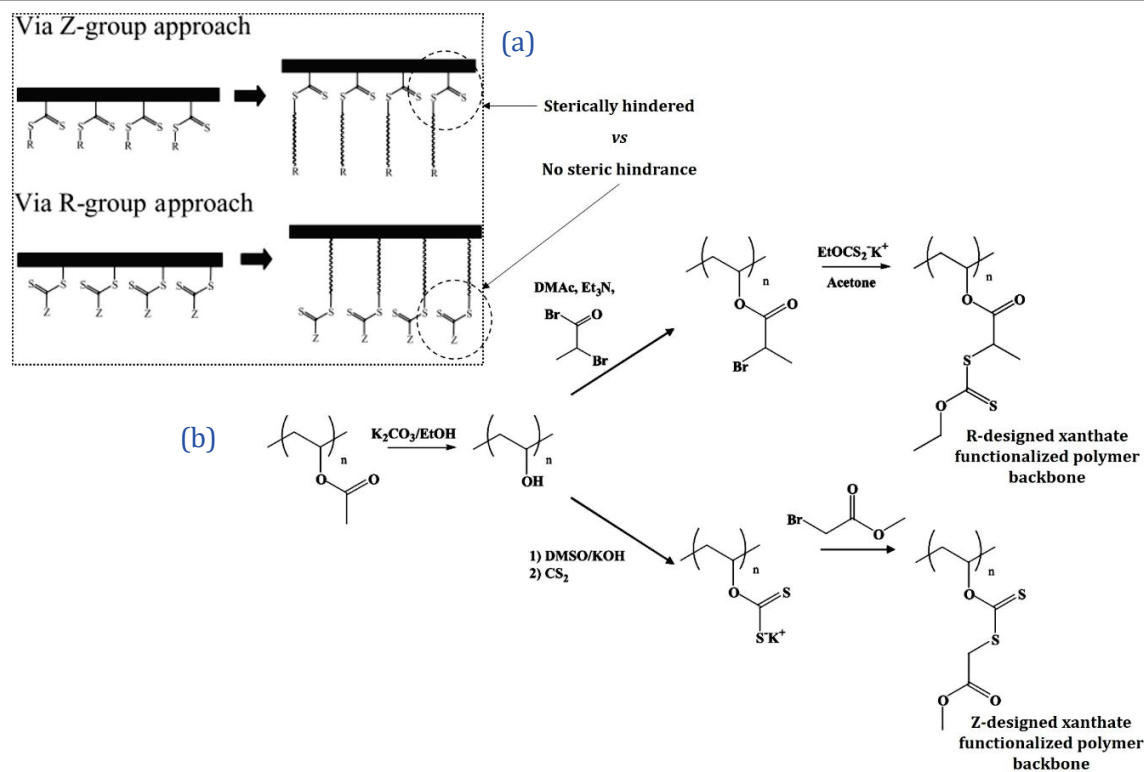


Figure I-27: (a): General scheme of comb polymers obtained *via* RAFT/MADIX polymerization, employing the Z-group of R-group approach and (b): synthetic approach to R- and Z- designed xanthate functionalized polymer backbones for the synthesis of PVAc combs. Reprinted from ref [56] and [117] with permissions from the publishers.

Indeed, to undergo transfer to the RAFT agent, the radical has to reach the xanthate moiety close to the main polymer backbone. Upon conversion, molar mass of the polymer increased and thus, the xanthate functionality was hindered. The propagating radical thus rather terminated with another radical and generated a dead polymer. As a consequence, the molar mass deviated from the theoretical value. On the contrary, R-designed xanthate functionalized polymer backbones were soluble in VAc and the xanthate functionality was not hindered. The R-group approach was thus suitable for the synthesis of PVAc comb.<sup>[117]</sup>

In the star synthesis experiments, the authors successfully synthesized 3 and 4-armed PVAc, starting from R- and Z-designed multifunctional CTA.<sup>[119]</sup> Once again, lower control of the polymerizations was observed when the Z-designed multifunctional RAFT/MADIX agent was used. This was once again attributed to steric hindrance. Hydrolysis of these PVAc star polymers resulted in the formation of P(VOH-*s*-VAc) stars. The R-group methodology seemed more adapted to form well-defined star polymers as it was possible to hydrolyze the acetate functionality without causing any destruction of the basic polymer structure. By contrast, the hydrolysis of stars generated by the Z-group approach resulted in destruction of the architecture, as the process also cleaved the xanthate linkage at the nexus of the arms. In a

second time, attempts were made to extend the scope of the R-designed multifunctional xanthate agents to the polymerization of vinyl esters with bulky pendant groups such as vinyl pivalate (VP) or VeoVa.<sup>[118]</sup> Polymerization rates and conversions were lower than the ones obtained with VAc, and this was attributed to the bulkiness of the side chains affecting monomer and radical reactivity.

Despite all the aforementioned examples reporting the synthesis of diverse and well-defined structures of amphiphilic VOH-based copolymers, it appears that these polymeric materials have never been considered as stabilizer candidates for the emulsion polymerization. One can expect that the better control over the dispersity and the molar masses of the copolymer may affect the stabilizing efficiency of P(VOH-*s*-VAc) and the final properties of the latex, compared to a P(VOH-*s*-VAc) obtained by FRP.



## VI. Motivation and objectives of this work

P(VOH-*s*-VAc) copolymers obtained by partial hydrolysis of PVAc are of practical importance for many applications, including as stabilizer for the preparation of VAc-based latexes by emulsion polymerization. Indeed, P(VOH-*s*-VAc) is one of the most widely used stabilizer as it is cost effective and easily available. It participates to the stabilization of the particles both by grafting and adsorption mechanisms. However, all the stabilizer chains are not involved in the stabilization of the particles. Free P(VOH-*s*-VAc) is present in the aqueous phase after complete polymerization, and can impact the final properties of the end products.

Currently, P(VOH-*s*-VAc) is mostly obtained by hydrolysis of PVAc synthesized by FRP. But FRP does not allow to synthesize perfectly reproducible PVAc polymers from one batch to another, and variations in the microstructure of the polymer are unavoidable. Consequently, the production of P(VOH-*s*-VAc) is not reproducible from one batch to another either, and this proved to have an impact on the latex characteristics. Additionally, depending on the experimental procedure to hydrolyze the PVAc, the microstructure of the resulting P(VOH-*s*-VAc) can be different, and this may drastically affect the stabilizing efficiency of the amphiphilic copolymer.

The present project aims to synthesize alternative amphiphilic copolymers, which mimic the properties of the commercially used P(VOH-*s*-VAc). These new macromolecular stabilizers must incorporate VOH units and must be able to stabilize PVAc latexes with a better involvement in particle stabilization.

The synthesis of the targeted amphiphilic copolymers relies on reversible addition-fragmentation chain transfer (RAFT/MADIX) polymerization that allows the formation of well-defined polymer architectures, and potentially to get rid of process variation. The question we posed in regard to the existing systems are:

- (i) Is it possible to obtain stable latexes with P(VOH-*s*-VAc) of lower molar masses and narrower molar mass distributions compared to a commercial P(VOH-*s*-VAc) obtained by FRP, namely Mowiol 4-88?
- (ii) Does the incorporation of more hydrophobic units to the structure enhance the adsorption and grafting efficiency of the stabilizer onto the polymer particles of the latex?
- (iii) What is the impact of the structure of the stabilizer onto the characteristics of the latex?
- (iv) Are those new macromolecular stabilizers suitable to be used in industrial applications such as mortar and spray drying?

To answer these questions, the manuscript is divided in six parts (including this one). Now that the main concepts used thorough this manuscript were defined in this chapter, the next

four chapters investigate the impact of the incorporation of more hydrophobic comonomer units (*i.e.*, VeoVa and VL (CoM)), and the influence of different structures of amphiphilic copolymers (statistical (**Chapter II** and **III**), block (**Chapter IV**) and gradient (**Chapter V**) copolymers) incorporating VOH, VAc and CoM units, onto their ability to efficiently stabilize polymer particles. In the last chapter (**Chapter VI**), the copolymers which provided the most promising results in terms of latex stability and adsorption and grafting efficiency onto the particles were then synthesized on a larger scale to be further characterized and to be tested in various fields of applications (*e.g.*, mortar formulation, and spray drying).

## References

- [1] R. Arshady, *Colloid Polym. Sci.* **1992**, *270*, 717–732.
- [2] L. I. Atanase, S. Bistac, G. Riess, *Soft Matter* **2015**, *11*, 2665–2672.
- [3] B. M. S. Budhlall, Grafting Reactions in the Emulsion Polymerization of Vinyl Acetate Using Poly(Vinyl Alcohol) as Emulsifier. Ph.D Dissertation, Lehigh University, **1999**.
- [4] K. Yuki, T. Sato, H. Maruyama, J. Yamauchi, T. Okaya, *Polym. Int.* **1993**, *30*, 513–517.
- [5] E. Frauendorfer, M. Babar, T. Melchin, "Monitoring of Vinyl Acetate–Ethylene Processes: An Industrial Perspective", in Polymer Reaction Engineering of Dispersed Systems. Volume II, Springer International Publishing, **2017**.
- [6] S. M. El-Aasser, S. D. Sudol, "Emulsion Polymerization and Emulsion Polymers", in Features of Emulsion Polymerization, Wiley, **1997**.
- [7] A. Allahverdi, K. Kianpur, M. R. Moghbeli, *Iran. J. Mater. Sci. Eng.* **2010**, *7*, 1–6.
- [8] T. Goto, Influence Des Paramètres Moléculaires Du Latex Sur l'hydratation, La Rhéologie et Les Propriétés Mécaniques Des Composites Ciment/Latex. Ph.D Dissertation, Université Pierre et Marie Curie - Paris VI, **2006**.
- [9] S. Carrà, A. Sliepcevich, A. Canevarolo, S. Carrà, *Polymer.* **2005**, *46*, 1379–1384.
- [10] J. C. Daniel, C. Pichot, "Latex à Base d'acétate de Vinyle".in Les Latexes Synthétiques, Lavoisier, **2006**.
- [11] P. A. Lovell, F. J. Schork, *Biomacromolecules* **2020**, *21*, 4396–4441.
- [12] T. P. Davis, K. Matyjaszewski, *Handbook of Radical Polymerization*, John Wiley & Sons, **2002**.
- [13] R. S. Porter, *Emulsion Polymers and Emulsion Polymerization*, ACS Symposium Series, Las Vegas, **1981**.
- [14] J. M. Asua, *J. Polym. Sci. Part A Polym. Chem.* **2004**, *42*, 1025–1041.
- [15] W. D. Harkins, *J. Chem. Phys.* **1946**, *14*, 47–48.
- [16] W. D. Harkins, *J. Am. Chem. Soc.* **1947**, *69*, 1428–1444.
- [17] W. V. Smith, R. H. Ewart, *J. Chem. Phys.* **1948**, *16*, 592–599.
- [18] C.-S. Chern, "Particle Nucleation Mechanism" in Principles and Applications of Emulsion Polymerization, John Wiley & Sons, **2008**.
- [19] Y. H. Erbil, "Vinyl Acetate Emulsion Polymerization and Copolymerization with Acrylic Monomers", CRC Press, **2000**.
- [20] H.-S. Chern, "Emulsion Polymerization Kinetics" in Principles and Applications of Emulsion Polymerization, John Wiley & Sons, **2008**.
- [21] S. W, *Freudenberg H. Br. US227163*, **1940**.
- [22] J. E. Bristol, N. Turnbull, *US2,614,088* **1952**.
- [23] W. R. Cornthwaite, D. Wilmonington, H. W. Bryant, *US2485141A*, **1949**.
- [24] X. S. Chai, F. J. Schork, A. DeCinque, K. Wilson, *Ind. Eng. Chem. Res.* **2005**, *44*, 5256–5258.
- [25] Peter J. Canterino, *US2694052A*, **1954**.
- [26] S. Binauld, L. Delafresnaye, B. Charleux, F. Dagosto, M. Lansalot, *Macromolecules* **2014**, *47*, 3461–3472.
- [27] G. S. Magallanes González, V. L. Dimonie, E. D. Sudol, H. J. Yue, A. Klein, M. S. El-Aasser, *J. Polym. Sci. Part A Polym. Chem.* **1996**, *34*, 849–862.
- [28] M. S. El-Aasser, "Emulsion Polymerization of Vinyl Acetate", Applied Science Publishers LTD, **1981**.
- [29] B. Jacobi, *Angew. Chemie* **1952**, *64*, 539–543.

- [30] W. J. Priest, *J. Phys. Chem.* **1952**, *56*, 1077–1082.
- [31] A. Brandrup, E. H. Immergut, "Polymer Handbook", 3rd Edition, Wiley-Interscience, New York, **1989**.
- [32] H. De Bruyn, The Emulsion Polymerization of Vinyl Acetate. Ph.D Dissertation, University of Sydney, **1999**.
- [33] P. Harriott, *J. Polym. Sci.* **1971**, *9*, 1153–1163.
- [34] J. Ugelstad, P. . Mork, J. . AAsen, *J. Polym. Sci. Part A Polym. Chem.* **1967**, *5*, 2281–2288.
- [35] N. De Rybel, P. H. M. Van Steenberge, M. F. Reyniers, D. R. D'hooge, G. B. Marin, *Macromolecules* **2019**, *52*, 4555–4569.
- [36] S. Harrisson, X. Liu, J. N. Ollagnier, O. Coutelier, J. D. Marty, M. Destarac, *Polymers.* **2014**, *6*, 1437–1488.
- [37] D. Britton, F. Heatley, P. A. Lovell, *Macromolecules* **1998**, *31*, 2828–2837.
- [38] "Wacker's product overview. Date of consultation: 12.05.2022," can be found under wacker.com, **2022**.
- [39] O. W. Smith, M. J. Collins, P. S. Martin, D. R. Bassett, *Prog. Org. Coatings* **1993**, *22*, 19–25.
- [40] "Vinyl neodecanoate technical datas sheet. Date of consultation: 09.08.22," can be found under www.hexion.com, **2022**.
- [41] M. J. Unzué, A. Urretabizkaia, J. M. Asua, *J. Appl. Polym. Sci.* **2000**, *78*, 475–485.
- [42] B. Schroeter, S. Bettermann, H. Semken, T. Melchin, H. P. Weitzel, W. Pauer, M. Chemistry, *Ind. Eng. Chem. Res.* **2019**, *58*, 12939–12952.
- [43] L. I. Jacob, W. Pauer, B. Schroeter, *RSC Adv.* **2022**, *12*, 14197–14208.
- [44] A. Agirre, H. P. Weitzel, W. D. Hergeth, J. M. Asua, *Chem. Eng. J.* **2015**, *266*, 34–47.
- [45] A. Agirre, I. Calvo, H. P. Weitzel, W. D. Hergeth, J. M. Asua, *Ind. Eng. Chem. Res.* **2014**, *53*, 9282–9295.
- [46] O. J. Deane, J. R. Lovett, O. M. Musa, A. Fernyhough, S. P. Armes, *Macromolecules* **2018**, *51*, 7756–7766.
- [47] S. J. Bohorquez, J. M. Asua, *J. Polym. Sci. Part A Polym. Chem.* **2008**, 6407–6415.
- [48] S. J. Bohórquez, J. M. Asua, *Macromolecules* **2008**, *41*, 8597–8602.
- [49] P. H. H. Araújo, J. C. De La Cal, J. M. Asua, J. C. Pinto, "Computer Aided Chemical Engineering: Modeling Particle Size Distribution (PSD)" in Emulsion Copolymerization Reactions in a Continuous Loop Reactor, Elsevier, **2000**.
- [50] B. M. Budhlall, E. D. Sudol, V. L. Dimonie, A. Klein, M. S. El-Aasser, *J. Polym. Sci. Part A Polym. Chem.* **2001**, *39*, 3633–3654.
- [51] E. Ogur, "Polyvinyl Alcohol: Materials, Processing and Applications", Smithers Rapra Technology, United Kingdom, **2005**.
- [52] F. L. Marten, in *Encycl. Polym. Sci. Technol. Vol. 8*, **2002**.
- [53] G. Mark, H. F.; Bikales, N. M.; Overberger, C. G.; Menges, *Vinyl Alcohol Polymers*, **1985**.
- [54] *WACKER Brochure. IHS Chem. Week Spec. Publ.* **2014**.
- [55] Y. Nagara, T. Nakano, Y. Okamoto, Y. Gotoh, M. Nagura, *Polymer (Guildf).* **2001**, *42*, 9679–9686.
- [56] G. Moad, C. Barner-Kowollik, "The Mechanism and Kinetics of the RAFT Process: Overview, Rates, Stabilities, Side Reactions, Product Spectrum and Outstanding Challenges" in Handbook of RAFT Polymerization, WILEY-VCH, **2008**.
- [57] T. J. Markley, Grafting Reactions of Vinyl Acetate onto Poly(Vinyl Alcohol-Co-Vinyl Acetate). Ph.D Dissertation, University of Lehigh, **1994**.

- [58] T. Moritani, Y. Fujiwara, *Macromolecules* **1976**, *10*, 532–535.
- [59] L.-I. Atanase, Contribution à l'étude Des Complexes Poly(Vinyle Alcool-Vinyle Acétate)/Tensioactifs Anioniques: Caractéristiques Colloïdales Des Nanogels et Extension Aux Copolymères à Blocs. Ph.D Dissertation, Université de Haute Alsace - Mulhouse, **2011**.
- [60] R. F. B. Davies, G. E. J. Reynolds, *J. Appl. Polym. Sci.* **1968**, *12*, 47–58.
- [61] T. Congdon, P. Shaw, M. I. Gibson, *Polym. Chem.* **2015**, *6*, 4749–4757.
- [62] C. Pichot, J. Guillot, A. Guyot, *J. Macromol. Sci. Part A - Chem.* **1974**, *8*, 1073–1086.
- [63] S. Aruldass, V. Mathivanan, A. R. Mohamed, C. T. Tye, *J. Environ. Chem. Eng.* **2019**, *7*.
- [64] M. Fabíni, S. Bobula, M. Rusina, V. Macho, M. Harustiak, *Polymer (Guildf)*. **1994**, *35*, 2201–2204.
- [65] *Cleanese Chemicals. Celvol Product Brochure. Polyvinyl Alcohol in Emulsion Polymerization*, **2004**.
- [66] WACKER, *Method for Producing Vinyl Ester Polymers Having Specifically Settable Dispersity and Low Polydispersity.*, **2013**, US 9,650,507.
- [67] M. Shiraishi, K. Toyoshima, *Br Polym J* **1973**, *5*, 419–432.
- [68] T. Moritani, Molecular Structures and Functional Modifications of Poly(Vinyl Alcohol). Ph.D. Dissertation, University of Tokyo, **1998**.
- [69] D. K. Marten, F. L.; Famili, A.; Mohanty, *U.S. Patent 4 772 663*, 1988. (*Air Products and Chemicals Inc.*), **1988**.
- [70] F. L. Marten, C. W. Zvanut, "*Poly(Vinyl Alcohol) Developments*", Finch, C.A; Ed Wjley, **1992**, 57-76.
- [71] D. Ha. P. Napper, "*Polymeric Stabilization of Colloidal Dispersions*", Academic Press Inc, San Diego, **1983**.
- [72] S. Carrà, L. Malcovati, A. Sliepcevich, G. Storti, S. Carrà, "*Stabilization Mechanisms in Vinyl Acetate Emulsion Polymerization Stabilized by Poly(Vinyl Alcohol)*" in *Polymer Colloids*, American Chemical Society, Washington DC, **2001**.
- [73] N. Kim, E. D. Sudol, V. L. Dimonie, M. S. El-Aasser, *Macromolecules* **2003**, *36*, 5573–5579.
- [74] F. D. Hartley, *J. Polym. Sci.* **1959**, *34*, 397–417.
- [75] C. M. Gilmore, G. W. Poehlein, F. J. Schork, *J. Appl. Polym. Sci.* **1993**, *48*, 1449–1460.
- [76] G. S. M. Gonzalez, V. L. . Dimonie, E. D. Sudol, H. J. Yue, A. Klein, M. S. El-Aasser, *J. Polym. Sci. Part A Polym. Chem.* **1996**, *34*, 849–862.
- [77] J. W. Vanderhoff, N. J. Earhart, V. L. Dimonie, S. M. El-Asser, *Makromol. Chem* **1990**, *35*, 477–497.
- [78] S. Okamura, T. Yamashita, T. Motoyama, *Kobunshi Kagaku* **1985**, *15*, 170.
- [79] G. G. D. S. Magallanes, Grafting Reactions in the Emulsion Polymerization of Vinyl Acetate Using Poly(Vinyl Alcohol) as Emulsifier. Ph.D Dissertation, Lehigh University, **1996**.
- [80] A. D. Jenkins, R. G. Jones, G. Moad, *Pure Appl. Chem.* **2010**, *82*, 483–491.
- [81] S. Perrier, *Macromolecules* **2017**, *50*, 7433–7447.
- [82] H. R. Lamontagne, B. H. Lessard, *ACS Appl. Polym. Mater.* **2020**, *2*, 5327–5344.
- [83] K. Matyjaszewski, *Macromolecules* **2012**, *45*, 4015–4039.
- [84] G. David, C. Boyer, J. Tonnar, B. Ameduri, P. Lacroix-Demazes, B. Boutevin\*, P. Lacroix-Desmazes, B. Boutevin, *Chem. Rev.* **2006**, *106*, 3936–3962.
- [85] J. Demarteau, A. Debuigne, C. Detrembleur, *Chem. Rev.* **2019**, *119*, 6906–6955.
- [86] S. Yamago, *J. Polym. Sci. Part A Polym. Chem.* **2006**, *44*, 1–12.



- [87] S. A. N. H. Thang, *"Fundamentals of RAFT Polymerization"*, RCS Publication, **2013**.
- [88] H. Fischer, *Chem. Rev.* **2001**, *101*, 3581–3610.
- [89] H. Arslan, *"Block and Graft Copolymerization by Controlled/Living Radical Polymerization Methods"* in IntechOpen, **2013**.
- [90] M. H. Stenzel, C. Barner-Kowollik, *Mater. Horizons* **2016**, *3*, 471–477.
- [91] M. C. Iovu, K. Matyjaszewski, *Macromolecules* **2003**, *36*, 9346–9354.
- [92] Y. Kwak, A. Goto, T. Fukuda, Y. Kobayashi, S. Yamago, *Macromolecules* **2006**, *39*, 4671–4679.
- [93] G. Moad, E. Rizzardo, S. H. Thang, *Polymer*. **2008**, *49*, 1079–1131.
- [94] B. Y. K. Chong, T. P. T. Le, G. Moad, E. Rizzardo, S. H. Thang, *Macromolecules* **1999**, *32*, 2071–2074.
- [95] P. Corpart, D. Charmot, T. Biadatti, S. . Zard, D. Michelet, *Method for Block Copolymer Synthesis by Controlled Radical Polymerization*, WO1998058974, **1998**.
- [96] S. Z. Zard, *Macromolecules* **2020**, *53*, 8144–8159.
- [97] D. J. Keddie, G. Moad, E. Rizzardo, S. H. Thang, *Macromolecules* **2012**, *45*, 5321–5342.
- [98] A. Favier, M. T. Charreyre, *Macromol. Rapid Commun.* **2006**, *27*, 653–692.
- [99] C. Bergerbit, RAFT Polymerization of Ethylene for the Synthesis of Polar-Apolar Olefin Block Copolymers. Ph.D Dissertation., Université Claude Bernard Lyon 1, **2019**.
- [100] M. Guerre, S. M. Wahidur Rahaman, B. Améduri, R. Poli, V. Ladmiral, *Polym. Chem.* **2016**, *7*, 6918–6933.
- [101] A. C. Rodriguez, Industrial Application of Supercritical Carbon Dioxide, PhD dissertation, Univeristé Claude Bernard Lyon 1, **2018**.
- [102] T. Okaya, *Polymer Having Thiol End Group*, **1984**, US4565854A.
- [103] E. Girard, X. Liu, J. D. Marty, M. Destarac, *Polym. Chem.* **2014**, *5*, 1013–1022.
- [104] A. A. A. Smith, T. Hussmann, J. Elich, A. Postma, M. H. Alves, A. N. Zelikin, *Polym. Chem.* **2012**, *3*, 85–88.
- [105] H. R. Hedayati, M. Khorasani, M. Ahmadi, N. Ballard, *Polymer*. **2022**, *246*, 124674.
- [106] Y. Geng, D. E. Discher, *Polycaprolactone Worm Micelles in Degradable Polymers and Materials*, in Degradable Polymers and Materials, ACS synopsis series, **2006**, 168–182.
- [107] R. C. Hayward, D. J. Pochan, *Macromolecules* **2010**, *43*, 3577–3584.
- [108] C. Booth, G. E. Yu, V. M. Nace, *"Block Copolymers of Ethylene Oxide and 1,2-Butylene Oxide"* in Amphiphilic Block Copolymers, Self-Assemblies and applications Elsevier, **2000**.
- [109] D. C. Tully, J. M. J. Fréchet, *Chem. Commun.* **2001**, *2*, 1229–1239.
- [110] Y. Y. Won, H. T. Davis, F. S. Bates, *Macromolecules* **2003**, *36*, 953–955.
- [111] H. Makino, T. Nishikawa, M. Ouchi, *Chem. Commun.* **2021**, *57*, 7410–7413.
- [112] M. H. Repollet-Pedrosa, R. L. Weber, A. L. Schmitt, M. K. Mahanthappa, *Macromolecules* **2010**, *43*, 7900–7902.
- [113] F. W. Speetjens, M. K. Mahanthappa, *Macromolecules* **2015**, *48*, 5412–5422.
- [114] M. Uchiyama, K. Satoh, M. Kamigaito, *Giant* **2021**, *5*, 100047.
- [115] Y.-Y. Tong, Rui Wang, N. Xu, F.-S. Du, Z.-C. Li, *J. Polym. Sci. Part A. Polym. Chem.* **2009**, *47*, 4494–4504.
- [116] J. Muller, F. Marchandeanu, B. Prelot, J. Zajac, J. J. Robin, S. Monge, *Polym. Chem.* **2015**, *6*, 3063–3073.
- [117] J. Bernard, A. Favier, T. P. Davis, C. Barner-Kowollik, M. H. Stenzel, *Polymer*. **2006**, *47*,

1073–1080.

- [118] J. Bernard, A. Favier, L. Zhang, A. Nilasaroya, T. P. Davis, C. Barner-Kowollik, M. H. Stenzel, *Macromolecules* **2005**, *38*, 5475–5484.
- [119] M. H. Stenzel, T. P. Davis, C. Barner-Kowollik, *Chem. Commun.* **2004**, *4*, 1546–1547.

---

# Chapter II

Synthesis of well-defined P(VOH-*s*-VAc) by  
alcoholysis of RAFT/MADIX synthesized  
poly(vinyl acetate).

Evaluation as stabilizers for the emulsion  
copolymerization of VAc and VeoVa

---

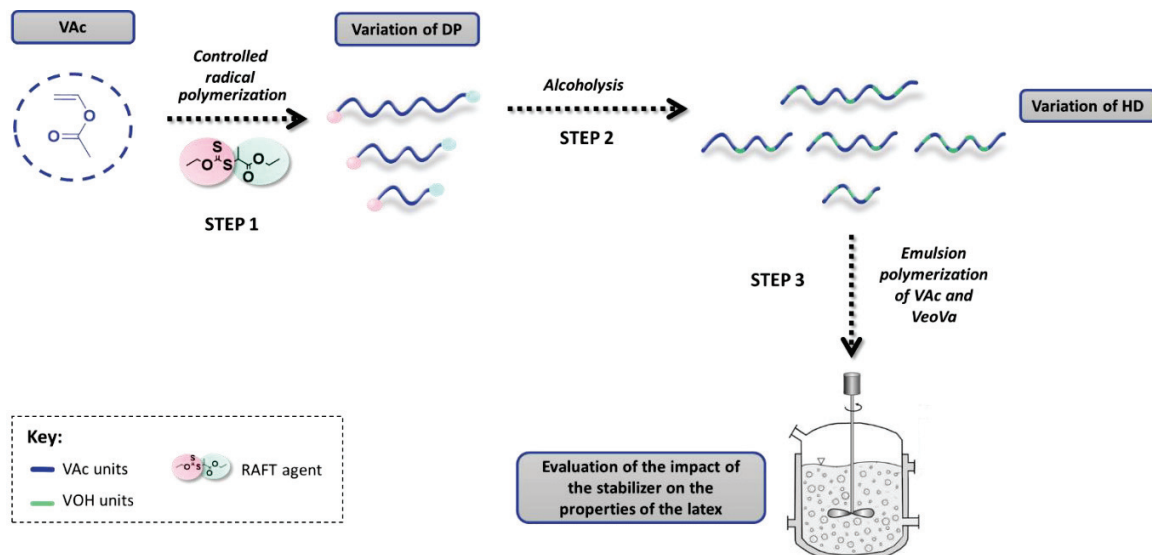




## Table of content

I. INTRODUCTION.....	92
II. RAFT/MADIX POLYMERIZATION OF VAC.....	93
III. ALCOHOLYSIS OF THE WELL-DEFINED PVAc.....	102
III.1 General introduction on the alcoholysis of PVAc and the associated method of characterization.....	102
III.2 Alcoholysis of the library of PVAc obtained by RAFT/MADIX polymerization.....	109
III.2.1 Set up of the alcoholysis parameters.....	109
III.2.2 In-depth characterization of the P(VOH-s-VAc).....	112
III.2.3 Reproducibility testing of the alcoholysis of 75_PVAc on different batches.....	112
III.3 Influence of the DP of the PVAc on the kinetics of alcoholysis.....	113
III.4 Study of the microstructure of the well-defined P(VOH-s-VAc) by NMR, and chain-end analysis.....	115
IV. (SELF-)ORGANIZATION IN WATER.....	118
IV.1 Organization in water.....	119
IV.2 Surface tension.....	124
IV.3 Conclusion on the (self-)organization of P(VOH-s-VAc) in water.....	126
V. EMULSION COPOLYMERIZATION OF VAc AND VEOVA STABILIZED WITH MOWIOL 4-88 AND THE RAFT/MADIX-SYNTHESIZED P(VOH-s-VAc).....	127
V.1 Set up of the experimental parameters for the emulsion copolymerization of VAc and VeoVa.....	130
V.2 Influence of the hydrolysis degree at fixed DP = 75 and fixed amount of stabilizer (10 wt.% based on monomers).....	134
V.3 Influence of the polymerization degree at fixed HD = 88% and fixed amount of stabilizer (10 wt.% based on monomers).....	135
V.3.1 Kinetics of the polymerizations and colloidal features.....	136
V.3.2 Adsorbed and grafted stabilizer.....	142
V.3.3 Evaluation of alkali resistance of the latex stored at high pH.....	144
V.4 Influence of the amount of stabilizer at fixed DP = 75 and HD = 88%.....	146
V.4.1 Colloidal features of the latex.....	146
V.4.2 Adsorbed and grafted stabilizer.....	148
VI. CONCLUSION.....	149

## I. Introduction

It is now well established that the composition and architecture of partially alcoholized poly(vinyl acetate) PVAc (*i.e.*, molar mass, average PVAc and PVOH sequence length and the distribution of these sequences along the chain ( $\beta$ ), 1,2-glycol and carbonyl content, and the presence of hydrolysable and non-hydrolysable branches) determine its properties as a stabilizer. All of these characteristics are difficult to control in the synthesis of commercial P(VOH-*s*-VAc), and therefore ostensibly similar grades provided by the same producer may behave differently in emulsion polymerization.

This chapter is dedicated to the synthesis of a library of well-defined P(VOH-*s*-VAc) copolymers with different degrees of polymerization (DP) and degrees of hydrolysis (HD). The aim is to evaluate the ability of such copolymers to stabilize a latex and compare the stabilization efficiency to a referent commercial P(VOH-*s*-VAc) named Mowiol 4-88 (Kuraray). This chapter will also serve as a basis to define a standard reference and be able to assess the performances of the new structures which will be developed later, and which will incorporate more hydrophobic units (VL and VeoVa).

In a first step, analogous polymers to the commercial P(VOH-*s*-VAc) were obtained after alcoholysis of PVAc synthesized by RAFT. In a second step, the conditions for the alcoholysis of these PVAc were optimized to obtain P(VOH-*s*-VAc) with different hydrolysis degrees in a reasonable amount of time. Finally, these polymers were evaluated as stabilizer candidates in the emulsion copolymerization of VAc and VeoVa. The resulting latexes were analyzed in terms of stability, particle size and particle size distribution (PSD), and the amount of adsorbed and grafted stabilizer was determined. The latexes prepared in the presence of well-defined P(VOH-*s*-VAc)s were compared to a latex obtained with Mowiol 4-88.

## II. RAFT/MADIX polymerization of VAc

As mentioned in **Chapter I**, RDRP of VAc is rather difficult to achieve due to the poor stability of the corresponding propagating radical. Nevertheless, RAFT polymerization based on xanthates and dithiocarbamates have been reported to give the most successful results.<sup>[1],[2]</sup> The first report of RAFT polymerization of VAc using xanthates was patented in 1998.<sup>[3]</sup> Shortly after, in 2000, the use of dithiocarbamates was published by Rizzardo *et al.*<sup>[4]</sup> and simultaneously by Destarac *et al.*<sup>[5]</sup> Since then, the literature flourished with numerous examples of RAFT polymerization of VAc, using different RAFT/MADIX agents and polymerization conditions.<sup>[6-14]</sup> However, as mentioned in **Chapter I, Section IV.2.3**, the preparation of well-defined PVAc with a low dispersity ( $\mathcal{D}$ ) and high chain-end fidelity remains difficult, because of head-to-head additions, occurring when a  $-\text{CH}(\text{OAc})^\bullet$  (head) radical adds onto the head of a VAc monomer and forms a  $-\text{CH}_2-\text{CH}(\text{OAc})-\text{CH}(\text{OAc})-\text{CH}_2^\bullet$  radical. At some point, the formation of this  $-\text{CH}_2^\bullet$  radical will immediately be followed by a xanthate exchange reaction and thus be terminated by a  $-\text{CH}(\text{OAc})\text{CH}_2\text{-X}$  group (noted  $\text{PVAc}_\text{T}\text{-X}$  for brevity, where X is the xanthate (**Figure II-1 (a)**). These chains are very likely to be reactivated much more slowly than their regularly terminated analogues  $-\text{CH}_2\text{CH}(\text{OAc})\text{-X}$  (noted  $\text{PVAc}_\text{H}\text{-X}$ , **Figure II-1 (b)**), because of the poor stability provided by the primary carbon. This renders the chains less reactivatable by affecting their ability to fragment.

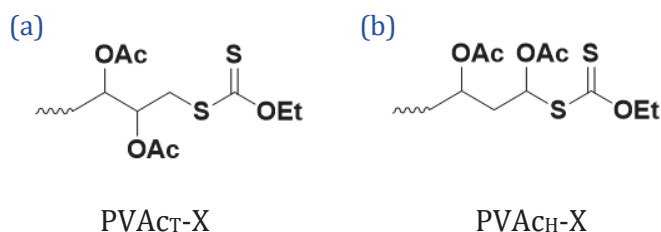


**Figure II-1: Dormant chains resulting from (a) head-to-head and (b) head-to-tail propagation of VAc followed by addition to a xanthate during RAFT/MADIX polymerization.**

The accumulation of these less reactive end-groups was shown to slow down the degenerative chain transfer process. As a consequence, molar mass distributions are significantly broadened and chain-end functionality ( $\Psi$ ) is negatively affected.<sup>[15-17]</sup>  $\Psi$  is defined as the fraction of re-activatable polymer chains functionalized by a xanthate (*i.e.*,  $\text{PVAc}_\text{H}\text{-X}$ ). Guerre *et al.*<sup>[16]</sup> synthesized three different PVAc-X with DP = 18, 96 and 115, using ethyl-*S*-(1-methoxycarbonyl)ethyl dithiocarbonate (most well-known as Rhodixan A1) as CTA and azobisisobutyronitrile (AIBN) with a ratio [CTA]:[AIBN] = 5. The polymerizations were performed for 14 h at 60 °C in bulk and nonafluoro-*tert*-butyl alcohol. The authors then performed <sup>1</sup>H NMR end-group analysis (based on attributions similar to the ones shown in

**Figure II-3** for one of our PVAc polymer) to calculate the proportions of the different types of PVAc chains (PVAc<sub>H</sub>-X, PVAc<sub>T</sub>-X and dead chains, shortened PVAc<sub>H</sub>-H). They found that when performed in bulk, the polymerization yielded a higher proportion of PVAc<sub>T</sub>-X for high DP (28 mol.% for DP = 18 and 90 mol.% for DP = 115). At fixed DP = 115, they obtained 67 mol.% of PVAc<sub>T</sub>-X in nonafluoro-*tert*-butyl alcohol, which highlighted the influence of the solvent in the occurrence of the reverse addition of the VAc units. In any case, they obtained approximately 10 mol.% of PVAc<sub>H</sub>-H. Similar results were obtained by Koumura *et al.*<sup>[18]</sup> for the ITP of VAc performed in different fluoroalcohols.<sup>[18]</sup> The authors showed that among the fluoroalcohols, the use of fluorodiol improved the control over the molar mass, resulting in narrow molar mass distribution. Finally, Levere *et al.*<sup>[14]</sup> demonstrated that performing MADIX polymerization of vinyl acetate in ethyl acetate (EtAc) produced polymers with near-complete monomer conversion, high molar masses and control of molar masses and distributions (from 7 900 g mol<sup>-1</sup> to 250 000 g mol<sup>-1</sup> with *D* varying from 1.4 to 1.8). The polymerizations were carried out at 70 °C with *S*-benzyl-*O*-ethyl dithiocarbonate and AIBN, with a ratio [CTA]:[AIBN] = 5. The authors also provided evidence of acceptable chain-end functionality by successful extension of their macroCTA PVAc-X with additional VAc. Another advantage of ethyl acetate is that it is considered as an environmentally friendly solvent. In spite of the difficulties resulting from head-to-head additions, RAFT/MADIX polymerization proved the most robust RDRP technique to synthesize well-defined PVAc.<sup>[19]</sup>

In the present work, the controlled polymerization of VAc was attempted using *O*-ethyl-*S*-(1-ethoxycarbonyl)ethyl dithiocarbonate (CTA) RAFT/MADIX agent, which is derived from the commercially available Rhodixan A1. The polymerizations were carried out in EtAc at 60 °C for 6 to 24 h with [CTA]:[AIBN] = 5. Depending on the DP, the final product was recovered as an amorphous polymer (DP = 20) or as a powder (40 ≤ DP ≤ 200) after purification. The general synthesis route is described in **Figure II-2**, and the detailed protocol is described in the **Experimental Section .III.1**.

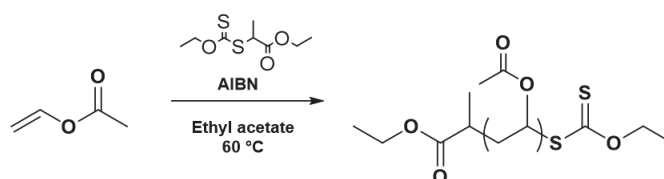


**Figure II-2: General reaction scheme for the synthesis of PVAc-X in EtAc at 60 °C.**

Several DP from 20 to 200 were targeted. For clarity's sake, the polymers with different DP will be referred to as DP\_PVAc, with DP the average polymerization degree of the polymer.

As mentioned above, the paper from Guerre *et al.*<sup>[16]</sup> provided the attribution of the <sup>1</sup>H NMR signals to the structure of PVAc, and a detailed analysis of the chain-ends of a PVAc-X macroCTA prepared by RAFT/MADIX polymerization. An example of <sup>1</sup>H NMR spectrum of 75\_PVAc synthesized by RAFT/MADIX and with the attributions based on Guerre's work is provided in **Figure II-3**. The identification of the chain-ends of the RAFT/MADIX agent (signals *f* and *g*, **Figure II-3**) also makes it possible to determine a degree of polymerization (obtained from the integration of the peak *h* from 4.7 to 5.3 ppm), and therefore the number-average molar mass by NMR (**Equation 6**). However, this requires assuming that all the polymer chains were initiated by the RAFT/MADIX agent, thus neglecting the chains resulting from the initiator as well as the termination reactions.

$$M_n(\text{NMR}) = \text{DP} \cdot M_{\text{VAc}} + M_{\text{RAFT}} \quad (6)$$

With  $M_{\text{VAc}}$  and  $M_{\text{RAFT}}$  the molar masses of VAc (86.09 g mol<sup>-1</sup>) and of the RAFT/MADIX agent (222 g mol<sup>-1</sup>), respectively.

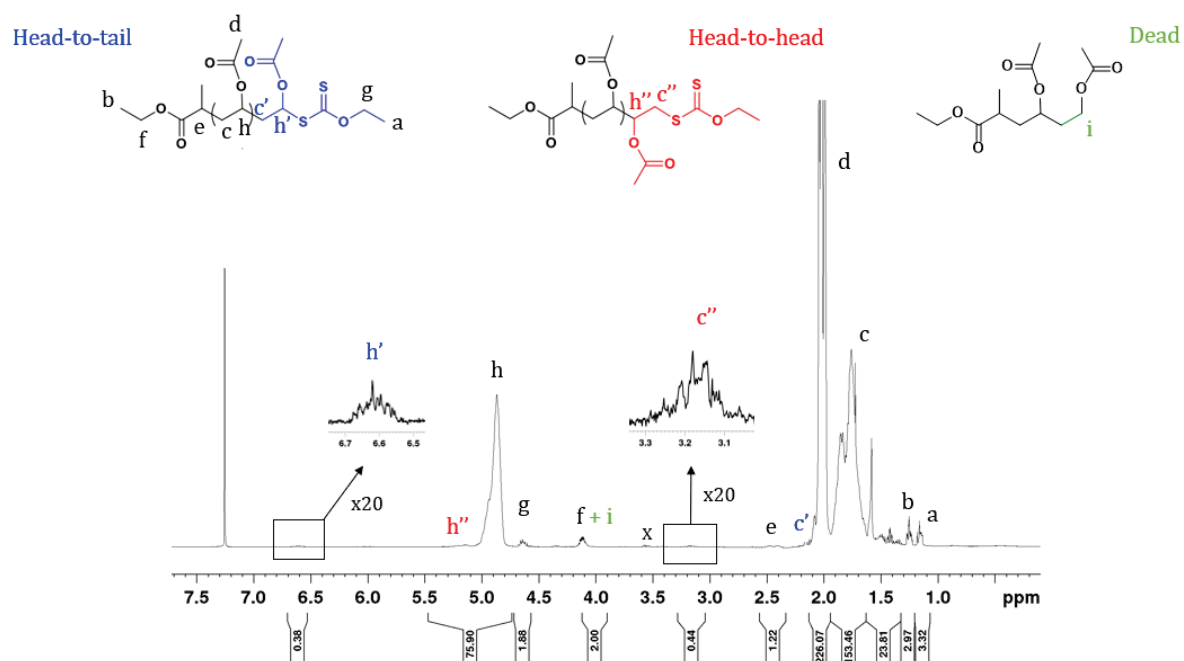


**Figure II-3:** <sup>1</sup>H NMR spectrum of purified 75\_PVAc in CDCl<sub>3</sub>, 256 scans at R.T. (25 °C).

The kinetics of the polymerizations (DP = 20, 75, 100 and 200) were followed by <sup>1</sup>H NMR. This was achieved by integrating the signals of the residual monomer CH protons (4.5 – 4.6 ppm) against the polymer backbone CH protons (4.7 – 5.4 ppm) (see **Appendix 2**, for the

detailed calculation). The theoretical number-average molar mass ( $M_{n(\text{theo.})}$ ) was calculated using **Equation 7**.<sup>[20]</sup>

$$M_{n(\text{theo.})} = \frac{[M] \cdot M_{\text{mon}} \cdot c}{[\text{CTA}]} + M_{\text{CTA}} \quad (7)$$

Where  $[M]$  is initial concentration of monomer,  $[\text{CTA}]$  is the initial concentration of RAFT/MADIX agent,  $M_{\text{mon}}$  is the molar mass of the monomer,  $c$  is the fractional conversion and  $M_{\text{CTA}}$  is the molar mass of the RAFT agent.

**Table II-1** provides a summary of the characteristics of the different synthesized PVAc polymers.

**Table II-1: Summary of the characteristics of the PVAc obtained by xanthate mediated RAFT/MADIX polymerization in EtAc at 60 °C for 6 to 24 h.**

Designation	Polymerization Time (h)	VAc conv. (%) <sup>a</sup>	$M_n$ (theo.) (g mol <sup>-1</sup> ) <sup>b</sup>	$M_n$ (NMR) (g mol <sup>-1</sup> ) <sup>c</sup>	$M_n$ (SEC) (g mol <sup>-1</sup> ) <sup>d</sup>	Dispersity ( $\bar{D}$ ) <sup>d</sup>
20_PVAc	6	94	2240	2180	2130	1.17
40_PVAc	6	90	4100	3750	3500	1.20
60_PVAc	6	90	6190	5500	5800	1.35
75_PVAc	6	80	6030	5600	6300	1.30
100_PVAc	7	88	9740	9600	9400	1.50
200_PVAc	24	86	15 980	16 800	15 100	1.50

<sup>a</sup> Conversion based on <sup>1</sup>H NMR calculations by comparing monomer and polymer resonances

<sup>b</sup> Theoretical molar mass of the polymer calculated from conversion

<sup>c</sup> Experimental molar mass of the polymers calculated from end group analysis by <sup>1</sup>H NMR comparing polymer chain-end and main chain resonances

<sup>d</sup> Experimental molar mass of the polymers calculated by SEC-THF using universal calibration

An example of <sup>1</sup>H NMR spectrum obtained after purification of the 75\_PVAc is shown in **Figure II-3**. The attribution of the signals of the purified polymer, and the calculations for the determination of the DP are also described. High conversions of VAc (from 80 to 94%) were achieved in an acceptable amount of time (from 6 to 7 h) for 20 ≤ DP ≤ 100 (**Table II-1**). It took however 24 h to reach 86% conversion for 200\_PVAc.

For every system, the conversion was plotted as a function of reaction time (**Figure II-4 (a)**). An induction period of 1 h was observed regardless of the targeted DP. This interval corresponds to the period during which the RAFT/MADIX agent is consumed.<sup>[21],[22],[23]</sup> **Figure II-4 (b)** shows indeed that the intensity of signal *b* (4.4 ppm) characteristic of the methine proton from the RAFT agent decreases from 0 to 60 min, and is shifted at 2.4 ppm after 60 min, corresponding to the methine proton *b'* of the macroCTA after addition of a growing macroradical.

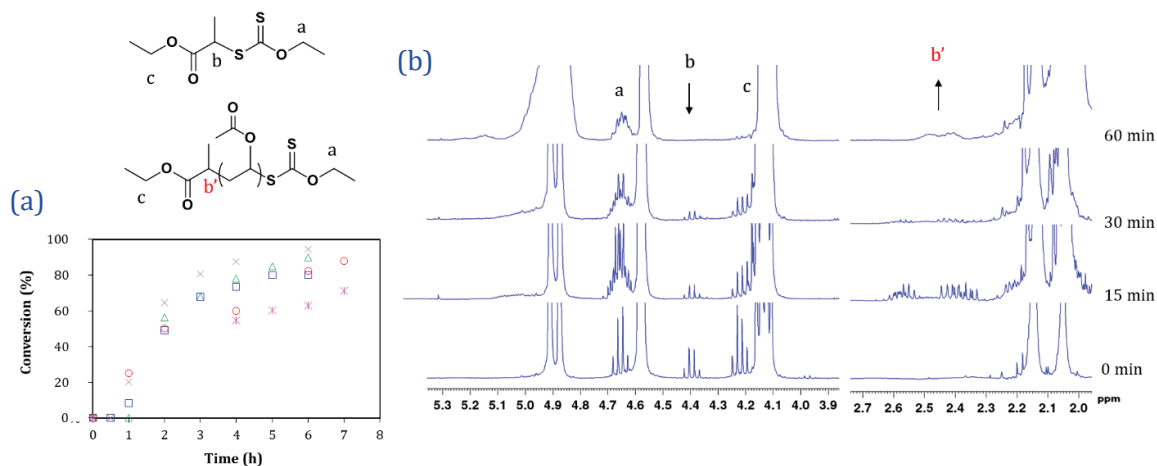


**Figure II-4:** (a) Evolution of conversion *versus* time for 20\_PVAc (×), 40\_PVAc (Δ), 75\_PVAc (□), 100\_PVAc (○) and 200\_PVAc (\*), and (b) <sup>1</sup>H NMR spectra of 75\_PVAc obtained during the polymerization in the presence of *O*-ethyl-*S*-(1-ethoxycarbonyl)ethyl dithiocarbonate.

Size exclusion chromatography (SEC) was used to measure the number-average molar mass ( $M_n$ ) and dispersity ( $\mathcal{D}$ ) of the polymers. In addition, as mentioned above, <sup>1</sup>H NMR spectroscopy was also used to measure the  $M_n$  of the polymers by integrating appropriate protons from the chain-end and the polymer backbone.

For  $20 \leq \text{DPs} \leq 75$ , the chromatograms were both narrow and mostly symmetrical (**Figure II-5**). The corresponding dispersity ( $\mathcal{D}$ ) of the resulting polymers remained almost constant at around 1.2 up to 65 - 70% monomer conversion and then increased gradually with further increase of monomer conversion (up to 1.3 for PVAc with DP = 75). Nevertheless, the experimental  $M_n$  values were closed to the theoretical ones (**Table II-1**) and the linear evolution of the molar masses with conversion attested a good control of the polymerizations (**Figure II-6, (a) and (b)**).



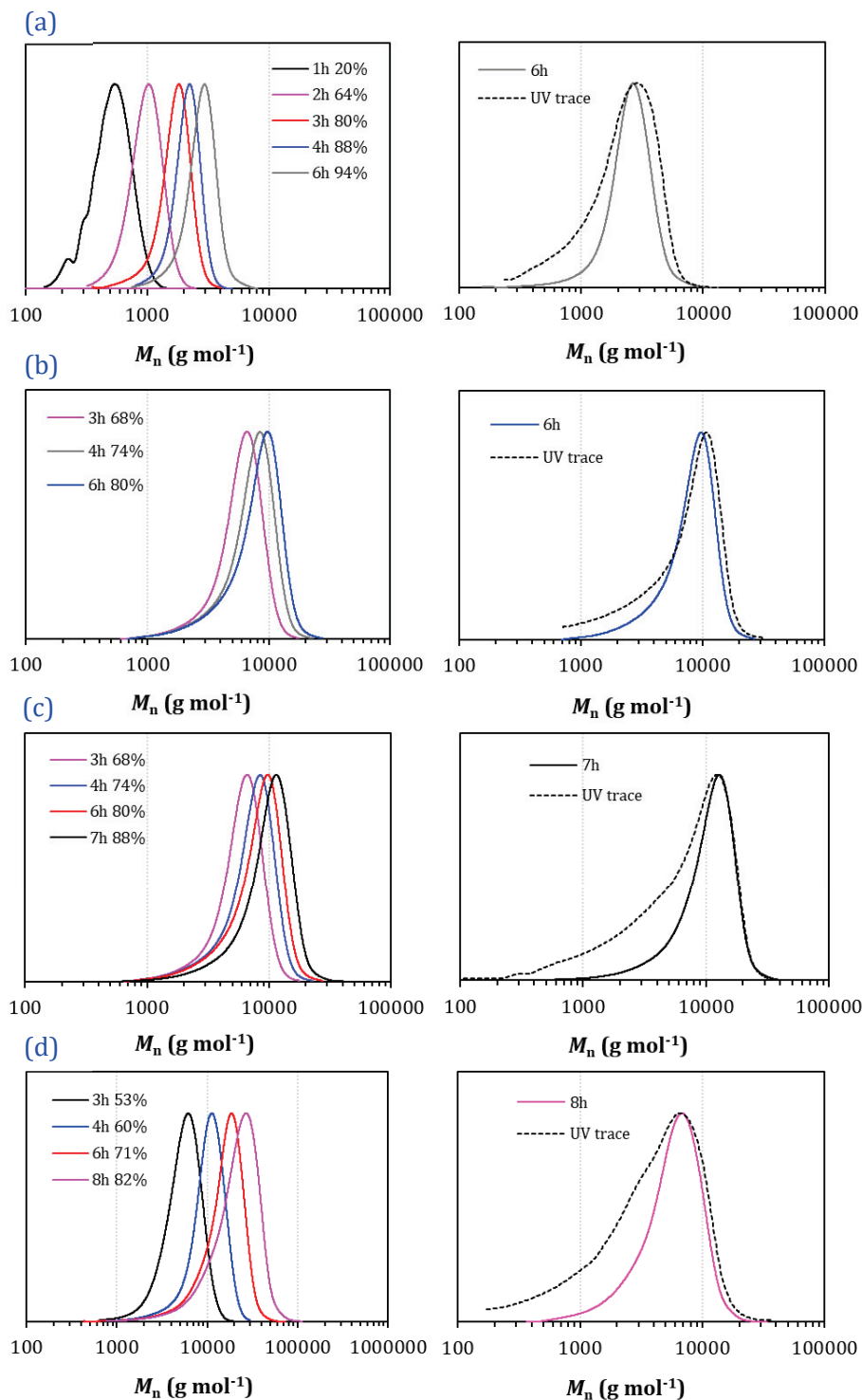


**Figure II-5: Normalized SEC-THF traces of the molar mass evolutions during RAFT/MADIX polymerizations of VAc for (a) DP = 20; (b) DP = 75; (c) DP = 100 and (d) DP = 200. Full lines correspond to the normalized RI trace. Dashed lines correspond to the normalized UV trace at 280 nm.**



However, when the DP increased further from 100 to 200, keeping the other conditions unchanged,  $\bar{D}$  tended to increase up to 1.5, and deviations of the experimental  $M_n$  from the theoretical ones were highlighted (Table II-1 entries 100\_PVAc and 200\_PVAc, and Figure II-6 (c) and (d)). Figure II-5 indeed shows that for high DP, the molar mass distribution became broader with conversion. These results compare well with the previously mentioned literature findings.<sup>[16]</sup>

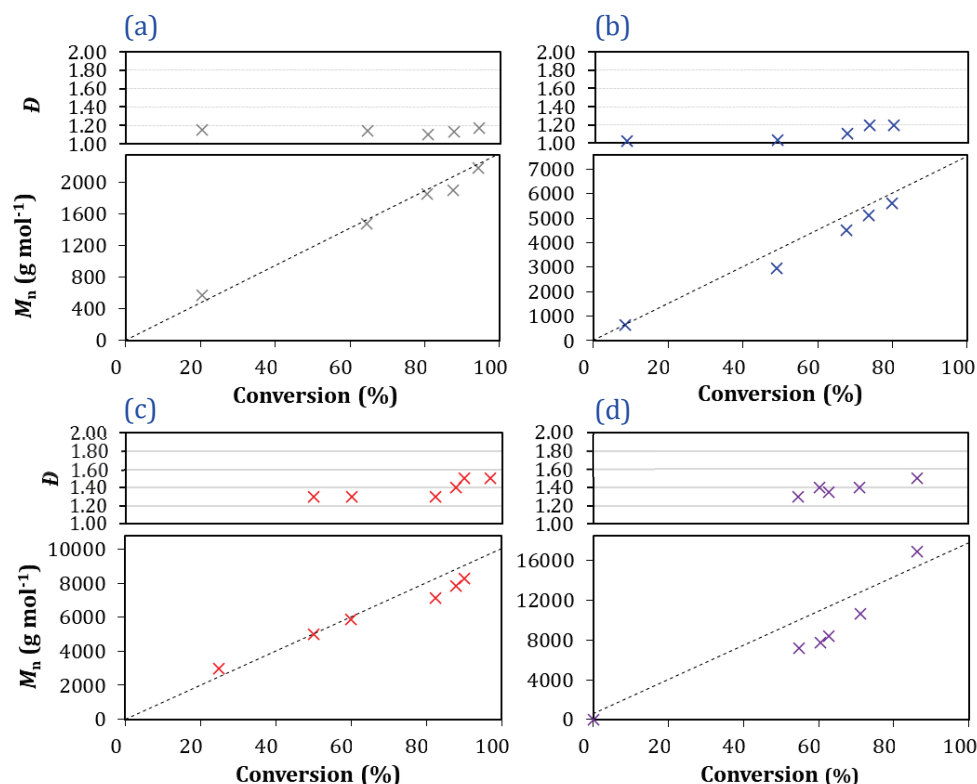


Figure II-6: Evolution of the molar masses (obtained by NMR) and dispersities (obtained by SEC) with the conversion of VAc, for (a) DP = 20; (b) DP = 75; (c) DP = 100 and (d) DP = 200. The polymerizations were performed at 60 °C in EtAc.  $\bar{D}$  was obtained by SEC-THF.

The UV/vis spectrum of the RAFT agent showed that the C=S bond absorbs at 280 nm (Experimental Section VI.3). For all the PVAc obtained, the UV trace of the SEC at 280 nm overlapped with the RI trace, and also highlighted the aforementioned broadening, which attested to the presence of the dithiocarbonate moiety in the unextended chains. These chains were attributed to the aforementioned PVAc<sub>T-X</sub>.

### Chain-end functionality

The  $^1\text{H}$  NMR spectra of every purified PVAc attested to the presence of the two fragments of the controlling agent on either side of the polymer chain, *via* the appearance of the resonances of the *e*, *f*, and *g* protons at 2.45, 4.1, and 4.6 ppm (an example for 75\_PVAc was provided in **Figure II-3**). These resonances correspond respectively to the protons of the methyl in  $\alpha$  and to the methylene belonging to the R group, and to the protons of the methylene in  $\alpha$  of the Z group of the original xanthate. These chains are normally terminated by a head-to-tail inserted VAc unit connected to the xanthate moiety (PVAc<sub>H-X</sub>) (**Figure II-3**, blue). Head-to-head inserted VAc units connected to xanthate moiety (PVAc<sub>T-X</sub>) (**Figure II-3**, red) are very likely to be reactivated much more slowly than their regularly head-to-tail terminated analogues. These chains thus tend to accumulate in the reaction medium as the RAFT/MADIX polymerization proceeds, which can explain the visible broadening in the molar mass distribution.

Assuming that only these three chain-end conformations are present in final polymer,  $\Psi$  is calculated by dividing the integral value of the terminal head-to-tail -CH- on the final unit (PVAc<sub>H-X</sub>, **Figure II-3**, *h'*,  $\delta = 6.5 - 6.7$  ppm) by the sum of the integrals *h'*, *c''* and *i* (**Equation 8**). The signal of PVAc<sub>H-H</sub> (integral *i*, **Figure II-3**) overlaps with the signal of the methine protons of the xanthate moiety (signal *f*, **Figure II-3**), so it is necessary to subtract the integral *g* (corresponding to the methine protons of the other xanthate moiety), to isolate the real value of integral *i*.

$$\Psi = \frac{\int_{6.50}^{6.70} [\text{CH}]_{h'} \text{d}\delta}{\int_{6.50}^{6.70} [\text{CH}]_{h'} \text{d}\delta + \int_{3.18}^{3.51} \frac{[\text{CH}_2]_{c''}}{2} \text{d}\delta + \int_{3.95}^{4.13} \frac{[\text{CH}_2]_{f+i}}{2} \text{d}\delta - \int_{4.51}^{4.52} \frac{[\text{CH}_2]_g}{2} \text{d}\delta} \quad (8)$$

**Figure II-7** provides an estimation of  $\Psi$  for the different DP of the synthesized PVAc.

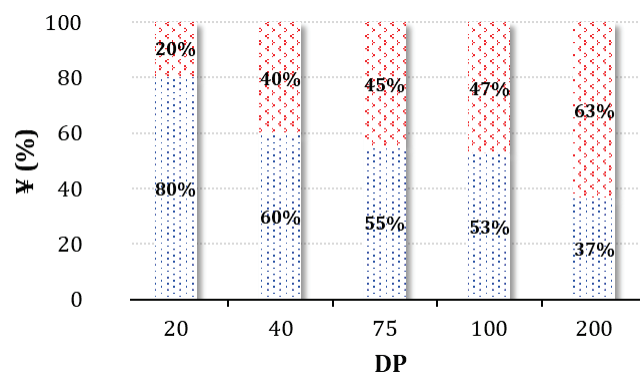


**Figure II-7:** Chain-end functionality ( $\Psi$ ) of the synthesized PVAc depending on their DP with in **blue** the molar fraction of head-to-tail (PVAc<sub>H</sub>-X) and in **red** the molar fraction of head-to-head (PVAc<sub>T</sub>-X) terminated structures and dead chains (PVAc<sub>H</sub>-H).

According to **Figure II-7**, the higher the DP, the lower the chain-end functionality of the PVAc, which is consistent with an accumulation of PVAc<sub>T</sub>-X chains with conversion. This result aligns with Guerre and Koumura's observation, highlighted at the beginning of this Section.

After synthesis and in-depth characterizations of the above-mentioned range of well-defined PVAc, the second step is now to alcoholize these polymers to turn them into a range of well-defined P(VAc-*s*-VOH) copolymers.

### III. Alcoholysis of the well-defined PVAc

#### III.1 General introduction on the alcoholysis of PVAc and the associated method of characterization

The alcoholysis (or more abusively referred to as hydrolysis in the literature) reaction to turn PVAc into P(VOH-*s*-VAc) was first introduced by Herrman and Haehnel in 1924.<sup>[24]</sup> As mentioned in **Chapter I**, several ways of preparing P(VOH-*s*-VAc) from PVAc exist, and each one of these will lead to a unique type of structure in terms of tacticity, distribution of the acetate and hydroxyl groups along the chain, structural irregularities and DP.<sup>[25-29]</sup> Additionally, Dawkins *et al.*<sup>[30]</sup> highlighted the existence of a distribution of the HD in commercial P(VOH-*s*-VAc)s samples *via* high-performance liquid chromatography. For instance, a P(VOH-*s*-VAc) with HD = 72.5 mol.% was found to have chains with HD ranging from 65 to 85 mol.%.

Among the different structures, P(VOH-*s*-VAc) with a blocky-like structure can be obtained by alcoholysis. When employed as stabilizer in emulsion polymerization, this blocky structure is considered to produce more stable latexes than those featuring a random distribution of acetyl groups. The most common way to obtain this “blocky” structure is by alkali catalysis with sodium hydroxide (NaOH) or potassium hydroxide (KOH) in methanol. The cause of this blockier distribution has been explained by the fact that the rate of hydrolysis is higher for the acetyl groups neighboring a hydroxyl group. Therefore, the hydrolysis reaction proceeds along the chain like the opening of a zipper.<sup>[31]</sup>

As mentioned in **Chapter I, Section III.1** several grades of P(VOH-*s*-VAc) exist depending on their hydrolysis degree and viscosity (related to their molar mass):

- Fully hydrolyzed PVAc (PVOH): HD higher than 97%,
- Moderately hydrolyzed PVAc (P(VOH-*s*-VAc): HD from 90 to 96%,
- Partially hydrolyzed PVAc (P(VOH-*s*-VAc)): HD from 84 to 89%,

Experimentally, it has been proved that partially hydrolyzed PVAc provided optimal stabilization.<sup>[32]</sup> For such grades, VAc and VOH signals are visible on <sup>1</sup>H and <sup>13</sup>C NMR spectra. This makes it possible to determine the HD and the distribution of the PVAc and PVOH sequences by analysis of the relative intensities of the -CH, -CH<sub>2</sub> and -CH<sub>3</sub> groups of P(VOH-*s*-VAc).<sup>[33],[29]</sup> Moritani and Fujiwara were the first to report the combination of <sup>1</sup>H and <sup>13</sup>C NMR to study the composition of P(VOH-*s*-VAc).<sup>[33]</sup>

As an illustration, **Figure II-8** shows an example of the <sup>1</sup>H NMR spectrum of the polymer obtained after alcoholysis of our 75\_PVAc. The assignments of the main signals were based

on Moritani and Fujiwara's work, with regard to the diads,<sup>[33]</sup> and according to Velden and Beulen's work, with regard to the triads.<sup>[34]</sup> The attribution of the tacticity was based on Uchiyama's work.<sup>[35]</sup> Triads can also be observed in <sup>13</sup>C NMR or HSQC (**Figure II-9**).

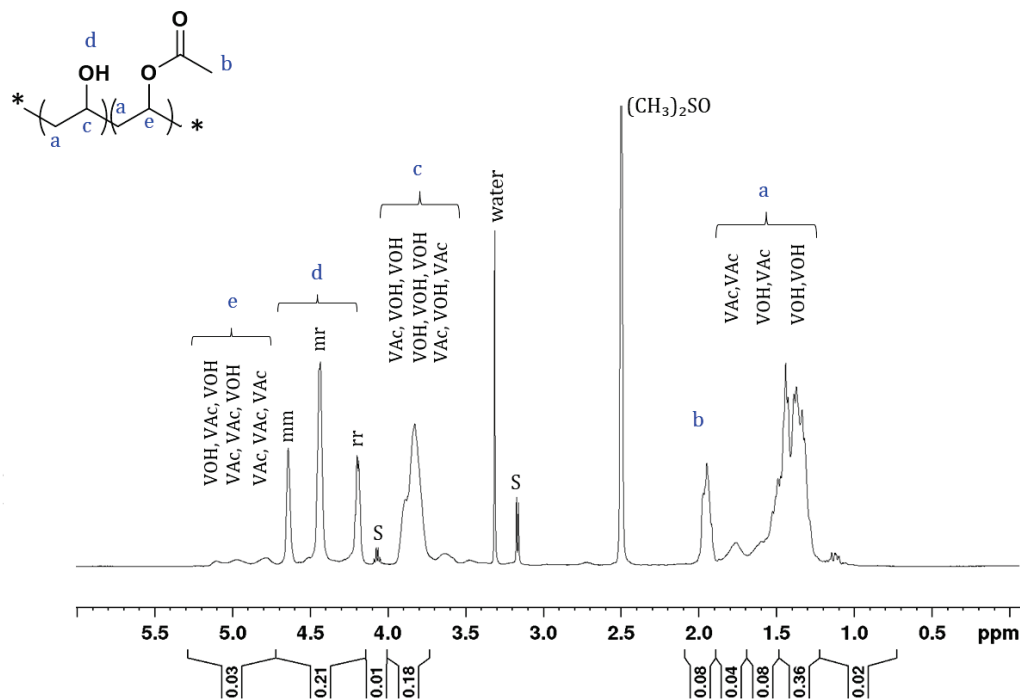


**Figure II-8:** <sup>1</sup>H NMR spectrum of partially hydrolyzed 75\_P(VOH-*s*-VAc) (HD = 88%) in DMSO-*d*<sub>6</sub> at R.T., 256 scans, with attribution of the diads and triads. mm, mr and rr correspond to triads tacticity of VOH units. S corresponds to signals of residual methanol.

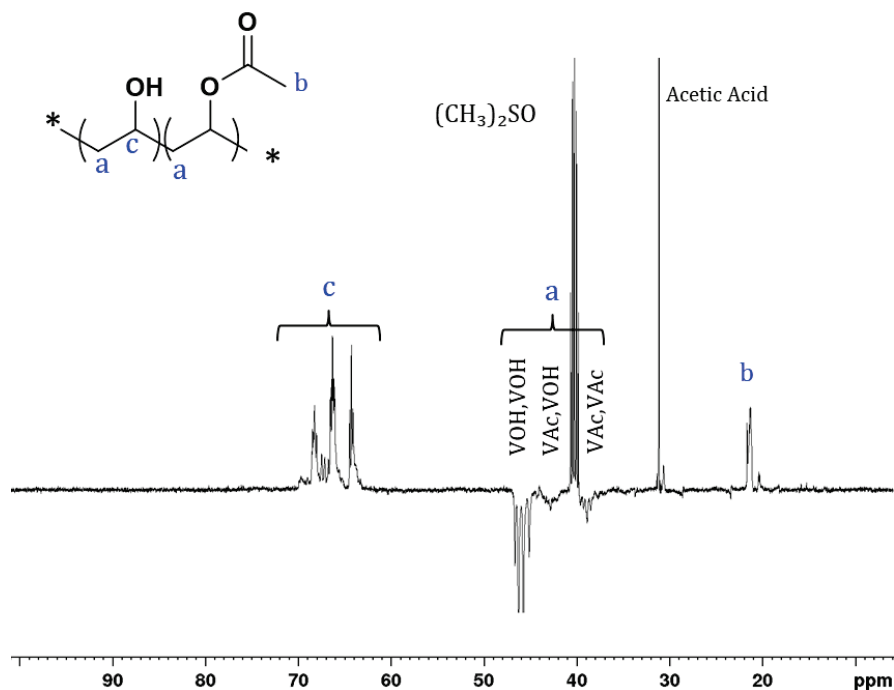


Figure II-9: DEPT 135 spectrum of partially hydrolyzed 75\_PVAc: 75\_P(VOH-s-VAc) (HD = 88%) in DMSO-d<sub>6</sub> at R.T., 6 K scans.

According to Bugada and Rudin,<sup>[36]</sup> the characteristics of P(VOH-s-VAc), namely the HD, the average length of PVAc and PVOH sequences ( $n_0^{\text{VAc}}$  and  $n_0^{\text{VOH}}$  respectively), as well as the “blockiness index” ( $\beta$ ), can be calculated using different diads in the spectral range of <sup>1</sup>H NMR spectrum between 1.4 -1.8 ppm.

The molar composition in alcohol units ( $F_{\text{VOH}}$ ), which also corresponds to HD are given according to **Equation 9**.

**From <sup>1</sup>H NMR:**

$$F_{\text{VOH}} = \text{HD} = 100 \times \frac{\int_{3.7}^{3.9} [\text{CH}]_c}{\int_{3.7}^{3.9} [\text{CH}]_c + \int_{1.85}^{2.0} \frac{[\text{CH}_3]_b}{3}} \quad (9)$$

Where the  $\int_{3.7}^{3.9} [\text{CH}]_c$  integral corresponds to the methine protons of the VOH units, and the  $\int_{1.85}^{2.0} \frac{[\text{CH}_3]_b}{3}$  integral corresponds to the methyl protons of the VAc units (signals *c* and *b* respectively, **Figure II-8**).

Another way to calculate the composition of the copolymer is by considering the signals which belong to the diads:

**Both from  $^{13}\text{C}$  and  $^1\text{H}$  NMR:**

$$F_{\text{VOH}} = \text{HD} = 100 \times \frac{\int [\text{CH}]_{(\text{VOH,VOH})} + \frac{1}{2} \times \int [\text{CH}]_{(\text{VOH,VAc})}}{\int [\text{CH}]_{(\text{VOH,VAc})} + \int [\text{CH}]_{(\text{VOH,VOH})} + \int [\text{CH}]_{(\text{VAc,VAc})}} \quad (10)$$

$$F_{\text{VAc}} = 100 \times \frac{\int [\text{CH}]_{(\text{VAc,VAc})} + \frac{1}{2} \times \int [\text{CH}]_{(\text{VOH,VAc})}}{\int [\text{CH}]_{(\text{VOH,VAc})} + \int [\text{CH}]_{(\text{VOH,VOH})} + \int [\text{CH}]_{(\text{VAc,VAc})}} \quad (11)$$

The molar fraction of each type of diads is given by the formulas 12 to 14.

$$F_{(\text{VAc,VAc})} = 100 \times \frac{\int [\text{CH}]_{(\text{VAc,VAc})}}{\int [\text{CH}]_{(\text{VOH,VAc})} + \int [\text{CH}]_{(\text{VAc,VAc})} + \int [\text{CH}]_{(\text{VOH,VOH})}} \quad (12)$$

$$F_{(\text{VOH,VAc})} = 100 \times \frac{\int [\text{CH}]_{(\text{VOH,VAc})}}{\int [\text{CH}]_{(\text{VOH,VAc})} + \int [\text{CH}]_{(\text{VAc,VAc})} + \int [\text{CH}]_{(\text{VOH,VOH})}} \quad (13)$$

$$F_{(\text{VOH,VOH})} = 100 \times \frac{\int [\text{CH}]_{(\text{VOH,VOH})}}{\int [\text{CH}]_{(\text{VOH,VAc})} + \int [\text{CH}]_{(\text{VAc,VAc})} + \int [\text{CH}]_{(\text{VOH,VOH})}} \quad (14)$$

The average length of PVAc and PVOH sequences,  $n_0^{\text{VAc}}$  and  $n_0^{\text{VOH}}$ , respectively, are available *via* **Equations 15** and **16**.

$$n_0^{\text{VAc}} = \frac{\int_{1.85}^{2.0} \frac{[\text{CH}_3]_{\text{b}}}{3}}{\frac{1}{2} \times \int_{1.54}^{1.68} [\text{CH}]_{(\text{VOH,VAc})}} \quad (15)$$

$$n_0^{\text{VOH}} = \frac{\int_{3.7}^{3.9} [\text{CH}]_{\text{c}}}{\frac{1}{2} \times \int_{1.54}^{1.68} [\text{CH}]_{(\text{VOH,VAc})}} \quad (16)$$

Finally,  $\beta$  was already introduced in **Chapter I** and is calculated *via* **Equation 17**.

$$\beta = \frac{\frac{1}{2} \times \int [\text{CH}]_{(\text{VOH,VAc})}}{\int \frac{[\text{CH}_3]_{\text{b}}}{3} + \int [\text{CH}]_{\text{c}}} \quad (17)$$

Where the  $\int [\text{CH}]_{(\text{VOH,VAc})}$ ,  $\int [\text{CH}]_{(\text{VOH,VOH})}$  and  $\int [\text{CH}]_{(\text{VAc,VAc})}$  integrals correspond to the methine protons of the diads.



## From Fourier-transform infrared spectroscopy (FTIR):

The HD of the P(VOH-*s*-VAc) can also be characterized by FTIR. **Table II-2** and **Figure II-10** show the characteristic bands of P(VOH-*s*-VAc) and their respective assignments.<sup>[37]</sup>

**Table II-2: Vibration modes and band frequencies in P(VOH-*s*-VAc).**

Identification	Chemical group	Wavenumber (cm <sup>-1</sup> )
I	VOH units	O-H from the intermolecular and intramolecular hydrogen bonds 3550 - 3200
II	VOH + VAc units	C-H 2840 - 3000
III	VAc units	C=O 1750 - 1735
IV	VOH + VAc units	C-H <sub>2</sub> 1460 - 1417

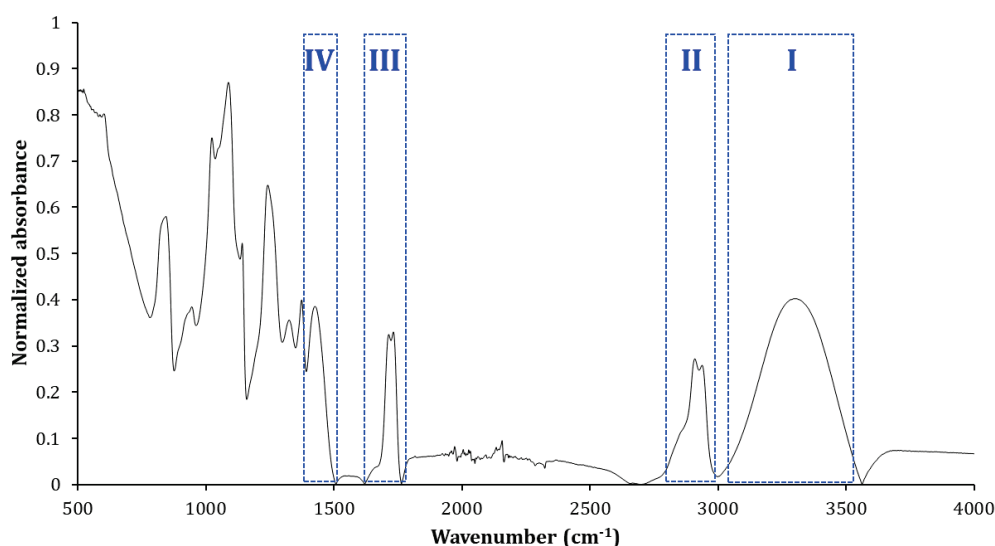


**Figure II-10: FTIR spectrum of 75\_P(VOH<sub>0.88</sub>-*s*-VAc<sub>0.12</sub>) with the corresponding band attributions related to VOH and VAc units.**

The HD is related to the number of acetate groups, meaning that a higher HD represents a lower number of acetate groups in the macromolecule. This correlation is calculated through the ratio of the bands C=O (1750 cm<sup>-1</sup>) and CH<sub>2</sub> (1450 cm<sup>-1</sup>).<sup>[37]</sup>

Mansur *et al.* founded a correlation between the HD of different grades of commercial P(VOH-*s*-VAc) and the ratio of the C=O and C-H bands *via* **Equation 18**.

$$HD = a * \frac{A_{1750}}{A_{1450}} + b \quad (18)$$

Where  $A_{1750}$  is the absorbance of the C=O bond of the VAc units;  $A_{1450}$  is the absorbance of the CH<sub>2</sub> bonds in the P(VOH-s-VAc) and a and b are coefficients related to the calibration curve. Mansur *et al.*'s calibration curve was re-plotted and used for the determination of the HD of our polymers, to crosscheck the HD obtained by <sup>1</sup>H NMR with another technique. As an example, **Figure II-11** shows the calibration curve of the HD *versus* the ratio of the C=O and CH<sub>2</sub> bands for different grades of commercial P(VOH-s-VAc) used by Mansur *et al.* (black crosses), and the value obtained for Mowiol 4-88 (red cross).

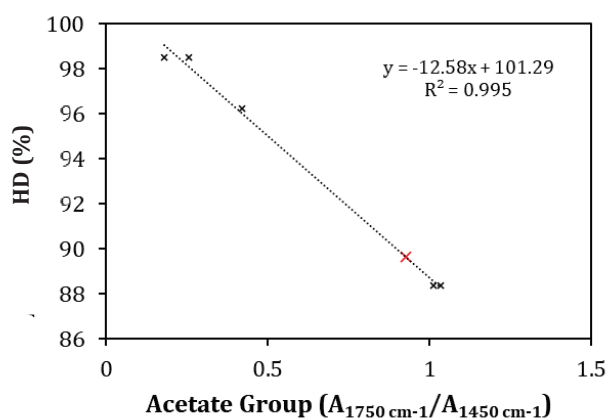


**Figure II-11: Hydrolysis degree related to acetate group ( $A_{1750} \text{ cm}^{-1} / A_{1450} \text{ cm}^{-1}$ ) based on Mansur *et al.*'s work, and result obtained for Mowiol 4-88 (x).**

The value of HD for Mowiol 4-88 was in accordance with the correlation curve obtained by Mansur and co-workers.

These different analysis techniques were applied to determine the main characteristics of Mowiol 4-88 (**Table II-3**). <sup>1</sup>H NMR data showed that Mowiol 4-88 accounts approximately 20 VOH units and 3 VAc units per sequence in average. Similar HD were obtained both by <sup>1</sup>H NMR (HD = 88%) and IR (HD = 89%).

**Table II-3: Characteristics of Mowiol 4-88.  $M_w$  and DP were provided by Wacker.**

Entry	DP	$M_w$ (g mol <sup>-1</sup> )	HD <sub>NMR</sub> (%) <sup>a</sup>	HD <sub>IR</sub> (%) <sup>b</sup>	$\beta$ <sup>a</sup>	$n_0^{\text{VOH}}$ <sup>a</sup>	$n_0^{\text{VAc}}$ <sup>a</sup>
<b>Mowiol 4-88</b>	Avg. 500	23 000 – 25 000	88	89	0.4	19.7	2.7

<sup>a</sup> Determined by <sup>1</sup>H NMR in DMSO-d<sub>6</sub> using **Equations 9,17,16 and 15**

<sup>b</sup> Determined by FTIR using **Equation 18**

## III.2 Alcoholysis of the library of PVAc obtained by RAFT/MADIX polymerization

### III.2.1 Set up of the alcoholysis parameters

Acetate groups are alcoholized by ester interchange with methanol in the presence of NaOH (**Figure II-12**). The protocol is described in the **Experimental Section IV.1**. PVAc copolymers of different DPs were dissolved in methanol and alcoholized *via* the addition of a predetermined amount of a methanolic NaOH solution ( $3.1 \times 10^{-2} \text{ mol mL}^{-1}$ ) at 30 °C. This amount was determined according to a targeted ratio [VAc]:[NaOH], where [VAc] is the number of equivalents of VAc units and NaOH is the number of equivalents of sodium hydroxide. The number of VAc equivalents was determined by dividing the mass of PVAc introduced in the reaction medium with the molar mass of VAc. The number of NaOH equivalents was then adapted, by determining the volume of basic methanolic solution to introduce in the reaction medium, depending on the targeted [VAc]:[NaOH] ratio. After a determined amount of time, NaOH was neutralized by addition of acetic acid to stop the alcoholysis. The polymer was washed several times with methanol and filtered. The final polymer was then dried under vacuum and recovered as a yellowish powder.  $^1\text{H}$  NMR and IR were used to determine the hydrolysis degree (HD) and follow the kinetics of the alcoholysis. The determination of HD is based on **Equation 9**.

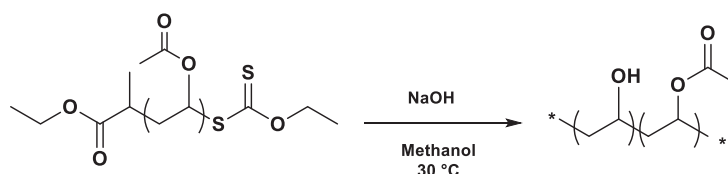


**Figure II-12:** General scheme for the alcoholysis of the RAFT-synthesized PVAc.

---

At first, drastic conditions [VAc]:[NaOH] = 1:1 were used. **Figure II-13** shows the  $^1\text{H}$  NMR spectra of 75\_PVAc ( $M_n$  (NMR) = 5600 g mol $^{-1}$ ,  $D = 1.3$ ) and 75\_PVOH (fully alcoholized 75\_PVAc), with their corresponding assignments.<sup>[38]</sup> After alcoholysis, most of the -CH $_2$ -signal is shifted from 1.54 ppm (*c*) to 1.06 ppm (*c'*). The signals expected for the OH groups (*h*) (taking into account the possible diads) is well defined and observed at 4.2 – 4.7 ppm. Near complete alcoholysis of 75\_PVAc was achieved after only 8 min (HD = 97%).

This [VAc]:[NaOH] ratio led to fast hydrolysis kinetics, and was obviously not suitable to target partially alcoholized grade of P(VOH-*s*-VAc) (*i.e.*, HD = 84 – 90 %) in the case of the alcoholysis of the PVAc's obtained by xanthate mediated RAFT/MADIX. Therefore, it was necessary to adapt the alcoholysis settings.

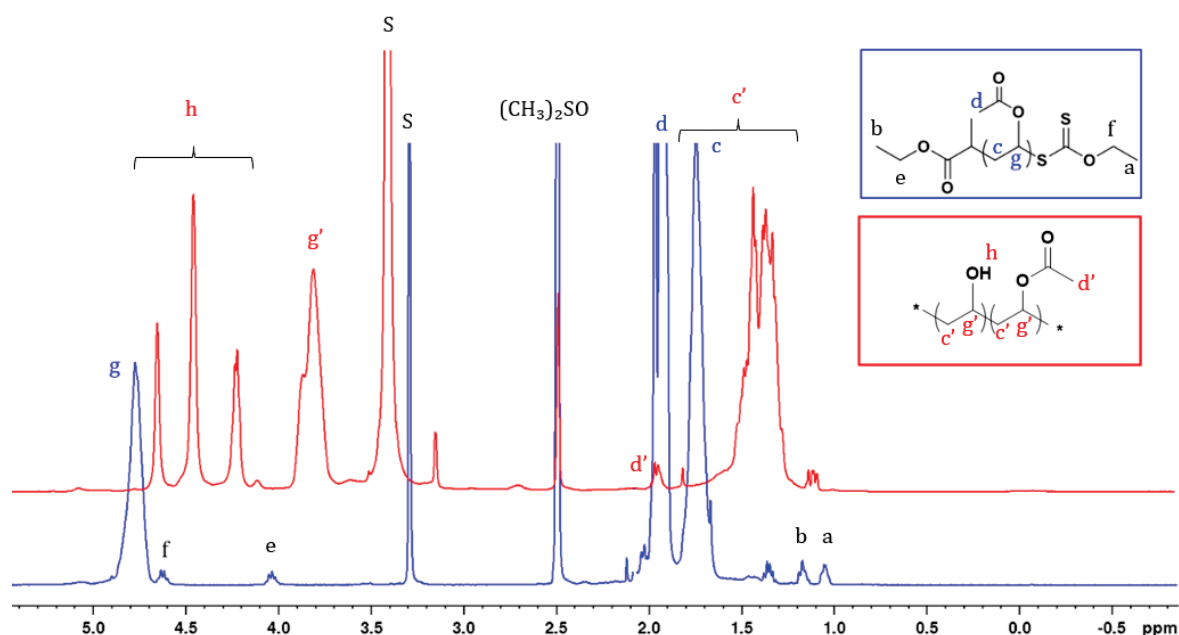


Figure II-13:  $^1\text{H}$  NMR spectra of 75\_PVAc (blue) and the corresponding fully alcoholized 75\_PVOH (red) in  $\text{DMSO-d}_6$ , 256 scans, and their related structures. The alcoholysis was performed in MeOH at 30 °C for 8 min with a [VAc]:[NaOH] ratio of 1:1. S refers to water present in  $\text{DMSO-d}_6$ .

In a second time, four experiments with different [VAc]:[NaOH] ratios were carried out. Different volumes of the solution of NaOH in methanol were added to a solution of 75\_PVAc in methanol, at constant concentration of acetate group ([VAc] = 3.1 mol L<sup>-1</sup>). Time zero was recorded as the moment the two solutions were mixed together. Samples were withdrawn at predetermined time intervals and quenched with acetic acid. At the end of the reaction, P(VOH-*s*-VAc)s were obtained as white gels in methanol. The product of the hydrolysis, after four successive methanol washes was dried at 60 °C overnight, and afforded a yellowish powder.

The average length of the PVAc and PVOH sequences and the blockiness index of the P(VOH-*s*-VAc) obtained after 4 h of hydrolysis were calculated as a function of the diads *via*  $^1\text{H}$  NMR, based on Moritani and Fujiwara's work in the region 1.2 - 1.9 ppm, *via* the integration of (VAc,VAc), (VAc,VOH) and (VOH,VOH) signals in the range 1.87 - 1.68; 1.68 - 1.54 and 1.54 - 1.27 ppm respectively. HD was determined by  $^1\text{H}$  NMR and double checked by FTIR analysis. All the results are summarized in **Table II-4**.

**Table II-4: Characteristics of various 75\_P(VOH-s-VAc) obtained from alcoholysis of 75\_PVAc, calculated as a function of diads from  $^1\text{H}$  NMR spectra in DMSO- $d_6$ .**

Experiment	[VAc]:[NaOH]	HD <sub>4 h</sub> (NMR) (%) <sup>a</sup>	$\beta$ <sup>b</sup>	$n_0^{\text{VOH c}}$	$n_0^{\text{VAc c}}$
1	1:0.01	-	-	-	-
2	1:0.025	97	0.7	45	2
3	1:0.05	97	0.8	42	2
4	1:0.1	98	0.7	38	2

<sup>a</sup> Determined by  $^1\text{H}$  NMR in DMSO- $d_6$  and using Equation 9

<sup>b</sup> Determined by Equation 17

<sup>c</sup> Determined by Equation 15 and 16

Experiment 1 was based on scaling down Wacker's protocol to 3 g using 75\_PVAc, after the determination of Wacker's [VAc]:[NaOH] ratio, which was found to be 1:0.01. However, this experiment showed no hydrolysis, even after 24 h. This could be due to scale-down limitations such as volume effect, different stirring, less precise control of the temperature and so forth.

Three other ratios were then tested and provided more adapted kinetics (Figure II-14). Experiments 2, 3 and 4 provided almost fully alcoholized polymer after 4 h (Table II-4). At such hydrolysis grade, the blockiness index can be questioned, but it seems that the average length of the PVAc and PVOH sequences remains the same regardless of the [VAc]:[NaOH] ratio.

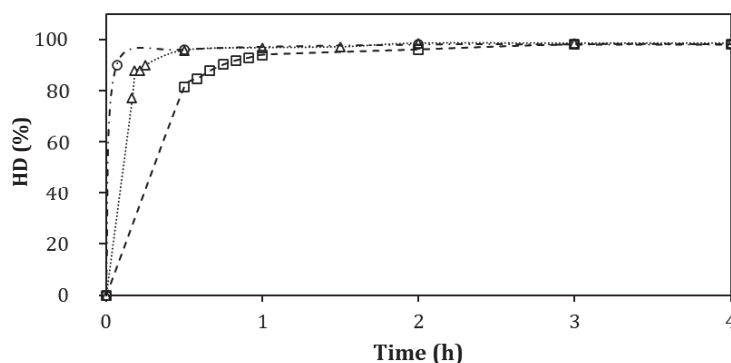


**Figure II-14: Kinetics of the alcoholysis of 75\_PVAc with [VAc]:[NaOH] ratio of 1:0.025 (□, experiment 2), 1:0.05 (△, experiment 3), 1:0.1 (○, experiment 4).**

Figure II-14 shows that the alcoholysis of experiment 4 was far too fast to ensure control over the alcoholysis rate, with 90% alcoholysis reached after only 5 min. Experiments 2 and 3 show slower alcoholysis rates. Mowiol 4-88, the commercial P(VOH-s-VAc) used as a benchmark in this chapter has a  $84\% < \text{HD} < 88\%$ . Such HD is reached after 40 min for experiment 2 and after 13 min for experiment 3. Experiment 2 was both slow enough to stop the alcoholysis at the desired HD in a sufficiently short timescales, and to allow for reaching

88% of hydrolysis after 45 min. Therefore, a ratio  $[VAc]:[NaOH] = 1:0.025$  was chosen for future alcoholysis reactions.

### III.2.2 In-depth characterization of the P(VOH-s-VAc)

In-depth characterizations of 75\_P(VOH<sub>0.88</sub>-s-VAc<sub>0.12</sub>) obtained during the alcoholysis of 75\_PVAc with a ratio  $[VAc]:[NaOH] = 1:0.025$  (and neutralized after 45 min) are provided in **Figure II-15**. **Figure II-15 (a)** shows that the blockiness index remained between 0 and 1 throughout the hydrolysis, which is indicative of a block-like structure. When the hydrolysis degree reached 88% (after 45 min), the average number of VAc and VOH units per sequence was 2 and 19, respectively, which are similar to that of Mowiol 4-88.

**Figure II-15 (b)** shows consistent results: upon alcoholysis,  $F_{VAc}$  decreased with the increase in  $F_{VOH}$  (HD) units, which resulted in an increase in the percentage of (VOH,VOH) diads and a decrease in the (VAc,VAc) ones. When HD = 88% was reached, the polymer contains 81%, 16% and 3% of (VOH,VOH), (VAc,VOH) and (VAc,VAc) diads, respectively.

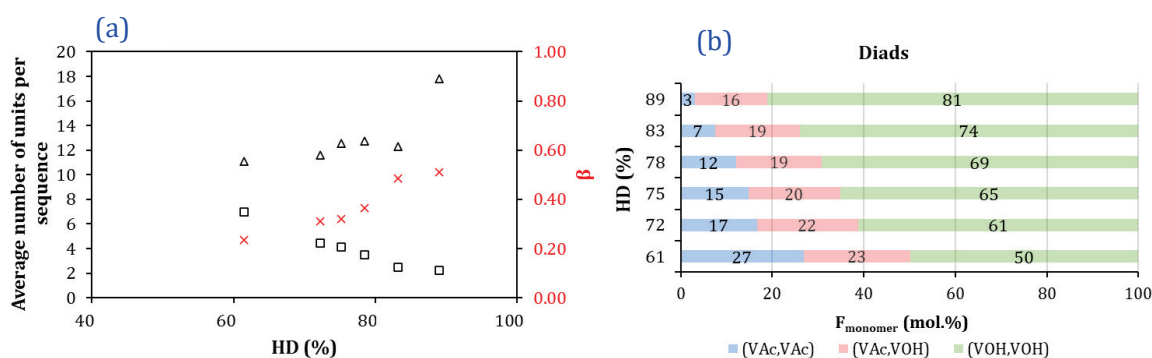


**Figure II-15: (a)**  $n_0^{VAc}$  (□);  $n_0^{VOH}$  (Δ) and blockiness index (×) versus HD and **(b)** evolution of the representative fraction of each diad with HD. These data were extracted from  $^1H$  NMR analyses in DMSO- $d_6$  as previously described.

### III.2.3 Reproducibility testing of the alcoholysis of 75\_PVAc on different batches

The previous experiments showed that with a fine tuning of the  $[VAc]:[NaOH]$  ratio, it was possible to influence the alcoholysis rate of PVAc. In our hands, the ratio 1:0.025 seemed to be the most appropriate to reach HD = 88% in less than one hour, but was long enough to allow stopping the reaction at a desired higher HD. To assess reproducibility, this experiment was carried out three additional times: two times on 3 g of PVAc with similar molar masses (5500 - 6300 g mol<sup>-1</sup>) but from different batches of 75\_PVAc, and one time on a larger scale

(45 g of the initial batch of 75\_PVAc used as the reference experiment ( $M_n(\text{NMR}) = 5600 \text{ g mol}^{-1}$ ,  $D = 1.3$ ).

**Figure II-16** shows excellent reproducibility of the hydrolysis on a 3 g system for three different batches, as both experiments  $\times$  and  $\times$  reached 88% hydrolysis after 40 - 43 min and showed a perfect overlay with the reference experiment. For each experiment, a gelation was observed after 30 min. FTIR analysis showed both 88 and 89% alcoholysis for the reproducibility tests on 3 g scale, respectively.

This experiment was then scaled up on a 45 g batch of 75\_PVAc to test its robustness. The gel point was reached after 32 min and HD = 88% was obtained after 43 min. **Figure II-16** shows once again a perfect overlay of this experiment with the reference plot.

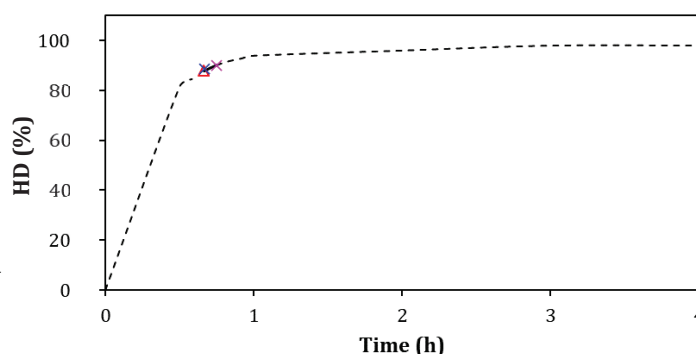


**Figure II-16:** Reproducibility tests for the alcoholysis of 75\_PVAc with ( $\times$ ) the first reproducibility test on 3 g with a different batch than the reference; ( $\times$ ) the second reproducibility test on 3 g and again another batch; and ( $\Delta$ ) the third reproducibility test on the scaled-up experiment: 45 g of the batch used for the reference experiment. (---) represents the reference kinetics.

### III.3 Influence of the DP of the PVAc on the kinetics of alcoholysis

As presented in the first section of this Chapter, several PVAc with different DPs were synthesized. Once set the experimental conditions for the alcoholysis of the RAFT/MADIX-synthesized PVAc, the aim of this section was then to study the influence of the DP of the polymer on the kinetics of the alcoholysis. 20\_PVAc, 75\_PVAc, 100\_PVAc and 200\_PVAc were alcoholized. The reactions were performed at 30 °C in methanol with  $[\text{VAc}]:[\text{NaOH}] = 1:0.025$ . The kinetics of these reactions were studied for 2 h (**Figure II-17**). Samples were taken from the reaction media, quenched in acetic acid and analyzed by  $^1\text{H}$  NMR in DMSO- $d_6$ .

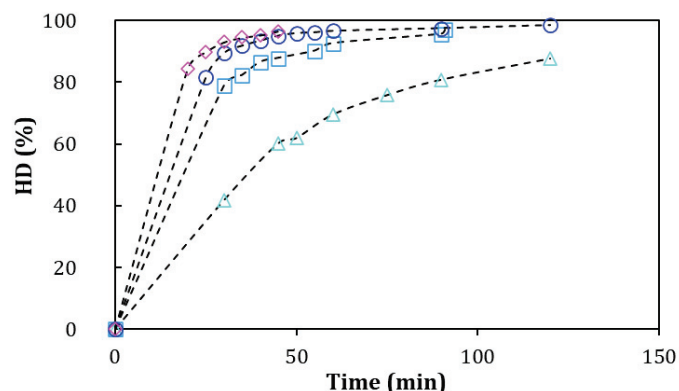


Figure II-17: Hydrolysis degree *versus* time for different DPs of PVAc: 20\_PVAc ( $\blacktriangle$ ); 75\_PVAc ( $\blacksquare$ ), 100\_PVAc ( $\bullet$ ) and 200\_PVAc ( $\blacklozenge$ ). [VAc]:[NaOH] = 1:0.025.

It can be clearly observed that the higher the DP (at fixed mass concentration of PVAc in methanol), the faster the alcoholysis (**Figure II-17**). This may be due to the aforementioned opening zipper mechanism. Indeed, at fixed mass concentration of PVAc, the higher the molar mass, the fewer the number of chains in the reaction medium. Therefore, when the hydrolysis starts on one chain, the hydrolysis is fast. In contrast, when the molar mass is low, there are more chains in the reaction medium, and it takes longer to start the hydrolysis process on each chain.

Finally, several P(VOH-s-VAc) copolymers with different DPs and HDs were synthesized to be able to test the corresponding range as stabilizer candidates in the emulsion copolymerization of VAc and VeoVa. The final characteristics of these materials are gathered in **Table II-5**.



**Table II-5: Library of the RAFT-synthesized P(VOH-*s*-VAc) stabilizer candidates for the emulsion copolymerization of VAc and VeoVa and their main characteristics.**

Entry *	$M_n$ before alcoholysis (g mol <sup>-1</sup> ) <sup>a</sup>	$M_n$ after alcoholysis (g mol <sup>-1</sup> ) <sup>b</sup>	Structure after alcoholysis	HD (%) <sup>c</sup>	$\beta$ <sup>c</sup>	$n_0^{\text{VOH}}$ <sup>c</sup>	$n_0^{\text{VAc}}$ <sup>c</sup>
20_PVOH <sub>0.88</sub>	2200	1080	20_P(VOH <sub>0.88</sub> - <i>s</i> -VAc <sub>0.12</sub> )	88	0.8	9	1.3
75_PVOH <sub>0.88</sub>	5600	3680	75_P(VOH <sub>0.88</sub> - <i>s</i> -VAc <sub>0.12</sub> )	88	0.5	19	2.0
75_PVOH <sub>0.91</sub>	6500	3320	75_P(VOH <sub>0.91</sub> - <i>s</i> -VAc <sub>0.09</sub> )	91	0.5	24	2.1
75_PVOH <sub>0.94</sub>	5600	3260	75_P(VOH <sub>0.94</sub> - <i>s</i> -VAc <sub>0.06</sub> )	94	0.7	42	3.0
75_PVOH <sub>0.97</sub>	5600	3170	75_P(VOH <sub>0.97</sub> - <i>s</i> -VAc <sub>0.03</sub> )	97	0.7	45	2.0
100_PVOH <sub>0.88</sub>	9600	5300	100_P(VOH <sub>0.88</sub> - <i>s</i> -VAc <sub>0.12</sub> )	88	0.4	19.5	2.0
200_PVOH <sub>0.88</sub>	16 800	9420	200_P(VOH <sub>0.88</sub> - <i>s</i> -VAc <sub>0.12</sub> )	88	0.4	20	2.5

\* P(VOH<sub>0.88</sub>-*s*-VAc<sub>0.12</sub>) was shortened in PVOH<sub>HD</sub> with the corresponding subscripted HD

<sup>a</sup> Determined by <sup>1</sup>H NMR via **Equation 6**

<sup>b</sup> Determined by **Equation 51**, considering retention of the DP after alcoholysis

<sup>c</sup> Determined by <sup>1</sup>H NMR via **Equations 9, 15, 16 and 17**

**Table II-5** shows that at fixed HD = 88%, the average length of the PVOH and PVAc sequences are about 19 and 2 units, respectively, regardless of the DP (except for 20\_PVAc where the average length of the PVOH sequences is 9 units). As expected, at fixed DP = 75, the average number of the VOH units per sequence of PVOH increases with increasing the HD. All the polymers obtained with the set experimental parameters have a blocky-like structure.

Noteworthy, the estimation of  $M_n$  after alcoholysis via **Equation 51** is true if the P(VOH-*s*-VAc) is linear.<sup>[39]</sup> This information can be verified by <sup>1</sup>H NMR. Knowing the DP of the polymer before alcoholysis (thanks to the presence of the xanthate moiety on each chain extremity), it is possible to cross check that this DP is similar for the alcoholized polymer. Additionally, Ballard *et. al.*<sup>[40]</sup> demonstrated the *quasi*-retention of the molar masses for RAFT-synthesized P(VOH-*s*-VAc) compared to the ones synthesized by FRP, because of limited chain branching occurring during RAFT/MADIX polymerization. We, therefore assumed retention of the polymerization degrees before and after alcoholysis of our polymers.

### III.4 Study of the microstructure of the well-defined P(VOH-*s*-VAc) by NMR, and chain-end analysis

It is now well established that thiocarbonylthio groups undergo reaction with nucleophiles. Thus, the alcoholysis of the RAFT-synthesized PVAc will surely affect the xanthate extremity,

resulting in thiol-terminated polymeric chains.<sup>[41-43]</sup> Tong *et al.*<sup>[44]</sup> stated that under basic hydrolysis conditions, the terminal xanthate Z group of a PVAc could give rise to the formation of conjugated unsaturated aldehyde, which provided the yellowish color to the final product according to the reactions presented in **Figure II-18**.

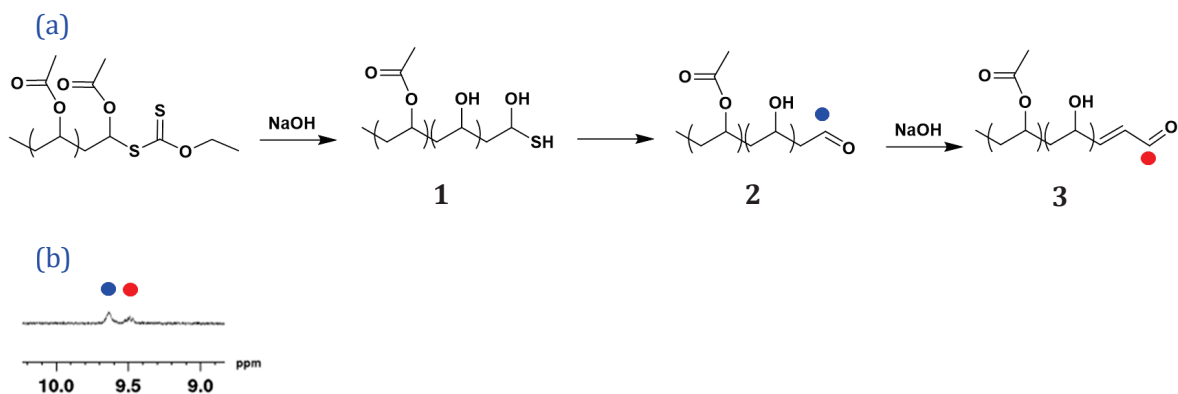


**Figure II-18:** (a) Chemical formula of the obtained products after basic alcoholysis of PVAc obtained by RAFT/MADIX polymerization, proposed by Tong *et al.*<sup>[44]</sup> and (b) <sup>1</sup>H NMR evidence of the presence of these end groups in our 75\_P(VOH<sub>0.88</sub>-S-VAc<sub>0.12</sub>) after alcoholysis of 75\_PVAc.

These functions were indeed detected by <sup>1</sup>H NMR in our products, for instance here for 75\_P(VOH<sub>0.88</sub>-S-VAc<sub>0.12</sub>) (**Table II-5, 75\_PVOH<sub>0.88</sub>**), with a signal at 9.6 ppm which was attributed to -CH=O (specie 2) and 9.5 ppm which was attributed to -C=C-CH=O (specie 3) (**Figure II-18**). To cross-check this attribution, <sup>13</sup>C NMR was run on 75\_P(VOH<sub>0.88</sub>-S-VAc<sub>0.12</sub>), with the different hypothesized chain-end groups and their possible assignments (**Figure II-19**). The main attributions of the polymer are represented by colored stickers and are based on Moritani<sup>[33]</sup> and Budhlall's<sup>[32]</sup> works. The different possible chain-end functions are represented on the right of the spectrum with different colors, and the hypothetical assignments of the chain-ends are defined by corresponding-colored letters. If the pink structure with the conjugated unsaturated aldehyde structures was present in the polymer, the alkene characteristic signals of -C=C- and -C=C- from specie 3 would be visible between 110 to 140 ppm. These signals were not present on the <sup>13</sup>C NMR spectrum, which was surprising and can question the presence of such end group functionality. Except for the purple structure where the C=S was not identified, the other attributions fit quite well with the proposed chain-end structures of specie 2. However, this technique did not allow to exclude the presence of specie 1, and it is likely that a mixture of both species 1 and 2 are present in the polymer.

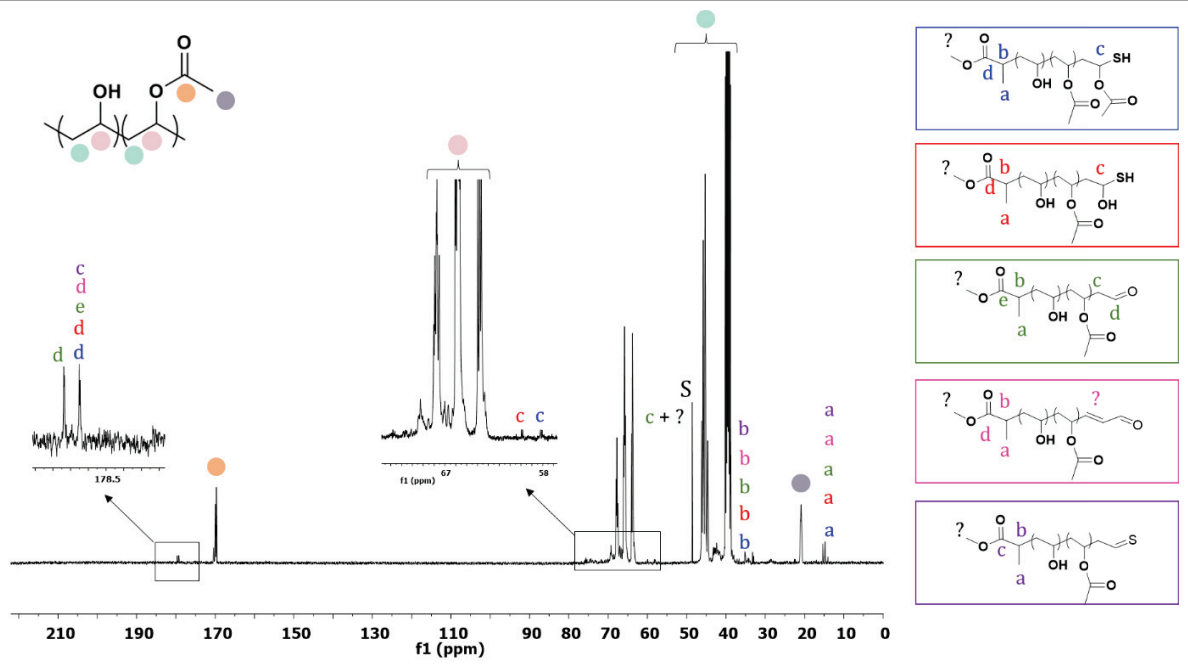


Figure II-19: <sup>13</sup>C NMR spectrum of 75\_P(VOH<sub>0.88</sub>-s-VAc<sub>0.12</sub>) in DMSO-d<sub>6</sub> at R.T. and the possible chain-end groups related with their hypothesized attributions. S corresponds to methanol traces.

#### IV. (Self-)Organization in water

In the last few decades, the self-assembly of amphiphilic copolymers in an aqueous medium has been widely studied due to their peculiar physical and chemical properties.<sup>[45][46],[47],[48]</sup> It is now well-established that low molar mass surfactants are molecules able to modify the surface properties of the liquid in which they are introduced (usually water).<sup>[49]</sup> The simultaneous presence of both hydrophilic and hydrophobic parts in the same molecule has been recognized as the key feature of these systems, which is responsible for their characteristic properties in solution. As a common feature, macromolecular stabilizers show interesting association phenomena in selective solvents, which results in particular rheological behavior and the formation of self-assembled structures.<sup>[47],[50–53]</sup> Dynamic light scattering (DLS), static light scattering (SLS) and surface tension measurements are of particular interest to get a better insight into conformational organization of these polymeric materials in water, and to get a better knowledge of their involvement in emulsion polymerization and the inherent stabilization process. For instance, DLS allows for the observation of aggregate formation (also referred to as pseudo-micelles) and characterization of their size.<sup>[48],[52],[54],[55]</sup>

Additionally, it was demonstrated by different authors that the adsorption of P(VOH-*s*-VAc) stabilizers at the interface between two immiscible liquids reduces the interfacial tension and thus enhances the emulsion stability.<sup>[56,57]</sup> Surface tension measurements were also carried out for selecting the optimal structure of P(VOH-*s*-VAc) as stabilizing agent (depending on its molar mass,  $\beta$  value or HD), for suspension polymerization systems, without carrying out the polymerization reaction.<sup>[58]</sup>

It was demonstrated that in the case of the commercial P(VOH-*s*-VAc) grades (including Mowiol 4-88), it is all the characteristics of the polymer (*i.e.*, molar mass, PVOH and PVAc sequence distributions and HD) that can affect their organization in water, and impact the nucleation mechanism when they are used as stabilizers for the emulsion polymerization of VAc.<sup>[52],[59]</sup> To the best of our knowledge, no investigation was performed on the aqueous organization of well-defined P(VOH-*s*-VAc) copolymers obtained by alcoholysis of RAFT-synthesized PVAc. The fact that these Mowiol-like P(VOH-*s*-VAc) were designed with a better control of the molar mass and dispersity may impact their micellization behavior compared to the commercial grades of P(VOH-*s*-VAc). The aqueous phase behavior of the RAFT-synthesized stabilizers was therefore studied and compared to that of the reference Mowiol 4-88. The presence of aggregates was studied by DLS for each P(VOH-*s*-VAc) with HD = 88%, regardless of their DPs.

Additionally, surface tension measurements of 2.5 wt.% dispersions (corresponding to the amount of stabilizer introduced in the emulsion polymerization systems (in **Section V**), based on the total volume of the reaction) of the different P(VOH-*s*-VAc) with various DP and

HD were carried out to study the influence of these parameters on the ability of the polymer to reduce the surface tension of water. This parameter will provide a useful guide for selecting an adequate stabilizing agent.<sup>[58]</sup>

All the RAFT-synthesized P(VOH-*s*-VAc) were found to be dispersible in water after approximately 15 to 30 min at R.T., while Mowiol 4-88 had to be heated to 70 °C for 20 min to ensure complete dissolution in water.

#### IV.1 Organization in water

Several authors carried out DLS studies to get a better insight on the aqueous phase conformation of P(VOH-*s*-VAc) copolymers, with differing architectures (molar mass, hydrolysis degree and blockiness index ( $\beta$ )) and concentrations.<sup>[47],[51],[60],[61]</sup> They found that a particular feature of these polymers is their strong tendency to form colloidal aggregates in water by inter- and intra-molecular hydrophobic interactions between the PVAc sequences. The proportion of these colloidal aggregates is influenced not only by the HD, but also by the molar mass and blockiness index of the polymer. In addition, free P(VOH-*s*-VAc) chains (unimers) were also present on the reported DLS traces (volume-average particle diameter ( $D_v$ ) in the range 5 to 15 nm).

Budhlall *et al.*<sup>[47]</sup> analyzed various commercial P(VOH-*s*-VAc) of different molar masses and blockiness index by DLS. The authors observed that the hydrodynamic volume ( $V_h$ , obtained from the intensity-weighted mean diameter ( $Z_{av}$ ) by DLS) increased with increasing  $\beta$  value and molar mass. By contrast, the cluster density,  $\rho_{agg}$ , or density of the polymer chains swollen or associated with the solvent, correspondingly decreased with increasing  $\beta$  value and molar masses. A schematic illustration of the proposed conformations is shown in **Figure II-20**. They also determined an aggregation number for these stabilizers,  $N_{agg}$  (**Equation 19**). This value estimates the average number of polymer chains per object, and was found to be close to unity, which suggested the absence of P(VOH-*s*-VAc) aggregates with respect to their experimental conditions (dispersions containing 1 wt/v.% of commercial P(VOH<sub>0.88</sub>-*s*-VAc<sub>0.12</sub>) at 25 °C).

$$N_{agg} = \frac{\rho_{agg} V_{agg}}{M_{agg}} = \frac{\rho_{agg} (4/3 \cdot \pi \cdot R_h^3)}{\frac{M_w}{N_A}} \quad (19)$$

With  $N_A$  the Avogadro's number;  $R_h$  the hydrodynamic radius and  $M_w = \bar{D} \cdot M_n$

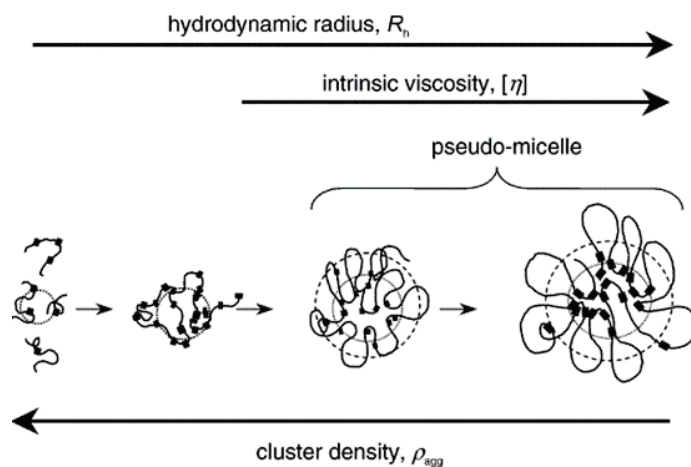


**Figure II-20: Schematic illustration of the conformational differences between P(VOH-s-VAc)s based on the blockiness index and DP in the presence of a polar (hydrophilic) solvent (e.g., water). With  $\rho_{agg} = 2.55 \cdot N_A / [\eta]$ ;  $\eta$  being the intrinsic viscosity. Reprinted from ref [47] with the permission from the publisher.**

Similarly, Atanase and Riess<sup>[52]</sup> highlighted that not all the P(VOH-s-VAc)s were subjected to the formation of pseudo-micelles in water (objects ranging from 30 to 100 nm) and that it depended on the HD of the stabilizer. With 1 wt.% P(VOH-s-VAc)s dispersions analyzed at 20 °C, they claimed that the relative amount of pseudo-micelles decreased from approximately 20 to 10 vol.% with HD increasing from 73 to 78%. Above 78% hydrolysis (e.g., HD = 88%), they observed a monomodal size distribution of objects with  $D_v$  ranging from 8.8 to 20.5 nm depending on the  $M_n$  of the P(VOH-s-VAc). The authors attributed this single population to “free chains” (or unimers) in water.

It is thus well established that partially hydrolyzed P(VOH-s-VAc) can adopt different conformations in aqueous solution, depending on their molecular weight, HD and  $\beta$ , but that unimers were found to be majority. These conformations likely play a role in regulating the grafting reactions in the aqueous phase and controlling the particle nucleation mechanism during the emulsion polymerization of vinyl acetate using P(VOH-s-VAc) as stabilizer. The study of the aqueous phase conformation of this kind of polymeric stabilizers could therefore be useful for the next section of this Chapter.

In this thesis, to mimic the emulsion polymerization composition (10 wt.% of stabilizer based on monomers, meaning 2.5 wt.% of stabilizer based on the total volume of the reaction), samples containing deionized water and 2.5 wt.% of each RAFT-synthesized P(VOH-s-VAc) with HD = 88% and different DP were prepared and analyzed by DLS. Their conformation in water was compared to that of Mowiol 4-88 *via* the analysis of the correlograms and the DLS distribution curves in intensity and in volume (**Figure II-21**).

The correlation function gives information about the signal-to-noise ratio as well as on the presence of aggregates. For a monomodal dispersion, the correlation function should be smooth, and with a single exponential decay. A non-linear baseline including several bumps indicates the presence of aggregates. The signal-to-noise ratio can be evaluated from the plateau value of the correlation function at small delay times, the so-called intercept. If the dispersion is stable, the value of the intercept will be in the range 0.85 – 1. Below 0.85, the solution is not diluted enough, and multiple diffusions may occur and disturb the measurement. The slope of the correlation function also provides information about the number, shape and distribution of the different populations in water: a slope break indicates the presence of either another population, or a non-spherical one.

The correlation curves of the dispersions that contained the RAFT-synthesized P(VOH-*s*-VAc) were reproducible over several runs, and the intercepts were in the range 0.85 – 1 for every system, which attests that the dilution was enough to avoid multiple diffusion, and that the signal-to-noise ratio was low. The values provided by the DLS were thus exploitable in our experimental conditions (2.5 wt.% dispersions at 25 °C). The correlation curves were however not smooth at small delay times, and also showed three different slopes between approximately 10 - 100, 100 - 1100 and above 1100  $\mu$ s (**Figure II-21**). In the case of the dispersion that contained Mowiol 4-88, only two different slopes ranging from 10 to 100 and 100 to 1000  $\mu$ s could be observed.

The signals in intensity confirmed the presence of the different populations for both dispersions of Mowiol 4-88 and the well-defined P(VOH-*s*-VAc) (**Figure II-21**). Population **A** ranging from 9 to 15 nm could correspond to free P(VOH-*s*-VAc) unimers, in agreement with the works of Budhlall *et al.*<sup>[47]</sup> and Atanase *et al.*<sup>[60]</sup> (**Figure II-21**). The other observed populations (**Figure II-21, B and C**) could correspond to pseudo-micelles or aggregates (which will be considered ranging from approximately 30 to 100 nm (population **B**) and from 100 to 1000 nm (population **C**), respectively). One can observe that there is only one population of aggregates for Mowiol 4-88 (**Figure II-21 and Table II-6**) with an average size of 172 nm, while two distinct populations are present in the case of the RAFT-synthesized P(VOH<sub>0.88</sub>-*s*-VAc<sub>0.12</sub>), regardless of their DP (**Figure II-21**), at approximately 50 nm and 300 to 800 nm (**Table II-6**).

Nevertheless, the volume distributions (**Figure II-21 and Table II-6**) show that the main population in the four dispersions is always population **A** from the DLS response in intensity (ranging from 9 to 15 nm and previously attributed to unimers). This population represents 100% of the signal detected in volume. This is in agreement with the literature findings,<sup>[52],[59]</sup> which means that these samples can be considered as free polymer dispersed in an aqueous medium at 20 – 25 °C.



Similar measurements were carried out at 55 °C (emulsion polymerization temperature that will be used in the following section) and provided similar trends (see **Appendix 5**), even though the correlation curves were not perfectly reproducible over several runs. This behavior was also observed by Atanase,<sup>[60]</sup> who attributed this to the beginning of formation of associates between unimers.

Noteworthy, the plot in intensity also shows that the  $D_v$  values (obtained by conversion of the intensity size distribution into a volume distribution using the Mie theory, taking into account the refractive index and absorption of the particles) must be considered with care as these calculations are not accurate, resulting from the uncertainty linked to that of the  $Z_{av}$ , due to the presence of several populations. Nevertheless, the volume distribution gives us some information on the main population present in water (bold values in **Table II-6**), which proved to be that with the smallest size. Indeed, the presence of pseudo-micelles and/or aggregates was only detectable in intensity distributions, not in volume.

In any case, the organization in water of these P(VOH-*s*-VAc) copolymers is still debated, and SLS or/and SAXS investigation could provide additional information.



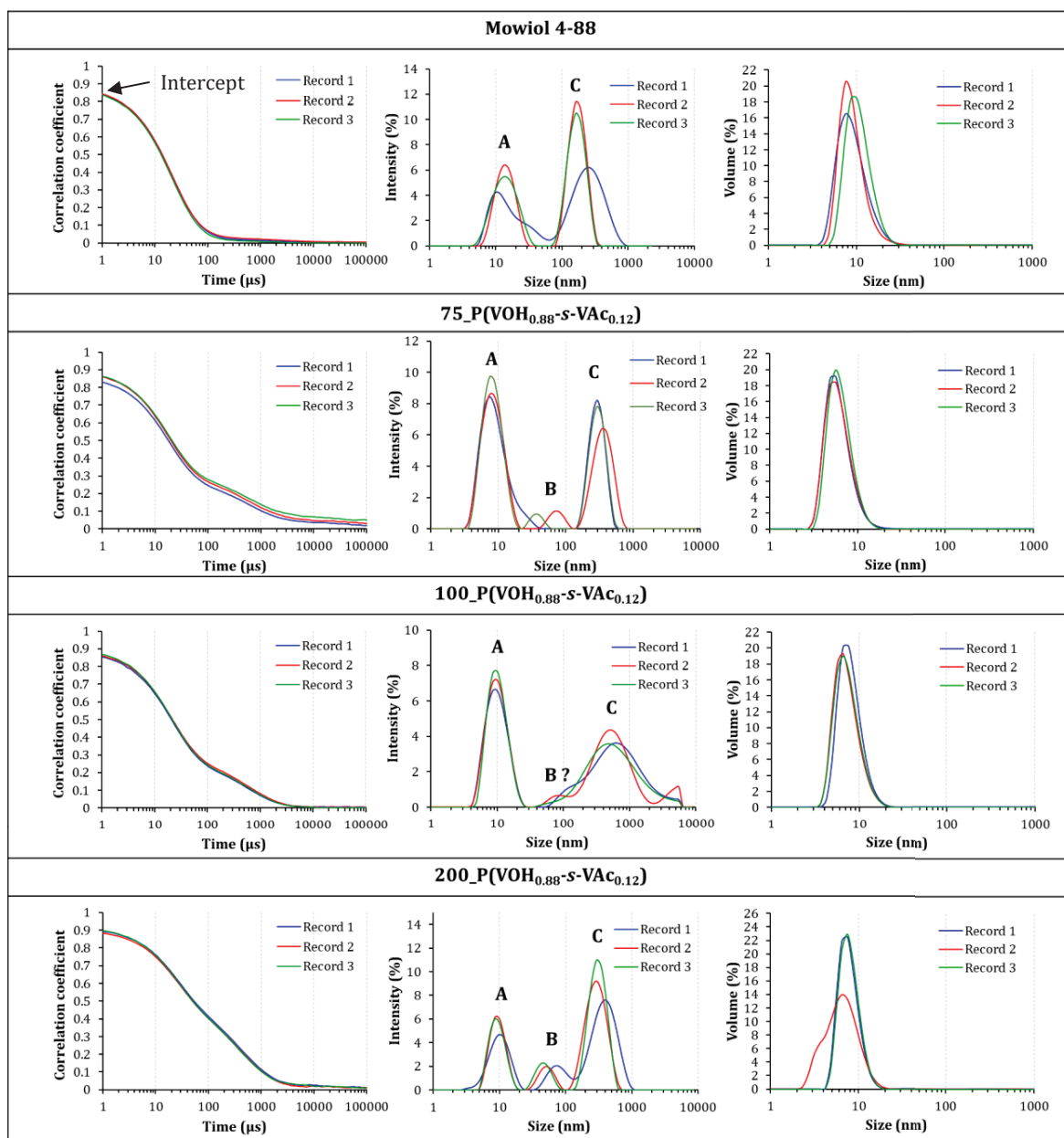


Figure II-21: Correlograms and DLS-size distributions in intensity and in volume for the 2.5 wt.% aqueous dispersions of Mowiol 4-88; 75\_P(VOH<sub>0.88</sub>-s-VAc<sub>0.12</sub>); 100\_P(VOH<sub>0.88</sub>-s-VAc<sub>0.12</sub>) and 200\_P(VOH<sub>0.88</sub>-s-VAc<sub>0.12</sub>).

Table II-6: DLS characteristics of P(VOH-*s*-VAc) in water at 25 °C.

Stabilizer	$M_n$ (g mol <sup>-1</sup> )	$Z_{av}$ (nm) <sup>a</sup> (Volume fraction (%))
Mowiol 4-88	8000*	<b>15</b> / 172 (100/0)
75_P(VOH <sub>0.88</sub> - <i>s</i> -VAc <sub>0.12</sub> )	3680	<b>9</b> / 45 / 300 (100/0/0)
100_P(VOH <sub>0.88</sub> - <i>s</i> -VAc <sub>0.12</sub> )	5300	<b>10</b> / 800 (100/0/0)
200_P(VOH <sub>0.88</sub> - <i>s</i> -VAc <sub>0.12</sub> )	9420	<b>10</b> / 50 / 300 (100/0/0)

<sup>a</sup> Determined by DLS

\* Average value provided by Wacker

**Bold** value: main population observed in volume

In the next chapters, the distributions in intensity will be considered as a first indication concerning the conformation of the copolymers in water. In case of the presence of several populations, the response in volume will only be considered to provide an information concerning the fraction of each population, and in the case where a single population is detected, the value of  $D_v$  could be considered as accurate.

In any case, the DLS data highlight that either Mowiol 4-88 or the well-defined P(VOH-*s*-VAc) with low molar masses and dispersities behave alike in water, with mostly the presence of unimers and only some minor aggregates. This observation could be surprising as a different organization could have been observed with the well-defined P(VOH-*s*-VAc) due to their lower molar masses. Again, the organization in water of such copolymers would require further investigation (such as SLS and SAXS for instance).

## IV.2 Surface tension

Surface tensions measurements were performed according to a protocol described in **Experimental Section VI.9**. Dispersions with 2.5 wt.% of the synthesized P(VOH<sub>0.88</sub>-*s*-VAc<sub>0.12</sub>) of different DPs but fixed HD = 88% were analyzed and compared to dispersions with 2.5 wt.% of Mowiol 4-88 (**Figure II-22**). Again, this concentration was chosen because in the following section emulsion polymerizations will be carried out with this amount of stabilizer.

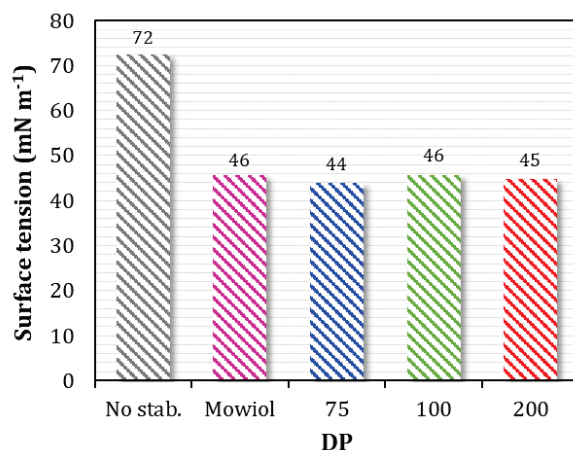


**Figure II-22:** Surface tension values of 2.5 wt.% stabilizer dispersions at 25 °C. Comparison between Mowiol 4-88 and P(VOH-*s*-VAc) copolymers with different DPs. The value measured for pure water is also provided.

**Figure II-22** shows that all the stabilizers have similar surface tension around 45 mN m<sup>-1</sup>. These results are consistent with O'Donnell *et al.*'s work.<sup>[62]</sup> The authors presented surface tension measurements of several commercially available P(VOH-*s*-VAc), with concentrations varying between 1 and 10 wt.%. It was found that these dispersions had a constant surface tension of 44.8 mN m<sup>-1</sup>. Below 1 wt.% a sharp rise in surface tension occurred, from which an apparent CAC of 0.25 wt.% was obtained.

Boscher *et al.*<sup>[63]</sup> and He *et al.*<sup>[56]</sup> demonstrated that the HD of P(VOH-*s*-VAc) had more effect on the interfacial tension than the molar mass. The results obtained with our well-defined 75\_P(VOH-*s*-VAc) are consistent with this assumption. Indeed, **Figure II-23** shows that, for a fixed DP of 75, the surface tension of 2.5 wt.% dispersions of P(VOH-*s*-VAc) increased with hydrolysis degrees from 42 mN m<sup>-1</sup> for HD = 80% and up to 63 mN m<sup>-1</sup> for HD = 97%. This result indicates that a better stabilization of the latex might be provided by P(VOH-*s*-VAc) with HD between 80 to 91%, and is consistent with the literature.<sup>[64]</sup>

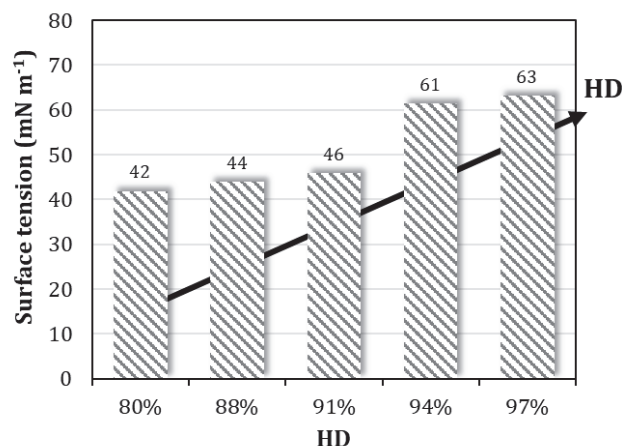


Figure II-23: Influence of the HD of 75\_P(VOH-s-VAc) on the surface tension (mN m<sup>-1</sup>).

### IV.3 Conclusion on the (self-)organization of P(VOH-s-VAc) in water

This section showed that Mowiol-like P(VOH-s-VAc), with a better control over the molar mass and dispersity, we did not get rid of the aggregation of the chains in water, which are not perfectly solvated. Surprisingly, these aggregates are of the same nature than those generated by Mowiol 4-88 (unimers with an average diameter of 10 nm). To further characterize these aggregates, it could be interesting to perform SLS and/or SAXS analysis to determine the number of aggregation (*i.e.*, number of polymer chains per aggregate) and the shape of these aggregates compared to those obtained with Mowiol 4-88. No significant influence was observed on the surface tension either.

A library of well-defined P(VOH-s-VAc) with different DPs and HDs was synthesized and presented in the previous sections.

The questions now are:

- Are these Mowiol-like copolymers, with lower molar masses and lower  $\bar{D}$ s than Mowiol 4-88, able to stabilize a latex?
- Do the unimers formed by these well-defined P(VOH-s-VAc) behave differently when used in emulsion polymerization compared to those formed from Mowiol 4-88?
- Is it possible to better control the nucleation mechanism induced by a well-defined stabilizer?

These questions will be addressed in the next section, where the stabilization efficiency of the different P(VOH-s-VAc) (with different HD ad DP) will be evaluated and compared to that of Mowiol 4-88.

## V. Emulsion copolymerization of VAc and VeoVa stabilized with Mowiol 4-88 and the RAFT/MADIX-synthesized P(VOH-s-VAc).

Budhlall *et al.*<sup>[65]</sup> and Carrà's<sup>[66]</sup> groups pushed the study of the organization of different grades of industrial P(VOH-s-VAc) further, to understand how the copolymer partakes in the emulsion polymerization kinetics. Indeed, the grafting reactions that occur on the stabilizer with VAc polymerization influence both particle nucleation and stabilization, in ways that were not completely understood. P(VOH-s-VAc) is also a major source of reproducibility issues coming from the synthesis route (macromolecular properties can vary widely in FRP from one batch to another). The authors highlighted that industrial-grades often present wide variations of macromolecular properties, particularly stereoregularity, intermolecular distribution of acetyl content,  $\beta$  value, broadness of molar mass distribution, and frequency of long-chain and short-chain branching.

No correlation was found between the rate of polymerization and the blockiness index of the stabilizer. Similarly, the number of particles ( $N_p$ ) was independent of the blockiness index. Grafted fraction also remained relatively constant regardless of  $\beta$ , and therefore the structure of P(VOH-s-VAc) did not seem to have a great effect on the chemistry of the process. The major difference was found to be the physically adsorbed fraction of stabilizer with respect to its structure: the amount of adsorbed P(VOH-s-VAc) was found to increase markedly with blockiness. This dependence could be explained in terms of the better stabilizing properties of the highly blocky P(VOH-s-VAc) grade, and greater affinity towards the particle surface (due to tails and loops structure).

One should keep in mind that besides the structure of the stabilizer, its specific organization in water will of course influence its stabilizing ability.

As highlighted in **Chapter I**, the kinetics of the emulsion polymerization of VAc is not trivial and follows a particular path when compared to systems in which more hydrophobic monomers are involved. Indeed, due to its high solubility in water, and because of transfer reactions occurring during its polymerization, VAc leads to the formation of oligoradicals that can migrate out of a polymer particle. This could induce a variation in the average number of radical per particle during the second stage of the polymerization ( $\bar{n} < 0.5$  or  $\bar{n} > 1$ ), and subsequently affect the kinetic profile of the polymerization.

When a macromolecule such as P(VOH-s-VAc) is used as stabilizer, the kinetics of the polymerization may also be impacted. This was related to the microstructure of the stabilizer and thus, its micellization efficiency. Budhlall *et al.*<sup>[65]</sup> investigated the influence of three different commercial P(VOH-s-VAc) with similar molar masses and HD, but different  $\beta$  values,

on the rate of polymerizations of VAc, initiated by potassium persulfate (KPS) ( $Sc = 10\%$ ). The polymerizations were carried out at  $60\text{ }^\circ\text{C}$  in a 1 L reactor equipped with a baffle and turbine impeller. The authors noted that there was no constant rate period in the evolution of the conversion with time, but that a maximum in the rate ( $R_{p\text{max}}$ ) was obtained at about the same conversion for all the experiments (26 – 28% conversion).

Another characteristic observed in the  $R_p$  curves for all the experiments was a plateau between about 50 and 75% conversion. They attributed this to the fact that they worked at low solids content, and that in these conditions and at these conversions, VAc partitions substantially between the aqueous and particle phases, which decreased the monomer concentration in the particles ( $[M]_p$ ), resulting in an increase in  $\bar{n}$  (correlated to an increase of the viscosity), thus increasing  $R_p$ . They also noted an evolution of  $N_p$  with conversion for all the P(VOH-*s*-VAc), indicating the existence of continuous nucleation. Nevertheless, no obvious relationship between  $R_p$  and  $N_p$  was obtained, and rates of polymerization were found to be relatively independent of the P(VOH-*s*-VAc) type. The final particle size distribution, for all the polymerizations were multimodal (particle diameter ranging from 20 to 100 nm), with limited coagulation. Nevertheless, it appeared that a larger fraction (number) of small particles was detected in the latexes stabilized with blockier P(VOH-*s*-VAc), which was considered as evidence that a blockier stabilizer possesses better emulsifier properties and is therefore able to stabilize more new particles. Finally, the authors evaluated the proportion of grafted P(VOH-*s*-VAc) with conversion. They observed a clear dependence between the amount of grafted P(VOH-*s*-VAc) and the grade of P(VOH-*s*-VAc) used: the higher the  $\beta$  value of the P(VOH-*s*-VAc), the lower the amount of grafts.

The authors attributed this observation to the fact that the P(VOH-*s*-VAc) with the highest  $\beta$  value would adsorb faster and more strongly at the surface of the nucleated particles and thus would reside a shorter time in the aqueous phase, where the grafting reactions can occur. This stronger adsorption behavior for the blockier structure was already presented previously and was studied in another paper from the same group, and was attributed to the aqueous conformation of the P(VOH-*s*-VAc) in water.<sup>[59]</sup> The authors highlighted that blockier P(VOH-*s*-VAc) would contain longer PVAc sequences compared to a less blocky P(VOH-*s*-VAc), and that the former would organize in water under the form of aggregates, with the VAc-rich core surrounded by VOH-rich loops and tails. By contrast, a less blocky P(VOH-*s*-VAc) would have a more extended conformation in the aqueous phase. These different conformations were directly correlated to the micellization efficiency of the P(VOH-*s*-VAc) and it was postulated that the structure able to form dense aggregates was more surface active than the more extended macromolecule.

Continuous nucleation in batch emulsion polymerization of VAc using P(VOH-*s*-VAc) as stabilizer was also reported by Herrera's group.<sup>[67]</sup> The authors showed that depending on the experimental conditions, unexpected secondary nucleation in the batch emulsion



polymerization of VAc might occur. They developed a mathematical model where this phenomenon was attributed to the existence of a steric barrier induced by the macromolecular stabilizer, which affects the oligoradical entry into the polymer particles, thus favoring the formation of new particles by homogeneous nucleation (**Figure II-24**).

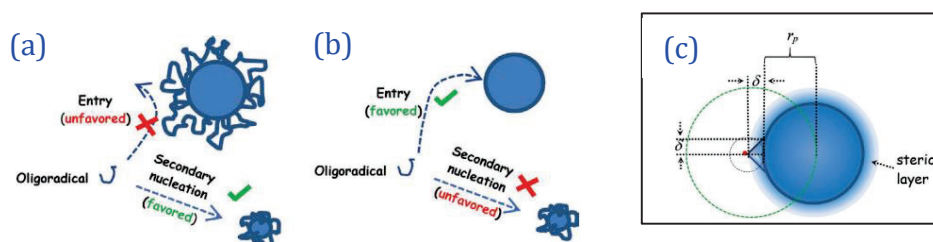


**Figure II-24: Scenarios for secondary nucleation and free-radical capture in particles for the emulsion polymerization of VAc in the presence of P(VOH-s-VAc) (a) with steric barrier or (b) without steric barrier. (c) Schematic representation of the particle geometry for mathematical modeling of an oligoradical passing through a steric barrier to collide with a particle.  $\delta$  = thickness of the steric layer. Adapted from ref [67] with permission from the publisher.**

The authors estimated the thickness of the steric barrier  $\delta$  through the root-mean-square end-to-end distance of a P(VOH-s-VAc) chain (in a good solvent), based on Hiemenz and Rajagopalan's calculations.<sup>[68]</sup> According to **Equation 20**, they found that  $\delta = 7.15$  nm for a P(VOH-s-VAc) with molar mass in the range 13 000 – 23 000 g mol<sup>-1</sup> (they set  $M_w = 18$  000 g mol<sup>-1</sup> as an average for the calculation).

$$\delta = 2 \cdot l \cdot \sqrt{DP} \quad (20)$$

With DP the degree of polymerization and  $l$  the length of the repeating unit, (about 0.25 nm for vinyl monomers). The term 2 accounts for angle restriction.<sup>[68]</sup>

Secondary nucleation was also highlighted by Agirre *et al.*<sup>[69]</sup> for the semi-continuous emulsion copolymerization of VAc and VeoVa using ascorbic acid/*tert*-butyl hydroperoxide (AsAc/TBHP) as redox initiating system, and by Donescu *et al.*<sup>[70]</sup> for the semi-continuous emulsion polymerization of VAc using hydrogen peroxide/iron(II) sulfate, both in the presence of P(VOH-s-VAc).

Finally, Lepizzera and Hamielec<sup>[71]</sup> highlighted the obtention of a bimodal PSD during the seeded emulsion polymerization of VAc using P(VOH-s-VAc) as stabilizer, thus highlighting the occurrence of a secondary nucleation. The authors compared the influence of two types of commercial P(VOH-s-VAc) with different molar masses ( $M_w = 26$  000 and 103 000 g mol<sup>-1</sup>), but similar HD (88%), and showed that the nucleation was more efficient when the P(VOH-

s-VAc) with the higher molar mass was used. They thus postulated that the propagating radical of a grafted P(VOH-s-VAc) (P(VOH-s-VAc)-*graft*-PVAc<sup>•</sup>) formed after transfer onto P(VOH-s-VAc) during the emulsion polymerization of VAc had a smaller diffusion coefficient than PVAc<sup>•</sup> propagating (oligo)radicals. Therefore, its rate of capture by seed particles is lower than that of PVAc<sup>•</sup> oligoradicals (and that of primary radicals). At some point, when the graft of PVAc reaches a certain size such that the overall structure of P(VOH-s-VAc)-*graft*-PVAc<sup>•</sup> is not soluble in water anymore, it will precipitate, leading to secondary nucleation. Thus, high molar masses P(VOH-s-VAc) with lower diffusion coefficient will most likely nucleate more particles than the low molar masses ones. The authors also demonstrated that the higher the initial P(VOH-s-VAc) load, the higher the number of particles nucleated.

To the best of our knowledge, no work has been published in the literature concerning latex stabilization with well-defined and low molar masses P(VOH-s-VAc)s. The aim of this study was thus to test the ability of the library of well-defined amphiphilic copolymers synthesized in the previous sections, to produce a latex, and determine the amount of absorbed and grafted stabilizer onto the particles, depending on the DP, HD and concentration of stabilizer in the emulsion polymerization system. These stabilizers were compared to the commercial grade of P(VOH-s-VAc) (Mowiol 4-88), which has a broader molar mass distribution and higher average molar mass.

### **V.1 Set up of the experimental parameters for the emulsion copolymerization of VAc and VeoVa**

At first, a few emulsion copolymerizations of VAc and VeoVa (with a fixed composition of 20 wt.% VeoVa and 80 wt.% VAc) were performed, using Mowiol 4-88 (**Table II-7**). The aim was to get used to the process and to develop reference experiments, which will then allow for a fair evaluation and comparison of the various VOH-based polymers as stabilizers.

Wacker provided a semi-batch protocol, in which the initiator is the AsAc/TBHP redox couple, the targeted solid content is 53 wt.% and the final latex volume is 1 L.  $1.15 \times 10^{-4}$  and  $6.72 \times 10^{-5}$  wt.% (based on monomers) of AsAc and TBHP respectively were used in this protocol.

This protocol was thus adapted to a 75 mL reactor targeting a solid content of 20 wt.% without feed of monomers but keeping similar AsAc/TBHP fractions as in Wacker's protocol. AsAc was introduced into the reactor with water, monomers and Mowiol 4-88, while a solution of TBHP was fed into the polymerization medium with a pump over a 50 min period, Polymerizations were stopped after 2 h. The detailed protocol is described in the **Experimental Section V.2**. The monomer conversion was followed by gravimetry. The



diameters of the particles and their distribution in the final latex were characterized by DLS and cryo-TEM.

**Table II-7: Emulsion copolymerizations of VAc and VeoVa carried out with Mowiol 4-88 as stabilizer.**

Entry *	Wt.% Stabilizer	Wt.% AsAc / wt.% TBHP (based on monomers)	Z <sub>av</sub> (nm) <sup>a</sup>	PdI <sup>a</sup>
<b>ER-Mowiol-0</b>	0	1.15 x 10 <sup>-4</sup> / 6.27 x 10 <sup>-5</sup>	-	-
<b>ER-Mowiol-1</b>	5	1.15 x 10 <sup>-4</sup> / 6.27 x 10 <sup>-5</sup>	260	0.03
<b>ER-Mowiol-2</b>	7	1.15 x 10 <sup>-4</sup> / 6.27 x 10 <sup>-5</sup>	195	0.02

\* ER refers to redox-initiated emulsion polymerization and is followed by the name of the stabilizer used in the experiment, and the label of the experiment

<sup>a</sup> Determined by DLS

Polymerizations were carried out at 55 °C for 2 h. Sc = 20%, with fixed composition of 20 wt.% VeoVa and 80 wt.% VAc

Emulsion polymerization **ER-Mowiol-0** (Table II-7) was carried out as a reference, without stabilizer, to verify that no stabilization could be ensured without stabilizer. This experiment provided a precipitate with two distinct phases: the polymer and the water, confirming that a stabilizer was required in this polymerization system to provide a stable dispersion.

Emulsion polymerization **ER-Mowiol-1** provided a stable latex that however sedimented after a few days, meaning that with this experimental set up, 5 wt.% of stabilizer was not sufficient to ensure a good stability of the dispersion. **ER-Mowiol-2** (7 wt.% of Mowiol 4-88 based on monomers) provided a white fluid latex after 50 min and reached 80% conversion after 2 h (Figure II-25). The average particle size was 195 nm, with a low polydispersity (Table II-7). Some coagulum (1 wt.% with respect to the latex) formed on the stirring anchor during the polymerization, but this did not impact the kinetics and did not lead to any further destabilization of the latex.

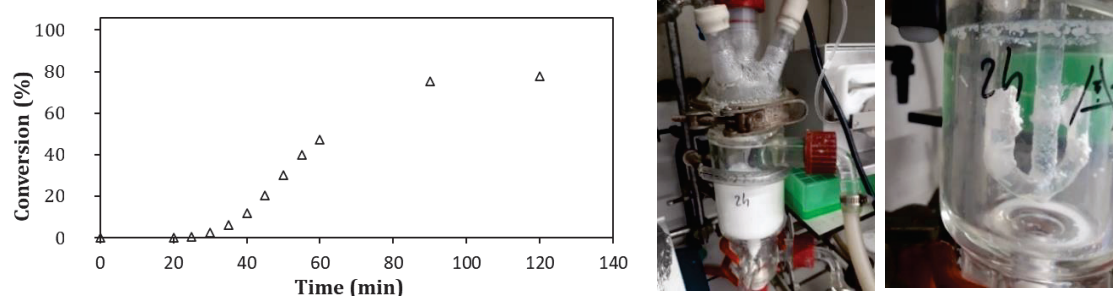


**Figure II-25: Conversion versus time plot for ER-Mowiol-2 experiment (Table II-7) and visual aspect of the final latex and aggregates.**

Once the experimental conditions were established, Mowiol 4-88 was replaced by the RAFT/MADIX-synthesized 100\_P(VOH<sub>0.88</sub>-s-VAc<sub>0.12</sub>) (Table II-8).

**Table II-8 : Set up of the experimental parameters for the emulsion copolymerization of VAc and VeoVa with the RAFT-synthesized P(VOH-s-VAc).**

Entry *	Stabilizer	Wt.% Stabilizer	Wt.% AsAc / wt.% TBHP (based on monomers)
ER-100_PVOH-1	100_P(VOH <sub>0.88</sub> -s-VAc <sub>0.12</sub> )	7	0.0110 / 0.0067
ER-100_PVOH-2	100_P(VOH <sub>0.88</sub> -s-VAc <sub>0.12</sub> )	10	0.0110 / 0.0067
ER-100_PVOH-3	100_P(VOH <sub>0.88</sub> -s-VAc <sub>0.12</sub> )	10	0.046 / 0.027
ER-100_PVOH-4	100_P(VOH <sub>0.88</sub> -s-VAc <sub>0.12</sub> )	10	0.092 / 0.054
ER-Mowiol-3	Mowiol 4-88	10	0.092 / 0.054

\* ER refers to redox-initiated emulsion polymerization and is followed by the name of the stabilizer used in the experiment, and the label of the experiment. 100\_P(VOH<sub>0.88</sub>-s-VAc<sub>0.12</sub>) was shortened to 100\_PVOH

Polymerizations were carried out at 55 °C for 2 h. Sc = 20%, with fixed composition of 20 wt.% VeoVa and 80 wt.% VAc

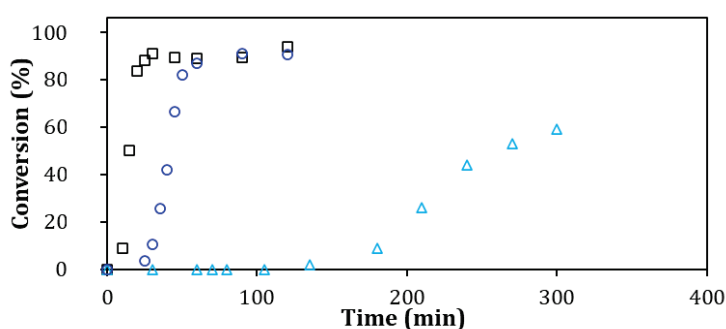


**Figure II-26: Conversion versus time curves for emulsion copolymerization of VAc and VeoVa adapted from Wacker's protocol. ( $\Delta$ ) ER-100\_PVOH-3; ( $\circ$ ) ER-100\_PVOH-4 and ( $\square$ ) ER-Mowiol-3.**

Emulsion polymerizations were first carried out with 7 wt.% of 100\_P(VOH<sub>0.88</sub>-s-VAc<sub>0.12</sub>) and similar ratio of AsAc/TBHP as above (respectively 0.011 and 0.062 wt.% based on monomers) (Table II-8, ER-100\_PVOH-1). However, no conversion occurred even after 24 h. Therefore, the amount of stabilizer was increased to 10 wt.%, keeping AsAc and TBHP content the same (Table II-8, ER-100\_PVOH-2). Again, no conversion occurred after 24 h. Thus, the amount of AsAc was set to 0.046 wt.% (4 times the initial amount) and further to 0.092 wt.% (8 times the initial amount) (both with 10 wt.% of 100\_P(VOH<sub>0.88</sub>-s-VAc<sub>0.12</sub>)) to eventually observe 60% conversion after 6 h and about 90% conversion after 1 h, respectively (Figure II-26 and Table II-8, ER-100\_PVOH-3 and ER-100\_PVOH-4).

The presence of an induction period for the experiments performed with 100\_P(VOH<sub>0.88</sub>-s-VAc<sub>0.12</sub>) is not well understood. Possible explanations are: (i) the well-defined P(VOH-s-VAc) copolymers are less efficient stabilizers (ii) the presence of some water-soluble inhibitor or retarder such as methanol, acetaldehyde or thiol (which could be present at the extremities of the RAFT-obtained P(VOH-s-VAc)), that are by-products coming from the hydrolysis step. These by products could act as transferring agents in the emulsion copolymerization of VAc and VeoVa, providing radicals that are less reactive (or not reactive at all) compared to the propagating oligoradicals, leading to a degradative transfer and loss of reactivity.<sup>[71-73]</sup> To

overcome these limitations, more initiator must be fed inside the polymerization medium. The new initiator ratio (0.092 wt.% based on monomers) will be kept as the reference for the next experiments.

The emulsion copolymerization of VAc with VeoVa, stabilized with 10 wt.% Mowiol 4-88 was carried out again with this new amount of initiator as a reference experiment (**Table II-8, ER-Mowiol-3**). A fluid white latex was obtained after 30 min. **Figure II-26** shows the kinetic profile obtained for the different experiments.

The rate of polymerization ( $R_p$ ) was defined in **Chapter I, Section II.2.2**.  $R_p$  is (among other parameters) proportional to the monomer consumption.  $S_{max}$  was determined as the slope of the conversion-time plot obtained by gravimetric analysis, in the area where the conversion evolves linearly with time (**Table II-9** and **Figure II-27**). This value provides indirect information on the rate of polymerization, and therefore, on the efficiency of the stabilizer.

**Table II-9: Emulsion copolymerization of VAc and VeoVa, stabilized with 10 wt.% (based on monomers) of either Mowiol 4-88 or 100\_P(VOH<sub>0.88</sub>-s-VAc<sub>0.12</sub>).**

Entry	$S_{max}$ (s <sup>-1</sup> )	$Z_{av}$ (nm)	PdI
ER-Mowiol-3	0.075	150	0.02
ER-100_PVOH-4	0.037	240	0.1

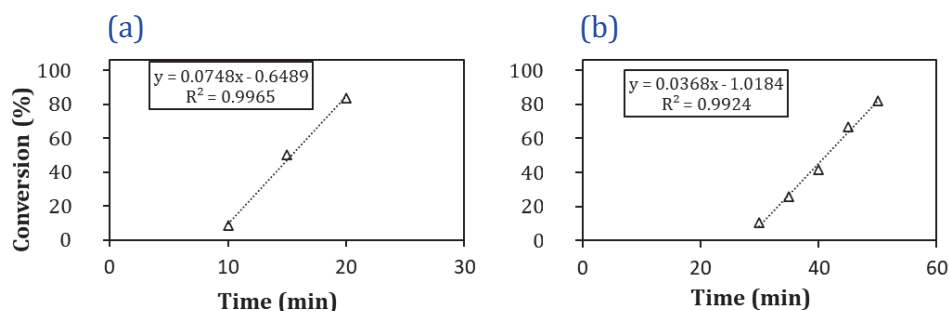


**Figure II-27: Conversion versus time plot in the linear region, for the latexes stabilized with (a) Mowiol 4-88 and (b) 100\_P(VOH<sub>0.88</sub>-s-VAc<sub>0.12</sub>), to determine the  $S_{max}$ .**

**Table II-9** shows that the monomer consumption was faster with Mowiol 4-88 than with 100\_P(VOH<sub>0.88</sub>-s-VAc<sub>0.12</sub>), and that the size of the particles was smaller for the latex **ER-Mowiol** than that of the latex obtained with the RAFT-synthesized 100\_P(VOH<sub>0.88</sub>-s-VAc<sub>0.12</sub>) (193 versus 240 nm, respectively). The mechanism of nucleation and stabilization efficiency likely differs from one system to the other. It is worth mentioning that Mowiol 4-88 has a broad dispersity. Therefore, a large panel of chains having different molar masses is involved in the stabilization process, and this heterogeneity has already proven to be beneficial in some processes.<sup>[25]</sup> The dispersed state of the stabilizer in water can also play a role. It

remains however difficult to assign the observed kinetic difference to a specific characteristic of the stabilizer employed at this stage.

Well-defined P(VOH-*s*-VAc) obtained by RAFT/MADIX polymerization with different molar masses and hydrolysis degrees were then investigated as stabilizer candidates.

## V.2 Influence of the hydrolysis degree at fixed DP = 75 and fixed amount of stabilizer (10 wt.% based on monomers)

As presented in **Section III.3** several P(VOH-*s*-VAc) were synthesized with either different DP and/or HD. All of them were dispersible in water at R.T. after a few minutes and provided transparent solutions. In this section the influence of the HD on the characteristics of the polymer particles in the resulting latex (*i.e.*,  $Z_{av}$ , PDI and adsorption and grafting efficiency of the stabilizer) is investigated, at fixed DP = 75 and fixed amount of stabilizer (10 wt.%). The emulsion copolymerizations were performed with 75\_P(VOH<sub>0.88</sub>-*s*-VAc<sub>0.12</sub>), 75\_P(VOH<sub>0.91</sub>-*s*-VAc<sub>0.09</sub>), 75\_P(VOH<sub>0.94</sub>-*s*-VAc<sub>0.06</sub>) and 75\_P(VOH<sub>0.97</sub>-*s*-VAc<sub>0.03</sub>). The experiments were carried out following the protocol described in the **Experimental Section V.2**.

**Figure II-28** gathers the features of the 4 latexes obtained. The particle size and PDI was determined by DLS. The amount of adsorbed and grafted stabilizer onto the particles was determined after ultracentrifugation as described in **Experimental Section VI.8**. In the following, the amount of adsorbed stabilizer will be defined as the amount of stabilizer that is strongly adsorbed at the surface of the polymer particles (original P(VOH-*s*-VAc)), while the grafted stabilizer will refer to the stabilizer that has been chemically grafted by VAc during the emulsion polymerization process (modified P(VOH-*s*-VAc) by grafting). As explained in **Chapter I** and previously in the introduction of this Section, the fractions of both the unmodified and modified P(VOH-*s*-VAc) participate to the stabilization and will be found at the particle surface at the end of the polymerization. Ultracentrifugation provides a fair evaluation of the free P(VOH-*s*-VAc) that remained in the aqueous phase and did not participate to the stabilization. It is thus possible to determine the total fraction of grafted and adsorbed stabilizer that effectively participated to the stabilization of the latex *via* this method. However, the distinction between the grafted and adsorbed fractions is not possible, and would require the use of selective solubilization of the two fractions,<sup>[74]</sup> which is time consuming and was not considered as relevant for this thesis.

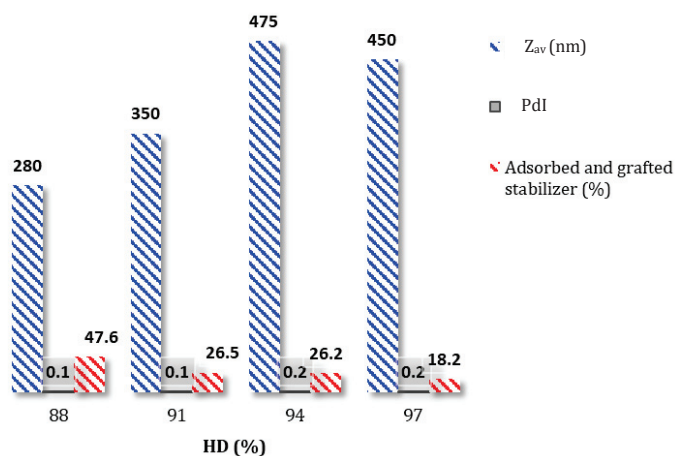


**Figure II-28: Main characteristics of the latexes stabilized with the well-defined 75\_P(VOH-s-VAc)s with different HDs.**

For the same reaction time (2 h), **Figure II-28** shows that the higher the HD, the larger the particles and simultaneously, the lower the amount of adsorbed and grafted stabilizer. Usually, both adsorption and grafting participate to the stabilization of the polymer particles, but that adsorption plays a major role into it. It is now well established that grafting sites where transfer reactions take place on the stabilizer (and thus reinitiation can happen), is more likely the methyl protons from the VAc units.<sup>[75]</sup> This grafting renders the stabilizer amphiphilic and allows it to become surface active and stabilize the particles. As the HD increases, there are therefore fewer grafting sites and when transfer and reinitiation take place, the corresponding growing PVAc graft radicals require several more hydrophobic units to be added to give the overall structure enough surface activity. In this case, the stabilization is probably mostly provided by adsorption of the stabilizer onto the particle. Additionally, the higher the HD, the smaller the PVAc sequences that are responsible of the pre-assembly of the stabilizer in water and provide a site for particle nucleation. The PVAc sequences are also responsible for the strong adsorption of the stabilizer at the surface of the particles. Therefore, the stabilizer is both less strongly anchored and adsorbed to the particles, and is most likely within the aqueous phase, which can explain the increase in the particle size for the latexes stabilized with stabilizer with high HD. Partial destabilization of the latexes was observed during storage when the HD was higher than 91%.

### **V.3 Influence of the polymerization degree at fixed HD = 88% and fixed amount of stabilizer (10 wt.% based on monomers)**

Based on the previous section, it was found that a P(VOH-s-VAc) with HD = 88% provided optimum adsorption and grafting onto the polymer particle with the highest conversion. In

this section, the influence of the DP of the stabilizer onto the characteristics of the polymer particles forming the latex was investigated, at fixed HD of 88%.

Emulsion polymerizations with a fixed amount of 10 wt.% (based on monomers, 2.5 wt.% based on the total weight) of 75\_P(VOH<sub>0.88-s</sub>-VAc<sub>0.12</sub>), 100\_P(VOH<sub>0.88-s</sub>-VAc<sub>0.12</sub>) and 200\_P(VOH<sub>0.88-s</sub>-VAc<sub>0.12</sub>) were performed. This implies that the higher the DP, the lower the initial number of stabilizer macromolecules. These latexes were characterized by DLS, cryo-TEM and the amount of adsorbed and grafted stabilizer was determined after ultracentrifugation. In addition, the evolution of pH upon storage was followed for four weeks at pH 4, 6, 8, 10 and 12.

From now on and simplicity's sake, experiments **ER-Mowiol-3** and **ER-100\_PVOH-4** will be designed as **ER-Mowiol 4-88** and **ER-100\_PVOH**.

### V.3.1 Kinetics of the polymerizations and colloidal features

The kinetics of the polymerizations were followed gravimetrically (**Figure II-29**).

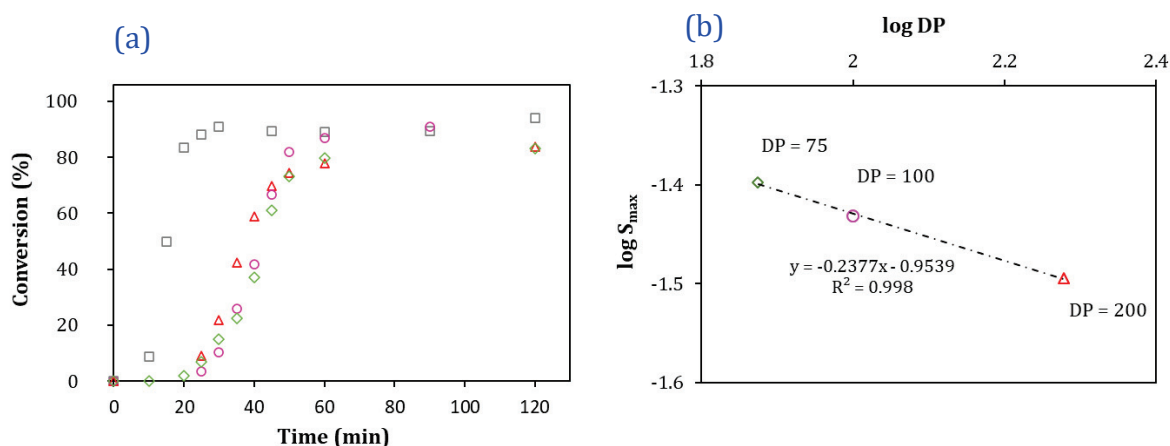


**Figure II-29 : (a)** Kinetics of the emulsion copolymerization of VAc with VeoVa, stabilized with 10 wt.% of (□) Mowiol 4-88; (◇) 75\_P(VOH<sub>0.88-s</sub>-VAc<sub>0.12</sub>); (○) 100\_P(VOH<sub>0.88-s</sub>-VAc<sub>0.12</sub>) and (△) 200\_P(VOH<sub>0.88-s</sub>-VAc<sub>0.12</sub>). **and (b)** plot of S<sub>max</sub> as function of the DP for these experiments.

Typically, for the systems stabilized with the well-defined P(VOH-s-VAc), conversion *versus* time curves exhibit a short induction period (of approximately 20 min), followed by a rapid increase in the polymerization rate, and high conversions (up to 85%) was reached after 1 h (**Figure II-29, (a)**). The curves appear to become nearly linear between 25 to 45 min, which could be interpreted as a constant rate period.



The evolution of the particle size (and PDI), and consequently of  $N_p$ , with time (and thus conversion) was followed by DLS. Unfortunately, the dispersity was higher than 0.1 for most of the samplings in the experiments carried out with 100\_P(VOH<sub>0.88</sub>-s-VAc<sub>0.12</sub>) and 200\_P(VOH<sub>0.88</sub>-s-VAc<sub>0.12</sub>). Therefore, the simple cumulant fitting is not accurate and more than one single population is present. In this case, the  $Z_{av}$  value was not accurate either, and its use would be irrelevant. The plot of  $N_p$ , with conversion for the system stabilized with 100\_P(VOH-s-VAc) is nevertheless available in **Appendix 3** as an illustration of this poor fit.

Nonetheless, the experiment performed with 75\_P(VOH<sub>0.88</sub>-s-VAc<sub>0.12</sub>) and Mowiol 4-88 provided PDI < 0.1 for most of the samplings, which allowed further investigation on the kinetics (**Figure II-30**).

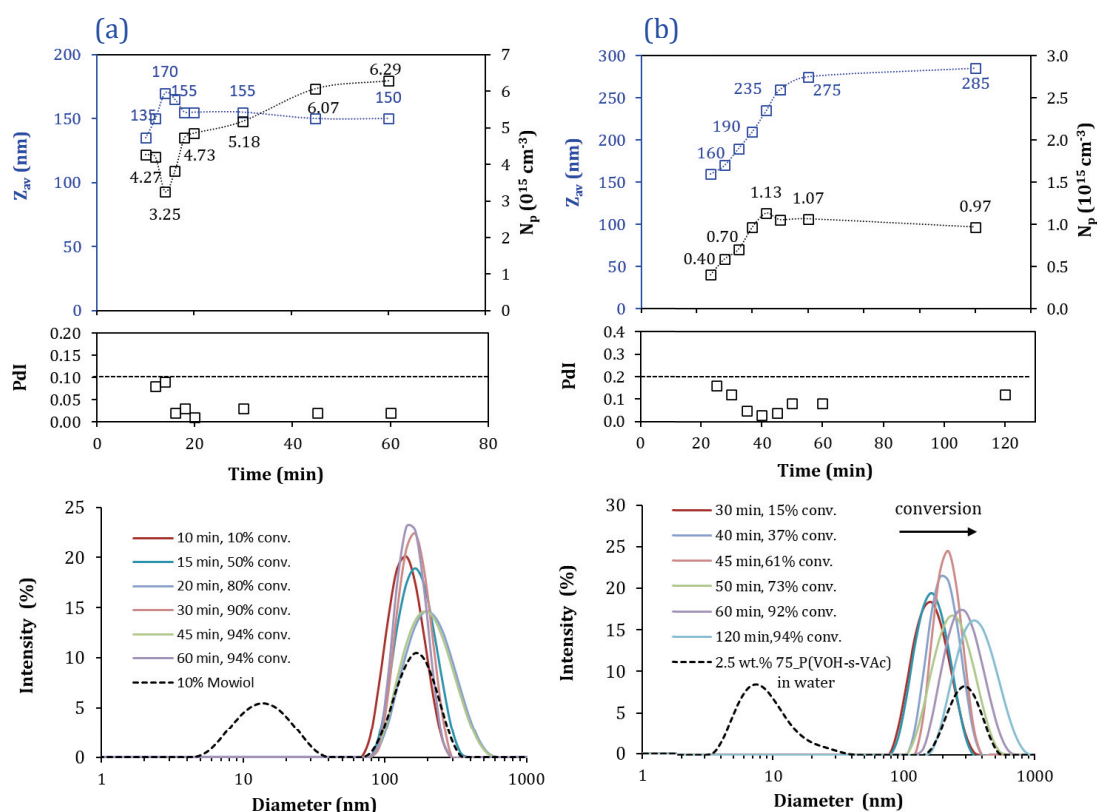


**Figure II-30: Evolution of the particle size ( $Z_{av}$ ) (blue) and of the number of particles ( $N_p$ ) (black) with time for the emulsion copolymerization of VAc and VeoVa for (a) ER-Mowiol and (b) ER-75\_PVOH, and the corresponding PDI. The evolution of the corresponding DLS-size distributions in intensity are also provided.**

**Figure II-30 (a)** shows that for the latex obtained with Mowiol 4-88,  $N_p$  decreased between 10 and 15 min (corresponding to 10 and 50% conversion, respectively) from 4.27 to 3.25  $\times 10^{15}$  particles  $\text{cm}^{-3}$ , before it increased again from 15 to 60 min (94% conversion, 6.29 to

$3.25 \times 10^{15}$  particles  $\text{cm}^{-3}$ ). This profile is similar to that observed by Herrera and coworkers,<sup>[67]</sup> thus confirming the occurrence of a secondary nucleation.

Adversely, for the latex obtained with 75\_P(VOH<sub>0.88</sub>-s-VAc<sub>0.12</sub>) (**Figure II-30 (b)**),  $N_p$  increased between 25 and 45 min (corresponding to 10 and 61% conversion, respectively) from 0.40 to  $1.13 \times 10^{15}$  particles  $\text{cm}^{-3}$  (which represent a gain of approximately  $70 \times 10^{15}$  particles  $\text{cm}^{-3}$ ). This could be attributed to a long nucleation period, and explains why the PSD of particles in the resulting latex was broad. After 60% conversion, the  $N_p$  remains relatively constant, while the  $Z_{av}$  kept increasing, which could be due to particle growth. These observations obtained from the DLS could suggest the occurrence of continuous nucleation during the polymerization stabilized by Mowiol 4-88 and the RAFT-synthesized stabilizers.

The presence of unimers in the aqueous dispersions of Mowiol 4-88 and 75\_P(VOH<sub>0.88</sub>-s-VAc<sub>0.12</sub>) observed by DLS in **Section IV.1** were no more visible in the samples withdrawn from the polymerization medium during the reaction (**Figure II-30**).

Additionally, **Figure II-29 (a)** and **Figure II-30** showed that the inhibition period was longer, and that the final  $N_p$  was lower for the RAFT-synthesized stabilizer compared to Mowiol 4-88. This behavior could indicate that the well-defined P(VOH<sub>0.88</sub>-s-VAc<sub>0.12</sub>) are less surface active compared to Mowiol 4-88. The comparison of both systems is nevertheless not straightforward because the nature of the stabilizers is much different. Indeed, Mowiol 4-88 has a high  $\bar{D}$  and an average DP of approximately 550, while the P(VOH-s-VAc) obtained by alcoholysis of the RAFT-synthesized PVAc have all similar  $M_n$  (low  $\bar{D}$ ) and low DP ranging from 75 to 200. The only common feature between these systems is their average HD, blockiness index and average length of PVOH sequences.

Nevertheless, in light of these results, it seems that high dispersity of the stabilizer could be beneficial for an efficient stabilization. More precisely, it is likely that it exists a synergy between adsorption and grafting, provided by the different molar masses of the P(VOH-s-VAc). Budhlall postulated that adsorption played a key role in the stabilization of the particles, but that grafting was also important.<sup>[32]</sup> It is thus possible that the long P(VOH-s-VAc) chains from Mowiol 4-88 are more prone to adsorb thanks to numerous PVAc sequences, while the short chains are more sensitive to grafting, because small grafts are required before they become hydrophobic enough (approximately HD = 82%)<sup>[76]</sup> to be surface active. In that context we hypothesized that the RAFT-synthesized P(VOH-s-VAc) (with low  $M_n$  and low  $\bar{D}$ ) would be more prone to grafting.

Furthermore, as mentioned in the introduction of this Section, it turns out that Lepizzera and Hamielec<sup>[71]</sup> demonstrated that the propagating radicals originating from transfer reaction taking place onto P(VOH-s-VAc) had a lower diffusion coefficient compared to PVAc<sup>•</sup> oligoradicals (and to primary radicals). It could thus explain the lower nucleation efficiency of the RAFT-synthesized P(VOH-s-VAc), resulting in delayed nucleation time and lower number of particles generated compared to the latex that contains Mowiol 4-88. This could



also explain why more initiator was also required for this system compared to Mowiol 4-88. Nevertheless, this hypothesis must be considered with care as further investigation is required to conclude. For instance, it could be interesting to evaluate the fraction of adsorbed and grafted stabilizer in the latexes that contain the RAFT-synthesized P(VOH-s-VAc) *via* selective solubilization of the two fractions as developed by El-Asser and coworkers.<sup>[74]</sup>

$S_{max}$  values of all the experiments were determined from the kinetics and correspond to the section where the slope is (nearly) linear. The values are reported in **Table II-10**, while a dependence of the DP of the stabilizer on the  $S_{max}$  values of the systems was highlighted in **Figure II-29 (b)**. It was observed that  $S_{max}$  depends on the DP to the power -0.25. This could be explained by the fact that longer chains require longer grafts before they become insoluble in water and therefore before they become surface active. Moreover, this could also be due to the fact that for similar wt.% of stabilizer introduced in the reactor, the number of chains (available for the stabilization) decreases of a factor 1.7 from DP = 200 to DP = 75. The dependence of the  $R_p$  with the molar mass of P(VOH-s-VAc) was also observed by Lepizzera<sup>[71]</sup> and Budhlall.<sup>[32]</sup> For instance, Budhlall *et al.* compared the  $R_p$  of two commercial P(VOH-s-VAc) (Poval 217, DP = 1750 and Poval 205, DP = 480) in batch emulsion polymerization of VAc. They highlighted a longer induction period and lower  $R_p$  when the polymerization was carried out with the P(VOH-s-VAc) of low molar mass (Poval 205), and concluded that Poval 217 was thus a better stabilizer.

**Table II-10:  $S_{max}$  values determined from the kinetics of the emulsion polymerizations stabilized with 10 wt.% (based on monomers) of the RAFT-synthesized P(VOH<sub>0.88</sub>-s-VAc<sub>0.12</sub>), with different DPs or with Mowiol 4-88.**

Entry	Stabilizer (10 wt.% based on monomers)	$S_{max}$ (s <sup>-1</sup> )	R <sup>2</sup>
ER-Mowiol	Mowiol 4-88	0.075	0.996
ER-75_PVOH	75_P(VOH <sub>0.88</sub> -s-VAc <sub>0.12</sub> )	0.040	0.994
ER-100_PVOH	100_P(VOH <sub>0.88</sub> -s-VAc <sub>0.12</sub> )	0.037	0.992
ER-200_PVOH	200_P(VOH <sub>0.88</sub> -s-VAc <sub>0.12</sub> )	0.032	0.999

Considering these results, it seems that broad molar mass distribution and high DP (provided by Mowiol 4-88) are more beneficial for the stabilization efficiency of P(VOH-s-VAc) than well-defined structure with similar  $M_n$  and low  $\bar{D}$  (The RAFT-synthesized P(VOH-s-VAc)).

With a fixed amount of 10 wt.% of stabilizer, it was expected that the higher the DP, the smaller the particles, as the surface coverage of the particle should be more efficient. The results obtained from DLS did not follow this hypothesis. Nevertheless, due to the high PSD, the  $Z_{av}$  provided by DLS is not accurate. Indeed, DLS struggles to cope with polydispersity as big particles hinder the small ones, which may distort the average particle diameter of the

particles in the latex. The samples were thus analyzed by cryo-TEM which provided an average diameter in number and a polydispersity index (**Table II-11**).

**Table II-11: Particle size comparison from the latexes ER-Mowiol; ER-75\_PVOH; ER-100\_PVOH and ER-200\_PVOH obtained by DLS and cryo-TEM.**

Entry	$Z_{av}$ (nm) <sup>a</sup>	PdI <sup>a</sup>	$D_n$ (nm) <sup>b</sup>	$D_v$ (nm) <sup>b</sup>	$D_w/D_n$ <sup>b</sup>	$N_p$ ( $10^{15}$ cm <sup>-3</sup> ) <sup>c</sup>
ER-Mowiol	150	0.05	145	150	1.07	7.3
ER-75_PVOH	285	0.07	240	250	1.20	1.4
ER-100_PVOH	240	0.10	185	205	1.20	2.0
ER-200_PVOH	255	0.10	185	215	1.40	1.6

<sup>a</sup> Obtained by DLS

<sup>b</sup> Obtained by cryo-TEM

<sup>c</sup> Calculated via **Equation 49**

Noteworthy, the average particle size provided by DLS was systematically higher than that obtained by cryo-TEM analysis, because the measurements takes the stabilizing layer into account, while this is not the case for the cryo-TEM.

Nevertheless, cryo-TEM pictures confirmed both the suspected broad PSD of the particles stabilized with the RAFT-synthesized P(VOH-*s*-VAc), and the expected trend where the average particle size decreases with the molar mass of the stabilizer ( $D_n = 240$  nm, 185 nm and 185 nm, respectively for the latexes stabilized with 75\_P(VOH<sub>0.88</sub>-*s*-VAc<sub>0.12</sub>), 100\_P(VOH<sub>0.88</sub>-*s*-VAc<sub>0.12</sub>) and 200\_P(VOH<sub>0.88</sub>-*s*-VAc<sub>0.12</sub>)( **Table II-11**).

It can also be noted that when the DP of the P(VOH-*s*-VAc) increases, the polydispersity also increases (**Figure II-31**). This might explain why the DLS results are surprising. The number of particles was not significantly affected by the DP of the stabilizer for the emulsion polymerization stabilized with the well-defined P(VOH-*s*-VAc) (approximately  $1.4$  to  $2 \times 10^{15}$  cm<sup>-3</sup>), while it was about seven times this amount for the latex obtained with Mowiol 4-88. This is consistent with the previous observations from the kinetics, where the stabilization efficiency of Mowiol 4-88 was better than that of the RAFT-synthesized P(VOH-*s*-VAc). Nevertheless, the values of  $N_p$  must once again be considered with care because the calculations are affected by the uncertainty on the average diameter, due to the broad particle size distribution.

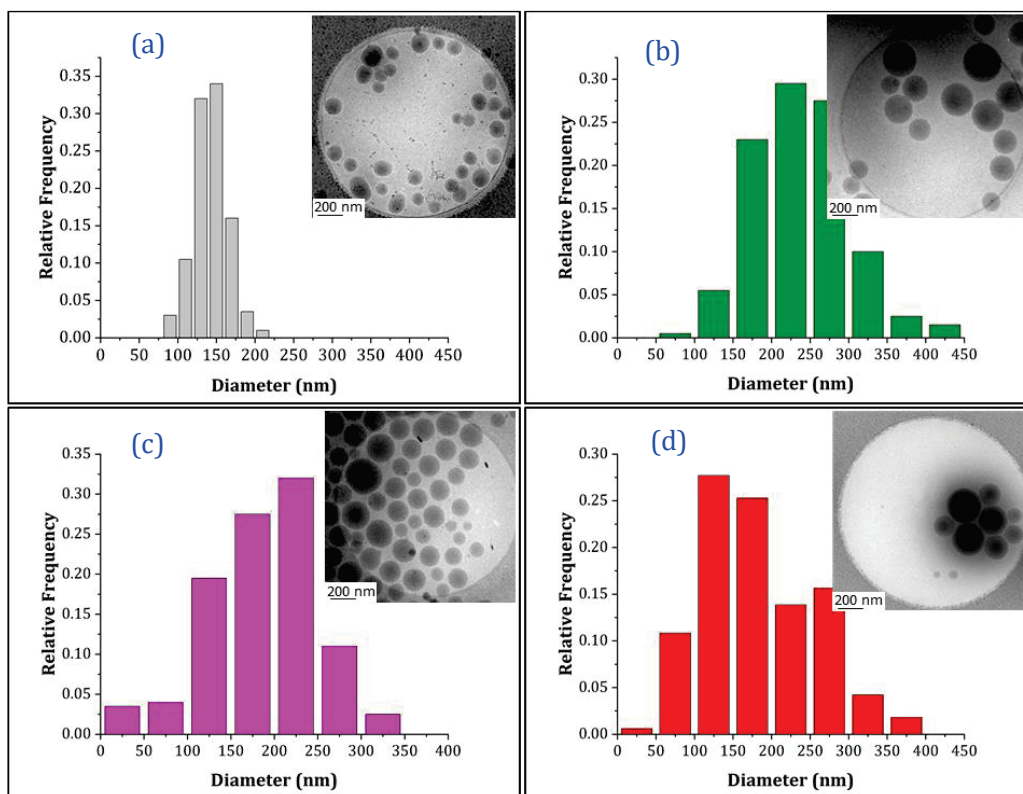


Figure II-31: Particle size distribution (PSD) obtained by cryo-TEM out of 200 particles and cryo-TEM pictures of the latexes (a) ER-Mowiol ; (b) ER-75\_PVOH; (c) ER-100\_PVOH and (d) ER-200\_PVOH; Scale bar = 200 nm.

Both **Figure II-31** and **Table II-11** show that the PSD was slightly broader in **ER-200\_PVOH** than in **ER-100\_PVOH** and **ER-75\_PVOH**, with a higher fraction of small particles, which could traduce better emulsifier properties for 200\_P(VOH<sub>0.88s</sub>-VAc<sub>0.12</sub>), which is thus able to stabilize more new particles. As mentioned in the introduction of this Section, Herrera's group showed that the thickness of the stabilizer layer at the particle interface was proportional to its DP.<sup>[67]</sup> By transposition of their findings to the present work, a possible explanation for the increase of the polydispersity as the DP of the P(VOH-*s*-VAc) increases could be the thickening of the steric barrier, which hinders free-radical entry in particles and therefore favors the secondary nucleation. It could also be an effect of coagulation processes occurring over the course of polymerization. The DLS also provided PDI values higher than 0.1 for the samples withdrawn during the emulsion polymerizations performed with P(VOH<sub>0.88s</sub>-VAc<sub>0.12</sub>) with DP = 100 and 200, but the PDI were lower in the case of DP = 75. This observation is consistent with the previous assumption that continuous/secondary nucleation occurs when the DP increases.

### V.3.2 Adsorbed and grafted stabilizer

One of the objectives of this research work is to enhance the adsorption and grafting of the stabilizer onto PVAc-based polymer particles. Carrà *et al.*<sup>[77]</sup> performed batch emulsion polymerizations of VAc in the presence of different commercial P(VOH-s-VAc) (including Mowiol 4-88) and reported that approximately 45% of Mowiol was adsorbed and grafted onto the polymer particles (17% grafted and 28% adsorbed). The authors used the selective solubilization of the different fractions of the stabilizer in the latex (free, grafted or adsorbed) developed by El Asser and coworkers.<sup>[78]</sup> This method is time and solvent consuming, and it was decided commonly with our industrial partner that the degree of precision provided by this multi-step separation method would not be relevant for the present research work, as the aim is to determine the overall fraction of adsorbed and grafted stabilizer, without distinction between the two.

To determine the amount of adsorbed and grafted stabilizer, the latex was centrifuged two times at 60 000 rpm for 1 h and 5 °C. The supernatant was separated from the pellet, and the solid content of this supernatant was evaluated after evaporation of the water at 60 °C for 48 h. It was assumed that the strongly adsorbed and grafted stabilizer remained in the pellet, while the free stabilizer that did not participate to particle stabilization would remain in the supernatant. Besides, it is worth mentioning that Fleer *et al.*<sup>[79]</sup> showed that the adsorption of P(VOH-s-VAc) was essentially irreversible. It was also assumed that the supernatant did not contain water-soluble chains formed during the emulsion polymerization. To cross check on this last assumption, the content of the dry supernatant was analyzed by <sup>1</sup>H NMR in DMSO-d<sub>6</sub>. An example of the supernatant of the latex obtained with 75\_P(VOH<sub>0.88</sub>-s-VAc<sub>0.12</sub>) and the corresponding analysis is provided in **Appendix 4**, and confirmed that only free stabilizer was present in the supernatant.

The determination of adsorbed and grafted stabilizer was therefore carried out, as presented in **Experimental Section**, and based on **Equation 58**. The results are given in **Table II-12**. Approximately 45% of Mowiol 4-88 was adsorbed and grafted onto the polymer particles, which correlates well with Carrà's findings and validates that the ultracentrifugation method provides a fair evaluation of this amount.

The amount of grafted and adsorbed stabilizer was found to decrease with increasing DP (**Table II-12**). A possible reason for this could be that the smaller the DP, the lower the fraction of PVAc sequences. Therefore, the stabilizer would require smaller grafts of PVAc (or less grafts per chain), before it becomes too hydrophobic to remain in water, and consequently, would be more quickly surface active for the stabilization of the particles. Another hypothesis could be the presence of the aforementioned aldehyde-end group (formed after alcoholysis of the RAFT-synthesized PVAc), which is known to be a chain

transfer agent in the polymerization of VAc. Thus, there could be an effect of anchoring the stabilizer, and the lower the DP, the higher the fraction of aldehyde end-group in the system. The results also showed that the amount of grafted and adsorbed stabilizer was slightly higher when the latex was stabilized with Mowiol 4-88 (45%) than for the RAFT-synthesized 75\_P(VOH<sub>0.88</sub>-s-VAc<sub>0.12</sub>) (44%), even though the average molar mass of Mowiol 4-88 was higher than that of the RAFT-synthesized P(VOH-s-VAc). This result might come from the fact that there is a synergy between adsorption of the stabilizer at the surface of existing particles, and grafting onto the P(VOH-s-VAc), which increases the hydrophobicity of the stabilizer and allows the nucleation of new particles. It is likely that the high dispersity of Mowiol 4-88 is advantageous as it provides P(VOH-s-VAc) of different molar masses and therefore, favors both the homogeneous and the micellar nucleation modes (the latter resulting from grafting and aggregation of grafted P(VOH-s-VAc) chains, followed by radical entry).

Based on the assumption that the stabilizer that is adsorbed onto the particles does not desorb during the ultracentrifugation process, it was possible to calculate the surface area occupied per macromolecule of stabilizer ( $A_s$ ), using **Equation 21**.

$$A_s = \frac{M_n}{m_{\text{Ads\&grafted}} * N_A} * S_{\text{tot latex}} \quad (21)$$

With  $m_{\text{Ads\&grafted}} = m_{\text{stabilizer}} * \text{wt.\%Ads\&grafted}$  the mass of adsorbed stabilizer obtained from **Equation 59** in **Experimental Section VI.8**,  $N_A$  the Avogadro's number and  $S_{\text{tot latex}} = N_p * \pi * D_v^2$ . with  $D_v$  obtained by cryo-TEM. The results are given in **Table II-12**.

**Table II-12: Determination of the specific surface area occupied by one macromolecule of stabilizer on a P(VAc-co-VeoVa) particle ( $A_s$ ).**

Entry*	Stabilizer	$M_n$ (g mol <sup>-1</sup> ) <sup>a</sup>	%Ads&grafted <sup>b</sup>	$S_{\text{tot latex}}$ (x10 <sup>6</sup> cm <sup>-2</sup> ) <sup>c</sup>	$A_s$ (Å <sup>2</sup> per molecule) <sup>d</sup>
<b>ER-Mowiol</b>	Mowiol 4-88	8000	45	4.9	960
<b>ER-75_PVOH</b>	75_P(VOH <sub>0.88</sub> -s-VAc <sub>0.12</sub> )	3680	44	2.8	260
<b>ER-100_PVOH</b>	100_P(VOH <sub>0.88</sub> -s-VAc <sub>0.12</sub> )	5300	39	3.3	490
<b>ER-200_PVOH</b>	200_P(VOH <sub>0.88</sub> -s-VAc <sub>0.12</sub> )	8340	22	2.9	1 210

<sup>a</sup> Obtained by **Equation 51**

<sup>b</sup> Obtained by **Equation 58**

<sup>c</sup> Obtained by **Equation 50**

<sup>d</sup> Obtained by **Equation 61**

The  $A_s$  value obtained for Mowiol 4-88 correlates well with the value obtained by Rocha-Botello *et al.*<sup>[67]</sup> ( $A_s = 750 \text{ \AA}^2$  per molecule) and Lankveld and Liklema<sup>[80]</sup> ( $A_s = 920 \text{ \AA}^2$  per molecule) for similar grades of P(VOH-s-VAc). Nevertheless, this value must be consider as

indicative only, because it is obtained *via* **Equation 21**, which requires the  $M_n$  of the copolymer.  $M_n$  of Mowiol 4-88 is an average value but is far from accurate due to high  $\bar{D}$  (*i.e.*, 2.5 – 3). For instance, Bohorquez *et al.*<sup>[81]</sup> and Kim *et al.*<sup>[82]</sup> reported higher values:  $A_s = 2016$  and  $1880 \text{ \AA}^2$ , respectively. Nevertheless, this estimation still provides a fair mean to evaluate the surface covered by a stabilizer as a first approximation, and allows for comparison from one stabilizer to the other (especially in the case of the RAFT- synthesized P(VOH-*s*-VAc), where the  $\bar{D}$  is lower).

For the RAFT-synthesized P(VOH-*s*-VAc), the higher the molar mass, the larger the estimated surface covered per macromolecule. This is consistent with the fact that for a higher DP, the hydrophobic and hydrophilic sequences are numerous, which might provide a better deployment of the stabilizer onto the surface of the particle, and therefore, a better surface coverage. This, together with the previously highlighted lower nucleation efficiency, could also explain the observation that for a higher DP, a larger fraction of small particles was produced, even if the amount of adsorbed and grafted stabilizer was lower. Indeed, at fixed amount of stabilizer in the polymerization medium (10 wt.% based on monomers), a lower amount of stabilizer was required to efficiently stabilize the particles, and therefore, the surplus remains in the aqueous phase because it is not surface active enough to generate new particles.

### V.3.3 Evaluation of alkali resistance of the latex stored at high pH

The latexes obtained with Mowiol 4-88 and the RAFT-synthesized P(VOH<sub>0.88</sub>-*s*-VAc<sub>0.12</sub>) were stored at different pH (4, 6, 8, 10 and 12) in the fridge over 4 weeks, and the pH was measured every week (**Figure II-32**). At week 4, the size of the particles was measured again by DLS (**Figure II-33**).



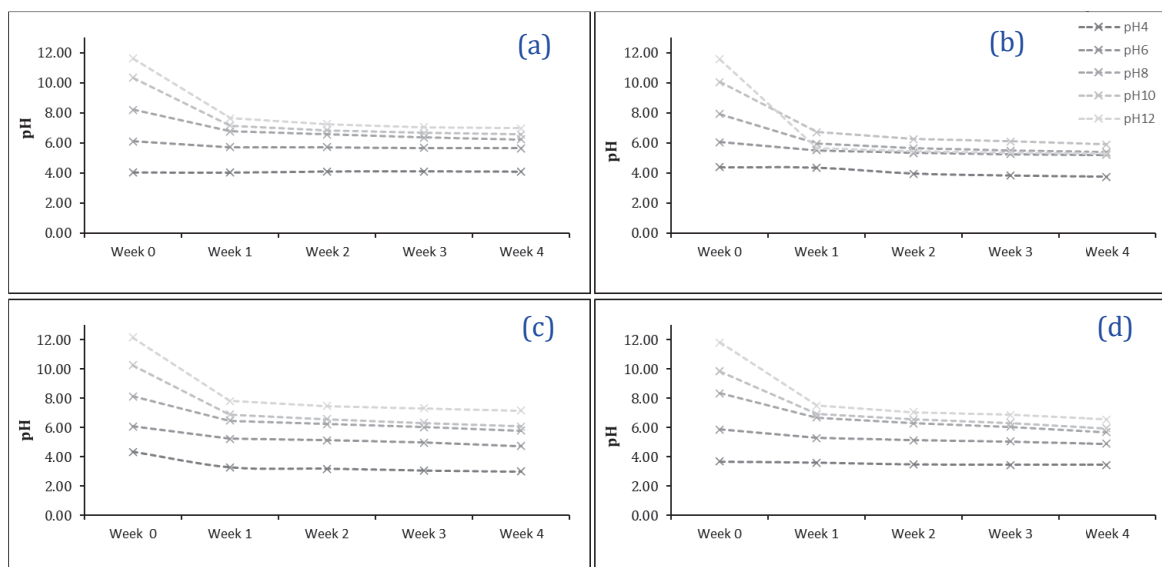


**Figure II-32: Evolution of the pH of the latexes obtained with 10 wt.% of (a) Mowiol 4-88; (b) 75\_P(VOH<sub>0.88</sub>-s-VAc<sub>0.12</sub>); (c) 100\_P(VOH<sub>0.88</sub>-s-VAc<sub>0.12</sub>) and (d) 200\_P(VOH<sub>0.88</sub>-s-VAc<sub>0.12</sub>) stored in the fridge over four weeks. At week 0, the pH was set to 4, 6, 8, 10 and 12 and was then measured every week for four weeks.**

No evolution of pH was observed in any of the systems when the latexes were stored at pH 4. In contrast, for the samples stored at pH 6, 8, 10 and 12, the pH decreased with time. This may be caused by the hydrolysis of VAc units from either the stabilizer, and the polymer particles which generates sodium acetate when  $\text{pH} > \text{pK}_a + 1$ , with  $\text{pK}_a = 4.8$ . It can be noted that the hydrolysis level reaches a plateau around pH 6.

The particle size of the latex obtained with the RAFT-synthesized P(VOH-s-VAc) was not impacted by this hydrolysis, while coagulum was visible in the latex obtained with Mowiol 4-88 and stored at pH 12. This was also visible by DLS as the  $Z_{av}$  was higher after 4 weeks of storage in the fridge at this pH (**Figure II-33**).

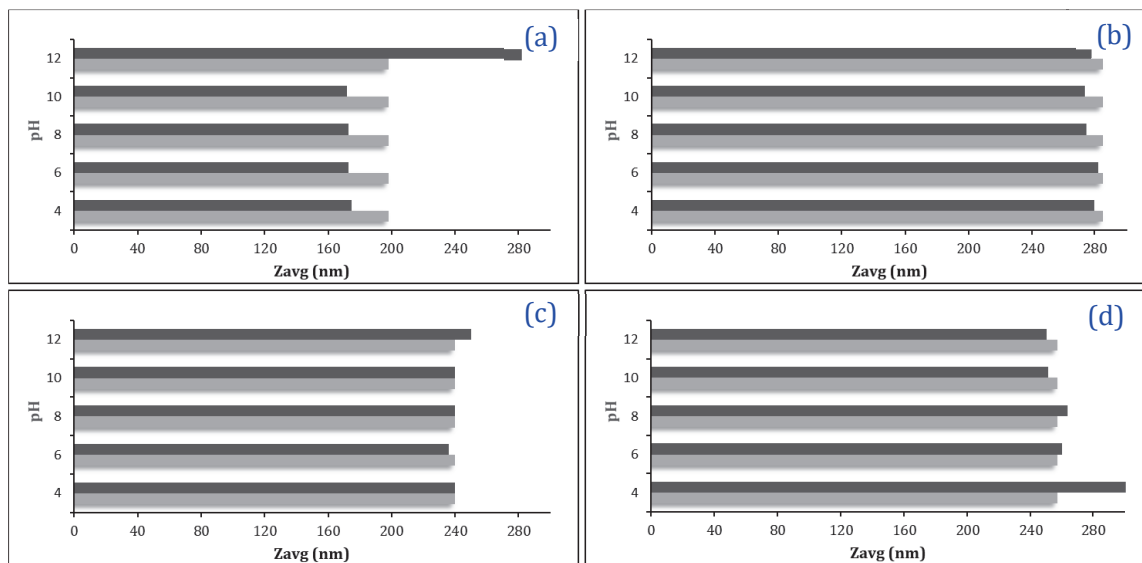


**Figure II-33:  $Z_{av}$  of the latex at week 0 and after storage for four weeks at different pH, measured by DLS for the latexes stabilized with 10 wt.% of (a) Mowiol 4-88; (b) 75\_P(VOH<sub>0.88</sub>-s-VAc<sub>0.12</sub>); (c) 100\_P(VOH<sub>0.88</sub>-s-VAc<sub>0.12</sub>) and (d) 200\_P(VOH<sub>0.88</sub>-s-VAc<sub>0.12</sub>). ■ : Week 0 and ▨ : Week 4.**

All the latexes stabilized with Mowiol 4-88 or the RAFT-synthesized P(VOH-s-VAc) were sensitive to hydrolysis at pH ranging from 6 to 12. The resistance to hydrolysis was not enhanced by the RAFT-synthesized structures.

#### V.4 Influence of the amount of stabilizer at fixed DP = 75 and HD = 88%

The previous study showed that at fixed amount of stabilizer, the use of 75\_P(VOH<sub>0.88</sub>-s-VAc<sub>0.12</sub>) led to the larger amount of grafted/adsorbed stabilizer onto the particles, but also to larger particle size in comparison to the latexes obtained with Mowiol 4-88 or 100\_P(VOH<sub>0.88</sub>-s-VAc<sub>0.12</sub>) and 200\_P(VOH<sub>0.88</sub>-s-VAc<sub>0.12</sub>). Therefore, it was decided to study the influence of the amount of 75\_P(VOH<sub>0.88</sub>-s-VAc<sub>0.12</sub>) on the particle size. Emulsion copolymerizations of VAc with VeoVa were then performed with 7, 10, 15 and 20 wt.% of 75\_P(VOH<sub>0.88</sub>-s-VAc<sub>0.12</sub>) (based on monomers).

##### V.4.1 Colloidal features of the latex

It was expected that the higher the amount of stabilizer, the smaller the particles, as more stabilizer would be available to stabilize more particles. DLS showed that the polymer particles were again polydisperse.  $Z_{av}$  is therefore not accurate, and the latexes were thus analyzed by cryo-TEM (Table II-13). The results obtained by cryo-TEM followed the expected trend.



**Table II-13: Particle size comparison from the latexes stabilized with different amounts of 75\_P(VOH<sub>0.88</sub>-s-VAc<sub>0.12</sub>) via DLS and cryo-TEM.**

Entry	Wt.% of stabilizer	Z <sub>av</sub> (nm) <sup>a</sup>	PdI <sup>a</sup>	D <sub>n</sub> (nm) <sup>b</sup>	D <sub>v</sub> (nm) <sup>b</sup>	D <sub>w</sub> /D <sub>n</sub> <sup>b</sup>	N <sub>p</sub> (10 <sup>15</sup> cm <sup>-3</sup> ) <sup>c</sup>
ER-75_PVOH-7%	7	1400	0.3	-	-	-	-
ER-75_PVOH-10%	10	285	0.1	240	250	1.2	1.4
ER-75_PVOH-15%	15	310	0.3	155	190	1.6	3.4
ER-75_PVOH-20%	20	525	0.5	95	195	2.0	9.3

<sup>a</sup> Obtained by DLS

<sup>b</sup> Obtained by cryo-TEM

<sup>c</sup> Obtained via Equation 49

Besides, **Figure II-34** showed that the latex which contained 7 wt.% stabilizer did not provide spherical particles, but non spherical objects that would result from particle coagulation, which might be the sign of limited aggregation of the particles. This suggests that this amount of stabilizer was too low to provide a good stabilization of particles.

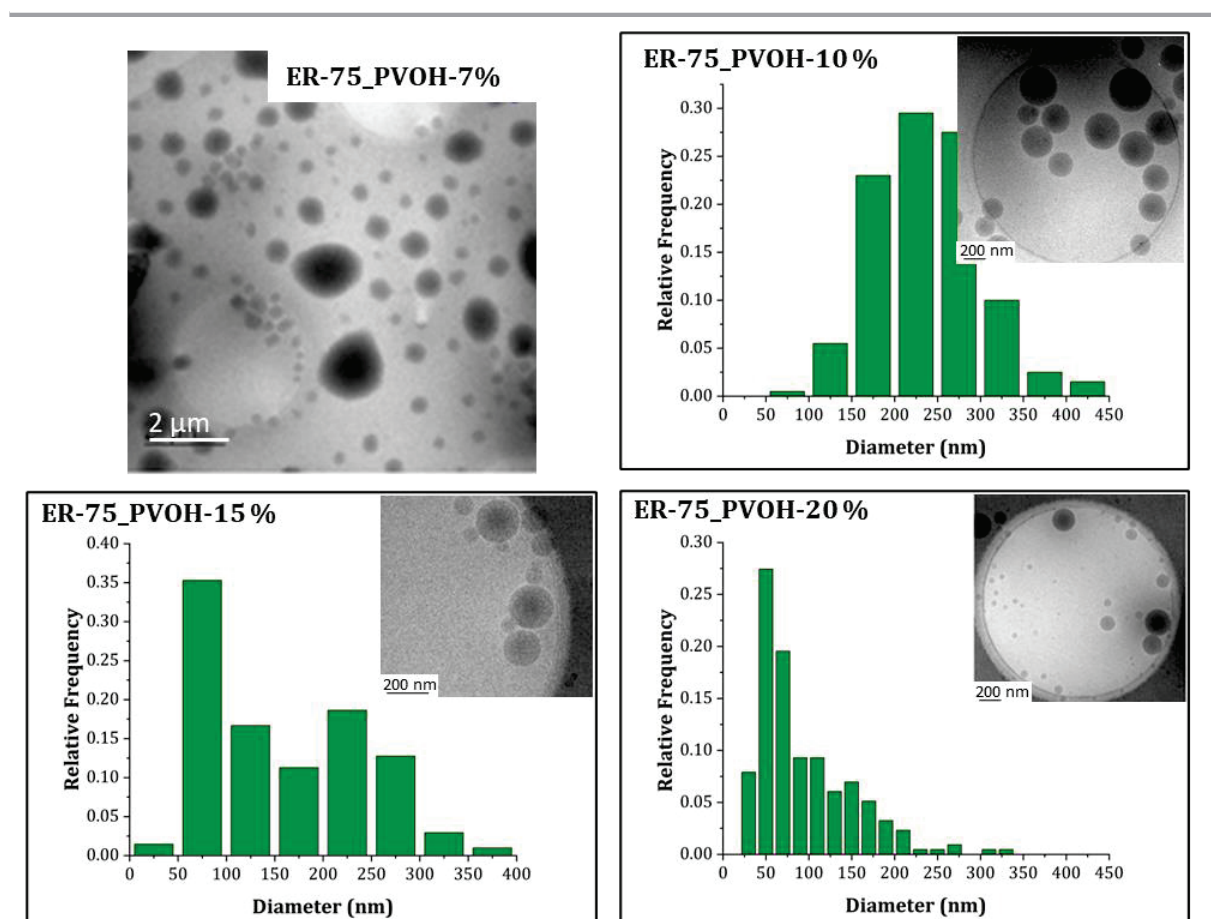


**Figure II-34 : Particle size distribution and related cryo-TEM snapshots of the latexes stabilized with 7, 10, 15 and 20 wt.% of 75\_P(VOH<sub>0.88</sub>-s-VAc<sub>0.12</sub>).Figure II-34 : Particle size distribution and related cryo-TEM snapshots of the latexes stabilized with 7, 10, 15 and 20 wt.% of 75\_P(VOH<sub>0.88</sub>-s-VAc<sub>0.12</sub>)**

Eventually,  $N_p$  increased accordingly with the stabilizer content. The  $N_p$  values, together with the observed increase of polydispersity, likely highlight the occurrence of intensive continuous nucleation (**Table II-13**). This result compares well the literature findings, where Lepizzera and Hamielec<sup>[71]</sup> highlighted that P(VOH-*s*-VAc)-*graft*-PVAc• macroradicals had a smaller diffusion coefficient than the PVAc• oligoradicals, and are thus more likely prone to form new particles by “aggregation” and induce continuous nucleation.

#### V.4.2 Adsorbed and grafted stabilizer

The centrifugation experiments showed that the amount of adsorbed and grafted stabilizer remains essentially the same regardless of the amount of stabilizer (*ca.* 36 - 38 %), except for the experiment carried out with 10 wt.% of stabilizer (wt.%<sub>Ads&graft</sub> was approximately 44%) (**Table II-14**).

This result was consistent with the above observations from cryo-TEM analyses, where it was observed that the higher the amount of stabilizer, the higher the number of particles. Thus, the percentage of adsorbed and grafted stabilizer should not evolve significantly. The deviation obtained with 10 wt.% of stabilizer was not explained though, and might come from experimental error.

**Table II-14: Estimation of the specific surface area occupied by 75\_P(VOH<sub>0.88</sub>-*s*-VAc<sub>0.12</sub>) on a P(VAc-*co*-VeoVa) particle ( $A_s$ ), depending on its wt.% percentage.**

Entry	Wt.% <sub>Ads&amp;Grafted</sub> <sup>a</sup>	$S_{tot\ latex}$ (x10 <sup>6</sup> cm <sup>-2</sup> ) <sup>b</sup>	$A_s$ (Å <sup>2</sup> /molecule) <sup>c</sup>
ER-75_PVOH-7%	38	-	-
ER-75_PVOH-10%	44	2.8	260
ER-75_PVOH-15%	36	3.9	300
ER-75_PVOH-20%	36	4.6	260

<sup>a</sup> Obtained by **Equation 58**

<sup>b</sup> Obtained by **Equation 50**

<sup>c</sup> Obtained by **Equation 61**

The estimation of the  $A_s$  values, depending on the percentage of stabilizer introduced in the system, are gathered in **Table II-14**. As expected, the specific surface area covered by 75\_P(VOH<sub>0.88</sub>-*s*-VAc<sub>0.12</sub>) was not significantly impacted by the initial load of stabilizer. The surface covered by one macromolecule was approximately 260 Å<sup>2</sup> when the amount of stabilizer is 10 and 20 wt.% (based on monomers). Surprisingly, it reaches 300 Å<sup>2</sup> when 15 wt.% of stabilizer was introduced into the reactor. This experiment was carried out a second time and led to the exact same result. The reason for this difference is not well understood. Still,  $A_s$  remains in the same range for each experiment.

## VI. Conclusion

**Chapter I** highlighted that the kinetics of the emulsion polymerization of VAc stabilized with commercial P(VOH-*s*-VAc)s including Mowiol 4-88 was not trivial and still debated. In this Chapter, we investigated the syntheses of RAFT/MADIX P(VOH-*s*-VAc) and their use as stabilizers in the emulsion copolymerization of VAc with VeoVa.

First, experimental parameters for successful synthesis of well-defined PVAc by RAFT/MADIX were identified. The control of the polymerization was not optimal, due to unavoidable accumulation in the polymerization medium of less reactive PVA<sub>CT</sub>-X species.

The alcoholysis step of the PVAcS was optimized to be reproducible and to target different VOH contents. Indeed, P(VOH-*s*-VAc) with different HD, DP and concentrations in water were thus obtained (HD ranging from 88 to 98% and DP, ranging from 75 to 200). The study of the aqueous behavior of these copolymers by surface tension measurements and DLS showed similarities with Mowiol 4-88, with mainly the presence of free chains (10 nm) and some aggregates ranging from 100 to 1000 nm.

No data were available in the literature concerning the ability of low molar mass and well-defined P(VOH-*s*-VAc) to stabilize a latex. After optimizing the conditions for emulsion copolymerization of VAc and VeoVa, the influence of the characteristics of such stabilizers (*i.e.*, HD and DP) onto the characteristics of the latex (nucleation mechanism, particle size, PSD, adsorption and grafting efficiency) was evaluated.

To reach conversions comparable to those achieved with Mowiol 4-88 (80 - 90%), the amount of initiator had to be significantly increased (up to 8 times). This was attributed to the presence of by-products retarders or inhibitors in the stabilizers, coming from the alcoholysis step (and possibly from the chain-end extremities of the RAFT-synthesized P(VOH-*s*-VAc)).

Continuous nucleation and low nucleation efficiency was also highlighted. The resulting PSD was large compared to the system containing Mowiol 4-88, leading us to consider that Mowiol-like P(VOH-*s*-VAc) with low molar mass and low  $\bar{D}$  was probably not beneficial to improve the stabilization efficiency. It was postulated that the presence of several chains with different molar masses and HD in the composition of Mowiol 4-88 induced a synergy between several modes of stabilization (either adsorption and grafting) that is lost in the well-defined P(VOH-*s*-VAc) and that leads to less polydisperse polymer particles (even if secondary nucleation was nevertheless present). The small chains require smaller grafts before they become surface active. Thus, the RAFT-synthesized P(VOH-*s*-VAc) are more likely to be prone to grafting reactions and aggregation of the grafted chains followed by radical entry, than homogeneous nucleation *via* adsorption of the stabilizer onto the surface of the particles.

The properties of the final latexes were compared to those of a latex obtained with Mowiol 4-88. It was demonstrated that at fixed HD (88%) and fixed amount of stabilizer (10 wt.% based on monomers), the higher the DP, the larger the amount of stabilizer that remains in water.

In addition, for a fixed DP (75) and fixed HD (88%), it was highlighted that increasing the stabilizer concentration impacted the dispersity of the latex as a result of a suspected steric hindrance of the protective corona of the formed particles that affects the entry of propagating radicals.

Nevertheless, the amount of adsorbed and grafted stabilizer remains low even with the optimized conditions (44% maximum) and was not significantly improved when compared to the latex obtained with Mowiol 4-88 (45%).

Therefore, the next aim of this work is to investigate the impact of additional hydrophobic units along the copolymer chain to try to beneficially impact its adsorption and grafting efficiency. In the next chapter, different architectures of stabilizers, incorporating VL or VeoVa comonomers were synthesized and will be evaluated as stabilizer candidates for the emulsion copolymerization of VAc with VeoVa.

## References

- [1] G. Moad, E. Rizzardo, S. H. Thang, *Polymer*. **2008**, *49*, 1079–1131.
- [2] M. Destarac, “On the Critical Role of RAFT Agent Design in Reversible Addition-Fragmentation Chain Transfer (RAFT) Polymerization”, in *Polymer Reviews*, *51:2*, 163–187, Taylor & Francis Group, **2011**.
- [3] P. Corpart, D. Charmot, T. Biadatti, S. Zard, D. Michelet, *Method for Block Copolymer Synthesis by Controlled Radical Polymerization*, WO1998058974, **1998**.
- [4] E. Rizzardo, J. Chiefari, R. T. A. Mayadunne, G. Moad, S. H. Thang, “Synthesis of Defined Polymers by Reversible Addition-Fragmentation Chain Transfer: The RAFT Process” in *ACS Symposium Series, Vol. 768*, American Chemical Society, Washington DC, **2000**.
- [5] M. Destarac, D. Charmot, X. Franck, S. Z. Zard, *Macromol. Rapid Commun.* **2000**, *21*, 1035–1039.
- [6] M. L. Coote, L. Radom, *Macromolecules* **2004**, *37*, 590–596.
- [7] A. Postma, T. P. Davis, G. Li, G. Moad, M. S. O’Shea, *Macromolecules* **2006**, *39*, 5307–5318.
- [8] G. Pound, J. B. McLeary, J. M. McKenzie, R. F. M. Lange, B. Klumperman, *Macromolecules* **2006**, *39*, 7796–7797.
- [9] V. Malepu, C. D. Petruczok, T. T. Tran, T. Zhang, M. Thopasridharan, D. A. Shipp, *ACS Symp. Ser.* **2009**, *1024*, 37–47.
- [10] M. Benaglia, J. Chiefari, Y. K. Chong, G. Moad, E. Rizzardo, S. H. Thang, *J. Am. Chem. Soc.* **2009**, *131*, 6914–6915.
- [11] M. R. Wood, D. J. Duncalf, S. P. Rannard, S. Perrier, *Org. Lett.* **2006**, *8*, 553–556.
- [12] M. H. Stenzel, L. Cummins, G. E. Roberts, T. P. Davis, P. Vana, C. Barner-Kowollik, *Macromol. Chem. Phys.* **2003**, *204*, 1160–1168.
- [13] V. K. Patel, N. K. Vishwakarma, A. K. Mishra, C. S. Biswas, B. Ray, *J. Appl. Polym. Sci.* **2012**, *125*, 2946–2955.
- [14] M. E. Levere, P. Chambon, S. P. Rannard, T. O. McDonald, *J. Polym. Sci. Part A Polym. Chem.* **2017**, *55*, 2427–2431.
- [15] P. E. Dufils, G. David, B. Boutevin, G. Woodward, G. Otter, A. Guinaudeau, S. Mazières, M. Destarac, *J. Polym. Sci. Part A Polym. Chem.* **2012**, *50*, 1997–2007.
- [16] M. Guerre, M. Semsarilar, F. Godiard, B. Améduri, V. Ladmiral, *Polym. Chem.* **2017**, *8*, 1477–1487.
- [17] K. Koumura, K. Satoh, M. Kamigaito, *Polym. J.* **2009**, *41*, 595–603.
- [18] K. Koumura, K. Satoh, M. Kamigaito, Y. Okamoto, *Macromolecules* **2006**, *39*, 4054–4061.
- [19] S. Harrisson, X. Liu, J. N. Ollagnier, O. Coutelier, J. D. Marty, M. Destarac, *Polymers*. **2014**, *6*, 1437–1488.
- [20] S. Perrier, *Macromolecules* **2017**, *50*, 7433–7447.
- [21] M. Drache, G. Schmidt-Naake, in *Macromol. Symp.*, **2007**, pp. 397–405.
- [22] J. B. McLeary, F. M. Calitz, J. M. McKenzie, M. P. Tonge, R. D. Sanderson, B. Klumperman,

- Macromolecules* **2005**, *38*, 3151–3161.
- [23] J. B. McLeary, F. M. Calitz, J. M. McKenzie, M. P. Tonge, R. D. Sanderson, B. Klumperman, *Macromolecules* **2004**, *37*, 2383–2394.
- [24] G. Mark, H. F.; Bikales, N. M.; Overberger, C. G.; Menges, "Vinyl Alcohol Polymers" in Encyclopedia of polymer science and technology, Volume 8, John Wiley & Sons **1985**.
- [25] M. S. El-Aasser, "Emulsion Polymerization of Vinyl Acetate", Applied Science Publishers LTD, **1981**.
- [26] S. Aruldass, V. Mathivanan, A. R. Mohamed, C. T. Tye, *J. Environ. Chem. Eng.* **2019**, *7*.
- [27] A. S. Dunn, C. J. Tonge, S. A. B. Anabtawi, "The Effects of Poly(vinyl alcohols) on the polymerization of vinyl acetate", in Emulsion Polymerization, ACS symposium series Washington, DC, **1976**, pp. 24–33.
- [28] L. I. Atanase, S. Bistac, G. Riess, *Soft Matter* **2015**, *11*, 2665–2672.
- [29] A. K. and M. S. E.-A. B.M. Budhall, K. Landfester, D. Nagy, E.D. Sudol, V.L. Dimonie, *Macromol.Symp.* **2000**, 63–84.
- [30] J. V. Dawkins, T. A. Nicholson, A. J. Handley, E. Meehan, A. Nevin, P. L. Shaw, *Polymer.* **1999**, *40*, 7331–7339.
- [31] T. Moritani, Molecular Structures and Functional Modifications of Poly(Vinyl Alcohol). Ph.D. Dissertation, University of Tokyo, **1998**.
- [32] B. M. S. Budhlall, Grafting Reactions in the Emulsion Polymerization of Vinyl Acetate Using Poly(Vinyl Alcohol) as Emulsifier. Ph.D Dissertation, Lehigh University, **1999**.
- [33] T. Moritani, Y. Fujiwara, *Macromolecules* **1976**, *10*, 532–535.
- [34] G. Van der Velden, J. Beulen, *Macromolecules* **1982**, *15*, 1071–1075.
- [35] M. Uchiyama, K. Satoh, M. Kamigaito, *Giant* **2021**, *5*, 100047.
- [36] D. C. Bugada, A. Rudin, *Polymer* **1984**, *25*, 1759–1766.
- [37] H. S. Mansur, C. M. Sadahira, A. N. Souza, A. A. P. Mansur, *Mater. Sci. Eng. C* **2008**, *28*, 539–548.
- [38] I. Korbog, S. Mohamed Saleh, *Int. J. Environ. Stud.* **2016**, *73*, 226–235.
- [39] L.-I. Atanase, Contribution à l'étude Des Complexes Poly(Vinyle Alcool-Vinyle Acétate)/Tensioactifs Anioniques: Caractéristiques Colloïdales Des Nanogels et Extension Au Copolymères à Blocs. Ph.D Dissertation, Université de Haute Alsace - Mulhouse, **2011**.
- [40] H. R. Hedayati, M. Khorasani, M. Ahmadi, N. Ballard, *Polymer.* **2022**, *246*, 124674.
- [41] G. Moad, C. Barner-Kowollik, "The Mechanism and Kinetics of the RAFT Process: Overview, Rates, Stabilities, Side Reactions, Product Spectrum and Outstanding Challenges", in Handbook of RAFT Polymerization, Wiley-VCH **2008**.
- [42] Y. A. Kabachii, S. Y. Kochev, *Polym. Sci. - Ser. A* **2006**, *48*, 717–722.
- [43] G. Moad, E. Rizzardo, S. H. Thang, *Chem. - An Asian J.* **2013**, *8*, 1634–1644.
- [44] Y.-Y. Tong, Y.-Q. Dong, F.-S. Du, Z.-C. Li, *J. Polym. Sci. Part A Polym. Chem.* **2009**, *47*, 1901–1910.
- [45] Y. Mai, A. Eisenberg, *Chem. Soc. Rev.* **2012**, *41*, 969–5985.



- [46] S. J. Holder, N. A. J. M. Sommerdijk, *Polym. Chem.* **2011**, *2*, 1018–1028.
- [47] B. M. Budhlall, K. Landfester, E. D. Sudol, V. L. Dimonie, A. Klein, M. S. El-Aasser, *Macromolecules* **2003**, *36*, 9477–9484.
- [48] G. H. Li, C. G. Cho, *Colloid Polym. Sci.* **2005**, *283*, 946–953.
- [49] N. Sarkar, *J. Phys. Chem. B* **2021**, *125*, 9917–9920.
- [50] P. Ra, D. Armando, Z. Wever, F. Picchioni, A. A. Broekhuis, *Chem. Rev.* **2015**, 8504–8563.
- [51] B. Wang, S. Mukataka, E. Kokufuta, M. Ogiso, M. Kodama, *J. Polym. Sci., Part B Polym. Phys.* **2000**, *38*, 214–221.
- [52] L. I. Atanase, G. Riess, *Colloids Surfaces A Physicochem. Eng. Asp.* **2010**, *355*, 29–36.
- [53] I. Piirma, *Makromol. Chemie. Macromol. Symp.* **1990**, *35–36*, 467–475.
- [54] J. Muller, F. Marchandea, B. Prelot, J. Zajac, J. J. Robin, S. Monge, *Polym. Chem.* **2015**, *6*, 3063–3073.
- [55] J. H. Jeong, H. S. Kang, S. R. Yang, J. D. Kim, *Polymer (Guildf)*. **2002**, *44*, 583–591.
- [56] Y. He, T. Howes, J. D. Litster, *J. Chem. Eng. Japan* **2004**, *37*, 181–186.
- [57] Y. He, T. Howes, J. D. Litster, G. H. Ko, *Colloids Surfaces A Physicochem. Eng. Asp.* **2002**, *207*, 89–104.
- [58] E. Mendizabal, J. R. Castellanos-Ortega, J. E. Puig, *Colloids and Surfaces* **1992**, *63*, 209–217.
- [59] B. M. Budhlall, K. Landfester, E. D. Sudol, V. L. Dimonie, A. Klein, M. S. El-Aasser, *Macromolecules* **2003**, *36*, 9477–9484.
- [60] L. I. Atanase, G. Riess, *Polymers*, **2011**, *3*, 1065–1075.
- [61] N. J. Crowther, D. Eagland, *J. Chem. Soc. Faraday Trans. 1 Phys. Chem. Condens. Phases* **1986**, *82*, 2791–2799.
- [62] J. T. O'Donnell, R. B. Mesrobian, A. E. Woodward, *J. Polym. Sci.* **1958**, *28*, 171–177.
- [63] V. Boscher, R. Helleboid, T. Lasuye, B. Stasik, G. Riess, *Rev. Roum. Chim.* **2009**, *54*, 527–531.
- [64] S. M. El-Aasser, S. D. Sudol, "Features of Emulsion Polymerization", in *Emulsion Polymerization and Emulsion Polymers*, Wiley-VCH, **1997**.
- [65] B. M. Budhlall, E. D. Sudol, V. L. Dimonie, A. Klein, M. S. El-Aasser, *J. Polym. Sci. Part A Polym. Chem.* **2001**, *39*, 3633–3654.
- [66] S. Carrà, L. Malcovati, A. Slipevich, G. Storti, S. Carrà, "Stabilization Mechanisms in Vinyl Acetate Emulsion Polymerization Stabilized by Poly(Vinyl Alcohol)" in *Polymer Colloids*, American Chemical Society, Washington DC, **2001**.
- [67] G. Rocha-Botello, R. Olvera-Guillen, J. Herrera-Ordonez, M. Cruz-Soto, D. Victoria-Valenzuela, *Macromol. React. Eng.* **2019**, *13*, 1–9.
- [68] P. C. Hiemenz, R. Rajagopalan, "Principles of Colloid and Surface Chemistry", Marcel Dekker INC, New York, **1997**.
- [69] A. Agirre, I. Calvo, H. P. Weitzel, W. D. Hergeth, J. M. Asua, *Ind. Eng. Chem. Res.* **2014**, *53*, 9282–9295.
- [70] D. Donescu, K. Gosa, I. Languri, *Acta Polym.* **1989**, *40*, 49–52.

- [71] S. M. Lepizzera, A. E. Hamielec, *Macromol. Chem. Phys.* **1994**, *195*, 3103–3115.
- [72] J. . Troyan, *rubber chem .* **1948**, *63*, 585–595.
- [73] A. S. Dunn, "The Polymerization of Aqueous Solutions of Vinyl Acetate" in Emulsion Polymerization of Vinyl Acetate, (Eds.: S.M. El-Asser, J.W. Vanderhoff), Applied Science Publishers LTD, **1981**, pp. 11–29.
- [74] G. S. M. Gonzalez, V. L. . Dimonie, E. D. Sudol, H. J. Yue, A. Klein, M. S. El-Aasser, G. S. Magallanes González, V. L. . Dimonie, E. D. Sudol, H. J. Yue, A. Klein, M. S. El-Aasser, *J. Polym. Sci. Part A Polym. Chem.* **1996**, *34*, 849–862.
- [75] P. A. Lovell, F. J. Schork, *Biomacromolecules* **2020**, *21*, 4396–4441.
- [76] J. W. Vanderhoff, N. J. Earhart, V. L. Dimonie, S. M. El-Asser, *Makromol. Chem* **1990**, *35*, 477–497.
- [77] S. Carrà, A. Slipecevic, A. Canevarolo, S. Carrà, *Polymer.* **2005**, *46*, 1379–1384.
- [78] H. Egret, V. L. Dimonie, E. David Sudol, A. Klein, M. S. El-Aasser, *J. Appl. Polym. Sci.* **2001**, *82*, 1739–1747.
- [79] G. Fleer, L. . Koopal, J. Lyklema, *Polymer* **1972**, 689.
- [80] J. M. G. Lankveld, J. Lyklema, *J. Colloid Interface Sci.* **1972**, *41*, 454–465.
- [81] S. J. Bohorquez, J. M. Asua, *J. Polym. Sci. Part A Polym. Chem.* **2008**, 6407–6415.
- [82] N. Kim, E. D. Sudol, V. L. Dimonie, M. S. El-Aasser, *Macromolecules* **2003**, *36*, 5573–5579.





# Chapter III

## Synthesis and evaluation as stabilizer of P(VAc-*s*-CoM-*s*-VAc) statistical copolymers

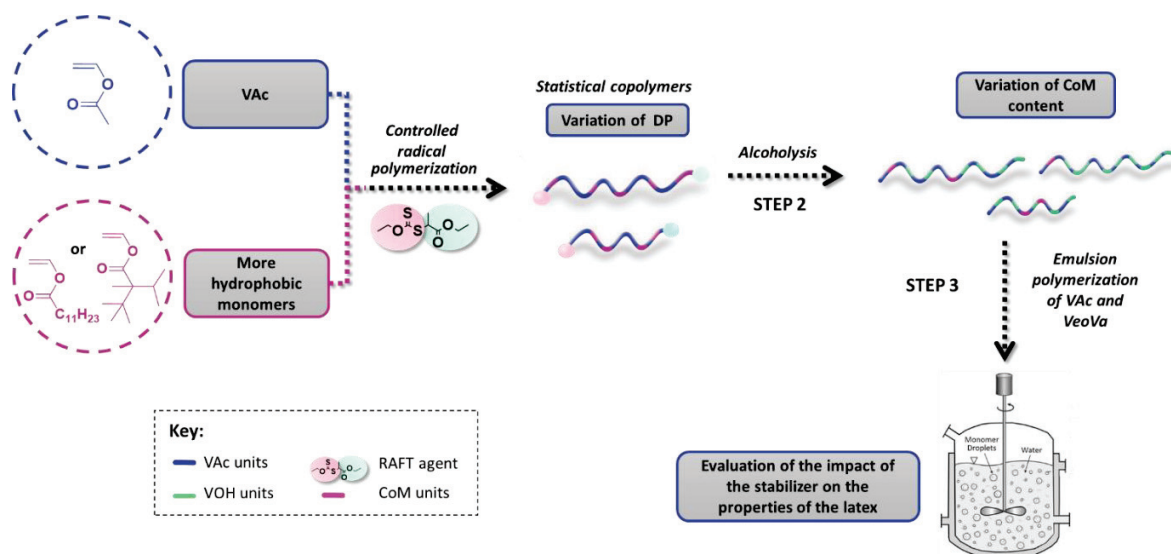


## Table of content

I. INTRODUCTION.....	158
II. RAFT/MADIX COPOLYMERIZATION OF VAC WITH VEOVA OR VL .....	160
II.1 General procedure.....	160
II.2 Characterization of P(VAc-s-VL) copolymers.....	161
II.3 Characterization of P(VAc-s-VeoVa) copolymers.....	164
III. ALCOHOLYSIS OF P(VAC-S-VL) AND P(VAC-S-VEOVA) COPOLYMERS .....	169
III.1 Alcoholysis of P(VAc <sub>0.90</sub> -s-VL <sub>0.10</sub> ).....	169
III.2 Alcoholysis of P(VAc-s-VeoVa).....	173
III.3 Conclusion on the alcoholysis of the statistical copolymers .....	176
IV. (SELF-)ORGANIZATION OF THE COPOLYMERS IN WATER.....	177
IV.1 Dispersibility of the statistical copolymers in water .....	177
IV.2 Organization of the copolymer in water: DLS study .....	179
IV.3 Surface tension.....	184
IV.4 Conclusion.....	185
V. EMULSION COPOLYMERIZATION OF VAC AND VEOVA WITH P(VOH-S-CoM-S-VAC) COPOLYMERS	187
V.1 Screening with KPS.....	187
V.2 Emulsion copolymerization of VAc and VeoVa initiated by a redox couple.....	188
V.2.1 VL-based statistical copolymer stabilizers .....	188
A. Kinetics of the polymerizations and colloidal features .....	188
B. Adsorbed and grafted stabilizer .....	192
C. Evaluation of the alkali resistance of the latexes stored at different pH .....	193
D. Reproducibility: evaluation of the robustness of the synthesis, alcoholysis and stabilization efficiency of P(VOH-s-VL-s-VAc) statistical copolymer.....	195
V.2.2 VeoVa-based statistical copolymer stabilizers.....	197
A. Kinetics of the polymerizations and colloidal features .....	197
B. Adsorbed and grafted stabilizer .....	202
C. Evaluation of the alkali resistance of the latex ER-S10 at different pH.....	202
VI. CONCLUSION .....	204

## I. Introduction

The first part of our research (**Chapter II**) focused on the optimization of the experimental conditions leading to innovative P(VOH-*s*-VAc) polymeric stabilizers. After adapting the industrial protocol of emulsion polymerization to a lab scale, it was possible to use well-defined P(VOH-*s*-VAc) to efficiently stabilize P(VAc-*co*-VeoVa) latexes. However, despite the variation of several parameters (*i.e.*, the DP, HD, and amount of the stabilizer), attempts to increase the fraction of adsorbed and grafted stabilizer onto the particles compared to the latexes obtained with Mowiol 4-88 were unsuccessful.

In the following Chapters, the impact of the incorporation of additional hydrophobic units into the P(VOH-*s*-VAc) structures is studied. It is hoped that, the incorporation of these hydrophobic moieties would increase the affinity of the stabilizer with the particles, and therefore enhance its adsorption and grafting onto the particles. In that purpose, two comonomers were selected, VeoVa and vinyl laurate (VL).

The use of controlled radical polymerization techniques such as NMP, ATRP and RAFT for the synthesis of amphiphilic copolymers is already widely documented in the literature.<sup>[1]</sup> These techniques give the possibility to prepare well-defined structures and tailored macromolecules with almost no limitation. Two monomers can be used to make either statistical, block or gradient copolymers simply by varying how the monomers are introduced in the polymerization medium and/or by playing with their reactivity ratios. The reactivity ratios for the copolymerization of VAc and VeoVa are 0.99 and 0.92, respectively.<sup>[2],[3]</sup> As these reactivity ratios are almost equal, VAc and VeoVa should be added with comparable rates to the growing macroradical, and a statistical (or random) copolymer should be formed. The reactivity ratios for the copolymerization of VAc and VL are 1.4 and 0.7, respectively.<sup>[3],[4]</sup> In this case, the copolymerization will lead to gradient copolymer. We indeed expect the structure of the copolymer formed during the RAFT/MADIX copolymerization of these two monomers to be initially rich in VAc units before being enriched in VL units upon VAc consumption.

To the best of our knowledge, while homopolymerization and block copolymerization of VeoVa are described in the literature,<sup>[5],[6],[7]</sup> there is no published data detailing the statistical RAFT/MADIX copolymerization of VAc and VeoVa or VAc and VL. Only one article refers to the synthesis of different copolymer architectures (statistical, gradient, block) based on *N*-vinylpyrrolidone (NVP) and VL<sup>[8]</sup> using RAFT/MADIX polymerization. In addition to varying compositions and molar masses, the authors compared the aqueous solution properties of the corresponding copolymers (surface tension, CAC and size of the aggregates) highlighting the significant impact of the architectures on these properties. The block copolymer yielded a much sharper cut-off in the surface tension plot than the other two copolymers. The block and gradient copolymers both show single peaks in the DLS distribution, providing pseudo-micelles and aggregates in a ~ 25 - 200 nm size range (depending on the composition and

architecture of the copolymers). The statistical copolymer however showed a bimodal distribution. The authors found that the more block-like structures were likely to self-assemble in water.

This Chapter is dedicated to the study of various statistical copolymers (as illustrated on the front page). The syntheses will be presented in a first part, followed by the alcoholysis in a second one. Then, the investigation of the organization of the statistical stabilizers will be presented in a third section. Finally, the statistical copolymers which were dispersible in water will be tested in emulsion copolymerization of VAc and VeoVa, and the resulting latexes will be characterized.

To ease the designation of these copolymers, the following notations will be used throughout the chapter:  $DP\_P(VAc_w-s-CoM_y)$  for the statistical structures before hydrolysis, and  $DP\_P(VOH_z-s-CoM_y-s-VAc_w)$  and for the structures after hydrolysis. DP refers to the DP of the statistical copolymer. w, y and z refer to the molar fraction of VAc, CoM and VOH units, respectively. CoM refers to either VeoVa or VL units.

## II. RAFT/MADIX copolymerization of VAc with VeoVa or VL

### II.1 General procedure

The experimental setup and conditions to copolymerize VAc with the CoM are similar to the ones described in **Chapter II** for VAc. The general synthesis routes are described in **Figure III-1**. Polymerizations were carried out at 60 °C in EtAc. *O*-ethyl-*S*-(1-ethoxycarbonyl)ethyl dithiocarbonate (CTA) was used as RAFT/MADIX agent and AIBN was used as the initiator. The ratio [monomers]:[CTA]:[AIBN] was 95:1:0.2 or 130:1:0.2, depending on the targeted DP. The concentration of VeoVa was varied from 1 to 10 mol.%, while it was fixed to 10 mol.% when VL was used. The reasons for this choice will be explained later in the alcoholysis **Section III.1**. The detailed protocol for the synthesis and purification is available in **Experimental Section III.3**. Monomer conversion was followed by <sup>1</sup>H NMR in CDCl<sub>3</sub> and molar masses by SEC-THF analyses, from samples withdrawn from the polymerization medium at different times. After a predetermined polymerization time (6 or 8 h depending on the conversion), the polymerization medium was cooled to stop the reaction. High yields (up to 84%) were obtained. **Table III-1** sums up the main characteristics of the synthesized copolymers.

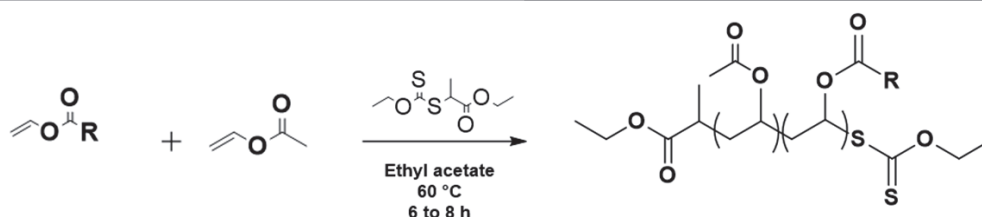


**Figure III-1:** General reaction scheme for the synthesis of P(VAc-*s*-CoM)-X in EtAc at 60 °C, with R = C<sub>9</sub>H<sub>19</sub> from the VeoVa units or C<sub>11</sub>H<sub>23</sub> from the VL units.

---

After purification, a white powder (for the VeoVa-based structures) or as a sticky solid (for the VL-based structures) were obtained. Over the course of the three years, several batches of statistical copolymers were synthesized and similar structures with reproducible DP = 75 ± 10 units and 100 ± 10 units were obtained according to <sup>1</sup>H NMR. The determination of the DP and composition of the copolymer by <sup>1</sup>H NMR is described elsewhere (**Figure III-2** and **Figure III-4**).

The characteristics of the statistical copolymers are summarized in **Table III-1**.

**Table III-1: Summary of the characteristics of P(VAc-s-CoM)-X copolymers synthesized in EtAc at 60 °C, for 6 to 8 h.**

Designation	VAc conv. (%) <sup>a</sup>	CoM conv. (%) <sup>a</sup>	$M_n$ (theo.) (g mol <sup>-1</sup> ) <sup>b</sup>	$M_n$ (NMR) (g mol <sup>-1</sup> ) <sup>c</sup>	$M_n$ (SEC) (g mol <sup>-1</sup> ) <sup>d</sup>	Dispersity ( $\bar{D}$ ) <sup>d</sup>
75_P(VAc <sub>0.90-s</sub> -VL <sub>0.10</sub> )	85	93	6500	6920	8400	1.36
100_P(VAc <sub>0.90-s</sub> -VL <sub>0.10</sub> )	87	88	12 200	12 900	15 000	1.40
100_P(VAc <sub>0.90-s</sub> -VeoVa <sub>0.10</sub> )	83	96	10 000	8500	10 800	1.40
100_P(VAc <sub>0.95-s</sub> -VeoVa <sub>0.05</sub> )	85	83	8950	8350	11 900	1.30
100_P(VAc <sub>0.97-s</sub> -VeoVa <sub>0.03</sub> )	88	91	8630	9460	12 260	1.40
100_P(VAc <sub>0.98-s</sub> -VeoVa <sub>0.02</sub> )	84	83	8800	8470	10 200	1.40
100_P(VAc <sub>0.99-s</sub> -VeoVa <sub>0.01</sub> )	80	99	10 210	9180	12 300	1.30

<sup>a</sup> Individual conversion based on <sup>1</sup>H NMR calculations comparing monomer and polymer resonances

<sup>b</sup> Theoretical molar mass of the statistical copolymers calculated from conversion

<sup>c</sup> Experimental molar mass of the statistical copolymers, calculated from end group analysis by <sup>1</sup>H NMR comparing polymer chain-end and main chain resonances

<sup>d</sup> Experimental molar mass of the statistical copolymers calculated by SEC-THF using PS calibration

The evolution of the overall conversion with time was plot using molar conversion,  $X_{mol}$ , calculated from the individual monomer conversions *via* <sup>1</sup>H NMR (**Equation 22**).

$$X_{mol.} (\%) = X_{VAc} \times f_{VAc,0} + X_{CoM} \times f_{CoM,0} \quad (22)$$

Where  $f_{VAc,0}$  and  $f_{CoM,0}$  is, respectively, the initial molar fractions of VAc and CoM in the monomer mixture.

In general, when the individual molar conversions of each monomer are different and the molar masses of the monomers are different, the overall weight conversion should be considered for the plot of the evolution of  $M_n$  as a function of conversion, using the following relationship (**Equation 23**).<sup>[9]</sup>

$$\text{Overall weight conversion (\%)} = X_{wt}(\%) = X_{VAc} * W_{VAc,0} + X_{CoM} * W_{CoM,0} \quad (23)$$

Where  $X_{VAc}$  and  $X_{CoM}$  are the individual conversion of each monomer (VAc and CoM, respectively); and  $W_{VAc,0}$  and  $W_{CoM,0}$  are the initial weight fraction of VAc and CoM, respectively. If the reaction is controlled, then the molar mass should increase linearly with the overall weight conversion.<sup>[10]</sup>

## II.2 Characterization of P(VAc-s-VL) copolymers

A <sup>1</sup>H NMR spectrum of 100\_P(VAc<sub>0.90-s</sub>-VL<sub>0.10</sub>) obtained after purification is presented in **Figure III-2**. The attribution of the different signals is also provided.

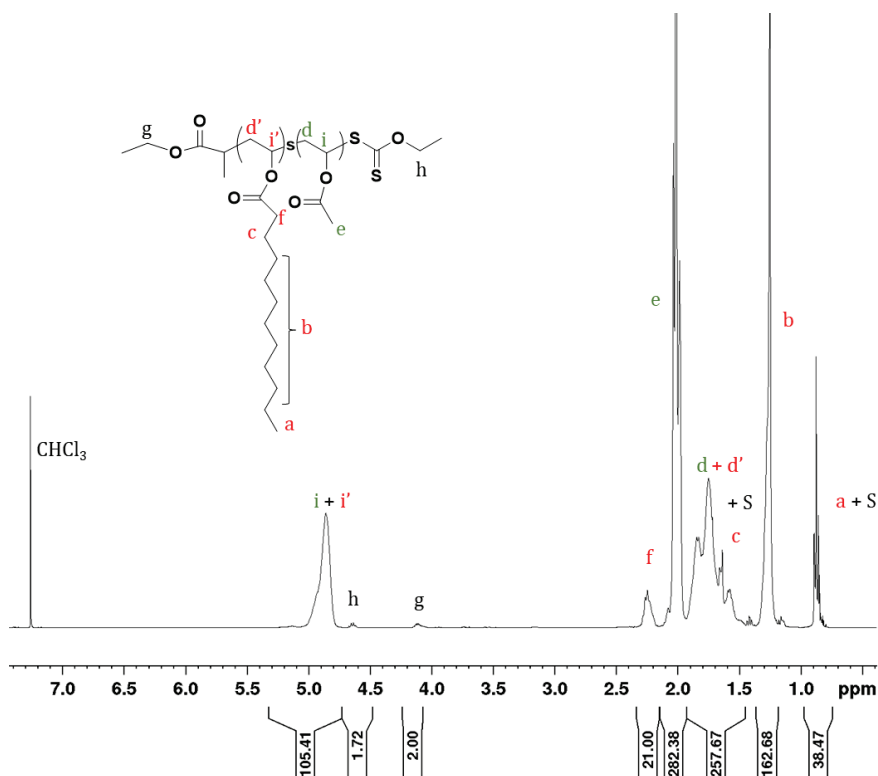


Figure III-2:  $^1\text{H}$  NMR spectrum of 100\_P(VAc<sub>0.90</sub>-s-VL<sub>0.10</sub>) in  $\text{CDCl}_3$  at R.T. S refers to residual petroleum ether from the purification.

Two areas of integration are defined to determine the composition and molar mass of the copolymer, according to **Equation 24** to **28**.  $M_n$  was calculated assuming that 100% of the chains were functionalized with the R group of the controlling agent (ethoxy) and using the integral of the corresponding resonance  $g$  as a reference. The DP is then obtained from the integration of the peak ( $i + i'$ ), and the average number of VL and VAc units per chains is provided by **Equations 24** and **25**, respectively.

$$(\text{VL}) = \frac{\int_{2.15}^{2.32} [\text{CH}_2]_f}{2} \quad \text{and} \quad (\text{VAc}) = \frac{\int_{4.7}^{5.3} [\text{CH}]_{i+i'} - (\text{VL})}{4.7} \quad (24) \text{ and } (25)$$

$$F_{\text{VL}} = 100 \times \frac{(\text{VL})}{(\text{VL}) + (\text{VAc})} \quad \text{and} \quad F_{\text{VAc}} = 100 \times \frac{(\text{VAc})}{(\text{VL}) + (\text{VAc})} \quad (26) \text{ and } (27)$$

$$M_n(\text{NMR}) = (\text{VL}) * M_{\text{VL}} + (\text{VAc}) * M_{\text{VAc}} + M_{\text{RAFT}} \quad (28)$$



With (VL) and (VAc) the average number of VL and VAc units per chain, respectively, and  $F_{VAc}$  and  $F_{VL}$  the molar fraction of VL and VAc, respectively;  $M_{VL}$ ,  $M_{VAc}$  and  $M_{RAFT}$  are the molar masses of VL, VAc and the RAFT/MADIX agent.

The plots of  $M_n$  (NMR) versus overall conversion for the statistical copolymerizations of VAc and VL are shown in **Figure III-3**.

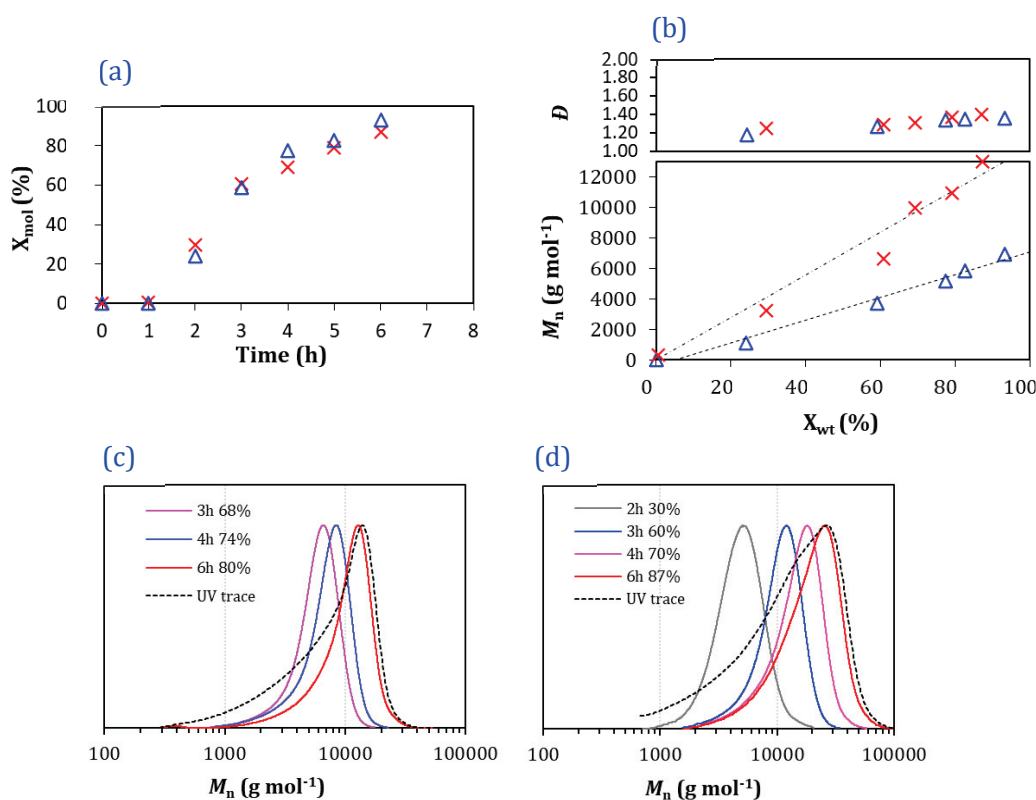


**Figure III-3:** RAFT/MADIX copolymerizations of VAc and VL in EtAc. Variation of the DP at fixed  $F_{VL} = 10$  mol.%: ( $\Delta$ ) targeted DP = 75; ( $\times$ ) targeted DP = 100;  $T = 60$  °C;  $[CTA]:[AIBN] = 5$ . **(a)** Evolution of the overall monomer conversion ( $X_{mol}$ ) with time; **(b)** Evolution of  $M_n$  (NMR) and  $\bar{D}$  with conversion; **(c)** and **(d)** Normalized SEC-THF traces of the molar mass evolutions with conversion for 75\_P(VAc-s-VL) and 100\_P(VAc-s-VL), respectively. Full lines = RI detector and dashed lines = UV detector at 280 nm.

DP of 75 and 100 were targeted for this copolymer, as it was previously demonstrated in **Chapter II** that good results in terms of particle size, PSD and stability were obtained for 75\_P(VOH-s-VAc) and 100\_P(VOH-s-VAc) when used as stabilizers. Both experiments showed linear evolution of the molar mass with conversion and narrow molar mass distributions (**Figure III-3**). Indeed,  $\bar{D}$  remained low for both experiments (1.3 and 1.4 for DP = 75 and 100, respectively, **Table III-1** entries 1 and 2), which attests the good control of the

polymerizations. Nevertheless, the SEC traces become slightly broader when the DP increases from 75 to 100 units (**Figure III-3 (c) and (d)**). The UV trace confirmed this broadening. This observation was attributed to competitive head-to-head additions that lead to the accumulation of less activated polymer chains, as already highlighted in the case of PVAc in **Chapter II**.

### II.3 Characterization of P(VAc-s-VeoVa) copolymers

**Figure III-4** provides a  $^1\text{H}$  NMR spectrum of 100\_P(VAc<sub>0.95</sub>-s-VeoVa<sub>0.05</sub>) obtained after purification, and the corresponding attribution of the different signals.

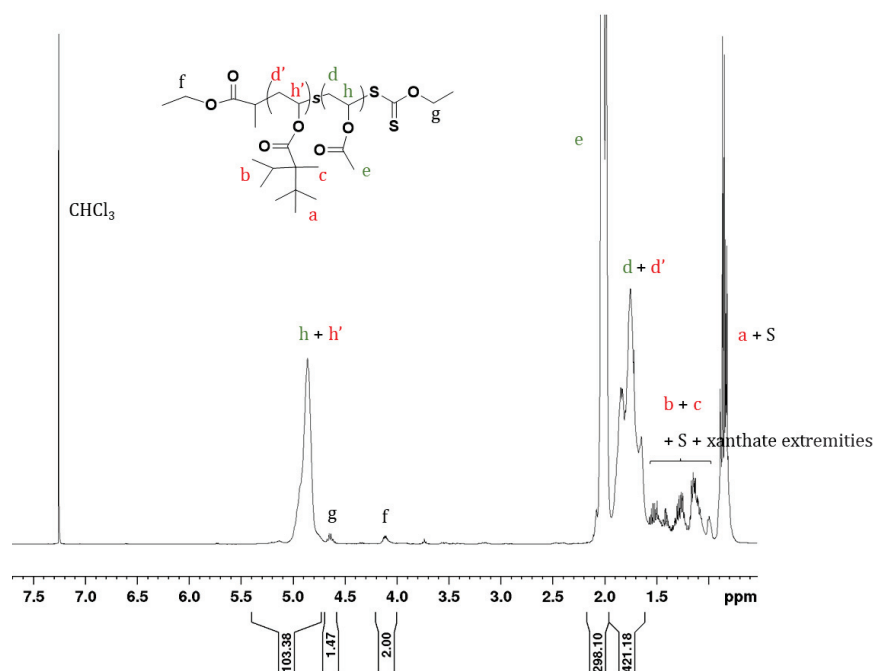


**Figure III-4:**  $^1\text{H}$  NMR spectrum of 100\_P(VAc<sub>0.95</sub>-s-VeoVa<sub>0.05</sub>) in  $\text{CDCl}_3$  at R.T. S refers to residual petroleum ether from the purification.

As for the VL-based statistical copolymers, it is possible to determine the average number of monomer units per polymer chain, thanks to the chain extremities (signals *f* and *g*, **Figure III-4**). The calculation is based on **Equations 29** and **30**. **Equation 33** also provides an evaluation of  $M_n$  (considering that all the chains were initiated by the RAFT/MADIX agent). The composition of the copolymer is determined by **Equations 31** and **32**. The global DP is then obtained from the integration of the signal ( $h + h'$ ).

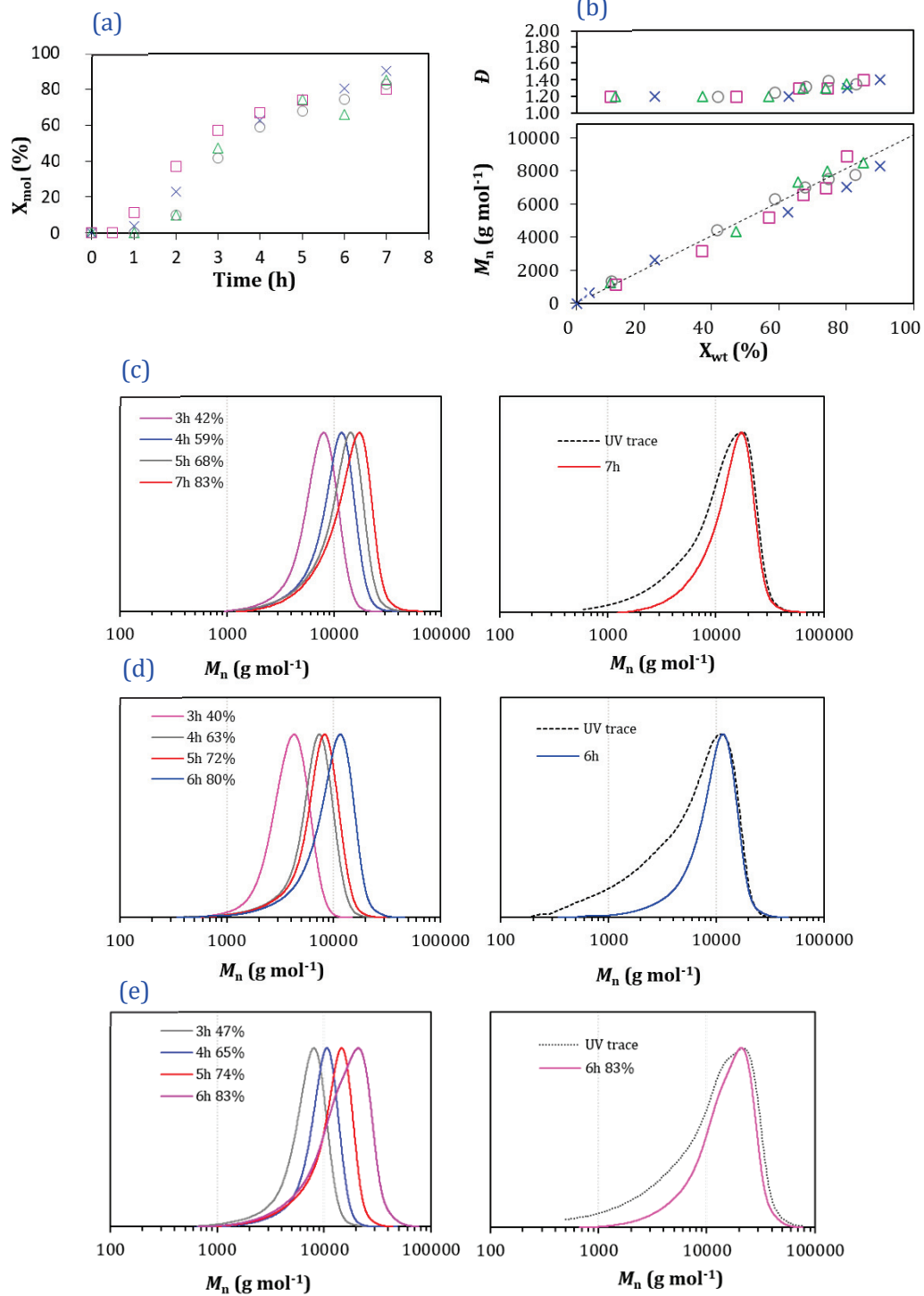
$$(\text{VAc}) = \int_{1.93}^{2.15} \frac{[\text{CH}_3]_e}{3} \quad \text{and} \quad (\text{VeOVA}) = \int_{4.7}^{5.3} [\text{CH}]_{\text{h+h}'} - (\text{VAc}) \quad (29) \text{ and } (30)$$

$$F_{\text{VAc}} = 100 \times \frac{(\text{VAc})}{(\text{VeOVA}) + (\text{VAc})} \quad \text{and} \quad F_{\text{VeOVA}} = 100 \times \frac{(\text{VeOVA})}{(\text{VeOVA}) + (\text{VAc})} \quad (31) \text{ and } (32)$$

$$M_n (\text{NMR}) = (\text{VeOVA}) * M_{\text{VeOVA}} + (\text{VAc}) * M_{\text{VAc}} + M_{\text{RAFT}} \quad (33)$$

With (VeOVA) and (VAc) the average number of VeOVA and VAc units per chain, respectively;  $F_{\text{VeOVA}}$  and  $F_{\text{VAc}}$  the molar fraction of VeOVA and VAc, respectively and  $M_{\text{VeOVA}}$ ,  $M_{\text{VAc}}$  and  $M_{\text{RAFT}}$  the molar masses of VeOVA, VAc and the RAFT/MADIX agent.

All the syntheses targeted a DP = 100, and  $F_{\text{VeOVA}}$  was varied from 10 to 1 mol.%. Similar to the VL-based statistical copolymers, the kinetics of the copolymerizations of VAc and VeOVA were followed by  $^1\text{H}$  NMR. An induction period of one hour was observed in all the studied systems, and the variation of  $F_{\text{VeOVA}}$  did not seem to affect the kinetics of the polymerization (**Figure III-5 (a)**). The plots of  $M_n$  versus overall conversion are provided in **Figure III-5 (b)**. For all the experiments, linearity of molar mass with overall conversion was observed. SEC-THF analyses showed that the molar mass distributions of the copolymers remained narrow for all samples (dispersity lower than 1.4 at 80% conversion). These results confirmed that the polymerizations were well controlled, regardless of the fraction of VeOVA (**Figure III-5**).



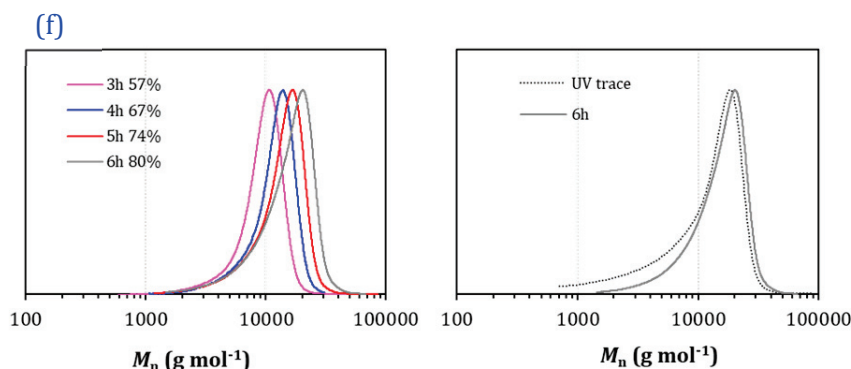


**Figure III-5:** RAFT/MADIX copolymerizations of VAc and VeoVa in EtAc. Variation of  $F_{\text{VeoVa}}$ : (○) 10 mol.%; (×) 5 mol.%; (△) 2 mol.% and (□) 1 mol.%.  $T = 60\text{ }^{\circ}\text{C}$ ;  $[\text{CTA}]:[\text{AIBN}] = 5$ . **(a)** Evolution of the overall monomer conversion ( $X_{\text{mol}}$ ) with time; **(b)** Evolution of  $M_n$  (NMR) and  $D$  with  $X_{\text{wt}}$  and **(c)** to **(f)**: SEC-THF traces of the molar mass evolutions with conversion of 100\_P(VAc-*s*-VeoVa)s for different fractions of VeoVa in the copolymer: **(c)** 10 mol.% **(d)** 5 mol.% **(e)** 2 mol.% and **(f)** 1 mol.%. Full lines correspond to normalized RI traces and dashed lines are the normalized UV traces at 280 nm. The percentage value refers to the conversion.

The UV trace did not perfectly overlap with the RI signal for SEC analyses. Again, this could be because of the accumulation of chains undergoing head-to-head addition that generates a 2,1-inserted vinyl ester monomer unit connected to the xanthate extremity, which are difficult to further reactivate during the polymerization. Due to its bulky structure, one can nevertheless anticipate that the VeoVa could have an influence on the proportion of these defects. Indeed, due to steric hindrance, it can be reasonably assumed that if the last unit connected to the xanthate moiety is a VeoVa unit, then regular head-to-tail addition of a VAc unit onto the macroradical released from the addition fragmentation step would be favored. The same trend would hold for a VeoVa addition on a macroradical carrying a vinyl acetate ultimate unit. This is schematically represented in **Figure III-6**.

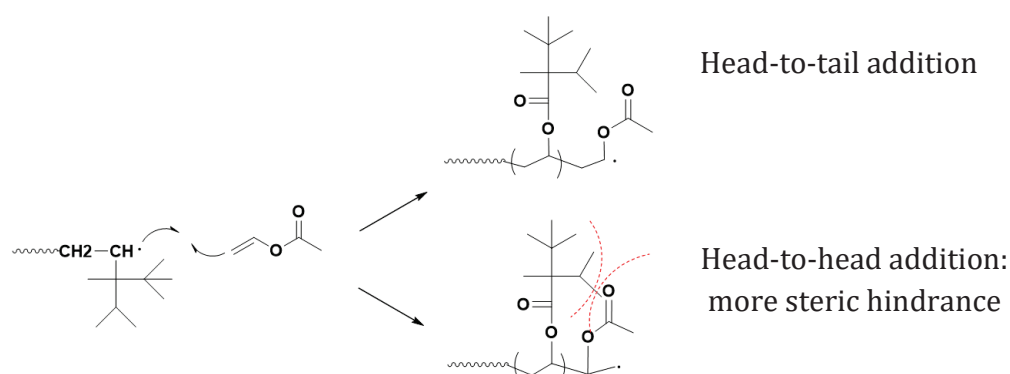


**Figure III-6:** Scheme of the head-to-tail *versus* head-to-head addition of a VAc inserted unit, where the last unit of the macroradical was VeoVa, and the corresponding steric hindrance induced by the VeoVa unit.

VeoVa is used in small amount compared to VAc, but if this phenomenon is indeed taking place, it might affect the amount of accumulated less reactivatable chains and potentially improve the livingness of the chains (¥).

To verify this hypothesis, the same calculations, previously used in **Chapter II, Section II (Equation 8)** for the determination of ¥ were performed on the 100\_P(VAc-s-VeoVa) copolymers with different  $F_{\text{VeovVa}}$ , and compared to the ones performed on 100\_PVAc (**Figure III-7**).

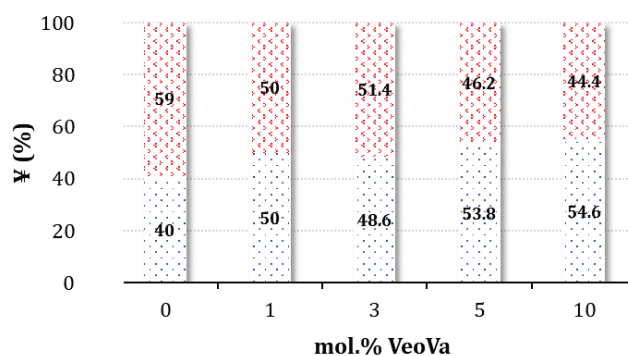


**Figure III-7:** Chain-end functionality (¥) of the synthesized 100\_P(VAc-s-VeoVa) depending on  $F_{\text{VeovVa}}$  with in blue the molar fraction of head-to-tail and in red the molar fraction of head-to-head inserted monomer unit connected to the xanthate moiety.

**Figure III-7** shows that the higher the proportion of VeoVa in the copolymer, the higher the chain-end fidelity. This tends to confirm the hypothesis that the addition of VeoVa units improves the control of the polymerization of VAc by decreasing the number of head-to-head defects. The dispersities of the polymerizations were also slightly lower than the ones observed for 100\_PVAc (1.3 to 1.4 *versus* 1.5, respectively), which is an additional contribution to confirm the hypothesis (**Table III-1**). These results also showed that head-to-head additions and accumulation of less reactivatable chains cannot be completely erased as 44.4% of such chains are formed when 10 mol.% of VeoVa is employed (**Figure III-7**). The main focus of this study was to eventually synthesize stabilizers that are dispersible in water, and it will be demonstrated in the future sections that the higher the VeoVa content, the lower the dispersibility. Therefore, no further investigation was performed at this stage on the improvement of the control of VAc polymerization by the addition of VeoVa.

### III. Alcoholysis of P(VAc-*s*-VL) and P(VAc-*s*-Veova) copolymers

To the best of our knowledge, no work has ever been carried out on the direct alcoholysis of P(VAc-*s*-VL) statistical copolymers. Congdon *et al.*<sup>[11]</sup> studied the effect of more hydrophobic side chains (acetyl, propanoyl and butanoyl) onto the thermal properties of modified P(VOH-*s*-VAc). The authors first completely alcoholized RAFT-synthesized PVAc with different DPs, before they partially alkanoyled the obtained PVOH with vinyl acetate, vinyl butanoate and vinyl propionate in a second step. No data is therefore available in the literature concerning the ability of a vinylic monomer with a long alkyl chain (such as VL), inserted in a copolymer, to resist an alkaline medium. In contrast, Veova is a highly branched ester, known to be resistant to alcoholysis.<sup>[12]</sup> Davies *et al.*<sup>[13]</sup> studied the alkaline hydrolysis of copolymers obtained by emulsion copolymerization, and in particular of VAc-based copolymers. The authors demonstrated that the rate of hydrolysis was reduced with increasing the proportion of branched hydrophobic vinyl comonomers (*e.g.*, Veova). It was concluded that the major factors affecting the hydrolysis was the steric effect arising from the copolymer microstructure. This resistance can be explained by a neighboring group steric effect.<sup>[14]</sup> Yang and coworkers<sup>[15]</sup> observed a similar behavior when they synthesized well-defined block copolymers of VAc and Veova in the presence of isopropylxanthic disulfide. The resulting block copolymer, PVAc-*b*-PVeova was hydrolyzed and yielded PVOH-*b*-PVeova. The presence of unhydrolyzed Veova units was demonstrated by <sup>1</sup>H NMR in DMSO-*d*<sub>6</sub> (despite a relatively limited solubility of the copolymer in this solvent). Additionally, due to its steric hindrance, not only is Veova resistant to hydrolysis, but it also protects a few neighboring acetate groups (an average of 2 units was reported in the literature).<sup>[12],[16]</sup> This behavior is referred to as the umbrella effect.

For the scope of this research work, alcoholysis conditions (based on the hydrolysis study of PVAc in **Chapter II**), with a [monomer]:[NaOH] ratio of 1:0.025 was used for the statistical P(VAc-*s*-VL) and P(VAc-*s*-Veova) copolymers. The hydrolysis degree and the composition of the copolymer with hydrolysis time were determined by <sup>1</sup>H NMR. The protocol is detailed in the **Experimental Section IV.2**.

#### III.1 Alcoholysis of P(VAc<sub>0.90</sub>-*s*-VL<sub>0.10</sub>)

As no information related to the alcoholysis of VL-based polymers is available in the literature, the attribution of the NMR signal was performed by comparison of the spectra obtained for 100\_P(VAc<sub>0.90</sub>-*s*-VL<sub>0.10</sub>) (before alcoholysis), P(VOH-*s*-VL-*s*-VAc) obtained after alcoholysis and 75\_P(VOH<sub>0.88</sub>-*s*-VAc<sub>0.12</sub>) studied in **Chapter II (Figure III-8)**.

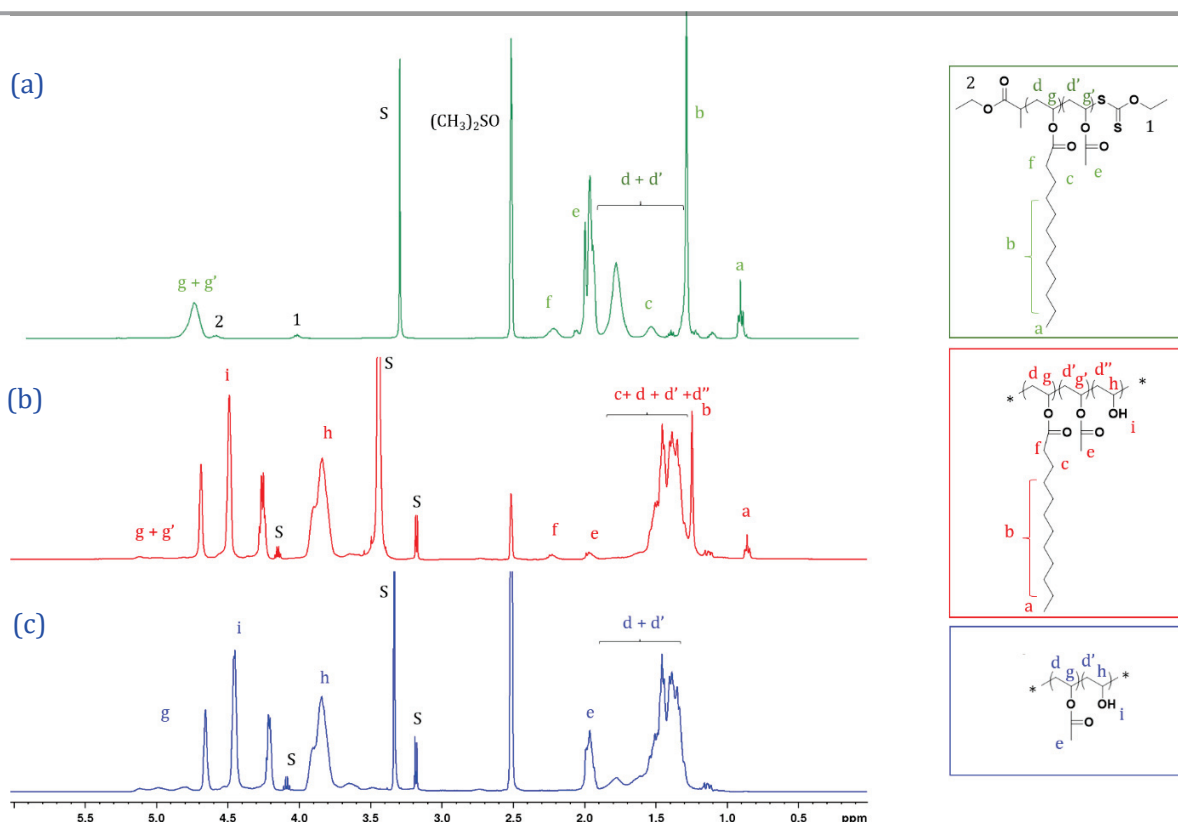


**Figure III-8:**  $^1\text{H}$  NMR spectra of (a)  $100\text{-P}(\text{VAc}_{0.90}\text{-s-VL}_{0.10})$ , (b)  $100\text{-P}(\text{VOH}_z\text{-s-VL}_y\text{-s-VAc}_w)$  and (c)  $75\text{-P}(\text{VOH}_{0.88}\text{-s-VAc}_{0.12})$  in  $\text{DMSO-d}_6$  at R.T., 256 scans, and their respective attributions. The alcoholysis was performed in MeOH at  $30^\circ\text{C}$  for 2 h with a ratio  $[\text{VAc}+\text{VL}]:[\text{NaOH}] = 1:0.025$  for (b) and 40 min with a ratio  $[\text{VAc}]:[\text{NaOH}] = 1:0.025$  for (c). S refers to residual methanol or water from the  $\text{DMSO-d}_6$ .

The molar fractions of VOH ( $F_{\text{VOH}}$ ), VAc ( $F_{\text{VAc}}$ ) and VL ( $F_{\text{VL}}$ ) in the copolymer were determined using the following set of equations (based on **Figure III-8 (b)**), allowing the kinetics of the alcoholysis to be monitored by  $^1\text{H}$  NMR (**Figure III-9**).



$$\begin{aligned}
 \text{HD} = F_{\text{VOH}} &= 100 \times \frac{\int_{3.7}^{3.9} [\text{CH}]_{\text{h}}}{\int_{3.7}^{3.9} [\text{CH}]_{\text{h}} + \int_{1.8}^{2.1} \frac{[\text{CH}_3]_{\text{e}}}{3} + \int_{2.2}^{2.35} \frac{[\text{CH}_2]_{\text{f}}}{2}} \\
 F_{\text{VAc}} &= 100 \times \frac{\int_{1.8}^{2.1} \frac{[\text{CH}_3]_{\text{e}}}{3}}{\int_{3.7}^{3.9} [\text{CH}]_{\text{h}} + \int_{1.8}^{2.1} \frac{[\text{CH}_3]_{\text{e}}}{3} + \int_{2.2}^{2.35} \frac{[\text{CH}_2]_{\text{f}}}{2}} \\
 F_{\text{VL}} &= 100 \times \frac{\int_{2.2}^{2.35} \frac{[\text{CH}_2]_{\text{f}}}{2}}{\int_{3.7}^{3.9} [\text{CH}]_{\text{h}} + \int_{1.8}^{2.1} \frac{[\text{CH}_3]_{\text{e}}}{3} + \int_{2.2}^{2.35} \frac{[\text{CH}_2]_{\text{f}}}{2}}
 \end{aligned} \tag{34}$$

One can first note that the presence of sodium acetate and lauric acid as by-products of the hydrolysis of VAc and VL units, are visible at 1.6 ppm and 2.3 ppm in the NMR spectra. The last NMR spectrum (**Figure III-9 (a)**, n°5) corresponds to the final sample, after the hydrolysis was stopped, and the polymer was washed several times with methanol and filtered, before being dried under vacuum. These by-products are consistently no longer visible in this spectrum, showing the efficiency of the washing process.

The evolutions of the composition of the copolymers with both DP = 75 and 100 show that the alcoholysis was slightly faster for the VAc units than for the VL units (**Figure III-9 (b)** and **(c)**).

Finally, even after 2 h of alcoholysis under the conditions used, the signals corresponding to the methyl protons of the VAc units (e) and the methylene protons of the VL units (f), at 2 and 2.3 ppm, respectively, were still slightly visible on the NMR spectrum, which attests that not all the VAc and VL units could be hydrolyzed.

The alcoholysis of 100\_P(VAc<sub>0.90</sub>-s-VL<sub>0.10</sub>) was carried out a second time on the same batch of copolymer at a larger scale (45 g) and a third time with a different batch of 100\_P(VAc<sub>0.90</sub>-s-VL<sub>0.10</sub>), and provided comparable results (**Table III-2**, entries **S2.1** to **S2.3**). Eventually, to later evaluate the impact of F<sub>VL</sub> on the dispersibility of the copolymers, **Table III-2** also gathers several polymers obtained by stopping the alcoholysis at different times and featuring different compositions in VL, VOH and VAc units.

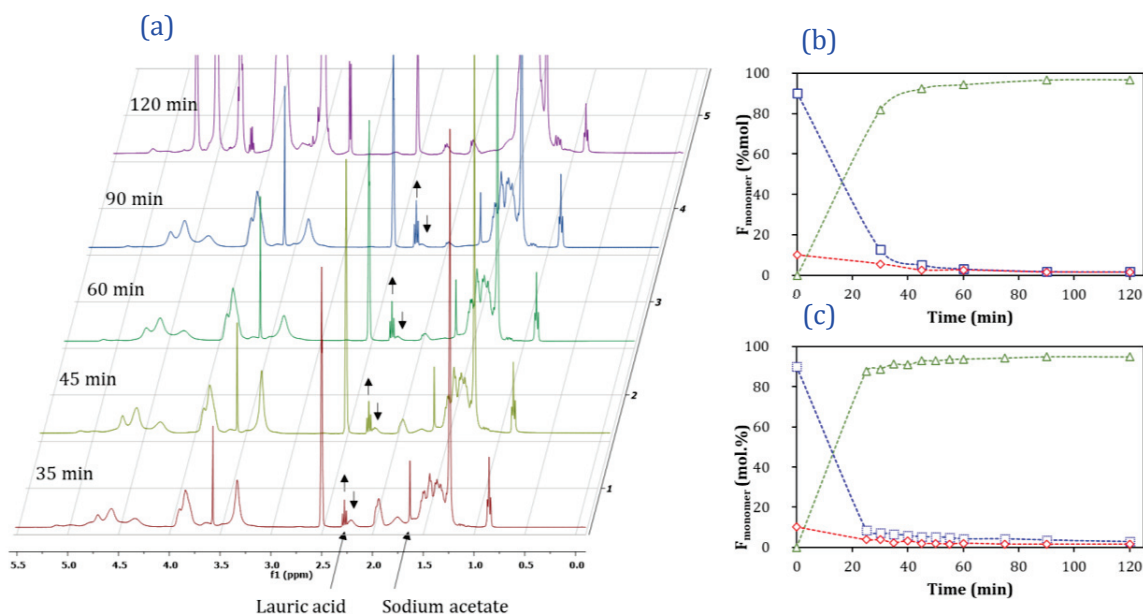


Figure III-9: (a)  $^1\text{H}$  NMR spectra of the samples withdrawn at different times during the alcoholysis of  $100\text{-P}(\text{VAc}_{0.90}\text{-S-VL}_{0.10})$  with  $[\text{VAc+VL}]:[\text{NaOH}] = 1:0.025$ , and plots of the kinetics of the alcoholysis for (b)  $100\text{-P}(\text{VAc}_{0.90}\text{-S-VL}_{0.10})$  and (c)  $75\text{-P}(\text{VAc}_{0.90}\text{-S-VL}_{0.10})$ . Evolution the molar fractions of VOH ( $\text{--}\Delta\text{--}$ ), VAc ( $\text{--}\square\text{--}$ ) and VL ( $\text{--}\diamond\text{--}$ ) units with alcoholysis time. The black arrows successively show the appearance of the by-product lauric acid while the VL units are alcoholized with time.

Table III-2: Library of  $\text{P}(\text{VOH-s-VL-s-VAc})$  statistical copolymers obtained after alcoholysis of  $\text{P}(\text{VAc-s-VL})$  for different amount of time (from 25 min to 2 h depending on the targeted composition) at  $30^\circ\text{C}$  in methanol.

Entry	Structure before hydrolysis	Structure after hydrolysis
S1	$75\text{-P}(\text{VAc}_{0.90}\text{-S-VL}_{0.10})$	$75\text{-P}(\text{VOH}_{0.957}\text{-S-VL}_{0.015}\text{-S-VAc}_{0.028})$
S2.1		$100\text{-P}(\text{VOH}_{0.970}\text{-S-VL}_{0.015}\text{-S-VAc}_{0.015})$
S2.2		$100\text{-P}(\text{VOH}_{0.966}\text{-S-VL}_{0.016}\text{-S-VAc}_{0.018})$
S2.3		$100\text{-P}(\text{VOH}_{0.966}\text{-S-VL}_{0.015}\text{-S-VAc}_{0.019})$
S3	$100\text{-P}(\text{VAc}_{0.90}\text{-S-VL}_{0.10})$	$100\text{-P}(\text{VOH}_{0.96}\text{-S-VL}_{0.02}\text{-S-VAc}_{0.02})$
S4		$100\text{-P}(\text{VOH}_{0.91}\text{-S-VL}_{0.04}\text{-S-VAc}_{0.05})$
S5		$100\text{-P}(\text{VOH}_{0.86}\text{-S-VL}_{0.05}\text{-S-VAc}_{0.09})$

### III.2 Alcoholysis of P(VAc-s-VeoVa)

The degree of alcoholysis and composition of the different 100\_P(VOH<sub>z</sub>-s-VeoVa<sub>y</sub>-s-VAc<sub>w</sub>) were determined by <sup>1</sup>H NMR analyses performed in DMSO-d<sub>6</sub>. The assignments were made based on the attributions reported in the paper from Gu *et al.*<sup>[5]</sup> The spectrum was compared to the spectra of 100\_P(VAc<sub>0.90</sub>-s-VeoVa<sub>0.10</sub>) before hydrolysis and of 75\_P(VOH<sub>0.88</sub>-s-VAc<sub>0.12</sub>) (Figure III-10).

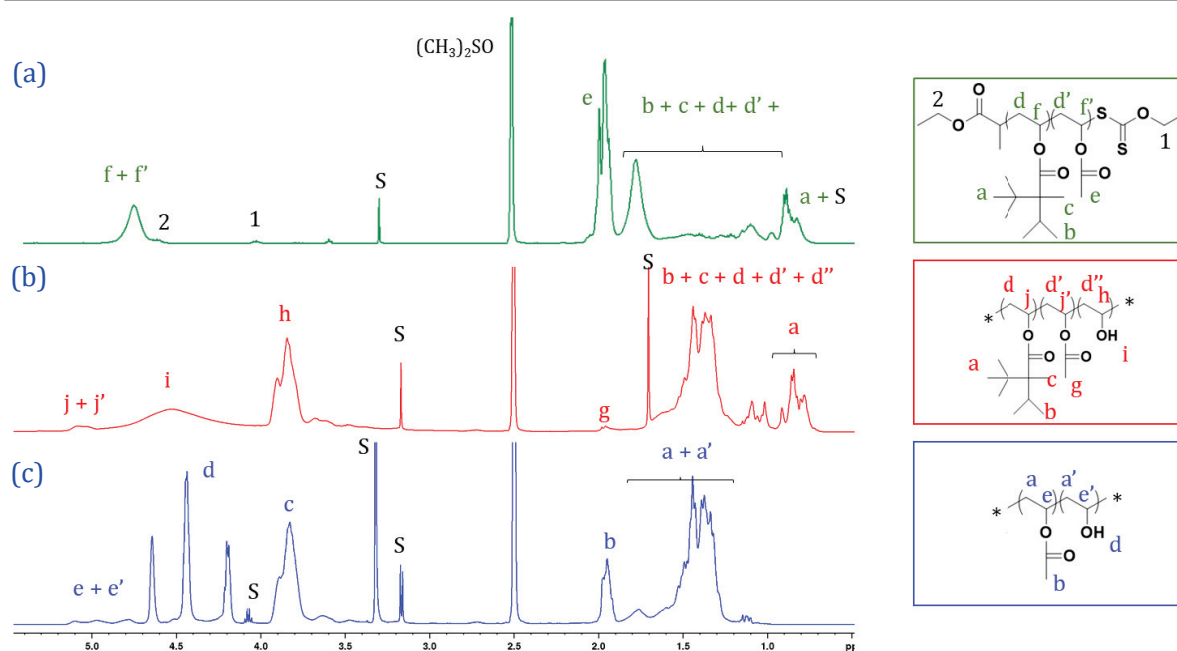


Figure III-10: <sup>1</sup>H NMR spectra of (a) 100\_P(VAc<sub>0.90</sub>-s-VeoVa<sub>0.10</sub>); (b) 100\_P(VOH-s-VAc-s-VeoVa) and (c) 75\_P(VOH<sub>0.88</sub>-s-VAc<sub>0.12</sub>) in DMSO-d<sub>6</sub> at R.T., 256 scans, and their respective assignments. The alcoholysis was performed in MeOH at 30 °C for 2 h with a ratio [VAc+VeoVa]:[NaOH] = 1:0.025 for (b) and 40 min with a ratio [VAc]:[NaOH] = 1:0.025 for (c). S refers to residual solvents: methanol or acetic acid residues and water from the DMSO-d<sub>6</sub>.

The molar fractions of VOH ( $F_{\text{VOH}}$ ), VAc ( $F_{\text{VAc}}$ ) and VeoVa ( $F_{\text{VeoVa}}$ ) were calculated using the following set of equations (based on Figure III-10 (b)), allowing the kinetics of the alcoholysis of the statistical copolymers to be monitored by <sup>1</sup>H NMR (Figure III-11).

$$\begin{aligned}
 \text{HD} = F_{\text{VOH}} &= 100 \times \frac{\int_{3.7}^{3.9} [\text{CH}]_{\text{h}}}{\int_{3.7}^4 [\text{CH}]_{\text{h}} + \int_{1.8}^{2.1} \frac{[\text{CH}_3]_{\text{g}}}{3} + \int_{0.66}^{0.95} \frac{[\text{CH}_3]_{\text{a}}}{9}} \\
 F_{\text{VAc}} &= 100 \times \frac{\int_{1.8}^{2.1} \frac{[\text{CH}_3]_{\text{g}}}{3}}{\int_{3.7}^4 [\text{CH}]_{\text{h}} + \int_{1.8}^{2.1} \frac{[\text{CH}_3]_{\text{g}}}{3} + \int_{0.66}^{0.95} \frac{[\text{CH}_3]_{\text{a}}}{9}} \\
 F_{\text{VeOVA}} &= 100 \times \frac{\int_{0.66}^{0.95} \frac{[\text{CH}_3]_{\text{a}}}{9}}{\int_{3.7}^4 [\text{CH}]_{\text{h}} + \int_{1.8}^{2.1} \frac{[\text{CH}_3]_{\text{g}}}{3} + \int_{0.66}^{0.95} \frac{[\text{CH}_3]_{\text{a}}}{9}}
 \end{aligned} \tag{35}$$

**Figure III-11** confirms that VeoVa units are not sensitive to hydrolysis, as  $F_{\text{VeOVA}}$  remained constant throughout the alcoholysis process. However, the  $F_{\text{VAc}}$  decreased as the VAc units were hydrolyzed and converted into VOH ones (indicated by an increase in  $F_{\text{VOH}}$  for every system). The alcoholysis of 100\_P(VAc<sub>0.90</sub>-s-VeoVa<sub>0.10</sub>) was performed a second time and provided similar results confirming the robustness of the process (**Table III-3**, entry **S6.2**).

Additionally, **Figure III-10 (b)** shows that under these alcoholysis conditions (2 h with a ratio [VAc+VeoVa]:[NaOH] = 1:0.025), the signal corresponding to the methyl protons of VAc units (*g*) at 1.8 – 2.1 ppm was still (merely) visible in the NMR spectrum and accounted for 2 mol.%, which indicates that not all the VAc units were hydrolyzed. This can be attributed to the aforementioned umbrella effect provided by the VeoVa units neighboring VAc units.<sup>[12],[16]</sup>

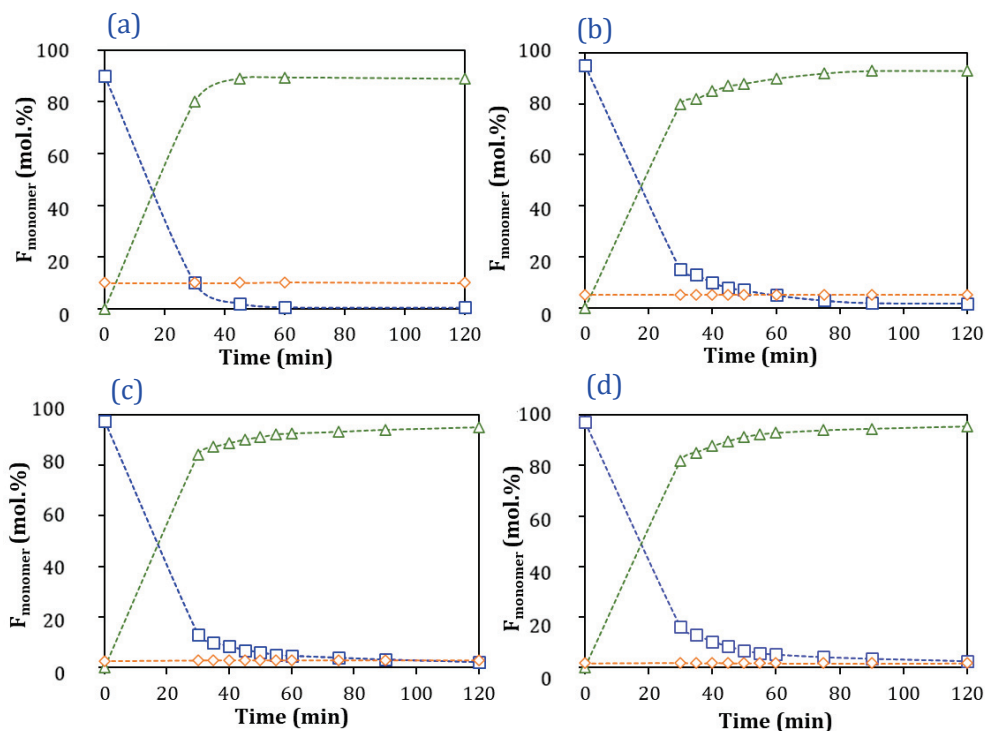


Figure III-11: Kinetics of the alcoholysis of (a) 100\_P(VAc<sub>0.90-s</sub>-VeoVa<sub>0.10</sub>), (b) 100\_P(VAc<sub>0.95-s</sub>-VeoVa<sub>0.05</sub>), (c) 100\_P(VAc<sub>0.97-s</sub>-VeoVa<sub>0.03</sub>) and (d) 100\_P(VAc<sub>0.99-s</sub>-VeoVa<sub>0.01</sub>) with [VAc+VeoVa]:[NaOH] = 1:0.025. Evolution of the molar fractions of VOH (---△---), VAc (---□---) and VeoVa (---◇---).

Table III-3: Library of 100\_P(VOH-s-VeoVa-s-VAc) statistical copolymers obtained after alcoholysis of P(VAc-s-VeoVa) for 2 h at 30 °C in methanol.

Entry	Structure before hydrolysis	Structure after hydrolysis
S6.1	100_P(VAc <sub>0.90-s</sub> -VeoVa <sub>0.10</sub> )	100_P(VOH <sub>0.88-s</sub> -VeoVa <sub>0.10-s</sub> -VAc <sub>0.02</sub> )
S6.2		100_P(VOH <sub>0.875-s</sub> -VeoVa <sub>0.10-s</sub> -VAc <sub>0.02</sub> )
S7	100_P(VAc <sub>0.95-s</sub> -VeoVa <sub>0.05</sub> )	100_P(VOH <sub>0.93-s</sub> -VeoVa <sub>0.05-s</sub> -VAc <sub>0.018</sub> )
S8	100_P(VAc <sub>0.97-s</sub> -VeoVa <sub>0.03</sub> )	100_P(VOH <sub>0.95-s</sub> -VeoVa <sub>0.03-s</sub> -VAc <sub>0.02</sub> )
S9	100_P(VAc <sub>0.98-s</sub> -VeoVa <sub>0.02</sub> )	100_P(VOH <sub>0.96-s</sub> -VeoVa <sub>0.02-s</sub> -VAc <sub>0.02</sub> )
S10	100_P(VAc <sub>0.990-s</sub> -VeoVa <sub>0.011</sub> )	100_P(VOH <sub>0.975-s</sub> -VeoVa <sub>0.010-s</sub> -VAc <sub>0.015</sub> )

### III.3 Conclusion on the alcoholysis of the statistical copolymers

The previous results show that it was necessary to synthesize different batches of P(VAc-*s*-VeOVA) with different compositions in VeOVA to get different compositions in hydrophobic CoM in the corresponding copolymers after hydrolysis. This is quite convenient because it is easier to fix the desired amount of CoM before hydrolysis with no risk to over-alcoholized the structure in the subsequent step. There is thus no need to control the kinetics of the alcoholysis. Nevertheless, a shift in DP can be obtained from one batch to another, and this difference can also impact the properties of the resulting stabilizer candidates after hydrolysis.

For the VL-based structures, however, different fractions of VL were targeted (from the same initial batch but different experiments), simply by neutralizing the alcoholysis at different times. This required a good knowledge of the kinetic profiles, but did not bring too much of a difficulty as the alcoholysis proved to be robust and reproducible.

#### IV. (Self-)Organization of the copolymers in water

As the copolymers synthesized during this work are meant to be used as stabilizers for emulsion polymerization, we thought it could be interesting to explore some of their features in water such as their dispersibility, their potential nano-organization and the surface tension of corresponding solution or dispersion.

##### IV.1 Dispersibility of the statistical copolymers in water

To mimic the emulsion polymerization composition (10 wt.% of stabilizer based on monomers, meaning 2.5 wt.% of stabilizer based on the total volume of the reaction), samples containing deionized water and 2.5 wt.% of each stabilizer candidates (from **S1** to **S10** in **Table III-2** and **Table III-3**) were prepared. The dispersibility of the statistical copolymers was first tested at R.T. ( $23 \pm 2$  °C). When the polymer did not dissolve after 2 h, the temperature was increased at 55 °C for 2 extra hours. If the polymer remained insoluble, the same procedure was carried out at 70 and 90 °C (**Table III-4**).

**Table III-4: Summary of the dispersibility of 75\_P(VOH-*s*-VL-*s*-VAc), 100\_P(VOH-*s*-VL-*s*-VAc) and 100\_P(VOH-*s*-VeoVa-*s*-VAc), with different hydrolysis degrees and molar composition of CoM.**

Stabilizer	Dispersibility at given temperature*			
	R.T.	55 °C	70 °C	90 °C
<b>S1:</b> 75_P(VOH <sub>0.957</sub> - <i>s</i> -VL <sub>0.015</sub> - <i>s</i> -VAc <sub>0.028</sub> )	⊗	⊗	⊖	-
<b>S2.2:</b> 100_P(VOH <sub>0.966</sub> - <i>s</i> -VL <sub>0.016</sub> - <i>s</i> -VAc <sub>0.018</sub> )	⊗	⊗	⊖	-
<b>S3:</b> 100_P(VOH <sub>0.96</sub> - <i>s</i> -VL <sub>0.02</sub> - <i>s</i> -VAc <sub>0.02</sub> )	⊗	⊗	⊖	-
<b>S4:</b> 100_P(VOH <sub>0.91</sub> - <i>s</i> -VL <sub>0.04</sub> - <i>s</i> -VAc <sub>0.05</sub> )	⊗	⊗	⊖	-
<b>S5:</b> 100_P(VOH <sub>0.86</sub> - <i>s</i> -VL <sub>0.05</sub> - <i>s</i> -VAc <sub>0.09</sub> )	⊗	⊗	⊗	⊗
<b>S6.1:</b> 100_P(VOH <sub>0.88</sub> - <i>s</i> -VeoVa <sub>0.10</sub> - <i>s</i> -VAc <sub>0.02</sub> )	⊗	⊗	⊗	⊗
<b>S7:</b> 100_P(VOH <sub>0.93</sub> - <i>s</i> -VeoVa <sub>0.05</sub> - <i>s</i> -VAc <sub>0.018</sub> )	⊗	⊗	⊗	⊗
<b>S8:</b> 100_P(VOH <sub>0.95</sub> - <i>s</i> -VeoVa <sub>0.03</sub> - <i>s</i> -VAc <sub>0.02</sub> )	⊗	⊗	⊖	⊖
<b>S9:</b> 100_P(VOH <sub>0.96</sub> - <i>s</i> -VeoVa <sub>0.02</sub> - <i>s</i> -VAc <sub>0.02</sub> )	⊗	⊖	✓	-
<b>S10:</b> 100_P(VOH <sub>0.975</sub> - <i>s</i> -VeoVa <sub>0.01</sub> - <i>s</i> -VAc <sub>0.015</sub> )	⊗	⊖	✓	-

\*A red cross indicates that the polymer is insoluble in water. An orange line indicates that it is insoluble at R.T. and higher temperatures, but dispersible or soluble at R.T., after heating at higher temperature. A green tick indicates that the copolymer is soluble at the mentioned temperature and remains dispersible when the solution is brought back to R.T.

**S5** was insoluble in water, regardless of the temperature. The VL-based statistical structures with HD between 91 and 96% (from **S1** to **S4**) were also not soluble at R.T. or 70 °C, but when the dispersions were cooled from 70 °C to R.T., the copolymers became visually dispersible and provided stable turbid dispersions to transparent dispersions (depending on the HD) (**Figure III-12**).

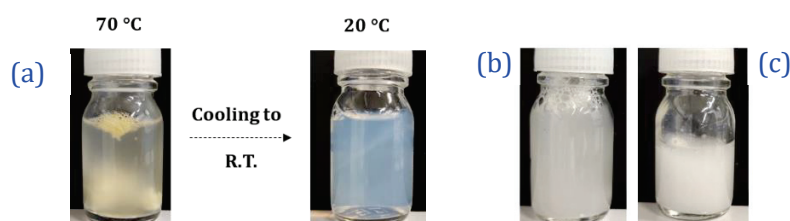


**Figure III-12** : Photographs of (a) **S2.1** from 70 °C to R.T. (b) **S3** back to R.T. after 2 h at 70 °C and (c) **S4** back to R.T. after 2 h at 70 °C.

These data show that the copolymers tend to form aggregates in water depending on the thermal treatment the samples undergo. This behavior could be explained by a reorganization of the hydrophobic and hydrophilic moieties, to minimize the interactions with water at elevated temperature. **S2.1** showed similar behavior to the three previously mentioned copolymers, but the dispersion was more transparent upon cooling. This may indicate a better dispersibility, or a formation of smaller aggregates. **S1** and **S2.1** showed similar behavior, suggesting that the DP did not have much impact on the dispersibility of the polymer in this case.

The statistical copolymer with  $F_{\text{VeOVA}} = 10$  mol.% (**S6.1**) was insoluble in water at R.T., 55, 70 and 90 °C, forming a compact solid regardless of the temperature. This solid remained in water after the solution was cooled to R.T. (**Figure III-13 (a)**). This copolymer, (with  $F_{\text{VeOVA}} = 10$  mol.%), was the first one to be synthesized. Considering that the amount of CoM should strongly impact the dispersibility in water, the fraction of VeoVa in the copolymer was then decreased to 5, 2 and 1 mol.%. These copolymers were thus successively synthesized, hydrolyzed and dispersed in deionized water. The copolymer containing 5 mol.% of VeoVa (**S7**) was not more soluble than the one containing 10 mol.%. **S8** ( $F_{\text{VeOVA}} = 3$  mol.%) was not soluble at R.T., nor at 55 °C, but slightly dispersible at 70 °C. Increasing the temperature did not help to solubilize it further and a precipitate appeared after the agitation was stopped and the solution was cooled down to R.T. (**Figure III-13 (b)**). Finally, **S9** ( $F_{\text{VeOVA}} = 2$  mol.%) was not soluble at R.T. but was slightly dispersible at 55 °C after 2 h. The temperature was then increased to 70 °C and a clear solution was obtained (**Figure III-13 (c)**). The polymer remained well-dispersed in water after the solution was cooled to R.T. (**Figure III-13 (c)**). Therefore,  $F_{\text{VeOVA}}$  was further decreased to 1 mol.% (**S10**) to see if this would improve the



dispersibility of the copolymer in water at lower temperature. Unfortunately, **S9** already contained only 2 mol.% of VeoVa and it was difficult to obtain a drastic difference in composition to visualize an effect on the dispersibility of the copolymer. Nevertheless, it seemed that **S10** provided a visually clearer solution than **S9** (**Figure III-13 (d)**).

---

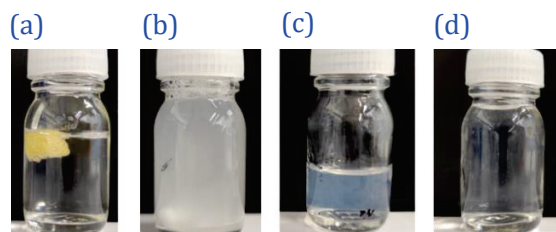
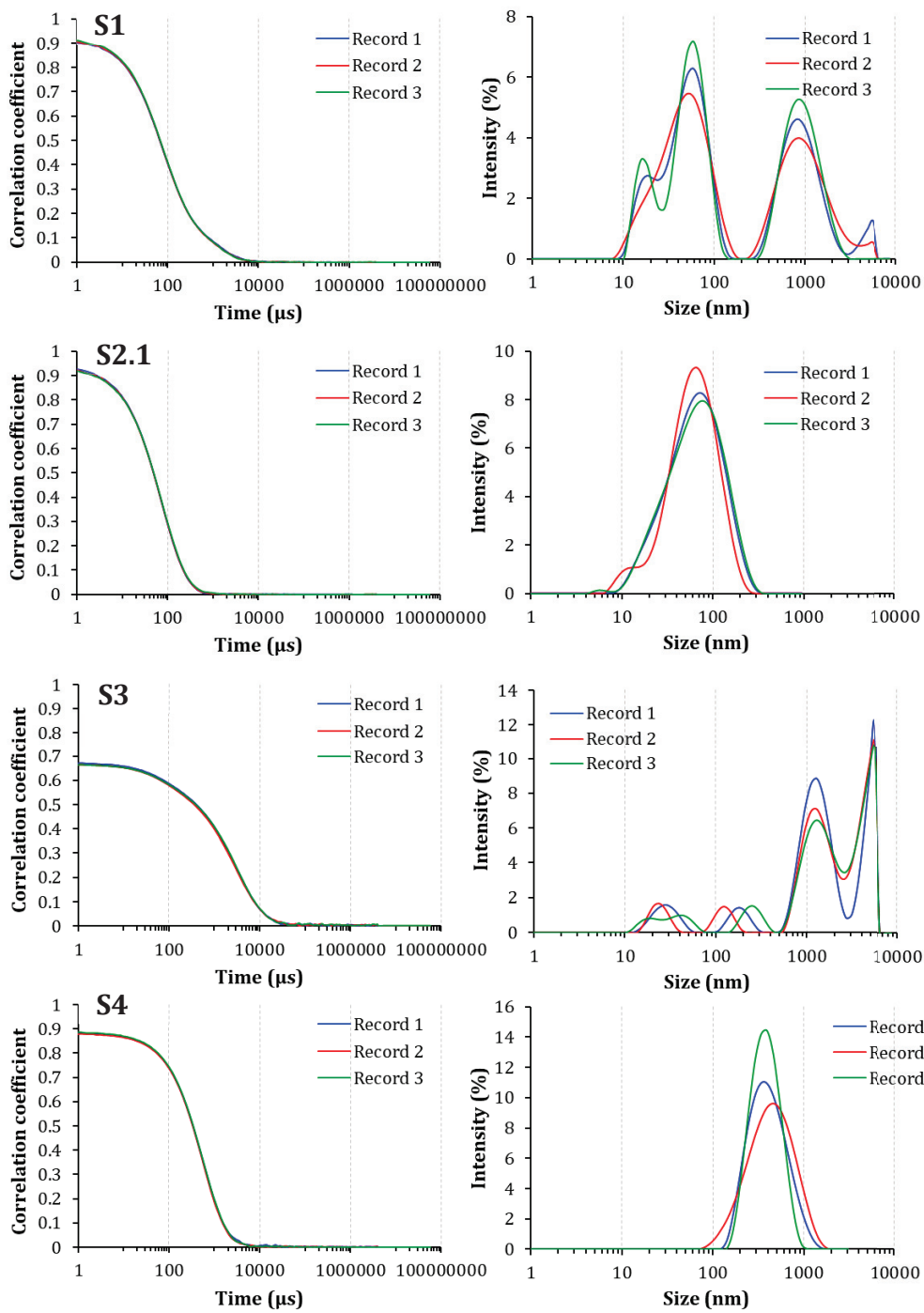


**Figure III-13:** Visual aspect of **(a)** and **(b)** S6.1 and S8 back to R.T. after 2 h at 90 °C; **(c)** and **(d)** S9 and S10 back to R.T. after 2 h at 70 °C.

---

## IV.2 Organization of the copolymer in water: DLS study

Self-assembly properties of **S1**, **S2.1**, **S3**, **S4**, **S9** and **S10** amphiphilic statistical copolymers were evaluated by DLS (**Figure III-14**). These stabilizer were chosen because they provided acceptable miscibility with water compared to the others. The solutions were analyzed without further dilution.



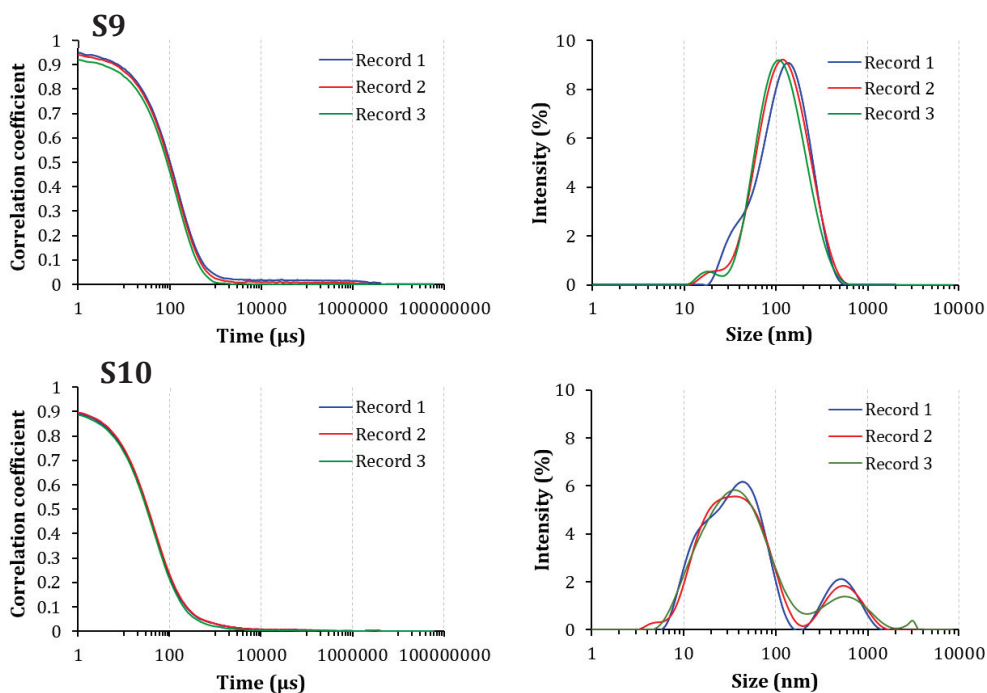


Figure III-14: DLS-size distributions in intensity for the 2.5 wt. % aqueous solution of the VL-based (S1 and S2.1, S3 and S4) and VeoVa-based (S9 and S10) statistical copolymers that are dispersible in water.

Table III-5: DLS analyses of the dispersible statistical copolymers after alcoholysis, including Mowiol 4-88 and the reference 75\_(PVOH<sub>0.88</sub>-S-VAc<sub>0.12</sub>) for comparison. The measurements were performed in water at 25 °C.

Entry	$M_n$ (g mol <sup>-1</sup> ) <sup>a</sup>	$Z_{av}$ (nm) <sup>b</sup>	PdI
Mowiol 4-88	8000*	15 / 172	>0.1
75_(PVOH <sub>0.88</sub> -S-VAc <sub>0.12</sub> )	4520	10 / 300	>0.1
<b>S1</b> : 75_P(VOH <sub>0.957</sub> -S-VL <sub>0.015</sub> -S-VAc <sub>0.028</sub> )	3550	20 / 90 / >1000**	>0.1
<b>S2.1</b> : 100_P(VOH <sub>0.970</sub> -S-VL <sub>0.015</sub> -S-VAc <sub>0.015</sub> )	4735	80	>0.1
<b>S3</b> : 100_P(VOH <sub>0.96</sub> -S-VL <sub>0.02</sub> -S-VAc <sub>0.02</sub> )	4850	25 / 200 / >1000**	>0.1
<b>S4</b> : 100_P(VOH <sub>0.91</sub> -S-VL <sub>0.04</sub> -S-VAc <sub>0.05</sub> )	5340	130	>0.1
<b>S9</b> : 100_P(VOH <sub>0.96</sub> -S-VeoVa <sub>0.02</sub> -S-VAc <sub>0.02</sub> )	4790	<b>20</b> / 120	0.1
<b>S10</b> : 100_P(VOH <sub>0.975</sub> -S-VeoVa <sub>0.01</sub> -S-VAc <sub>0.015</sub> )	4670	<b>25</b> / 600	>0.1

<sup>a</sup> Calculated by Equation 52 in Experimental

<sup>b</sup> Obtained by DLS

\* Average value calculated via  $M_w = 20\ 000 - 24\ 000$  and  $\bar{D} = 2.5 - 3$

\*\* No main population detected by the volume response of the DLS

**Bold** value = main population observed in volume, see Appendix 5

As mentioned in **Chapter II**, the correlation function gives precious information about the signal-to-noise ratio as well as on the presence of aggregates. This information is provided by the value of the intercept (which should be in range 0.85 – 1 for homogenous dispersions), the shape and slope of the correlation coefficient, and by the presence of slope breaks. Intercepts of the correlation curves are in the range 0.85 – 1 for almost every dispersion, except for **S3** (copolymer with  $F_{VL} = 2$  mol.%). The correlation curve of the dispersion that contained **S3** also showed at least two different slopes between 100 and 200  $\mu\text{s}$  and above 200  $\mu\text{m}$ , **Figure III-14**), and the signal in intensity confirmed the presence of four different movements. This can be either attributed to the presence of four different populations, or to a unique non-spherical population (which is less likely). Visually (**Figure III-12 (b) and (c)**), one can also observe that the dispersions that contained **S3** and **S4** were more turbid and viscous than the dispersion that contained **S2.1** (**Figure III-12 (a)**), which could suggest either the presence of big aggregates or non-spherical objects observed by DLS. The dispersion that contains **S3** (with  $F_{VL} = 2$  mol.%) seems to be the limit between two different configurations of the VL-based statistical copolymers in water: below 2 mol.% of VL in the copolymer, a single population with an average size of 80 nm is dispersed in water (which could be attributed to a pseudo-micelle configuration) (**S2.1, Figure III-14**). When the copolymer contains 2 mol.% of VL units, two main populations are visible: a small one in the range 25 - 100 nm, and a large one above 100 nm. This behavior was probably due to the statistical copolymer aggregates forming both single-chain folded micelles as well as multi-chain aggregates, thus appearing in the distributions as two separate size aggregates (**S3, Figure III-14**).

Finally, above 4 mol.% of VL, a single but large population is visible in the range 100 – 1000 nm (with an average diameter of 130 nm, **Table III-5**), which could be attributed to the presence of aggregates only (**S4, Figure III-14**). It is likely that at such CoM content ( $F_{VL} = 4$  mol.%), the copolymer reached a limit in dispersibility, and it tends to minimize the hydrophobic-hydrophilic interactions *via* a favorable organization in water. In summary, for similar DP = 100 but different composition of VL, one can observe that the objects detected by the DLS became larger with increasing the VL content, and the number of the populations fluctuated. This behavior would surely affect the micellization and thus stabilization efficiency of the copolymer. Nevertheless, this trend must be considered with care as the correlation curve for **S3** was not perfectly accurate (intercept way below 0.85, **Figure III-14**).

Additionally, based on the comparison of the DLS results of solutions that contained **S1** and **S2.1**, single-chain folding could be dictated by the relative amount of the hydrophobic units and their relative distribution along the backbone of the polymer chain. Indeed, for similar VL content (1.5 mol.%) but different DP, it was observed that the copolymer with DP = 75 provided a multi-modal distribution, with a population of large aggregates of approximately 1000 nm, a population in with an average size of 90 nm and another one in the range 15 - 20 nm (**S1, Figure III-14**). By contrast, the copolymer with DP = 100 presented only one

population (**S2**, **Figure III-14** with  $Z_{av} = 80$  nm). This behavior seems to indicate that both the CoM content and the molar mass impact the solution behavior of the copolymer.

Similarly, the copolymer with  $F_{Veova} = 1$  mol.% and  $DP = 100$  (**S10**) also presents two populations (one at approximately 10 - 30 nm and one in the range 30 - 100 nm). In these cases, 1 to 1.5 mol.% CoM corresponds to an average of 1 to 2 units per chains. It is possible that the copolymers with  $F_{Veova} = 1$  mol.% and  $F_{VL} = 1.5$  mol.% do not significantly impact the organization of the copolymer in water when compared to the standard P(VOH-s-VAc), which also provided a population at 10 nm (**Chapter II**). In fact, it is likely that some of the polymer chains in **S1**, **S2** and **S9** do not carry a CoM unit, and that the resulting copolymers are in fact a mixture of P(VOH-s-CoM-s-VAc) and P(VOH-s-VAc), which could explain the presence of two distinct populations.

For the VeoVa-based copolymers, it was more complicated to conclude on a correlation between the VeoVa content in the copolymer and the behavior of the copolymer in water, as only two samples were dispersible in water (**S9** and **S10**). Nevertheless, the size of the population detected by DLS was larger for the copolymer containing 2 mol.% VeoVa than the one containing 1 mol.% ( $Z_{av} = 25$  and 160 nm *versus* 20 and 600 nm, respectively, **Table III-5** and **Figure III-14**).

In any case, the results obtained by DLS were consistent with the visual observations made on the polymers dispersed in water: turbid dispersions contained larger aggregates than clear dispersions.

Noteworthy, the main population of the water dispersible VeoVa-based statistical copolymers exhibited smaller value of  $Z_{av}$  compared to the VL-based statistical copolymers with similar DP and similar CoM content. Indeed, for CoM content of 1 - 1.5 mol.%,  $Z_{av} = 25$  nm for the VeoVa-based copolymers and 80 nm for VL-based ones (**Table III-5**, entries **S10** and **S2.1**). At higher content (2 mol.%),  $Z_{av} = 25$  nm (and approximately 600 nm for the second population) when VeoVa is used against 200 nm (and higher than 1000 nm for the second population) for VL (**Table III-5**, entries **S9** and **S3**). This difference in conformation could be related to the stronger hydrophobic character of VeoVa, leading to a more important contraction of the core of the aggregates, to limit the interaction of the hydrophobic moieties with water. It could also be due to the fact that the reactivity ratios of VAc and VeoVa (0.99 and 0.92,<sup>[2]</sup> respectively) favors a more random distribution of the VeoVa units along the polymer chain compared to the VAc/VL system (VAc and VL reactivity ratios are 1.4 and 0.7,<sup>[3]</sup> respectively). As synthesized with a RDRP technique such as RAFT/MADIX, the P(VAc-s-VL) copolymers are rich in VAc at the beginning of the chain. This would lead to a block-like gradient distribution of the PVL sequences along the chain (before and after alcoholysis), resulting in longer hydrophobic sequences which will interact together and longer hydrophilic loops deployed in water, as schematized in **Figure III-15**.

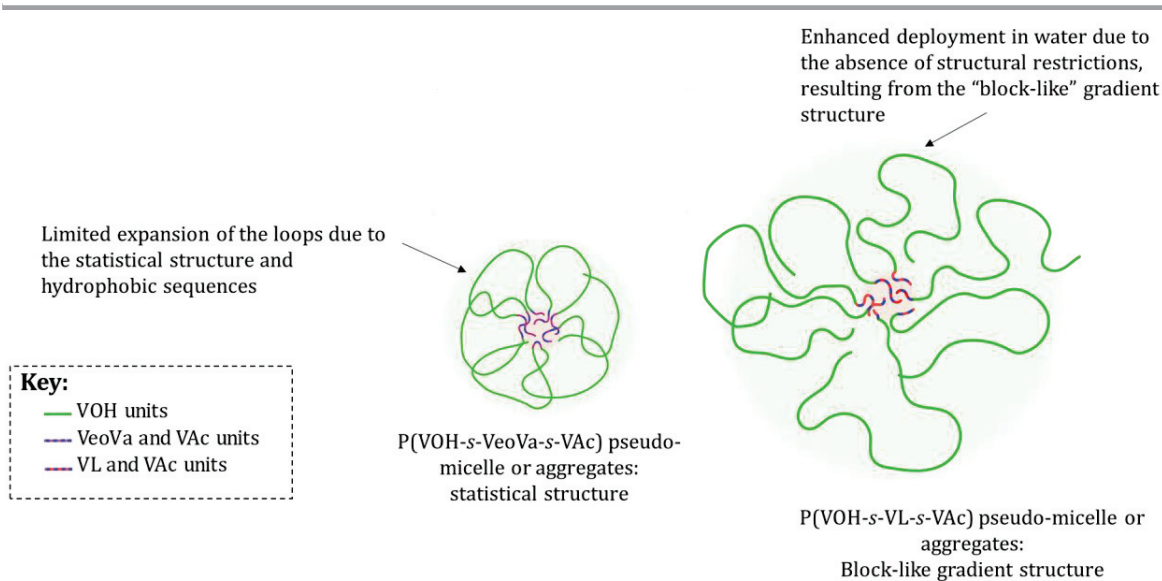


**Figure III-15: Scheme of the different hypothesized conformations of P(VOH-s-VeoVa-s-VAc) and P(VOH-s-VL-s-VAc) in water considering the different reactivity ratios of the comonomers and the resulting repartition of the CoM units along the polymer backbone after alcoholysis.**

---

These results show that the nature of the hydrophobic CoM and the amount of CoM has an impact on the micellization behavior of the statistical copolymers. To enlarge the vision, one can note that previously published data where copolymers containing VP and VL units, with different structures and composition were analyzed in solution, and provided aggregates in a similar range to what was observed here ( $\sim 25 - 200$  nm).<sup>[8]</sup> To further characterize the size, shape and conformation of these aggregates, it could be interesting to perform SLS and/or SAXS analysis.

### IV.3 Surface tension

Surface tension measurements of dispersions that contained 2.5 wt.% of the copolymers that are dispersible in water (after the thermal treatment) were performed, to evaluate their micellization ability (**S1**, **S2**, **S3**, **S9** and **S10**). The results of the measurement were compared to the RAFT-synthesized 100\_P(VOH<sub>0.88</sub>-s-VAc<sub>0.12</sub>) (**Figure III-16, (a)**). The trend suggests that the higher the molar fraction of VeoVa in the copolymer, the lower the measured surface tension. Additionally, this result shows that even a small fraction of VeoVa (*i.e.*, 1 mol.%) strongly affects the surface tension of the solution, compared to 100\_P(VOH<sub>0.88</sub>-s-VAc<sub>0.12</sub>). Similarly, surface tension of the solutions containing 2.5 wt.% of the dispersible VL-based statistical copolymers was carried out and compared to 100\_P(VOH<sub>0.88</sub>-s-VAc<sub>0.12</sub>) and 75\_P(VOH<sub>0.88</sub>-s-VAc<sub>0.12</sub>) (**Figure III-16 (b)**).



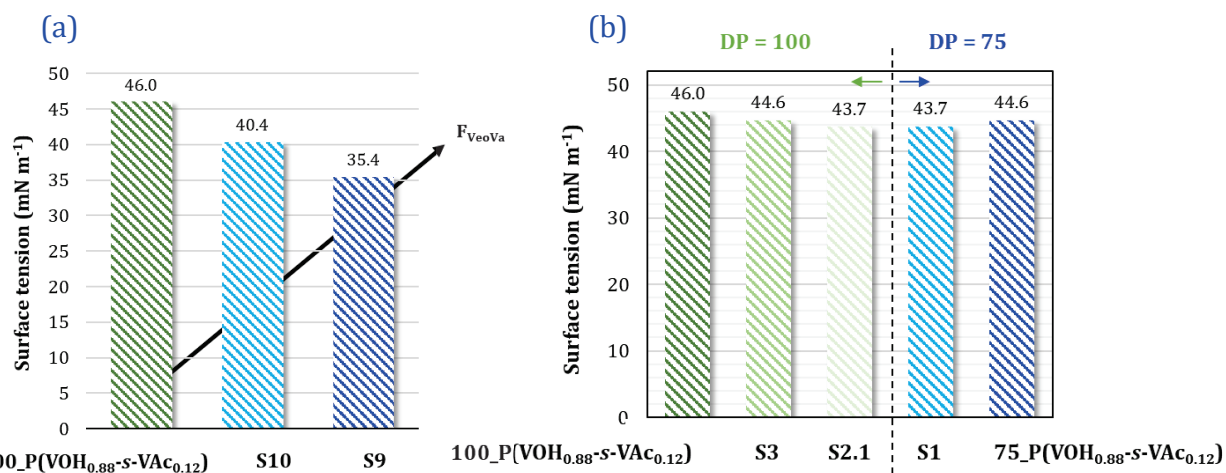


**Figure III-16: (a)** Influence of  $F_{\text{Veova}}$  in  $100\_P(\text{VOH-s-VeoVa-s-VAc})$  on the surface tension of 2.5 wt.% stabilizer dispersions at 25 °C, in comparison to  $100\_P(\text{VOH}_{0.88}\text{-s-VAc}_{0.12})$  and **(b)** Influence of  $F_{\text{VL}}$  in  $100\_P(\text{VOH-s-VL-s-VAc})$  (green) or of the DP at fixed  $F_{\text{VL}} = 1.5$  mol.% (comparison of S1, DP = 75 (blue) and S2.1, DP = 100 (green)) on the surface tension of 2.5 wt.% stabilizer dispersions at 25 °C. Comparison is made with  $100\_P(\text{VOH}_{0.88}\text{-s-VAc}_{0.12})$  and  $75\_P(\text{VOH}_{0.88}\text{-s-VAc}_{0.12})$ . The dispersions were obtained after the thermal treatment.

Concerning the VL-based statistical structures, it seems that there is no major difference between the surface tension of the copolymers. Regardless of their  $F_{\text{VL}}$  or their DP, they provided similar surface tensions when compared to the ones measured for  $P(\text{VOH}_{0.88}\text{-s-VAc}_{0.12})$ s at DP = 100 and 75 (**Figure III-16 (b)**). The dispersions showed lower surface tension than pure water (measured at 71.5 mN m<sup>-1</sup> at 25 °C), but higher than the ones obtained with the VeoVa-based copolymers. These results indicate that the VL-based statistical stabilizers are less surface active than the VeoVa-based ones.

It is worth noting that surface tension measurement of  $100\_P(\text{VOH}_{0.97}\text{-s-VL}_{0.015}\text{-s-VAc}_{0.015})$  (**S2.1**) could not be performed as not enough material was available for this characterization. Surface tension analyses were thus performed with a second batch of this copolymer (**S2.2**), but it will be discussed later in this Chapter, as it will highlight reproducibility issues associated with slight variations of the microstructure of the copolymers from one batch to another.

#### IV.4 Conclusion

The trends observed in the DLS and surface tension data indicate that the nature of the monomer is the primary governing factor in determining the solution properties of these statistical copolymers. VL-based statistical copolymers provided larger aggregates compared to the VeoVa-based stabilizers, and their surface tensions were systematically higher, regardless of the VL content. By contrast, a higher VeoVa content tended to decrease the size

of the aggregates and the surface tension. These behaviors could affect the stabilization efficiency of the particles in the emulsion polymerization process. This is why the previous copolymers that are either easily dispersible in water were considered as stabilizer candidates and were further tested in emulsion polymerization systems in the following section.



## V. Emulsion copolymerization of VAc and VeoVa with P(VOH-s-CoM-s-VAc) copolymers

### V.1 Screening with KPS

Before being tested with in the redox initiated system, the dispersible stabilizer candidates (**S1**, **S2.1**, **S3**, **S4**, **S9** and **S10**) were tested in a protocol of emulsion copolymerization of VAc with VeoVa on a small scale (10 mL round bottom flask with magnetic stirring), using a thermal initiation. If the thermal initiated emulsion polymerization is successful, then the stabilizers will further be tested on a 75 mL reactor with a redox initiation. This strategy allowed for fast screening of the most promising stabilizers before envisioning larger scales that require a larger quantity of stabilizer and monomer. The targeted solid content was 20 wt.% and 1 wt.% KPS based on monomers was used to initiate the polymerization. 10 wt.% stabilizers (based on monomers) were introduced in the reaction medium, according to the protocol described in the **Experimental Section V.1**. The following table summarizes the main results obtained for the studied systems.

**Table III-6: Emulsion copolymerization of VAc and VeoVa performed with the stabilizer candidates and KPS as initiator, for 2 h at 70 °C. Sc = 20%.**

Entry *	Stabilizer	Latex after storage for 24 h		
		Stability	Z <sub>av</sub> (nm)	PdI
ET-0	None	Sedimentation	>1000	1
ET-Mowiol	Mowiol 4-88	Yes	200	0.04
ET-100_PVOH	100_P(VOH <sub>0.88</sub> -S-PVAc <sub>0.12</sub> )	Yes	320	0.1
ET-S1	<b>S1</b> : 75_P(VOH <sub>0.970</sub> -S-VL <sub>0.015</sub> -S-VAc <sub>0.015</sub> )	Yes	<b>500</b> + 1000	0.6
ET-S2.1	<b>S2.1</b> : 100_P(VOH <sub>0.970</sub> -S-VL <sub>0.015</sub> -S-VAc <sub>0.015</sub> )	Yes	<b>100</b> + 1000	0.5
ET-S3	<b>S3</b> : 100_P(VOH <sub>0.96</sub> -S-VL <sub>0.02</sub> -S-VAc <sub>0.02</sub> )	Sedimentation	>1000	-
ET-S4	<b>S4</b> : 100_P(VOH <sub>0.91</sub> -S-VL <sub>0.04</sub> -S-VAc <sub>0.05</sub> )	Sedimentation	>1000	-
ET-S9	<b>S9</b> : 100_P(VOH <sub>0.96</sub> -S-VeoVa <sub>0.02</sub> -S-VAc <sub>0.02</sub> )	Yes	650	0.2
ET-S10	<b>S10</b> : 100_P(VOH <sub>0.972</sub> -S-VeoVa <sub>0.015</sub> -S-VAc <sub>0.013</sub> )	Yes	450	0.2

\* ET refers to thermal-initiated emulsion polymerization and is followed by the name of the stabilizer used in the experiment P(VOH<sub>0.88</sub>-S-VAc<sub>0.12</sub>) was shortened to PVOH.

**Bold** value = main population

A first blank experiment was performed without stabilizer to evaluate the potential of the initiator to self-stabilize a latex in our conditions. (**Table III-6, ET-0**). It yielded a latex with very large particles ( $> 1000$  nm) that rapidly sedimented after 24 h. The lack of stability of this latex is then a benchmark reference to evaluate the performance of the stabilizers employed. As a reference, the experiment performed with 10 wt.% Mowiol 4-88 based on monomers provided a stable and isometric latex, with an average particle diameter of 200 nm (**Table III-6, entry ET-Mowiol**). Unstable latexes were obtained with **S3** and **S4**. In contrast, the others, that showed good dispersibility, yielded stable latexes with  $Z_{av} < 1000$  nm (**ET-S1, ET-S2.1, ET-S9** and **ET-S10**). Hence, the corresponding copolymers (**S1, S2.1, S9** and **S10**) were tested in a 75 mL reactor, following an adapted protocol described in **Chapter II**.

## V.2 Emulsion copolymerization of VAc and VeoVa initiated by a redox couple.

Emulsion copolymerizations of VAc and VeoVa, were performed in the presence of the selected VL and VeoVa-based statistical stabilizer candidates according to the protocol set up in **Chapter II** with the RAFT-synthesized P(VOH-s-VAc) stabilizers. The polymerizations were all performed in a 75 mL glass reactor at 55 °C for 2 h, using AsAc and TBHP as redox initiating system (AsAc/TBHP = 0.092/0.054 wt.% based on monomers). Prior polymerization, the stabilizer (10 wt.% based on monomers) was dispersed in a water premix, according to the thermal treatment described in the previous section.

### V.2.1 VL-based statistical copolymer stabilizers

#### A. Kinetics of the polymerizations and colloidal features

Kinetics of the emulsion copolymerizations of VAc and VeoVa performed with **S1** and **S2.1** (both containing 1.5 mol% of VL) were compared to the one carried out with 75\_P(VOH<sub>0.88</sub>-s-VAc<sub>0.12</sub>) (**Figure III-17 (a)**) and 100\_P(VOH<sub>0.88</sub>-s-VAc<sub>0.12</sub>) (**Figure III-17 (b)**). As in **Chapter II**,  $S_{max}$  was determined as the slope of the conversion-time plot, in the area where the conversion evolves linearly with time.

**Table III-7: Estimation of  $S_{max}$  for the emulsion copolymerizations performed with 10 wt.% of 75\_P(VOH<sub>0.88</sub>-S-VAc<sub>0.12</sub>); 100\_P(VOH<sub>0.88</sub>-S-VAc<sub>0.12</sub>); S1: 75\_P(VOH<sub>0.970</sub>-S-VL<sub>0.015</sub>-S-VAc<sub>0.015</sub>) and S2.1: 100\_P(VOH<sub>0.970</sub>-S-VL<sub>0.015</sub>-S-VAc<sub>0.015</sub>), obtained from the slopes of the conversion *versus* time.**

Entry *	Stabilizer (10 wt.% based on monomers)	$S_{max}$ (s <sup>-1</sup> )	R <sup>2</sup>	Coagulum (wt.% based on monomers and stabilizer)
ER-75_PVOH	75_P(VOH <sub>0.88</sub> -S-VAc <sub>0.12</sub> )	0.040	0.996	0
ER-S1	S1	0.048	0.999	15
ER-100_PVOH	100_P(VOH <sub>0.88</sub> -S-VAc <sub>0.12</sub> )	0.037	0.992	0
ER-S2.1	S2.1	0.036	0.97	10

\* ER refers to redox-initiated emulsion polymerization and is followed by the name of the stabilizer used in the experiment; P(VOH<sub>0.88</sub>-S-VAc<sub>0.12</sub>) was shortened to PVOH.

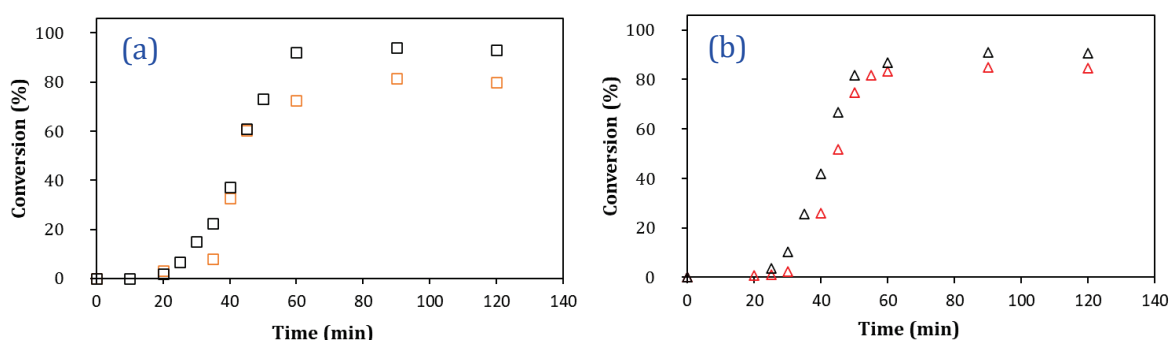


**Figure III-17: Kinetics of the emulsion copolymerizations of VAc and VeoVa stabilized with 10 wt.% of (a) (□) 75\_P(VOH<sub>0.88</sub>-S-VAc<sub>0.12</sub>) and (□) S1: 75\_P(VOH<sub>0.970</sub>-S-VL<sub>0.015</sub>-S-VAc<sub>0.015</sub>); and (b) (Δ) 100\_P(VOH<sub>0.88</sub>-S-VAc<sub>0.12</sub>) and (Δ) S2.1: 75\_P(VOH<sub>0.970</sub>-S-VL<sub>0.015</sub>-S-VAc<sub>0.015</sub>).**

For each experiment, conversion *versus* time curves exhibit a short induction period (approximately 30 min), followed by a rapid increase in the rate of polymerization. The latter seems to be constant from 40 to 60 min, before the system reached a plateau from 60 to 120 min. Both VL-based stabilizers showed similar kinetic profiles and  $S_{max}$  than the corresponding P(VOH-s-VAc) with similar DP (**Table III-7** and **Figure III-17**), with good accuracy (correlation coefficient  $R^2$  close to unity). The conversion reached approximately 80% with both VL-based stabilizers. However, the latex obtained with 75\_P(VOH<sub>0.957</sub>-S-VL<sub>0.015</sub>-S-VAc<sub>0.028</sub>) (**S1**) sedimented after 5 days, whilst the one stabilized with 100\_P(VOH<sub>0.970</sub>-S-VL<sub>0.015</sub>-S-VAc<sub>0.015</sub>) (**S2.1**) remained stable for several months (it is actually still stable after two years). Latexes stabilized with 75\_P(VOH<sub>0.88</sub>-S-VAc<sub>0.12</sub>) and 100\_P(VOH<sub>0.88</sub>-S-VAc<sub>0.12</sub>) were also stable for very long times (two years from now). Additionally, some coagulum was present on the anchor and on the wall of the reactor at the end of the polymerizations. This coagulum was recovered, dried for 48 h in an oven at 100 °C and weighted. It represented 15 wt.% (2.25 g) and 10 wt.% (1.5 g) of the amount of monomer and stabilizer introduced in the reactor for the experiments using **S1** and **S2.1**, respectively. No coagulum was observed in the case of the emulsion polymerizations carried out in the presence of Mowiol 4-88 or the well-defined P(VOH-s-VAc). In light of these results, it seems

that the DP of the copolymer plays a role in the stabilization efficiency. In addition, the presence of a very small amount of CoM hydrophobic units has a strong impact on the stabilization of the particles. As DP 100 seemed to provide better results than DP 75, the VeoVa-based statistical stabilizers further developed focused on a DP = 100. The enhanced stabilization efficiency of **S2.1** compared to **S1** could be related to the different conformations of the copolymers previously observed in the aqueous phase. **S1** showed larger and more polydisperse aggregates when dispersed in water than **S2.1**. It could be possible that these aggregates do not participate (or in a lesser extent) to the stabilization of the forming polymer particles, which explains the higher amount of coagulum.

The latexes were analyzed by both DLS and cryo-TEM, except for the latex obtained in the presence of **S1**, which was not observed by electron microscopy because it sedimented too quickly (**Table III-8**). Due to the polydispersity of the latexes, 200 particles were analyzed from each sample to obtain a representative distribution.

**Table III-8: Particle size comparison from the latexes stabilized with 10 wt.% of Mowiol 4-88; 100\_P(VOH<sub>0.88</sub>-s-VAc<sub>0.12</sub>); S1 and S2.1 obtained by DLS and cryo-TEM.**

Entry	$Z_{av}$ (nm) <sup>a</sup>	PdI <sup>a</sup>	$D_n$ (nm) <sup>b</sup>	$D_v$ (nm) <sup>b</sup>	$D_w/D_n$ <sup>b</sup>	$N_p$ (10 <sup>15</sup> cm <sup>-3</sup> ) <sup>c</sup>
<b>ER-Mowiol</b>	195	0.05	145	150	1.07	7.3
<b>ER-100_PVOH<sub>0.88</sub></b>	240	0.1	185	205	1.2	2.0
<b>ER-100_PVOH<sub>0.97</sub></b>	330	0.07	270	270	1.2	0.8
<b>ER-S1</b>	> 1000	0.7	-	-	-	-
<b>ER-S2.1</b>	285	0.5	84	97	1.5	22

<sup>a</sup> Obtained by DLS

<sup>b</sup> Obtained by cryo-TEM

<sup>c</sup> Calculated *via* **Equation 50**

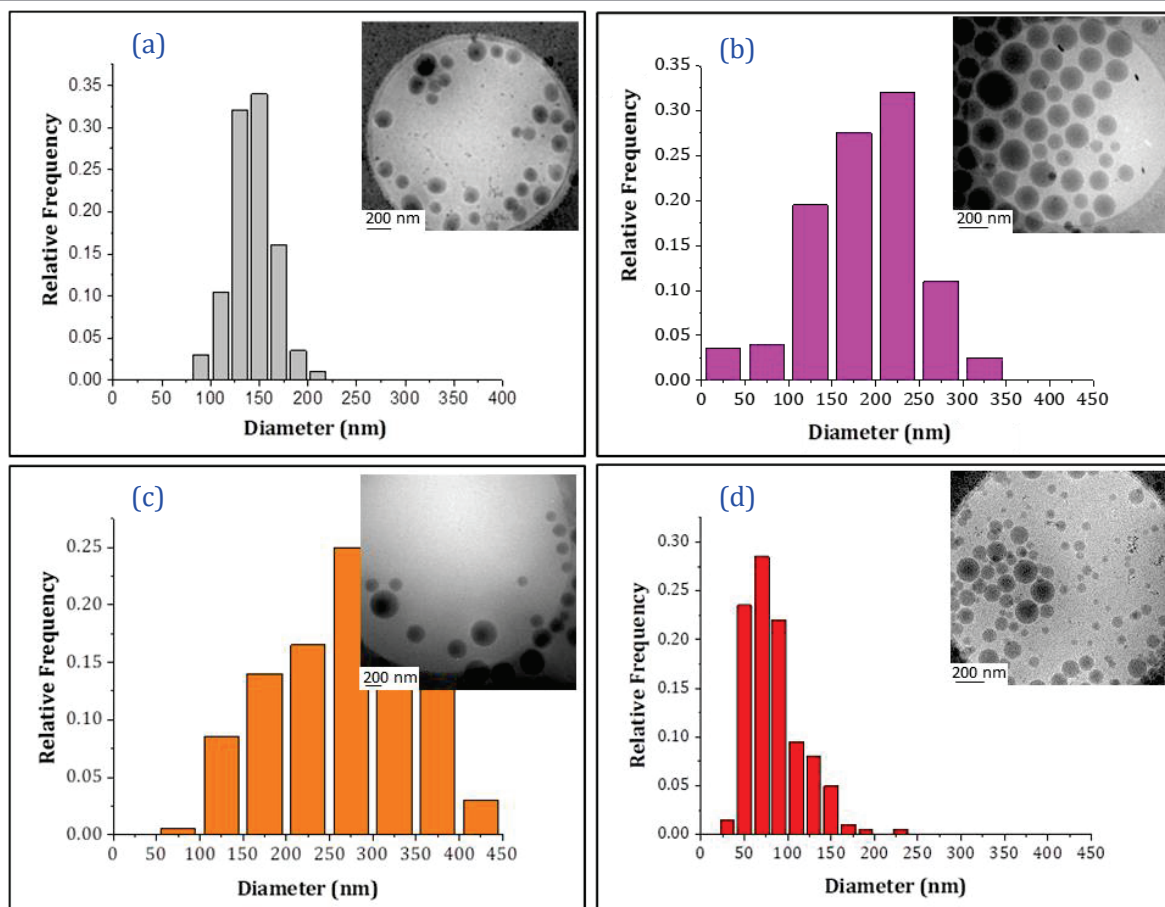


Figure III-18: Particle size distribution (PSD) obtained by cryo-TEM out of 200 particles and cryo-TEM pictures of the latexes stabilized with 10 wt.% of (a) Mowiol 4-88 (grey); (b) 100\_P(VOH<sub>0.88</sub>-S-VAc<sub>0.12</sub>) (magenta) and (c) 100\_P(VOH<sub>0.97</sub>-S-VAc<sub>0.03</sub>) (orange) and S2.1: 100\_P(VOH<sub>0.97</sub>-S-VL<sub>0.015</sub>-S-VAc<sub>0.015</sub>) (red). Scale bar: 200 nm.

For each experiment, the particle size measured by DLS was different from the one measured by cryo-TEM. A first explanation can lie in the fact that the DLS response takes into account the stabilizing layer, while the cryo-TEM does not.

DLS analysis showed that the particles of **ER-S2.1** were larger than the ones of **ER-75\_PVOH<sub>0.88</sub>** or **ER-Mowiol**. This contradicts the cryo-TEM observations, which clearly show the presence of smaller particles in **ER-S2.1**. However, it is worth noting that the three latexes stabilized with the RAFT-synthesized copolymers provided polydisperse particles, and that the DLS has some limitations in the attribution of the average particle size in this case. Indeed, large particles tend to “hide” the small ones for the calculation.

Particle sizes from cryo-TEM are thus probably more reliable, even if one has to carefully choose the photos used to calculate the particle size, in order to have the most realistic view

of the whole sample. Both **Table III-8** and **Figure III-18** show that even though the polydispersity was higher, the particle size determined by cryo-TEM for the latex obtained with **S2.1 (ER-S2.1,  $D_n = 84$  nm)** was significantly lower than that of the latex obtained with 100\_P(VOH<sub>0.88</sub>-s-VAc<sub>0.12</sub>) (**ER-75\_PVOH<sub>0.88</sub>,  $D_n = 185$  nm**) or Mowiol 4-88 (**ER-Mowiol,  $D_n = 145$  nm**). It was also observed that the latex obtained with 100\_P(VOH<sub>0.97</sub>-s-VAc<sub>0.03</sub>) (**Table III-8, entry ER-75\_PVOH<sub>0.97</sub>**), which had a similar HD and DP than **S2.1**, showed a much larger particle size and PSD. This result confirms that the introduction of very low VL content (1.5 mol.%) has a strong impact on the properties of the latex. It also suggests a better involvement of **S2.1** into the stabilization of the polymer particles compared to **S1** (lower DP) and the well-defined P(VOH-s-VAc) obtained in **Chapter II**.

### ***B. Adsorbed and grafted stabilizer***

The amount of adsorbed and grafted stabilizer **S2.1** was estimated after ultracentrifugation of the latexes **ER-S2.1** (as explained in **Experimental Section VI.8**) and compared to that of Mowiol 4-88, 100\_P(VOH<sub>0.88</sub>-s-VAc<sub>0.12</sub>) (the reference experiment) and 100\_P(VOH<sub>0.97</sub>-s-VAc<sub>0.03</sub>) (with similar DP and HD) (**Table III-9**). 77% of 100\_P(VOH<sub>0.97</sub>-s-VL<sub>0.015</sub>-s-VAc<sub>0.015</sub>) (**S2.1**) was found to be adsorbed or grafted onto the latex particles. In comparison with 45% for Mowiol 4-88 and approximately 40% for the well-defined reference 100\_P(VOH<sub>0.88</sub>-s-VAc<sub>0.12</sub>) (from **Chapter II**) (**Table III-9, entry ER-100\_PVOH<sub>0.88</sub>**). With 100\_P(VOH<sub>0.97</sub>-s-VAc<sub>0.03</sub>) (similar DP and HD as **S2.1**), the amount of adsorbed and grafted stabilizer drastically dropped to 21% (**Table III-9, entry ER-100\_PVOH<sub>0.97</sub>**). This result shows that the integration of VL units in the stabilizer structure improves the adsorption and grafting ability onto the polymer particles, even at low VL content (*i.e.*,  $F_{VL} = 1.5$  mol.%). This might be due to the long alkyl chain of the VL units, which increases the hydrophobic interactions with the particle and leads to a stronger adsorption onto the surface of the particle (**Table III-9**).

**Table III-9: Determination of the specific surface area occupied by S2.1 on a P(VAc-co-VeoVa) particle ( $A_s$ ), comparison with Mowiol 4-88, 100\_P(VOH<sub>0.97</sub>-S-VAc<sub>0.03</sub>) and 100\_P(VOH<sub>0.88</sub>-S-VAc<sub>0.12</sub>).**

Entry	Stabilizer	%Ads&Grafted <sup>a</sup>	S <sub>tot</sub> latex (x10 <sup>6</sup> cm <sup>2</sup> ) <sup>b</sup>	M <sub>n</sub> (g mol <sup>-1</sup> ) <sup>c</sup>	A <sub>s</sub> (Å <sup>2</sup> ) <sup>d</sup>
ER-Mowiol	Mowiol 4-88	45	4.9	8000	960
ER-100_PVOH <sub>0.88</sub>	100_P(VOH <sub>0.88</sub> -S-VAc <sub>0.12</sub> )	40	3.3	5 300	490
ER-100_PVOH <sub>0.97</sub>	100_P(VOH <sub>0.97</sub> -S-VAc <sub>0.03</sub> )	21	1.9	4 840	560
ER-S2.1	S2.1: 100_P(VOH <sub>0.970</sub> -S-VL <sub>0.015</sub> -S-VAc <sub>0.015</sub> )	77	6.6	5 100	480

<sup>a</sup> Obtained by Equation 59

<sup>b</sup> Obtained by Equation 50

<sup>c</sup> Obtained by Equation 51

<sup>d</sup> Obtained by Equation 61

**Table III-9** shows that the total surface of the latex obtained with **S2.1** is larger than that of the latexes obtained with Mowiol 4-88 and the well-defined P(VOH-s-VAc) copolymers, which attests for a better stabilization efficiency of the VL-based statistical copolymers, even with only  $F_{VL} = 1.5$  mol.%.

The estimated surface area occupied by one macromolecule of **S2.1** is similar to that covered by 100\_P(VOH<sub>0.88</sub>-S-VAc<sub>0.12</sub>) and slightly lower than that occupied by 100\_P(VOH<sub>0.97</sub>-S-VAc<sub>0.03</sub>) (**Table III-9**). This result is surprising because one could expect that the surface covered by 100\_P(VOH<sub>0.88</sub>-S-VAc<sub>0.12</sub>) would be larger, due to the fact that this copolymer has longer PVAc sequences strongly adsorbed at the surface of the particle compared to 100\_P(VOH<sub>0.97</sub>-S-VAc<sub>0.03</sub>). Again, these results must be taken with care because the calculation is based on polydisperse polymer particles. The calculation was also made with the assumption that all the stabilizer chains were located at the surface of the particles.

### C. Evaluation of the alkali resistance of the latexes stored at different pH

The latex **ER-S2.1** was stored in a fridge (3 – 5 °C) at pH 4, 6, 8, 10 and 12. The evolution of pH was followed over a four-week period. NaOH 0.1 N or 0.5 N was used to set the pH at  $t_0$ . The results are presented in **Figure III-19**, which also displays the results of the same study carried out for the latex synthesized with Mowiol 4-88.



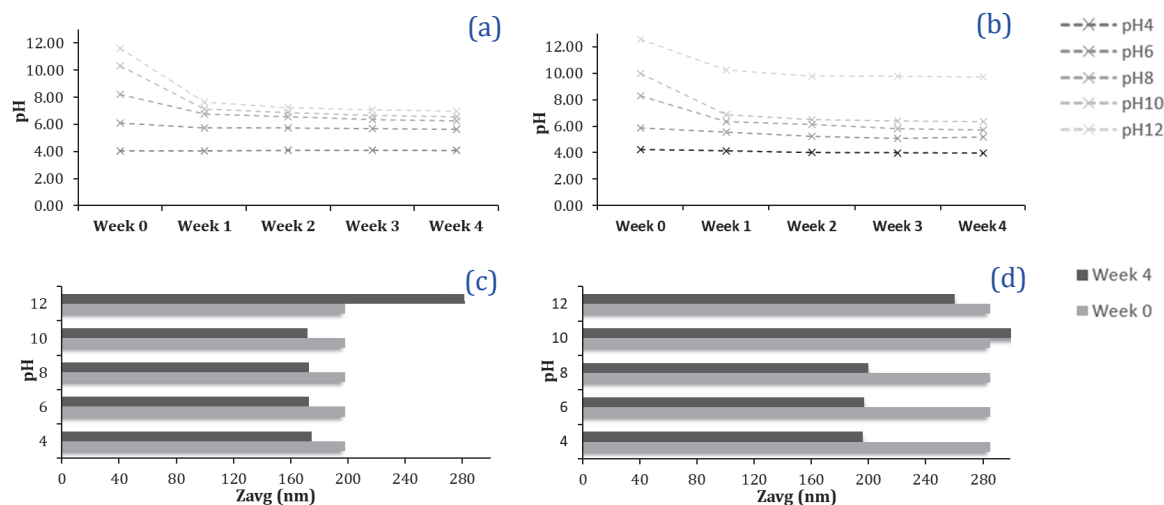


**Figure III-19: Evolution of the pH of the latexes obtained with 10 wt.% of (a) Mowiol 4-88 and (b) S2.1, and their respective particle size measured by DLS (respectively (c) and (d)) after 4 weeks of storage in the fridge. At week 0, the pH was set at 4, 6, 8, 10 and 12 and was then followed for 4 weeks.**

Similar to the latex **ER-Mowiol**, the pH of **ER-S2.1** remained constant over the weeks as long as it was initially set below 8. At pH 8 and 10, it tends to decrease to reach a plateau value close to 7, once again similarly to the latex obtained with Mowiol 4-88. However, at pH 12 the pH decreases less for **ER-S2.1** than for **ER-Mowiol**: a plateau at pH 10 was reached for the first latex instead of pH 7 for **ER-Mowiol** (Figure III-19, (a) and (b)).

Concerning the particle size, Figure III-19 (c) and (d) show a decrease both for the latexes **ER-Mowiol** and **ER-S2.1** when stored at pH 4, 6 and 8 over a four-week period. In addition, a destabilization of the latex **ER-Mowiol** was visible at pH 12 (flocculate and larger particle size, Figure III-19 (c)). In contrast, the latex **ER-S2.1** at pH 10 and 12 seemed stable (no visible flocculation and similar particle size after 4 weeks, Figure III-19 (d)).

This behavior at pH 12 is not well understood yet, but suggests that the stabilizer provides a better stability and resistance to the polymer particles, against hydrolysis. This behavior can be an asset for applications in mortar or for high pH paints.

One possible explanation is that VL units from the stabilizer are probably hydrolyzed and generate lauric acid in close proximity of the particle surface. The excess of sodium hydroxide would instantaneously turn the lauric acid into sodium laurate, which is a known efficient surfactant, and could prevent further hydrolysis of the particles by anionic repulsion of NaOH. Therefore, the combination of both the polymer stabilizer and sodium laurate could enhance the stability of the latex by, not only steric, but also electrostatic stabilization. This could explain why the latex is still stable at pH 10 and 12 after 4 weeks of storage, while the latex obtained with Mowiol 4-88 and the RAFT-synthesized P(VOH-s-VAc) are not.



To tentatively show the formation of sodium laurate under these conditions, a sample of the latex at pH 12 was centrifugated, dried at 60 °C for 48 h and analyzed by <sup>1</sup>H NMR in DMSO-d<sub>6</sub>. It was thought that the presence of the characteristic signal of sodium laurate could be visible on the NMR spectrum at 2.2 ppm. Unfortunately, due to the very low VL content in the stabilizer, this signal was not visible on the spectrum and did not allow us to conclude.

This experiment was carried out again on a new batch of latex to confirm the observed enhanced stability at pH 12 of the latex prepared with **S2.1**.

***D. Reproducibility: evaluation of the robustness of the synthesis, alcoholysis and stabilization efficiency of P(VOH-s-VL-s-VAc) statistical copolymer.***

A fresh batch of the same stabilizer was synthesized to perform reproducibility experiments (**Appendix 8** and **Table III-2, S2.2**). The synthesis of the copolymer seemed robust as similar DP ± 10 and molar fractions of VL, VAc and VOH units after alcoholysis were obtained. The results concerning the kinetics, particle size, storage stability at different pH and adsorption of the stabilizer onto the particles of the two latexes are summarized in **Figure III-20**.

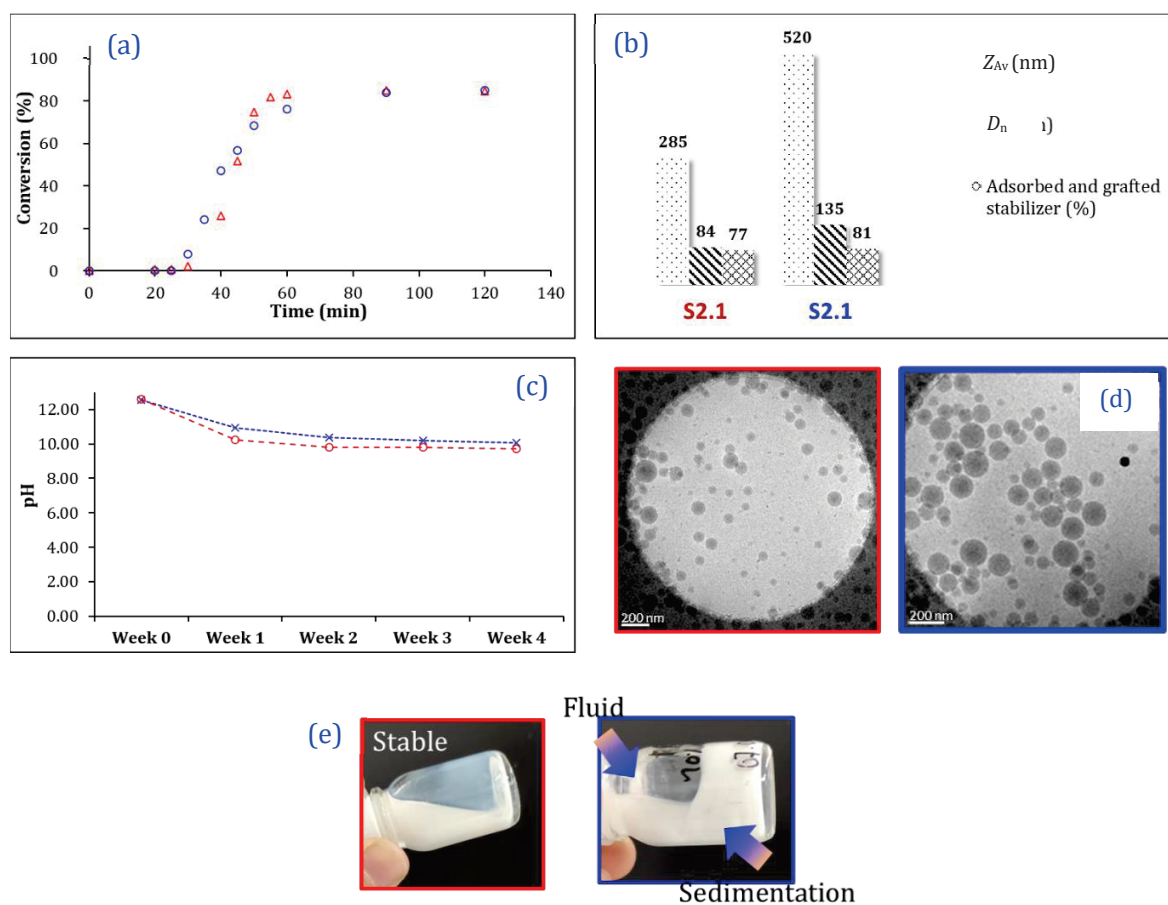


**Figure III-20: Emulsion copolymerizations of VAc and VeoVa with 10 wt.% of S2.1 (in red) and S2.2 (in blue).** (a) Conversion versus time plots; (b)  $Z_{av}$ ,  $D_n$  obtained by cryo-TEM and percentage of adsorbed and grafted stabilizer for the formed latexes; (c) Storage stability of the latexes for four weeks at pH 12; (d) cryo-TEM pictures of the two latexes (the scale bar in both images is 200 nm); and (e) Pictures of the two latexes after 4 weeks of storage in the fridge.

Figure III-20 (a) shows that similar kinetic profiles were obtained for both emulsion copolymerizations. The amount of grafted and adsorbed stabilizer remained the same (80.6 versus 77% +/- 4%, Figure III-20 (b)), and the same evolution of the pH over 4 weeks was nevertheless observed for both latexes (Figure III-20 (c)) confirming that the latexes were similarly prevented from hydrolysis when stored at pH 12.

However, the average particle size ( $D_n$ ) in each latex was significantly different (135 versus 84 nm with S2.1 and S2.2, respectively), and the reproduced latex showed partial decantation after one week, while the first batch was still stable after several months (Figure III-20, (e)). Nevertheless, the second dispersion was easily recovered by manual shaking. The slight variations in the DP, the blockiness, and thus the location of the VL units in the copolymer stabilizer chains may explain this sometimes-strong variations of latex properties. This anyway emphasizes that the colloidal stability of the final latex is strongly

dictated by small variations of structure of the copolymer stabilizer. This further shows the importance to master the preparation of these stabilizers but also opens up great possibilities to improve the stability of this type of latex.

The results presented in this section show that the incorporation of even a small amount of VL units in the stabilizer had a significant impact on the dispersibility of the polymer, and the latex properties. For example, the particle size was reduced and the amount of adsorbed and grafted stabilizer was higher compared to the latexes obtained either with Mowiol 4-88 or the well-defined P(VOH-s-VAc) with similar DP and HD. The hydrophobicity provided by the VL units seems to increase the hydrophobic interactions with the particles and improve the stabilizer anchorage into the particle.

The polydispersity of the polymer particles stabilized with the VL-based statistical copolymer stabilizer is however higher than the one of the latexes stabilized with Mowiol 4-88. The problem of variability in the properties of the P(VOH-s-VAc) was already reported in the literature,<sup>[17],[18]</sup> and a slight change in the microstructure of the stabilizer proved to drastically impact the properties of the final latex. It is likely that the structure of the stabilizers synthesized in the laboratory differ from one batch to another (blockiness, distribution of the VL and VOH units along the polymer backbone etc.), which could explain the issue of sedimentation encountered with the latex obtained with a different batch of 100\_P(VOH-s-VL-s-VAc).

Nevertheless, the results obtained in this section are encouraging and will be built upon in the following section, where the hydrophobic units VL in the stabilizer were replaced by VeoVa.

## V.2.2 VeoVa-based statistical copolymer stabilizers

### A. Kinetics of the polymerizations and colloidal features

Kinetics of the emulsion copolymerizations of VAc and VeoVa stabilized with 100\_P(VOH<sub>0.96</sub>-s-VeoVa<sub>0.02</sub>-s-VAc<sub>0.02</sub>) (**S9**) and 100\_P(VOH<sub>0.975</sub>-s-VeoVa<sub>0.010</sub>-s-VAc<sub>0.015</sub>) (**S10**) were followed and compared to the systems stabilized with Mowiol 4-88 and 100\_P(VOH<sub>0.88</sub>-s-VAc<sub>0.12</sub>) (**Figure III-21**).

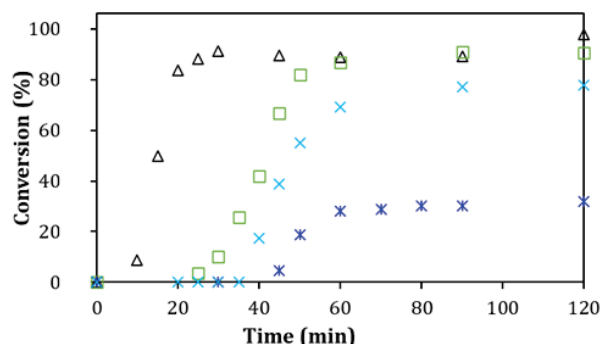


Figure III-21: Kinetics of the emulsion copolymerizations of VAc and VeoVa with 10 wt.% of (Δ) Mowiol 4-88; (□) 100\_P(VOH<sub>0.88</sub>-S-VAc<sub>0.12</sub>); (×) S9: 100\_P(VOH<sub>0.96</sub>-S-VeoVa<sub>0.02</sub>-S-VAc<sub>0.02</sub>) and (×) S10: 100\_P(VOH<sub>0.975</sub>-S-VeoVa<sub>0.010</sub>-S-VAc<sub>0.015</sub>).

The latex obtained with **S10** reached 78% conversion after 1 h (and then subsequently plateaued), while the one stabilized with **S9** reached a maximum conversion of 30% (**Figure III-21**). The amount of initiator was multiplied by 1.5 based on the first experiment (AsAc = 0.13 against 0.092 wt.% based on monomers). At this concentration, 78% conversion was achieved for the system that contained **S9** (**Figure III-22**). To try and increase the conversion further, the concentration was multiplied by two compared to the first experiment (AsAc = 0.18 wt.% based on monomers). The induction period was gradually reduced with the increasing concentration of radicals. However, no improvement in the conversion was observed and it once again reached a plateau at 78% (**Figure III-22**).

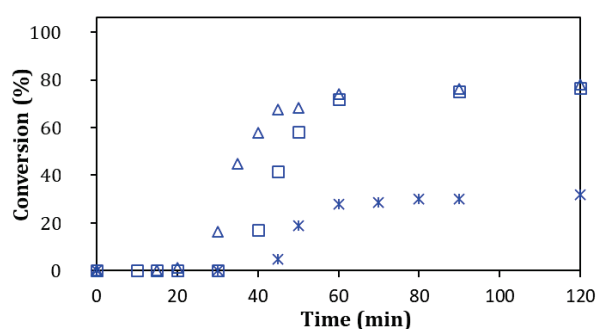


Figure III-22: Kinetics of the emulsion copolymerization of VAc and VeoVa with 10 wt.% of S9 with different amount of initiator (AsAc, based on monomers): (×) 0.092 wt.%; (□) 0.13 wt.% and (Δ) 0.18 wt.%.

No explanation for this observation has been found yet, but it is believed that degradative chain transfer might occur in the polymerization medium, which might be responsible for the lack of initiation, and thus induce the inhibition. This degradative chain transfer could be due to the presence of residual acetic acid, visible on the <sup>1</sup>H NMR spectra of the copolymers containing VeoVa units, in a higher proportion than in the other copolymers. These species

are still present after several washes and drying of the copolymers, and may act as chain transfer agent during the emulsion copolymerization of VAc and VeoVa, with slower (or not at all) reactivation of the resulting radical. Another hypothesis was that the presence of VeoVa units in the stabilizing shell, provided by the structure and composition of the stabilizer may also induce degradative transfer of the oligoradicals onto the methyl, methylene or methine protons of the VeoVa side group, when the oligoradical intends to migrate inside the particle. It could be that the radical resulting from such transfer is not as reactive as the oligoradical because of the steric hindrance provided by the bulky side group of VeoVa units. An accumulation of such degradative transfer onto the VeoVa units of the stabilizer inside the stabilizing shell could thus induce an additional rate retardation of the polymerization (or even an inhibition).

$S_{\max}$  values obtained from the conversion curve for the experiments carried out with **S9** and **S10** are gathered in **Table III-10**, and compared to the ones obtained for the experiments **ER-Mowiol** and **ER-100\_PVOH**.  $S_{\max}$  was not affected by the fraction of VeoVa, inserted in the copolymer, but was lower than the ones obtained for the latexes that contained the RAFT-synthesized P(VOH-*s*-VAc) with similar DP (even after the increase in initiator concentration), confirming that the radical entry was affected by the structure of the stabilizer, or the presence of by products from the alcoholysis step.

**Table III-10:  $S_{\max}$  of the emulsion polymerization systems stabilized by Mowiol 4-88 (ER-Mowiol); 100\_P(VOH<sub>0.88</sub>-*s*-VAc<sub>0.12</sub>) (ER-100\_PVOH); S9 (ER-S9) and S10 (ER-S10).**

Entry	$S_{\max}$ (s <sup>-1</sup> )	R <sup>2</sup>
ER-Mowiol	0.075	0.996
ER-100_PVOH	0.037	0.994
ER-S9	0.026	0.993
ER-S10	0.028	0.998

The particle size and particle size distributions were determined *via* DLS and cryo-TEM analyses (**Table III-11**). Once again, a large PSD was observed for the particles stabilized with the RAFT-synthesized stabilizers DP\_P(VOH-*s*-VeoVa-*s*-VAc) (PDI > 0.2 and  $D_w/D_n > 1.2$ ).

**Table III-11: Particle size comparison for the latexes obtained with 10 wt.% of Mowiol 4-88; 100\_P(VOH<sub>0.88</sub>-S-VAc<sub>0.12</sub>); 100\_P(VOH<sub>0.96</sub>-S-VeoVa<sub>0.02</sub>-S-VAc<sub>0.02</sub>) (S9) and 100\_P(VOH<sub>0.975</sub>-S-VeoVa<sub>0.01</sub>-S-VAc<sub>0.015</sub>) (S10) obtained par DLS and cryo-TEM.**

Entry	Stabilizer	Z <sub>av</sub> (nm) <sup>a</sup>	PdI <sub>a</sub>	D <sub>n</sub> (nm) <sup>b</sup>	D <sub>v</sub> (nm) <sup>b</sup>	D <sub>w</sub> /D <sub>n</sub> <sup>b</sup>	N <sub>p</sub> (10 <sup>15</sup> cm <sup>-3</sup> ) <sup>c</sup>
ER-Mowiol	Mowiol 4-88	195	0.05	145	150	1.07	7.3
ER-100_PVOH	100_P(VOH <sub>0.88</sub> -S-VAc <sub>0.12</sub> )	240	0.1	185	205	1.2	2.0
ER-S9	S9: 100_P(VOH <sub>0.96</sub> -S-VeoVa <sub>0.02</sub> -S-VAc <sub>0.02</sub> )	300	0.4	115	130	1.2	8.6
ER-S10	S10: 100_P(VOH <sub>0.975</sub> -S-VeoVa <sub>0.01</sub> -S-VAc <sub>0.015</sub> )	360	0.2	135	160	1.7	4.5

<sup>a</sup> Obtained by DLS

<sup>b</sup> Obtained by cryo-TEM

<sup>c</sup> Obtained by Equation 49

The data provided by DLS highlighted narrower PSD and smaller number-average particle diameter for **ER-S9** compared to **ER-S10**; **Figure III-23**, suggesting that the stabilizer with the higher fraction of VeoVa ( $F_{\text{VeoVa}} = 2$  mol.% in **S9**) had better emulsifier properties and was thus able to stabilize more new particles compared to **S10** ( $F_{\text{VeoVa}} = 1$  mol.%).

In light of these results, it seems that the fraction of VeoVa inserted in the stabilizer affects the particle size and PSD, (even at very low VeoVa content), so that the higher the VeoVa content, the smaller the particle size and PSD.

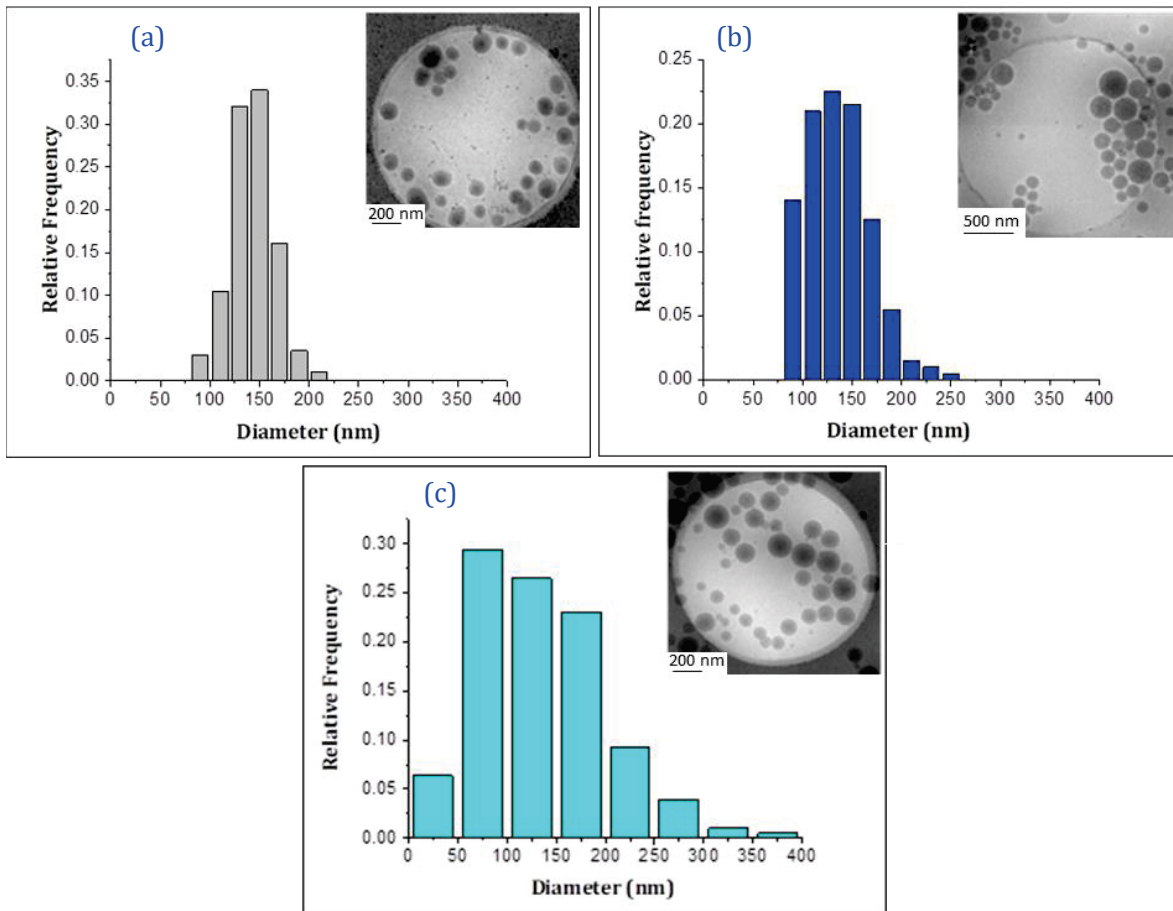
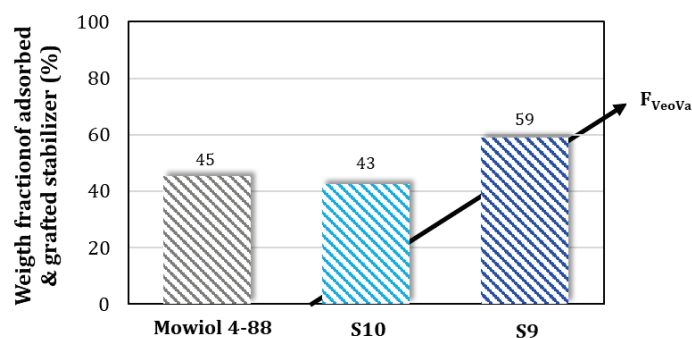


Figure III-23: Particle size distribution (PSD) obtained by cryo-TEM out of 200 particles and cryo-TEM pictures of the latexes stabilized with 10 wt.% of (a) Mowiol 4-88, scale bar: 200 nm (grey); (b) S9, scale bar: 500 nm (blue), and (c) S10, scale bar: 200 nm (cyan).

### B. Adsorbed and grafted stabilizer

The amount of adsorbed and grafted stabilizers **S9** and **S10** are compared to that of Mowiol 4-88 in **Figure III-24**.



**Figure III-24:** Weight percentage of adsorbed and grafted stabilizer obtained for the latexes stabilized with 10 wt.% of Mowiol 4-88; S10: 100\_P(VOH<sub>0.975</sub>-S-VeoVa<sub>0.01</sub>-S-VAC<sub>0.015</sub>) and S9: 100\_P(VOH<sub>0.96</sub>-S-VeoVa<sub>0.02</sub>-S-VAC<sub>0.02</sub>), after ultracentrifugation.

Approximately 43% of the stabilizer was adsorbed or grafted onto the particles in the latex obtained with **S10** (with  $F_{\text{VeoVa}} = 1$  mol.%), which is slightly lower than with Mowiol 4-88. However, this amount reached 59% when the latex contained **S9** (with  $F_{\text{VeoVa}} = 2$  mol.%). This increase could be a result of the increased number of VeoVa units in the stabilizer. To confirm this hypothesis, it would be interesting to perform a third emulsion polymerization with a VeoVa-based statistical copolymer with higher molar fraction of VeoVa. However, this will raise water dispersibility issues of the copolymer.

Nevertheless, in light of the results obtained in this section, it seems that the VeoVa-based statistical copolymers are more efficient to stabilize a latex than the VL-based ones, or than the regular P(VOH-s-VAc). These results correlate well with the lower values of surface tension which were obtained with this copolymer compared to the values obtained with Mowiol 4-88 and the well-defined P(VOH-s-VAc) synthesized in **Chapter II**, and tends to confirm that this copolymer is more surface active than the regular P(VOH-s-VAc).

### C. Evaluation of the alkali resistance of the latex ER-S10 at different pH

To compare with the VL-based statistical copolymer the latex **ER-S10** was stored 5 °C at different pH (6, 8, 10 and 12). The evolution of the pH was followed every week for four weeks and is compared to the results obtained for **ER-Mowiol** and **ER-S2.1** (**Figure III-25**).



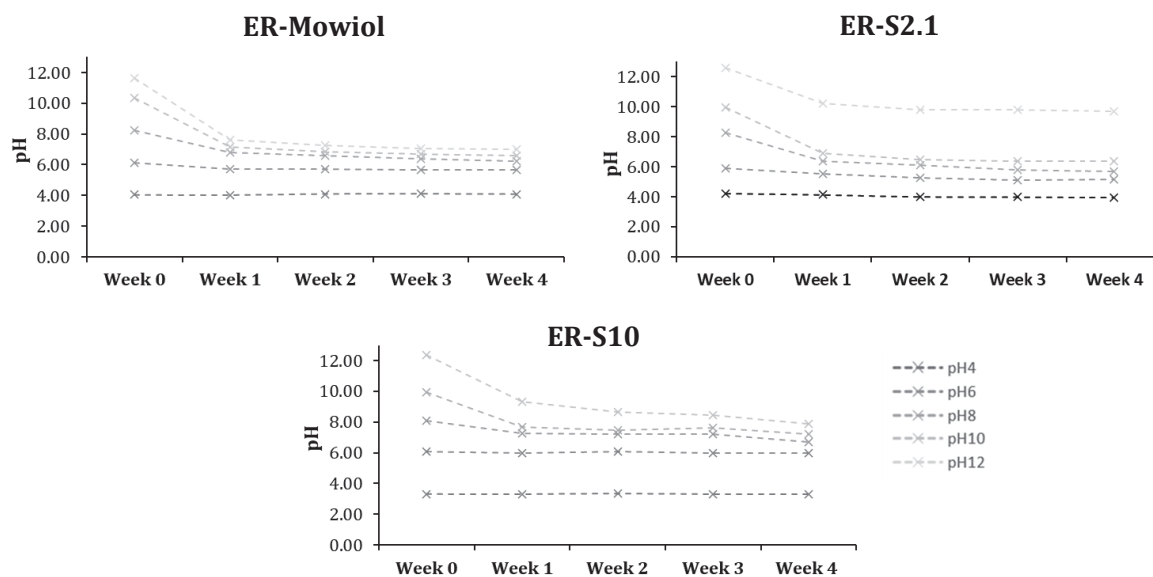


**Figure III-25: Evolution of the pH of the latexes ER-Mowiol; ER-S2.1 and ER-S10 obtained with 10 wt.% of Mowiol 4-88; 100\_P(VOH<sub>0.970</sub>-s-VL<sub>0.015</sub>-s-VAC<sub>0.015</sub>) and 100\_P(VOH<sub>0.975</sub>-s-VeoVa<sub>0.01</sub>-s-VAC<sub>0.015</sub>) respectively, stored in the fridge for four weeks. At week 0, the pH was set at 4, 6, 8, 10 and 12.**

The evolution of pH of the latex **ER-S10** (which contained 10 wt.% of 100\_P(VOH<sub>0.975</sub>-s-VeoVa<sub>0.01</sub>-s-VAC<sub>0.015</sub>)) provided similar trend that of **ER-Mowiol**: for a pH set below 8, no evolution of the pH was observed over the weeks, while for a pH set at 10 or 12, the pH of the latex decreases over weeks to reach a plateau. Nevertheless, this plateau was reached at a higher pH for **ER-S10** (pH = 8 - 9) compared to **ER-Mowiol** (pH = 7 - 8). The plateau reached by **ER-S2.1** (with similar CoM content and DP but VL units instead of VeoVa), set at pH 12, was approximately reached at pH 10. It was previously hypothesized that the VL units were hydrolyzed when the latex was stored at pH 12, releasing sodium laurate which could prevent further hydrolysis of the polymer particle by anionic repulsions. The present result highlights that the presence of VL units is not the only parameter providing alkali resistance to the latex at high pH. Indeed, **S10** also seemed to prevent the polymer particles from extensive hydrolysis compared to Mowiol 4-88, but in a lesser extent than **S2.1**. It is thus likely that the presence of the CoM affects the hydrolysis of the latex at high pH, either by steric hindrance or/and ionic repulsion of sodium hydroxide (in the case of the VL-based statistical copolymer), and enhanced the alkali resistance of the polymer particles.

## VI. Conclusion

This part of the project aimed to investigate the feasibility of designing new polymeric stabilizer structures based on P(VOH-*s*-VAc), and incorporating more hydrophobic units of VeoVa and VL. The present Chapter investigated the simplest structure which can be obtained by RAFT/MADIX polymerization, namely the statistical structure. The synthesis of statistical copolymers of VAc and VL or VeoVa (CoM) was indeed straightforward and provided a library of P(VAc-*s*-CoM) copolymers with different DPs and CoM contents. These structures were then alcoholized into P(VOH-*s*-VAc-*s*-CoM) and tested in emulsion copolymerization to evaluate their ability to stabilize a latex of P(VAc-*co*-VeoVa). The alcoholysis study highlighted that VeoVa units remained untouched during this step. It was therefore possible to directly tune the composition of the P(VAc-*s*-VeoVa) copolymer. On the contrary, the VL units were sensitive to the alcoholysis, but in a lesser extent than the VAc ones. It was then possible to target different composition of VL in the final copolymer, by stopping the alcoholysis at different times.

After alcoholysis, the dispersibility of the statistical copolymers was drastically limited by the presence of the more hydrophobic CoM units. Indeed, in our conditions, the copolymers were insoluble in water if the amount of CoM units exceeded 2 mol.% (corresponding to an average of 2 - 3 CoM units per chain). Nevertheless, we managed to successfully disperse the copolymers with  $F_{\text{CoM}} \leq 2$  mol.% after a thermal treatment, and these structures provided long lasting stable latexes, and visibly impacted the particle size and particle size distribution, with an enhanced amount of adsorbed and grafted stabilizer onto the particles compared to the latexes obtained with the commercial Mowiol 4-88 or the RAFT-synthesized P(VOH-*s*-VAc). Up to ca 59% and 77% of adsorbed and grafted stabilizer was obtained for the latexes containing the VeoVa and VL-based statistical structures, respectively. Both the VL and VeoVa-based copolymers also provided the latex with enhanced resistance to high pH upon storage, with even higher alkali resistance provided by the copolymer which contained the VL units. This behavior could benefit some industrial applications such as mortar or high pH paints.

However, some limitations were also encountered such as the sensitivity of the stabilization system to slight variations in the chemical composition or structure of the copolymer stabilizer, as shown with a freshly synthesized batch of the same VL-based stabilizer. No reproducibility experiments were nevertheless carried out with the VeoVa-based statistical copolymer stabilizers. Besides, when the VeoVa-based stabilizer candidates were used in emulsion polymerization, the conversion plateaued at 70%, even when the amount of initiator was increased. This behavior is not well understood but could be attributed to a

possible degradative chain transfer or to the steric hindrance provided by the VeoVa units, which could prevent the entry of the propagating in the particles, loci of the polymerization. At this stage of the project, it was commonly decided with our industrial partner to focus on the development of the VL-based copolymers as **S2.1** (with  $F_{VL} = 1.5$  mol.%) provided latexes with enhanced results in terms of stability, adsorption and grafting, and pH resistance compared to the ones obtained with the RAFT-synthesized P(VOH-s-VAc) and P(VOH-s-VeoVa-s-VAc). Nevertheless, we were still facing some limitations in terms of dispersibility issue and poor reproducibility.

So far, it seems clear that a balance must be found between the dispersibility issues of the copolymer and the improved characteristic of the latex. In order to improve the dispersibility, macromolecular engineering must be reconsidered, and different structures could alternatively be tested. The RAFT/MADIX technique allows for the design of various copolymer architectures. The literature concerning the investigation of different well-controlled architectures of amphiphilic copolymers incorporating VeoVa or VL units is seldom. As mentioned in the introduction of this chapter, one paper was nevertheless found, and the authors investigated the influence of the architecture of well-defined copolymers of NVP and VL on the aqueous solution properties of the copolymers.<sup>[8]</sup> The authors claimed that the more block-like structures were likely to self-assemble in water and decreased the surface tension more readily than statistical structures. Additionally, it was already highlighted in **Chapters I** and **II**, that the solution properties of amphiphilic copolymers are dictated by many factors, including the hydrophilicity/hydrophobicity of the repeating units, molar mass, and the microstructure of the polymer chain. These observations combined, it came to our mind that it was worth investigating block copolymers as an alternative structure to the statistical one. This could provide different dispersibility and micellization behaviors. Different structures of block copolymers incorporating PVeoVa, PVL and PVAc blocks were thus investigated and are presented in **Chapter IV**.

## References

- [1] P. Ra, D. Armando, Z. Wever, F. Picchioni, A. A. Broekhuis, *Chem. Rev.* **2015**, 8504–8563.
- [2] T. P. Davis, K. Matyjasezowski, "*Handbook of Radical Polymerization*", John Wiley & Sons, **2002**.
- [3] C. F. Cordeiro, F. P. Petrocelli, "*Vinyl acetate polymers*", in Encyclopedia of polymer science and technology, John Wiley & Sons, New York, **1970**, pp. 416–451.
- [4] L. J. Young, *J. Polym. Sci.* **2010**, *54*, 411–455.
- [5] Y. Gu, J. He, C. Li, C. Zhou, S. Song, Y. Yang, *Macromolecules* **2010**, *43*, 4500–4510.
- [6] J. Bernard, A. Favier, L. Zhang, A. Nilasaroya, T. P. Davis, C. Barner-Kowollik, M. H. Stenzel, *Macromolecules* **2005**, *38*, 5475–5484.
- [7] M. Destarac, D. Taton, S. Z. Zard, T. Saleh, Y. Six, *ACS Symp. Ser.* **2003**, *854*, 536–550.
- [8] K. A. Knapp, I. M. Nuñez, D. A. Shipp, *Polymer* **2018**, *141*, 54–61.
- [9] X. G. Qiao, M. Lansalot, E. Bourgeat-Lami, B. Charleux, *Macromolecules* **2013**, *46*, 4285–4295.
- [10] S. Perrier, *Macromolecules* **2017**, *50*, 7433–7447.
- [11] T. Congdon, P. Shaw, M. I. Gibson, *Polym. Chem.* **2015**, *6*, 4749–4757.
- [12] J. C. Daniel, C. Pichot, "*Latex à Base d'acétate de Vinyle*". in Les Latexes Synthétiques, Lavoisier, **2006**.
- [13] R. F. B. Davies, G. E. J. Reynolds, *J. Appl. Polym. Sci.* **1968**, *12*, 47–58.
- [14] O. W. Smith, M. J. Collins, P. S. Martin, D. R. Bassett, *Prog. Org. Coatings* **1993**, *22*, 19–25.
- [15] Y. Gu, J. He, C. Li, C. Zhou, S. Song, Y. Yang, *Macromolecules* **2010**, *43*, 4500–4510.
- [16] E. R. Coatings, **n.d.**, 1–11.
- [17] M. S. El-Aasser, "*Emulsion Polymerization of Vinyl Acetate*", Applied Science Publishers LTD, **1981**.
- [18] K. Noro, *Br. Polym. J.* **1970**, 128–134.
- [19] H. De Bruyn, The Emulsion Polymerization of Vinyl Acetate. Ph.D Dissertation, University of Sydney, **1999**.



---

# Chapter IV

Synthesis and evaluation as stabilizer of PCoM-*b*-P(VOH-*s*-VAc) (or reverse order P(VOH-*s*-VAc)-*b*-PCoM) block copolymers

---

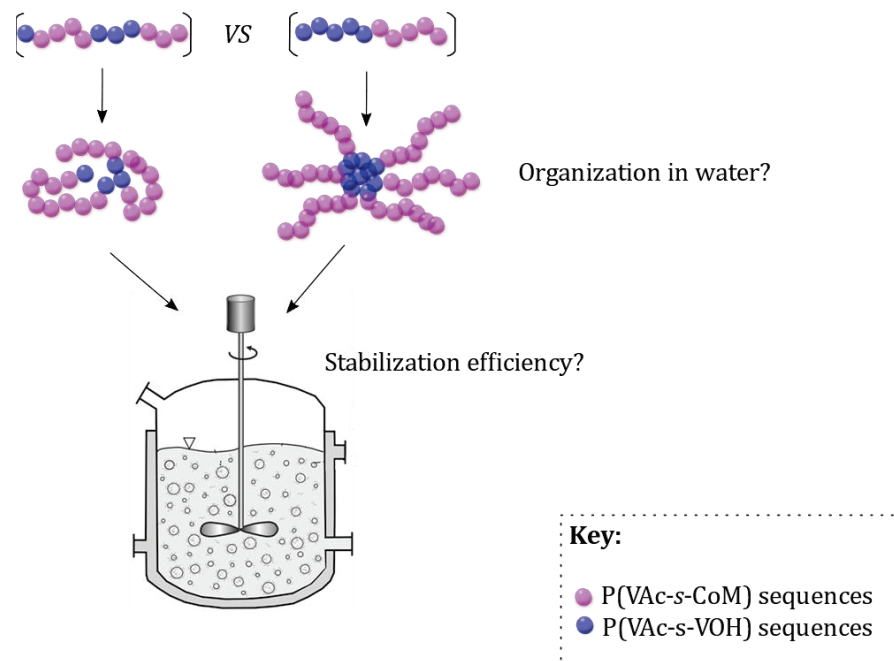


## Table of content

I. INTRODUCTION .....	210
II. SYNTHESIS OF THE BLOCK COPOLYMERS .....	213
II.1 RAFT/MADIX polymerization of VeoVa or VL.....	213
II.1.1 Synthesis and characterization of low molar mass PVeova (DP 5 and 10) for further block copolymer synthesis.....	213
II.1.2 Evaluation of the extent of head-to-head additions in PVeova-X synthesis .....	215
II.2 Synthesis and characterizations of low molar mass PVL homopolymers for further block copolymerization synthesis .....	220
II.3 Chain extension of PVeova and PVL with VAc.....	223
II.4 Conclusion on the synthesis of block copolymers.....	226
III. ALCOHOLYSIS OF THE BLOCK COPOLYMERS.....	228
III.1 Alcoholysis of the VeoVa-based block copolymers.....	228
III.2 Alcoholysis of the VL-based block copolymers .....	230
IV. (SELF-) ORGANIZATION OF THE BLOCK COPOLYMERS IN WATER .....	234
IV.1 Dispersibility of the block copolymers in water.....	234
IV.2 Organization of the block copolymers in water: DLS study.....	235
IV.3 Surface tension.....	237
IV.4 Conclusion .....	238
V. EMULSION COPOLYMERIZATION OF VAC AND VEOVA WITH THE SELECTED BLOCK COPOLYMER CANDIDATES .....	239
V.1 Kinetics of the polymerizations and colloidal features of the latexes .....	239
V.2 Adsorbed and grafted stabilizer .....	245
V.3 Evaluation of the alkali resistance of the latexes at different pH .....	246
VI. CONCLUSION .....	247

## I. Introduction

Amphiphilic stabilizers are usually described as macromolecules that contain both hydrophilic and hydrophobic moieties and can be located at the interface of water-oil systems. The influence of the polymer architecture on the properties of such amphiphilic polymers has raised interest for decades, and it is now well-established that amphiphilic random copolymers with hydrophobic and hydrophilic units can undergo intramolecular aggregation in water.<sup>[1,2]</sup> Amphiphilic block copolymers, on the other hand, will mostly give intermolecular aggregation (see scheme on the front page).<sup>[3-5]</sup> These different behaviors in water will most likely provide different properties to the resulting latex. The most common hydrophobic blocks are based on polystyrene, polyacrylates, polyolefins, or non-water-soluble polyethers. Hydrophilic blocks are made of either negatively or positively charged monomers, such as vinylic or acrylic monomers bearing sulfonate, carboxylic acid, phosphonic, or amino groups, or neutral blocks, which are essentially poly(ethylene glycol) (PEG).<sup>[3]</sup>

A quick literature review showed that no work has been published concerning the synthesis of block copolymers containing PVL hydrophobic block with P(VOH-*s*-VAc) as more hydrophilic block (after alcoholysis of a PVAc block). However, Yuankai *et al.*<sup>[6]</sup> reported the RAFT/MADIX block copolymerization of VAc and VeoVa in benzene at 60 °C, using AIBN as the initiator and isopropylxanthic disulfide (DIP) as the controlling agent. The authors obtained well-defined PVAc-*b*-PVeova, with different PVeova molar masses ( $M_{n,PVeova} = 10\ 200$  to  $38\ 300\ \text{g mol}^{-1}$ ). After hydrolysis of these block copolymers, the authors highlighted that the resulting P(VOH-*s*-VAc)-*b*-PVeova were insoluble in most of the solvents tested (THF, DMF, *N*-methylpyrrolidone, chloroform, dichloromethane, cyclohexane, toluene, and benzene), but were partially soluble in DMSO at 80 °C. They also claimed the successful synthesis of PVeova, even though they observed a deviation of the molar mass of PVeova with conversion compared to the theoretical values, and obtained relatively high dispersity ( $\bar{D} = 1.5$ , polymerization time = 30 h). No explanation on the behavior of this system was provided by the authors in this article. Barner-Kowollik and coworkers<sup>[7]</sup> successfully synthesized well-defined PVAc star polymers *via* RAFT/MADIX polymerization starting from multifunctional xanthate agents in bulk, and reached 40% conversion in 3 h. When they adapted this synthesis to vinylic esters with more bulky pendant groups such as vinyl pivalate and VeoVa, the authors reached significantly lower conversions (64% in 24 h and 45% in 22 h, respectively). They attributed this difference with the PVAc system to the steric hindrance of the side chain in close proximity with the xanthate moiety, which might restrict the access of the macroradicals to the C=S bond. Nevertheless, the molar masses increased relatively linearly with conversion (up to 50%), and the samples exhibited comparable molar mass distributions ( $\bar{D} = 1.4$ ) to the ones from the works of Yuankai.

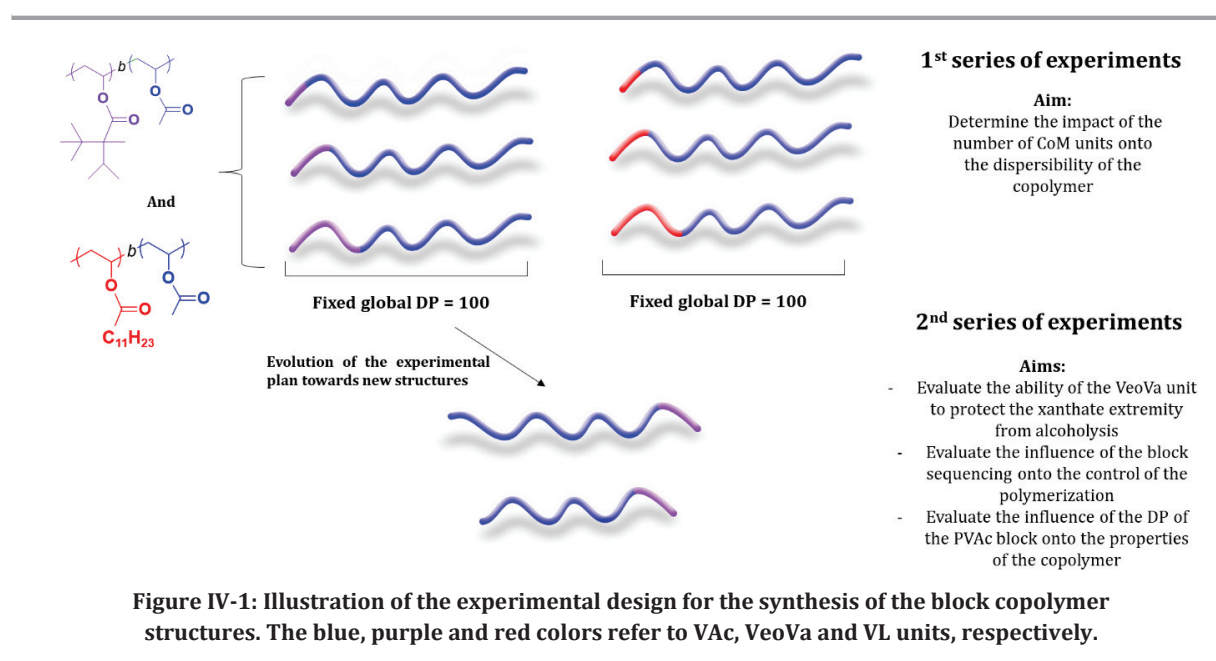


This literature review highlights that the synthesis of well-defined PVL-*b*-P(VOH-*s*-VAc) has never been reported, nor has the use of amphiphilic block copolymers of either PVL-*b*-P(VOH-*s*-VAc) or PVeOVA-*b*-P(VOH-*s*-VAc) as stabilizers for emulsion polymerization systems.

Thus, we synthesized a library of block copolymers with a block of either PVeOVA or PVL (with different molar masses), and a block of PVAc, which were then alcoholized to generate a hydrophilic P(VOH-*s*-VAc) block. The results are presented in **Sections II** and **III**, respectively. In **Section IV**, the dispersibility and aqueous phase conformation of the block copolymers was evaluated. When they were sufficiently dispersible in water, the most promising candidates were then tested in emulsion polymerization, to evaluate their ability to stabilize P(VAc-*co*-VeOVA) latexes. This is discussed in **Section V**.

It was demonstrated in **Chapter III** that the VeOVA units were not sensitive to hydrolysis, and that they were able to protect some neighboring monomer units against it, thanks to the umbrella effect. Therefore, we wondered if the xanthate moiety could benefit from this protection during the alcoholysis step if the last monomer unit connected to the xanthate extremity was a VeOVA. In that case, the resulting P(VOH-*s*-VAc)-*b*-PVeOVA-X block copolymer could proceed as a reactive stabilizer, and provide a different stabilization efficiency compared to the reverse structure PVeOVA-*b*-P(VOH-*s*-VAc). In that purpose, PVAc-*b*-PVeOVA block copolymers were also synthesized.

To bring some clarity, the following scheme illustrates the experimental design that was followed for the synthesis of these block copolymer series (**Figure IV-1**).



Besides, to ease the designation of the copolymers, the following notations will be used through this Chapter: DP1\_PVAc-X or DP1\_PCoM-X for the polymer before chain extension, and DP1\_PVAc-*b*-DP2\_PCoM or DP1\_PCoM-*b*-DP2\_PVAc for the polymers after chain extension, with DP1 and DP2 referring to the DP of the first and second block, respectively.

## II. Synthesis of the block copolymers

In this section, we first synthesized PVeoVa and PVL polymers with different DPs. Indeed, we intended to synthesize well-defined PCoM with both low and high molar masses. The low molar mass PCoM will then be used as macroCTA to synthesize well-defined PCoM-*b*-PVAc block copolymer. For the high molar mass PCoM, the aim was to investigate the ability of bulky vinyl ester monomer to homopolymerize, and, when used in RAFT/MADIX polymerization, to compare the chain-end functionality with that obtained for PVAc. First, the homopolymerization of VeoVa, and characterizations of the resulting PVeoVas are presented. Then, similar synthesis procedures were applied to obtain a library of well-defined PVL. Finally, chain extensions of PVeoVa and PVL with VAc (or reversely of PVAc with VeoVa) will be investigated. **Figure IV-2** outlines the general synthetic routes of these block copolymers.

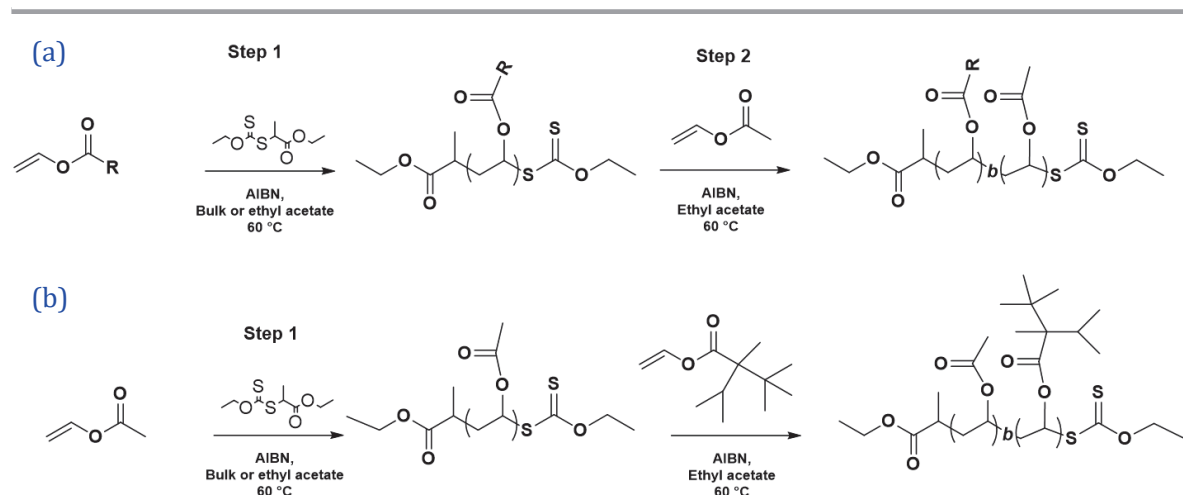


**Figure IV-2:** General reaction scheme for the synthesis of (a) PCoM-*b*-PVAc and (b) PVAc-*b*-PVeoVa. With R = C<sub>9</sub>H<sub>19</sub> (VeoVa) or C<sub>11</sub>H<sub>23</sub> (VL).

### II.1 RAFT/MADIX polymerization of VeoVa or VL

In this subsection, a library of PVeoVa with different DPs was synthesized as a first block.

#### II.1.1 Synthesis and characterization of low molar mass PVeoVa (DP 5 and 10) for further block copolymer synthesis

The results from **Chapter III** showed that only a small fraction of VeoVa allowed to maintain acceptable dispersibility of the statistical copolymer structures. Therefore, in this chapter, PVeoVa-*X* homopolymers with targeted DP = 5 and 10 were synthesized using *O*-ethyl-*S*-(1-

ethoxycarbonyl)ethyl dithiocarbonate as CTA, with a ratio [CTA]:[AIBN] = 5 according to the protocol described in **Experimental, Section III.4**. The polymer was soluble in most of the purification solvents. Methanol was found to be the best solvent in hands.

**Table IV-1: Main characteristics of the PVeOva-X homopolymers synthesized in bulk at 60 °C for 3 to 4 h.**

Designation	Time (h)	Monomer conv. (%) <sup>a</sup>	$M_n$ (theo.) (g mol <sup>-1</sup> ) <sup>a</sup>	$M_n$ (NMR) (g mol <sup>-1</sup> ) <sup>b</sup>	$M_n$ (SEC) (g mol <sup>-1</sup> ) <sup>c</sup>	Dispersity ( $\bar{D}$ )
10_PVeOva	4	68	2200	1800	2800	1.08
5_PVeOva	3	70	1190	1210	1390	1.10

<sup>a</sup> Theoretical molar mass of PVeOva calculated from conversion

<sup>b</sup> Experimental molar mass of PVeOva calculated from end group analysis by <sup>1</sup>H NMR comparing polymer chain-end and main chain resonances

<sup>c</sup> Experimental molar mass of PVeOva calculated by SEC-THF using universal calibration

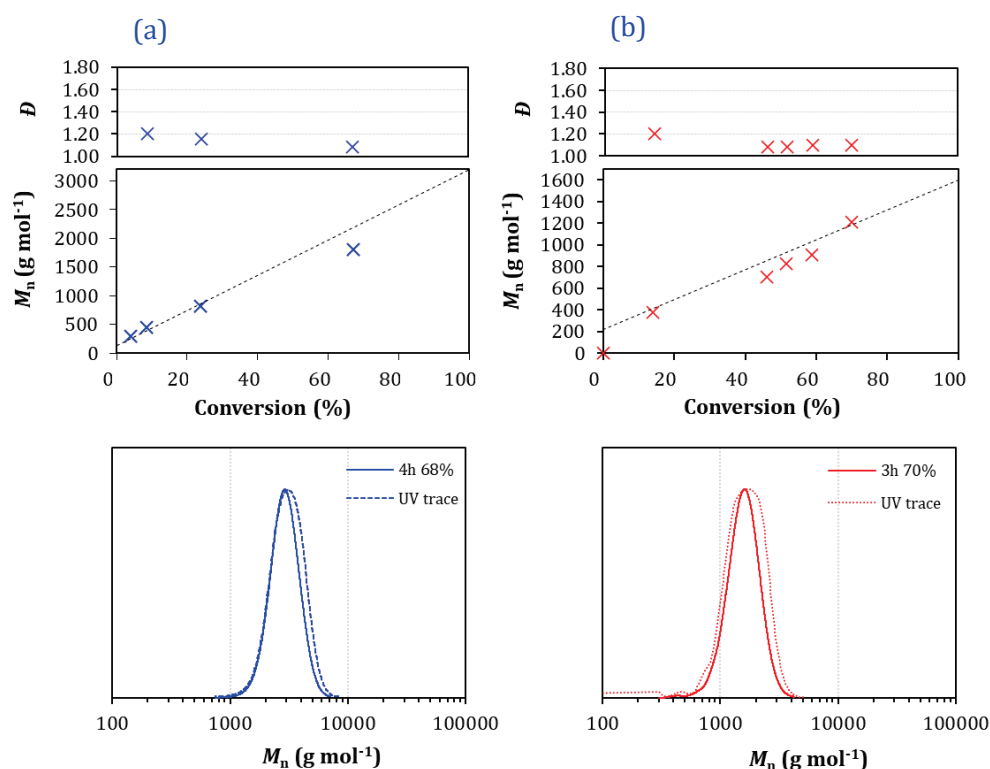


**Figure IV-3: Evolution of  $M_n$  (NMR) versus conversion for (a) 10\_PVeOva and (b) 5\_PVeOva, and the respective normalized SEC-THF traces of the final polymers with RI detector (full colored lines) and UV detector at 280 nm (dashed lines). Experimental data (X); Theoretical data (---).  $\bar{D}$  was obtained by SEC-THF.**

The resulting PVeOva had a low dispersity (less than 1.10) and the theoretical  $M_n$  closely matched that calculated from the <sup>1</sup>H NMR and obtained by SEC-THF (**Table IV-1**). Finally, the linearity of the evolution of the  $M_n$  with the conversion and the symmetry of the SEC traces attest good control of the polymerizations (**Figure IV-3**). These results suggest that for DP 5 and 10, the xanthate moiety (X) is likely to be present at the end of each polymer chain, which

would allow for chain extension of these macroCTA and therefore the ability to synthesize well-defined block copolymers.

### II.1.2 Evaluation of the extent of head-to-head additions in PVeOVA-X synthesis

It has already been reported that the steric hindrance provided by the bulky side group (T) in radical polymerization of vinyl monomers  $H_2C=CHT$  reinforced the stabilization of the radical, and limited the occurrence of head-to-head additions.<sup>[8]</sup> In that line, a part of this study was also to assess the ability of VeoVa to homopolymerize and evaluate the occurrence of head-to-head additions, in comparison with the polymerization of VAc (see **Chapter II, Section II**). Hence, the experimental conditions were very similar to those used for the polymerization of VAc, and the DP at 100% conversion was set to 80, to target DP = 75 (**Table IV-2**, entry **1**). Kinetics of the polymerizations are available in **Appendix 7**.

**Table IV-2: Experimental conditions and results obtained for the RAFT/MADIX homopolymerization of VeoVa with targeted DP = 75, at 60 °C.**

Exp.	Time (h)	[CTA]:[AIBN]	Solvent	Conv. (%) <sup>a</sup>	Experimental DP <sup>b</sup>	$M_n$ (theo.) (g mol <sup>-1</sup> ) <sup>c</sup>	$M_n$ (SEC) (g mol <sup>-1</sup> ) <sup>d</sup>	$\bar{D}$ <sup>d</sup>
1	7	5	EtAc	22	23	3760	4825	1.20
2	8	5	Bulk	34	39	5760	7970	1.17
3	7	3	EtAc	4	-	855	-	-
4	24	3	EtAc	74	60	12 000	11 790	1.30
5	7	3	Bulk	45	46	7590	9350	1.17

<sup>a</sup> Conversion based on <sup>1</sup>H NMR calculations by comparing monomer and polymer resonances

<sup>b</sup> DP calculated *via* the equation  $M_n = DP \cdot M_{VeoVa} + M_{RAFT}$  with  $M_{VeoVa}$  and  $M_{RAFT}$  the molar mass of VeoVa and the RAFT/MADIX agent, respectively, and  $M_n$  obtained by SEC-THF using universal calibration

<sup>c</sup> Theoretical molar mass of the polymer calculated from conversion

<sup>d</sup> Experimental molar mass of the polymers obtained *via* SEC-THF using universal calibration

At first, the polymerization of VeoVa was performed in EtAc with a ratio [CTA]:[AIBN] = 5 (**Table IV-2**, entry **1**). An induction period of 4 h was observed, and only 22% conversion was reached after 7 h (compared to 80% conversion for the polymerization of VAc after 6 h). Another limitation of these experiments when performed in EtAc was the low amount of polymer recovered after purification in methanol. When performed in bulk with the same [CTA]:[AIBN] ratio of 5, a similar induction period was observed, and 34% conversion was reached after 8 h (**Table IV-2**, entry **2**). To increase the polymerization rate, the initiator concentration was increased. With the ratio [CTA]:[AIBN] = 3, surprisingly only 4% conversion was reached after 7 h, and 74% conversion after 24 h in EtAc (corresponding to DP = 60) (**Table IV-2** entries **3** and **4**, respectively). The induction period lasted for 6 h. Finally, the same reaction was performed in bulk. This time, the conversion reached 45% (corresponding to DP = 40 and with an induction period of 3 h) (**Table IV-2**, entry **5**), before the magnetic stirrer stopped as the viscosity of the polymerization medium increased.

The results of these experiments show that for high DP, the RAFT polymerization of VeoVa was not straightforward and some delay in the polymerization were highlighted compared to that of VAc (where the induction time was approximately 1 h, regardless of the DP). Nevertheless, the theoretical  $M_n$  fitted quite well with the experimental ones determined by SEC using a universal calibration, and the molar mass distributions remained narrow for every experiment, which attest good control of the polymerizations (**Table IV-2**).

A few examples of VeoVa homopolymerization and of copolymerization of VeoVa with VAc can be found in the literature and were already mentioned in the introduction of this Chapter.<sup>[6,7]</sup> The authors also faced difficulties in reaching high conversion for the VeoVa homopolymerization, and attributed this behavior to the bulkiness of the side chains, affecting monomer and radical reactivity, and limiting the access of the radicals to the xanthate moiety.<sup>[6]</sup> In line with these observations, the experimental conditions employed in the present work did not allow reaching the targeted DP = 75.

The aim of this set of experiments was also to determine the chain-end functionality (¥) of PVeoVa compared to that of PVAc, which is directly linked to the configuration of the inserted last monomer unit connected to the xanthate moiety. Indeed, it was previously mentioned in **Chapter II (Section II)**, that PVAc• radicals had the tendency to undergo head-to-head additions and led to the formation of less-reactivable CH(OAc)CH<sub>2</sub>-X terminated chains (noted PVAc<sub>T</sub>-X), which were slow to fragment and thus accumulated in the polymerization medium, leading to a broad molar mass distribution and high dispersities. ¥ was thus defined as the ratio between chains that are normally terminated by a head-to-tail inserted VAc unit connected to the xanthate moiety (PVAc<sub>H</sub>-X) with all the possible chain-end configurations (PVAc<sub>H</sub>-X, PVAc<sub>T</sub>-X, and dead chains) **Chapter II, Section II**.

¥ of PVeoVas (from **Table IV-2**, entries **4** and **5**) and PVAc (40\_PVAc and 60\_PVAc from **Chapter II, Section II, Table II-1**) with similar DPs (*i.e.*, 40 and 60, **Table IV-3**) were determined by <sup>1</sup>H NMR as described in **Chapter II, Equation 8** for PVAc. In the following, Exp. **4** will be referred to as 40\_PVeoVa and Exp. **5** as 60\_PVeoVa.

**Table IV-3: Main characteristics of PVeoVa-X and PVAc-X homopolymers.**

Designation	$M_n$ (theo.) (g mol <sup>-1</sup> ) <sup>a</sup>	$M_n$ (SEC) (g mol <sup>-1</sup> ) <sup>b</sup>	Dispersity ( $\mathcal{D}$ )	¥ (%)
40_PVeoVa	7590	9350	1.17	100
60_PVeoVa	12 000	11 790	1.30	100
40_PVAc	4100	3500	1.20	60
60_PVAc	6190	5800	1.35	55

<sup>a</sup>Theoretical molar mass calculated from conversion determined by <sup>1</sup>H NMR

<sup>b</sup> Experimental molar mass calculated by SEC-THF using universal calibration

$^1\text{H}$  NMR characterizations of PVeOVA were difficult as broadening of the signals occurred. Indeed, limited resolution of the signal was obtained with most of the organic solvents including acetone, DMF, *N*-methylpyrrolidone, chloroform, dichloromethane, cyclohexane, toluene, and benzene.<sup>[6]</sup>  $\text{CDCl}_3$  was finally the most adapted solvent for PVeOVA, even though the typical (1-ethoxycarbonyl)ethyl fragment of the xanthate ( $\alpha$ -end) overlapped with the polymer backbone and monomer signals (4.6 - 5.3 ppm) (**Figure IV-4**). Nevertheless, the ethyl signal of the *O*-ethyl fragment of the xanthate ( $\omega$ -end) was visible in the range 4.1 - 4.3 ppm. As previously shown in **Chapter II**, characteristic signals of the xanthate end-groups were clearly identified for PVAc: a complex signal centered at 6.60 ppm assigned to the -CH- of the terminal VAc unit in PVAc<sub>H</sub>-X chains; a broad signal ranging from 3.1 to 3.5 ppm corresponding to the -CH<sub>2</sub>- of the terminal VAc unit in PVAc<sub>T</sub>-X chains. Similarly, for PVeOVA-X, the signal centered at 6.60 ppm, corresponding to terminal VeoVa unit in PVeOVA<sub>H</sub>-X, was visible in the  $^1\text{H}$  NMR spectrum, while the signal that would correspond to the -CH<sub>2</sub>- of the terminal VeoVa unit in PVeOVA<sub>T</sub>-X chains was not.

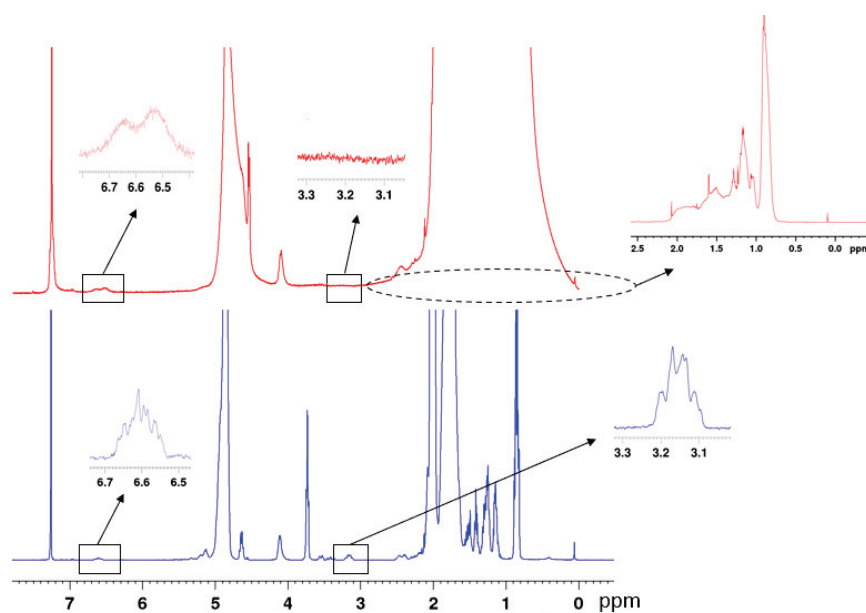


**Figure IV-4:**  $^1\text{H}$  NMR spectra of 60\_PVeOVA-X (red) and 60\_PVAc-X (blue) in  $\text{CDCl}_3$ , 256 scans at R.T. with an insert (x10) on the signal of head-to-head inserted monomer unit connected to the xanthate moiety (3.08 - 3.3 ppm) and on the signal of head-to-tail inserted monomer unit connected to the xanthate moiety (6.4 - 6.7 ppm).

Based on the  $^1\text{H}$  NMR spectra, chain-end functionality was determined to be 100% for both 40 and 60\_PVeOVA, while it was only 60 and 55% for 40 and 60\_PVAc, respectively (**Table IV-3**). A possible explanation would be that the steric hindrance provided by VeoVa only allows for regular head-to-tail addition of the next monomer units. To confirm this hypothesis, extensions of 60\_PVAc-X and 60\_PVeOVA-X were carried out in EtAc with 200 VAc



equivalents at 60 °C and with [60\_PVeoVa-X]:[AIBN] or [60\_PVAc-X]:[AIBN] = 5 for 6 h. The resulting polymers were purified by precipitation in cold petroleum ether for PVAc-*b*-PVAc and in a water:methanol 50:50 mixture (v/v) for PVeoVa-*b*-PVAc. The resulting polymers were characterized by SEC-THF (**Figure IV-5 (a)** and **(b)**).

To quantify the proportion of chains that were extended with VAc and those which were not, deconvolution of the chromatograms was performed *via* an automated program in Origin software (**Figure IV-5 (c)** and **(d)**). The SEC chromatograms provide a response according to the concentration of the polymer. The concentrations of the polymers in THF were similar (3 mg mL<sup>-1</sup>), so it is possible to compare the area under the peaks of each signal provided by the SEC after deconvolution (**Figure IV-5 (c)** and **(d)**). The response provided by the deconvolution is probably not the exact value of the proportion of chains that were effectively extended, but it provides a reasonable comparison of the two systems. The area of each deconvoluted peak is given by **Equations 36** and **37**.

$$S_1 = K (dn/dC)_1 C_1 \text{ and } S_2 = K (dn/dC)_2 C_2 \quad \text{(36) and (37)}$$

With  $S_1$  the area of the deconvoluted peak of the PVAc-X or PVeoVa-X macroCTA that has not been chain extended;  $S_2$  the area of the deconvoluted peak of the polymer after extension with VAc (*i.e.*, PVAc-*b*-PVAc or PVeoVa-*b*-PVAc);  $K$ , the Mark-Houwink coefficients of the system (considering  $K_{PVAc} = 15.8 \cdot 10^{-3} \text{ mL g}^{-1}$  also for PVeoVa-*b*-PVAc),  $(dn/dC)_1$  and  $(dn/dC)_2$  the refractive index increment of PVAc-X (or PVeoVa-X) macroCTA and the block copolymers after extension, respectively; and  $C_1$  and  $C_2$  the concentration, respectively, of PVAc-X (or PVeoVa-X) macroCTA that has not been extended, and of the block copolymer after extension with VAc. Due to the close nature of the vinyl monomers VAc and VeoVa, it was considered as a first approximation that  $(dn/dC)_1$  and  $(dn/dC)_2$  values were similar (*i.e.*, 1.467 at 20 °C, Malvern data).



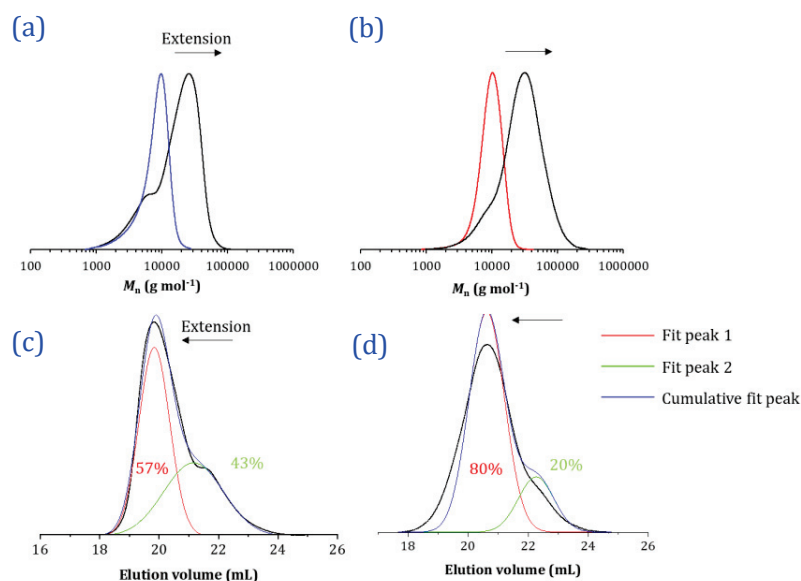


**Figure IV-5: Extension of (a) 60\_PVAc and (b) 60\_PVeoVa, where the colored chromatogram corresponds to the polymer before extension and the black trace to the polymer after extension; and (c) and (d) the corresponding deconvolutions of the SEC traces after extension. Note that for deconvolution, the SEC traces were plot as a function of the elution volume, which changes the order of the peaks compared to (a) and (b) traces.**

Typical shouldering of the SEC trace was observed for the chain extension of 60\_PVAc (**Figure IV-5, (a)**). This shoulder overlapped with the trace of the original PVAc, and was attributed to un-extended macroCtA chains, most likely corresponding to less reactivable  $\text{CH}(\text{OAc})\text{CH}_2\text{-X}$  terminated chains and a possible contribution of dead chains. The extension of 60\_PVeoVa-X with VAc was successful, as a clear shift of the SEC trace towards higher molar masses was observed (**Figure IV-5 (b)**). Nevertheless, the molar mass distribution also highlighted a shouldering but it seemed to occur to a lesser extent than for the extension of 60\_PVAc. The deconvolution of the chromatograms confirmed that the extension of the chains of 60\_PVeoVa-X was 20% more efficient than the extension of the 60\_PVAc-X chains. This highlights a better functionalization of 60\_PVeoVa-X, which is probably due to the occurrence of fewer head-to-head insertions of the last monomer units connected to the xanthate moiety. Interestingly, after deconvolution, the area under the SEC trace corresponding to the polymer after extension, suggested that 57% of the chains were successfully extended, which was self-consistent with the  $^1\text{H}$  NMR calculations. However, 100% functionality was calculated in the case of the extension of 60\_PVeoVa-X by  $^1\text{H}$  NMR, and the area under the SEC traces after extension of the polymer indicate that only 80% of the chains were successfully extended. This value is somehow still consistent with the one obtained by  $^1\text{H}$  NMR, but with a higher deviation. The accuracy of both techniques used to determine the chain-end functionality can be questionable. For example, the resolution of the NMR signal of homopolymer 60\_PVeoVa-X was not perfect, and it is likely that the chain-end signal at 3.03 – 3.3 ppm (which corresponds to the signal of PVeoVa-X) is not well defined.

Also, the deconvolution of the SEC chromatograms relies on a mathematical equation, which tries to fit the original chromatograms as precisely as possible, but in the case where both signals overlap, an error in the fit is possible. This is why the values returned by the deconvolution cannot be considered as exact values. Nevertheless, the trend given by the two techniques is in agreement and confirms a better functionalization of the PVeOVA chains compared to that of the PVAc ones.

Building on these results it is most likely that chain extension of PVeOVA with VAc will lead to more well-defined block copolymers in comparison with chain extension of PVAc with VeOVA.

In the following section, VeOVA was replaced by VL, and PVL-X homopolymers with different targeted DP were synthesized (5, 10 and 20 units).

## **II.2 Synthesis and characterizations of low molar mass PVL homopolymers for further block copolymerization synthesis**

VL homopolymerizations were carried out in bulk at 60 °C and stopped at approximately 80% conversion. A ratio [CTA]:[AIBN] = 5 was used and the ratio [VL]:[CTA] was adapted accordingly to the targeted DP, *i.e.*, 20, 10 and 5. PVL was difficult to purify by precipitation, because it was soluble in most of the solvents tested, namely petroleum ether, hexane, heptane, cyclohexane, methanol:water 50:50 (v/v) and pentane. However, the polymer precipitated as a viscous oil in cold methanol. The polymer was denser than methanol, which allowed for recovery of the polymer as an oil after decantation. The purification process was performed three times and yielded 75% of the expected mass of polymer (**Table IV-4**).

**Table IV-4: Main characteristics of the PVL-X homopolymers synthesized in bulk at 60 °C for 4 to 6 h.**

Designation	Time (h)	Conv. (%) <sup>a</sup>	$M_n$ (theo.) (g mol <sup>-1</sup> ) <sup>a</sup>	$M_n$ (NMR) (g mol <sup>-1</sup> ) <sup>b</sup>	$M_n$ (SEC) (g mol <sup>-1</sup> ) <sup>c</sup>	Experimental DP <sup>c</sup>	$\mathcal{D}$ <sup>d</sup>
20_PVL	4	77	3700	4360	4670	18	1.08
10_PVL	6	77	2840	2610	3250	10	1.11
5_PVL	6	84	1550	1530	1880	5	1.14

<sup>a</sup> Theoretical molar mass of PVL calculated from conversion

<sup>b</sup> Experimental molar mass of PVL calculated from end group analysis by <sup>1</sup>H NMR comparing polymer chain-end and main chain resonances

<sup>c</sup> Calculated from  $M_n$  (NMR):  $DP = (M_n - M_{RAFT})/M_{VL}$  with  $M_{RAFT}$  and  $M_{VL}$  the molar masses of the RAFT/MADIX agent and VL monomer, respectively

<sup>d</sup> Experimental molar mass of PVL calculated by SEC-THF using universal calibration

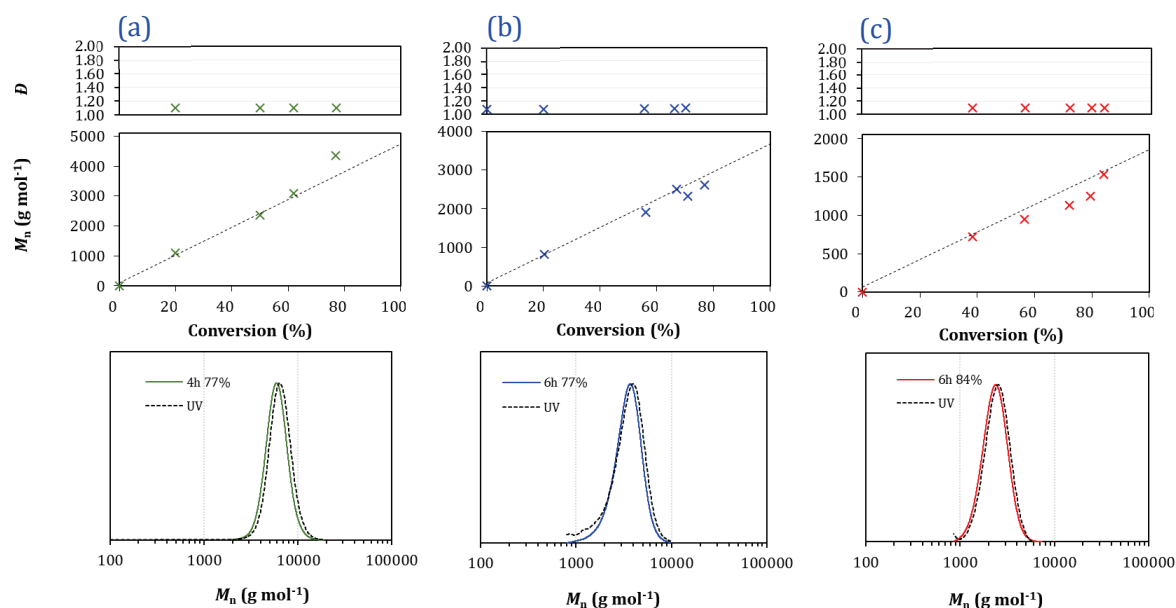


**Figure IV-6: Evolution of  $M_n$  (NMR) versus monomer conversion for (a) 20\_PVL; (b) 10\_PVL and (c) 5\_PVL and the respective normalized SEC-THF traces of the polymers after purification with RI detector (full colored lines) and UV detector at 280 nm (dashed black lines). Experimental data (X); Theoretical data (-.-).  $\mathcal{D}$  was obtained by SEC-THF.**

**Figure IV-6** and **Table IV-4** show that the polymerizations were well controlled and that polymers with different DP closed to the target, with low dispersity ( $\mathcal{D} = 1.1$ ), were synthesized. This low dispersity suggested that the xanthate moiety was likely to be present at the end of each polymer chain, which would allow for chain extension of PVL-X. To confirm this hypothesis, the proportion of regularly  $\text{CH}_2\text{CH}(\text{OC}_{12}\text{H}_{23})\text{-X}$  terminated chains (PVL<sub>H</sub>-X) was compared to the proportion of less-reactivable  $\text{CH}(\text{OC}_{12}\text{H}_{23})\text{CH}_2\text{-X}$  terminated chains (PVL<sub>T</sub>-X) via <sup>1</sup>H NMR to evaluate the chain-end fidelity (¥) of 20\_PVL-X, as previously presented in **Chapter II, Section II**. **Figure IV-7** provides an example of <sup>1</sup>H NMR spectrum of 20\_PVL and the relevant assignments.

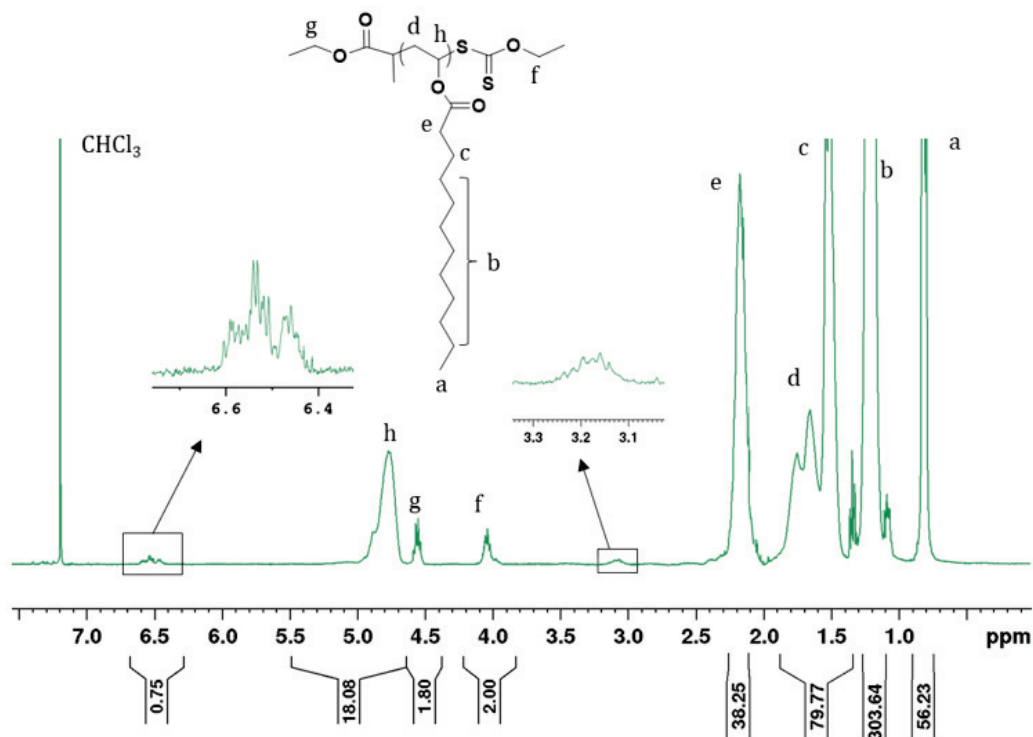


Figure IV-7:  $^1\text{H}$  NMR spectrum of 20\_PVL-X in  $\text{CDCl}_3$ , 256 scans at R.T. with an insert (x10) on the head-to-tail inserted monomer unit connected to the xanthate moiety signal (3.08 - 3.3 ppm) and head-to-head inserted monomer unit connected to the xanthate moiety signal (6.4 - 6.7 ppm).

In contrast to the  $^1\text{H}$  NMR spectrum of 60\_PVeoVa-X, the one from 20\_PVL-X shows well-resolved signals characteristic of  $\text{PVL}_T\text{-X}$  at 3.08 - 3.3 ppm (**Figure IV-7**). This could be related to a steric hindrance provided by the VL units that is less efficient than the one provided by a VeoVa unit to suppress the reverse addition defect. According to the  $^1\text{H}$  NMR, in the case of 20\_PVL-X, this signal corresponded to 11% of the chains (**Table IV-5**).

Table IV-5: Chain-end functionality determined by  $^1\text{H}$  NMR for the PVL-X

Designation	¥ (%) <sup>a</sup>
20_PVL-X	89
10_PVL-X	96
5_PVL-X	99
20_PVAc-X	80

<sup>a</sup> Determined using **Equation 8** from **Chapter II**.

For similar DP = 20, the loss of chain-end functionality of 20\_PVAc-X was determined to be 20% in **Chapter II**. If the steric hindrance provided by the VL units is not sufficient to completely eliminate head-to-head additions, it seems nevertheless that the long alkyl chain

already decreases their occurrence. These results (both for PVeOVA and PVL) are in agreement with the literature findings.<sup>[8]</sup>

### II.3 Chain extension of PVeOVA and PVL with VAc

Extension of the homopolymers from **Table IV-1** and **Table IV-4** were performed with 140 VAc units in EtAc and stopped to target approximately a total DP of  $100 \pm 10$  units. [PCoM]:[AIBN] ratio of 5 was used for the extensions. The extensions of 75\_PVAc and 100\_PVAc were also performed with 10 VeOVA equivalents (and stopped to target about 5 VAc units in the final structures), to compare the influence of the quality of the extension relative to the block order, on the properties of the resulting alcoholized copolymers (*i.e.*, micellization ability, and later on, stabilization efficiency) (**Figure IV-10**). The protocol is provided in **Experimental, Section III.4**. The molar mass of the block copolymers was determined by <sup>1</sup>H NMR, making the assumption that all the starting chains were successfully extended. **Figure IV-8** to **Figure IV-10** also shows the SEC traces of the polymers before (black traces) and after extension (colored traces).

**Table IV-6: Summary of the structures obtained after extension of PVeOVA-X, PVL-X with VAc and of PVAc-X and with VeOVA, in EtAc at 60 °C.**

Designation	MacroCTA	monomer conv. (%) <sup>a</sup>	$M_n$ (theo.) (g mol <sup>-1</sup> ) <sup>b</sup>	$M_n$ (NMR) (g mol <sup>-1</sup> ) <sup>c</sup>	$M_n$ (SEC) (g mol <sup>-1</sup> ) <sup>d</sup>	Dispersity ( $\mathcal{D}$ ) <sup>d</sup>
10_PVeOVA- <i>b</i> -90_PVAc	10_PVeOVA	60	13 540	10 840	11 610	1.40
5_PVeOVA- <i>b</i> -95_PVAc	5_PVeOVA	68	10 560	9820	12 120	1.40
75_PVAc- <i>b</i> -5_PVeOVA	75_PVAc	50	6950	7170	8800	1.50
100_PVAc- <i>b</i> -5_PVeOVA	100_PVAc	60	10 430	10 500	13 600	1.50
20_PVL- <i>b</i> -80_PVAc	20_PVL	60	11 320	10 280	15 560	1.60
10_PVL- <i>b</i> -90_PVAc	10_PVL	66	11 690	10 850	12 450	1.60
5_PVL- <i>b</i> -95_PVAc	5_PVL	78	12 260	11 560	10 370	1.40

<sup>a</sup> Conversion of the chain extension step from the crude sample calculated by <sup>1</sup>H NMR by comparing monomer (VAc or VeOVA) and polymer resonances

<sup>b</sup> Theoretical molar mass of the block copolymer calculated from conversion

<sup>c</sup> Experimental molar mass of the block copolymer calculated from end group analysis by <sup>1</sup>H NMR comparing polymer chain-end and main chain resonances

<sup>d</sup> Experimental molar mass of the block copolymer calculated by SEC-THF using PS calibration

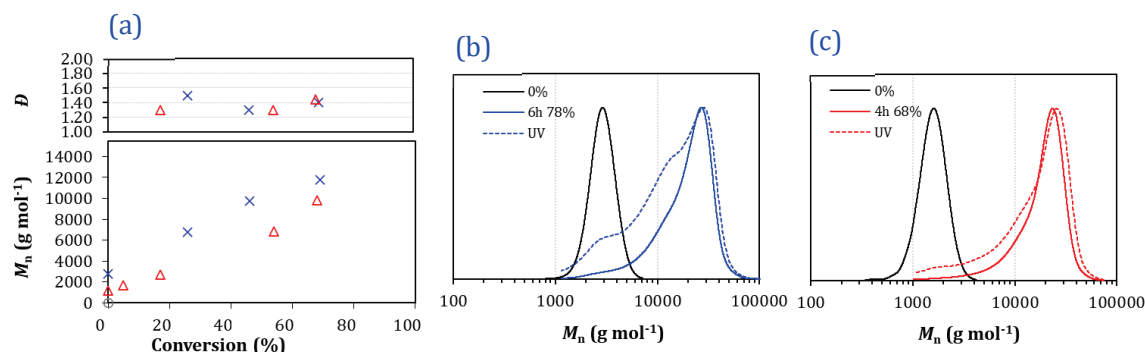


**Figure IV-8:** RAFT/MADIX extension of PVeOVA with VAc, in EtAc at 60 °C, with [PVeOVA]:[AIBN] = 5. Targeted composition of VAc in the second block = 100 units. **(a)** Evolution of  $M_n$  (NMR) and  $\bar{D}$  with the conversion of VAc for the extension of (x) 10\_PVeOVA and (Δ) 5\_PVeOVA, and their corresponding normalized SEC-THF traces before (black) and after extension (colored trace), respectively **(b)** and **(c)**. Full lines correspond to the RI traces and dashed lines correspond to the UV traces at 280 nm of the block copolymer after extension.

In the case of the extensions of PVeOVA-X (**Figure IV-8**) and PVL-X (**Figure IV-9**) macroCTAs,  $M_n$  increased relatively linearly with conversion (**Figure IV-8 (a)** and **Figure IV-9 (a)**). RI traces from the chromatograms showed a clear shift of the molar mass distributions towards higher values, which confirmed the successful extensions. The UV traces overlapped with the resulting RI signals of the polymers after extensions, which confirmed the presence of the xanthate extremity in the resulting block copolymers and therefore confirmed that these extensions were successfully controlled. Nevertheless, for DP1 = 10 (for the VeOVA and VL-based block copolymers, **Figure IV-8 (b)** and **Figure IV-9 (c)**) and for DP1 = 5 and 20 (for the VL-based block copolymer, **Figure IV-9 (b)** and **(d)**), the UV trace also highlighted two shoulders. The first of which overlapped with the trace of PVeOVA or PVL before extension. This indicates that not all the PVeOVA or PVL were involved in the extension. It is difficult to determine the exact fraction of chains that did not extend, but from the previous results obtained by NMR and for the extension of PVeOVA and PVAc homopolymers of high DP with VAc (**Section II.1**), one can expect that the fraction of non-extended chains coming from the PVeOVA block (and to a certain extent also that of PVL block) is not high. The second shoulder was attributed to the loss of functionality that might occur during the extension with VAc, probably due to the aforementioned competitive head-to-head additions that lead to the accumulation of less activated polymer chains, as already highlighted in the case of PVAc in **Chapter II**. Additionally, when it comes to the synthesis of block copolymers, one has to keep in mind that the quality of the final block is also impacted by the efficiency of reinitiation of the starting chains and the amount of initiator used during the chain extension. This inevitably leads to the existence of several species *i.e.*, homopolymers of the first and the second block, respectively that can pollute the final block copolymer structure.

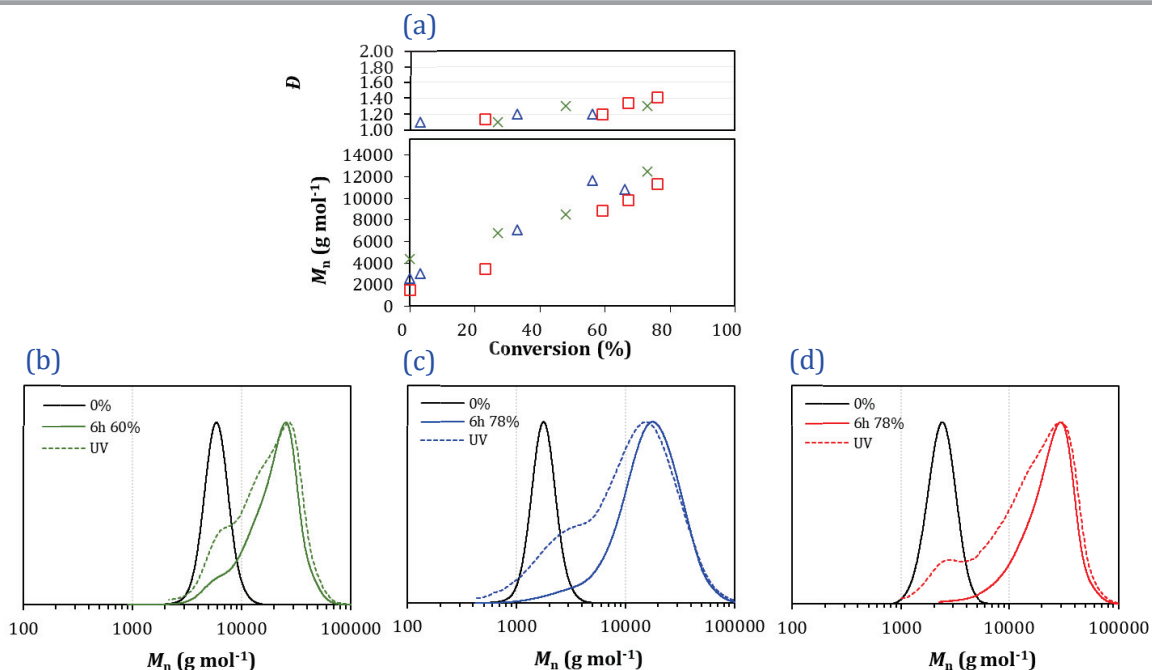


**Figure IV-9:** RAFT/MADIX extension of PVL-X with VAc, in EtAc at 60 °C with [PVL-X]:[AIBN] = 5. Targeted DP of VAc in the second block = 100 units. **(a)** Evolution of  $M_n$ (NMR) and  $\bar{D}$  with the conversion of VAc for the extension of (×) 20\_PVL, (Δ): 10\_PVL and (□) 5\_PVL, and their corresponding normalized SEC-THF traces before (black) and after extension (colored trace), respectively **(b)**, **(c)** and **(d)**. Full lines correspond to the RI traces and dashed lines correspond to the UV traces at 280 nm of the block copolymer after extension.

Nevertheless, good agreement was observed between,  $M_n$  (NMR) and  $M_n$  (theo.), and dispersities remained low (**Table IV-6**, **Figure IV-8 (a)** and **Figure IV-9 (a)**). This supports that relatively well-controlled block copolymers have been successfully synthesized.

For the chain extension performed from the PVAc macroCTA, the UV trace of the polymer extended with VeoVa units was broad and overlapped with both the first RI trace (corresponding to the PVAc before extension), and with the second RI trace (which corresponds to the resulting block copolymer after extension) (**Figure IV-10 (b)** and **(c)**). This observation appeared to be similar regardless of the DP of the first block, even if the RI trace seemed narrower for 75\_PVAc-*b*-5-PVeoVa than for 100\_PVAc-*b*-5-PVeoVa (**Figure IV-10 (b)** and **(c)**). It was already highlighted in **Chapter II** that the higher the DP of PVAc-X, the lower the xanthate functionality. It was therefore not surprising that for DP = 75 and 100 ( $\bar{Y} = 55$  and 53%, respectively), all the chains were not efficiently extended with the addition of VeoVa. The determination of the DP of the PVeoVa block by <sup>1</sup>H NMR must also be taken with care, because it was assumed that all the chains were successfully extended for the calculation, which was obviously not the case for the second series of experiments, where the macroCTAs are PVAc blocks. Furthermore, it did not make sense to plot the evolution of  $M_n$  with conversion. Nevertheless, of the higher value of  $M_n$  obtained from <sup>1</sup>H NMR after



extension (**Figure IV-10 (a)**) and the clear shift of  $M_n$  towards higher values obtained by SEC attest an extension of the initial polymers.

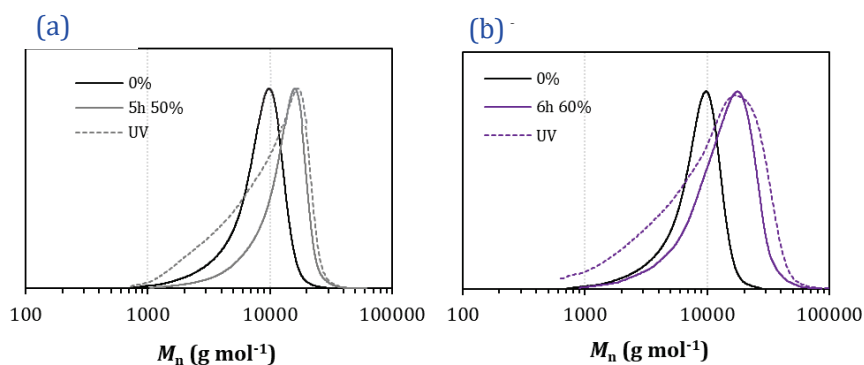


**Figure IV-10** : SEC-traces of the extensions of **(a)** 75\_PVAc-X and **(b)** 100\_PVAc-X with VeoVa, in EtAc at 60 °C with [PVAc-X]:[AIBN] = 5. Targeted DP of VeoVa in the second block = 5. Black traces correspond to PVAc-X before extension; colored traces correspond to the polymer after extension. Full lines correspond to the RI traces and dashed lines correspond to the UV traces at 280 nm of the block copolymer after extension.

## II.4 Conclusion on the synthesis of block copolymers

As demonstrated in the above sections, the syntheses of the block copolymers PVeoVa-*b*-PVAc, PVAc-*b*-PVeovVa and PVL-*b*-PVAc were not straightforward. It was indeed difficult to synthesize PVeovVa-X, with high DP, because of the bulkiness of the monomer. The synthesis of PVL-X homopolymers provided low yields, due to the high solubility of the polymer in most of the purification solvents in hand. Nevertheless, PVeovVa-X and PVL-X homopolymers, with DP ranging from 5 to 10 (and up to 20 for PVL), were successfully synthesized in a controlled manner, and further extended with VAc. This extension was not straightforward either, and relative control of the second block was achieved. In a second series of experiments, PVAc-X with DP = 75 and 100 were synthesized and chain extended with VeoVa. The control of the polymerizations was limited because of the loss of chain-end functionality during the synthesis of the first block of PVAc, resulting from the accumulation of less-reactive polymer chains which did not participate to the chain extension with VeoVa.

However, the syntheses of PVAc-*b*-PVeovVa block copolymers were carried out with a specific purpose, in order to verify an alternative hypothesis. It was demonstrated in **Chapter II** that the VeoVa units were not sensitive to hydrolysis, and that they were able to protect some neighboring units against it, thanks to the umbrella effect. Therefore, it was thought that if the last unit connected to the xanthate was VeoVa, the xanthate extremity might benefit from this protection. If the xanthate extremity is still present at the end of the block copolymer after alcoholysis, then the block copolymer could act as a reactive stabilizer (at least for the chains that have been successfully chain extended during the second step and carry a PVeovVa



block). In that case, the block sequencing would have an impact on the stabilization efficiency of the latex.

To validate this hypothesis,  $^1\text{H}$  and  $^{13}\text{C}$  NMR in depth characterization of P(VOH-*s*-VAc)-*b*-PVeOVA were carried out after alcoholysis, as well as preliminary extension experiment of the block copolymer with VAc. Unfortunately, this investigation is not conclusive at this stage and would require more time and further experiments to conclude. Nevertheless, these preliminary results are available in **Appendix 6**.

*In conclusion*, it was possible to synthesize well-defined block copolymers PVeOVA-*b*-PVAc, PVAc-*b*-PVeOVA and PVL-*b*-PVAc by RAFT/MADIX polymerization, but it is important to keep in mind that the final polymers were not pure block copolymers, but a mixture of block copolymers and homopolymers (from the first and second block, as well as some unavoidable dead chains). The next section investigates the alcoholysis of these block copolymers.

### III. Alcoholysis of the block copolymers

#### III.1 Alcoholysis of the VeoVa-based block copolymers

It was previously observed that during the alcoholysis of the statistical VeoVa-based stabilizers the VeoVa units were maintained (**Chapter III**). Therefore, it was expected that this behavior would be similar when VeoVa-based block copolymers are alcoholized, and hence the kinetics was not followed by  $^1\text{H}$  NMR. The block copolymers were solubilized in MeOH and alcoholized for 2 h, following the protocol described in the **Experimental Section IV.2**. After neutralization with acetic acid, three washes with methanol and filtration, the alcoholized block copolymers were recovered as yellowish powders, and analyzed by  $^1\text{H}$  NMR in DMSO- $d_6$ .

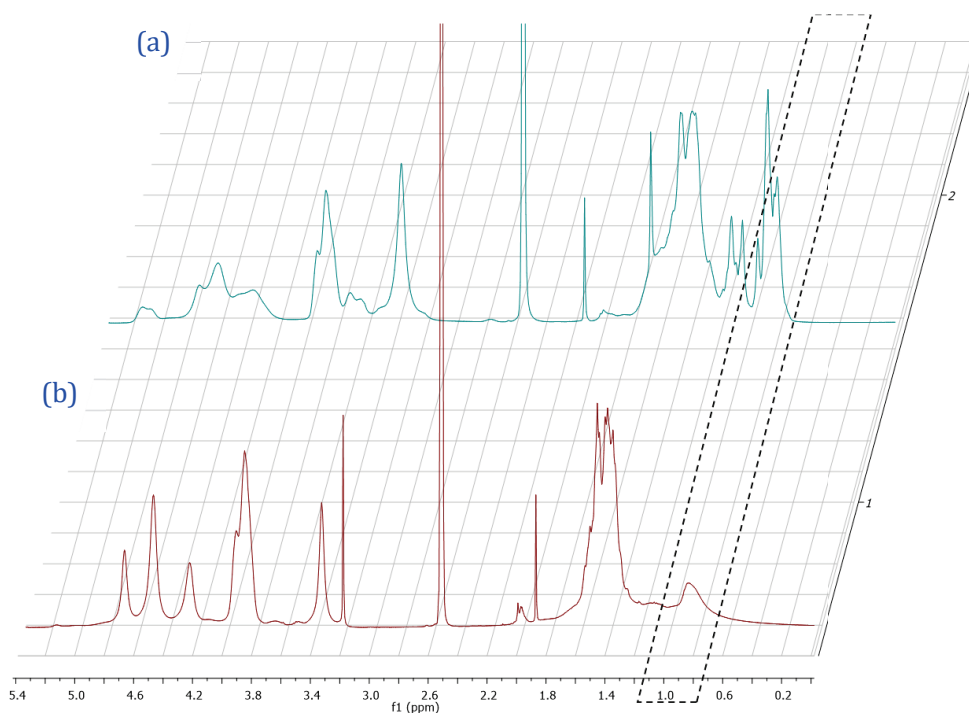


**Figure IV-11: (a)**  $^1\text{H}$  NMR spectrum of  $100\_P(\text{VOH}_{0.875}\text{-s-VeoVa}_{0.100}\text{-s-VAc}_{0.025})$  and **(b)**  $^1\text{H}$  NMR spectrum of  $10\_P\text{VeoVa-b-}90\_P(\text{VOH-s-VAc})$  in DMSO- $d_6$  at R.T. Dashed lines highlight the low definition of the VeoVa signal in DMSO- $d_6$  for the block copolymer compared to the one in the statistical copolymer (with similar VeoVa content), that is well-defined.

The dissolution of the block copolymers in DMSO- $d_6$  was not as straightforward as for the statistical copolymers. It was necessary to carefully heat the NMR tube to 100 °C for 15 min to obtain a clear solution, but this procedure also produced a lot of foam. Nevertheless, the definition of the signals was no better in the other deuterated solvents ( $\text{D}_2\text{O}$ ,  $\text{CDCl}_3$ ,  $\text{CDOD}_3$ ).

**Figure IV-11** shows that for similar fraction of VeoVa in the copolymer (*i.e.*, 10 mol.%), the signal corresponding to the VeoVa units (0.7 – 1.1 ppm) seemed more intense and with a better resolution in the statistical copolymer than in the block copolymer. This first indicates that the calculation of the composition of the block copolymer will probably be tainted with error. This is also the sign that the copolymers do not move in the same way, and therefore that the block structure probably influences the arrangement of the chains in DMSO. This would already reflect a different conformation of the polymer in a hydrophilic solvent, that will probably also have some consequences onto the organization of the block copolymer in water.

To get further insight into the organization of these block copolymers in DMSO, they were put in DMSO at 100 °C. Back at 25 °C, turbid dispersions were obtained, which were then analyzed by DLS. **Figure IV-12** provides an example of the results obtained for 100\_P(VOH<sub>0.935</sub>-S-VAC<sub>0.015</sub>)-b-5\_PVeoVa<sub>0.050</sub> (**B3**, **Table IV-7**) and 75\_P(VOH<sub>0.924</sub>-S-VAC<sub>0.016</sub>)-b-5\_PVeoVa<sub>0.060</sub> (**B4**, **Table IV-7**).

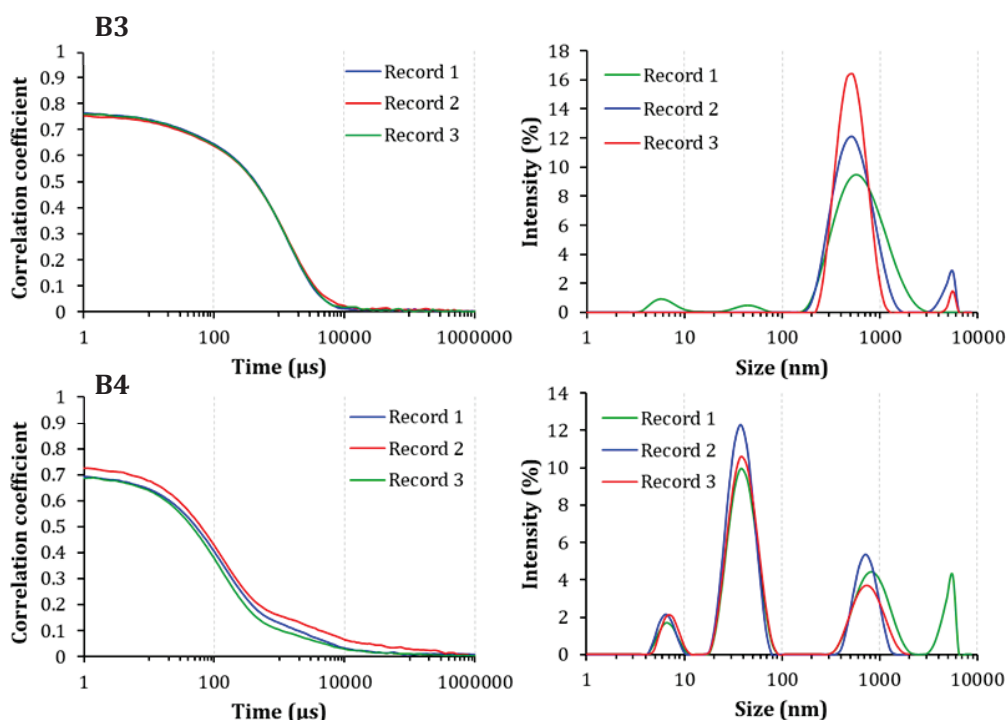


**Figure IV-12:** DLS-size distribution in intensity of B3 and B4 in DMSO and their related correlated coefficient curves.

In both cases, the correlogram fits are inaccurate (**Figure IV-12**), resulting in inconsistent determination of the object sizes over several runs. This indicates that the dispersions

contain either objects that are not spherical, different types of objects, or a combination of both. The suspected low solubility of the PVeOVA block in DMSO at room temperature, even after preheating at 100 °C as performed for <sup>1</sup>H NMR analyses, could be contributing to this result and could explain why the determination of F<sub>VeOVA</sub> in the copolymer by <sup>1</sup>H NMR was not accurate (**Table IV-7**).

VeOVA is known to be resistant to hydrolysis.<sup>[9]</sup> Therefore, it was postulated that the molar fraction of VeOVA remained the same after the 2 h step of alcoholysis. Calculations were thus based on the initial molar fraction of VeOVA units determined in the structure of the polymer before alcoholysis (by <sup>1</sup>H NMR in CDCl<sub>3</sub>); and adapted to determine the molar fractions of VAc and VOH units in the resulting copolymer after alcoholysis. **Table IV-7** summarizes the characteristics of the alcoholized VeOVA-based block copolymers, and compares to the inaccurate values obtained by <sup>1</sup>H NMR.

**Table IV-7: Library of VeOVA-based block copolymers alcoholized for 2 h at 30 °C in methanol.**

Entry	Structure before alcoholysis *	Structure after alcoholysis **	VeOVA/VOH/VAc content calculated via <sup>1</sup> H NMR
<b>B1</b>	10_PVeOVA- <i>b</i> -90_PVAc	10_PVeOVA <sub>0.10</sub> - <i>b</i> -90_P(VOH <sub>0.86</sub> - <i>s</i> -VAc <sub>0.04</sub> )	0.076/0.906/0.018
<b>B2</b>	5_PVeOVA- <i>b</i> -95_PVAc	5_PVeOVA <sub>0.05</sub> - <i>b</i> -95_P(VOH <sub>0.90</sub> - <i>s</i> -VAc <sub>0.05</sub> )	0.015/0.968/0.017
<b>B3</b>	100_PVAc- <i>b</i> -5_PVeOVA	100_P(VOH <sub>0.935</sub> - <i>s</i> -VAc <sub>0.015</sub> )- <i>b</i> -5_PVeOVA <sub>0.050</sub>	0.015/0.980/0.015
<b>B4</b>	75_PVAc- <i>b</i> -5_PVeOVA	75_P(VOH <sub>0.934</sub> - <i>s</i> -VAc <sub>0.016</sub> )- <i>b</i> -5_PVeOVA <sub>0.050</sub>	0.019/0.966/0.015

\* Note that the DP of the second block is the targeted DP.

\*\* The composition of the block copolymers was determined by <sup>1</sup>H NMR, considering that the VeOVA units were not alcoholized

### III.2 Alcoholysis of the VL-based block copolymers

The solubilization of the different VL-based block copolymers in methanol was not as immediate in comparison to the statistical structures. The solutions were stirred for half an hour at 32 °C before the addition of the basic methanolic solution. The block copolymers 5\_PVL-*b*-95\_PVAc and 10\_PVL-*b*-90\_PVAc provided clear dispersions, while 20\_PVL-*b*-80\_PVAc led to a turbid dispersion. The three block copolymers were alcoholized for 2 h, following the protocol described in the **Experimental Section IV.2**, and the kinetics of the alcoholysis was followed by <sup>1</sup>H NMR in DMSO-*d*<sub>6</sub> (**Figure IV-13**).

After neutralization by acetic acid, three washes with methanol and filtration, the alcoholized block copolymers were recovered as white powders, and also analyzed by <sup>1</sup>H NMR in DMSO-*d*<sub>6</sub>.

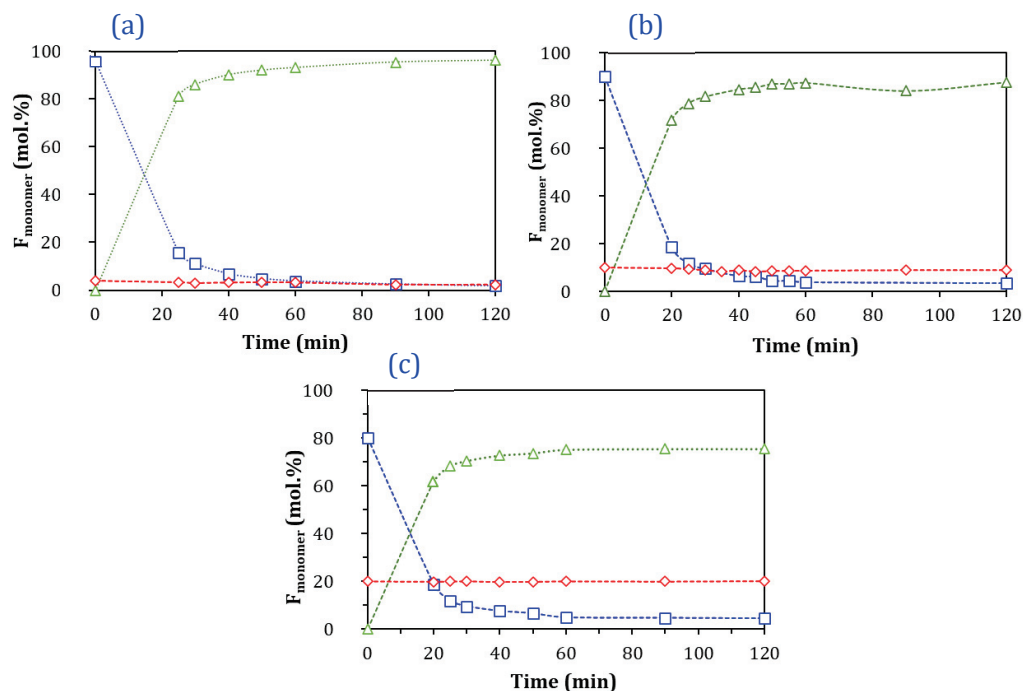


**Figure IV-13:** Kinetics of the alcoholysis of (a) 20\_PVL-*b*-80\_PVAc; (b) 10\_PVL-*b*-90\_PVAc and (c) 5\_PVL-*b*-95\_PVAc and the corresponding molar fractions of VOH ( $\text{--}\triangle\text{--}$ ), VAc ( $\text{--}\square\text{--}$ ) and VL ( $\text{--}\diamond\text{--}$ ) units with alcoholysis time. [VAc + VL]:[NaOH] ratio 1:0.025.

The VL content for 20\_PVL-*b*-80\_PVAc remained at 20% over the course of the alcoholysis, (**Figure IV-13 (a)**). In comparison, for 10\_PVL-*b*-90\_PVAc the amount of VL units slightly decreased, from 10% to 8.8% after 2 h (**Figure IV-13 (b)**). For a similar proportion of VL units in the analogous 100\_P(VAc<sub>0.90-s</sub>-VL<sub>0.10</sub>) statistical copolymer, the amount of VL decreased to 1.5% after 2 h of alcoholysis. Finally, the VL content decreased from 5% to 2.5% after 2 h of alcoholysis of 5\_PVL-*b*-100\_PVAc. This study shows that the VL units were less affected (if affected at all) by the alcoholysis when the structure of the copolymer was blocky, compared to the statistical structure (**Chapter III, Section III.1**). These results suggest that the longer the PVL block (*i.e.*, here, DP = 20), the harder it is to alcoholize the VL units. This might be due to the lower solubility of the PVL block in comparison to the PVAc block in methanol. Therefore, it is likely that the block copolymer self-assembles in methanol with a VL-rich core and VAc-rich shell (**Figure IV-14**). As a result, the VAc units are more available to be alcoholized. To confirm this hypothesis, the three copolymers were dispersed in MeOH and analyzed by DLS (**Figure IV-15**).

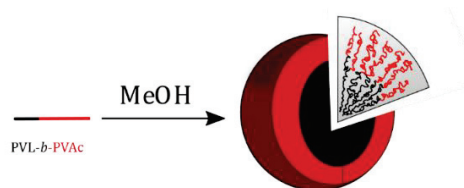


Figure IV-14: Scheme of the hypothesized organization of PVL-*b*-PVAc in methanol.

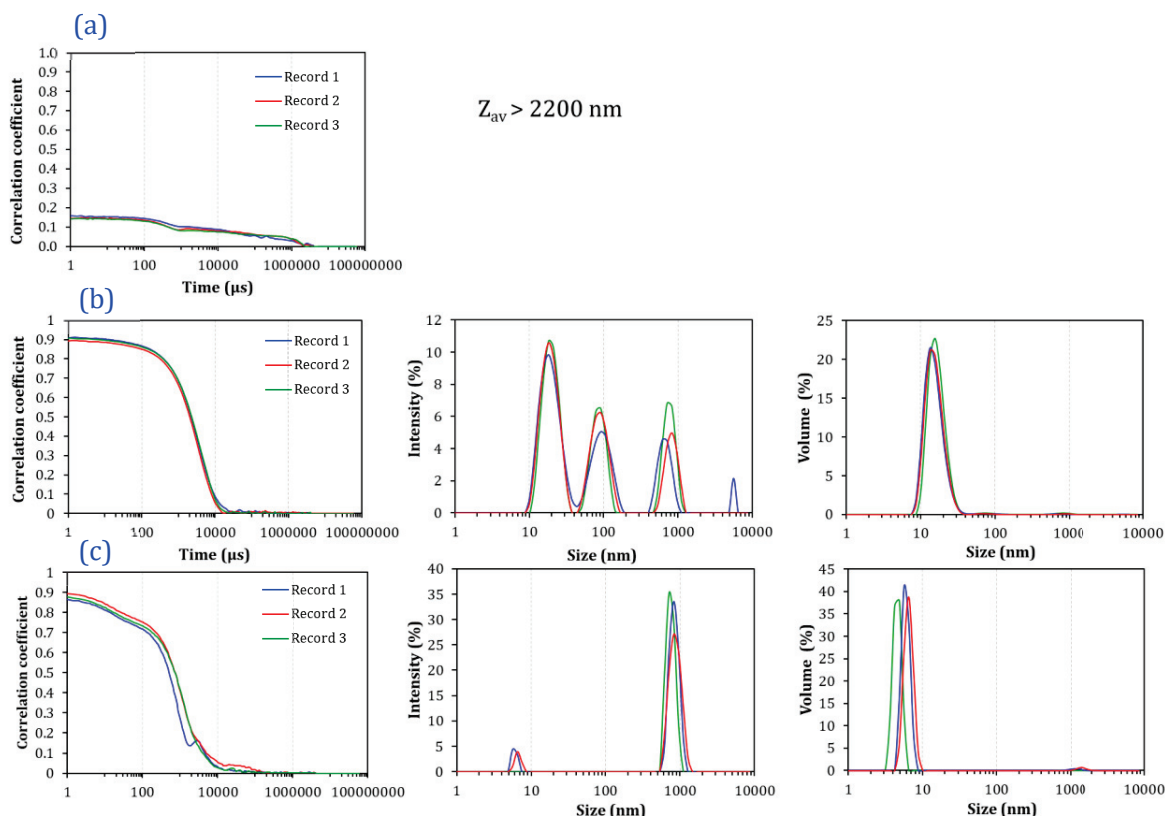


Figure IV-15: DLS-size distributions in intensity and volume for (a) 20\_PVL-*b*-80\_PVAc; (b) 10\_PVL-*b*-90\_PVAc and (c) 5\_PVL-*b*-95\_PVAc in methanol and their related correlation coefficient curves.

Apart from 20\_PVL-*b*-80\_PVAc which seemed to sediment in the DLS tank (the value of the intercept was well below 0.85), the two other samples tested provided clear solutions. The correlograms (b) **Figure IV-15** were perfectly reproducible over several runs, while some deviations were visible in (c). Nevertheless, the correlogram fits were accurate (in the range 0.85 – 1) in both cases, which attests of the presence of an arrangement of the polymer chains (either in the range unimers (10 – 30 nm), pseudo-micelles (30 – 100 nm) and aggregates (100 – 1000 nm)). The distribution in volume showed that the main population in both cases was the small one in the range 8 – 20 nm (unimers). Large aggregates were nevertheless still visible in the range 1000 nm.

This result is consistent with the fact that the VL units from the first block were not alcoholized at all in the case of 20\_PVL-*b*-80\_PVAc (because the copolymer is not dispersible in MeOH). However, a few VL units were hydrolyzed in the other two block copolymers which formed aggregates in methanol.

This result must be taken with care because the presence of several objects in the dispersion might disrupt the measurement and lead to a wrong interpretation of the DLS data. Furthermore, it does not demonstrate that the self-assembly of unimers or aggregates avoids sodium hydroxide to penetrate inside the core of these objects. In addition, it was previously highlighted that in the case of the statistical structures, the kinetics of alcoholysis was faster for the VAc units than for the VL units when they were randomly distributed along the polymer backbone. Therefore, due to the block organization, and because of the “zipper” mechanism already presented in **Chapter II**, it is likely that the VAc units are first affected by the alcoholysis (since more readily available), and that it keeps hydrolyzing immediate VAc neighbors before the VL units. In the block structure, the VL units are also more hindered by the long alkyl chains from their neighbors and are therefore probably less available for hydrolysis.

**Table IV-8** summarizes the mains characteristics of the alcoholized block copolymers.

**Table IV-8: Library of PVL-*b*-P(VOH-*s*-VAc) obtained after alcoholysis of the VL-based block copolymers (from 20 min to 2 h depending on the targeted composition) at 30 °C in methanol.**

Entry	Structure before alcoholysis	Alcoholysis time (min)	Structure after alcoholysis
<b>B5</b>	20_PVL- <i>b</i> -80_PVAc	120	20_PVL <sub>0.20</sub> - <i>b</i> -80_P(VOH <sub>0.75</sub> - <i>s</i> -VAc <sub>0.05</sub> )
<b>B6</b>	10_PVL- <i>b</i> -90_PVAc	120	9_PVL <sub>0.09</sub> - <i>b</i> -90_P(VOH <sub>0.87</sub> - <i>s</i> -VAc <sub>0.04</sub> )
<b>B7</b>		120	2.5_PVL <sub>0.025</sub> - <i>b</i> -95_P(VOH <sub>0.955</sub> - <i>s</i> -VAc <sub>0.020</sub> )
<b>B8</b>	5_PVL- <i>b</i> -95_PVAc	30	2.5_PVL <sub>0.025</sub> - <i>b</i> -95_P(VOH <sub>0.900</sub> - <i>s</i> -VAc <sub>0.075</sub> )
<b>B9</b>		20	2.5_PVL <sub>0.027</sub> - <i>b</i> -95_P(VOH <sub>0.830</sub> - <i>s</i> -VAc <sub>0.014</sub> )

The alcoholysis of 5\_PVL-*b*-95\_PVAc was performed several times on different experiments using the same starting batch of block copolymer, and the hydrolysis was stopped at different times to target different compositions of VAc in the resulting copolymer. The reason for this was to determine if the VAc content could later on have an impact on the water dispersibility of this structure (**Table IV-8**, entries **B7** to **B9**).



## IV. (Self-) Organization of the block copolymers in water

### IV.1 Dispersibility of the block copolymers in water

Similar to the statistical structures, the dispersibility of 2.5 wt.% dispersions of the different block copolymers was tested at different temperatures (**Table IV-9**).

**Table IV-9: Summary of the dispersibility of PVeOVA-*b*-P(VOH-*s*-VAc), P(VOH-*s*-VAc)-*b*-PVeOVA and PVL-*b*-P(VOH-*s*-VAc) with different degrees of hydrolysis and molar fractions of CoM.\***

Stabilizer	Dispersibility at given temperature			
	R.T.	55 °C	70 °C	90 °C
<b>B1:</b> 10_PVeOVA <sub>0.10</sub> - <i>b</i> -90_P(VOH <sub>0.86</sub> - <i>s</i> -VAc <sub>0.04</sub> )	⊗	⊗	⊗	⊗
<b>B2:</b> 5_PVeOVA <sub>0.05</sub> - <i>b</i> -95_P(VOH <sub>0.90</sub> - <i>s</i> -VAc <sub>0.05</sub> )	⊗	⊗	⊙	-
<b>B3:</b> 100_P(VOH <sub>0.935</sub> - <i>s</i> -VAc <sub>0.015</sub> )- <i>b</i> -5_PVeOVA <sub>0.050</sub>	⊗	⊗	⊙ (15 min)	-
<b>B4:</b> 75_P(VOH <sub>0.934</sub> - <i>s</i> -VAc <sub>0.016</sub> )- <i>b</i> -5_PVeOVA <sub>0.050</sub>	⊗	⊖	⊙	-
<b>B5:</b> 20_PVL <sub>0.20</sub> - <i>b</i> -80_P(VOH <sub>0.75</sub> - <i>s</i> -VAc <sub>0.05</sub> )	⊗	⊗	⊗	⊗
<b>B6:</b> 9_PVL <sub>0.09</sub> - <i>b</i> -90_P(VOH <sub>0.87</sub> - <i>s</i> -VAc <sub>0.04</sub> )	⊗	⊗	⊗	⊗
<b>B7:</b> 2.5_PVL <sub>0.025</sub> - <i>b</i> -95_P(VOH <sub>0.955</sub> - <i>s</i> -VAc <sub>0.020</sub> )	⊗	⊗	⊗	⊗
<b>B8:</b> 2.5_PVL <sub>0.025</sub> - <i>b</i> -95_P(VOH <sub>0.900</sub> - <i>s</i> -VAc <sub>0.075</sub> )	⊗	⊗	⊗	⊗
<b>B90:</b> 2.5_PVL <sub>0.027</sub> - <i>b</i> -95_P(VOH <sub>0.830</sub> - <i>s</i> -VAc <sub>0.014</sub> )	⊗	⊗	⊗	⊗

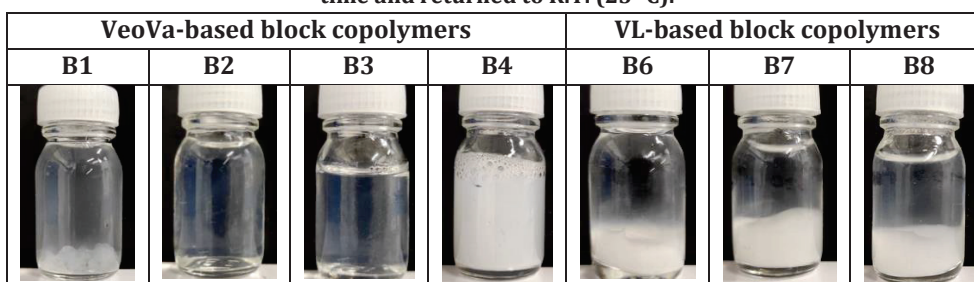
\*A red cross indicates that the polymer is insoluble in water. An orange line indicates that it is insoluble at R.T. and higher temperature, but dispersible or soluble at R.T., after having been heated at higher temperature. A green tick indicates that the copolymer is dispersible at the mentioned temperature, and remains dispersible when the solution is brought back at R.T.

In general, the majority of the block copolymers were insoluble in water. None of the PVL-based block copolymers were soluble nor dispersible in water, even at low VL content (**B7** to **B9**, with  $F_{VL} = 2.5$  mol.%) (**Table IV-10**). The PVeOVA-based block copolymers proved to be slightly more dispersible, **B1** being the only insoluble copolymer (**Table IV-10**). Surprisingly, **B2** (which contained an average of 5 VeoVa units) provided a transparent solution at 70 °C and remained dispersible in water after being cooled to R.T.

This observation explains why 5 VeoVa units were targeted for the second series of experiments, when it came to the synthesis of the reverse block order copolymer PVAc-*b*-PVeOVA.



**Table IV-10: Pictures of the dispersible VeoVa and VL-based block copolymers that were heated for the stated time and returned to R.T. (23 °C).**



The lack of solubility of the VL-based block copolymers could have been predicted from the results obtained for the VL-based statistical structures. It has already been mentioned that the reactivity ratios of VAc and VL were different (1.4 and 0.7 respectively), and that it might lead to some gradient block copolymer structures. The copolymers resulting from this “statistical” polymerization were poorly dispersible in water after alcoholysis, while the “true” statistical VeoVa-based structures were slightly more dispersible in water. Therefore, it is not surprising that when all the VL units are located in the same block, the solubility of the resulting copolymer after alcoholysis was not improved compared to the “statistical” structures. VL-based statistical structure with  $F_{VL} = 1.5$  mol.% (**S2** from **Chapter III**) provided acceptable dispersibility in water to allow for its use in the emulsion polymerization step. To investigate the solubility of the VL-based block copolymer further, it would have been interesting to target 1.5 mol.% of VL units in the resulting structure after alcoholysis. Nevertheless, many other systems were being tested at the same time, and some other provided interesting results (see **Chapter V**). This is why no further syntheses and alcoholyses were carried out with the VL-based block copolymers at this stage.

## IV.2 Organization of the block copolymers in water: DLS study

Aqueous dispersions containing 2.5 wt.% (corresponding to the amount of stabilizer introduced in the emulsion polymerization systems, based on the total volume of the reaction) of VeoVa-based block copolymers 5\_PVeoVa<sub>0.05</sub>-*b*-95\_P(VOH<sub>0.90</sub>-*s*-VAc<sub>0.05</sub>) (**B2**), 100\_P(VOH<sub>0.935</sub>-*s*-VAc<sub>0.015</sub>)-*b*-5\_PVeoVa<sub>0.050</sub> (**B3**) and 75\_P(VOH<sub>0.934</sub>-*s*-VAc<sub>0.016</sub>)-*b*-5\_PVeoVa<sub>0.050</sub> (**B4**) were prepared and analyzed by DLS (**Figure IV-16**).

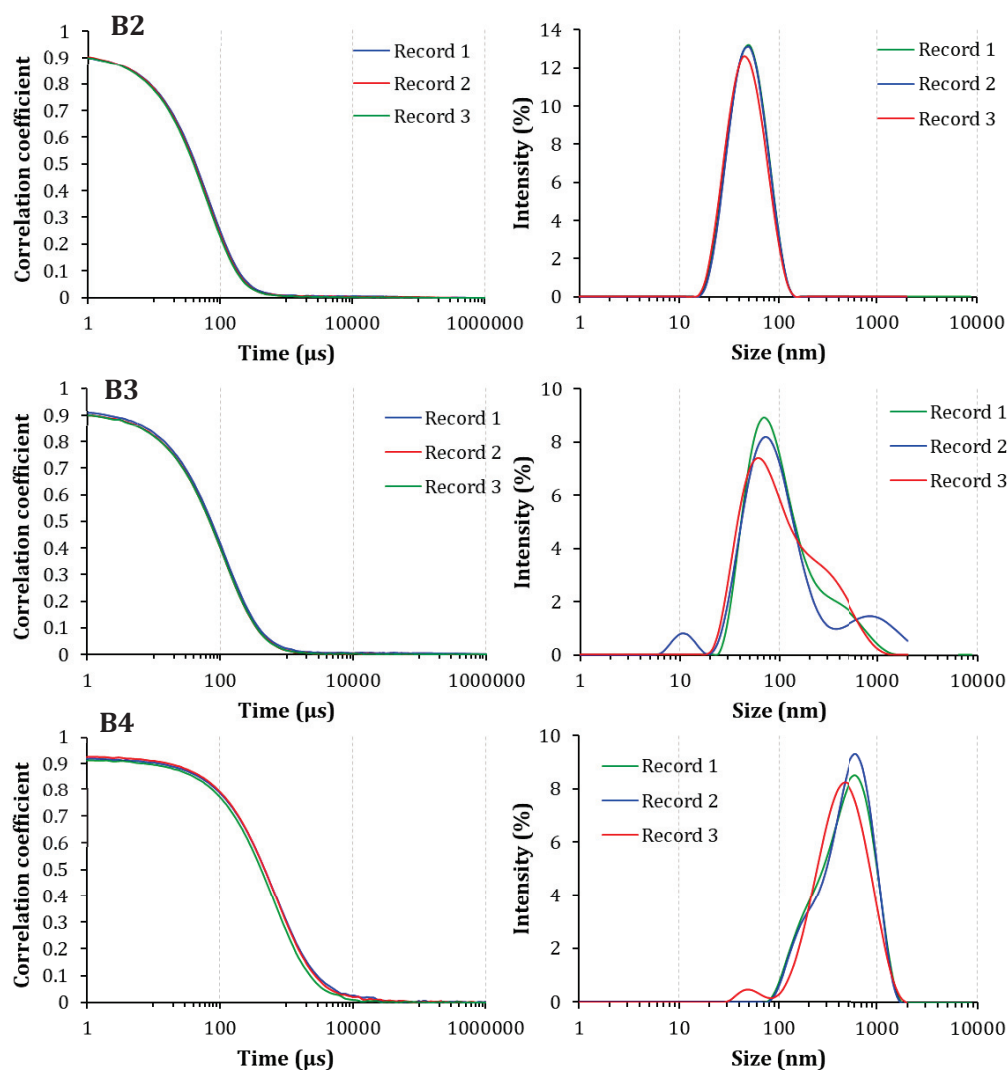


**Figure IV-16:** DLS-size distributions in intensity for the 2.5 wt.% aqueous solution of 5\_PVeoVa<sub>0.05</sub>-b-95\_P(VOH<sub>0.90</sub>-s-VA<sub>C0.05</sub>) (**B2**); 100\_P(VOH<sub>0.935</sub>-s-VA<sub>C0.015</sub>)-b-5\_PVeoVa<sub>0.050</sub> (**B3**) and 75\_P(VOH<sub>0.934</sub>-s-VA<sub>C0.016</sub>)-b-5\_PVeoVa<sub>0.050</sub> (**B4**).

All the correlograms in **Figure IV-16** were reproducible over several runs, which confirms the presence of nano-objects in the corresponding dispersions. The correlation function and the DLS trace in intensity for the dispersion that contained **B2** were reproducible over several runs, which indicates that these nano-objects were mostly spherical. The  $Z_{av}$  was determined to be 52 nm with good accuracy (**Table IV-11**), which belongs to the range of pseudo-micelles as defined in **Chapter II**. The correlogram fits of **B3** and **B4** are also accurate and reproducible over several runs, but the intensity was different, resulting in the inconsistent determination of the size of the objects over several runs (**Figure IV-16**). This result could be consistent with the broad molar mass distribution of the stabilizers **B3** and **B4**, resulting from the limited control over the extension of the PVAc macroCTAs. It is likely

that there are several chains of various molar masses in the solution, forming aggregates of different sizes.

**Table IV-11: DLS characteristics of the dispersions of VeoVa-based block copolymers obtained after alcoholysis and thermal treatment, and comparison with Mowiol 4-88 and the references 75\_P(VOH<sub>0.88</sub>-s-VAc<sub>0.12</sub>) and 100\_P(VOH<sub>0.88</sub>-s-VAc<sub>0.12</sub>). The measurements were performed in water at 25 °C.**

Entry	Z <sub>av</sub> (nm) <sup>a</sup> (Volume fraction (%))	PdI <sup>a</sup>
<b>Mowiol 4-88</b>	<b>15</b> / 172 (100/0)	0.2
<b>75_P(VOH<sub>0.88</sub>-s-VAc<sub>0.12</sub>)</b>	<b>9</b> / 45 / 300 (100/0/0)	0.3
<b>100_P(VOH<sub>0.88</sub>-s-VAc<sub>0.12</sub>)</b>	<b>10</b> / 800 (100/0)	0.7
<b>B2: 5_PVeoVa<sub>0.05</sub>-b-95_P(VOH<sub>0.90</sub>-s-VAc<sub>0.05</sub>)</b>	52	0.2
<b>B3: 100_P(VOH<sub>0.935</sub>-s-VAc<sub>0.015</sub>)-b-5_PVeoVa<sub>0.050</sub></b>	<b>130</b> /4000 (98.7/1.3)	0.4
<b>B4: 75_P(VOH<sub>0.934</sub>-s-VAc<sub>0.016</sub>)-b-5_PVeoVa<sub>0.050</sub></b>	<b>530</b> /5000 (88/12)	0.6

<sup>a</sup> Obtained by DLS

**Bold** value: main population observed in volume

### IV.3 Surface tension

The surface tension of the VL-based block copolymer could not be evaluated as the copolymers were not fully dispersible in water (**Table IV-10**). Therefore, the following results only concern the surface tension of the VeoVa-based block copolymer dispersions, and more specifically, **B2**, **B3** and **B4**.

**Table IV-12: Surface tension of the VeoVa-based block copolymers B2, B3 and B4 dispersed in water after thermal treatment. The dispersions contained 2.5 wt.% of copolymer. Measurements were performed at 25 °C.**

Entry	Surface tension (mN m <sup>-1</sup> )
Mowiol 4-88	46
75_(PVOH <sub>0.88</sub> -s-VAc <sub>0.12</sub> )	44
100_(PVOH <sub>0.88</sub> -s-VAc <sub>0.12</sub> )	46
<b>B2:</b> 5_PVeoVa <sub>0.05</sub> -b-95_P(VOH <sub>0.90</sub> -s-VAc <sub>0.05</sub> )	37
<b>B3:</b> 100_P(VOH <sub>0.935</sub> -s-VAc <sub>0.015</sub> )-b-5_PVeoVa <sub>0.050</sub>	56
<b>B4:</b> 75_P(VOH <sub>0.934</sub> -s-VAc <sub>0.016</sub> )-b-5_PVeoVa <sub>0.050</sub>	34

**Table IV-12** shows that **B2** and **B4** provided lower surface tensions (37 and 34 mN m<sup>-1</sup>, respectively) compared to Mowiol 4-88 and the RAFT-synthesized P(VOH<sub>0.88</sub>-s-VAc<sub>0.12</sub>) (approximately 45 mN m<sup>-1</sup>), thus suggesting a better micellization efficiency.

#### IV.4 Conclusion

This section highlighted that the dispersibility and conformation in water of the VL and VeoVa-based block copolymers was drastically affected by the structure of the copolymer. Similar to what has previously been highlighted in **Chapter III**, a slight variation in the structure (not only the addition of a more hydrophobic CoM but also its position in the chain) significantly affected the aqueous phase conformation of the copolymer. The order of the more hydrophobic and more hydrophilic blocks also seemed to affect the phase conformation of the copolymer, probably also because the quality of the synthesis is affected. In the following section, the block copolymers which were sufficiently dispersible in water (namely **B2**, **B3** and **B4**) are tested as stabilizer candidates for the emulsion copolymerization of VAc and VeoVa.

## V. Emulsion copolymerization of VAc and VeoVa with the selected block copolymer candidates

In **Chapters III**, it was systematically observed that the dispersions of copolymers which had high surface tension and low dispersibility in water did not provide stable latexes. In light of these results, it was decided to skip the screening with KPS for the block copolymer structures as performed in the previous chapter, and to directly test the dispersible ones in emulsion copolymerization of VAc and VeoVa initiated by the redox couple.

The protocol was set up in **Chapter II** and is detailed in **Experimental Section V.2**, except that the concentration of initiator was increased compared to the initial protocol (AsAc/TBHP = 0.14/0.08 against 0.092/0.054 wt.% based on monomers), because similarly to the systems stabilized with the statistical structures, a plateau was reached at 50% conversion. 5\_PVeoVa<sub>0.05</sub>-b-95\_P(VOH<sub>0.90</sub>-s-VAc<sub>0.05</sub>) (**B2**), 100\_P(VOH<sub>0.935</sub>-s-VAc<sub>0.015</sub>)-b-5\_PVeoVa<sub>0.050</sub> (**B3**) and 75\_P(VOH<sub>0.934</sub>-s-VAc<sub>0.016</sub>)-b-5\_PVeoVa<sub>0.050</sub> (**B4**) gave stable dispersions in water and were thus evaluated as stabilizer candidates.

### V.1 Kinetics of the polymerizations and colloidal features of the latexes

Kinetics of the polymerizations were followed gravimetrically over a 2 h period.

Table IV-13: Estimation of  $S_{max}$  for the emulsion polymerizations stabilized with 10 wt.% B2; B3 and B4, obtained from the slopes of the conversion *versus* time plots.

Entry*	Stabilizer (10 wt.% based on monomers)	$S_{max}$ (s <sup>-1</sup> )	R <sup>2</sup>
ER-B2	B2: 5_PVeoVa <sub>0.05</sub> -b-95_P(VOH <sub>0.90</sub> -s-VAc <sub>0.05</sub> )	0.033	0.986
ER-B3	B3: 100_P(VOH <sub>0.935</sub> -s-VAc <sub>0.015</sub> )-b-5_PVeoVa <sub>0.050</sub>	0.038	0.970
ER-B4	B4: 75_P(VOH <sub>0.934</sub> -s-VAc <sub>0.016</sub> )-b-5_PVeoVa <sub>0.050</sub>	0.034	0.999

\* ER refers to redox-initiated emulsion polymerization and is followed by the name of the stabilizer used in the experiment.

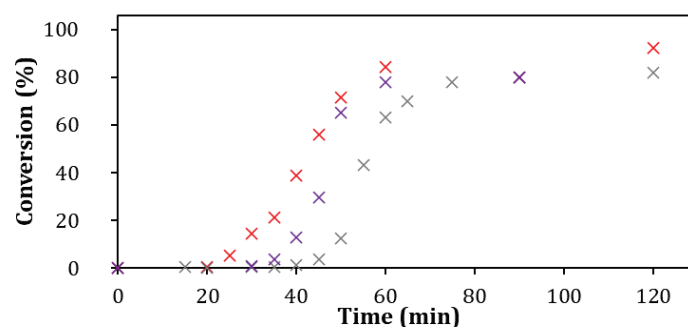


Figure IV-17: Kinetics of the emulsion copolymerizations of VAc and VeoVa with 10 wt.% of (X) B2; (X) B3 and (X) B4.

High conversions (from 80 to 91%) and stable latexes were obtained after 2 h with all the copolymers (**Figure IV-17**). In addition,  $S_{\max}$  values were similar (**Table IV-13**).

The main difference between these systems is the induction period, which varied from one system to another. This could be either due to the presence of residual methanol or acetic acid from the purification step of the stabilizer, which can act as transfer agents producing less reactive radicals, or, as hypothesized in **Chapter III Section V.2.2** to the presence of the VeoVa units in the stabilizer. It was indeed observed that VeoVa-based statistical copolymers induced a longer induction period when used in emulsion copolymerization of VAc and VeoVa compared to the other stabilizers, and that the conversion reached a plateau. It was thus hypothesized that the radicals from the growing chains could abstract a hydrogen from the bulky side group of the VeoVa units of the stabilizer, and that the resulting radical was less reactive.

It is difficult to explain the differences in the kinetics based on the structure of the copolymers because of the complexity of their architecture (resulting from the synthesis step). Nevertheless, another possible explanation for the delayed induction period could lie in the aqueous phase conformation of the block copolymers before emulsion (regardless of their initial structure). Indeed, it was highlighted in **Section IV** that **B2** formed rather defined objects in water ( $Z_{av} = 52$  nm), previously attributed to the pseudo-micelle conformation range. Adversely, **B3** and **B4** formed aggregates in range 100 – 1000 nm. It is possible that the pseudo-micelles present in **ER-B2** were used as nanoreactors, thus providing a better nucleation efficiency in **ER-B2** (with both adsorption and grafting of the stabilizer onto the particles) than in **ER-B3** and **ER-B4**, hence leading to a smaller induction period. Noteworthy, this result is consistent with that obtained in **Chapter III**, where the presence of dense aggregates of statistical copolymer dispersed in water before emulsion provided low nucleation efficiency. Nevertheless, the PDI obtained by DLS on the samples withdrawn from the polymerization medium for **ER-B2** were systematically higher than 0.1 (in range 0.4 – 0.5), thus suggesting broad particle size distribution and the occurrence of continuous nucleation, leading us to consider that the presence of pseudo micelles in water was not exclusively used as nanoreactors in this system.

Nevertheless, fluid latexes without coagulum and long-lasting stability (at least six months) were obtained with these three stabilizers.

The particle size of the latexes was measured by DLS and cryo-TEM (**Figure IV-18** and **Table IV-14**).

**Table IV-14: Main characteristics for the latexes obtained with 10 wt.% of B2: 5\_PVeoVa<sub>0.05</sub>-b-95\_P(VOH<sub>0.90</sub>-s-VAc<sub>0.05</sub>), B3: 100\_P(VOH<sub>0.935</sub>-s-VAc<sub>0.015</sub>)-b-5\_PVeoVa<sub>0.050</sub> and B4: 75\_P(VOH<sub>0.934</sub>-s-VAc<sub>0.016</sub>)-b-5\_PVeoVa<sub>0.050</sub>**

Entry *	Z <sub>av</sub> (nm) <sup>a</sup>	Pdl <sup>a</sup>	D <sub>n</sub> (nm) <sup>b</sup>	D <sub>v</sub> (nm) <sup>b</sup>	D <sub>w</sub> /D <sub>n</sub> <sup>b</sup>	N <sub>p</sub> (10 <sup>15</sup> cm <sup>-3</sup> ) <sup>c</sup>	%Ads&grafted <sup>d</sup>
ER-B2	370	0.5	170	195	1.4	3.0	80
ER-B3	230	0.2	82	200	2.7	9.5	35
ER-B4	280	0.3	100	135	1.3	13.6	64

<sup>a</sup> Obtained by DLS

<sup>b</sup> Obtained from cryo-TEM

<sup>c</sup> Calculated *via* Equation 49

<sup>d</sup> Calculated *via* Equation 58

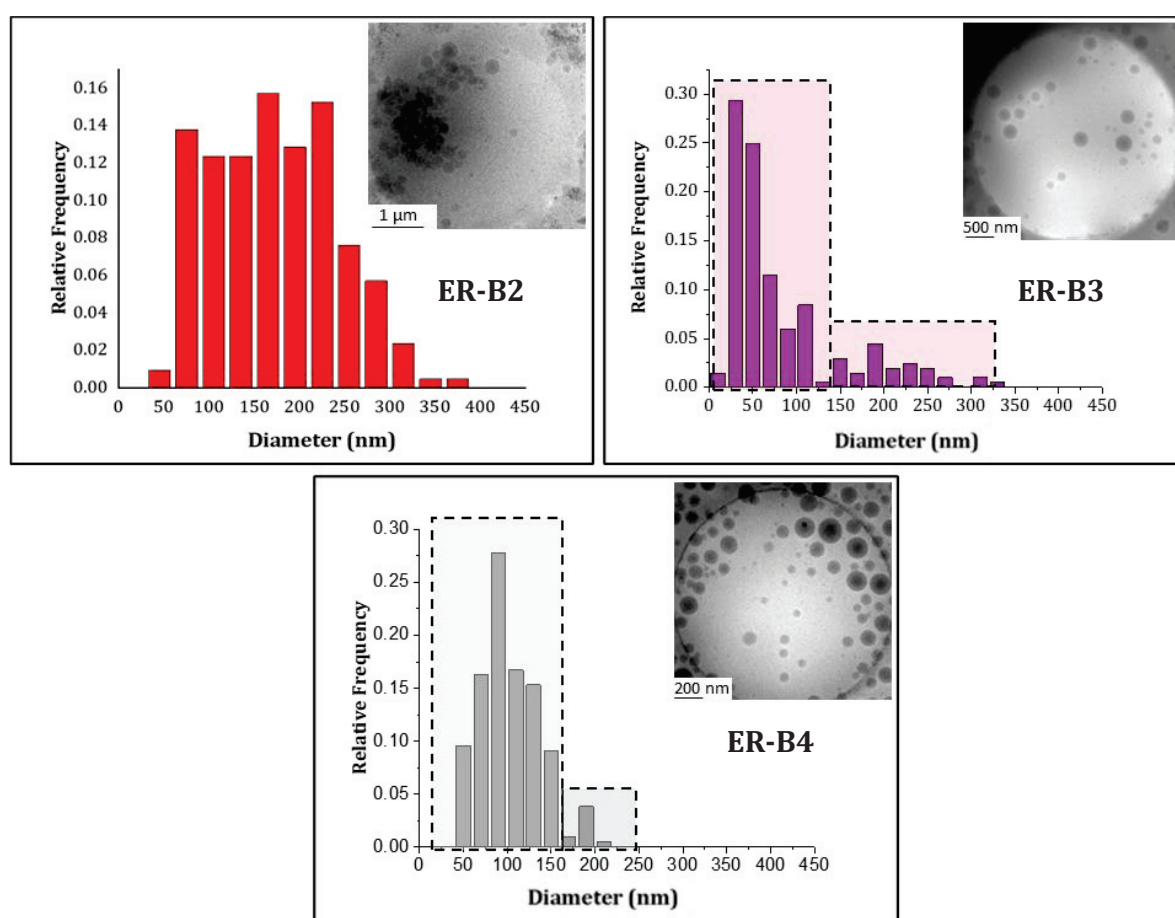


**Figure IV-18: Particle size distribution obtained by cryo-TEM out of 200 particles and cryo-TEM pictures of the latexes stabilized with 10 wt.% of B2 (red); B3 (purple) and B4 (grey).**

**Table IV-14** together with **Figure IV-18** show that once again, the latexes obtained with the RAFT-synthesized structures are polydisperse. One interesting trend was that the position of the PVeoVa block seemed to significantly influence the particle size distribution, and this



might be correlated to the quality of the synthesis which led to a mixture of different species depending on the block sequencing (this aspect will be further discussed later in the reproducibility test). Focusing on the cryo-TEM results, it can be seen that the latex obtained with the P(VOH-*s*-VAc)-*b*-PVeOVA structures (namely **B3** (100\_P(VOH<sub>0.935</sub>-*s*-VAc<sub>0.015</sub>)-*b*-5\_PVeOVA<sub>0.050</sub>) and **B4** (75\_P(VOH<sub>0.934</sub>-*s*-VAc<sub>0.016</sub>)-*b*-5\_PVeOVA<sub>0.050</sub>, **Figure IV-18**) presented smaller particles than the ones obtained with the PVeOVA-*b*-P(VOH-*s*-VAc) structure (**B2**, **Figure IV-18**), suggesting a better involvement of the stabilizers in the nucleation process. Additionally, it also seems that in the case of the latexes stabilized with **B3** and **B4**, two distinct populations were visible on the cryo-TEM histograms (as highlighted by the boxes on the histograms, **Figure IV-18**). One possible explanation could be that these two populations result from the presence of (at least) two kinds of stabilizers that have different stabilization modes. VeoVa is known to be resistant to the alcoholysis, and to be able to protect close neighbors from it. Therefore, as hypothesized in the introduction of this chapter, in the block copolymers where PVeOVA was built in second position, it is possible that the xanthate extremity was not (or less) impacted by the alcoholysis and was still present at the end of the chain that have been successfully chain extended with VeoVa, and the resulting P(VOH-*s*-VAc)-*b*-PVeOVA could act as a reactive stabilizer. Nevertheless, not all the chains participated to the extension, due to the fact that the chain-end functionality of 75\_PVAc and 100\_PVAc were not 100% as demonstrated in **Chapter II, Section II**. In that case, at least two populations of stabilizers are present in the resulting crude: the reactive one (P(VOH-*s*-VAc)-*b*-PVeOVA-X, which was chain extended before alcoholysis)) and the non-reactive one (P(VOH-*s*-VAc), which were not chain extended before alcoholysis, and other species resulting from the extension: dead chains and a fraction of homopolymer from the second bloc). These populations possibly lead to a different stabilization mechanism during the emulsion polymerization. Some elements could confirm this hypothesis, but it has never been proved in the frame of this research work (See **Appendix 6**).

Fresh batches of 5\_PVeOVA-*b*-95\_PVAc (**B2.2**) and 75\_PVAc-*b*-5\_PVeOVA (**B4.2**) were synthesized and alcoholized to test the overall robustness of the strategy. The characterizations of these new batches are provided in **Appendix 8**. Following the same protocol as for **B2**, the synthesis of **B2.2** showed limited robustness. The calculation of  $M_n$  via <sup>1</sup>H NMR provided higher values after purification (16 000 g mol<sup>-1</sup> for **B2.2** versus 9820 g mol<sup>-1</sup> for **B2**), and the SEC traces did not perfectly overlap. However, similar fractions of VOH, VAc and VeoVa were calculated via <sup>1</sup>H NMR after alcoholysis. The limited robustness of the synthesis of 75\_PVAc-*b*-5\_PVeOVA might impact the aqueous phase behavior and stabilization efficiency of the copolymer.

In contrast, <sup>1</sup>H NMR analysis provided comparable  $M_n$  for **B4** and **B4.2** (7170 and 8000 g mol<sup>-1</sup>, respectively), and the SEC traces overlapped accordingly. After alcoholysis, similar fractions of the different comonomer units (VOH, VeoVa and VAc) were calculated via <sup>1</sup>H NMR.



As suspected, **B2.2** was not fully dispersible in water, regardless of the temperature (from 55 °C to 90 °C for 2 h) and remained turbid even after the temperature was cooled at R.T. (**Figure IV-19 (a)**). The emulsion copolymerization of VAc and VeoVa was nevertheless carried out with **B2.2**. After an inhibition of ca. 15 min, conversion increased up to 55% after 30 min (**Figure IV-19 (b)**) before flocculation occurred. The failure in reproducing the emulsion polymerization conducted with **B2** with its analogue **B2.2** shows the poor robustness of the overall strategy in the particular case of P<sub>VeO</sub>Va-*b*-P(VOH-*s*-VAc) copolymer structure. This might indeed be related to the fact that targeting a very low DP with RAFT (and anyway with any RDRP techniques) is always tricky since the chains are always part of a distribution in which different DPs are produced. The <sup>1</sup>H NMR spectra before and after alcoholysis suggested that the structures were similar, but their solubility was different. This could be due to the difficulty to perfectly target 5 VeoVa units in the first block.<sup>[10]</sup>

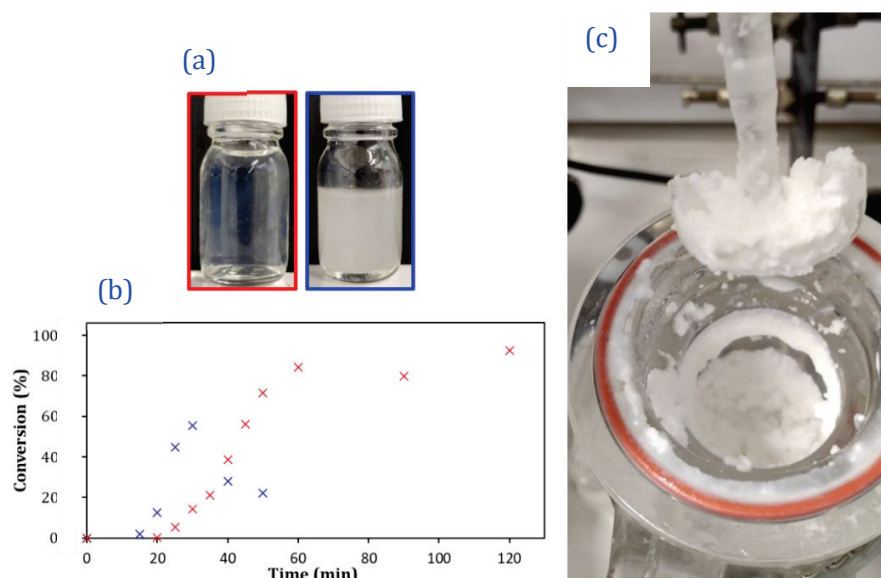


**Figure IV-19:** (a) Visual aspect of the 2.5 wt.% of **B2** (red) and **B2.2** (blue) dispersed in water after thermal treatment. (b) Kinetics of the emulsion copolymerization of VAc and VeoVa with 10 wt.% of (X) **B2** and (X) **B2.2**. The copolymerizations were performed in a 75 mL glass reactor at 55 °C for 2 h and (c) photograph of the reactor content after polymerization.

The same reproducibility experiment was carried out with 75\_PVAc-*b*-5\_PVeoVa copolymer structure **B4.2**, analogous to **B4**. The results concerning the kinetics, particle size and adsorption of the stabilizer on the particles of the two latexes are summarized in **Figure IV-20**.

Very similar results were obtained for both experiments in terms of kinetics, particle size and percentage of adsorbed and grafted stabilizer. These results show that surprisingly, minor

variation in the  $M_n$  and composition of the ill-defined stabilizer did not affect the stabilization efficiency when the copolymer was used in emulsion.

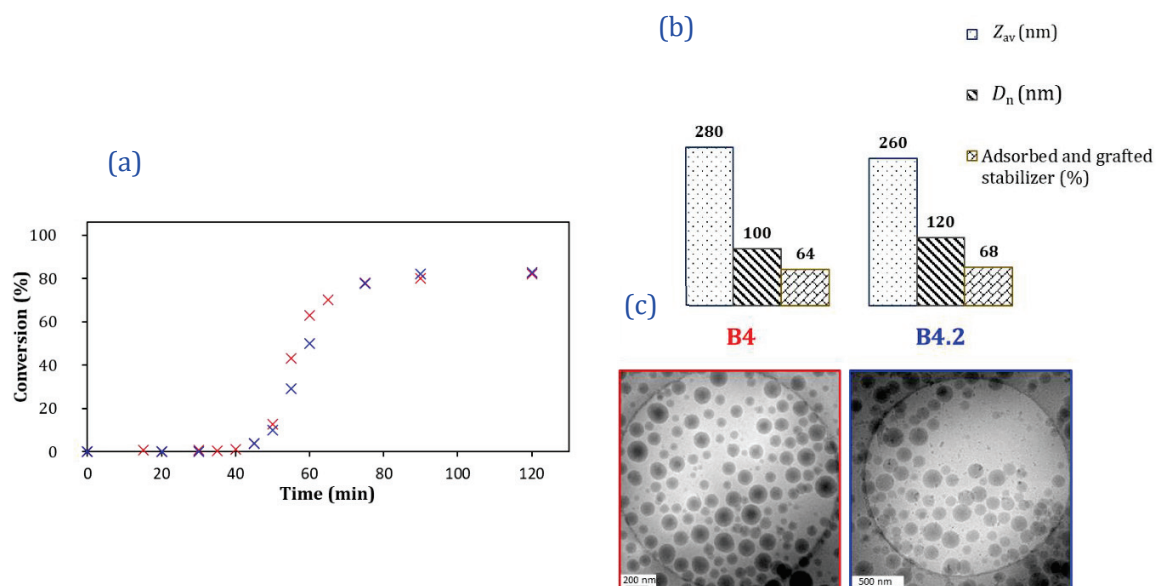


Figure IV-20: (a) Kinetics of the emulsion copolymerizations of VAc and VeoVa with 10 wt.% of (X) B4 and (X) B4.2; (b)  $Z_{av}$ ,  $D_n$  obtained by cryo-TEM and percentage of adsorbed and grafted stabilizer for the latexes stabilized with 10 wt.% of B4. (red) and B4.2 (blue) and (c) related cryo-TEM pictures corresponding to the respective latexes.

As a conclusion, on the top of the difficulty in precisely targeting low molar mass blocks with RDRP, one has to keep in mind that in the particular case of RAFT, when it comes to the synthesis of block copolymers, the quality of the final block is impacted by the efficiency of reinitiation of the starting chains and the amount of initiator used during the chain extension. Both parameters indeed impact the amount of homopolymers (of the first and the second block, respectively) that can pollute the final block copolymer structure. Slight variations in the behavior of the polymerizations might lead to differences in the dispersibility of the final product and their efficiency when used as stabilizers in emulsion. This study on the reproducibility of the overall strategy employing either P(VeOVA-*b*-P(VOH-*s*-VAc)) or P(VOH-*s*-VAc)-*b*-P(VeOVA) shows that differences are less for the latter. As a result, we decided to focus on the use of this class of block copolymers in the following.

## V.2 Adsorbed and grafted stabilizer

The amount of adsorbed and grafted stabilizer was determined after ultracentrifugation. The results are summarized in **Table IV-15**.

**Table IV-15** Fraction of adsorbed and grafted stabilizer obtained after ultracentrifugation of the latexes obtained with 10 wt.% of VeoVa-based block copolymers. Estimation of the specific surface area occupied by the stabilizers onto a P(VAc-s-VeoVa) polymer particle ( $A_s$ ).

Entry	Stabilizer	%Ads&grafted <sup>a</sup>	$S_{tot\ latex}$ ( $\times 10^6\text{ cm}^{-2}$ ) <sup>b</sup>	$M_n$ ( $\text{g mol}^{-1}$ ) <sup>c</sup>	$A_s$ ( $\text{\AA}^2$ ) <sup>d</sup>
ER-B3	B3: 100_P(VOH <sub>0.935</sub> -s-VAc <sub>0.015</sub> )-b-5_PVeoVa <sub>0.050</sub>	35	4.7	5460	900
ER-B4	B4: 75_P(VOH <sub>0.934</sub> -s-VAc <sub>0.016</sub> )-b-5_PVeoVa <sub>0.050</sub>	64	5.4	4570	420
ER-B4.2	B4.2: 75_P(VOH <sub>0.928</sub> -s-VAc <sub>0.020</sub> )-b-5_PVeoVa <sub>0.052</sub>	68	4.8	4780	355

<sup>a</sup> Obtained by Equation 58

<sup>b</sup> Obtained by Equation 50

<sup>c</sup> Obtained by Equation 52

<sup>d</sup> Obtained by Equation 61

Comparable fractions were obtained for the latex obtained with **B3** and the RAFT-synthesized 100\_P(VOH<sub>0.88</sub>-s-VAc<sub>0.12</sub>) from **Chapter II** (35% and 39 %, respectively, **Table IV-15**). This suggests that the efficiency of the extension of the 100\_PVAc was limited, due to the previously mentioned low chain-end functionality. This stabilizer contains a majority 100\_P(VOH-s-VAc) chains (resulting from of unextended PVAc before alcoholysis, and dead chains), and potentially a low amount of 100\_P(VOH-s-VAc)-b-5-PVeoVa chains (resulting from PVAc chains which were efficiently chain-extended with VeoVa before alcoholysis), which was not sufficient to improve the adsorption and grafting efficiency on the particles. In contrast, the latex obtained with **B4** provided higher fraction of adsorbed and grafted stabilizer compared to the one obtained with 75\_P(VOH<sub>0.88</sub>-s-VAc<sub>0.12</sub>) from **Chapter II** (approximately 64% against 44%, respectively). This result is consistent with cryo-TEM pictures which, as previously mentioned, highlighted rather small polymer particles and low polydispersity, thus suggesting a good involvement of the stabilizer onto the polymer particles. Similar adsorption and grafting efficiency were obtained with **B4.2**, thus confirming the robustness of the synthesis.

Noteworthy, **B4** also contains residual 75\_P(VOH-s-VAc) from the macroCTA 75\_PVAc that has not been chain extended with VeoVa before alcoholysis (and a fraction of PVeoVa formed during the extension). However, it seems that in this case, the extension provided sufficient 75\_P(VOH-s-VAc)-b-5\_PVeoVa chains to improve the affinity of the overall crude with the polymer particles, and increase the grafting and adsorption efficiency. In fact, it is likely that the presence of a mixture of chains with different molar masses and natures (either

homopolymers from the first and second block and the desired block copolymer structure) were beneficial for the stabilization and adsorption and grafting efficiency of the copolymer.

The estimated surface area occupied by one stabilizer was in the range of the values estimated for the RAFT-synthesized statistical copolymers from the previous chapters ( $A_s = 260 - 490 \text{ \AA}^2$  for the RAFT-synthesized P(VOH-*s*-VAc) with similar DPs = 75 and 100, and from 260 to 600  $\text{\AA}^2$  for the statistical structures, depending on the CoM content and nature of the CoM). This result might be surprising as we expected a different behavior for the block copolymers, but it can also be related to the aforementioned presence of several types of stabilizers in the overall crude, which could disturb a traditional arrangement of the block copolymers at the surface of the particles. Additionally, the determination of  $A_s$  in the case of block copolymers must be considered with care as the calculation requires the molar mass of the copolymer. In **Chapters II** and **III**, the statistical structures provided copolymers with low dispersities, which allowed to determine  $M_n$ , and thus  $A_s$  with acceptable accuracy. In the present case, the synthesis of block copolymers led to broad molar mass distribution, which entailed the estimation of  $A_s$  with a relative error (similar to that of Mowiol 4-88).  $A_s$  must be considered here as an indicative value only.

### V.3 Evaluation of the alkali resistance of the latexes at different pH

The alkali resistance of the latexes obtained with 100\_P(VOH<sub>0.935-s</sub>-VAc<sub>0.015</sub>)-*b*-5\_PVeoVa<sub>0.050</sub> (**B3**) and 75\_P(VOH<sub>0.934-s</sub>-VAc<sub>0.016</sub>)-*b*-5\_PVeoVa<sub>0.050</sub> (**B4**) was investigated at different pH: 4, 6, 8, 10 and 12, and compared to the latex obtained with Mowiol 4-88.

A trend similar to that obtained for the latex obtained with Mowiol 4-88 was obtained for the latexes obtained with the VeoVa-based block copolymers: at pH below 8 the latexes remained unhydrolyzed over time, but the latexes where the pH was set above 8 were progressively hydrolyzed with time. No protection against the hydrolysis was provided by the block copolymer stabilizers. The evolution of pH with time for these latexes is provided in **Appendix 9**.

## VI. Conclusion

In this Chapter, a series of block copolymers of PVL-*b*-PVAc, PVeOVA-*b*-PVAc and PVAc-*b*-PVeOVA were synthesized, alcoholized and used as stabilizers in emulsion polymerization.

The synthesis of block copolymers brought a new level of difficulty compared to the statistical structures, because the quality of the final blocks was impacted by the efficiency of reinitiation of the starting chains, and led to a mixture of homopolymers from the first and second block, and the desired structure of block copolymer.

None of the PVL-*b*-P(VOH-*s*-VAc) were dispersible in water. To efficiently disperse PVeOVA-*b*-P(VOH-*s*-VAc) block copolymer in water, the targeted DP of the PVeOVA block must be low. Indeed, the block copolymer was not soluble when the VeOVA content exceeded 5 mol.% (representing approximately  $DP_{\text{PVeOVA}} = 5$  in our conditions), The synthesis of PVeOVA-*b*-P(VOH-*s*-VAc) block copolymers with a low DP first block was tricky and was not robust, because it is elusive to target very low DPs with RAFT, since the chains are always part of a distribution of DPs.

Therefore, the strategy was to reverse the block sequencing, and different P(VOH-*s*-VAc)-*b*-PVeOVA block copolymers were synthesized. Once again, a mixture of different structures was present in the final product, but stable latexes were nevertheless obtained with enhance involvement of the stabilizer onto the particles, and higher grafting and adsorption efficiency compared to the RAFT-synthesized P(VOH-*s*-VAc) and Mowiol4-88 developed **in Chapter II**. Up to 68% was obtained for a block copolymer that contained 5 mol.% of VeOVA. The idea also behind setting the PVeOVA block in the second position was that the VeOVA units could perhaps protect the xanthate extremity against hydrolysis (thanks to the umbrella effect), thus potentially providing reactive stabilizers. Some elements could confirm this hypothesis, as illustrated in **Appendix 6**, and by the fact that two distinct populations of particles seemed visible in the resulting latexes (against a broad PSD in the case of PVeOVA-*b*-P(VOH-*s*-VAc) and other RAFT-synthesized stabilizers so far). Nevertheless, except from this empirical assumption, this hypothesis has never been proved in the frame of this research work. Finally, if the robustness of the synthesis and stabilizing efficiency proved to be limited for the PVeOVA-*b*-PVAc structures, it was successful for the PVAc-*b*-PveOVA.

## References

- [1] K. Nakashima, P. Bahadur, *Adv. Colloid Interface Sci.* **2006**, 123–126, 75–96.
- [2] C. Booth, G. E. Yu, V. M. Nace, "Block Copolymers of Ethylene Oxide and 1,2-Butylene Oxide, in Amphiphilic block copolymers", in *Amphiphilic Block copolymers Self-Assembly and Applications*, Elsevier, **2000**.
- [3] P. Ra, D. Armando, Z. Wever, F. Picchioni, A. A. Broekhuis, *Chem. Rev.* **2015**, 8504–8563.
- [4] B. M. Budhlall, K. Landfester, E. D. Sudol, V. L. Dimonie, A. Klein, M. S. El-Aasser, *Macromolecules* **2003**, 36, 9477–9484.
- [5] S. R. George, C. A. Sanders, G. A. Deeter, J. D. Campbell, B. Reck, M. F. Cunningham, *Macromolecules* **2022**.
- [6] Y. Gu, J. He, C. Li, C. Zhou, S. Song, Y. Yang, *Macromolecules* **2010**, 43, 4500–4510.
- [7] J. Bernard, A. Favier, L. Zhang, A. Nilasaroya, T. P. Davis, C. Barner-Kowollik, M. H. Stenzel, *Macromolecules* **2005**, 38, 5475–5484.
- [8] K. J. Saunders, *Organic Polymer Chemistry*, Springer, **1976**.
- [9] E. Ogur, "Polyvinyl Alcohol: Materials, Processing and Applications", Smithers Rapra Technology, United Kingdom, **2005**.
- [10] G. Gody, P. B. Zetterlund, S. Perrier, S. Harriison, *Nat. Commun.* **2016**, 7, 1–8.



---

# Chapter V

## Synthesis and evaluation as stabilizer of P(VOH-*s*-VAc)-*b*-P(VOH-*s*-CoM-*s*-VAc) "hybrid" block copolymers

---

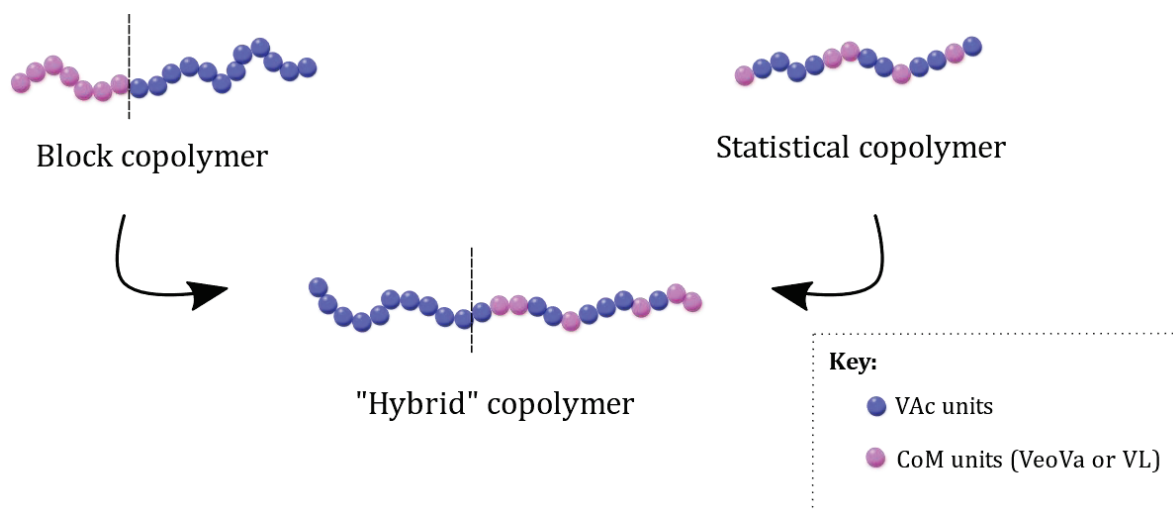




## Table of content

I. INTRODUCTION .....	252
II. SYNTHESIS AND CHARACTERIZATIONS OF THE “HYBRID” PVAc-B-P(VAc-s-CoM) STRUCTURES ..	253
II.1 Variation of the molar fraction of VeoVa in 75_PVAc-b-P(VAc-s-VeoVa) <sub>y/z</sub> .....	254
II.2 Variation of the DP of PVAc (DP1) in PVAc-b-P(VAc-s-VeoVa) <sub>y/z</sub> .....	257
II.3 Synthesis of PVAc-b-P(VAc-s-VL) <sub>y/z</sub> .....	261
II.4 Conclusion on the synthesis of the hybrid structures.....	262
III. ALCOHOLYSIS OF THE HYBRID COPOLYMERS.....	263
IV. (SELF-)ORGANIZATION OF THE HYBRID COPOLYMERS IN WATER .....	265
V. EMULSION COPOLYMERIZATION OF VAc AND VEOVA STABILIZED WITH THE SELECTED HYBRID COPOLYMERS .....	271
V.1 Emulsion copolymerization of VAc and VeoVa stabilized with the CoM-based hybrid stabilizers.....	271
V.1.1 Kinetics of the polymerizations and colloidal features of the latexes.....	271
V.1.2 Adsorbed and grafted stabilizer.....	279
VI. CONCLUSION .....	281

## I. Introduction

**Chapters II, III and IV** proved that it was possible to design new structures of polymeric stabilizers incorporating VOH and more hydrophobic units, for the emulsion copolymerization of VAc and VeoVa, with improved adsorption and grafting onto the particles. The integration of more hydrophobic CoM units such as VeoVa and VL into different architectures played a major role in this behavior and allowed for a better compatibilization of the stabilizer with the particles, leading to less free stabilizer in the aqueous phase. The dispersibility in water of these new structures was however an important issue and insolubility was faced for the statistical structures when the fraction of CoM inserted units exceeded 2 mol.%. Moving to block copolymer structures incorporating a PCoM block, up to 5 mol.% of VeoVa units could be added in the polymer chain, allowing for acceptable dispersibility of the stabilizer and yielded stable latexes.

In light of the previous results, as long as the final structure remains dispersible in water, it seems that the higher the CoM fraction, the better the adsorption and grafting onto the polymer particles and that block copolymer structures seemed to perform better. It was therefore thought that the use of copolymers obtained by alcoholysis of PVAc-*b*-P(VAc-*s*-CoM), also called hybrid with respect to the previous statistical and block structures, could lead to the introduction of enough CoM in the copolymer while still allowing the dispersibility in water. The present chapter aims at identifying such structures by optimizing the localization of the CoM units in the chains.

To the best of our knowledge, this particular structure, containing VOH units, has never been synthesized nor tested as stabilizer in emulsion polymerization.

To ease the designation of the copolymers, the following notations will be used through this Chapter: DP1\_PVAc-*b*-DP2\_P(VAc-*s*-CoM)<sub>y/z</sub> for the hybrid structures before alcoholysis, with y and z the global molar composition in CoM and VAc units, respectively. DP1 and DP2 refer to the DP of the first and second block of the hybrid copolymer.

First, the synthesis and characterization of a library of hybrid copolymers will be presented. These copolymers will then be alcoholized and their aqueous phase conformation will be investigated *via* DLS and surface tension measurements. Finally, the hybrid copolymers that are dispersible in water will be tested in emulsion polymerization. The resulting latexes will be analyzed to evaluate the influence of the structure and composition of the hybrid copolymers onto the stabilization efficiency.

## II. Synthesis and characterizations of the “hybrid” PVAc-*b*-P(VAc-*s*-CoM) structures

As highlighted in **Chapter IV**, the quality of the synthesis of block copolymers can drastically affect the dispersibility and stabilization efficiency of the overall structures. Block copolymers obtained after extensions of 75\_PVAc and 100\_PVAc had broad molar mass distributions, but it proved to be beneficial when the copolymer (after alcoholysis) was used in emulsion: latexes were obtained in a reproducible way, with enhanced fraction of adsorbed and grafted stabilizer compared to the ones obtained with well-defined statistical structures.

In **Chapter II**, when 75\_P(VOH-*s*-VAc) was used in emulsion, it provided lower PSD and better adsorption and grafting efficiency to the polymer particles compared to 100\_P(VOH-*s*-VAc) and 200\_P(VOH-*s*-VAc). In **Chapter IV**, 75\_P(VOH-*s*-VAc)-*b*-PVeOVA also provided the best results when compared to 100\_P(VOH-*s*-VAc)-*b*-PVeOVA.

Thus, in a first series of experiments, we made the choice to chain extend 75\_PVAc with VAc and VeoVa to target the PVAc-*b*-P(VAc-*s*-VeoVa) hybrid structure (**Figure V-1 (a)**). To evaluate the influence of the composition of the statistical block, different fractions of VeoVa ( $F_{VeoVa}$  varying from 2 to 10 mol.%) were targeted.

Additionally, it was also highlighted in **Chapter II** that the smaller the DP, the higher the chain-end functionality of PVAc. In case of chain extension, the reinitiation should be more efficient for PVAc with low DP, and provide narrower molar mass distributions compared to PVAc with high DP. To evaluate the influence of the DP of the PVAc block, a library of hybrid copolymers with different DP1 (from 20 to 100), and fixed  $F_{VeoVa} = 5$  mol.% was synthesized.

The synthesis scheme of hybrid copolymers and a summary of the experimental design is illustrated in **Figure V-1**.

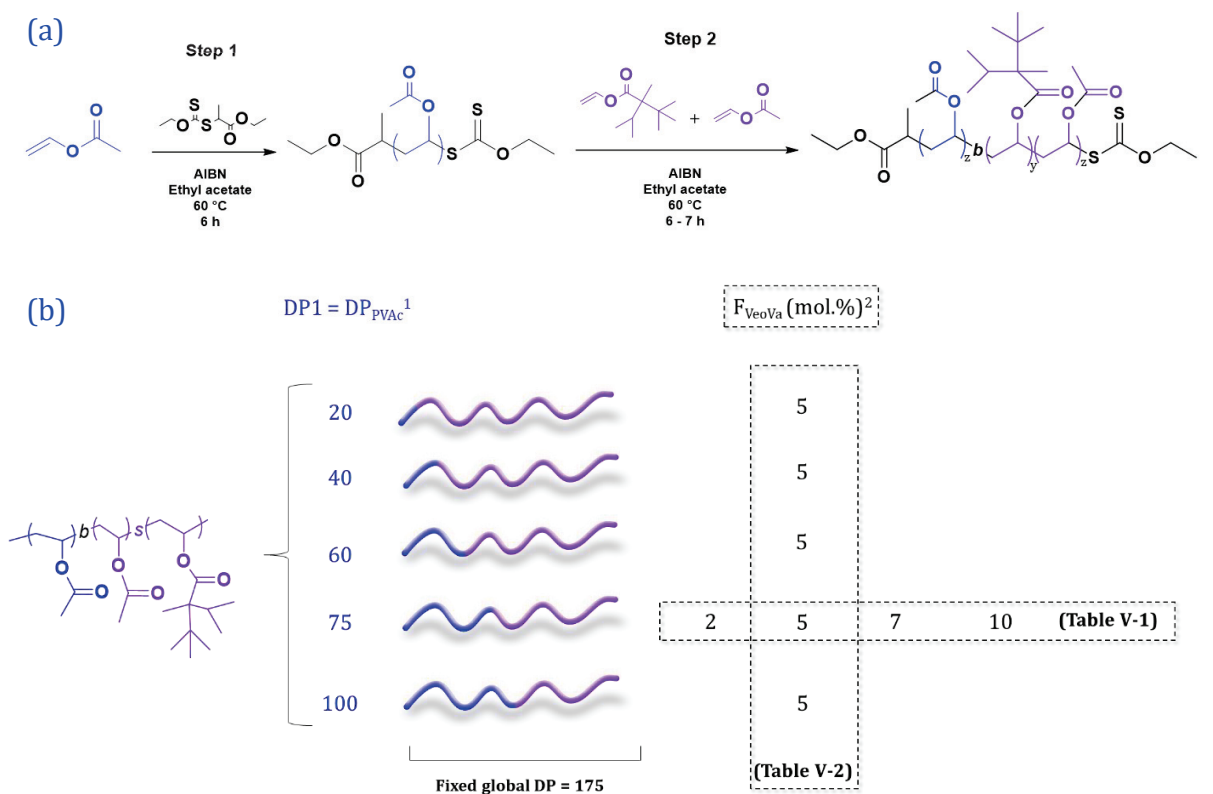


**Figure V-1: (a)** Synthesis of PVAc-*b*-P(VAc-*s*-VeoVa)-X in EtAc at 60 °C, and **(b)** general illustration of the experimental design for the hybrid copolymers syntheses. In all cases, the targeted overall DP was fixed at 175. The **blue** represents the first PVAc block. The **purple** represents the second statistical block. <sup>(1)</sup>: DP1 was determined by <sup>1</sup>H NMR in CDCl<sub>3</sub> after purification of the 1<sup>st</sup> block. <sup>(2)</sup>: Molar fraction VeoVa in the final structure, determined by <sup>1</sup>H NMR in CDCl<sub>3</sub> after purification of the copolymer.

## II.1 Variation of the molar fraction of VeoVa in 75\_PVAc-*b*-P(VAc-*s*-VeoVa)<sub>y/z</sub>

The first series of synthesis consisted of the extension of 75\_PVAc-X with different fractions of VAc and VeoVa. F<sub>VeoVa</sub> = 2, 5, 7 and 10 mol.% were targeted in the final composition of the hybrid copolymer. 75\_PVAc from **Chapter II** was used for the extension (see **Table V-3** below). The extensions were carried out in EtAc at 60 °C for 5 to 6 h with [75\_PVAc-X]:[AIBN] = 5. The detailed protocole is described in **Experimental, Section III.4.4** The conversion of VAc and VeoVa was determined *via* <sup>1</sup>H NMR, and the evaluation of the final molar mass, after purification of the polymer was determined by SEC-THF.

For the considered *M<sub>n</sub>*, the signal of the xanthate extremity was not always perfectly resolved in the NMR spectrum, which might affect the evaluation of the molar mass and average DP *via* this technique. Additionnaly, the determination of the overall DP (and thus DP2 of the

second block) is based on the assumption that all the 75\_PVAc-X were involved in the extension, which, in light of the SEC traces gathered in **Figure V-2**, was obviously not the case and might lead to a wrong estimation of the molar mass of the second block by  $^1\text{H}$  NMR. Therefore,  $^1\text{H}$  NMR will not be used anymore to evaluate the  $M_n$  of the hybrid copolymers after purification, but SEC.

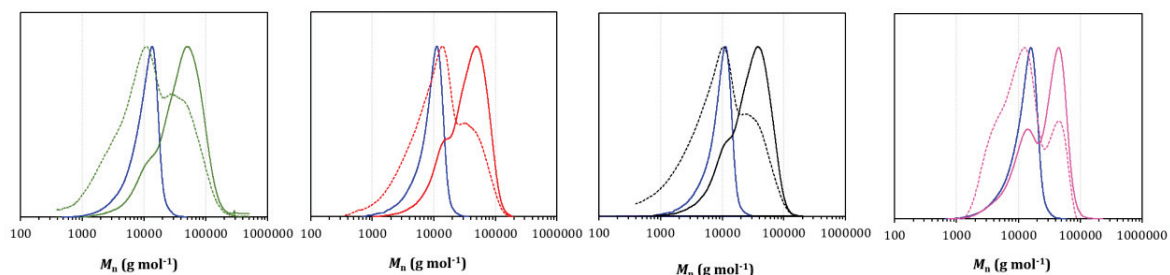


**Figure V-2:** SEC-THF traces of the molar mass evolutions of the chain extensions of 75\_PVAc-X with different fractions of VeoVa and VAc: (blue) 75\_PVAc-X before extension; 75\_PVAc-*b*-100\_P(VAc-*s*-VeoVa) with targeted  $F_{\text{VeoVa}}$  of 10 mol.% (green), 7 mol.% (red), 5 mol.% (black), 2 mol.% (pink) and their corresponding UV traces after extension at 280 nm (dashed lines).

After extension, the UV traces overlapped with the RI trace, which indicates that the hybrid copolymers were functionalized with the xanthate, indicating the successful extensions of 75\_PVAc-X. However, in all cases, broadening and shouldering of the SEC traces were visible at low molar masses (**Figure V-2**). This shoulder was attributed to the slow consumption of 75\_PVAc-X, due to the presence of  $\text{CH}(\text{OAc})\text{CH}_2\text{-X}$  terminated chains which are slow to fragment ( $\text{PVAc}_T\text{-X}$ ) and to dead chains ( $\text{PVAc}_H\text{-H}$ ). To evaluate the fraction of chains that were efficiently chain extended, the SEC chromatograms were deconvoluted using Origin Software (**Figure V-3**). The surface of each deconvoluted peak is given by **Equations 38** and **39**.

$$S_1 = K \left(\frac{dn}{dC}\right)_1 C_1 \quad \text{and} \quad S_2 = K \left(\frac{dn}{dC}\right)_2 C_2 \quad \text{(38) and (39)}$$

With  $S_1$  the area of the deconvoluted peak of the 75\_PVAc-X that has not been chain extended;  $S_2$  the area of the deconvoluted peak of the polymer after extension with VAc and VeoVa;  $K$  the Mark-Houwink coefficients of the system (considering  $K_{\text{PVAc}} = 15.8 \cdot 10^{-3} \text{ mL g}^{-1}$  also for the polymer after extension),  $(dn/dC)_1$  and  $(dn/dC)_2$  the refractive index increments of PVAc and of the copolymer after extension, respectively; and  $C_1$  and  $C_2$  the concentration of PVAc that has not been extended, and of the copolymer after extension with VAc and VeoVa, respectively. Due to the close nature of the vinyl monomers VAc and VeoVa (and later on, VL), it was considered as a first approximation that  $(dn/dC)_1$  and  $(dn/dC)_2$  were similar (*i.e.*, 1.467 at 20 °C).

Again, a particular care was taken to weight the same mass of polymer for each SEC analysis in order to get comparable results. Nevertheless, the values of the areas under the curve calculated by Origin can, under no circumstance, be considered as absolute values, but these deconvolutions make it possible to obtain a trend on the effectiveness of the chain extensions. The results obtained after deconvolution of the SEC traces showed that the extensions of 75\_PVAc was more efficient when 10, 7 and 5 mol.% of VeoVa were targeted compared to the polymer were 2 mol.% of VeoVa was targeted (**Figure V-3**). This result is consistent with that obtained in **Chapter III**, where it was highlighted that the higher the VeoVa content in the statistical structures, the higher the chain-end functionality.

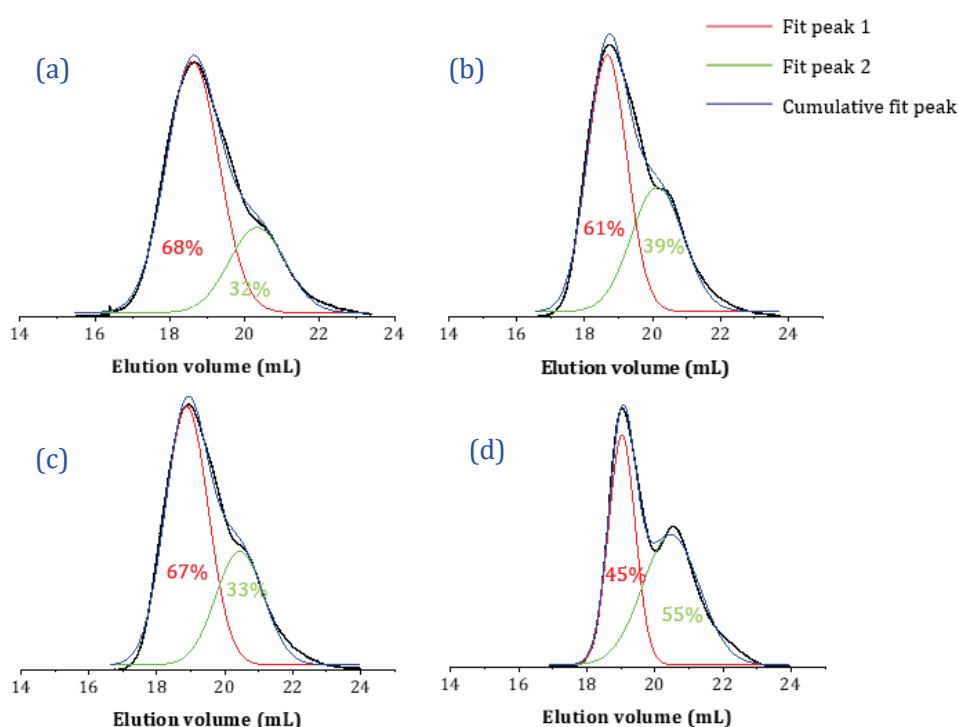


**Figure V-3:** Deconvolution of the SEC chromatograms of (a) 75\_PVAc-*b*-100\_P(VAc-*s*-VeoVa)<sub>0.90/0.10</sub>; (b) 75\_PVAc-*b*-100\_P(VAc-*s*-VeoVa)<sub>0.93/0.07</sub>; (c) 75\_PVAc-*b*-100\_P(VAc-*s*-VeoVa)<sub>0.95/0.05</sub> and (d) 75\_PVAc-*b*-50\_P(VAc-*s*-VeoVa)<sub>0.98/0.02</sub>.

Furthermore, the  $\bar{D}$  were quite high and increased when the VeoVa content decreased, which could indicate a lack of control of the polymerization due to the presence of VAc and the unavoidable head-to-head defect (**Table V-1**).

**Table V-1: Main characteristics of the 75\_PVAc-*b*-P(VAc-*s*-VeOVA) hybrid copolymers with different  $F_{\text{VeOVA}}$ , obtained by extension of 75\_PVAc-X in EtAc at 60 °C with  $[75\_PVAc-X]:[AIBN] = 5$ .**

Designation *	Overall conversion ( $X_{\text{wt.}}\%$ ) <sup>a</sup>	$M_n$ (theo.) ( $\text{g mol}^{-1}$ ) <sup>b</sup>	$M_n$ (SEC) ( $\text{g mol}^{-1}$ ) <sup>c</sup>	Dispersity ( $\bar{D}$ ) <sup>c</sup>
75_PVAc- <i>b</i> -100_P(VAc- <i>s</i> - VeOVA) <sub>0.90/0.10</sub>	60	24 200	21 500	1.8
75_PVAc- <i>b</i> -100_P(VAc- <i>s</i> - VeOVA) <sub>0.93/0.07</sub>	60	23 360	21 000	1.8
75_PVAc- <i>b</i> -100_P(VAc- <i>s</i> - VeOVA) <sub>0.95/0.05</sub>	67	22 000	28 000	1.9
75_PVAc- <i>b</i> -50_P(VAc- <i>s</i> - VeOVA) <sub>0.98/0.02</sub>	20	9 900	29 600	2.0

<sup>a</sup> Overall conversion based on <sup>1</sup>H NMR analyses

<sup>b</sup> Theoretical molar mass of the copolymers calculated from conversion

<sup>c</sup> Experimental molar mass of the copolymers calculated by SEC-THF using PS calibration

Nevertheless, most of the samples maintained dispersity values below 2. Only the copolymer 75\_PVAc-*b*-100\_P(VAc-*s*-VeOVA)<sub>0.98/0.02</sub> presented a lower monomer conversion than the other structures. This experiment was carried out a second time and led to the same conversion. This could be attributed to less efficient extension compared to the other systems, due to the presence of a higher fraction of PVAc<sub>H-H</sub> chains at the beginning of the extension, and the accumulation of less reactive chains over the course of the polymerization. These chains are slow to fragment, thus leading to lower conversion after 7 h.

In any case, all these results confirm the formation of the hybrid copolymers, but also highlight the presence of PVAc-X resulting from the macroCTA that has not been chain extended, and dead chains. It is also more than likely that the final polymer contains a small fraction of P(VAc-*s*-VeOVA) resulting from the reinitiation step.

## II.2 Variation of the DP of PVAc (DP1) in PVAc-*b*-P(VAc-*s*-VeOVA)<sub>y/z</sub>

In a second set of experiments, the DP of PVAc-X was varied from 20 to 100, with  $F_{\text{VeOVA}}$  set constant. To proceed, the overall targeted DP was fixed at 175 and the number of equivalents of VAc and VeOVA was adapted to DP1 value, to target  $F_{\text{VeOVA}} = 5$  mol.% in the overall structures.

The questions were:

1. As observed in **Chapter II**, the smaller the DP, the lower the fraction of PVAc<sub>T-X</sub>. Therefore, does the DP of the first block affects the quality of the extension?
2. Does the molar mass of the first PVAc block affects the dispersibility and the micellization efficiency of the hybrid copolymers after alcoholysis?

The syntheses of the first PVAc blocks with different DPs were described in **Chapter II, Section II**. **Table V-2** summarizes the characteristics of the first blocks which were used for the extensions in the present Chapter.

**Table V-2: Main characteristics of the first blocks of PVAc-X obtained by RAFT/MADIX polymerization in the presence of *O*-ethyl-*S*-(1-ethoxycarbonyl)ethyl dithiocarbonate in EtAc at 60 °C.**

Designation	VAc conv. (%) <sup>a</sup>	$M_n$ (theo.) (g mol <sup>-1</sup> ) <sup>b</sup>	$M_n$ (NMR) (g mol <sup>-1</sup> ) <sup>c</sup>	$M_n$ (SEC) (g mol <sup>-1</sup> ) <sup>d</sup>	Dispersity ( $\mathcal{D}$ ) <sup>d</sup>	¥ (%)
20_PVAc	94	2240	2180	2130	1.17	80
40_PVAc	90	4100	3750	3500	1.20	60
60_PVAc	90	6190	5500	5800	1.35	-
75_PVAc	80	6030	5600	6300	1.30	55
100_PVAc	88	9740	9600	9400	1.50	53

<sup>a</sup> Individual conversion based on <sup>1</sup>H NMR analyses

<sup>b</sup> Theoretical molar mass the polymers calculated from conversion

<sup>c</sup> Experimental molar mass of the polymers, calculated from end group analysis by <sup>1</sup>H NMR comparing polymer chain-end and main chain resonances

<sup>d</sup> Experimental molar mass of the polymers calculated by SEC-THF using PS calibration

<sup>1</sup>H NMR analysis suggested that the desired composition of VAc and VeoVa was successfully reached. The shift of the molar mass distributions towards higher values on the SEC traces indicated successful block copolymerizations (**Figure V-4**). The UV traces overlapped with the RI trace, which indicates that the hybrid copolymers were functionalized with the xanthate moiety and provide additional proof for successful extensions of PVAc-X.



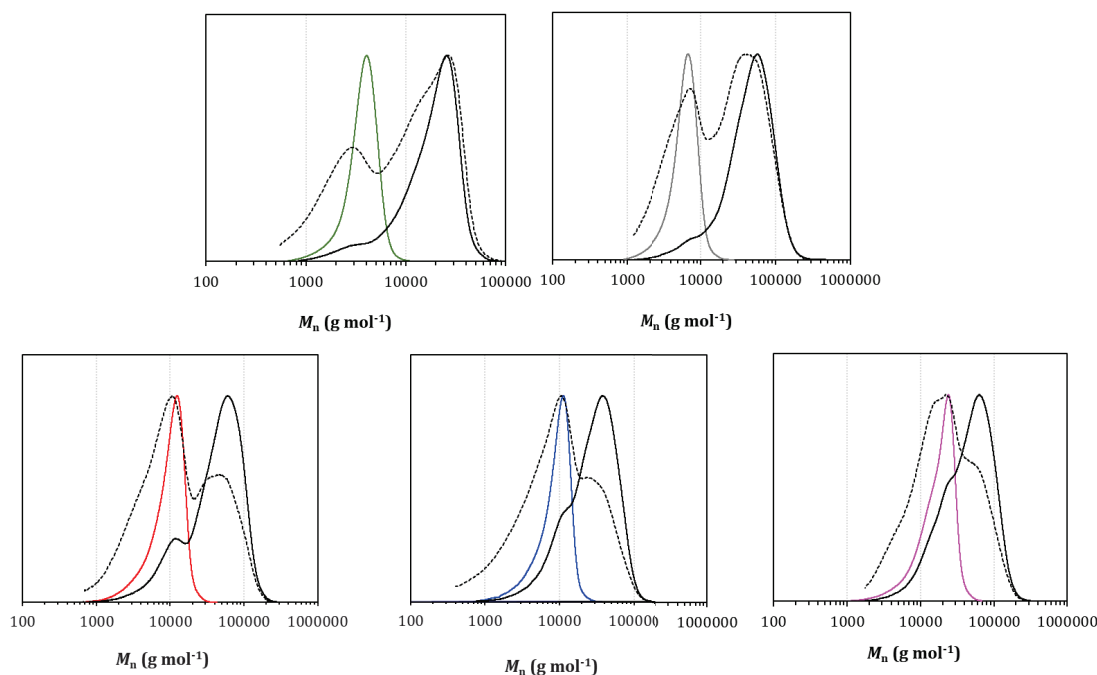


**Figure V-4:** SEC-THF traces of the molar mass evolutions of the extensions of PVAc-X with VAc and VeoVa. The colored traces correspond to PVAc-X polymers before extension: **(green):** 20\_PVAc-X; **(grey):** 40\_PVAc-X; **(blue):** 75\_PVAc-X and **(pink):** 100\_PVAc-X. The black traces correspond to the resulting polymers after extension with VAc and VeoVa. Full lines correspond to the normalized RI traces and dashed lines correspond to the normalized UV traces after extension at 280 nm. The targeted molar fraction of VeoVa was fixed at 5 mol.% for a targeted overall DP of 175.

Nevertheless, the SEC traces also revealed the presence of the typical shoulder (which overlapped with the SEC traces of the PVAc before extension) with high  $\bar{D}$  values (**Figure V-4**). These shoulders most likely originate from unconsumed PVAc macroCTAs. However, the SEC traces suggest that the lower the DP of the first block (DP1), the lower the amount of unextended PVAc macroCTA. Indeed, the shoulder seemed to progressively broaden from DP1 = 20 to DP1 = 100 (**Figure V-4**). This is consistent with the chain-end functionality determined by  $^1\text{H}$  NMR in **Chapter II**. As a reminder, it was determined to be 80% for  $\text{DP}_{\text{PVAc}} = 20$  and 53% for  $\text{DP}_{\text{PVAc}} = 100$ . This was confirmed by deconvolution studies (**Figure V-5**). With the exception of the extension of 100\_PVAc, all the other samples maintain dispersity values below 2 (**Table V-4**).

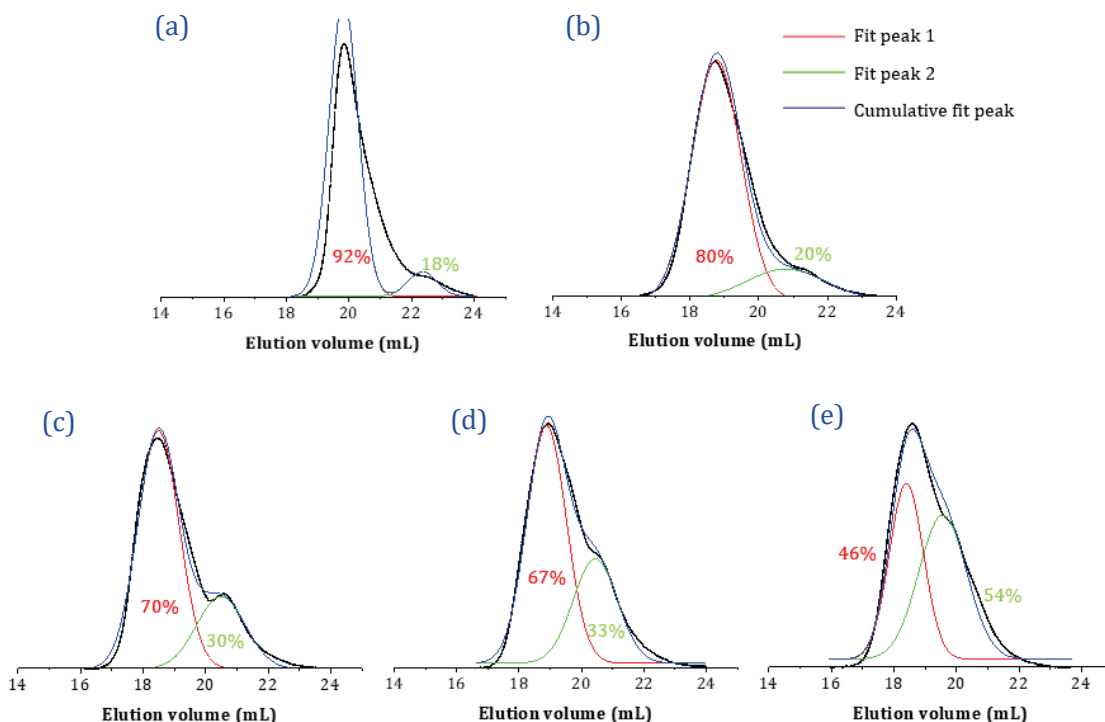


**Figure V-5:** Deconvolution of the SEC traces of **(a)** 20\_PVAc-*b*-155\_P(VAc-*s*-VeoVa)<sub>0.95/0.05</sub>; **(b)** 40\_PVAc-*b*-145\_P(VAc-*s*-VeoVa)<sub>0.95/0.05</sub>; **(c)** 60\_PVAc-*b*-115\_P(VAc-*s*-VeoVa)<sub>0.95/0.05</sub>; **(d)** 75\_PVAc-*b*-100\_P(VAc-*s*-VeoVa)<sub>0.95/0.05</sub> and **(e)** 100\_PVAc-*b*-75\_P(VAc-*s*-VeoVa)<sub>0.95/0.05</sub>.

**Table V-3:** Main characteristics of the PVAc-*b*-P(VAc-*s*-VeoVa)<sub>0.95/0.05</sub> hybrid copolymers obtained after extension of PVAc in EtAc at 60 °C with [PVAc-X]:[AIBN] = 5.

Designation	Overall conversion (X <sub>wt.</sub> %) <sup>a</sup>	M <sub>n</sub> (theo.) (g mol <sup>-1</sup> ) <sup>b</sup>	M <sub>n</sub> (SEC) (g mol <sup>-1</sup> ) <sup>c</sup>	Dispersity (Đ)
20_PVAc- <i>b</i> -155_P(VAc- <i>s</i> -VeoVa) <sub>0.95/0.05</sub>	86	20 280	11 500	1.6
40_PVAc- <i>b</i> -145_P(VAc- <i>s</i> -VeoVa) <sub>0.95/0.05</sub>	87	22 850	28 950	1.8
60_PVAc- <i>b</i> -115_P(VAc- <i>s</i> -VeoVa) <sub>0.95/0.05</sub>	65	19 900	23 130	1.8
75_PVAc- <i>b</i> -100_P(VAc- <i>s</i> -VeoVa) <sub>0.95/0.05</sub>	67	22 000	28 000	1.9
100_PVAc- <i>b</i> -75_P(VAc- <i>s</i> -VeoVa) <sub>0.95/0.05</sub>	67	22 000	29 600	2.6

<sup>a</sup> Overall conversion based on <sup>1</sup>H NMR analyses.

<sup>b</sup> Theoretical molar mass of the copolymers calculated from conversion

<sup>c</sup> Experimental molar mass of the copolymers calculated by SEC-THF using PS calibration

These results suggest that the optimum route to synthesize hybrid copolymers which contain a PVAc block and a statistical block based on VAc and VeoVa, is by chain extension of PVAc-X with low DP<sub>1</sub>, to avoid the accumulation of PVAc<sub>T</sub>-X chains in the first block, thus maintaining high chain-end functionality for the extension.

In light of these results, one has to keep in mind that the final product, obtained after purification, contained a mixture of the starting chains carrying or not (dead chains) a xanthate moiety, the desired hybrid copolymer and a fraction of the second block formed as a result of the use of free radical initiator for the reinitiation of the starting macroCTA.

Subsequently, a library of PVAc-*b*-P(VL-*s*-VAc) hybrid copolymers were also produced to evaluate the influence of the VL units.

### II.3 Synthesis of PVAc-*b*-P(VAc-*s*-VL)<sub>y/z</sub>

In **Chapter III**, it was demonstrated that VL units were less sensitive to alcoholysis than VAc ones and that it was possible to tune the HD by varying the hydrolysis time. Thus, a hybrid copolymer with  $F_{VL} = 10$  mol.% was synthesized, and different fractions of VL in the resulting copolymer after alcoholysis will be targeted later on from this starting material, simply by neutralization of the reaction at different times.

75\_PVAc-X was thus chain extended with VAc and VL, to target  $F_{VL} = 10$  mol.% in the final structure according to a protocol similar to the one employed for the VeoVa-based hybrid copolymers. Approximately 72% conversion was obtained (**Table V-4**). The final product after purification was analyzed by SEC-THF (**Figure V-6**).

**Table V-4:** Main characteristics of the 75\_PVAc-*b*-P(VAc-*s*-VL)<sub>0.90/0.10</sub> hybrid copolymer obtained after extension of 75\_PVAc-X in EtAc at 60 °C for 5 h with [75\_PVAc-X]:[AIBN] = 5.

Designation	Overall conversion (X <sub>wt.</sub> %) <sup>a</sup>	$M_n$ (theo.) (g mol <sup>-1</sup> ) <sup>b</sup>	$M_n$ (SEC) (g mol <sup>-1</sup> ) <sup>c</sup>	Dispersity ( $\mathcal{D}$ )
75_PVAc- <i>b</i> -100_P(VAc- <i>s</i> -VL) <sub>0.90/0.10</sub>	72	19 800	22 600	1.8

<sup>a</sup> Overall conversion based on <sup>1</sup>H NMR analysis

<sup>b</sup> Theoretical molar mass of the copolymers calculated from conversion

<sup>c</sup> Experimental molar mass of the copolymers calculated by SEC THF using PS calibration

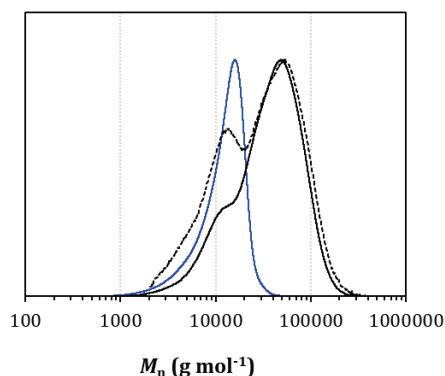


**Figure V-6:** SEC trace before (blue) and after (black) extension of 75\_PVAc in the presence of VAc and VL. Targeted  $F_{VL} = 10$  mol.%. Full lines correspond to the normalized RI traces and dashed lines correspond to the normalized UV trace at 280 nm after chain extension.

The visible shoulder in the SEC trace after extension showed that, again, not all the 75\_PVAc-X was reactivated during the extension. Nevertheless,  $\mathcal{D}$  remained below 2, and the shift of

the molar mass distributions towards higher values both with RI and UV detector at 280 nm indicate an effective chain extension of the first block towards the hybrid structure.

#### **II.4 Conclusion on the synthesis of the hybrid structures**

Similar to the VeoVa-based hybrid copolymer synthesis, chain extension was not perfectly controlled for the VL-based system, thus leading to a mixture of the desired hybrid structure, but with also PVAc that has not been chain extended, dead chains, and a fraction of the second block coming from the second step. Even though these structures were not well-defined, alcoholysis will be performed on the different hybrid structures in the next section, before their ability to act as stabilizers will be evaluated in the final section, hoping to evidence a potential synergistic effect of the presence of several types of stabilizer chains during the emulsion copolymerization of VAc and VeoVa. Indeed, it was highlighted in **Chapter II** that Mowiol 4-88 (with broad molar mass distribution) generated a higher number of smaller polymer particles in emulsion compared to the well-defined P(VOH-s-VAc) obtained after the alcoholysis of the RAFT-synthesized PVAc. Hence, high  $\mathcal{D}$  seemed beneficial for the stabilization of the particles. This aspect will be further investigated in the following sections.

### III. Alcoholysis of the hybrid copolymers

The alcoholysis of the hybrid structures was performed in methanol, following the same experimental procedure as described in **Chapter II**, with  $[\text{VAc}+\text{CoM}]:[\text{NaOH}] = 1:0.025$ . The kinetics of the alcoholysis were followed by  $^1\text{H}$  NMR (**Figure V-7**), and the molar fraction ( $F_{\text{monomer}}$ ) of each unit was determined by  $^1\text{H}$  NMR as explained in **Chapter III**.

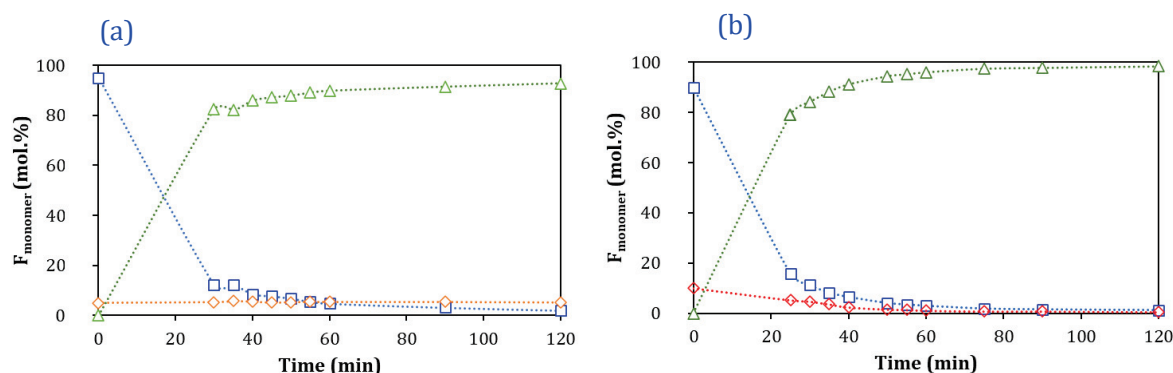


**Figure V-7:** Kinetics of the alcoholysis of (a) 75\_PVAc-*b*-100\_P(VAc-*s*-VeoVa)<sub>0.95/0.05</sub> and (b) 75\_PVAc-*b*-100\_P(VAc-*s*-VL)<sub>0.90/0.10</sub> with the evolution of molar fractions of VOH ( $\blacktriangle$ ), VAc ( $\square$ ); VeoVa ( $\blacklozenge$ ) and VL ( $\blacklozenge$ ) units.  $T = 30\text{ }^\circ\text{C}$ , 2 h,  $[\text{VAc}+\text{CoM}]:[\text{NaOH}] = 1:0.025$ .

**Figure V-7** shows that the kinetic profiles for the alcoholyses of the hybrid copolymers are similar to that of the statistical ones. Indeed, here again, VeoVa units were not affected by the alcoholysis (**Figure V-7 (a)**), while VL units were slowly alcoholized over time (**Figure V-7 (b)**).

Various molar fractions of VeoVa were obtained after alcoholysis of different samples of PVAc-*b*-P(VAc-*s*-VeoVa) (**Table V-5**). Two molar fractions of VL,  $F_{\text{VL}} = 1.5$  and 5 mol.%, were targeted with the same starting copolymer 75\_PVAc-*b*-100\_P(VAc-*s*-VL)<sub>0.90/0.10</sub>, simply by stopping the alcoholysis at different times (**Table V-5**).  $F_{\text{VL}} = 1.5$  mol.% was chosen to compare with the well-defined statistical copolymer that contained 1.5 mol.% of VL, and provided the best results for the VL-based statistical structures.  $F_{\text{VL}} = 5$  mol.% was chosen to evaluate the influence of the nature of the CoM in the hybrid structure and compare with the VeoVa-based hybrid copolymer that contains 5 mol.% of VeoVa.

To ease the designation of these different structures, they will be designed by the letter **H** for “hybrid” and be associated to a label. As it was not possible to determine the exact composition of VAc and VOH units in each block by  $^1\text{H}$  NMR, the overall composition of the resulting copolymers after alcoholysis will be depicted as follows: DP1\_P(VOH-*s*-VAc)-*b*-DP2\_P(VOH-*s*-CoM-*s*-VAc)<sub>w/y/z</sub> in which w, y and z are the global molar composition of VOH,

CoM and VAc units, respectively; DP1 and DP2 are the DPs of the first and second block of the hybrid copolymer, respectively.

**Table V-5: Library of P(VOH-s-VAc)-b-P(VOH-s-CoM-s-VAc) obtained after alcoholysis of the hybrid copolymers.**

Entry	Structure before hydrolysis	Structure after hydrolysis
H1	75_PVAc- <i>b</i> -100_P(VAc- <i>s</i> -VeoVa) <sub>0.90/0.10</sub>	75_P(VOH- <i>s</i> -VAc)- <i>b</i> -100_P(VOH- <i>s</i> -VeoVa- <i>s</i> -VAc) <sub>0.858/0.110/0.032</sub>
H2	75_PVAc- <i>b</i> -100_P(VAc- <i>s</i> -VeoVa) <sub>0.93/0.07</sub>	75_P(VOH- <i>s</i> -VAc)- <i>b</i> -100_P(VOH- <i>s</i> -VeoVa- <i>s</i> -VAc) <sub>0.911/0.075/0.014</sub>
H3	75_PVAc- <i>b</i> -100_P(VAc- <i>s</i> -VeoVa) <sub>0.95/0.05</sub>	75_P(VOH- <i>s</i> -VAc)- <i>b</i> -100_P(VOH- <i>s</i> -VeoVa- <i>s</i> -VAc) <sub>0.929/0.053/0.018</sub>
H4	75_PVAc- <i>b</i> -50_P(VAc- <i>s</i> -VeoVa) <sub>0.98/0.02</sub>	75_P(VOH- <i>s</i> -VAc)- <i>b</i> -50_P(VOH- <i>s</i> -VeoVa- <i>s</i> -VAc) <sub>0.96/0.02/0.02</sub>
H5	20_PVAc- <i>b</i> -155_P(VAc- <i>s</i> -VeoVa) <sub>0.95/0.05</sub>	20_P(VOH- <i>s</i> -VAc)- <i>b</i> -155_P(VOH- <i>s</i> -VeoVa- <i>s</i> -VAc) <sub>0.932/0.048/0.023</sub>
H6	40_PVAc- <i>b</i> -145_P(VAc- <i>s</i> -VeoVa) <sub>0.95/0.05</sub>	40_P(VOH- <i>s</i> -VAc)- <i>b</i> -145_P(VOH- <i>s</i> -VeoVa- <i>s</i> -VAc) <sub>0.935/0.047/0.018</sub>
H7	60_PVAc- <i>b</i> -115_P(VAc- <i>s</i> -VeoVa) <sub>0.95/0.05</sub>	60_P(VOH- <i>s</i> -VAc)- <i>b</i> -115_P(VOH- <i>s</i> -VeoVa- <i>s</i> -VAc) <sub>0.937/0.047/0.016</sub>
H8	100_PVAc- <i>b</i> -75_P(VAc- <i>s</i> -VeoVa) <sub>0.95/0.05</sub>	100_P(VOH- <i>s</i> -VAc)- <i>b</i> -75_P(VOH- <i>s</i> -VeoVa- <i>s</i> -VAc) <sub>0.932/0.052/0.016</sub>
H9		75_P(VOH- <i>s</i> -VAc)- <i>b</i> -100_P(VOH- <i>s</i> -VL- <i>s</i> -VAc) <sub>0.956/0.015/0.029</sub>
H10	75_PVAc- <i>b</i> -100_P(VAc- <i>s</i> -VL) <sub>0.90/0.10</sub>	75_P(VOH- <i>s</i> -VAc)- <i>b</i> -100_P(VOH- <i>s</i> -VL- <i>s</i> -VAc) <sub>0.85/0.05/0.10</sub>

#### IV. (Self-)Organization of the hybrid copolymers in water

Similar to the previous Chapters, aqueous dispersions containing 2.5 wt.% of the different hybrid structures were prepared at R.T. When the polymer did not dissolve after 2 h, the temperature was increased to 55 °C and the dispersion stirred for further 2 h. If the polymer remained insoluble, the temperature was increased further to 70 °C and finally 90 °C (**Table V-6**).

**Table V-6: Dispersibility of the VeoVa- and VL-based hybrid stabilizer candidates.**

Stabilizer	Dispersibility at given temperature			
	R.T.	55 °C	70 °C	90 °C
<b>H1:</b> 75_P(VOH-s-VAc)-b-100_P(VOH-s-VeoVa-s-VAc) <sub>0.858/0.110/0.032</sub>	⊗	⊗	⊗	⊗
<b>H2:</b> 75_P(VOH-s-VAc)-b-100_P(VOH-s-VeoVa-s-VAc) <sub>0.911/0.075/0.014</sub>	⊗	⊗	Partially	✔ (20 h)
<b>H3:</b> 75_P(VOH-s-VAc)-b-100_P(VOH-s-VeoVa-s-VAc) <sub>0.929/0.053/0.018</sub>	⊗	Partially	✔ (30 min)	-
<b>H4:</b> 75_P(VOH-s-VAc)-b-50_P(VOH-s-VeoVa-s-VAc) <sub>0.96/0.02/0.02</sub>	⊗	Partially	✔ (20 min)	-
<b>H5:</b> 20_P(VOH-s-VAc)-b-155_P(VOH-s-VeoVa-s-VAc) <sub>0.932/0.048/0.023</sub>	⊗	⊗	⊗	⊗
<b>H6:</b> 40_P(VOH-s-VAc)-b-145_P(VOH-s-VeoVa-s-VAc) <sub>0.935/0.047/0.018</sub>	⊗	⊗	⊗	⊗
<b>H7:</b> 60_P(VOH-s-VAc)-b-115_P(VOH-s-VeoVa-s-VAc) <sub>0.937/0.047/0.016</sub>	⊗	⊗	Partially	✔
<b>H8:</b> 100_P(VOH-s-VAc)-b-75_P(VOH-s-VeoVa-s-VAc) <sub>0.932/0.052/0.018</sub>	⊗	Partially	✔ (40 min)	-
<b>H9:</b> 75_P(VOH-s-VAc)-b-100_P(VOH-s-VL-s-VAc) <sub>0.956/0.015/0.029</sub>	⊗	⊗	—	-
<b>H10:</b> 75_P(VOH-s-VAc)-b-100_P(VOH-s-VL-s-VAc) <sub>0.85/0.05/0.10</sub>	⊗	⊗	—	-

\* A red cross indicates that the polymer is insoluble. An orange line indicates that it is insoluble at R.T. and higher temperature, but dispersible at R.T., after having been heated at higher temperature. A green tick indicates that the copolymer is dispersible at the mentioned temperature and remains dispersible when the solution is cooled at R.T. In case of different behavior (time, aspect...), it will be briefly described with a sentence.

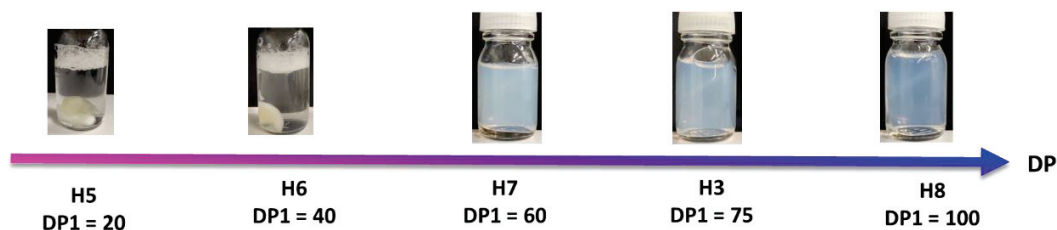
At fixed  $F_{\text{VeoVa}} = 5$  mol.%, the hybrid stabilizers were not soluble in water when the DP of the first P(VOH-s-VAc) block (DP1) was below 60 average units (regardless of the temperature) (**H5** and **H6**, **Figure V-8 (a)**). For DP1 = 75 and 100 (**H3** and **H8**, respectively), the polymers were partially dispersible at 55 °C, and provided turbid but homogeneous dispersions when the temperature was increased to 70 °C. **H7** (DP = 60) had to be heated to 90 °C to be dispersible. These dispersions remained homogeneous after cooling to R.T. (**Figure V-8 (a)**).

At fixed DP1 = 75, the polymers with  $F_{\text{VeOVA}}$  up to 7 mol.% were dispersible in water while they became insoluble for  $F_{\text{VeOVA}} = 10$  mol.% (**H2, H3, H4** and **H5, Figure V-8, (b)**).

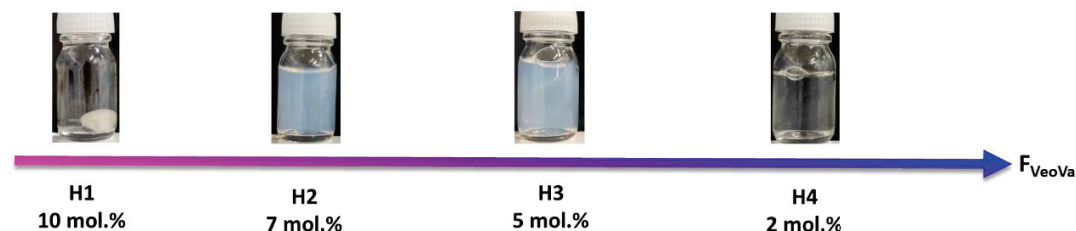
It is worth remembering that in the case of the statistical structures, the dispersibility in water was lost when the inclusion of VeoVa exceeded 2 mol.%. Not only the presence of the first hydrophilic P(VOH-s-VAc) block, but potentially also the presence of a mixture of different polymers with a broad molar mass distribution in the hybrid copolymer structures, seem thus to significantly improve the dispersibility of the overall structure.

The VL-based hybrid copolymers (**H9**, and **H10, Figure VI-8(c)**) provided a different behavior compared to the VeoVa-based system. Similar to the statistical structures, they were insoluble at R.T. nor at 70 and 90 °C, but became dispersible when the dispersions were cooled down to R.T. After this thermal treatment, both VL-based hybrid copolymers remained dispersible in water, even the one that contained 5 mol.% of VL.

(a) Variation of DP1 & Fixed VeoVa content = 5 mol.%



(b) Fixed DP1 = 75 & Variation of VeoVa content



(c) Fixed DP1 = 75 & Variation of VL content

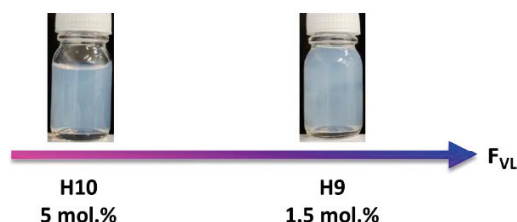


Figure V-8: Photographs of 2.5 wt.% aqueous dispersions containing (a) 75\_P(VOH-s-VAc)-b-100\_P(VOH-s-VL-s-VAc) with  $F_{\text{VL}} = 1.5$  and 5 mol.%; (b) 75\_P(VOH-s-VAc)-b-100\_P(VOH-s-VeoVa-s-VAc) with different  $F_{\text{VeOVA}}$  and (c) DP1\_P(VOH-s-VAc)-b-100\_P(VOH-s-VeoVa-s-VAc) with fixed  $F_{\text{VeOVA}} = 5$  mol.% and different DP1.



The self-assembly of the amphiphilic hybrid copolymers which were dispersible in water (*i.e.*, **H2**, **H3**, **H4**, **H7**, **H8**, **H9** and **H10**) was investigated by DLS. **H2** to **H4** are presented below to illustrate the behavior for the VeoVa-based copolymers in water. As **H7** and **H8** behaved the same, they were not inserted in this chapter but are available in **Appendix 5**. The size distribution of the pseudo-micelles was determined (**Figure V-9**).

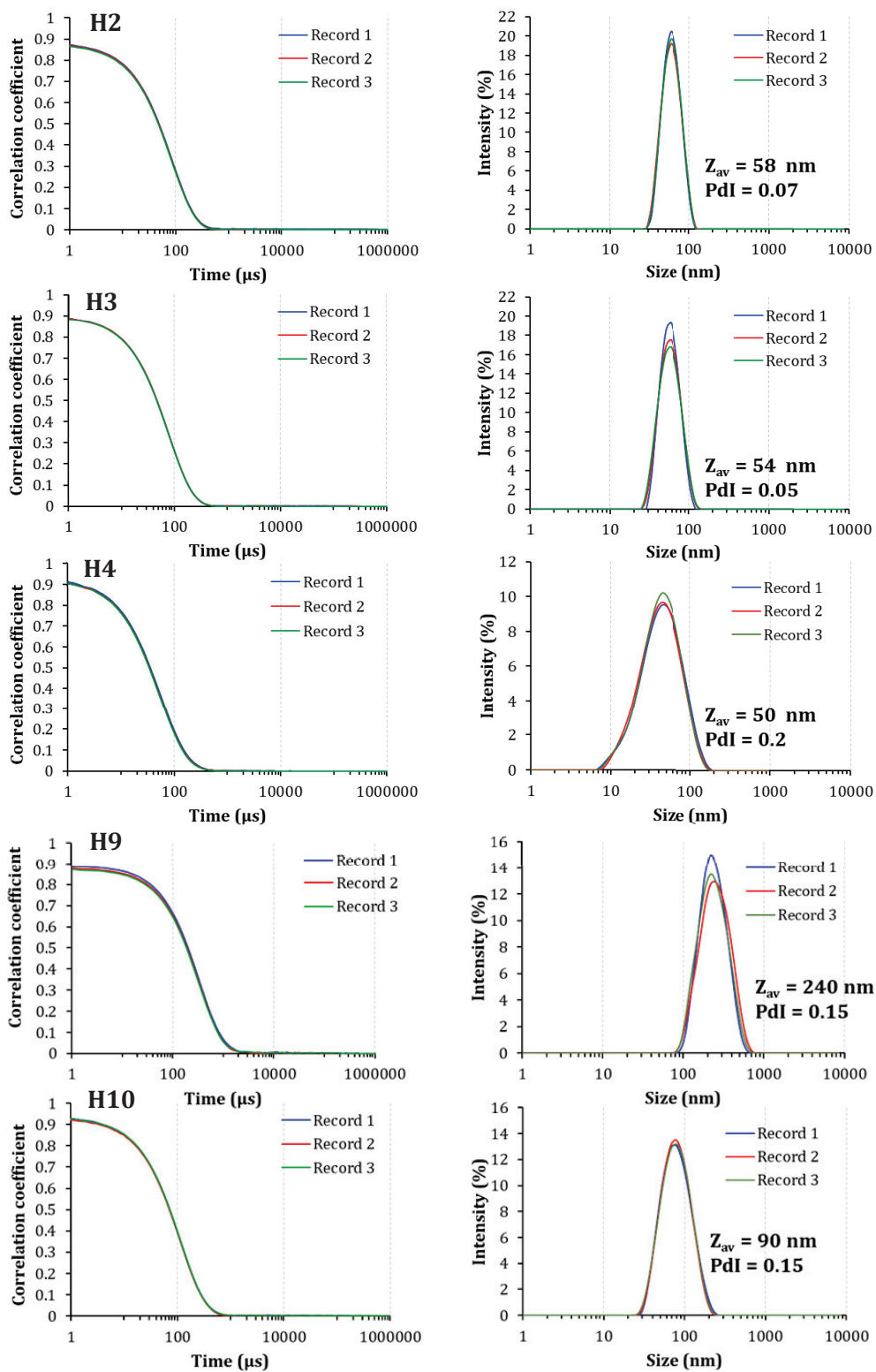


Figure V-9: Correlograms and DLS-size distributions in intensity for the 2.5 wt. % aqueous dispersions hybrid copolymers obtained after thermal treatment. Measurements were performed at 25 °C.

All the correlograms showed perfect reproducibility and the value of the intercept was systematically in the range 0.85 – 1. These results confirm the formation of quite monodisperse objects, despite the ill-defined nature of the copolymers they are made of.

For a fixed DP1 of 75, one could expect that the higher the CoM content, the smaller the  $Z_{av}$  value due to higher contraction of the hydrophobic core of the objects. This behavior was observed for the VL-based hybrid copolymers, where the  $Z_{av}$  values were 240 and 90 nm for **H9** ( $F_{VL} = 1.5$  mol.%), and **H10** ( $F_{VL} = 5$  mol.%), respectively. The same does not always hold true for VeoVa-based hybrid structures such as **H2** and **H4** for which  $F_{VeoVa}$  was 7 and 2 mol.% and  $Z_{av}$  values were 58 and 50 nm, respectively. This can probably be explained by the fact that the VL-based hybrid copolymers were obtained from the same and unique non-alcoholized structure simply by tuning the alcoholysis reaction times, while VeoVa-based hybrid copolymers are obtained from the full alcoholysis of their hydrophobic analogues. The definition of the latter is obviously entailed with the relative quality of the synthesis of the block copolymers discussed at the beginning of this chapter.

Noteworthy, the objects formed by the VeoVa-based hybrid copolymers were smaller (in the pseudo-micelle range from 30 to 100 nm) than the ones obtained with the VL-based hybrid ones (in the aggregate range, from 100 to 1000 nm, as defined in **Chapter II**).

Finally, comparing the  $Z_{av}$  values of the statistical structures from **Chapter III (Section IV.2)** to the ones of the hybrid structures, smaller values (*ca.*  $Z_{av} = 50 - 60$  nm) and more defined objects were obtained with the hybrid structures (as a reminder DLS data for the statistical copolymers provided large and multi-populated signals, in the range 20 to 1000 nm), even at low CoM content (from 1 to 2 mol.%). In contrast, the hybrid copolymers had a higher fraction of CoM units, and provided monodisperse objects, thus, leading to a better arrangement of the copolymers in water.

This being said, the behavior and variations from one system to another, and from one structure to another (*e.g.*, statistical versus hybrid) are difficult to apprehend, because the hybrid structures are in fact a mixtures of several structures coming from the synthesis, and there are no values associated with one system that can be commented on by looking at another (except the average fraction of CoM in the polymer).

Based on the results obtained in **Chapters II, III and IV**, all the stabilizer candidates which provided stable dispersions with surface tensions below  $46 \text{ mN m}^{-1}$  led to stable latexes while those with higher surface tensions provided latexes that sedimented or quickly destabilized. The determination of the surface tension thus seemed to provide a fair evaluation of the stabilizing efficiency of the amphiphilic copolymers, as already highlighted by Castellanos-Ortega *et al.*<sup>[5]</sup> (see **Chapter II, Section IV**). Surface tension of the previously identified

dispersible hybrid structures (obtained after thermal treatment) was evaluated in water at 25 °C (**Table V-7**).

**Table V-7: Surface tension of the VeoVa and VL-based hybrid copolymers in water. The dispersions contained 2.5 wt.% of copolymer, and were obtained after the thermal treatment of the copolymers, as previously described. Measurements were performed at 25 °C. Values previously measured for Mowiol 4-88 and 75\_(PVOH<sub>0.88</sub>-s-VAc<sub>0.12</sub>) are also indicated for the sake of comparison.**

Entry	Surface tension (mN m <sup>-1</sup> )
<b>Mowiol 4-88</b>	46
<b>75_(PVOH<sub>0.88</sub>-s-VAc<sub>0.12</sub>)</b>	44
<b>H2:</b> 75_P(VOH-s-VAc)-b-100_P(VOH-s-VeoVa-s-VAc) <sub>0.911/0.075/0.014</sub>	32
<b>H3:</b> 75_P(VOH-s-VAc)-b-100_P(VOH-s-VeoVa-s-VAc) <sub>0.929/0.053/0.018</sub>	34
<b>H4:</b> 75_P(VOH-s-VAc)-b-50_P(VOH-s-VeoVa-s-VAc) <sub>0.96/0.02/0.02</sub>	37
<b>H7:</b> 60_P(VOH-s-VAc)-b-115_P(VOH-s-VeoVa-s-VAc) <sub>0.937/0.047/0.016</sub>	35
<b>H8:</b> 100_P(VOH-s-VAc)-b-75_P(VOH-s-VeoVa-s-VAc) <sub>0.932/0.052/0.018</sub>	34
<b>H9:</b> 75_P(VOH-s-VAc)-b-100_P(VOH-s-VL-s-VAc) <sub>0.956/0.015/0.029</sub>	41
<b>H10:</b> 75_P(VOH-s-VAc)-b-100_P(VOH-s-VL-s-VAc) <sub>0.85/0.05/0.10</sub>	42

The VeoVa-based hybrid structures provided lower surface tensions than the VL-based ones (approximately 34 against 41 mN m<sup>-1</sup>, respectively) (**Table V-7**). Nevertheless, all the dispersions provided surface tension below 46 mN m<sup>-1</sup> and are thus strong candidates to be tested as stabilizers in the emulsion copolymerization of VAc with VeoVa.

This section highlighted a very particular aqueous phase behavior of the hybrid copolymers. Depending on their structure and composition, some of them were insoluble in water, regardless of the temperature. Nevertheless, when DP1 was higher than 40 units, we managed to disperse the copolymers *via* a thermal treatment (by different heating and cooling temperatures), resulting in monodisperse dispersions of objects of different sizes but in the pseudo-micelle range, in spite of the ill-defined nature of the copolymers they are made of (due to the poor controlled afforded during the synthesis, leading to a mixture of several structures in the final crude). The low surface tension obtained for the hybrid copolymers and the fact that they self-assemble in water, led us to consider them as stabilizer candidates in the emulsion copolymerization of VAc and VeoVa, which is the aim of the following section.

## V. Emulsion copolymerization of VAc and VeoVa stabilized with the selected hybrid copolymers

Now that we successfully synthesized, alcoholized and characterized the aqueous conformation of the most promising hybrid copolymers, let us investigate if they can meet the goal: perform efficient copolymerization of VAc and VeoVa.

The original aim in synthesizing hybrid copolymers with different DP1 in the first block was to evaluate the influence of such block on the stabilization efficiency of the overall structure after extension and alcoholysis. Here, we demonstrated that the resulting copolymers after alcoholysis were in fact a mixture of several structures, with P(VAc-*s*-VOH) resulting from the first block that has not been chain extended, a fraction of P(VOH-*s*-CoM-*s*-VAc) resulting from the reinitiation, and the desired P(VOH-*s*-VAc)-*b*-P(VOH-*s*-CoM-*s*-VAc) hybrid structure. The structure of the resulting polymer was thus clearly not defined, and hence, it does not make sense to compare the influence of the DP of the first block anymore, as several other parameters differed from one hybrid copolymer to the other.

The results obtained with the hybrid copolymers **H7** and **H8** will therefore not be presented in the following. However, even if the structure is not perfectly defined, the fraction of VeoVa determined by <sup>1</sup>H NMR is still accurate and can affect the micellization efficiency of the mixture of stabilizers. Emulsion copolymerizations of VAc with VeoVa were thus carried out with the selected VeoVa and VL-based hybrid stabilizer candidates (**H2**, **H3**, **H4**, **H9** and **H10**) according to the protocol established in **Chapter II**, with the RAFT-synthesized P(VOH-*s*-VAc) stabilizers.

### V.1 Emulsion copolymerization of VAc and VeoVa stabilized with the CoM-based hybrid stabilizers

#### V.1.1 Kinetics of the polymerizations and colloidal features of the latexes

The kinetics of the emulsion copolymerizations of VAc and VeoVa stabilized with the VeoVa-based hybrid copolymers were followed gravimetrically (**Figure V-10**).

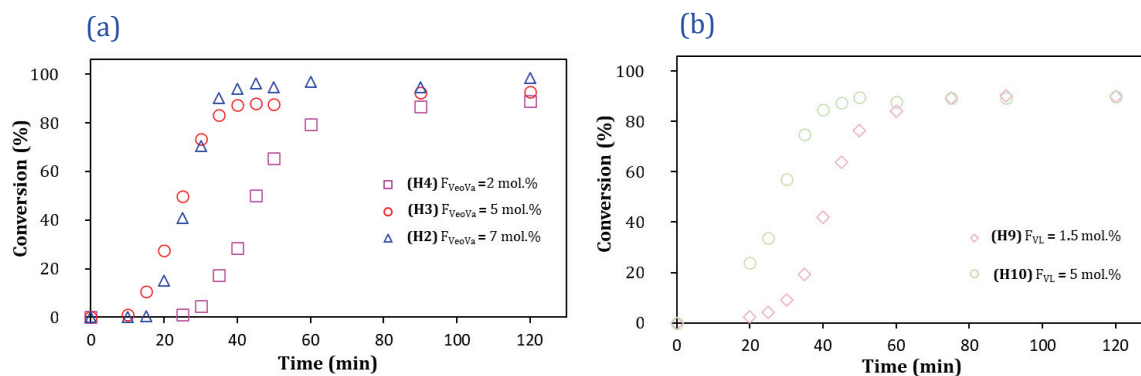


**Figure V-10 :** Kinetics of the emulsion copolymerizations of VAc and VeoVa stabilized with 10 wt.% of (a) the VeoVa-based hybrid copolymers H2, H3 and H4, fixed DP1 = 75 and variation of  $F_{VeoVa}$  from 2 to 7 mol.%, and (b) the VL-based hybrid copolymers H9 and H10, with DP1 = 75 and variation of  $F_{VL} = 1.5$  and 5 mol.%.

**Table V-8: Estimation of  $S_{max}$  for the emulsion copolymerizations stabilized with 10 wt.% of the selected hybrid stabilizer candidates, obtained from the slopes of the conversion versus time plots.**

Entry *	Stabilizer (10 wt.% based on monomers)	$S_{max}$ (s <sup>-1</sup> )	R <sup>2</sup>
ER-H2	H2: 75_P(VOH-s-VAc)-b-100_P(VOH-s-VeoVa-s-VAc) <sub>0.911/0.075/0.014</sub>	0.050	0.995
ER-H3	H3: 75_P(VOH-s-VAc)-b-100_P(VOH-s-VeoVa-s-VAc) <sub>0.929/0.053/0.018</sub>	0.046	0.999
ER-H4	H4: 75_P(VOH-s-VAc)-b-50_P(VOH-s-VeoVa-s-VAc) <sub>0.96/0.02/0.02</sub>	0.036	0.989
ER-H9	H9: 75_P(VOH-s-VAc)-b-100_P(VOH-s-VL-s-VAc) <sub>0.956/0.015/0.029</sub>	0.038	0.985
ER-H10	H10: 75_P(VOH-s-VAc)-b-100_P(VOH-s-VL-s-VAc) <sub>0.85/0.05/0.10</sub>	0.040	0.993

\* ER refers to redox-initiated emulsion polymerization and is followed by the label of the stabilizer used in the experiment. Polymerizations were performed at 55 °C using AsAc and TBHP as redox initiating system (AsAc/TBHP = 0.092/0.054 wt.% based on monomers).

All the experiments led to high conversions (up to approximately 97%). An induction period of only 15 min was observed for most of the systems (which is similar to that of **ER-Mowiol 4-88** observed in the previous chapters), except for **ER-H9** (CoM = VL, DP1 = 75,  $F_{VL} = 1.5$  mol.%) (**Figure V-10 (b)**), which showed an induction period of 20 min. All the latexes were stable, without coagulum for the experiments using the VeoVa-based stabilizers. However, approximately 15 wt.% (based on monomers and stabilizer content) of coagulum was formed in the experiment using the VL-based ones.

Noteworthy, when VeoVa-based statistical and block copolymers were tested in emulsion, the amount of initiator had to be increased (AsAc = 0.13 wt.% based on monomers) compared to the amount used in **Chapter II** for the RAFT-synthesized P(VOH-s-VAc) (AsAc = 0.092 wt.%), to reach similar conversion (approximately 80%). In contrast, in the present case, the same amount of initiator as in **Chapter II** (AsAc = 0.092 wt.% based on monomers) was used and provided high conversion.  $S_{max}$  (obtained from the slope of the kinetics profile) was also significantly higher in the present case (in range 0.036 - 0.050 s<sup>-1</sup>, **Table V-8**), compared to the VeoVa-based statistical stabilizers ( $S_{max}$  in range 0.026 s<sup>-1</sup>, **Chapter III, Section V.2.2**).

High values of  $S_{max}$  were also measured for the VL-bases hybrid copolymers (approximately 0.040, **Table V-8**).

These observations, together with the low values of surface tensions obtained in **Section IV** could indicate that the hybrid structures (and the associated structures with high dispersity) are more surface active than the statistical ones.

In addition, stable latexes were obtained with stabilizers that contained up to 7 mol.% of VeoVa (**H2**) (and  $F_{VL} = 5$  mol.%, **H10**) while no stabilization was obtained with statistical structures with  $F_{VeoVa} > 2$  mol.% (and  $F_{VL} > 1.5$  mol.%).

The samples withdrawn from the polymerization medium were analyzed by DLS. For the experiments carried out with the VeoVa-based stabilizers, most of them provided Pdl values below 0.1. It was thus possible to plot  $Z_{av}$  and the  $N_p$  as a function of the conversion (**Figure V-11**). The same was not true for the experiments carried out with the VL-based hybrid copolymers (see **Appendix 10**). In this case, this high polydispersity could be the sign of extensive continuous nucleation.

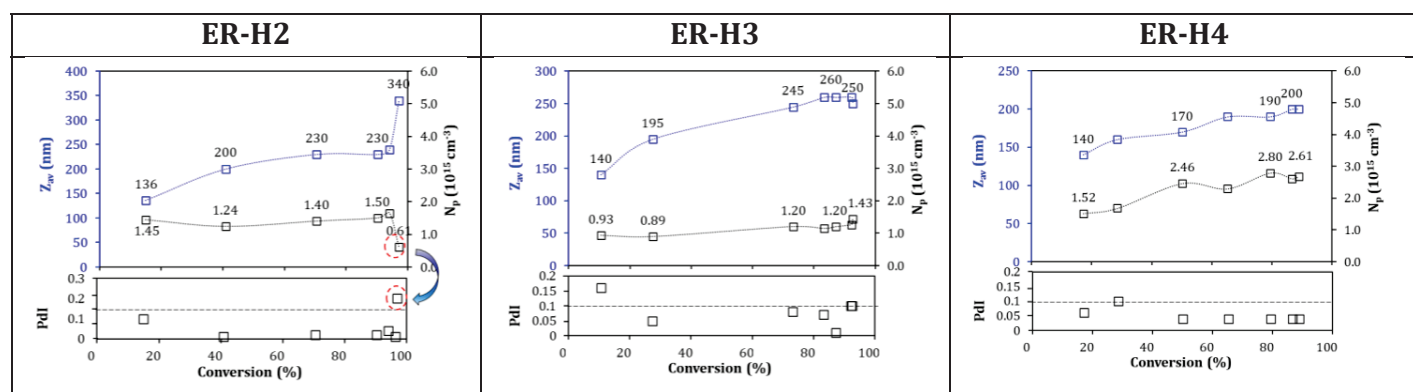


**Figure V-11:** Evolution of the particle size and number of particles with conversion for the emulsion copolymerizations stabilized with 75\_P(VOH-s-VAc)-b-100\_P(VOH-s-VeoVa-s-VAc)<sub>0.911/0.075/0.014</sub> (**ER-H2**), 75\_P(VOH-s-VAc)-b-100\_P(VOH-s-VeoVa-s-VAc)<sub>0.929/0.053/0.018</sub> (**ER-H3**) and 75\_P(VOH-s-VAc)-b-50\_P(VOH-s-VeoVa-s-VAc)<sub>0.96/0.02/0.02</sub> (**ER-H4**).



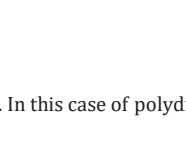
**Figure V-11** shows that  $N_p$  remained relatively constant (the increase was lesser than one unit) during the polymerization, for most of the systems stabilized with the VeoVa-based hybrid copolymers. Visible deviation from this trend was observed for the last measurement of the particle size of the latex **ER-H2** (96% conversion). In this case, the Pdl index was higher than 0.1, which can explain the fluctuations of the  $Z_{av}$  (and consequently the inconsistent values of  $N_p$ ). This could traduce a partial destabilization of the latex; with the occurrence of limited aggregation of the particles.



Globally, the particle size increased up to approximately 70 to 80% conversion, before it remained constant. The number of particles also remained relatively constant with conversion through the polymerization (**Figure V-11**). This behavior is different from the one observed for the latex obtained with most of the previously studied RAFT-synthesized stabilizers (from **Chapters II to IV**), and suggests a different mechanism of stabilization provided by the VeoVa-based hybrid structures. Obviously, the presence of well-defined preformed objects (pseudo-micelles) dispersed in water (as highlighted in **Section IV**) improved the nucleation efficiency compared to the previous systems where unimers (**Chapter II**) or aggregates (**Chapter III**) were present. These pseudo-micelles could act as nanoreactors (or seeds) for the emulsion copolymerization of VAc and VeoVa, hence decreasing the occurrence of continuous nucleation. To verify that these nano objects were still present at 55 °C (temperature of the emulsion polymerization), the 2.5 wt.% dispersions of **H2**, **H3** were analyzed by DLS at 55 °C (**Appendix 5**). As a general trend, the size of the objects slightly increased but remained well-defined and in the pseudo-micelle range (30 – 100 nm, defined in **Chapter II**).

To confirm this hypothesis, monomer swelling ability of the systems in the absence of polymerization was thus investigated. VAc monomer was added to dispersions containing 2.5 wt.% of **H2** (DP1 = 75,  $F_{VeoVa} = 7$  mol.%), **H3** (DP1 = 75,  $F_{VeoVa} = 5$  mol.%), 75\_P(VOH<sub>0.88</sub>-S-VAc<sub>0.12</sub>) and Mowiol 4-88, and stirred 15 min at 300 rpm. This was performed in the absence of initiator or increased temperature to avoid polymerization, allowing a thermodynamic equilibrium to be reached. The effect of using different weight fractions of the monomer was studied (0, 2.5 and 20 wt.%), and the characteristics of these emulsions (not polymerizations) are summarized in **Table V-9**. PSD for the different systems is provided in **Figure V-12**.

**Table V-9: Characteristics of emulsions prepared by addition of different amount of VAc to aqueous dispersions (2.5 wt.%) of Mowiol, 75\_P(VOH<sub>0.88</sub>-S-VAc<sub>0.12</sub>), H2: 75\_P(VOH-s-VAc)-b-100\_P(VOH-s-VeoVa-s-VAc)<sub>0.911/0.075/0.014</sub> and H3: 75\_P(VOH-s-VAc)-b-100\_P(VOH-s-VeoVa-s-VAc)<sub>0.929/0.053/0.018</sub> (obtained after thermal treatment)..**

Stabilizer in dispersion	Wt.% VAc	Z <sub>av</sub> (nm) <sup>a</sup>	D <sub>v</sub> (nm)	PdI	
Mowiol 4-88	0	15 / 172	-	0.2	
	2.5	12 / 71	-	0.4	
	20	> 1000	-	> 1000	
75_P(VOH <sub>0.88</sub> -S-VAc <sub>0.12</sub> )	0	10 / 298	-	0.4	
	2.5	6 / 36	-	0.3	
	20	> 1000	-	> 1000	
<b>H2</b>	0	98	98	0.1	
	2.5	84	84	0.1	
	20	100	100	0.1	
<b>H3</b>	0	40	40	0.08	
	2.5	44	44	0.1	
	20	97	-	0.6	

<sup>a</sup> Average particle size in intensity. The bold value is the main population when two peaks are detected by DLS. In this case of polydisperse samples, D<sub>v</sub> is not accurate and is therefore not provided.



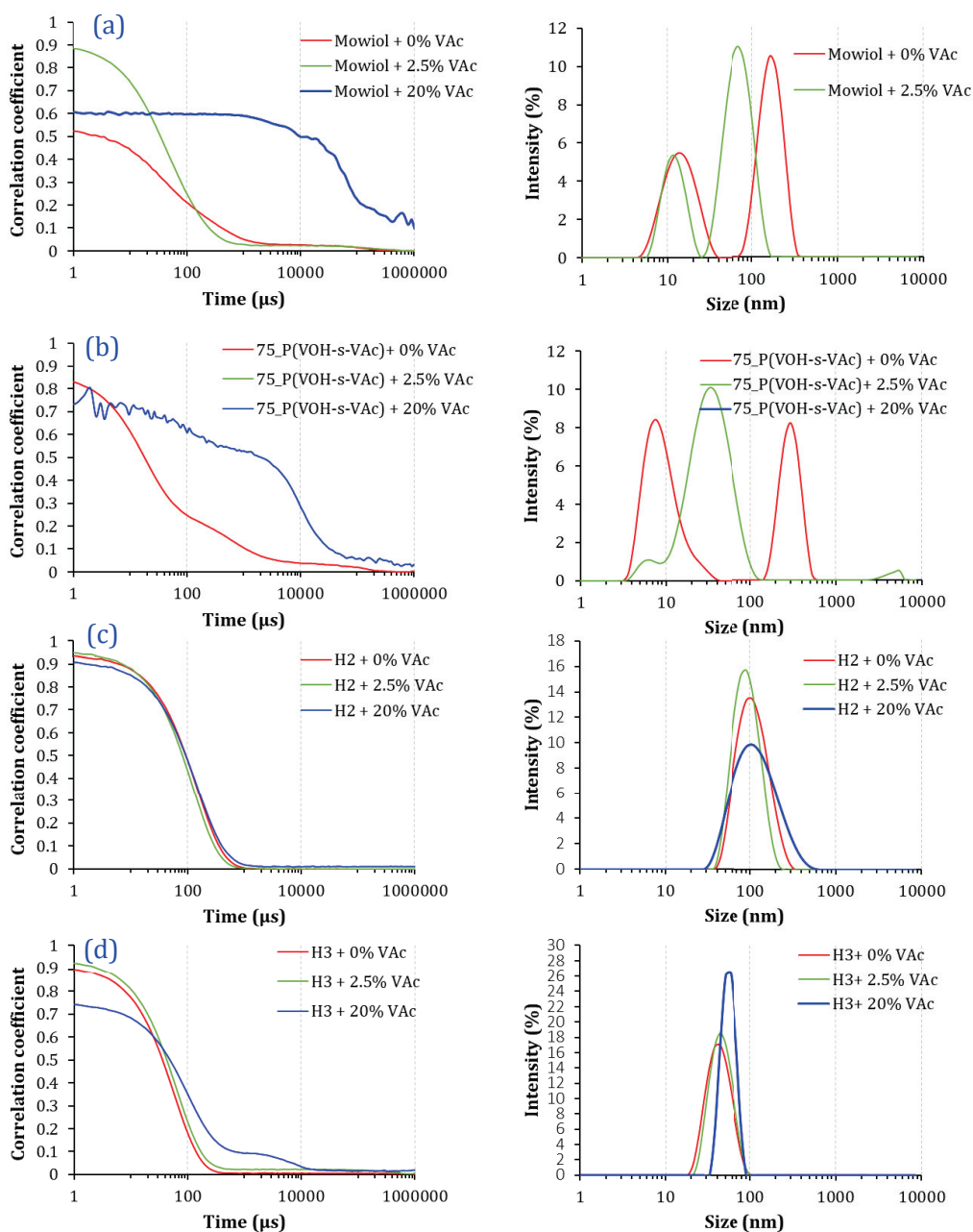


**Figure V-12:** DLS analysis of the dispersions containing 2.5 wt.% of **(a)** Mowiol 4-88; **(b)** 75\_P(VOH<sub>0.88</sub>-s-VAc<sub>0.12</sub>); **(c)** H2 and **(d)** H3 (obtained after thermal treatment to disperse the stabilizers in water), with (—): 0 wt.%; (—): 2.5 wt.% and (—): 20 wt.% VAc. DLS were performed at 25 °C.

Emulsions were prepared with 2.5 wt.% of VAc (limit of solubility of VAc in water) and 20 wt.% (Sc used in the emulsion polymerizations experiments). **Figure V-12** shows that for the emulsions which contained Mowiol 4-88 and the well-defined 75\_P(VOH<sub>0.88</sub>-s-VAc<sub>0.12</sub>), a mixture of nano-droplets were detected by DLS at 2.5 wt.% of VAc, similar to what was

observed without VAc. At 20 wt.% VAc, the emulsion which contained Mowiol 4-88 separated in two phases after 1 min, indicating that this emulsion was unstable. Similar observation was made with the emulsion containing 75\_P(VOH<sub>0.88</sub>-s-VAc<sub>0.12</sub>).

In contrast, homogeneous and stable dispersions were obtained with the hybrid stabilizers, up to 20 wt.% VAc, with slight increase in the particle size with increasing the concentration of VAc, indicating that VAc swells the pseudo-micelles. Monodisperse nanodroplets were present in the emulsions containing the hybrid stabilizers. This result provides additional proof that the stabilization mechanism provided by the VeoVa-based hybrid stabilizer differs from the one provided by P(VOH-s-VAc).

Noteworthy, in spite of the broad molar mass distribution, and the presence of different structures in the hybrid copolymer (resulting from the synthesis), some chains have nevertheless the desired hybrid structure (P(VOH-s-VAc)-*b*-P(VOH-s-VeoVa-s-VAc)). For these chains, it is likely that the VeoVa units are buried into the core of the dispersed objects before polymerization, and this could be beneficial for the formation of the defined pseudo-micelles observed by DLS.

To investigate further the nucleation mechanism of these new systems, it would be interesting to vary to amount of stabilizer in the system and see if there is a correlation between the  $N_p$  and the concentration of stabilizer ( $[S]$ ). Indeed, the number of particles is typically proportional to  $[S]^\alpha$ , where the exponent  $\alpha$  will be indicative of the type of nucleation mechanism. For instance, in the theoretical treatment of micellar nucleation proposed by Smith and Ewart, the exponent  $\alpha$  is 0.6,<sup>[6]</sup> whereas, in the presence of seeds, the exponent  $\alpha$  is 1. For typical micellar nucleation,  $\alpha$  is in the range 0 – 0.9. Values of  $\alpha$  greater than 1 are uncommon.<sup>[1]</sup> Unfortunately, this field was not further explored but is an interesting touchpoint for further research activities.

The particle size and particle size distributions of the polymer particles were analyzed by DLS and cryo-TEM (**Table V-10**).

**Table V-10: Particle size comparison for the latexes obtained with 10 wt.% of the selected hybrid stabilizers, obtained by DLS and cryo-TEM.**

Entry	Stabilizer (10 wt.% based on monomers)	$Z_{av}$ (nm) <sup>a</sup>	PdI <sup>a</sup>	$D_n$ (nm) <sup>b</sup>	$D_v$ (nm) <sup>b</sup>	$D_w/D_n$ <sup>b</sup>	$N_p$ ( $10^{15} \text{ cm}^{-3}$ ) <sup>c</sup>
ER-H2	H2: 75_P(VOH-s-VAc)-b-100_P(VOH-s-VeoVa-s-VAc) <sub>0.911/0.075/0.014</sub>	340	0.17	160	170	1.4	4.8
ER-H3	H3: 75_P(VOH-s-VAc)-b-100_P(VOH-s-VeoVa-s-VAc) <sub>0.929/0.053/0.018</sub>	250	0.10	205	210	1.1	2.9
ER-H4	H4: 75_P(VOH-s-VAc)-b-50_P(VOH-s-VeoVa-s-VAc) <sub>0.96/0.02/0.02</sub>	200	0.04	110	115	1.35	14
ER-H9	H9: 75_P(VOH-s-VAc)-b-100_P(VOH-s-VL-s-VAc) <sub>0.956/0.015/0.029</sub>	240	0.10	140	150	1.3	6.5
ER-H10	H10: 75_P(VOH-s-VAc)-b-100_P(VOH-s-VL-s-VAc) <sub>0.85/0.05/0.10</sub>	580	0.51	200	200	1.2	2.7

<sup>a</sup> obtained by DLS

<sup>b</sup> obtained by cryo-TEM

<sup>c</sup> Calculated via **Equation 49**

The comparison of the particle size and PSDs of the particles stabilized with **H2** (DP1 = 75,  $F_{\text{VeOVA}} = 7$  mol.%), **H3** (DP1 = 75,  $F_{\text{VeOVA}} = 5$  mol.%) and **H4** (DP1 = 75,  $F_{\text{VeOVA}} = 2$  mol.%) showed that for a similar structure, the VeoVa content had little influence on the particle size of the particles, and no clear correlation was found. ( $Z_{av} = 240$  nm before destabilization, 250 nm and 200 nm, respectively) The cryo-TEM analysis highlighted that **ER-H4** provided smaller particles, with a significantly higher  $N_p$ . The trend was less clear between the experiments **ER-H2** and **ER-H3** (**Table V-10**).

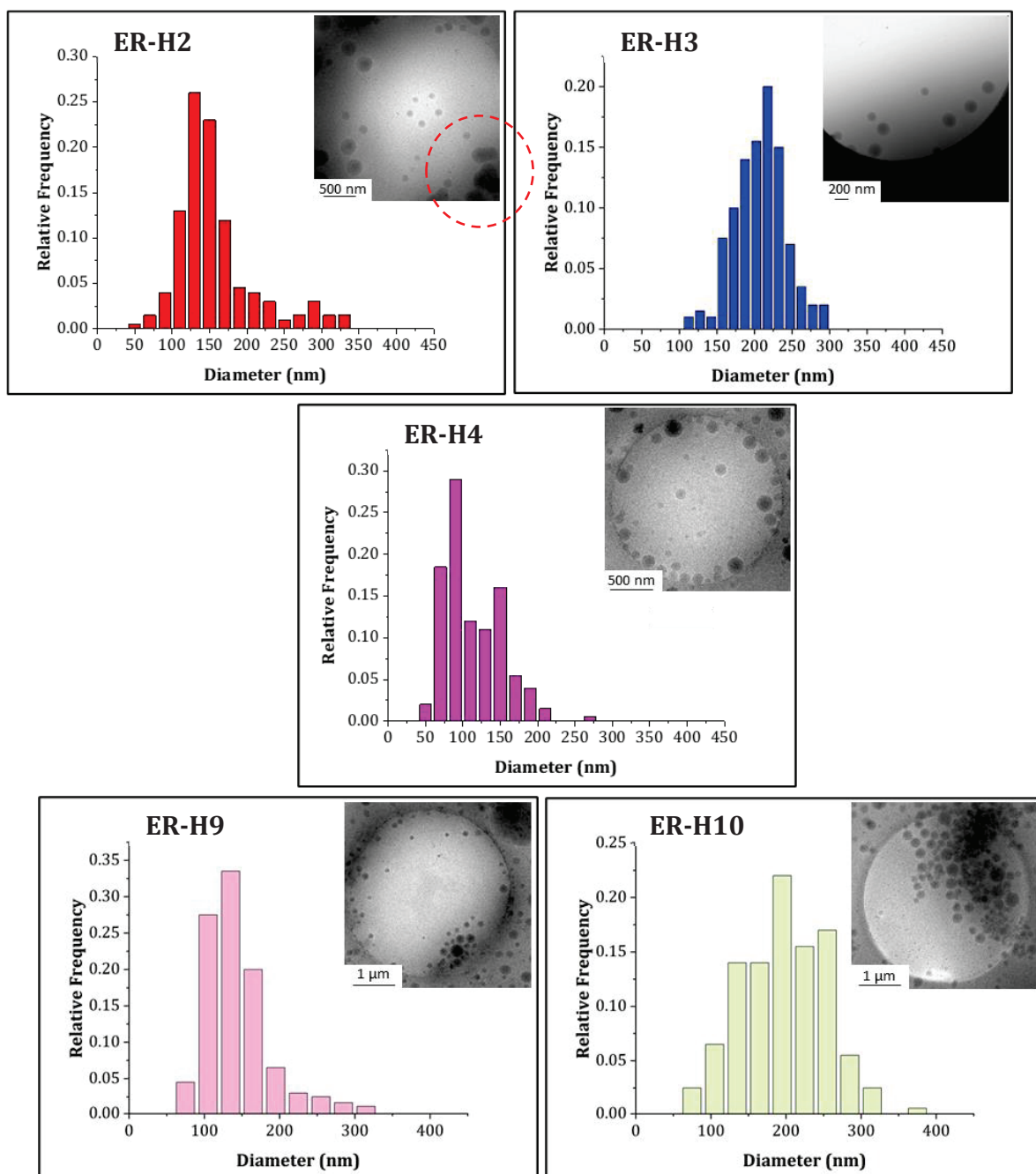


Figure V-13: Particle size distribution (PSD) obtained by cryo-TEM out of 200 particles and cryo-TEM pictures of the latexes ER-H2 (blue); ER-H3 (red); ER-H4 (pink); ER-H9 (mallow) and ER-H10 (green).

The cryo-TEM pictures of the latex obtained with H2 also highlighted some coalescence of the particles (Figure V-13, red circle). This observation is consistent with the results obtained by DLS where the particle size and particle size distribution significantly increased

from 240 to 340 nm at high conversion (approximately 98%), (**Figure V-11**, entry **ER-H2**) would indicate that 7 mol.% of VeoVa inserted in the hybrid stabilizer is close to the limit value that can be incorporated in the stabilizer before the stabilization efficiency of the copolymer is lost.

For the VL-based hybrid copolymer larger particles and larger particle size distributions were obtained when the fraction of VL inserted the stabilizer increased ( $D_n = 160$  versus 200 nm with **H9** ( $F_{VL} = 1.5$  mol.%) and **H10** ( $F_{VL} = 5$  mol.%), respectively).

Emulsion polymerization **ER-H10** (with **H10**,  $F_{VL} = 5$  mol.%) provided broader PSD compared to **ER-H3** (with **H3**,  $F_{VeoVa} = 5$  mol.%) suggesting that the nature of the hydrophobic copolymer plays a role in the nucleation efficiency of the particles. This result is consistent with the ones obtained in **Section IV**. Indeed, the VL-based hybrid copolymers dispersed in water provided aggregates (in range 90 – 240 nm), while the VeoVa-based ones organized as more defined and smaller objects (pseudo-micelles of approximately 50 nm). The size of the objects where the nucleation step is suspected to occur with these systems was smaller for the VeoVa-based hybrid copolymers, thus leading to smaller particles at the end of the polymerization compared to the VL-based ones.

The following study, which quantifies the amount of adsorbed and grafted stabilizer, will allow to know more about the mobilization of the amphiphilic hybrid block copolymers used for the stabilization of the formed latexes.

### V.1.2 Adsorbed and grafted stabilizer

The amount of adsorbed and grafted stabilizer was determined after ultracentrifugation, following the protocol described in **Experimental Section VI.8 (Table V-11)**. In the previous chapters (**II** and **III**), the specific surface area of the stabilizers was calculated *via Equation 61*, and used the  $M_n$ , assuming conservation of the polymerization degree after alcoholysis. This estimation was possible because the  $\bar{D}$  of the copolymers were low. In the present case, the estimation of  $A_s$  would not be relevant as the  $\bar{D}$  of the copolymers was high, and the value of  $M_n$  was thus not accurate. This value was therefore not considered here.

**Table V-11: Determination of the amount of adsorbed and grafted stabilizer. Comparison with Mowiol 4-88.**

Entry *	Stabilizer	%Ads&grafted <sup>a</sup>	S <sub>tot latex</sub> (x10 <sup>6</sup> cm <sup>-2</sup> ) <sup>b</sup>
ER-Mowiol	Mowiol 4-88	45	4.90
ER-H2	H2: 75_P(VOH-s-VAc)-b-100_P(VOH-s-VeoVa-s-VAc) <sub>0.911/0.075/0.014</sub>	90	4.35
ER-H3	H3: 75_P(VOH-s-VAc)-b-100_P(VOH-s-VeoVa-s-VAc) <sub>0.929/0.053/0.018</sub>	87	3.60
ER-H4	H4: 75_P(VOH-s-VAc)-b-50_P(VOH-s-VeoVa-s-VAc) <sub>0.96/0.02/0.02</sub>	67	3.57
ER-H9	H9: 75_P(VOH-s-VAc)-b-100_P(VOH-s-VL-s-VAc) <sub>0.956/0.015/0.029</sub>	86	4.60
ER-H10	H10: 75_P(VOH-s-VAc)-b-100_P(VOH-s-VL-s-VAc) <sub>0.85/0.05/0.10</sub>	88	3.40

<sup>a</sup> Obtained by Equation 58

<sup>b</sup> Obtained by Equation 50

All the latexes obtained with the hybrid stabilizers had a higher fraction of adsorbed and grafted stabilizer compared to the ones obtained with Mowiol 4-88 or the statistical stabilizers from **Chapter II** and **III (Table V-11)**, thus highlighting a better involvement of these copolymers into particle stabilization.

Additionally, and as previously suspected in **Chapter III** for the statistical structures, the fraction of adsorbed and grafted stabilizer increased with increasing the CoM content in the stabilizer. Indeed, this fraction increased from 67 to 87 and further up to 90% for the stabilizers incorporating 2, 5 and 7 mol.% of VeoVa (**H4**, **H3** and **H2**, respectively, **Table V-11**).

Similar trend was obtained with the VL-based hybrid copolymers, even if the difference between **H9** and **H10** was not very important, because high adsorption and grafting efficiency was already obtained with **H9** ( $F_{VL} = 1.5$  mol.%, %Ads&grafted = 86%).

In **Chapter II**, it was suggested that the main difference in particle nucleation efficiency between Mowiol 4-88 and the RAFT-synthesized copolymers was due to the small  $M_n$  and low  $\bar{D}$  obtained with the RAFT-synthesized copolymers. Mowiol 4-88 provided a broad molar mass distribution, and the stabilization of the particles was ensured both by adsorption (which is the main and more efficient pathway) and grafting. In the case of the RAFT-synthesized P(VOH-s-VAc), we hypothesized that grafting was more likely, hence nucleation was less efficient.

In the present case, with the hybrid structures, we already highlighted good nucleation efficiency thanks to the presence of preformed nanometric objects dispersed in water. It is thus likely that the particles are formed inside these nanoreactors, thus providing a good stabilization efficiency.

## VI. Conclusion

In summary, this chapter aimed to investigate the inclusion of a more hydrophilic block (P(VOH-*s*-VAc)) to the structure of the statistical copolymers (P(VOH-*s*-CoM-*s*-VAc)), which provided the best results in terms of ease for the synthesis and of stabilization efficiency in **Chapter III**. The limitation of these statistical copolymers was their poor dispersibility in water when the amount of CoM exceeded a certain percentage (approximately 2 mol.%). Thus, in **Chapter IV**, block copolymers were synthesized, and block copolymers P(VOH-*s*-VAc)-*b*-PVeOVA were more easily dispersible in water with up to  $F_{\text{VeOVA}} = 5$  mol.%. Adsorption and grafting efficiency was also slightly improved compared to the statistical structures (approximately 59% against 64% for the VeoVa-based statistical and block structures, respectively). However, the synthesis of such block copolymers proved to be rather difficult, and led to ill-defined structures.

The idea was therefore to combine both the block and the statistical structures, to investigate the dispersibility and the stabilization efficiency of what was called the hybrid copolymers P(VAc-*s*-VOH)-*b*-P(VOH-*s*-CoM-*s*-VAc). It was thought that the affinity of the hybrid structure with water could be enhanced thanks to the P(VOH-*s*-VAc) block, while still maintaining strong affinity with the polymer particles thanks to the presence of more hydrophobic CoM units in the second P(VOH-*s*-CoM-*s*-VAc) block. Several parameters were investigated and optimized, such as the amount of CoM, the DP of the original PVAc block and the nature of the CoM (either VeoVa or VL). However, the resulting hybrid block copolymers suffered from poor control during the extension of the first PVAc block, resulting once again into ill-defined amphiphilic copolymers after alcoholysis.

Nevertheless, we have succeeded in obtaining stable latexes with some of these hybrid structures, and the particles in these latexes had narrow PSD, almost as good as the one obtained with Mowiol 4-88. The synthesis did not allow us to compare the structures between them because of the ill-defined nature of these copolymers. However, after a thermal treatment, they were able to self-assemble in water into rather defined objects before polymerization. This allowed to use them as nanoreactors.

The grafting and adsorption efficiency was also improved compared to the latexes that contain Mowiol 4-88 and the RAFT-synthesized statistical and block copolymers synthesized so far.

Considering that these stabilizers could be industrialized and commercialized, a compromise must be found between the production cost and the stabilizing efficiency of the copolymer, regarding the content of CoM units. As a rough estimation from Sigma Aldrich, VeoVa, VL and VAc monomers cost 110, 170 and 30 € per liter, respectively, and the incorporation of 7 mol.% of VeoVa would increase the amount of adsorbed and grafted stabilizer from 87 to



90% only, compared to the stabilizer which contained 5 mol.% of VeoVa. This gain would very likely be not worth the cost increase. Besides this latex showed signs of instability which definitely leads us to definitively exclude it from the list of candidates for further development. The latex that contained the VeoVa-based hybrid copolymer with 2 mol.% of VeoVa led to poorer adsorption and grafting efficiency (67%). In light of these results, it seems that the stabilizer which contained 5 mol.% VeoVa was the best stabilizer candidate from the VeoVa-based hybrid stabilizers.

This is why a similar structure with 5 mol.% VL was synthesized. This stabilizer provided polydisperse particles, but high adsorption and grafting efficiency. The particle size of the latex could be decreased by decreasing the fraction of VL in the stabilizer without affecting the amount of adsorbed and grafted stabilizer.

As an illustration for this chapter, an idealistic configuration of the different stabilizing species involved in the stabilization of the polymers particles is provided in **Figure V-14**. Note that this is just an illustration to get a visual representation of the different structures of stabilizers (exemplified here with the VeoVa-based structures), and their possible interaction with the polymer particles.

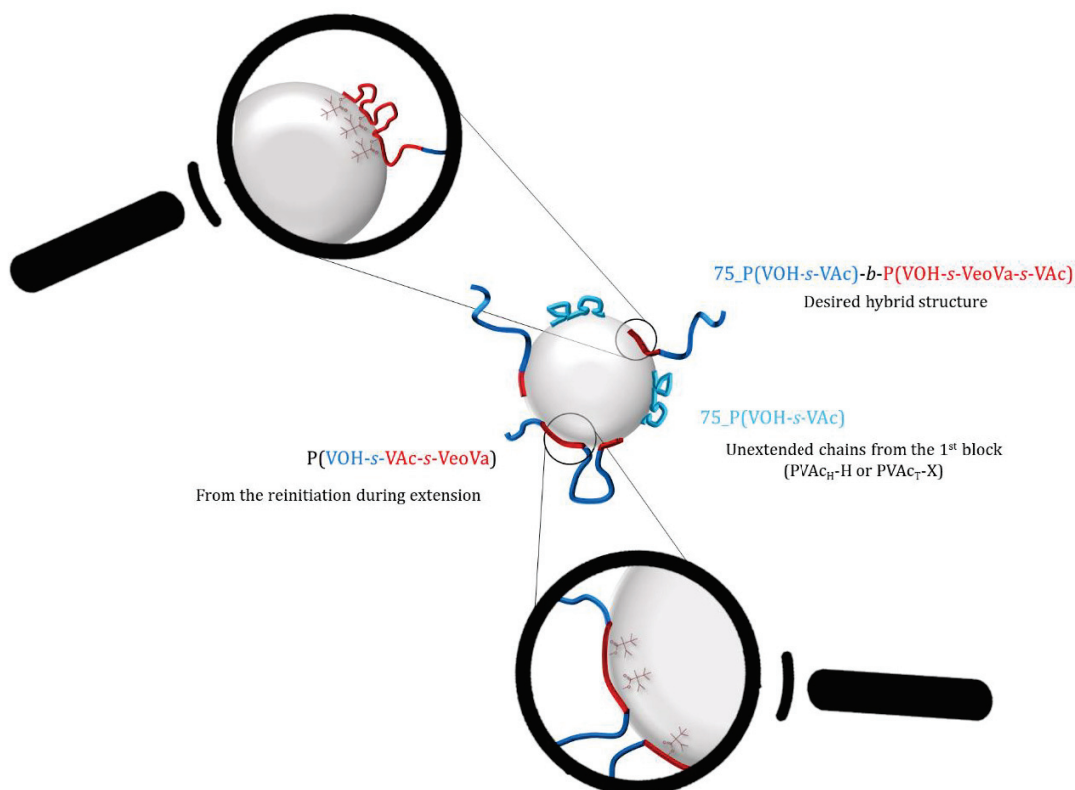


**Figure V-14:** Scheme of the hypothesized configuration of the different chains of VeoVa-based hybrid stabilizer at the surface of the polymer particles, resulting from poor chain extension efficiency of the first block during the synthesis step.



Based on the results obtained in **Chapters II to IV**, and the aim to find applications for the most promising stabilizer candidates, it was commonly decided with Wacker to try to scale up the syntheses of 75\_P(VOH<sub>0.88</sub>-s-VAc<sub>0.12</sub>) from **Chapter II** (selected as reference) 100\_P(VOH<sub>0.97</sub>-s-VL<sub>0.015</sub>-s-VAc<sub>0.015</sub>) (**S2**), which provided the best results from the statistical series in spite of its poor process reproducibility, 75\_P(VOH-s-VAc)-b-100\_P(VOH-s-VL-s-VAc)<sub>0.956/0.015/0.029</sub> (**H9**) and 75\_P(VOH-s-VAc)-b-100\_P(VOH-s-VeoVa-s-VAc)<sub>0.929/0.053/0.018</sub> (**H3**). The scale-up of the syntheses, alcoholyses and emulsion polymerizations were performed at Wacker in Burghausen over a 2-month period. This also allowed to test the reproducibility of our protocols for the hybrid structures, as it was not investigated before this internship at Wacker due to time limitation. The resulting latexes were tested in different applications, namely in mortar, spray drying and alkali resistance. Further characterizations of the selected stabilizers were also performed, such as the evaluation of their biodegradability. The results are discussed in **Chapter VI**.

## References

- [1] S. R. George, C. A. Sanders, G. A. Deeter, J. D. Campbell, B. Reck, M. F. Cunningham, *Macromolecules* **2022**.
- [2] G. Graziano, *Int. J. Biol. Macromol.* **2000**, *27*, 89–97.
- [3] T. Congdon, P. Shaw, M. I. Gibson, *Polym. Chem.* **2015**, *6*, 4749–4757.
- [4] F. Doberenz, K. Zeng, C. Willems, K. Zhang, T. Groth, *J. Mater. Chem. B* **2020**, *8*, 607–628.
- [5] E. Mendizabal, J. R. Castellanos-Ortega, J. E. Puig, *Colloids and Surfaces* **1992**, *63*, 209–217.
- [6] W. V. Smith, R. H. Ewart, *J. Chem. Phys.* **1948**, *16*, 592–599.



---

# Chapter VI

Selection of the most promising stabilizer candidates for the scale-up experiments and applications

---

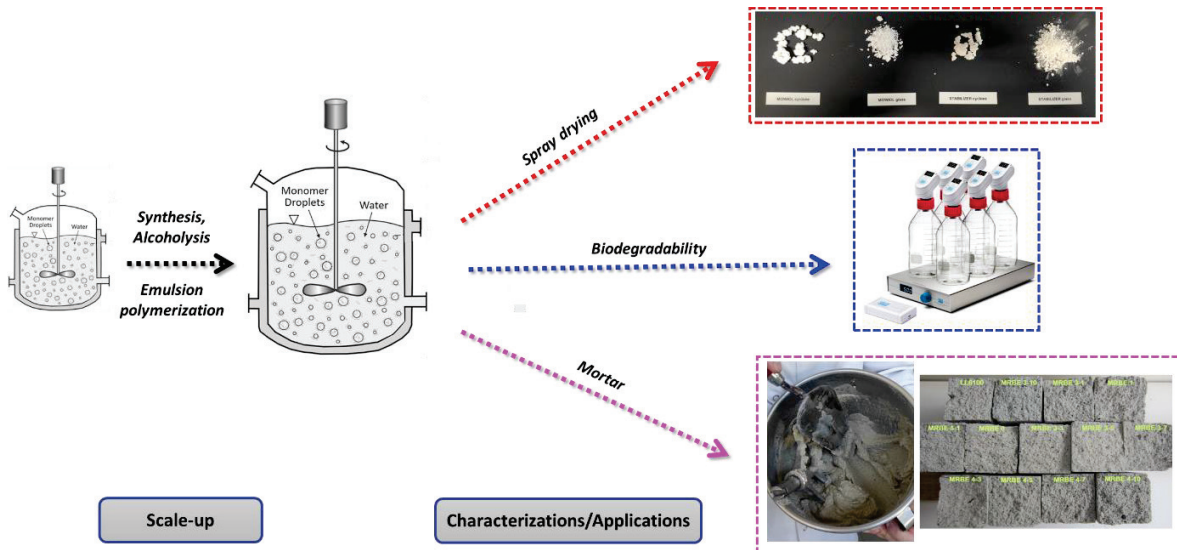


## Table of content

I. INTRODUCTION .....	288
II. SCALE-UP OF THE (CO)POLYMER SYNTHESSES .....	289
II.1 Materials.....	289
II.2 Polymerizations.....	289
II.3 Alcoholysis of the (co)polymers.....	290
II.4 Evaluation of the biodegradability of the stabilizers.....	292
III. SCALE-UP OF THE EMULSION COPOLYMERIZATIONS OF VAC AND VEOVA .....	296
III.1 Set up of the experimental parameters in a 1 L scale reactor .....	296
III.2 Influence of the amount of stabilizer on the stabilization of the particles .....	299
IV. EVALUATION OF THE PERFORMANCES OF THE LATEXES IN DIFFERENT APPLICATIONS .....	301
IV.1 Evaluation of the alkali resistance of the latexes at different pH .....	301
IV.2 Mortar application.....	303
IV.2.1 Visual observation of the formulations of mortars .....	308
IV.2.2 Tensile adhesion strength of the mortars .....	310
IV.2.3 Flexural (or bending) strength of the mortars .....	312
IV.2.4 Compressive strength of the mortars .....	314
IV.2.5 Density of the mortars.....	315
IV.2.6 Conclusion on the mortar application.....	317
IV.3 Spray drying.....	318
V. CONCLUSION .....	322

## I. Introduction

Over the course of the three years, several structures of stabilizers were synthesized and tested in the emulsion copolymerization of VAc and VeoVa. Among these structures, three were found to be promising to undergo further development, as they showed superior adsorption and grafting ability onto the polymer particles and better storage stability at high pH. These polymers are the statistical copolymer 100\_P(VOH<sub>0.97</sub>-s-VL<sub>0.015</sub>-s-VAc<sub>0.015</sub>) (**S2**) and the hybrid copolymers 75\_P(VOH-s-VAc)-*b*-100\_P(VOH-s-VL-s-VAc)<sub>0.956/0.015/0.029</sub> (**H10**) and 75\_P(VOH-s-VAc)-*b*-100\_P(VOH-s-VeoVa-s-VAc)<sub>0.929/0.053/0.018</sub> (**H3**).

In the attempt to characterize the corresponding systems further in an industrial context, with our industrial partner Wacker, the synthesis of these stabilizer candidates was scaled-up to evaluate: (i) the feasibility of pre-industrial synthesis and (ii) provide enough material for further characterizations.

The scale-up experiments were carried out in Burghausen, at Wacker's research and development center. Initially, the RAFT/MADIX polymerizations were adapted to be carried out in 500 mL mechanically stirred reactors. Then, the procedure for the alcoholyses was adapted to this large batch scale. Finally, the emulsion polymerizations were conducted in 1 L glass reactors and the ability to produce comparable polymers was assessed. These syntheses will be presented in a first section. After alcoholysis, the biodegradability of the stabilizers was evaluated.

The last section is dedicated to the evaluation of the mechanical properties of the latexes in industrial applications such as mortar and spray drying. Further investigation was also performed to evaluate the alkali resistance of the latexes stabilized with the RAFT-synthesized stabilizers.

## II. Scale-up of the (co)polymer syntheses

The first step of this scale-up process was to produce a higher quantity of the selected polymers. The polymerizations were scaled-up by a factor of five compared to the synthesis performed in Lyon, and were conducted in a 500 mL reactor with a mechanical stirrer.

### II.1 Materials

Polymerizations were carried out using VAc, VL and VeoVa (Wacker, 99%) as monomers along with AIBN (Sigma Aldrich, 98%) as initiator and RAFT/MADIX agent *O*-ethyl-*S*-(1-ethoxycarbonyl)ethyl dithiocarbonate (CTA) (synthesized as detailed in the **Experimental Section II**). The polymerizations were carried out in EtAc (Aldrich, 40 wt.%). Mowiol 4-88 (Kuraray), was used as the reference stabilizer for the emulsion copolymerizations of VAc and VeoVa. To simulate industrial processes, all chemicals were used without purification.

### II.2 Polymerizations

Quantities (monomer, solvent, initiator and CTA) were adapted from a 150 mL to a 500 mL reactor. Typical polymerization procedure is as follows:

Following deoxygenation (30 min), the monomer(s), the CTA, AIBN and the solvent were stirred at 160 rpm and heated to 62 °C *via* a thermostatic water bath. The reactions were left stirring (160 rpm) for 7 hours. The conversion was followed gravimetrically *via* a halogen moisture analyzer (thermal balance from Mettler Toledo, drying temperature range from 40 to 230 °C), until it reached 80%. After this time the polymerization medium was cooled down. The resulting products were precipitated/filtrated twice in cold petroleum ether and dried overnight in an oven at 40 °C. The resulting polymers were characterized by <sup>1</sup>H NMR in CDCl<sub>3</sub>.

After 7 h, 80 to 86% conversion was obtained for all the polymerizations. Such conversions were obtained after 6 h in the 150 mL round bottom flask reactions in Lyon. The difference in polymerization time can be attributed to differences in the reactor setup and are a consequence of the heating process in the 500 mL reactor taking more time after the degassing step. <sup>1</sup>H NMR analysis allowed for determination of the molar fraction of each monomer unit in the copolymers ( $F_{VAc}$  and  $F_{CoM}$ ). SEC-THF and <sup>1</sup>H NMR (for 75\_PVAc and 100\_P(VAc<sub>0.90</sub>-*S*-VL<sub>0.10</sub>)) were used to determine the  $M_n$  of the (co)polymers after purification (**Table VI-1**).

**Table VI-1: Characteristics of the (co)polymers synthesized in a 500 mL reactor at 60 °C in EtAc for 7 h.**

Designation	Overall Conversion (X <sub>w</sub> t%) <sup>a</sup>	F <sub>VAc</sub> <sup>b</sup> (%)	F <sub>CoM</sub> <sup>b</sup> (%)	M <sub>n</sub> (theo.) (g mol <sup>-1</sup> ) <sup>c</sup>	M <sub>n</sub> (NMR) (g mol <sup>-1</sup> ) <sup>c</sup>	M <sub>n</sub> (SEC) (g mol <sup>-1</sup> ) <sup>e</sup>	<i>D</i>
75_PVAc	86	100	-	7200	6 700	7220	1.38
100_P(VAc <sub>0.90</sub> -s-VL <sub>0.10</sub> )	80	90	10	18 000	10 500	14 200	1.40
75_PVAc- <i>b</i> -100_P(VAc- <i>s</i> -Veova) <sub>0.95/0.05</sub>	80	95	5	21 750	-	25 900	1.50
75_PVAc- <i>b</i> -100_P(VAc- <i>s</i> -VL) <sub>0.90/0.10</sub>	85	90	10	26 500	-	28 300	1.80

<sup>a</sup> Overall conversion determined gravimetrically

<sup>b</sup> Molar fraction of VAc and CoM in the (co)polymers, obtained by <sup>1</sup>H NMR (**Appendix 2**)

<sup>c</sup> Theoretical molar mass the (co)copolymers calculated from conversion

<sup>d</sup> Experimental molar mass of the (co)polymers calculated by SEC THF using PS calibration

According to this analysis method, higher conversion was reached for the extension of 75\_PVAc with VAc and VeoVa (or VL) in a glass reactor with mechanical stirring compared to the ones obtained on a small scale, in a round bottom flask with magnetic stirring and calculated *via* <sup>1</sup>H NMR (*e.g.*, 80% conversion for the VeoVa-based copolymer against approximately 67% on a smaller scale (**Chapter V, Section II**). This can be caused by a better stirring efficiency, of the polymerization medium, even when the viscosity increases at high conversion, which allows a better homogenization of the reaction and a better diffusion of the monomers and radicals.

The synthesis of 100\_P(VAc<sub>0.90</sub>-s-VL<sub>0.10</sub>) was robust as comparable *M<sub>n</sub>* and *D* were obtained after scale-up.

Hybrid copolymers with similar F<sub>VAc</sub> and F<sub>CoM</sub> than the ones obtained on a small scale were also synthesized, with a good overlay of the SEC traces (see **Appendix 11**), suggesting that the syntheses were also robust.

### II.3 Alcoholysis of the (co)polymers

Alcoholysis was first performed on 80 g of 75\_PVAc-*b*-100\_P(VAc-*s*-VL), to set up the experimental parameters in a 500 mL double-walled glass reactor equipped with a mechanical stirrer. The temperature was controlled and monitored using a thermostat (Julabo) and jacked reactor connected to a water bath, set at 32 °C. After the polymer was fully dissolved in methanol, a predetermined amount of sodium hydroxide solution ([VAc+VL]:[NaOH] of 1:0.025 used in the previous chapters, see **Experimental Section IV.2**) was introduced into the reaction medium, under stirring at 160 rpm. Regular samples were withdrawn from the reactor and quenched with acetic acid. Methanol was evaporated from these samples before <sup>1</sup>H NMR analysis in DMSO-*d*<sub>6</sub> was performed for the kinetic studies.

The evolution of the viscosity of the reaction medium was also recorded and allowed for a precise determination of the gel point time. The gel point is defined as the time when the



viscosity of the reaction medium starts to increase, indicating that the polymer starts to become insoluble in methanol after a certain hydrolysis degree (of approximately 70 mol.%). In the case where the  $[VAc+VL]:[NaOH]$  ratio was 1:0.025 (similar to the one used for the small scaled reaction), the gel point of the solution was reached after only 10 min (**Figure VI-1, (a) pink**), while it took visually approximately 20 min for the small-scaled reactions with similar ratio. It was believed that scaling effects and differences in homogenization led to shortened gel points times. Therefore, this ratio was decreased to 1:0.015 (**Figure VI-1, (a) blue**).

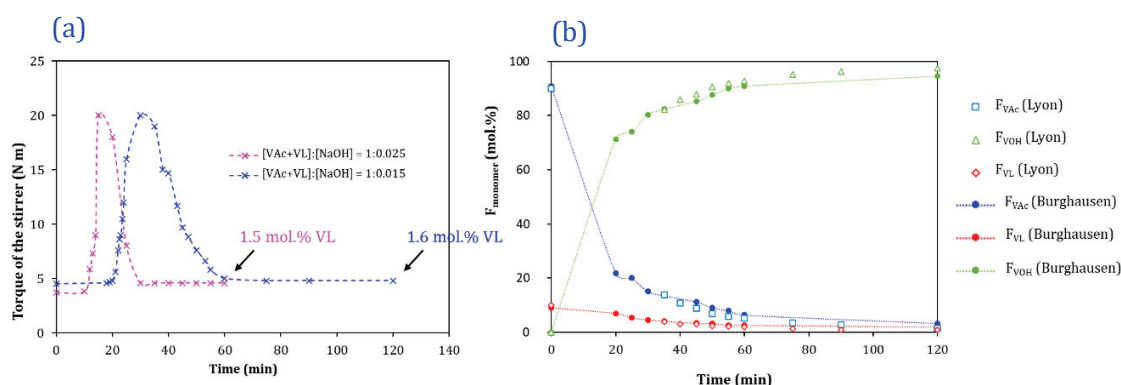


**Figure VI-1:** (a) Evolution of the viscosity of the reaction media for a ratio  $[VAc+VL]:[NaOH] = 1:0.025$  (×) and 1:0.015(×); (b) comparison of the kinetics depending on the scale and the  $[VAc+VL]:[NaOH]$  ratio, with the unfilled shapes corresponding to the experiment performed on a 45 g scale in Lyon and  $[VAc+VL]:[NaOH]$  ratio = 1:0.025, while filled shapes correspond to the experiment performed on 80 g scale in Burghausen and  $[VAc+VL]:[NaOH]$  ratio = 1:0.015. The alcoholyses were performed in methanol at 32 °C.

**Table VI-2** together with **Figure VI-1 (a)** show that the alcoholysis was faster when performed on a large scale with a ratio  $[VAc+VL]:[NaOH] = 1:0.025$ .

This ratio had to be adapted to 1:0.015 to meet similar kinetic profile as the one obtained on a small scale (**Figure VI-1, (b)**).

$^1H$  NMR of the final product was performed in  $DMSO-d_6$  to determine the composition of the copolymer for both scaled-up alcoholyses. It was observed that the targeted fraction of VL ( $F_{VL} = 1.5 - 2$  mol.%) was reached after 1 h in the case where the  $[VAc+VL]:[NaOH]$  ratio was 1:0.025 and after 2 h when this ratio was 1:0.015 (**Figure VI-1, (a)**). **Table VI-2** summarizes the final compositions of the copolymers, depending on the  $[VAc+VL]:[NaOH]$  ratio used for the alcoholyses.

**Table VI-2: Characteristics of 75\_P(VOH-s-VAc)-b-100\_P(VOH-s-VL-s-VAc) copolymer, obtained after alcoholysis of 75\_PVAc-b-100\_P(VL-s-VAc), with different [VAc+VL]:[NaOH] ratios and different scales.**

Exp.	[VAc+VL]:[NaOH] ratio	Scale (g)	Reaction time (h)	F <sub>VOH</sub> (%) <sup>a</sup>	F <sub>VL</sub> (%) <sup>a</sup>	F <sub>VAc</sub> (%) <sup>a</sup>
A	1:0.025	45	2	95.6	1.50	2.9
B	1:0.025	80	1	96.6	1.50	1.90
C	1:0.015	80	2	96.0	1.60	2.40

<sup>a</sup> Molar fraction of VOH, VL and VAc in the copolymer, calculated *via* <sup>1</sup>H NMR

The ratio [Monomer]:[NaOH] = 1:0.015 was then used to alcoholize 300 g of material for the three different (co)polymers previously synthesized. Alcoholyses times were adapted to the systems to reach the desired fractions of VOH, VAc and CoM obtained in the previous Chapters. After alcoholysis, the stabilizers were washed three times with methanol, filtrated and dried under vacuum at 40 °C for 6 h. The composition of the final stabilizers was determined by <sup>1</sup>H NMR in DMSO-d<sub>6</sub> as described in the previous Chapters.

The characteristics of these polymers, after hydrolysis are summarized in **Table VI-3**.

**Table VI-3: Library of scaled-up stabilizers.**

Entry	Alcoholysis time (min)	Reference before alcoholysis	Structure after alcoholysis
L1	50	75_PVAc	75_P(VOH <sub>0.88</sub> -s-VAc <sub>0.12</sub> )
L2	120	100_P(VAc <sub>0.90</sub> -s-VL <sub>0.10</sub> )	100_P(VOH <sub>0.965</sub> -s-VL <sub>0.017</sub> -s-VAc <sub>0.018</sub> )
L3	120	75_PVAc-b-100_P(VAc-s-VeoVa) <sub>0.90/0.10</sub>	75_P(VOH-s-VAc)-b-100_P(VOH-s-VeoVa-s-VAc) <sub>0.90/0.05/0.05</sub>
L4	120	75_PVAc-b-100_P(VAc-s-VL) <sub>0.95/0.05</sub>	75_P(VOH-s-VAc)-b-100_P(VOH-s-VL-s-VAc) <sub>0.960/0.016/0.024</sub>

This section showed that after adapting the experimental parameters, the synthesis and the alcoholysis of the selected stabilizers were robust on a higher scale. In the following section, biodegradability of the stabilizers is evaluated.

#### II.4 Evaluation of the biodegradability of the stabilizers

P(VOH-s-VAc) is one of the rare synthetic polymer known to be biodegradable.<sup>[1]</sup> This behavior presents a major advantage in medical applications, such as drug delivery. However, when it is used as a stabilizer for the emulsion (co)polymerization of VAc for water-based applications (*e.g.*, paint), the growth of bacteria and the degradation of the stabilizer

can have negative effect on the properties of the final material, such as the occurrence of moist. Nevertheless, biodegradability of the stabilizers is a sought-after parameter, as they could be eluted from a test sample, being it a paint, a paper adhesive or wood adhesive and the like. A stabilizer should be readily biodegradable for the case of exposure to exterior influences (fire, or wash-out by rain for instance).

Biodegradability of the synthesized stabilizers was determined according to a standard procedure (OECD 301F) *via* measurement of oxygen consumption (Manometric Respirometry). A measured volume of inoculated mineral medium, containing a known concentration of test substance (100 mg test substance/L) as the nominal sole source of organic carbon, was stirred in a closed flask at a constant temperature ( $\pm 1$  °C) for up to 28 days. The consumption of oxygen was determined from the change in volume or pressure (or a combination of the two) in the apparatus. Evolved carbon dioxide was absorbed in a solution of potassium hydroxide. The amount of oxygen taken up by the microbial population during biodegradation of the test substance (corrected for uptake by blank inoculum, run in parallel) is expressed as a percentage of Theoretical Oxygen Demand (ThOD).

The biological oxygen demand (BOD) ( $\text{mg O}_2 \text{ mg}^{-1}$  test chemical) is the amount of oxygen consumed by micro-organisms when metabolizing a test compound. This value was calculated after each time period by dividing the oxygen uptake (mg) of the test chemical, corrected for that by the blank inoculum control, by the weight of the test chemical used (**Equation 40**).

$$\text{BOD} = \frac{\text{mg O}_2 \text{ uptake by test substance} - \text{mg O}_2 \text{ uptake by blank}}{\text{mg test substance in vessel}} \quad (40)$$

This value is compared to the theoretical oxygen demand (ThOD), which is the total amount of oxygen required to oxidize a chemical completely. It is calculated from the molecular formula (**Appendix 12**) and is also expressed as mg oxygen required per mg test compound.

The degradation of a material is expressed as the ratio of the BOD and ThOD. According to OECD 301F the pass level for ready biodegradability is 60% of ThOD in a 10-days window, within 28 days. The 10-days window begins when 10% of the ThOD is reached. Chemicals which reach the pass levels after the 28-days period are not deemed to be readily biodegradable. In order to check the procedure, reference compounds, which meet the criteria for ready biodegradability, are tested by setting up an appropriate vessel in parallel as part of normal test runs. Suitable compounds are aniline (freshly distilled), sodium acetate and sodium benzoate. These reference compounds all degrade in these methods even when no inoculum is deliberately added.

Due to the nature of biodegradation and of the mixed bacterial populations used as inocula, determinations were carried out in duplicate and the average values were plotted (**Figure VI-2**).

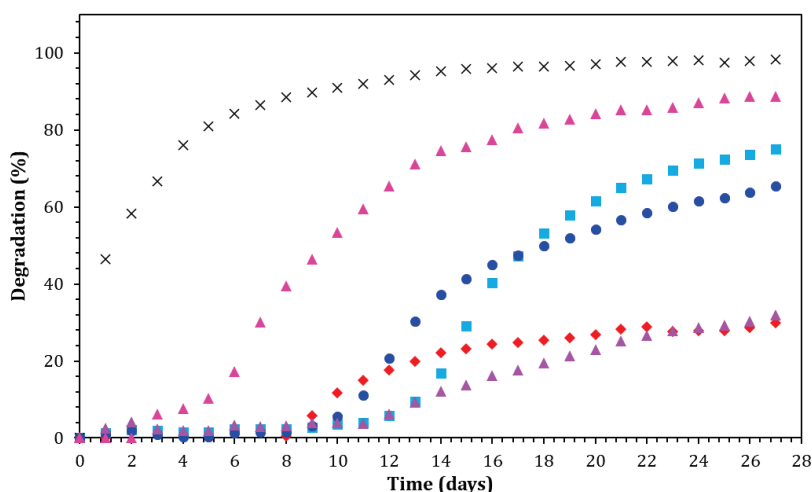


**Figure VI-2: Biodegradation of the stabilizers measured with manometric respirometer for 28-days according to OECD 301F, with (x) Sodium benzoate (reference); (▲): Mowiol 4-88; (■) 75\_P(VOH<sub>0.88</sub>-s-VAC<sub>0.12</sub>) (L1); (●) 100\_P(VOH<sub>0.965</sub>-s-VL<sub>0.017</sub>-s-VAC<sub>0.018</sub>) (L2); (▲) 75\_P(VOH-s-VAC)-b-100\_P(VOH-s-VeoVa-s-VAC)<sub>0.9/0.05/0.05</sub> (L3) and (◆) 75\_P(VOH-s-VAC)-b-100\_P(VOH-s-VL-s-VAC)<sub>0.960/0.016/0.024</sub> (L4).**

The pass level, according to OECD 301F, was reached for Mowiol 4-88 and 75\_P(VOH<sub>0.88</sub>-s-VAC<sub>0.12</sub>) (L1), which can be classified to be readily biodegradable. On the other hand, 100\_P(VOH<sub>0.965</sub>-s-VL<sub>0.017</sub>-s-VAC<sub>0.018</sub>) (L2) did not fulfill the 10-days window criterion. However, it was biodegradable because it reached 60% of ThOD. No official term for classification was found so far for this polymer. The other two samples, 75\_P(VOH-s-VAC)-b-100\_P(VOH-s-VeoVa-s-VAC)<sub>0.90/0.05/0.05</sub> (L3) and 75\_P(VOH-s-VAC)-b-100\_P(VOH-s-VL-s-VAC)<sub>0.960/0.016/0.024</sub> (L4) were poorly biodegradable as they did not reach the 10-day window nor the 60% of the ThOD. The main difference usually lies in the so called-lag-phase: long chains are longer to break into smaller species. Other properties, like blockiness, will also affect biodegradability.

The RAFT-synthesized stabilizers presented in this work, have smaller DP than the reference Mowiol 4-88. Therefore, the composition of the polymer and its structure can explain the difference in biodegradability observed: the presence of residual MeOH and sulfur from the xanthate extremity is one possible explanation for the 10-days period delay. The lower degradability of the stabilizers that contain the CoM is also noticeable. The presence of VL and VeoVa can therefore have an impact on the chain cut. Finally, poor degradability of L3

and **L4** compared to relative degradability of **L2** can be attributed to the block structures, compared to the statistical structure of the latter. Based on these results, **L3** and **L4** are not suitable for exterior paint or adhesive formulations, because they are not biodegradable. This result can still find other fields of applications. Indeed, lack of degradation means the properties of the latex would not change with time. This could be interesting in mortar for instance, when we need the material to last for several decades.

Next, the robustness of the emulsion polymerization using these selected stabilizers was evaluated in 1 L glass reactors.

### III. Scale-up of the emulsion copolymerizations of VAc and VeoVa

#### III.1 Set up of the experimental parameters in a 1 L scale reactor

Emulsion copolymerizations were performed in a 1 L jacked glass reactor equipped with a metallic anchor. The protocol described in the **Experimental Section V.2** was adapted to this scale. The volume of the fed TBHP solution was kept constant (10 mL), but the concentration of the solution was increased to meet the required ratio of [monomers]:[initiator] set up in **Chapter II**. This solution was fed over a 50-min period.

The experiment carried out with 10 wt.% of Mowiol 4-88 (**Table VI-4**, entry **ER-M1**), provided a stable and isometric latex (**Figure VI-4 (a)** and **(b)**). 88% conversion was reached after 50 min (end of the feeding time), which increased to 93% after 2 h. A longer inhibition period was observed for the 1 L experiment compared to the one carried out on a 75 mL scale (**Figure VI-3**), which is a common scaling feature. The particle size obtained from the intensity-weighted mean diameter ( $Z_{av}$ ) by DLS was 130 nm, which was comparable to the one obtained in the 75 mL reactor ( $Z_{av} = 150$  nm). However, an induction period of 18 min was observed in these conditions, in comparison to only 8 min with the same conditions in the small reactor. Again, this is usually a known and common scaling effect.

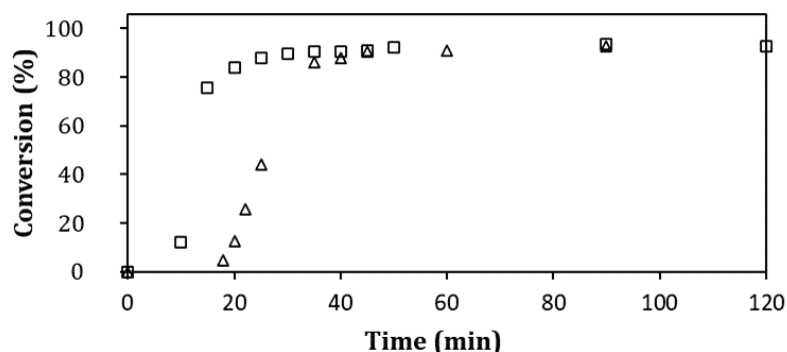


**Figure VI-3:** Kinetics of the emulsion copolymerizations of VAc and VeoVa stabilized with 10 wt.% Mowiol 4-88, carried out in a 75 mL scale (□) and in a 1 L scale (Δ) reactors, with similar initiator concentrations ( $AsAc/TBHP = 0.092/0.054$  wt.% based on monomers).

**Table VI-4: Experimental parameters for the emulsion copolymerization of VAc and VeoVa, stabilized with Mowiol 4-88 or L3 in a 1 L reactor.**

Entry	Stabilizer	AsAc/TBHP conc. (wt.% based on monomers)	Conv.2h (%)	Z <sub>av</sub> (nm)
ER-M1	Mowiol 4-88	0.092 / 0.054	93	130
ER-L3-1	L3: 75_P(VOH- <i>s</i> -VAc)- <i>b</i> -100_P(VOH- <i>s</i> -VeoVa- <i>s</i> -VAc) <sub>0.90/0.05/0.05</sub>	0.092 / 0.054	58	-
ER-L3-2	L3	0.184 / 0.110	95	270

The same experiment was carried out with 10 wt.% 75\_P(VOH-*s*-VAc)-*b*-100\_P(VOH-*s*-VeoVa-*s*-VAc)<sub>0.90/0.05/0.05</sub> (L3) (Table VI-4, entry ER-L3-1). Only 58% conversion was reached at the end of the feeding time. Therefore, an additional feed of TBHP was introduced in the polymerization medium, which increased the conversion to 84% after 2 h. This polymerization was performed a second time, with increased initiator concentration (AsAc = 0.184 wt.% based on monomers, Table VI-4, entry 2). This time a conversion of 87% was reached at the end of the feeding time (50 min), and further increased to 95% after 2 h. The resulting latex was stable and the PSD was narrow, which is similar to the results obtained at smaller scale (Figure VI-4 (c) and (d)).

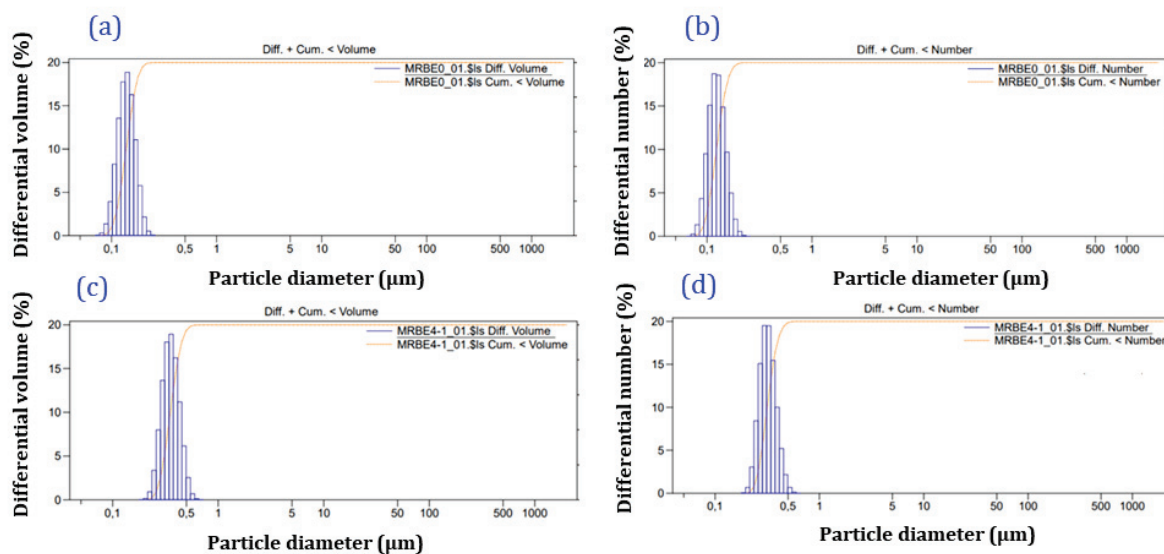


**Figure VI-4: Particle size distribution in volume and number, measured by the mastersizer for experiment ER-M1: (a) and (b) and for experiment ER-L3-2: (c) and (d).**

This new initiator ratio was kept as the reference for the following experiments. After the experimental parameters for the synthesis of 1 L latexes were established, the same experiment was carried out with the other stabilizers (L1, L2 and L4). The particle size distributions obtained *via* the mastersizer device are provided in Appendix 13. The latexes



were stable, but some of them provided coagulum (approximately 4 wt.% for the latex containing 75\_P(VOH<sub>0.88</sub>-s-VAc<sub>0.12</sub>) (**ER-L1**) (located on the anchor), 18 wt.% for the containing 100\_P(VOH<sub>0.965</sub>-s-VL<sub>0.017</sub>-s-VAc<sub>0.018</sub>) (**ER-L2**) and 7 wt.% for the latex containing the VL-based hybrid copolymer (**ER-L4**). No coagulum was obtained in **ER-L3** (with the VeoVa-based hybrid copolymer). **ER-L2** sedimented after three days and was therefore not further characterized.

For simplicity's sake, experiments **ER-L3-2** will now be shortened to **ER-L3** and the experiment carried out with 10 wt.% Mowiol 4-88 and 0.184 wt.% of AsAc will be designed as **ER-M**.

At first, the robustness of the systems containing 10 wt.% of the stabilizers was evaluated. Particle size, PSD and fraction of adsorbed and grafted stabilizer was determined and compared to the results obtained in the 75 mL scale reactor (**Figure VI-5**).

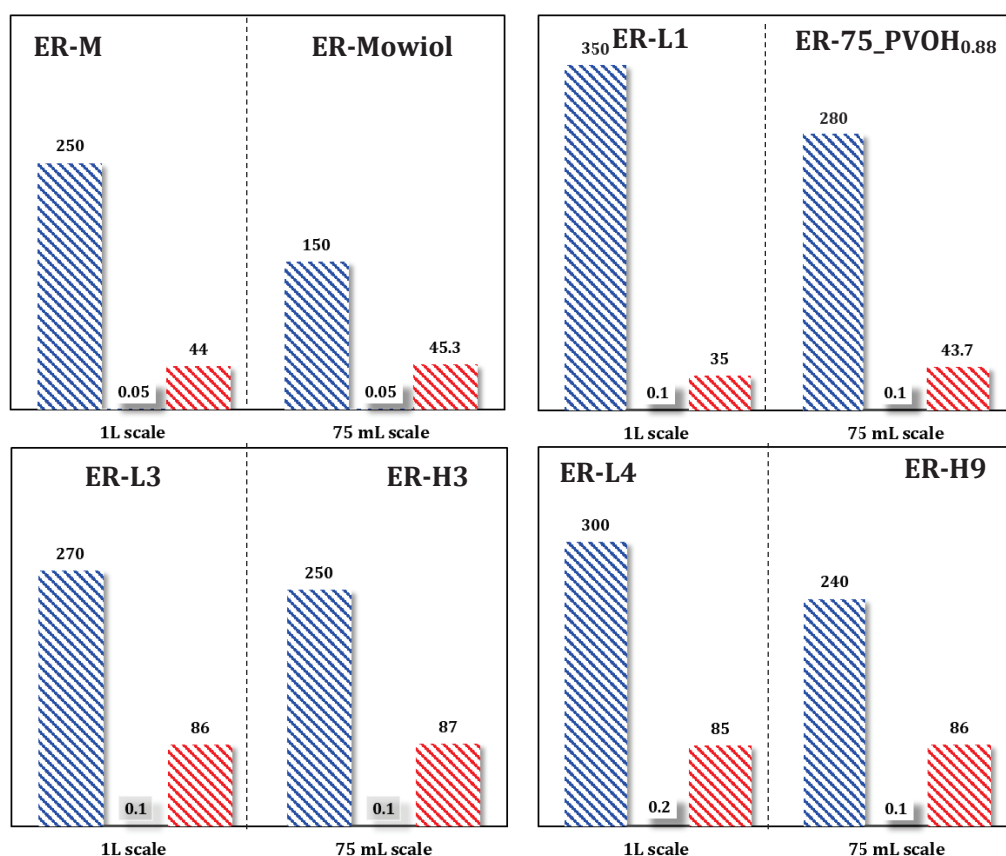


**Figure VI-5:** Colloidal features of the latexes and fraction of adsorbed and grafted stabilizer obtained for the latexes prepared with 10 wt.% of Mowiol 4-88; 75\_P(VOH<sub>0.88</sub>-s-VAc<sub>0.12</sub>) (L1); 75\_P(VOH-s-VAc)-b-100\_P(VOH-s-VeoVa-s-VAc)<sub>0.90/0.05/0.05</sub> (L3) and 75\_P(VOH-s-VAc)-b-100\_P(VOH-s-VL-s-VAc)<sub>0.960/0.016/0.024</sub> (L4) for the experiment carried out either in a 75 mL or in a 1L scale reactor. With (▨): Z<sub>av</sub> (nm) determined by DLS; (▨) the PDI and (▨) the molar fraction of adsorbed and grafted stabilizer determined after ultracentrifugation.



The particle size obtained in the 1 L scale reactor were slightly larger than the ones obtained in the 75 mL reactor (of approximately 20 to 80 nm for the experiments performed with the RAFT-synthesized stabilizers **L1**, **L3** and **L4**, and 100 nm for the experiment carried out with Mowiol 4-88). Again, this can be attributed to scaling effects, but also to the synthesis of new batches of stabilizers, which might not be perfectly identical to the ones used at smaller scale. Mastersizer-size distribution in volume highlighted the presence of aggregates (in the micrometer scale) for **ER-L1** ( $D_{v50} = 540$  nm and  $D_{v75} = 7\,690$  nm) and **ER-L4** ( $D_{v50} = 1\,400$  nm and  $D_{v75} = 4\,900$  nm), (**Appendix 12**). In both cases, the large populations can be attributed to the coagulum. The distribution in number did not show these large populations, suggesting that they are a minority in the latex.

In contrast, the latexes **ER-Mowiol** and **ER-L3** (containing the VeoVa-based hybrid stabilizer), were relatively isometric (**Figure VI-4**).

Additionally, very close values of adsorbed and grafted stabilizer were obtained, either with the 75 mL and 1 L scales (**Figure VI-5**). This result highlights that the emulsion polymerization process was not too sensitive to slight variations in the nature and composition of the stabilizers. This is a good first indication of scalability.

The previous sections demonstrated that the synthesis, alcoholysis and stabilization ability of the selected copolymers **L1**, **L3** and **L4** was reproducible on a larger scale. It was already demonstrated in **Chapter II**, that a minimum of 7 wt.% of P(VOH<sub>0.88</sub>-*S*-VAc<sub>0.12</sub>) (**L1** here) was required to obtain a stable latex. It is now interesting to determine the minimum amount of hybrid copolymer required to ensure the stabilization of the particles.

Thus, in a second set of experiments, the amount of stabilizer used in the polymerization medium was decreased from 10 to 7, 5 and 3 wt.% (based on monomer).

### **III.2 Influence of the amount of stabilizer on the stabilization of the particles**

1 L batches were performed with 3, 5, 7 and 10 wt.% of hybrid stabilizers **L3** and **L4** (**Figure VI-6**).

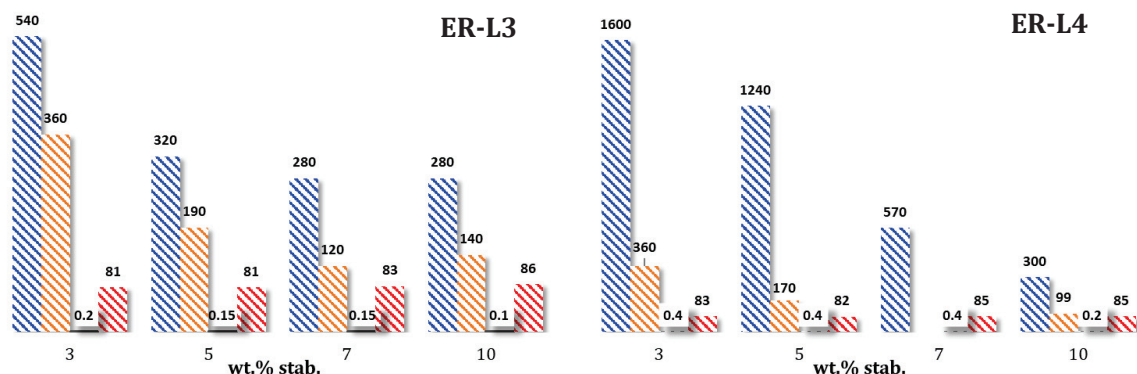


**Figure VI-6:** Colloidal features of the latexes and fraction of adsorbed and grafted stabilizer obtained for the latexes prepared with 3, 5, 7 and 10 wt.% of 75\_P(VOH-s-VAc)-b-100\_P(VOH-s-VeoVa-s-VAc)<sub>0.90/0.05/0.05</sub> (L3) and 75\_P(VOH-s-VAc)-b-100\_P(VOH-s-VL-s-VAc)<sub>0.960/0.016/0.024</sub> (L4) in a 1 L scale reactor. With (▨):  $Z_{av}$  (nm) determined by DLS; (▨):  $D_n$  (nm) obtained by Cryo-TEM; (▨): the PdI and (▨): the fraction of adsorbed and grafted stabilizer determined after ultracentrifugation.

All the latexes were stable, but coagulum (from 5 to 18 wt.% based on monomers and stabilizer) was systematically obtained with the different experiments carried out with L4. Using only 3 wt.% of stabilizer provided a stable latex both with L3 and L4, but decantation was observed after one week for the latex containing the VL-based stabilizer L4, and two months for the one containing the VeoVa-based hybrid copolymer L3. The same was true for the latex obtained with 5 wt.% of the VL-hybrid copolymer (decantation occurred after three weeks). At such Sc (20 wt.%), this decantation was expected because the particle size of the latexes stabilized with 3 and 5 wt.% of VL-based hybrid copolymer exceeded 1  $\mu\text{m}$ . Nevertheless, the dispersions were easily recovered by manual shaking. In contrast, the latexes that contain 5, 7 and 10 w.% of the VeoVa-based hybrid stabilizer remained homogeneous over months.

Figure VI-6 shows that the characteristics of the latex are a function of the stabilizer content. Additionally, the hybrid copolymer that contains VeoVa units (L3) provided smaller particles compared to that obtain with the VL-based hybrid copolymer (L4). This result is consistent with the one obtained in Chapter V, where it was highlighted that the VeoVa-based copolymer was a better stabilizer than the VL-based one.

The fraction of adsorbed and grafted stabilizer did not differ much with respect to the amount of stabilizer in the system, or with the nature of the comonomer in the hybrid structures. This shows that the stabilizers are involved in the stabilization process, and they are more compatible with the polymer than with the aqueous phase (Figure VI-6).

This set of latexes will now be evaluated in different applications.

## IV. Evaluation of the performances of the latexes in different applications

P(VAc-co-VeoVa) latexes are widely used in many applications such as paints, adhesives and mortar. Depending on the application, the final product must possess different properties (mechanical strength and pH stability for instance), and the latex plays a key role in these properties.

Thus, additional investigations on the alkali resistance of our latexes were performed, following those presented in the previous chapters (storage of the latex at low temperature). Then, the latexes were tested in mortar formulations. Finally, spray drying of the latex was also intended. The results are presented in this section.

### IV.1 Evaluation of the alkali resistance of the latexes at different pH

In the previous Chapters, the extent of hydrolysis of the polymer particles was followed over a four weeks period for some latexes stored at low temperature at different pH (ranging from 4 to 12). It was highlighted that the statistical structure that contained VL units (and to a certain extent those containing VeoVa also), provided a better resistance to hydrolysis of the latex at high pH (*e.g.*, 12). This resistance can be useful in applications such as paints or mortar formulation. For instance, within the manufacturing process of a paint, there are several factors that can destabilize the product, and this destabilization is often accompanied by a decrease in pH. This can induce a negative impact on the film characteristics and properties, such as low adhesion, poor quality color, poor texture, low gloss, procreation of bacteria and consequently a bad smell of the paint.<sup>[2-4]</sup> At pH between 5 and 9, water based paints are prone to the growth of microorganisms. Organic matters such as a nutriment and water, lead the formation of colonies aerobically (with air) or anaerobically (without air). The latter are responsible for bad odor produced during fermentation or putrefaction.<sup>[5]</sup>

In the previous Chapters, it was shown that when exposed to a high pH, the pH of the latexes containing P(VOH-s-VAc) quickly decreased to pH 6 – 7 as a result of hydrolysis of VAc units of the polymer particles. The resistance to the development of bacteria can therefore not be achieved. Little improvement was obtained when statistical P(VOH-s-VeoVa-s-VAc) was used as stabilizer, when the pH of the latex was set at 12. A decrease from pH 12 to 8 was observed within four weeks. The kinetics of this decrease was slower than for the latex obtained with Mowiol 4-88 and the RAFT-synthesized 75\_P(VOH<sub>0.88</sub>-s-VAc<sub>0.12</sub>): the pH decreased from 12 to 7 after only one week. However, it was observed that P(VOH-s-VL-s-VAc) prevented the hydrolysis of the latex to a certain extend: a plateau was reached at pH 9.5 - 10.5 over the course of the four weeks. It was thought that the hydrolysis of VL units released sodium laurate in the dispersed medium, which acted as a protective anionic stabilizer and repulsive charge towards sodium hydroxide.

However, this characteristic has not been tested for the latexes that contain the hybrid copolymers yet.

As 100\_P(VOH<sub>0.965</sub>-S-VL<sub>0.016</sub>-S-VAc<sub>0.019</sub>) did not provide a stable latex, further investigation into the pH stability was not possible. However, it was possible to study the evolution of pH for the latexes **ER-L3-x** and **ER-L4-x** that contain different amount of 75\_P(VOH-s-VAc)-b-100\_P(VOH-s-VL-s-VAc)<sub>0.960/0.016/0.024</sub> (**L4**) and 75\_P(VOH-s-VAc)-b-100\_P(VOH-s-VeoVa-s-VAc)<sub>0.90/0.05/0.05</sub> (**L3**) (with x in **ER-L-x** referring to the wt.% of stabilizer in the latex).

Two standardized aging tests were performed at 40 °C, over a twelve days period. The first one consisted in studying the evolution of the pH of P(VAc-co-VeoVa) latexes previously synthesized, and containing different concentrations of the hybrid stabilizers (**Figure VI-7, (a)** and **(b)**). The second test consisted in studying the evolution of the pH of a poly(vinyl acetate-co-ethylene) (VAE) referent latex provided by Wacker, in which 4 wt.% of stabilizers **L1**, **L3** or **L4** were added as fillers (**Figure VI-7 (c)**). In any case, the pH was set at 11.5 at day 0, and the variation of pH was measured over days.

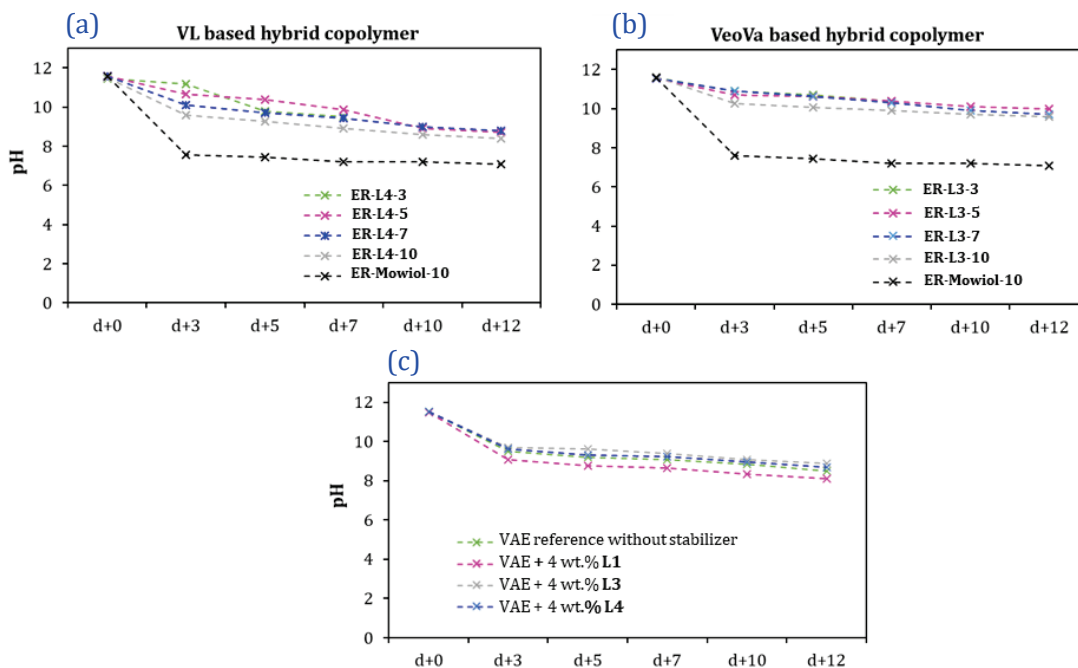


**Figure VI-7:** Aging test of the latexes stabilized with different wt.% of **(a)** the VL-based hybrid copolymer L4 and **(b)** the VeoVa-based hybrid copolymer L3 and **(c)** aging test for a reference VAE latex provided by Wacker with 4 wt.% of the different stabilizer candidates. The pH of the samples was set at 11.5 at day 0 and the latexes were stored in an oven at 40 °C.

**Figure VI-7 (a) and (b)** confirms the enhanced alkali resistance at pH 11.5 for the polymer particles stabilized with the hybrid copolymers compared to the ones stabilized with Mowiol 4-88. This aging test also highlighted that the VeoVa-based hybrid copolymer (**L4**) provided enhanced protection against hydrolysis to the polymer particles compared to the VL-based one (**L3**). Steric hindrance, provided by the VeoVa structure, and a higher proportion of VeoVa units in the structure of the stabilizer compared to VL ( $F_{\text{VeoVa}} = 5 \text{ mol.}\%$  versus  $F_{\text{VL}} = 1.6 \text{ mol.}\%$ , respectively), could limit the nucleophilic attack on the ester function of the stabilizer, and therefore, provided a better resistance of the polymer particles against hydrolysis.

**Figure VI-7 (c)** also highlights that the stabilizer did not provide this specific protection against hydrolysis when it is used as a filler. Indeed, the decrease of pH (thus the hydrolysis) of the reference VAE latex was similar when 4 wt.% of the different stabilizers were added to the latex compared to the reference latex without stabilizer.

These results show that the copolymer must be used as stabilizing agent in the system to provide resistance against hydrolysis of the overall polymer particles. This could indicate that the stabilizer must be in close contact with the polymer particles, either by strong adsorption or grafting, to ensure the protection, which is not efficient when it is simply added as a filler in the polymer matrix, and confirm that protections mentioned above may be at play in the stability against hydrolysis.

## IV.2 Mortar application

Mortars are formulated from one or more mineral binders (lime, Portland cement, plaster, gypsum) and/or organic (latex), granulate (or aggregates), additives and/or adjuvants.<sup>[6]</sup> Depending on the composition, mortars find applications in various fields such as masonry, insulation, renovation, or decoration.<sup>[6]</sup>

Latex-based mortars are also used in tile adhesives and external thermal insulation composite systems (ETICS).<sup>[7]</sup> These different industrial mortars can be conditioned in bags or silos for powdered products, in buckets for paste or ready-to-use products in mixer trucks as for concrete on large construction sites. Without the presence of the latex, water can be used to control the rheological properties of the mortar and allow the processability. It is possible to increase the fluidity of the mixture by increasing the quantity of mixing water. However, the disadvantage of such a practice is that the water/cement ratio (W/E) necessary to obtain a fluid paste is much higher than the water/cement ratio necessary for the optimal hydration of the cement (typically  $W/C_{\text{optimal}} = 0.3$ ).<sup>[8]</sup>

Under these conditions, when the material hardens, the excess water evaporates and is replaced by macroscopic pores in the cementitious matrix. Thus, the material obtained has

reduced mechanical performance compared to a material containing fewer pores. It has poor flexibility and low compressive strength. It is also vulnerable to chemical (carbonation, corrosion) and climatic attacks (in particular freeze-thaw and humidity which creates rapid biological fouling).

To overcome these limitations, adjuvants are used to the formulation of mortar. They also make it possible to modify (accelerate or delay) the hydration kinetics (hardening time) and the mechanical performance according to the requirements of the construction site. They are also the source of greater cohesion and better pumpability of the dough. The use of adjuvants was first patented at the beginning of the twentieth century.<sup>[9-12]</sup> Latexes have been used as building additives since 1924.<sup>[13]</sup> Their use became widespread in the 1960s.<sup>[14]</sup> Nowadays, the latexes most used in mortars are:

- PVAc or copolymers of VAc with ethylene (VAE), or VAc with VeoVa,
- Polystyrene or copolymers of styrene with different acrylate comonomers such as *n*-butyl acrylate,
- Poly(vinyl chloride) or copolymers of vinyl chloride with comonomers such as vinylidene chloride and vinyl propionate,
- Polyacrylates and their copolymers.<sup>[7]</sup>

The use of EVA-based latexes is more recent.<sup>[14]</sup> They provide a better resistance to hydrolysis than PVAc homopolymer, improve the processability of the mortar and decrease the required amount of water necessary for hydration.<sup>[15]</sup> These latexes are widely used in renovation work to constitute a bonding and fixing layer for most substrates.<sup>[6]</sup> They can also be used as bonding agent between bricks and plaster. This property is related to their high surface energy due to the presence of many polar functional groups in the latex.<sup>[16]</sup>

Latexes based on VAc and VeoVa are also widely used. Their applications are similar to those of VAE, and they provide better mechanical performance, flexibility and adhesion than P(VAc-*co*-ethylene) latexes.<sup>[16],[17]</sup>

If the latex increases the mechanical properties of the mortar, it also increases the time in which the paste can be easily processed after mixing, (*i.e.*, workability). This increase is often considered a side effect. Commercial mortar is a product that makes it possible to achieve an acceptable compromise between the desired properties and this side effect. Thus, to make the appropriate choice of the latex, the physico-chemical knowledge of the elements of the material needs to be treated and the cement/latex compatibility in the short and long term needs to be studied. Indeed, long-term compatibility determines the durability of structures or repairs.

The interaction between the polymer and the Portland cement is complex and has been extensively studied over the past decades. Portland cement is a mineral powder, whose property is to harden when in contact with water. For this reason, it is called a hydraulic binder. Several authors have proposed cement hydration models in the presence of a latex.<sup>[18-20]</sup> For example, according to Ohama<sup>[20]</sup>, a network structure is formed in which the cement hydrates and the polymeric phase interpenetrate to form a co-matrix. The formation of this co-matrix takes place in three steps:

**Step 1:** the latex is mixed with the cement and the latex particles are uniformly dispersed inside the cement paste, which leads to the formation of a hydrated gel, saturated with calcium hydroxide. The specific area of the cement surface increases upon hydration. The latex particles are partially deposited on the anhydrous cement grains and on the newly formed surfaces.<sup>[21]</sup>

**Step 2:** the cement progressively reacts with water to provide hydrated forms and the amount of capillary water decreases. The latex, which is trapped in the capillary pores, starts to flocculate with this decrease and forms a continuous layer of compact particles on the anhydrous gains and hydrated gel.

**Step 3:** the amount of water keeps decreasing due to the hydration reaction with the cement and due to evaporation, which leads to the coalescence of the compact layer of particles. A continuous film of polymer (or membranes) is formed and binds the cement hydrates together. This forms a three-dimensional network where the polymeric phase interpenetrates inside the partially hydrated cementitious phase. Thus, the properties of ordinary cement mortars are greatly improved by the latex. The microcracks that appear under stress and water evaporation are bridged by the polymer film or the membranes formed (**Figure VI-8**).



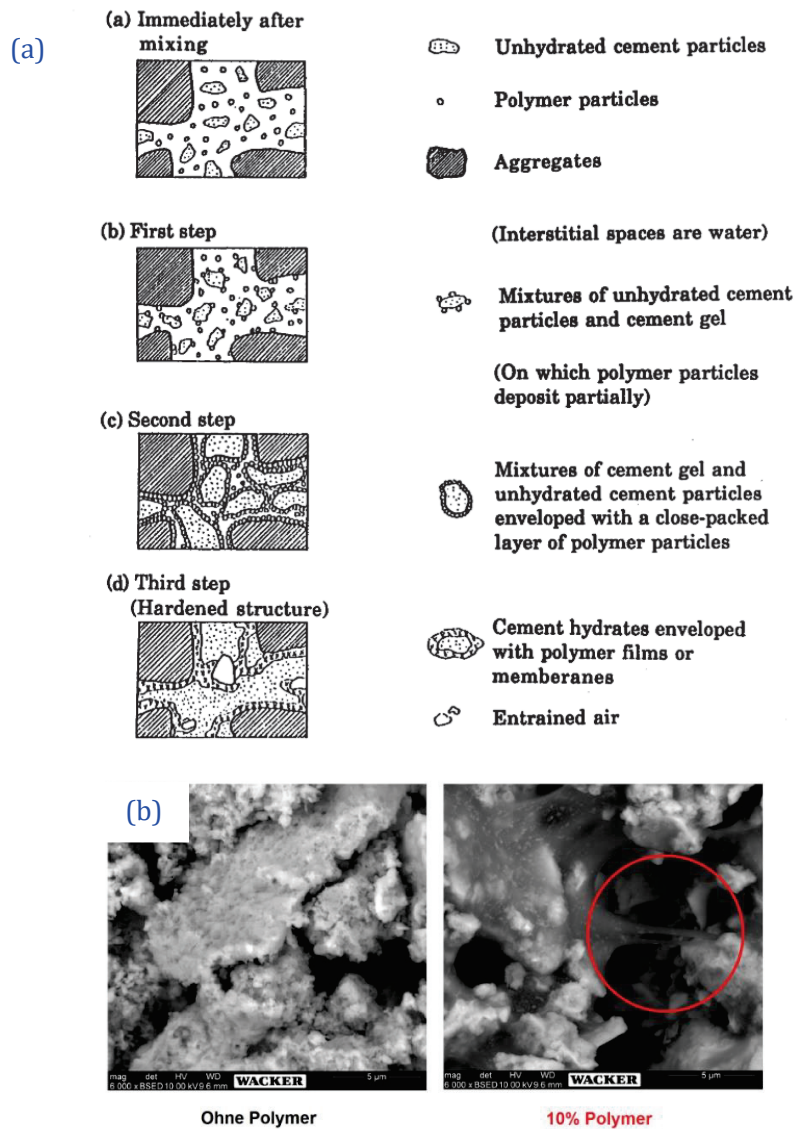


Figure VI-8: (a) Scheme of the formation of the cement/polymer co-matrix, reprinted from ref [22] and (b) Reflection electron microscopy (REM) image of a tile mortar without polymer (left) and with 10% of a reference polymer from Wacker (right). The red circle highlights the interaction between the mineral powder and the polymer.

The use of P(VOH-s-VAc) as stabilizer for the latex or its addition in aqueous solution to cement-based materials has a great influence on the performance of cement-based materials. The addition of a small amount of free P(VOH-s-VAc) can improve the workability and water retention of this material in the state of fresh mixing. P(VOH-s-VAc) can also delay the hydration of cement and the hydrolysis can affect the hydration process.<sup>[23],[24]</sup> Nguyen *et al.* showed that the chemical structure of P(VOH-s-VAc) can affect the hydration process of cement by producing acetate anion.<sup>[25]</sup> Additionally, polar groups such as hydroxyl groups



(OH) present in the stabilization system slow down the setting and reduce the final hardness of the formulations.

Nonetheless, to enhance the properties of the mortar, the polymer-based admixtures must fulfill general requirements such as:<sup>[26]</sup>

- High chemical stability towards the extremely active cations, such as calcium and aluminum ions, liberated during cement hydration,
- High mechanical stability under severers actions (shear in mortar mixing or transfer pumps etc.),
- No adverse influence on cement hydration,
- Formation of continuous polymer films in mortar, due to a lower MFFT than the application temperature, and high adhesion of the polymer film to cement hydrates and aggregates,
- Excellent water and alkali resistance,
- Thermal stability.

The quality requirements for the polymer latexes, specified in JIS A 6203 (Polymer Dispersions and Redispersible Polymer Powders for Cement Modifiers), are provided in **Table VI-5**.

**Table VI-5: Quality requirement for polymer latexes specified in JIS A 6203.**

Test item	Requirement
Appearance of the latex	Exclusive of coarse particles or coagula
Non-volatile matter	No less than 35.0 %
Adhesion <sup>a</sup>	Not less than 0.7 N mm <sup>-2</sup>
Flexural / bending strength	Not less than 5.0 N mm <sup>-2</sup>
Compressive strength	Not less than 15.0 N mm <sup>-2</sup>

<sup>a</sup>Adhesion to cement mortar

The previous section showed that the hybrid stabilizers improved the alkali resistance of the latex at high pH and prevented the hydrolysis of the polymer particle over time. Therefore, it was hypothesized that latexes stabilized with these new copolymers could improve the aforementioned limitation and provide different properties to the mortar.

Mortar formulations were prepared with latexes containing from 3 to 10 wt.% of 75\_P(VOH-s-VAc)-b-100\_P(VOH-s-VeoVa-s-VAc)<sub>0.90/0.05/0.05</sub> (**L3**) or 75\_P(VOH-s-VAc)-b-100\_P(VOH-s-VL-s-VAc)<sub>0.960/0.016/0.024</sub> (**L4**), and compared to systems containing 10 wt.% of the references Mowiol 4-88 and 75\_P(VOH<sub>0.88</sub>-s-VAc<sub>0.12</sub>) (**L1**). The dispersions were mixed with a standardized sand and cement. The water/cement ratio was set at constant value of 0.46, and

the amount of water was adjusted to reach constant ratio of water/polymer in all the samples to allow comparison. The protocol is provided in **Experimental Section VII.4**. Visual observations, tensile strength, compressive strength, adhesive strength and density tests were performed on the mortars containing the latexes with the aforementioned stabilizers, to evaluate their influence on the properties of the mortar.

#### **IV.2.1 Visual observation of the formulations of mortars**

Mortar formulations are supposed to be handled by construction workers, and hence they need to be fluid enough to facilitate the application, but not too fluid to allow good mechanical strength of the final product. Construction workers usually apply a protocol where a constant amount of water is added to the powder product, which contains standardized sand and the polymer with the stabilizer. The visual observation of the formulation is the first empirical test which must be performed when a new formulation of mortar is developed. Independently from the mechanical strength, it will give important information on the processability of the new material. The following table summarizes the visual observations that were made during the formulation of the mortar with the different stabilizers and amount of stabilizer used in the latexes. Green indicates an excellent processability, orange indicates that the processability was acceptable and red that the processability was not good: either too dry or too fluid.

**Table VI-6: Visual observations of the mortar formulations based on latexes obtained with different amount of the selected stabilizers (Mowiol 4-88, L1, L3 and L4). The colors (red, orange and green) give empirical indications onto the workability and processability (maneuverability) of the formulations.**

Entry*	stabilizer and wt.% contained in the latex used for the mortar application	Maneuverability	Evaluation
<b>MMowiol-10</b>	10 wt.% Mowiol	Poor mixing wettability 3 min, poor handling, very thick mix. Too dry	
<b>ML1-10</b>	10 wt.% <b>L1</b> (75_P(VOH <sub>0.88</sub> -s-VAc <sub>0.12</sub> ))	Poor mixing wettability after 3 min poor handling, very thick mix. Too dry	
<b>ML3-3</b>	3 wt.% <b>L3</b> 75_P(VOH-s-VAc)-b-100_P(VOH-s-VeoVa-s-VAc) <sub>0.90/0.05/0.05</sub>	Acceptable mixing wettability after 3 min. Acceptable handling, very thick mix. Too dry	
<b>ML3-5</b>	5 wt.% <b>L3</b>	Good mixing wettability after 3 min	
<b>ML3-7</b>	7 wt.% <b>L3</b>	Good mixing wettability after 3 min	
<b>ML3-10</b>	10 wt.% <b>L3</b>	Good mixing wettability after 3 min. Good handling, very airy	
<b>ML4-3</b>	3 wt.% <b>L4</b> 75_P(VOH-s-VAc)-b-100_P(VOH-s-VL-s-VAc) <sub>0.955/0.018/0.027</sub>	Acceptable mixing wettability after 3 min. Acceptable handling, very thick mix. Too dry	
<b>ML4-5</b>	5 wt.% <b>L4</b>	Good mixing wettability after 3 min	
<b>ML4-7</b>	7 wt.% <b>L4</b>	Good mixing wettability after 3 min	
<b>ML4-10</b>	10 wt.% <b>L4</b>	Mixing wettability ok after 3 min. good handling, very airy. Good adhesion on the support	

\* M refers to mortar and is followed by the code that has been used to design the stabilizer in the latex, and the wt.% of stabilizer in the latex

In general, the formulations that contained the latexes with 10 wt.% of Mowiol (**MMowiol-10**) and **L1** (**ML1-10**) presented limited wettability and processability. The ones that contained the latexes with 3, 5 and 7 wt.% of hybrid stabilizers **L3** and **L4** provided acceptable maneuverability. Finally, the formulations that contained the latexes obtained with 10 wt.% of the VeoVa-based (**L3**) and VL-based (**L4**) hybrid copolymers (**ML3-10** and **ML4-10**, respectively) provided excellent maneuverability and a very airy mortar after mixing.

## IV.2.2 Tensile adhesion strength of the mortars

To measure the tensile adhesion strength of the mortar, the formulations were square molded on standard gray concrete slab (50 x 50 x 4cm – 14 kg) (**Figure VI-9 (a)**). Four samples of the same formulation were prepared for repeatability tests. After 28 days of storage under standard climatic conditions (23 °C / 50 % humidity), an epoxy resin was then applied to the surface of the mortar samples to bond the tensile adhesion probe (**Figure VI-9 (d)**) for measurement.

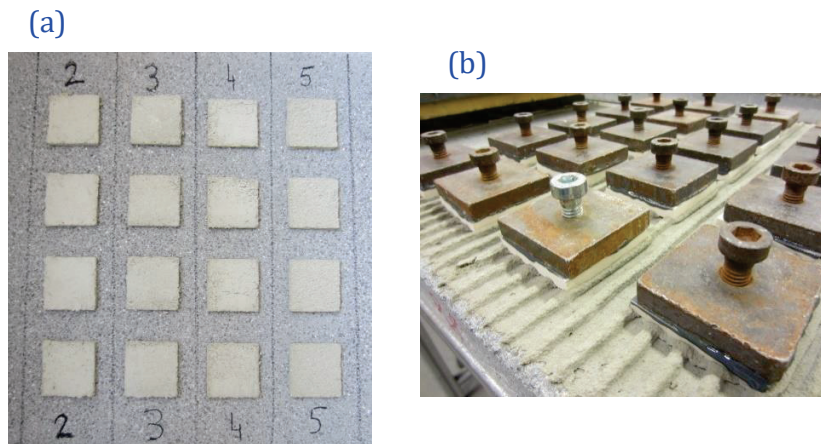


Figure VI-9: Pictures of (a) the samples molded onto a standard gray concrete slab of the KUKER brand and (b) application test to determine the cohesive strength of the mortar for tile adhesion.

The tensile adhesion strength ( $\text{N mm}^{-2}$ ) was calculated from the bond strength (kN), *via Equation 41*.

$$\text{Tensile adhesion strength (N mm}^{-2}\text{)} = \frac{\text{Bond strength (kN)} * 1000}{\text{Mortar sample area (mm}^2\text{)}} \quad (41)$$

The surface area of the pull head plate is  $50 \times 50 \text{ mm} = 2\,500 \text{ mm}^2$ .

Good mortar quality usually provides cohesive failure in the upper, middle or lower of the adhesive layer respectively. An adhesive failure within the epoxy resin or the substrate is not desired because it means that the mortar fails to bond properly with the substrate. Finally, substrate failure is rare. It means that both the cohesive strength and the adhesive strength of the mortar with the substrate are stronger than the substrate itself (**Figure VI-10**).

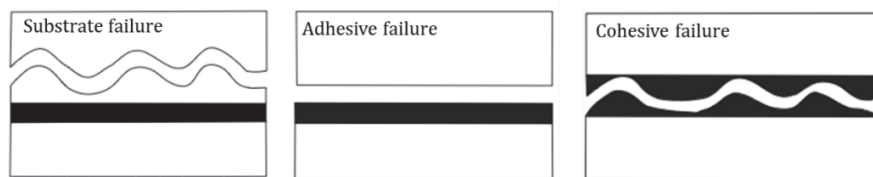


Figure VI-10 : Schematic representation of the failure modes.

The specifications to pass the adhesive test for new formulations of mortar are to reach a tensile shear strength of at least 0.7 MPa with cohesive failure (or substrate failure).

The results obtained with the different mortar formulations with the latexes containing 10 wt.% of Mowiol 4-88 of L1, and different wt.% of L3 and L4 are shown in Figure VI-11. Cohesive failures were obtained for all the samples.

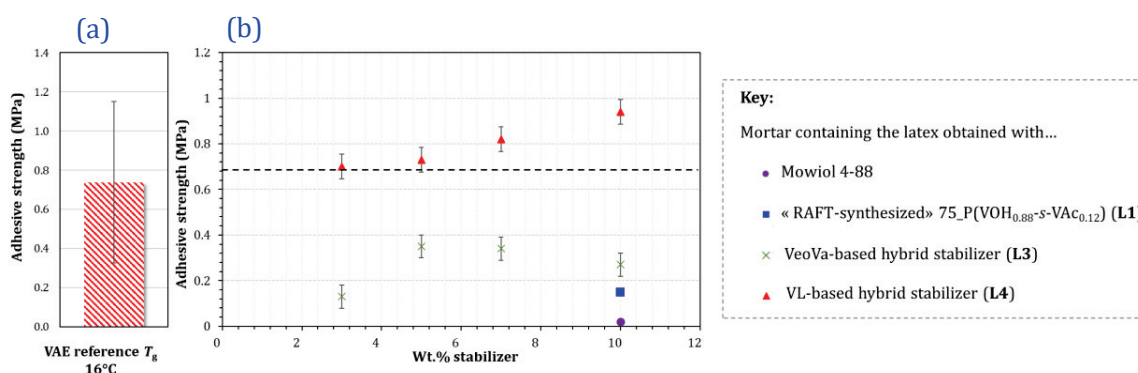


Figure VI-11: (a) Adhesive strength obtained for the mortar that contained the reference latex formulation provided by Wacker as benchmark and (b) influence of the amount and nature of the stabilizers on the adhesive strength of the mortar formulations. Dashed line represents the minimum strength to pass the test (*i.e.*, 0.7 MPa).

The adhesive strength of the mortar formulated with latexes obtained with 10 wt.% of the RAFT-synthesized stabilizer candidates was compared to a mortar containing a latex obtained with 10 wt.% of Mowiol 4-88 with a  $Sc = 20\%$ , synthesized in batch (similar protocol to the RAFT-synthesized stabilizer candidates, for comparison) (Figure VI-11 (b)). Wacker also provided VAE reference binder with  $T_g = 16^\circ\text{C}$ , containing 5 wt.% of P(VOH-*s*-VAc) (Figure VI-11 (a)). It was difficult to compare the results obtained with the reference to the ones obtained with Mowiol 4-88 and the RAFT-synthesized stabilizers, because the  $Sc$  of the latex and the protocol used for its synthesis were different from the others. Nevertheless, it can be used as a benchmark, and gives an indication on the adhesive strength that can be achieved by an existing and commercialized formulation (0.74 MPa).

At a fixed amount of stabilizer in the latex (10 wt.%), it was observed that the formulation with Mowiol 4-88 provided very low adhesive capacity (only 0.02 MPa, **Figure VI-11 (b)**) This result is surprising and remains unexplained.

In contrast, the adhesive strength of the formulations which contained latexes with 10 wt.% of the RAFT-synthesized 75\_P(VOH<sub>0.88</sub>-s-VAc<sub>0.12</sub>) (**ML2-10**) and the hybrid structures 75\_P(VOH-s-VAc)-*b*-100\_P(VOH-s-VeoVa-s-VAc)<sub>0.90/0.05/0.05</sub> (**ML3-10**) and 75\_P(VOH-s-VAc)-*b*-100\_P(VOH-s-VL-s-VAc)<sub>0.960/0.016/0.024</sub> (**ML4-10**) was successively improved: 0.15, 0.27 and 0.94 MPa, respectively. This result suggests that at a fixed amount of stabilizer, the adhesive properties of the mortar was impacted by the structure of the stabilizer.

As previously mentioned, the second objective of the scale-up experiments was to investigate the stability of the latexes and their properties with reduced amount of stabilizers. Therefore, the adhesive strength of formulations containing latexes with 3, 5, 7 and 10 wt.% of **L3** and **L4** were evaluated.

The formulations containing the VL-based hybrid structure **L4** provided excellent adhesive properties, with adhesive strength values higher than 0.7 MPa, regardless of the amount of stabilizer. A strong dependance was also visible between the VL-based hybrid copolymer content and the adhesive strength as increasing the amount of stabilizer improved the adhesive strength. The value reached up to 0.94 MPa for **ML4-10** (10 wt.% of **L4**, **Figure VI-11 (b)**).

Adversely no dependance was observed between the VeoVa-based hybrid stabilizer content (**L3**) and the adhesive strength. Optimal adhesive strength was reached for mortars that contained latexes stabilized with 5 and 7 wt.% of **L3** (0.35 for **ML3-5** and 0.34 MPa for **ML3-7**), but this strength decreased to 0.27 MPa when the latex contained 10 wt.% stabilizer (**ML3-10**).

Nevertheless, even if the benchmark value was not reached with **L3**, it provided better adhesive strength than the formulations containing either Mowiol 4-88 or the RAFT-synthesized 75\_P(VOH<sub>0.88</sub>-s-VAc<sub>0.12</sub>).

#### IV.2.3 Flexural (or bending) strength of the mortars

The three-point bending tests are carried out on specimens from the prism, measuring 4x4x16 cm, using a fatigue tensile testing machine (brand MTS), equipped with a force sensor of 20 or 100 kN according to the test (**Figure VI-12**), as described in **Experimental Section VII.4**. The crosshead descends at a fixed speed and applies a vertical force which continues on the base of the sample, and in turn stresses the latter in compression (**Figure VI-12**). Once a crack is initiated, it will propagate under the effect of increased load.



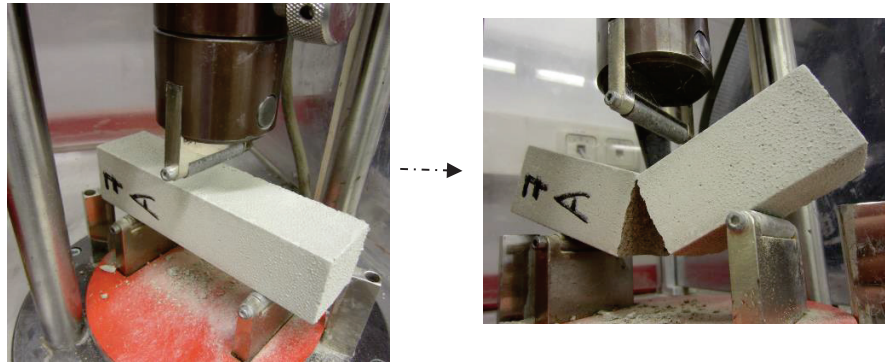


Figure VI-12: Pictures of the bending test carried out on a specimen from the prism with the MTS Systems multifunction press.

Similar to the adhesion strength, the flexural resistance of mortar formulations containing latexes stabilized with either 10 wt.% of different structures of stabilizer or formulations containing latexes with different amount of the same stabilizer was evaluated (Figure VI-13).

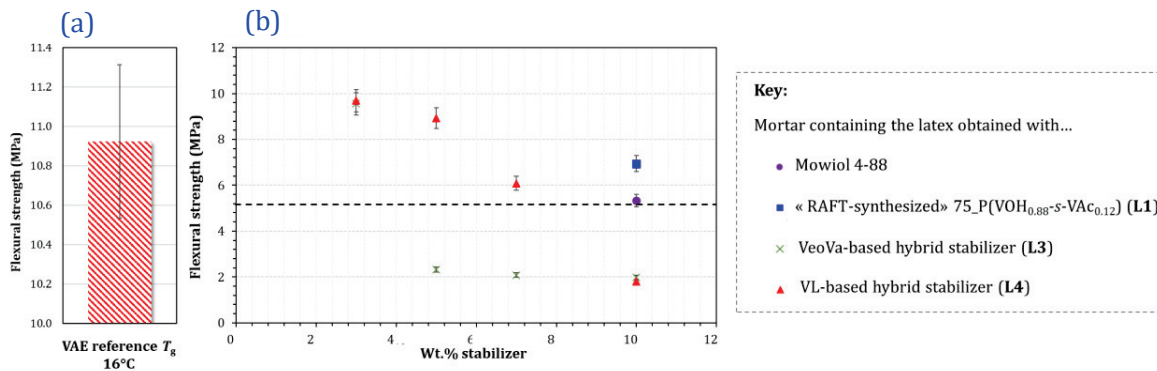


Figure VI-13: (a) Flexural strength obtained for the mortar that contained the reference latex formulation provided by Wacker as benchmark and (b) influence of the amount and nature of the stabilizers on the flexural strength of the mortars. Dashed line represents the minimum strength to pass the test (*i.e.*, 5 MPa).

The quality requirements for the mortar to pass the test (from JIS A 6203 standard) specifies a flexural strength of no less than 5.0 MPa. The mortar formulations that contained latexes obtained with 10 wt.% Mowiol 4-88 (**MMowiol-10**) and 75\_P(VOH<sub>0.88</sub>-S-VAc<sub>0.12</sub>) (**ML1-10**) passed the test, while the ones that contain latexes obtained with 10 wt.% of the hybrid structures **L3** and **L4** failed (Figure VI-13 (b)).

Nevertheless, the flexural strength of the formulation containing the hybrid stabilizer, was improved by decreasing their amount in the latex. Indeed, the flexural strength of the mortar formulations reach up to 9.55 and 9.69 MPa for **ML3-3** and **ML4-3** (mortar formulations with latexes containing 3 wt.% of the VeoVa and VL-based stabilizer, respectively). This value is well above the JIS A 6203 specifications, and close to the benchmark value provided by the reference mortar (10.9 MPa, **Figure VI-13 (a)**).

The quality specifications are also reached for the formulations **ML4-7** and **ML4-5**, which contained latexes obtained with 7 and 5 wt.% of the VL-based hybrid stabilizer, but not when the VeoVa-based hybrid stabilizer was added in the same proportions to the latex. These results highlight that both the structure and the amount of stabilizer in the latex admixture of the mortar play a role on the properties of the resulting mortar.

#### IV.2.4 Compressive strength of the mortars

The resistance and the compressive modulus are determined on the half-prisms recovered after the bending test (**Figure VI-14**).



**Figure VI-14: Picture of the compressive test carried out on a half prism with the MTS Systems multifunction press.**

Since the support/sample bearing surface is known, the software determines directly the stress  $\sigma'_m$  and the modulus  $E_c$  according to the acquisition data (force  $F'_m$  and displacement  $\varepsilon'_m$  at break) (**Equations 42 and 43**).

$$\sigma'_m = F'_m / S \quad (42)$$

$$E_c = \sigma'_m / \varepsilon'_m \quad (43)$$



The compressive resistance of mortar formulations containing latexes stabilized with either 10 wt.% of different structures of stabilizer, or formulations containing latexes with different amount of the same stabilizer was evaluated from the half prisms used in the flexural test (**Figure VI-15**).

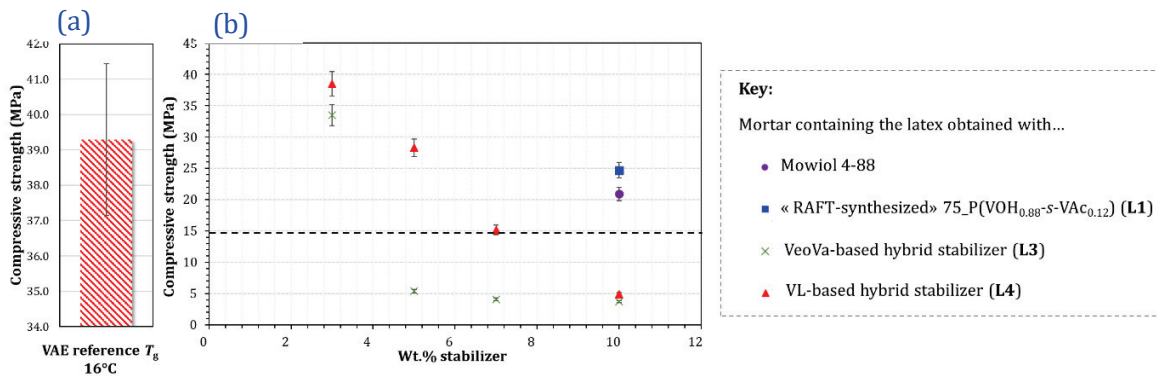


**Figure VI-15:** (a) Compressive strength obtained for the mortar that contained the reference formulation provided by Wacker as benchmark and (b) influence of the amount and nature of the stabilizers on the compressive strength of the mortar. Dashed line represents the minimum strength to pass the test (*i.e.*, 15 MPa).

The quality requirements for the polymer latexes (from JIS A 6203) specifies a compressive strength of no less than 15.0 MPa. **Figure VI-15 (b)** shows that the exact same behaviors were observed for the mortar formulations in terms of compressive and flexural resistance: formulations which contained 10 wt.% Mowiol 4-88 and 75\_P(VOH<sub>0.88</sub>-5-VAc<sub>0.12</sub>) passed the test, while it was necessary to decrease the amount of the hybrid stabilizer in the latex to reach mortar with compressive strength that met the JIS A 6203 standard.

Once again, the mortars that contained the VL-based hybrid stabilizer (**ML4-x**) provided higher compressive strengths (and met the quality requirement) with 7, 5 and 3 wt.% of stabilizer in the latex, compared to the one that contained the same amounts of VeoVa-based hybrid structure **L3**.

#### IV.2.5 Density of the mortars

With the introduction of composite materials, one challenge of the construction area is to develop light but resistant materials. Light mortar is often characterized by low density due to the presence of foam, which leads to air trapped in the final material after water evaporation. These structures tend to have poor modulus strength, because, once formed, the cracks can easily propagate. The presence of latex prevents the propagation of microcracks, since cement particles are bridged by the film of polymer formed. Some correlation between the mechanical properties and the density of the mortar were found (**Figure VI-16**).

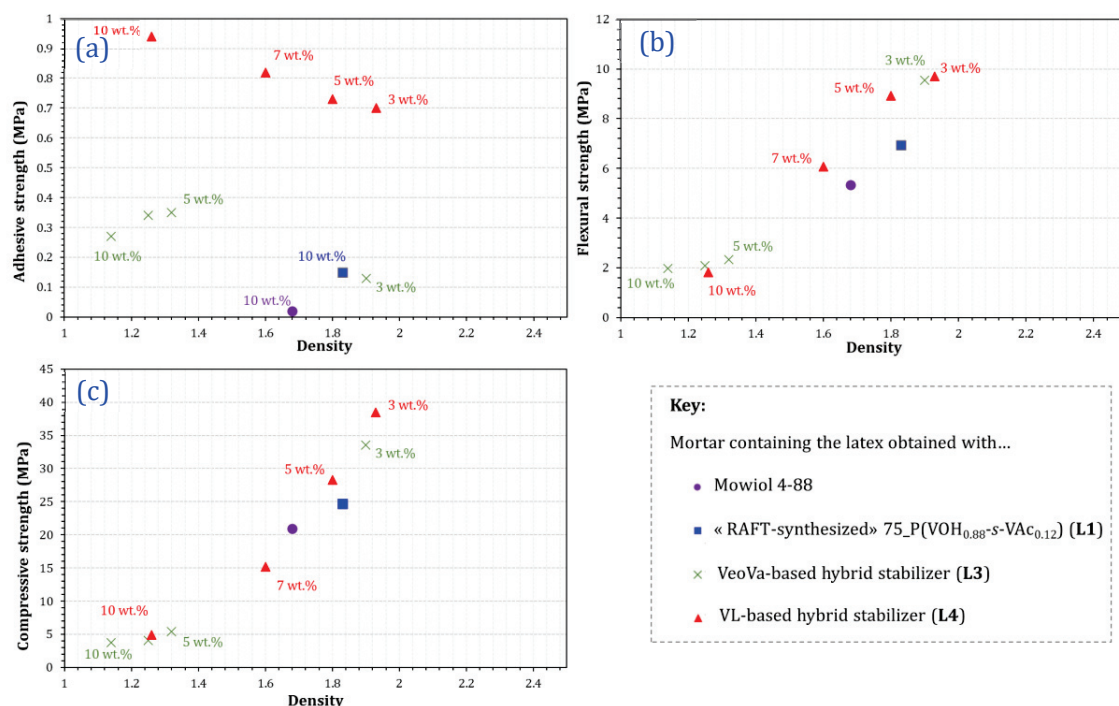


**Figure VI-16: Influence of the density on the mechanical properties of the mortar: (a) adhesive strength; (b) flexural strength and (c) compressive strength.**

**Figure VI-16 (b) and (c)** highlights a correlation between the compressive and flexural strength with the density. It was observed that for all the systems (regardless of the amount of stabilizer in the latexes), the flexural and compressive strength increased with increasing density of the mortar.

In contrast, the adhesive strength presented the reverse behavior: the higher the density, the lower the adhesive strength (**Figure VI-16 (a)**). Noteworthy, the mortars that contain the latex obtained with the VL-based hybrid copolymer provided excellent adhesive strength regardless of the density (from 0.92 to 0.7 MPa for a density ranging from approximately 1 to 2).

In addition, one can observe that the density of the mortar increased with decreasing amount of stabilizer in the latex. This is in line with the visual observation made in the previous section, where a higher amount of stabilizer produced an airier mortar. This observation highlights that, when the amount of hybrid stabilizer increases, more foam is generated in the formulations (during mixing), and this foam leads to air bubbles being entrapped in the mortar after the evaporation of water. This excess air entrapment resulted in a lower density of the resulting mortar after drying, and caused discontinuities of the formed monolithic network structure whose strength is then subsequently reduced.

#### IV.2.6 Conclusion on the mortar application

The results obtained with the different mortar formulation show that the VL-based hybrid stabilizer **L4** is the only stabilizer candidate that meets all the benchmark expectations. It provided excellent adhesion properties, compression and bending resistance (even higher than the reference and the quality requirement for polymer latexes specified in JIS A 6203), with slight variation regarding the amount of stabilizer introduced in the latex (from 3 to 10 wt.%), but always higher than the requirements to pass the tests. A good compromise can be found with this stabilizer to reach high adhesion level and high compressive and binding resistance. Indeed, it was shown that increasing the amount of **L4** improved the adhesion properties, but tended to decrease the compression and bending strength.

Mortar formulations containing Mowiol 4-88 and the RAFT-synthesized 75\_P(VOH-s-VAc) (**L1**) did not provide good adhesion properties, but they met the benchmark requirements for the compression and bending tests.

Finally, the formulation that contained the hybrid VeoVa-based stabilizer **L3** provided mixed results. None of the formulations met the adhesive strength fixed by the benchmark (regardless the amount of stabilizer in the latex), but the formulation which contained the latex obtained with 3 wt.% of **L3** met quality requirement for polymer latexes specified in JIS A 6203 for the compression and bending tests.

Based on these results, it is clear that both the quantity and the structure of the stabilizer played a role in the final properties of the mortar. Nevertheless, the interactions between the polymer and the cement are complex, so it is difficult to drive a precise conclusion about the exact role of each structure. Several hypotheses can be formulated, but further investigations are required to verify them:

1. The improved adsorption and grafting of the hybrid stabilizers (compared to Mowiol 4-88 and the RAFT-synthesized PVOH), could allowed for a better interaction between the polymer particles and the cement. Thus, a more homogeneous and continuous film surrounding the cement particles could be formed, which could improve the resistance of the mortar to compression and binding. Reflection electron microscopy could confirm or refute this hypothesis, by providing surface information.
2. In contrast to Mowiol 4-88 and the RAFT-synthesized P(VOH-s-VAc), the VL and VeoVa-based hybrid copolymers provided better alkali resistance to the polymer particles. This can also impact the polymer film formation and properties in the resulting mortar formulation.

3. Increasing the amount of stabilizer in the latexes tended to decrease the compressive and flexural strength. A possible explanation could be that the more the stabilizer, the smaller the polymer particles and particle size distributions, which is not favorable for flexural strength. Basically, Wacker uses latexes with particle size in the range of the micrometer to design mortar formulations. Another hypothesis could be that the excessive air load, due to foam forming during the mixing step, observed with the hybrid copolymers, and polymer inclusions caused discontinuities in the monolithic network. This resulted in low density mortar and can negatively affect the compressive strength.

### IV.3 Spray drying

As previously mentioned, polymeric materials are used as fillers to improve the properties of mortars. They are conditioned either as latexes or re-dispersible powders, mixed together with the cement and other fillers. In the case where the latex is mixed with the dry-mix component, the right ratio must be calculated to reach the desired properties in the final mortar. This is susceptible to human errors during mixing, and transport to the construction site is expensive (due to the weight of water). The use of re-dispersible powders presents a major advantage because it is a one-component system where the dry polymer is mixed together with the cement, sand and fillers, which only needs to be mixed with water on-site. It also presents the economic advantage of reducing transportation and packing costs and increases the product shelf life. [27],[15]

However, re-dispersibility of the polymer powder is not straightforward, particularly in the case of relatively soft polymers such as those used for these applications. A careful choice of the flow rate of the emulsion, inlet and outlet temperature must be investigated to reduce the chance of caking to occur.[28] Anti blocking agents such as clay or kaolin can also be used to reduce caking and improve the workability of the powder for re-dispersion.[26],[29]

The presence of free P(VOH-s-VAc) in the latex can have a negative impact on the viscosity of the final product after the spray drying process, when the powder is redispersed in water. It was believed that by replacing P(VOH-s-VAc) with a more hydrophobic stabilizer (hybrid structure), the amount of adsorbed and grafted stabilizer on the particles would be increased. Therefore, the affinity between the stabilizer and the particles would subsequently be improved, and the viscosity issue and caking occurring during the spray drying process could be limited. The previous Chapters already showed that the amount of adsorbed and grafted stabilizer was improved when a more hydrophobic stabilizer was used in the emulsion copolymerization of VAc and VeoVa.

We therefore investigated the impact of these stabilizers on the spray drying system, and the ability to re-disperse these powders in an aqueous medium which simulates mortar

composition. Lin Jindong *et al.*<sup>[30]</sup> already investigated the re-dispersibility of polymethyl methacrylate (PMMA) dispersions, stabilized with a thiol-terminated P(VOH-*s*-VAc). They showed that grafting of P(VOH-*s*-VAc)-*graft*-PMMA was formed during the emulsion polymerization process, and that good quality powder could be obtained by spray drying, without the use of additional filler. This powder was easily re-dispersed in water into sub-micron polymer dispersion. In the case of this present research work, hybrid structures and P(VOH-*s*-VAc) obtained by RAFT and after alcoholysis may also present a thiol end group, prone to grafting during the emulsion copolymerization of VAc and VeoVa. Therefore, it was believed that this could also have a positive impact on the spray drying system.

Spray drying tests are usually performed in pilot dryers in Burghausen with no less than 5 - 10 kg of latex, which was impossible to synthesize at a lab scale in the given 2-months period. Therefore, a lab scale dryer (Mini Spray Dryer B-290) was installed at the research and development center in Munich and the tests were conducted with 500 mL latex. A peristaltic pump was used to feed the dispersions to a fluid nozzle atomizer (inside diameter: 0.7 mm), which used compressed air from a compressor. The drying chamber (height: 400 mm; diameter: 100 mm) and the cyclone were made of thick transparent glass. The layout of the spray dryer is shown in **Figure VI-17**. Inlet drying air, after passing through an electric heater, flows concurrently with the spray through the main chamber. Dried powder was collected in the receivers from the bottom of the cyclone and in the drying chamber.

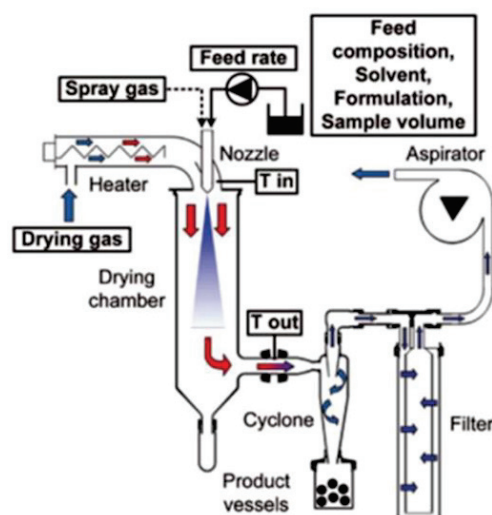


Figure VI-17: Scheme of the conventional spray-drying process, adapted from ref<sup>[31]</sup>.

Parameters such as feed flow rate, drying air temperature, and compressed air pressure for atomization were set and controlled through a computer. As this device was never used



before, it was necessary to set up the optimal experimental parameters to get the best powder possible. The first set of experiments consisted in the optimization of the inlet temperature and flow rate of the powder. The drying air flow rate and the feed temperature were kept at  $660 \text{ L h}^{-1}$  and  $25 \text{ }^\circ\text{C}$ , respectively. The inlet air temperature was varied from  $140$  to  $180 \text{ }^\circ\text{C}$ . Spray drying of the latexes stabilized with  $10 \text{ wt.}\%$  of Mowiol 4-88 and  $75\text{-P}(\text{VOH-s-VAc})\text{-}b\text{-}100\text{-P}(\text{VOH-s-VeoVa-s-VAc})_{0.90/0.05/0.05}$  (**L3**) were first performed with different air inlet and outlet temperatures ( $140, 150, 170, 180 \text{ }^\circ\text{C}$  and  $77, 85, 90 \text{ }^\circ\text{C}$ , respectively), with other parameters being constant.

After spray drying, the powder was both located inside the drying chamber and the cyclone. Both samples were collected and the label “glass” or “cyclone” were used to distinguish them (**Figure VI-18**).

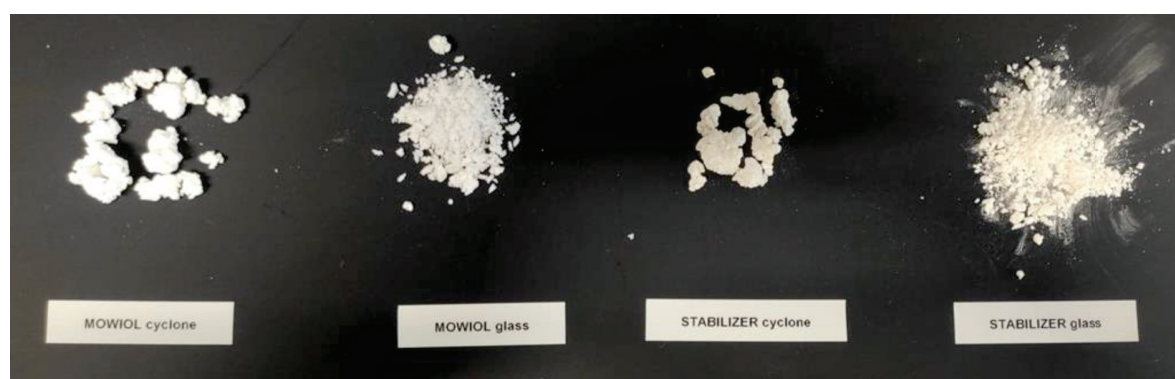


**Figure VI-18:** Example of powders (Mowiol and L3) spray dried at  $150 \text{ }^\circ\text{C}$  and recovered from the cyclone and the drying chamber.

**Figure VI-18** shows that, the powders recovered inside the cyclone and the drying chamber were visually different. The ones recovered from the cyclone were more agglomerated than the ones recovered from the drying chamber, which seemed finer. The agglomeration of the powders from the cyclone could be due to the presence of water inside the powder which was not successfully evaporated inside the drying chamber before the powder flew to the cyclone. This led to caking of the resulting powder. Similar aspects were obtained for the powers at higher temperatures.

Re-dispersion test of these spray dried powders was then carried out by mixing  $10 \text{ g}$  of the dried polymer powder with  $150 \text{ g}$  of standardized sand and  $30 \text{ g}$  of water. The mixture was homogenized by hand and mixed thoroughly in a dissolver, resulting in a milky dispersion with sand sediment. The sedimented sand was separated and the milky dispersion was analyzed *via* light scattering to determine the average particle size. None of the powders that contained Mowiol 4-88 were re-dispersible regardless of the temperature. The powders did not mix properly with the sand and water mixture, and it was therefore not possible to

characterize them. The powders that contained **L3**, which were recovered in the cyclone, were not re-dispersible either. Therefore, DLS was only performed with the re-dispersions that contained the powder with **L3** (and which were dried at different temperatures) (**Figure VI-19**).

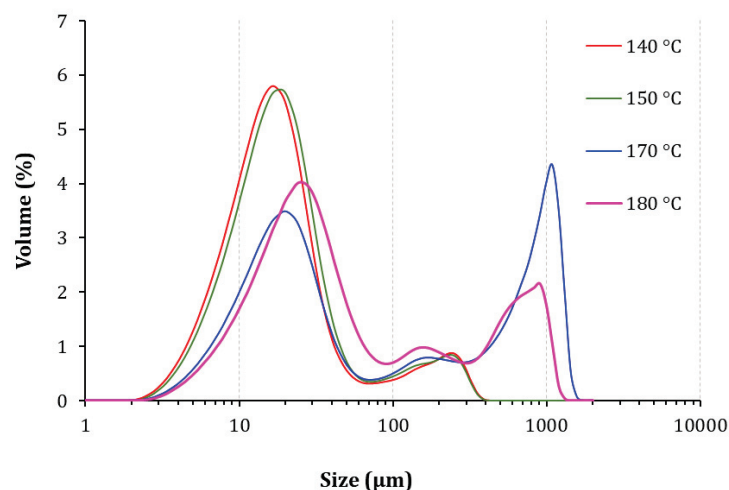


**Figure VI-19:** DLS-size distributions in intensity for the re-dispersions containing the powder L3 spray dried at different temperatures ranging from 140 °C to 180 °C.

**Figure VI-19** shows that larger particles were obtained after spray drying and redispersion of the powders, compared to the initial size before spray drying (in range 150 – 280 nm). The quality of the re-dispersion (and therefore the powder) was significantly affected by the spray drying temperatures, and none of the experimental conditions tried provided good enough quality of powders for re-dispersibility.

In spite of many attempts to optimize the parameters of the Büchi spray dryer, it was not possible to obtain a better-quality of powder to re-disperse them efficiently. The controllable parameters (temperature inlet and outlet) did not allow for complete removal of the water, which led to agglomeration of the powders inside the cyclone.

Ideally, an anticaking agent should be added to the mixture to prevent the powder from agglomerating. These anticaking agents are usually used at industrial scale in 14 m high drying chambers. It was not possible to add some in the lab scale büchi, as there was only one feed pipe for the latex. Also, the low Sc (20 wt.%) can be a limitation for spray drying at such small scale: it is difficult to remove all the water from the latex in such small drying chamber without using a too high temperature which could destroy to latex or alter its quality. Therefore, the spray drying experiments were not very conclusive and the parameters must be improved to further investigate the effect of the structure of the stabilizer (and its quantity) onto the powder properties.

## V. Conclusion

75\_P(VOH<sub>0.88</sub>-s-VAc<sub>0.12</sub>) (**L1**), 100\_P(VOH<sub>0.97</sub>-s-VL<sub>0.015</sub>-s-VAc<sub>0.015</sub>) (**L2**), 75\_P(VOH-s-VAc)-b-100\_P(VOH-s-VeoVa-s-VAc)<sub>0.93/0.05/0.02</sub> (**L3**) and 75\_P(VOH-s-VAc)-b-100\_P(VOH-s-VL-s-VAc)<sub>0.960/0.016/0.024</sub> (**L4**) were synthesized at a larger scale, and alcoholized.

Biodegradability tests was also provided to complete the characterization of the stabilizers of concern in this chapter.

Subsequently, 1 L batch latexes were obtained with these stabilizers, with acceptable reproducibility when compared to the 75 mL scale. All the latexes (except the one stabilized with **L2**) were stable and validated the scalability of the syntheses. Besides, this study showed that stable latexes could be obtained by decreasing the amount of stabilizer down to 3 wt.% for **L3** and 5 wt.% for **L4**.

By performing aging test at high pH (*e.g.*, 12) on the obtained latexes, we showed that the hybrid stabilizers provided an unexpected protection against hydrolysis over time, in contrast to the latexes stabilized with Mowiol 4-88 or the well-defined 75\_P(VOH<sub>0.88</sub>-s-VAc<sub>0.12</sub>), and that cannot be obtained when used as simple fillers.

When used in a mortar formulation, the amount of stabilizer in the latex had an influence on the mechanical strength. It was observed that an increase in stabilizer in the latex increased the adhesive properties of the latex. In contrast, the compressive and flexural strength were improved when the amount of stabilizer decreased.

Mortars that contained the latex obtained with **L4** systematically provided enhanced mechanical properties when compared to the mortar that contained the reference VAE latex provided by Wacker or the latex obtained with Mowiol 4-88 and **L1**. A correlation between the mechanical strengths and the density (and therefore the amount of stabilizer in the latex) was also highlighted.

These results showed that by adapting the composition of the latex, a library of mortars with different mechanical properties can be designed, allowing the targeting of various applications.

Eventually, spray drying tests of the latexes were not very conclusive. A small Büchi dryer was specifically installed in the laboratory to investigate the re-dispersibility of the powders obtained from the latexes. Unfortunately, in spite of the variation of the drying air temperature, the presence of residual moisture in the powders could not be avoided, affecting the re-dispersibility of the powders.



## References

- [1] R. Nagarkar, J. Patel, *Acta Sci. Pharm. Sci.* **2019**, 3, 34–44.
- [2] S. Lemain, B. Mensink, *Biocides in Paint. In-Can Preservatives in the Paint Industry: How to Stimulate Alternatives to Biocides*, **2021**.
- [3] P. Pandey, U. V Kiran, *J. Crit. Rev.* **2020**, 7.
- [4] *IPEL Brochure - Microbiological Control Solutions*, **2020**.
- [5] L. Etim, S. Antai, *Glob. J. Pure Appl. Sci.* **2014**, 20, 89.
- [6] K. Sandin, in *Build. Issues* (Eds.: C. Modena, F. Da Porto, M. Valluzzi), **1995**.
- [7] T. Goto, Influence Des Paramètres Moléculaires Du Latex Sur l'hydratation, La Rhéologie et Les Propriétés Mécaniques Des Composites Ciment/Latex. Ph.D Dissertation, Université Pierre et Marie Curie - Paris VI, **2006**.
- [8] C. Jolicoeur, M. A. Simard, *Cem. Concr. Compos.* **1998**, 20, 87–101.
- [9] L. H. Baekland, *US Patent N° 939.966.*, **1909**.
- [10] E. Varegyas, *French Patent N° 436.061*, **1911**.
- [11] Y. Jin, Interaction between Vinyl Acetate-Ethylene Latex Stabilized with Polyvinyl Alcohol and Portland Cement. PhD Dissertation., Technical University of Berlin, **2016**.
- [12] V. Lefebure, *British Patent N° 217279*, **1924**.
- [13] S. Chandra, Y. Ohama, *Polymers in Concrete*, **1994**.
- [14] H. Waron, C. Fiinch, *Applications of Synthetic Resin Latices*, **2001**.
- [15] S. Caimi, E. Timmerer, M. Banfi, G. Storti, M. Morbidelli, *Polymers (Basel)*. **2018**, 10.
- [16] M. Salomon and C. Majcherczyk, **1991**, 26–35.
- [17] R. Wang, P. M. Wang, L. J. Yao, *Constr. Build. Mater.* **2012**, 27, 259–262.
- [18] Y. Jin, D. Stephan, *SN Appl. Sci.* **2016**, 1.
- [19] R. D. Eash, H. H. Shafer, *Transp. Res. Rec.* **1975**, 1–8.
- [20] E. Sakai, S. Jun, *Cem. Concr. Res.* **1995**, 25, 127–135.
- [21] S. Zeng, N. R. Short, C. L. Page, *Adv. Cem. Res.* **1996**, 8, 1–9.
- [22] Y. Ohama, "Properties and Process Technology" in Handbook of Polymer Modified Concrete and Mortars Noyes Publications, New Jersey, **1995**.
- [23] A. Allahverdi, K. Kianpur, M. R. Moghbeli, *Iran. J. Mater. Sci. Eng.* **2010**, 7, 1–6.
- [24] D. D. Nguyen, L. P. Devlin, P. Koshy, C. C. Sorrell, *J. Therm. Anal. Calorim.* **2016**, 123, 489–499.
- [25] D. D. Nguyen, L. P. Devlin, P. Koshy, C. C. Sorrell, *J. Therm. Anal. Calorim.* **2016**, 123, 1439–1450.
- [26] Y. Ohama, *Cem. Concr. Compos.* **1998**, 20, 189–212.
- [27] X. Fan, L. Niu, *J. Adhes. Sci. Technol.* **2015**, 29, 296–307.
- [28] C. Yu, J. Ma, W. Wang, *Int. J. Food Eng.* **2010**, 6.
- [29] Z. Thomas Elwood, R. P. Bright, M. T. Phillips, *Redispersible Polymer Powders by Redistribution of Poly(Vinyl Alcohol) Dispersant.*, **1995**, US5473013A.
- [30] L. I. N. Jindong, Q. I. N. Shaoxiong, L. A. N. Renhua, C. Huanqin, **2007**, 261–265.
- [31] A. Sosnik, K. P. Seremeta, *Adv. Colloid Interface Sci.* **2015**, 223, 40–54.

---

# General Conclusion

---

**Impact on the adsorption & grafting efficiency**



- *Well-defined versus ill-defined copolymers*
- *Structure of the copolymer: statistical, block, hybrid*
- *Presence of more hydrophobic comonomer*
- *Molar mass,  $\mathcal{D}$ , blockiness index*

Amphiphilic poly(vinyl alcohol-*s*-vinyl acetate) P(VOH-*s*-VAc) copolymers are industrially obtained by alcoholysis of poly(vinyl acetate) (PVAc) and are among the cheapest and easiest macromolecular stabilizers to produce. They are widely used for the synthesis of vinyl acetate (VAc)-based latexes by emulsion polymerization. Much work has been devoted to examining the relationship between the P(VOH-*s*-VAc) structure and its aqueous properties. Indeed, the latter are dictated by many factors, the molar mass, the stereochemistry, the blockiness index and the arrangement of monomers within polymer chains. P(VOH-*s*-VAc) participates in the stabilization of the polymer particles *via* a synergy between grafting and adsorption. It was demonstrated that adsorption was the main stabilization pathway, but grafting was also important to a certain extent, and was mostly dependent on the HD of the stabilizer, while adsorption mainly relies on the molar mass and degree of blockiness. However, not all the chains are involved in the stabilization of the polymer particles, and free P(VOH-*s*-VAc) can also be found in the water phase at the end of the emulsion polymerization. This free P(VOH-*s*-VAc) can have negative impacts on the characteristics of the latex, when used in applications such as mortar and paints.

This research work aimed to develop new macromolecular stabilizers, that mimic the P(VOH-*s*-VAc) behavior, but with a better involvement in the stabilization of the polymer particles. It was thought that the addition of more hydrophobic comonomer units (CoM) such as vinyl neodecanoate (Veova) or vinyl laurate (VL) could enhance the compatibility of the stabilizer with the polymer particles, and therefore improve the adsorption and grafting efficiency. Several structures (*i.e.*, statistical and block) incorporating VAc, VOH and the CoM units were developed during this work, with some evaluated as stabilizer candidates for the emulsion copolymerization of VAc with Veova. To fully appreciate the structure-property relationships of these new copolymers, in-depth studies were carried out to understand the various effects and nuances each factor had on the properties of the latex. Reversible-deactivation radical polymerization (RDRP), namely reversible addition-fragmentation chain transfer (RAFT) / macromolecular design via interchange of xanthate (MADIX) in the present work, provided the capacity to make most of the copolymers (essentially the statistical structures), with good control over several structural features, most commonly molar mass, dispersity and chain-end functionality. The control of the syntheses of block copolymers was harder to achieve.

The questions we asked at the beginning of this research work were:

- (i) Is it possible to obtain stable latexes with P(VOH-*s*-VAc) of lower molar masses and narrower molar mass distributions compared to a commercial P(VOH-*s*-VAc) obtained by free radical polymerization, namely Mowiol 4-88?
- (ii) Does the incorporation of more hydrophobic units to the structure enhance the adsorption and grafting efficiency of the stabilizer onto the polymer particles of the latex?

- (iii) What is the impact of the structure of the stabilizer onto the characteristics of the latex?
- (iv) Are those new macromolecular stabilizers suitable to be used in industrial applications such as mortar and spray drying?

At the end of this project, we are now able to answer most of these questions.

(i). We indeed demonstrated that it was possible to use Mowiol-like P(VOH-*s*-VAc) copolymers with low molar mass and low  $\bar{D}$ , obtained by alcoholysis of chains formed by RAFT/MADIX polymerization of VAc, and still obtain stable latexes of P(VAc-*co*-VeoVa) after optimization of the experimental parameters. DLS study of the dispersions also highlighted some similarities in the aqueous phase configuration of both types of copolymers, with the presence of mostly unimers.

Nevertheless, nucleation efficiency proved lesser, and the extent of adsorption and grafting onto the polymer particles was not improved compared to the experiments carried out with Mowiol 4-88 (where it was 45%). It was postulated that the presence of several chains with different molar masses and HD in the composition of Mowiol 4-88 induced a synergy between several modes of stabilization (adsorption and grafting) that is lost in the well-defined P(VOH-*s*-VAc).

(ii). Therefore, the next aim of this research work was to investigate the impact of additional hydrophobic units along the copolymer chain to try to beneficially impact its adsorption and grafting efficiency onto the polymer particles. The more hydrophobic CoM units VL or VeoVa were identified as candidates because they were less impacted than VAc during alcoholysis, allowing the synthesis of well-defined P(VOH-*s*-VeoVa-*s*-VAc) and P(VOH-*s*-VL-*s*-VAc) with different degrees of polymerization (DPs) and CoM contents.

The main issue here was the poor dispersibility of these more hydrophobic copolymers, and only a limited fraction of inserted CoM in the structure (no more than 2 mol.%) allowed for the production of homogeneous dispersions containing aggregates observed by DLS.

Copolymers with 1 to 2 mol.% of CoM and DP = 75 and 100 were subsequently tested as stabilizer candidates in the emulsion copolymerization of VAc and VeoVa. It was shown that the latex obtained with DP = 75 was not a long-lasting stable latex, but stabilizers containing 1.5 mol.% of VL and 1 to 2 mol.% of VeoVa and DP = 100 provided stable latexes, with enhanced fraction of adsorbed and grafted stabilizer onto the particles (77 and 59%, respectively) compared to 100\_P(VOH<sub>0.88</sub>-*s*-VAc<sub>0.12</sub>) and Mowiol 4-88 (39% and 45%, respectively). They also provided to the latex resistance to hydrolysis at high pH (*i.e.*, 10 and 12) over time, where the latexes stabilized with Mowiol 4-88 or the well-defined P(VOH-*s*-VAc) failed. This characteristic was even more pronounced with the VL-based statistical copolymer than with the VeoVa-based one. This behavior might be partly attributed to the steric hindrance provided by the more hydrophobic CoM units.

Unfortunately, the reproducibility of the results obtained with 100\_P(VOH<sub>0.97</sub>-s-VL<sub>0.015</sub>-s-VAc<sub>0.015</sub>) proved to be limited.

(iii). Subsequently, with the aim to increase the CoM content in the copolymer and allow for its dispersibility in water, it was thought that block copolymers could be an alternative to the statistical structures. PVL-*b*-PVAc, PVeOVA-*b*-PVAc with low PCoM molar masses and CoM contents ranging from 5 to 20 mol.% were synthesized with rather good control, alcoholized, and the dispersibility of the resulting copolymers was tested in water. None of the VL-based block copolymers were dispersible in water, regardless of the temperature, and only 5\_PVeOVA-*b*-95\_P(VOH-*s*-VAc) provided a homogeneous dispersion after a thermal treatment, with formation of mostly defined pseudo-micelles in water. This copolymer also provided a stable latex in which adsorption and grafting of the copolymer onto the particles was enhanced. Unfortunately, poor reproducibility was obtained when a second batch of this copolymer was synthesized. The failure in reproducing the emulsion polymerization conducted with two different batches of 5\_PVeOVA-*b*-95\_P(VOH-*s*-VAc) highlights the poor robustness of the overall strategy in synthesizing PVeOVA-*b*-P(VOH-*s*-VAc) copolymer structure with small DP for the first block. This might indeed be related to the fact that targeting a very low DP with RDRP is always tricky, particularly with RAFT/MADIX, since the chains are always part of a distribution in which different DPs are produced.

We also investigated the synthesis of the reverse structure PVAc-*b*-PVeOVA. In this case, the extension of PVAc was not perfectly controlled and led to a broad molar mass distribution of the resulting block copolymer. Indeed, on the top of the difficulty in precisely targeting low molar mass blocks with RAFT, one has to keep in mind that when it comes to the synthesis of block copolymers, the quality of the final block is impacted by the efficiency of re-initiation of the starting chains and the amount of initiator used during chain extension, potentially leading to a mixture of several structures (*i.e.*, homopolymers of the first and the second block, and the desired block copolymer). Slight variations in the behavior of the polymerizations might lead to differences in the dispersibility of the final product and their efficiency when used as stabilizers in emulsion.

Nevertheless, P(VOH-*s*-VAc)-*b*-PVeOVA block copolymers (with  $F_{\text{VeOVA}}$  up to 5 mol.%) obtained after alcoholysis of the PVAc-*b*-PVeOVA were dispersible in water and self-assembled in aggregates. They also provided stable latexes with slightly improved adsorption and grafting efficiency compared to the statistical structures (up to 64%), and latexes were also obtained with good reproducibility.

These results showed that the synthesis of the statistical copolymers was straightforward and the adsorption and grafting of the corresponding alcoholized structures when used as stabilizers in the emulsion copolymerization of VAc and VeOVA were improved to a certain extent. However, the main limitations were the robustness and the limited dispersibility of these structures in water (when the CoM content exceeded 2 mol.%). Block copolymers

allowed for an increase in the amount of CoM incorporated (up to 5 mol.%), while maintaining acceptable dispersibility with water, and the adsorption and grafting efficiency was improved up to 64%.

As a general trend, it seemed thus that as long as the final structure remains dispersible in water, the higher the CoM content, the better the adsorption and grafting onto the polymer particles and that block copolymer structures seemed to perform better. It was therefore thought that the use of copolymers obtained by alcoholysis of P(VAc-*b*-P(VAc-*s*-CoM)), also called hybrid with respect to the previous statistical and block structures, could lead to the introduction of enough CoM in the chains while still allowing the dispersibility in water. Similar limitation was faced with respect to the synthesis of block copolymer, *i.e.*, broad molar mass distribution and presence of several structures in the final block copolymer, resulting in ill-defined hybrid copolymers. Nevertheless, the shift of the SEC trace towards higher molar masses highlighted efficient extension if not perfectly controlled. These hybrid structures were thus alcoholized and successfully dispersed in water after a thermal treatment. Surprisingly, they self-assembled into rather defined pseudo-micelles in water (at least for the VeoVa-based hybrid structures), both at 25 and 55 °C (emulsion copolymerization temperature). These nano-objects led to stable latexes with enhanced adsorption and grafting efficiency. VL-based hybrid structures with  $F_{VL} = 1.5$  and 5 mol.% also provided stable latexes, but the polymer particles were more disperse in size, suggesting a lower nucleation efficiency, or different affinity with the P(VAc-*co*-VeoVa) polymer particles.

These results highlighted that it was not required to synthesize well-defined copolymers to get stable latexes with enhanced affinity of the stabilizer with the polymer particles. On the contrary, the presence of a mixture of homo and copolymers resulting from the extension of the first PVAc block seemed beneficial for the stabilization, as long as this mixture of copolymers self-assembled into well-defined nanometric objects in water.

*As a conclusion* for point (iii), the design of new macromolecular stabilizers for the emulsion copolymerization of VAc and VeoVa, proved not only that the nature of the CoM, but also the CoM content and the structure of the copolymer played a significant role in the stabilization efficiency of the latex. The RAFT technique allowed the access to a wide range of structures with the formation of well-defined statistical copolymers, and a rather good control over the synthesis of the block and hybrid copolymers (with the concomitant presence of homopolymers). The limited control over the synthesis of the hybrid copolymer did not seem to be a limitation for the successful use of such structures as stabilizers. In contrast, it seemed beneficial to increase the affinity of the stabilizer with the polymer particles, resulting in high stabilization efficiency and enhanced amount of adsorbed and grafted stabilizer.

(iv). Among the various stabilizers developed, four structures were selected to test the robustness of the syntheses at a larger scale: 75\_P(VOH<sub>0.88</sub>-*s*-VAc<sub>0.12</sub>), 100\_P(VOH<sub>0.97</sub>-*s*-



VL<sub>0.015-s-VAc0.015</sub>), 75\_P(VOH-s-VAc)-b-100\_P(VOH-s-VeoVa-s-VAc)<sub>0.93/0.05/0.02</sub> and 75\_P(VOH-s-VAc)-b-100\_P(VOH-s-VL-s-VAc)<sub>0.956/0.015/0.029</sub>. The syntheses and alcoholyses were successful with good reproducibility at a larger scale. The biodegradability of these structures was evaluated. Mowiol 4-88 and 75\_P(VOH<sub>0.88-s-VAc0.12</sub>) passed the biodegradability test, while 100\_P(VOH<sub>0.97-s-VL0.015-s-VAc0.015</sub>) was poorly degradable and 75\_P(VOH-s-VAc)-b-100\_P(VOH-s-VeoVa-s-VAc)<sub>0.93/0.05/0.02</sub> and 75\_P(VOH-s-VAc)-b-100\_P(VOH-s-VL-s-VAc)<sub>0.960/0.016/0.024</sub> were not biodegradable at all. These results showed that not only the presence of a more hydrophobic unit affects the biodegradability, but also the structure of the copolymer (*e.g.*, the presence of a block).

The emulsion copolymerization of VAc and VeoVa stabilized with 75\_P(VOH<sub>0.88-s-VAc0.12</sub>), 75\_P(VOH-s-VAc)-b-100\_P(VOH-s-VeoVa-s-VAc)<sub>0.93/0.05/0.02</sub> and 75\_P(VOH-s-VAc)-b-100\_P(VOH-s-VL-s-VAc)<sub>0.960/0.016/0.024</sub> on a 1 L scale provided similar results to the ones carried out at 75 mL scale. Only the latex obtained with 100\_P(VOH<sub>0.97-s-VL0.015-s-VAc0.015</sub>) sedimented after a few days and was not suitable for further characterization.

Stable latexes were obtained with no less than 3 wt.% and 5 wt.% of VeoVa-based and VL-based hybrid copolymers, respectively, where, in our conditions, the minimum amount of 75\_P(VOH<sub>0.88-s-VAc0.12</sub>) required to obtain a stable latex was 10 wt.% (and 7 wt.% for Mowiol 4-88). These latexes were tested in various applications such as spray drying, aging test at high pH and in mortar formulations.

The spray drying tests were not conclusive because of the extensive presence of moisture in the resulting powders, which was not successfully removed despite the variation of the inlet air temperature. The resulting powders proved to be hardly dispersible. Further investigations must be carried out to improve the process. The addition of an anticaking agent or the use of a more adapted spray dryer for small scaled experiments could be an option.

The aging test at pH 11.5 and 40 °C confirmed the previous observations where the stabilizer which contains a more hydrophobic unit prevents the hydrolysis (and thus degradation) of the latex at high pH. This behavior could be of great interest for applications such as high pH paints or mortar.

Hence, the influence of the amount and nature of stabilizer in the latex onto the mechanical properties of a mortar formulation was investigated. When added to the mortar formulation, the latexes that contained the VL-based hybrid stabilizer always provided improved mechanical properties (depending on the percentage of stabilizer in the latex) compared to the reference latex provided by Wacker, or the latexes stabilized with Mowiol 4-88 and 75\_P(VOH<sub>0.88-s-VAc0.12</sub>), while the mortar with the latex containing the VeoVa-based hybrid copolymer provided mixed results. These results showed that it was possible to create a library of mortars for targeted applications by simply varying the stabilizer content and composition in the latex, which was already quite satisfying.



All in all, previous studies already showed that not only are the kinetics different, but also the evolution of the number of particles, the amount of grafted polymer, and subsequently, the final latex properties were affected by the microstructure of commercial P(VOH-*s*-VAc) (*i.e.*, blockiness index, HD, molar mass). This present research work also highlighted that several other parameters can influence these properties: the choice of the polymerization technique (either RAFT or FRP), the incorporation of more hydrophobic monomer units into the structure of the copolymer, the nature of the more hydrophobic monomer units and the structure of the stabilizer (*i.e.*, statistical, block or hybrid).

To go further, as it was highlighted that a mixed composition of stabilizers could be beneficial for the stabilization of the latex, it could be highly interesting to evaluate the stabilization efficiency, and extent of adsorption and grafting provided by mixing the structures developed over the course of these three years with Mowiol 4-88. It could also be beneficial to reduce the cost of production of the latex compared to a latex exclusively stabilized with the RAFT-synthesized structures.

Star copolymer structures were not investigated in the present work. Nevertheless, star poly(vinyl pyrrolidone) already proved to have excellent stabilization efficiency when used as stabilizers in suspension polymerization to prepare crosslinked P(VeoVa-*co*-ethylene glycol dimethacrylate) microspheres.<sup>[1]</sup> PVP star copolymer decreased the surface tension, and resulted in an isometric latex with small particle size, compared to the statistical and block structures. Star copolymers are also known to reduce the viscosity when used as additives in certain applications, such as in oil products. It could be of great interest to transfer the PVP star structure to the monomers used in this thesis, and evaluate the ability of a VAc, VOH and CoM-based star copolymer to act as a stabilizer in the emulsion copolymerization of VAc and VeoVa.

## Reference

- [1] U. T. . Nguyen, K. Eagles, P. T. Davis, W. Barner-Kowollik, M. H. Stenzel, *J. Polym. Sci. Part A Polym. Chem.* **2006**, *44*, 4372– 4383.



---

# Experimental procedures and characterization techniques

---

## Table of content

I. MATERIALS.....	334
II. SYNTHESIS OF THE RAFT AGENT.....	334
III. POLYMERIZATION PROCEDURES.....	336
III.1 Homopolymerization of VAc (Chapter II).....	336
III.2 Homopolymerization of VeoVa and VL (Chapter IV).....	336
III.3 Statistical copolymerization of VAc and VeoVa or VL (Chapter III).....	337
III.4 Block copolymerization of VAc and either VeoVa or VL (CoM) (Chapters IV and V).....	338
III.4.1 Chain extension of PVAc-X with VeoVa (Chapter IV).....	338
III.4.2 Chain extension of PCoM-X with VAc (Chapter IV).....	338
III.4.3 Chain extension of P(VAc <sub>0.90</sub> - <i>s</i> -VeoVa <sub>0.10</sub> )-X with VAc (Chapter V).....	338
III.4.4 Chain extension of PVAc-X with VAc and either VeoVa or VL (Chapter V).....	339
D. Extension of 75_PVAc-X.....	339
E. Extensions of PVAc-X of different DPs (DP1).....	339
IV. ALCOHOLYSIS PROCEDURES.....	340
IV.1 Alcoholysis of PVAc.....	340
IV.2 Alcoholysis of statistical and block copolymers.....	340
V. EMULSION COPOLYMERIZATION OF VAc AND VEOVA.....	342
V.1 Screening with KPS (Chapters II and III).....	342
V.2 Emulsion copolymerization of VAc and VeoVa initiated by a redox couple.....	342
V.3 Scale up of the emulsion polymerization to a 1000 mL reactor.....	343
VI. CHARACTERIZATION TECHNIQUES.....	345
VI.1 Nuclear magnetic resonance (NMR).....	345
VI.2 Size exclusion chromatography (SEC).....	345
VI.3 UV-visible spectroscopy.....	346
VI.4 Fourier-transform infrared (FTIR) spectroscopy.....	346
VI.5 Gravimetric analysis.....	347
VI.6 Dynamic light scattering (DLS).....	347
VI.7 Cryogenic electron transmission microscopy (Cryo-TEM).....	348
VI.8 Determination of the amount of adsorbed & grafted stabilizer.....	348
VI.9 Surface tension.....	350
VII. PROCEDURES FOR THE USE OF THE LATEXES IN VARIOUS FIELD OF APPLICATION.....	351
VII.1 pH stability.....	351
VII.2 pH stability for latexes stored in the fridge.....	351
VII.3 Aging tests: pH stability for latexes stored at 40 °C.....	351
VII.4 Mortar calorimetry.....	351
VII.4.1 Formulation.....	351
VII.4.2 Sample preparation and conditioning.....	352
VII.4.3 Measuring.....	352
VII.4.4 Evaluation.....	353
VII.5 Spray drying.....	354

## I. Materials

Vinyl acetate (VAc, Wacker, 99%), Vinyl neodecanoate (Versa®10, Wacker, 99%), Vinyl laurate (Versa®12, Wacker, 99%), Mowiol 4-88 (Wacker), 2,2'-azobis(isobutyronitrile) (AIBN, Aldrich, 98%), *tert*-butyl hydroperoxide solution (Aldrich, 70 wt.% in water), ascorbic acid (AsAc, Aldrich, 99%), ammonium iron(II) sulfate (Aldrich, 99%), 4-methoxyphenol (Aldrich, 99%), potassium persulfate (KPS, Aldrich, 99.99%), ethyl 2-bromopropionate (Aldrich, 99%), potassium ethyl xanthate (Aldrich, 99%), ethyl acetate (EtAc, Aldrich, >99.5%), tetrahydrofuran (THF, Fisher, HPLC grade), petroleum ether (Aldrich), acetone (Aldrich, >99.5%), dichloromethane (Aldrich, >99.5%), ethanol (Aldrich, >99.5%), methanol (Aldrich, >99.5%), sodium hydroxide (NaOH, Aldrich, >98%), acetic acid (Aldrich, >99%), formic acid (Aldrich, >99%), hydrochloric acid (Aldrich, 37%) (Wacker, 55 wt.% in water), were used as received.

Deuterated dimethyl sulfoxide (DMSO- $d_6$ , Fisher, 99.6%), and deuterated chloroform ( $CDCl_3$ , Fisher, 99.8%) were used for NMR characterizations.

## II. Synthesis of the RAFT agent

*O*-ethyl-*S*-(1-ethoxycarbonyl)ethyl dithiocarbonate (CTA) was synthesized according to a procedure adapted from the literature.<sup>[3]</sup>

Ethyl-2-bromopropionate (11.298 g, 0.062 mol) was dissolved in 100 mL of ethanol in a 250 mL round bottom flask. The reaction medium was cooled to 0 °C. Subsequently, potassium ethyl xanthate (12.005 g, 0.075 mol) was added to the solution over a period of 30 min. The resulting mixture was degassed with argon for 30 min and stirred at room temperature for 24 h. The mixture was then filtered and the solvent removed by rotary evaporation (40 °C, 175 mbar) to give a yellow liquid.

This liquid was dissolved in dichloromethane and a liquid-liquid extraction was performed with water (3 x 75 mL) to remove the remaining KBr. The product was then dried with  $MgSO_4$  and filtered. The solvent was removed under reduced pressure to give the pure product.

The  $^1H$  and  $^{13}C$  NMR spectra show no impurities in the final product, which was thus used without any further purification.

Yield: 89.15%.  $^1H$  NMR ( $CDCl_3$ ):  $\delta$  (ppm) = 4.60 (q,  $CH_3-CH_2-O$ ), 4.35 (q,  $S-CH-(CH_3)-C$ ), 4.18 (q,  $O-CH_2-CH_3$ ), 1.54 (d,  $CH_3-CH-$ ), 1.39 (t,  $CH_3-CH_2-O$ ), 1.26 (t,  $CH_3-CH_2-O$ ).

$^{13}C$  NMR:  $\delta$  (ppm) = 13.8 ( $CH_3-CH_2-O-R1$ ), 14.1 ( $CH_3-CH_2-O-R2$ ); 17 ( $CH_3-CH-R3$ ); 47.5 ( $-CH-S$ ); 61.7 ( $CH_3-CH_2-O-R1$ ); 70.4 ( $CH_3-CH_2-O-R2$ ); 171.4 ( $-C=O$ ); 212.3 ( $-C=S$ ).

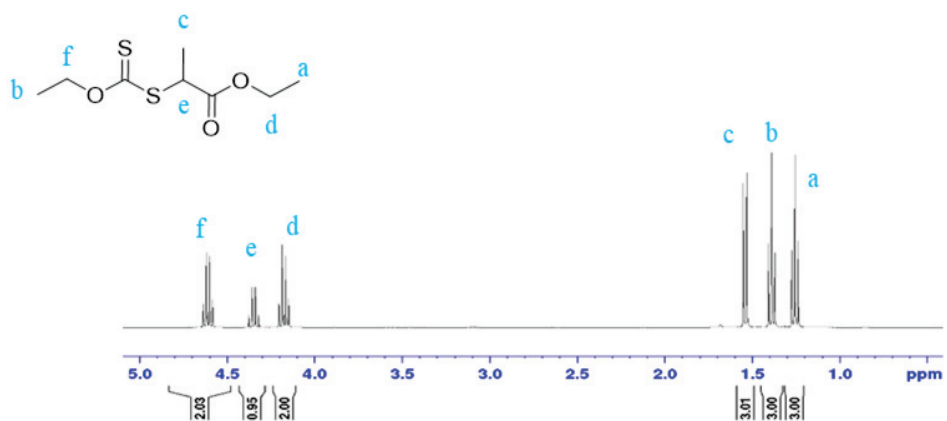


Figure VIII-1: <sup>1</sup>H NMR of *O*-ethyl-*S*-(1-ethoxycarbonyl)ethyl dithiocarbonate, CDCl<sub>3</sub>, R.T, 256 scans.

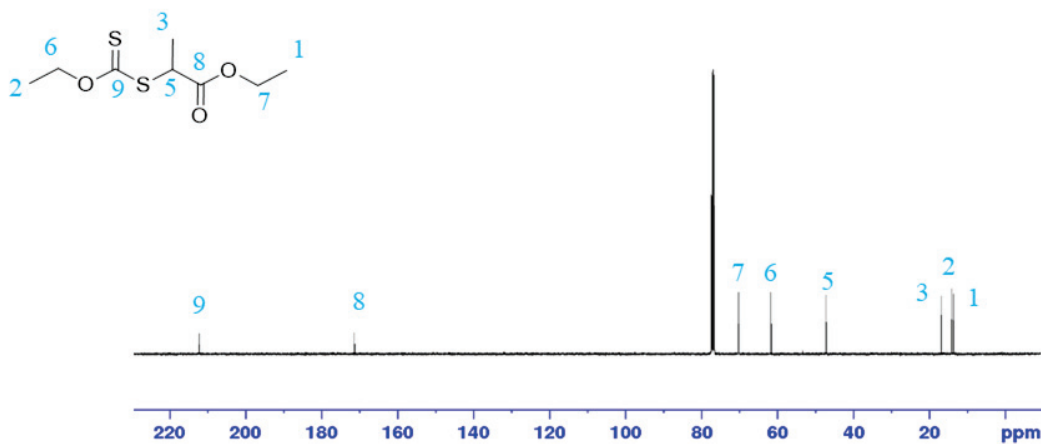


Figure VIII-2: <sup>13</sup>C NMR *O*-ethyl-*S*-(1-ethoxycarbonyl)ethyl dithiocarbonate, CDCl<sub>3</sub>, R.T, 12 K scans.

### III. Polymerization procedures

To stick to industrial conditions, in all the experiments described, the monomers and reactants were used without any further purification.

#### III.1 Homopolymerization of VAc (Chapter II)

Kinetic studies of the homopolymerization of VAc were carried out in EtAc at 60 °C with a ratio [CTA]:[AIBN] = 5. The [Monomer]:[CTA] ratio was adapted depending on the targeted DP (at 80% conversion) (**Figure VIII-1**). The individual conversion of the monomers was determined according to the calculations detailed in **Appendix 2**.

Table VIII-1: Experimental conditions for RAFT/MADIX polymerization of VAc.

Targeted DP (at 80% conversion)	[VAc]:[CTA]	[CTA]:[AIBN]
20	[25]:[1]	[1]:[0.2]
40	[50]:[1]	[1]:[0.2]
60	[75]:[1]	[1]:[0.2]
75	[95]:[1]	[1]:[0.2]
100	[130]:[1]	[1]:[0.2]
200	[250]:[1]	[1]:[0.2]

A typical polymerization procedure for the synthesis of 75\_PVAc is as follows: VAc (50 g, 580 mmol), CTA (1.36 g, 6.11 mmol), AIBN (0.2 g, 1.22 mmol) and EtAc (33 g) were introduced in a 150 mL three-necked round bottom flask connected to a condenser. The polymerization medium was degassed with nitrogen for 30 min. Then the mixture was placed in an oil bath at 60 °C and stirred at 300 rpm *via* a magnetic stirrer. The kinetics of the reaction was followed by <sup>1</sup>H NMR in CDCl<sub>3</sub> at R.T., and the polymerization was stopped at approximately 80% conversion. Number-average molar mass ( $M_n$ ) and distribution of molar masses ( $\mathcal{D} = M_w/M_n$ ) were followed by size exclusion chromatography (SEC) using THF as eluent (SEC-THF). The resulting polymers were then purified *via* two precipitations in cold petroleum ether/filtrations. The final product was dried under vacuum to afford a white powder. The solid was analyzed by <sup>1</sup>H NMR and SEC-THF.

#### III.2 Homopolymerization of VeoVa and VL (Chapter IV)

Kinetic studies of the homopolymerizations of VeoVa or VL (referred to as CoM) were carried out in EtAc or in bulk at 60 °C with a ratio [CTA]:[AIBN] = 3 and 5. The ratio [CoM]:[CTA] was adapted depending on the targeted DP: 5; 10; 20; 40 and 75 (**Table VIII-2**). The general procedure remains the same as for the homopolymerization of VAc. The polymers were dissolved in THF, precipitated in cold methanol and filtrated. This purification step was carried out three times and the final product was dried under vacuum.



**Table VIII-2: Experimental conditions for the RAFT/MADIX polymerization of either VeoVa or VL (CoM).**

Targeted DP	[CoM]:[CTA]	[CTA]:[AIBN]
5	[7]:[1]	[1]:[0.33]
10	[15]:[1]	[1]:[0.33]
20	[30]:[1]	[1]:[0.33]
40*	[85]:[1]	[1]:[0.33]

\* Only 45% conversion were reached for this experiment after 24 h

### III.3 Statistical copolymerization of VAc and VeoVa or VL (Chapter III)

Copolymerizations of VAc with either VeoVa or VL were carried out in EtAc at 60 °C, with a ratio [CTA]:[AIBN] = 5. The polymerization procedure was similar to the homopolymerization of VAc, except that this time, both VAc and the CoM were introduced in the round bottom flask.

The initial [VAc]:[CoM] ratio varied from [90]:[10] to [99]:[1] for VAc:VeoVa, but was kept at [90]:[10] for VAc:VL. Different DPs were targeted (75 and 100) (**Table VIII-3**).

**Table VIII-3 Experimental conditions for the RAFT/MADIX statistical copolymerization of VAc with either VeoVa or VL (CoM).**

Targeted DP (at 80% conversion)	[Monomers]:[CTA]	[CTA]:[AIBN]	[VAc]:[CoM]
75	[95]:[1]	[1]:[0.2]	[90]:[10]
100	[130]:[1]	[1]:[0.2]	[90]:[10]
100	[130]:[1]	[1]:[0.2]	[95]:[5]
100	[130]:[1]	[1]:[0.2]	[98]:[2]
100	[130]:[1]	[1]:[0.2]	[99]:[1]

For example, in a typical procedure for the statistical copolymerization of VAc with VeoVa, targeting 10 mol.% of VeoVa in the composition of the copolymer and DP = 100 (at 80% conversion), the procedure is as follows: VAc (40.14 g, 470 mmol), VeoVa (10.44 g, 52.7 mmol), CTA (0.9 g, 4.05 mmol), AIBN (0.13 g, 0.81 mmol) and EtAc (57 g) were introduced in a 250 mL three-necked round bottom flask and connected to a condenser. Then the mixture was placed in an oil bath at 60 °C and stirred at 300 rpm *via* a magnetic stirrer. Kinetics of the reaction was followed by <sup>1</sup>H NMR in CDCl<sub>3</sub> at R.T., and the individual conversion of the monomers was determined according to the calculations detailed in **Appendix 2**. The polymerization was stopped after approximately 80% conversion. The resulting polymers were then purified *via* two successive precipitations in cold petroleum ether/ filtration steps. The final product was dried under vacuum. Number average molar masses ( $M_n$ ) and distribution of molar masses ( $\mathcal{D}$ ) were followed by size exclusion chromatography using THF (SEC-THF).

### III.4 Block copolymerization of VAc and either VeoVa or VL (CoM) (Chapters IV and V)

#### III.4.1 Chain extension of PVAc-X with VeoVa (Chapter IV)

Chain extensions of PVAc-X (with  $DP_1 = DP_{PVAc} = 75$  and  $100$ ) were performed with VeoVa in EtAc at  $60\text{ }^\circ\text{C}$  with  $[PVAc-X]:[AIBN] = 5$ . The ratio:  $[VeoVa]:[PVAc-X]$  was set to  $10$ , to target a  $DP_2 = DP_{VeoVa} = 5$  at  $50\%$  conversion of VeoVa. For example, a typical procedure for the extension of  $75\_PVAc-X$  is as follows: VeoVa ( $6.5\text{ g}$ ,  $30\text{ mmol}$ ),  $75\_PVAc-X$  ( $20\text{ g}$ ,  $3.33\text{ mmol}$ ) and AIBN ( $0.11\text{ g}$ ,  $0.67\text{ mmol}$ ) were introduced in a  $50\text{ mL}$  three-necked round bottom flask and connected to a condenser. The polymerization medium was degassed for  $30\text{ min}$ . Then, the round bottom flask was introduced in an oil bath at  $60\text{ }^\circ\text{C}$  and polymerization proceeded under magnetic stirring at  $300\text{ rpm}$  until approximately  $50\%$  conversion. Kinetics of the reactions was followed by  $^1\text{H NMR}$  in  $\text{CDCl}_3$  at R.T., and the polymerization was stopped at approximately  $50\%$  conversion. Number average molar masses ( $M_n$ ) and distribution of molar masses ( $D$ ) were followed by size exclusion chromatography using THF (SEC-THF). The polymer was precipitated in a mixture of  $50:50\text{ v/v.}\%$  cold water and methanol, before filtration and drying under vacuum at R.T.

#### III.4.2 Chain extension of PCoM-X with VAc (Chapter IV)

Chain extensions of PVeoVa-X and PVL-X (PCoM-X) (with  $DP_1 = DP_{CoM} = 5, 10$  and  $20$ ) were performed in EtAc at  $60\text{ }^\circ\text{C}$ . The procedure remains the same as for the extension of PVAc-X. The ratio  $[VAc]:[PCoM-X]$  was adapted from  $DP_1$  to target an overall  $DP = 100$  after  $65 - 70\%$  conversion, with  $[PCoM-X]:[AIBN] = 5$ .

#### III.4.3 Chain extension of P(VAc<sub>0.90-s-VeoVa<sub>0.10</sub>)-X with VAc (Chapter V)</sub>

Chain extensions of P(VAc<sub>0.90-s-VeoVa<sub>0.10</sub>)-X was carried out in EtAc at  $60\text{ }^\circ\text{C}$  with a ratio  $[P(VAc_{0.90-s-VeoVa_{0.10}}-X):[AIBN] = 5$  and a ratio  $[VAc]:[P(VAc_{0.90-s-VeoVa_{0.10}}-X) = 150$ . The rest of the procedure is similar to that described for the other polymerizations.</sub>

### III.4.4 Chain extension of PVAc-X with VAc and either VeoVa or VL (Chapter V)

#### D. Extension of 75\_PVAc-X

Extensions of 75\_PVAc-X with VAc and VeoVa or VAc and VL were carried out in EtAc at 60 °C, with a ratio [75\_PVAc-X]:[AIBN] = 5. The polymerization procedure is similar to the extension of PVAc-X described above (**Section III.1**), except that this time, both VAc and VeoVa (or VL) were introduced in the round bottom flask. A global DP = 175 was targeted. Thus, DP2 = 200 was fixed, to reach approximately DP2 = 100 at the desired conversion (50 - 60%). The amount of CoM was calculated to target 2 to 10 mol.% in the global composition of the copolymer (taking into account the fraction of VAc from the macroCTA). Thus, the ratios [VAc]:[CoM] introduced in the polymerization medium for the extension varied from [97.5]:[2.5] to [86]:[14] (**Table VIII-4**).

**Table VIII-4: Experimental conditions for the extension of 75\_PVAc-X with VAc and CoM.**

Targeted global DP	Targeted DP2 (50 - 60% conversion)	[Monomers]:[75_PVAc-X]	Global targeted [VAc]:[CoM]	Introduced [VAc]:[CoM] for the extension
175	100	[200]:[1]	[90]:[10]	[86]:[14]
175	100	[200]:[1]	[93]:[7]	[90]:[10]
175	100	[200]:[1]	[95]:[5]	[92.5]:[7.5]
175	100	[200]:[1]	[98]:[2]	[97.5]:[2.5]

#### E. Extensions of PVAc-X of different DPs (DP1)

Extensions of PVAc-X of different DPs with VAc and VeoVa or VAc and VL were carried out in EtAc at 60 °C, with a ratio [PVAc-X]:[AIBN] = 5. The polymerization procedure is similar to that described for the extension of 75\_PVAc-X. A global DP = 175 was targeted, with a fixed global composition of [VAc]:[CoM] = [95]:[5]. This means that the ratio [Monomers]:[PVAc-X] was varied accordingly with DP1 to target a global DP = 175 at the desired conversion (50 - 60%) (**Table VIII-5**).

**Table VIII-5: Experimental conditions for the extension of PVAc-X with VAc and either VeoVa or VL.**

Targeted global DP	DP1 of PVAc	Targeted DP2 (at 50-60% conversion)	[Monomers]:[PVAc-X]	Global targeted [VAc]:[CoM]	Introduced [VAc]:[CoM] for the extension
175	20	155	[275]:[1]	[95]:[5]	[94.5]:[5.5]
175	40	135	[245]:[1]	[95]:[5]	[94.3]:[5.7]
175	60	115	[230]:[1]	[95]:[5]	[93.5]:[6.5]
175	75	100	[200]:[1]	[95]:[5]	[92.5]:[7.5]
175	100	75	[140]:[1]	[95]:[5]	[91.2]:[8.8]

## IV. Alcoholysis procedures

### IV.1 Alcoholysis of PVAc

The alcoholysis of PVAc ( $M_n = 2000 \text{ g mol}^{-1}$ ;  $6000 \text{ g mol}^{-1}$ ;  $10\,000 \text{ g mol}^{-1}$  and  $20\,000 \text{ g mol}^{-1}$ ) was performed with [VAc]:[NaOH] ratios varying from 1:0.01 to 1:0.1.

A typical procedure for the alcoholysis of 75\_PVAc with a [VAc]:[NaOH] = 1:0.025 is as follows: 75\_PVAc ( $M_n = 6400 \text{ g mol}^{-1}$ ,  $D = 1.3$ , 5 g, 58 mmol) was dissolved in MeOH (15 g, 18.9 mL) in a 50 mL round bottom flask with a silicon cap. The flask was then placed in an oil bath at 30 °C for 10 min, and the mixture was stirred with a magnetic stirrer at 250 rpm before the methanolic solution of NaOH was introduced. This solution was prepared as follows: NaOH pellets (0.46 g, 11.5 mmol) were dissolved in MeOH (20 mL) ( $C_{\text{NaOH}} = 0.575 \text{ mmol mL}^{-1}$ ). The volume of this solution, which had to be introduced into the round bottom flask, was calculated to meet a ratio [VAc]:[NaOH] = 1:0.025. Thus, 2.52 mL of the basic solution was introduced in the round bottom flask.

Time zero was recorded immediately after the basic solution was introduced in the reaction medium. The alcoholysis was conducted at 30 °C for a predetermined amount of time. Regular sampling was performed and each sample was neutralized with acetic acid until the pH reached 4-5. The alcoholized polymer was washed three times with methanol, recovered by filtration and dried under vacuum at 40 °C.  $^1\text{H}$  NMR characterizations were performed in DMSO at R.T. after complete dissolution of the P(VOH-*s*-VAc) in the NMR tube. To reach complete dissolution of the sample, the NMR tube was heated at 90 °C with a heat gun and cooled down at R.T before analysis.

### IV.2 Alcoholysis of statistical and block copolymers

To determine the volume of the basic solution required to meet the desired [monomer]:[NaOH] ratio, it is first required to calculate the number of moles of each monomer in the copolymer, according to the mole fraction (N) determined by  $^1\text{H}$  NMR, as follows:

The weight fraction (w) of each monomer in the copolymer is given by **Equations 44 and 45**.

$$w_{\text{VAc}} = \frac{f_{\text{VAc}} * M_{\text{VAc}}}{f_{\text{VAc}} * M_{\text{VAc}} + f_{\text{CoM}} * M_{\text{CoM}}} \quad (44)$$

$$w_{\text{CoM}} = 1 - w_{\text{VAc}} \quad (45)$$

With  $w_{VAc}$  and  $w_{CoM}$  the weight fraction of VAc and CoM, respectively,  $f_{VAc}$  and  $f_{CoM}$  the molar fraction of VAc and CoM, respectively, and  $M_{VAc}$  and  $M_{CoM}$  the molar mass of VAc and CoM, respectively.

Then, the number of moles of each monomer in a given mass of copolymer is determined *via*:

$$n_{VAc} = \frac{m_p * W_{VAc}}{M_{VAc}} \quad (46)$$

$$n_{CoM} = \frac{m_p * W_{CoM}}{M_{CoM}} \quad (47)$$

$$n_{tot} = n_{VAc} + n_{CoM} \quad (48)$$

With  $n_{VAc}$  and  $n_{CoM}$  the number of moles of VAc and CoM, respectively, in the mass  $m_p$  of copolymer, and  $n_{tot}$  the total molar amount of VAc and CoM in the copolymer.

The value  $n_{tot}$  allows to determine the number of moles of NaOH to introduce in the reaction medium, to alcoholize a mass  $m_p$  of copolymer.

For example, 100\_P(VAc<sub>0.90</sub>-S-VL<sub>0.10</sub>) ( $M_n = 12\,900 \text{ g mol}^{-1}$ ,  $D = 1.4$ ) is composed of 90 mol.% of VAc and 10 mol.% of VL. This represents 77 wt.% of VAc and 23 wt.% of VL. In 5 g of this copolymer,  $n_{VAc} = 44.7 \text{ mmol}$  and  $n_{VL} = 5.1 \text{ mmol}$ . Thus,  $n_{tot} = 49.8 \text{ mmol}$ . For a ratio [monomers]:[NaOH] = 1:0.025, it is then required to introduce 2.17 mL of the methanolic NaOH solution ( $C_{NaOH} = 0.575 \text{ mmol mL}^{-1}$ ).

The protocol for the alcoholysis of the statistical, block and hybrid copolymers is similar to that described for the alcoholysis of PVAc.

## V. Emulsion copolymerization of VAc and VeoVa

### V.1 Screening with KPS (Chapters II and III)

To achieve a screening of the potential stabilizer candidates, emulsion polymerizations were first carried out in a 10 mL round bottom flask with thermal initiation. Working on this small scale allowed for optimization and prevented wasting of monomers and stabilizers. Suitable stabilizers were subsequently tested on a larger scale.

0.1 g of the stabilizer candidate was dissolved in 4.1 g of water at either R.T. (23 °C), 55 °C, 70 °C or 90 °C. Following dissolution, once the temperature had reached R.T., potassium persulfate (KPS, 0.01 g, 0.037 mmol), VeoVa (0.2 g, 1.10 mmol) and VAc (0.8 g, 9.4 mmol) were added to the polymerization medium, which was then degassed for 10 min before being heated to 70 °C for 2 h. If stable, the resulting latex was analyzed by DLS.

### V.2 Emulsion copolymerization of VAc and VeoVa initiated by a redox couple

More standard emulsion polymerization conditions were then employed at a larger scale. Emulsion polymerizations were carried out in a 75 mL three-neck double-wall round-bottom glass reactor. The agitation was set at 160 rpm using a glass anchor. A condenser was used to minimize monomer loss. The sampling port, used to withdraw latex periodically, consisted of a Teflon tube connected to a syringe. After degassing of the initial medium for 40 min, a continuous flow of nitrogen was applied in the polymerization medium throughout the reaction. The temperature was set at 55 °C and controlled *via* a thermostatic bath. Each experiment yielded ca. 75 g of latex (**Figure VIII-3**, left).

The preparation of the emulsion polymerization was divided in two parts: redox premix and water premix. Typical protocol is as follows:

#### **Redox premix**

**[1]:** Ascorbic acid (0.350 g, 1.99 mmol, 0.092 wt.% based on monomers) and ammonium iron (II) sulfate (0.05 g, 0.128 mmol, 0.054 wt.% based on monomers) were dissolved in deionized water (25 g).

**[2]:** TBHP 70 wt.% (0.42 g, 4.66 mmol) was diluted in deionized water (10 mL). An aliquot of this solution (0.95 mL) was diluted further in deionized water (50 mL) and stored in the fridge.

#### **Water premix**

To prepare 75 g of latex, stabilizer powder (1.5 g to 3 g) was first dispersed in deionized water (38 g), either at R.T. or at temperatures ranging from 55 to 90 °C (depending on the

dispersibility of the stabilizer), using a magnetic stirrer. The pH was adjusted to 3.9 - 4.1 with formic acid (0.1 or 0.05 mol L<sup>-1</sup>), and this water premix was loaded into the reactor.

The redox premix **[1]** (1 mL) was then poured into the reactor with monomers (VeoVa = 3 g, 15.4 mmol; VAc = 12 g, 139 mmol) and additional deionized water (10 g). The reaction medium was degassed for 40 min and heated to 55 °C under stirring at 160 rpm. Once the polymerization temperature was reached, the redox premix **[2]** (10 mL) was fed to the reactor with a flow rate of 0.2 mL min<sup>-1</sup> *via* an automatic pump over a 50 min period. The reaction was stirred at 55 °C and 160 rpm for 2 h.

Samples were withdrawn periodically during the reaction with a syringe and quenched by 4-methoxyphenol. To follow the kinetics, the conversion was determined gravimetrically. The average size of the particle ( $Z_{av}$ ) and the dispersity (evaluated from the polydispersity index, PDI, provided by the software) were determined by dynamic light scattering (DLS). The number-average diameter ( $D_n$ ) was determined by cryogenic electron transmission microscopy (cryo-TEM). The final latex was stored in the fridge. The surface of the latex ( $S_{tot\ latex}$ , cm<sup>-2</sup>) and the number of particles ( $N_p$ , cm<sup>-3</sup>) is calculated *via* **Equations 49** and **50**.

$$N_p = \frac{6 \cdot x \cdot [M]_0}{\Pi \cdot D_v \cdot \rho} \quad (49)$$

$$S_{tot\ latex} = N_p \cdot \Pi \cdot D_v^2 \quad (50)$$

With  $x$  the conversion,  $[M]_0$  the initial concentration of monomer (g cm<sup>-3</sup>),  $D_v$  the volume diameter of the particles (cm) (obtained by cryo-TEM *via* **Equation 56**) and  $\rho$  the density of the polymer (considered to be the density of PVAc = 1.19).

### V.3 Scale up of the emulsion polymerization to a 1000 mL reactor

The emulsion polymerizations with the selected stabilizer candidates were performed in a 1000 mL double-walled glass reactor equipped with a mechanical stirrer. The temperature was controlled and monitored using a thermostat (Julabo) and jacketed reactor connected to a water bath, set at 55 °C (**Figure VIII-3**, right). Similar protocol was applied to that described for the 75 mL scale reaction, with quantities adjusted to produce 1000 mL of latex.

A water premix containing the stabilizer (10 g) and of water (200 g) was heated to 80 °C for 2 h, before being cooled to R.T. (25 °C). Water (569.7 g) was added to this premix and the pH of the solution was adjusted to 3.9 - 4.1. This premix was introduced into the reactor, with



Veova (40 g), VAc (160 g). A solution containing AsAc (2 mL, 0.092 g mL<sup>-1</sup>) and iron(II) sulfate ammonium salt (0.0536 g mL<sup>-1</sup>) was added to the reactor. The reaction media was degassed for 40 min under stirring at 150 rpm, and heated at 55 °C. At the end of this degassing time, the stirring speed was increased to 190 rpm and the TBHP solution (0.011 g mL<sup>-1</sup>) was fed inside the reactor *via* an automatic pump, at a rate of 0.2 mL min<sup>-1</sup> for 50 min. The polymerization was cooled down at 20 °C after 2 h. The conversion of the polymerization was followed gravimetrically *via* a Mettler balance. A Mastersizer device was used to determine the particle size and particle size distribution of the latex.

---



Figure VIII-3: 75 mL (left) and 1000 mL (right) glass reactors with the pump to feed the TBHP solution.

---

## VI. Characterization techniques

### VI.1 Nuclear magnetic resonance (NMR)

NMR spectra were recorded with a 5 mm BBFO+ probe with a z-gradient coil. Proton NMR spectra were recorded with a 5 mm BBFO+ probe with a z-gradient coil (D1 = 3 s, scans = 256, O1P = 110.0 ppm, O2P = 4.0 ppm, RO = 20 Hz). Carbon NMR spectra were recorded with a 10 mm SEX probe,  $^{13}\text{C}$  selective with a z-gradient coil. The pulse sequence used includes a decoupling proton with NOE effects, and a  $70^\circ$  spin excitation (D1 = 2 s, scans = 6144, O1P = 6.50 ppm, O2P = 6.18 ppm, RO = 20 Hz). The method is said to be "semiquantitative," and the NMR calculations were carried out between carbon atoms of the same nature (the  $-\text{CH}_2-$ ). Chemical shifts are given in parts per million (ppm) with the solvent peak as internal standard. The samples were diluted in  $\text{CDCl}_3$  or DMSO, at concentrations of approximately  $30 \text{ mg mL}^{-1}$  for  $^1\text{H}$  and  $90 \text{ mg mL}^{-1}$  for  $^{13}\text{C}$ .

### VI.2 Size exclusion chromatography (SEC)

Molar mass measurements were performed using a Viscotek system (Malvern Instruments), including a four-capillary differential viscometer, a differential refractive index detector (RI), and a UV detector. THF was used as the mobile phase at a flow rate of  $1 \text{ mL min}^{-1}$  at  $35^\circ\text{C}$ . All samples were injected at a concentration of  $3 - 6 \text{ mg mL}^{-1}$  after filtration through a  $0.45 \mu\text{m}$  PTFE membrane. The separation was carried out on three Polymer Standard Service columns Experimental part 309 (SDVB,  $5 \mu\text{m}$ ,  $300 \times 7.5 \text{ mm}$ ) and a guard column. The molar mass distributions were calculated by means of a conventional calibration curve based on polystyrene standards from  $470$  to  $270\,000 \text{ g mol}^{-1}$  or by a universal calibration based on polystyrene standards (Polymer Standards Service). The Omnisec software was used for data acquisition and data analysis

Finally, knowing the hydrolysis degree of P(VOH-*s*-VAc) (HD), one can calculate  $M_{n, \text{P(VOH-co-VAc)}}$  according to **Equation 51**.

$$M_{n, \text{P(VOH-co-VAc)}} = \text{DP} \times (M_{\text{VOH}} \times \text{HD} + M_{\text{VAc}} \times (1-\text{HD})) \quad (51)$$

With  $M_{\text{VOH}}$  and  $M_{\text{VAc}}$  the molar masses of vinyl alcohol ( $44 \text{ g mol}^{-1}$ ) and vinyl acetate ( $86.09 \text{ g mol}^{-1}$ ), respectively.

**Equation 51** is true if the P(VOH-*co*-VAc) is linear.<sup>[6]</sup> This information can be verified by  $^1\text{H}$  NMR. Knowing the DP of the polymer before alcoholysis (thanks to the presence of the chain-end extremities), it is possible to cross check that this DP is similar for the alcoholized polymer.

**Equation 51** can be generalized to more complex structures which incorporate the CoM units:

$$M_{n, \text{ stabilizer}} = DP \times (M_{\text{VOH}} \times F_{\text{VOH}} + M_{\text{VAc}} \times F_{\text{VAc}} + M_{\text{CoM}} \times F_{\text{CoM}}) \quad (52)$$

With  $F_{\text{VOH}}$ ,  $F_{\text{VAc}}$ , and  $F_{\text{CoM}}$  the molar fraction of the VOH, VAc and CoM units, respectively, determined by  $^1\text{H}$  NMR, and  $M_{\text{CoM}}$  the molar mass of the CoM (198 g mol $^{-1}$  for VeoVa and 226.36 g mol $^{-1}$  for VL).

### VI.3 UV-visible spectroscopy

UV-visible spectra were recorded using a Cary 100 UV-vis spectrophotometer from Agilent Technologies (from 180 to 900 nm), and Cary WinUV software. Measurements were carried out with quartz cells with an optical path of 10 mm (model 100-QS from the Hellma brand).

The UV/Vis analysis of 75\_PVAc highlighted two absorption bands at 227 and 280 nm, corresponding, respectively, to the absorptions of the C=O and C=S bonds, which attests of the presence of the dithiocarbonate function on the polymer (**Figure VIII-4**).

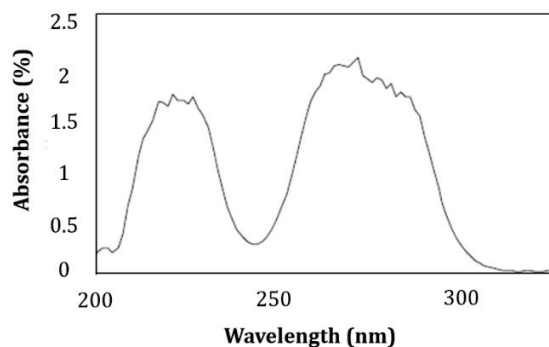


Figure VIII-4: UV-vis spectrum of 75\_PVAc in THF at R.T.

---

### VI.4 Fourier-transform infrared (FTIR) spectroscopy

FTIR measurements were performed on a Nicolet i550 FT-IR device at R.T. KBr pellets were prepared to record FTIR spectra. Each spectrum was carried out with 32 scans (to enhance the signal-to-noise ratio) from 4 000 to 400 cm $^{-1}$  at the speed of 0.20 cm s $^{-1}$ . The FTIR spectra were treated with Omnic software.

## VI.5 Gravimetric analysis

Gravimetric analysis is the traditional method to determine the solid content and the monomer conversion during emulsion polymerizations. The solid content is the mass percentage of the non-volatile species. A quantity of latex (approximately 0.3 g) is weighed and dried in an oven at 100 °C until it reaches a constant weight. The value of the dry extract (DE) gives the conversion to monomer (X) by means of the following relation:

$$X = \frac{\tau_{\text{polymer}}}{\tau_{\text{solid}}} = \frac{\text{DE} - \tau_{\text{NV}}}{\tau_{\text{solid}}} \quad (53)$$

with X is the monomer conversion;  $\tau_{\text{polymer}}$  the experimental monomer ratio;  $\tau_{\text{solid}}$  the theoretical polymer ratio at 100% conversion (initial mass of monomer/total mass); DE is the dry extract (proportion of solid product in the medium) and  $\tau_{\text{NV}}$  is the ratio of non-volatile species that are not the polymer (initiator or salts for instance).

## VI.6 Dynamic light scattering (DLS)

The intensity-weighted mean diameter (or Z-average diameter),  $Z_{\text{av}}$ , of the latex particles and the dispersity factor (PDI) were measured at 25 °C using a Zetasizer Nano Series (Nano ZS) from Malvern Instruments. Prior to measurements, the latex was diluted with water. The mean particle diameter was averaged over three consecutive runs. The data was collected at a 173° scattering angle using the fully automatic mode of the Zetasizer system.

DLS is based on the measurement of fluctuations in the intensity of the light scattered as a function of time, by particles in suspension subjected to Brownian motion. The frequency of fluctuations in the intensity, due to variations in position of the particle, differs according to the speed of movement, and therefore the size of the particle. This analysis provides not only the average size of the particle ( $Z_{\text{av}}$ ), but also information on the dispersity, *via* the polydispersity index (PDI). If  $0 < \text{PDI} < 0.08$ , the latex is considered monodisperse. If  $0.05 < \text{PDI} < 0.08$  the latex is almost monodisperse. If  $0.08 < \text{PDI} < 0.7$  the latex has a relative monodispersity. If  $\text{PDI} > 0.7$ , the latex is polydisperse.

## VI.7 Cryogenic electron transmission microscopy (Cryo-TEM)

Cryo-TEM is a type of transmission electron microscopy (TEM) where the sample is studied at cryogenic temperatures. A beam of electrons is transmitted through a specimen to form an image. This image is formed from the interaction of the electrons with the sample as the beam is transmitted through the specimen.

All cryo-TEM analyses were carried out using a JEOL 1400 Flash microscope. The diluted samples were dropped onto 300 Mesh holey carbon films (C-Flat 2/1) and quench-frozen in liquid ethane using a cryo-plunge Vitrobot (ThermoFisher). The specimens were then mounted on a precooled Fischione 2550 specimen holder, transferred in the microscope (JEOL 1400 Flash) and observed in low dose condition at an accelerating voltage of 120 kV. Image analysis was performed with Fiji analysis software.

The average particle size of the particles was calculated out of 200 particles using ImageJ software. The number-average of particles ( $D_n$ , nm), the weight-average diameter ( $D_w$ , nm) and the volume-average diameter ( $D_v$ , nm) are calculated *via* the following equations:

$$D_n = \frac{\sum n_i D_i}{\sum n_i} \quad (54)$$

$$D_w = \frac{\sum n_i D_i^4}{\sum n_i D_i^3} \quad (55)$$

$$D_v = \left( \frac{\sum n_i D_i^3}{n_i} \right)^{1/3} \quad (56)$$

$$PdI = D_w/D_n \quad (57)$$

Where  $n_i$  is the number of particles with diameter  $D_i$ .

## VI.8 Determination of the amount of adsorbed & grafted stabilizer

The amount of grafted and adsorbed stabilizer was determined after ultracentrifugation using a ThermoScientific Sorvall mTX150 device. It allows separation of the supernatant which contains the free stabilizer, from the pellet, which contains the polymer and the strongly adsorbed and grafted stabilizer.

A sample of latex (approximately 3 g) ( $m$ ) is centrifugated (2 times for 1 h at 60 000 rpm and 5 °C). The amount of stabilizer in  $m$  is defined as:  $m_1 = \text{fraction of stabilizer in the reactor} * m$ .

After centrifugation, the supernatant is collected in a pre-weighted vial. The solid content of the supernatant, which corresponds to free stabilizer in water, is determined by gravimetric analysis and noted  $m_2$ .

The fraction of adsorbed and grafted stabilizer in the centrifugated sample is therefore defined as:

$$\text{Wt.}\%_{\text{Ads\&grafted}} = 100 * (1 - m_2 / m_1) \quad (58)$$

This analysis is performed twice to get an average value of the adsorbed and grafted fraction of stabilizer. To verify that there is no soluble polymer in the supernatant,  $^1\text{H}$  NMR analysis on the dried product is performed in  $\text{DMSO-d}_6$ , to crosscheck that the HD remains the same as the one determined for the stabilizer. This verification provides a fair evaluation of the composition of the supernatant.

The total mass of adsorbed and grafted stabilizer in the reactor ( $m_a$ ) is then evaluated from the weight of stabilizer introduced into the reactor ( $m_{\text{stabilizer}}$ ):

$$m_{\text{Ads\&grafted}} = \text{wt.}\%_{\text{Ads\&grafted}} * m_{\text{stabilizer}} \quad (59)$$

The surface coverage ( $A_s$ ,  $\text{\AA}^2$  per molecule) was calculated *via* the determination of the stabilizer fraction of adsorbed and grafted stabilizer per unit area,  $\Gamma$  ( $\text{g cm}^{-2}$ ), and the molar mass ( $M_n$ ) of the stabilizer calculated from its chemical structure (based on **Equation 51**), where:

$$\Gamma = \frac{m_a}{S_{\text{tot latex}}} \quad (60)$$

Where  $S_{\text{tot latex}}$  determined *via* **Equation 50**.

$$A_s = \frac{M_n}{\Gamma * N_A} \quad (61)$$

With  $M_n$  the molar mass of the stabilizer ( $\text{g mol}^{-1}$ ) determined *via* **Equation 51** or **13** and  $N_A$  the Avogadro's number ( $\text{mol}^{-1}$ ).

## **VI.9 Surface tension**

The surface tension ( $\sigma$ ) of the aqueous solutions of the stabilizers at different polymer concentrations was measured by an automatic surface tensiometer (DY-300, Kyowa Interface Sci.) with Wilhelmy method using the automated DCAT11 tensiometer (DataPhysics Instruments GmbH, Filderstadt, Germany). Three measurements were performed and the presented result is the average. Measurements were carried out at 25 °C by circulating thermostatic water bath (with  $\pm 0.1$  °C accuracy) through the jacketed vessel containing the measuring solution.



## **VII. Procedures for the use of the latexes in various field of application**

### **VII.1 pH stability**

pH storage stability experiments were carried out on the most promising latexes, either stored in the fridge or at 40 °C.

### **VII.2 pH stability for latexes stored in the fridge**

Five samples (10 mL) of the latex were poured in 20 mL glass flasks. The pH of each sample was adjusted with NaOH or HCl to pH 4, 6, 8, 10 and 12. This was recorded as week 0. The samples were stored in the fridge and the pH was measured again once a week over a period of four weeks. At the end of week four, the particle size of the samples was measured by DLS.

### **VII.3 Aging tests: pH stability for latexes stored at 40 °C**

Aging tests were carried out at pH 11.5. The pH of 100 mL sample latexes was adjusted *via* a solution of a methylsiliconate Silres BS 16 (Wacker) used in mortar applications. The samples were stored in an oven at 40 °C and the pH was measured after day 3, 5, 7, 10, 12, 30, 60, 90 and 120.

### **VII.4 Mortar calorimetry**

The formulations of mortar with the latexes produced in Burghausen and the tests were carried out by the analytical service at Wacker. A general description of the mortar application tests was provided by Wacker and is as follows.

#### **VII.4.1 Formulation**

##### DIN mortar standard formulation:

900 g CEM I 42.5 R  
2.700 g Standardized sand (2 bags)  
135 g Dispersion (polymer/cement ratio PC: 0.20)  
450 g Water = water/cement ratio WC: 0.50

## VII.4.2 Sample preparation and conditioning

### Mortars and troweling compounds

- The powders are mixed in a mortar mixer
- Then the requisite amount of dispersion is added and the mixt again
- Molds for the adhesion test are then filled with the mortar formulation. The surface is smoothed by scraping off the excess mortar several times with a trowel. The test specimens from the mold between 20 and 24 hours after they have been made. The test specimens from the mold between 20 and 24 hours after they have been made.
- In parallel, prisms for flexural and compressive tests are filled with mortar. The surface is smoothed and the prisms are stored 28 days in standard climatic conditions (23 °C / 50% r.h.)

### VII.4.3 Measuring

- Measures of the tensile strength in bending and the compressive strength is performed in standard climatic conditions (23 °C / 50 % r.h.).
- Test 3 specimens per type of conditioning and mortar.
- Carry out the measurement using TestXpert test software.
- Switch on the ToniPRAX testing machine with the main switch.

#### A) Bending strength: Load-increase rate: 0.05 kN/s

The three-point bending test is a destructive test, carried on specimens from the prisms, measuring 4\*4\*16 cm, and using an MTS Systems multifunction press, equipped with a force sensor of 20 or 100 kN according to the test. This test makes it possible to evaluate the tensile strength by bending of the specimens, (*i.e.* the breaking stress). Cement is much more fragile in tension than in compression. It is the reason why the stretched (lower) part is cracked first. The rupture is initiated by a main crack initially activated by a lack of homogeneity of the material, and which propagates there under the effect of increased load. **Figure VIII-5** provides a picture of the test, and a schematical representation of the prism under bending stress during the test.

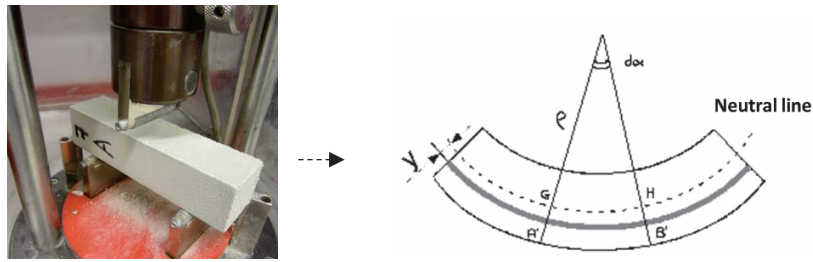


**Figure VIII-5: Picture of the three-bending test (left) and scheme of the prism, under bending stress during the test (right).**

The load was applied in force control at a rate of 0.05 kN/s. The prism is supported on each end and loaded at the middle until failure. The tensile strength is calculated by measuring the load required to split the sample in half over the section of the fracture.

B) Compressive strength: 1.5 N/mm<sup>2</sup>/sec.

The resistance and the compressive modulus are determined on the half-prisms recovered after the three-point bending test. Since the support/specimen bearing surface is known, the software determines directly the stress  $\sigma'_m$  and the modulus  $E_c$  according to the acquisition data:

$$\sigma'_m = F'_m/S \quad (62)$$

$$E_c = \sigma'_m / \varepsilon'_m \quad (63)$$

With  $F'_m$  the force and  $\varepsilon'_m$  the displacement at failure; S is the surface of the prism.

#### **VII.4.4 Evaluation**

Testing was performed on 3 bending-test readings and the 3 readings for the compressive strength test. The result is provided as a mean value, with a confidence range of the individual readings.

## VII.5 Spray drying

Spray drying experiments were performed in a Mini Spray dryer B-290 by the analytical service at Wacker. A peristaltic pump was used to feed polymer solution to a fluid nozzle atomizer (inside diameter: 0.7 mm), which used compressed air from a compressor. The spray drier was composed of a drying chamber (height: 400 mm; diameter: 100 mm) and a cyclone. 500 mL latex ( $Sc = 20\%$ ) were used for the experiments. The temperature of the latex before spray drying was kept constant at 25 °C. Air inlet temperature ( $T_{in}$ ) was set at 150 – 180 °C and the rate of feed flow was adjusted to keep the outlet temperature at the desired level. The air volume flow rate was 667 L h<sup>-1</sup>. The dried powders were collected and the re-dispersibility was evaluated as follows:

In a plastic recipient of 250 mL, add 75 g of standardized quartz sand (0.1 - 0.4 μm), 75 g of another standardized quartz sand (0.33 μm), 10 g of the latex powder, 0.6 of tylose powder, 30 of standardized synthetic mortar solution (pH = 7, contains minerals, sulfate dihydrate, kalium sulfate and sodium sulfate). The powders were stirred with an ultraturrax T25 for 1 min at 700 rpm before 80 g of deionized water was added. The mixture is then mixed with a spatula for 1 min and left for decantation for 2 min. Then, the mixture is introduced into decanters (**Figure VIII-6**). The amount of sedimented powder is measured after 1 h and 24 h. To pass the test, the height of sedimented powder should not overtake 3 cm inside the decanter. After 24 h, the particle size of the dispersion is measured by DLS. The latex is considered redispersible if the particle size of the dispersion is similar to that of the latex before spray drying.

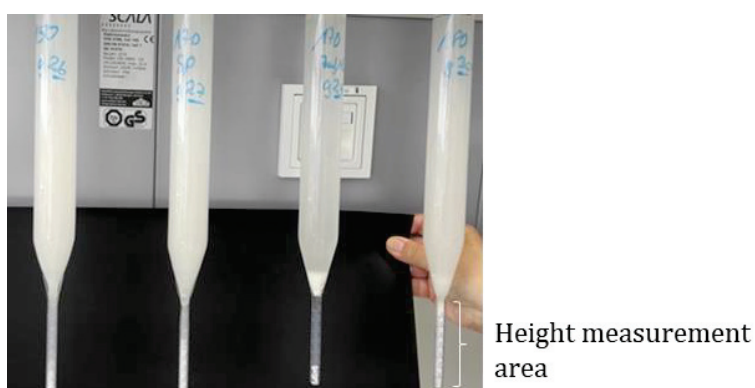


Figure VIII-6: Decanters for the evaluation of the redispersibility of the latex.

---

## References

- [1] D. J. Keddie, G. Moad, E. Rizzardo, S. H. Thang, *Macromolecules* **2012**, *45*, 5321–5342.
- [2] G. Moad, E. Rizzardo, S. H. Thang, *Aust. J. Chem.* **2012**, *65*, 985–1076.
- [3] J. R. Góis, A. V. Popov, T. Guliashvili, A. C. Serra, J. F. J. Coelho, *RSC Adv.* **2015**, *5*, 91225–91234.
- [4] R. A. Hutchinson, D. A. Paquet, J. H. McMinn, *Macromolecules* **1995**, *28*, 5655–5663.
- [5] E. . G. J.Brandrup, E.H. immergut, "*Polymer Handbook*" (4th Edition), **1999**.
- [6] L. I. Atanase, Contribution à l'étude Des Complexes Poly(Vinyle Alcool - Vinyle Acétate) / Tensioactifs Anioniques: Caractéristiques Colloïdales Des Nanogels et Extension Aux Copolymères à Blocs, PhD Dissertation, **2017**.

---

# Appendix

---

## Table of content

Appendix 1: $^1\text{H}$ NMR of the monomers .....	358
Appendix 2: Calculation of the average number of monomers in the polymer <i>via</i> the $^1\text{H}$ NMR for the kinetic studies .....	360
Appendix 3: Plot of $N_p$ as a function of conversion for the emulsion copolymerization of VAc and VeoVa stabilized with 100_P(VOH <sub>0.88</sub> - <i>s</i> -VAc <sub>0.12</sub> ) (Chapter II).....	371
Appendix 4: $^1\text{H}$ NMR analysis of the dry supernatant of 75_P(VOH <sub>0.88</sub> - <i>s</i> -VAc <sub>0.12</sub> ) to verify that only the stabilizer is present in the supernatant after centrifugation.....	372
Appendix 5: DLS analysis of the stabilizers in water: volume distributions at 25 °C and intensity distributions at 55 °C for the selected copolymers .....	373
Appendix 6: Investigation on the presence of the xanthate moiety after alcoholysis of P(VOH- <i>s</i> -VAc)- <i>b</i> -PVeova block copolymer .....	377
Appendix 7: Kinetics of VeoVa homopolymerization with targeted DP = 80 and different experimental conditions.....	382
Appendix 8: Main characteristics for the synthesis of two different batches of some copolymers.....	383
Appendix 9: Alkali resistance of the latexes stabilized by the VeoVa-based block copolymers stored at different pH.....	385
Appendix 10: Plot of $N_p$ and $Z_{av}$ as a function of conversion for ER-H9 and ER-H10 .....	386
Appendix 11: Overlay of the SEC traces of the (co) polymerization carried out in the 150- and 500-mL batch reactors .....	387
Appendix 12: Calculation and determination of suitable parameters for the biodegradability testing.....	388
Appendix 13: Mastersizer analyses of the latexes synthesized at Wacker .....	389
Appendix 14: List of communications and publications .....	392

## Appendix 1: $^1\text{H}$ NMR of the monomers

### Vinyl acetate (VAc)

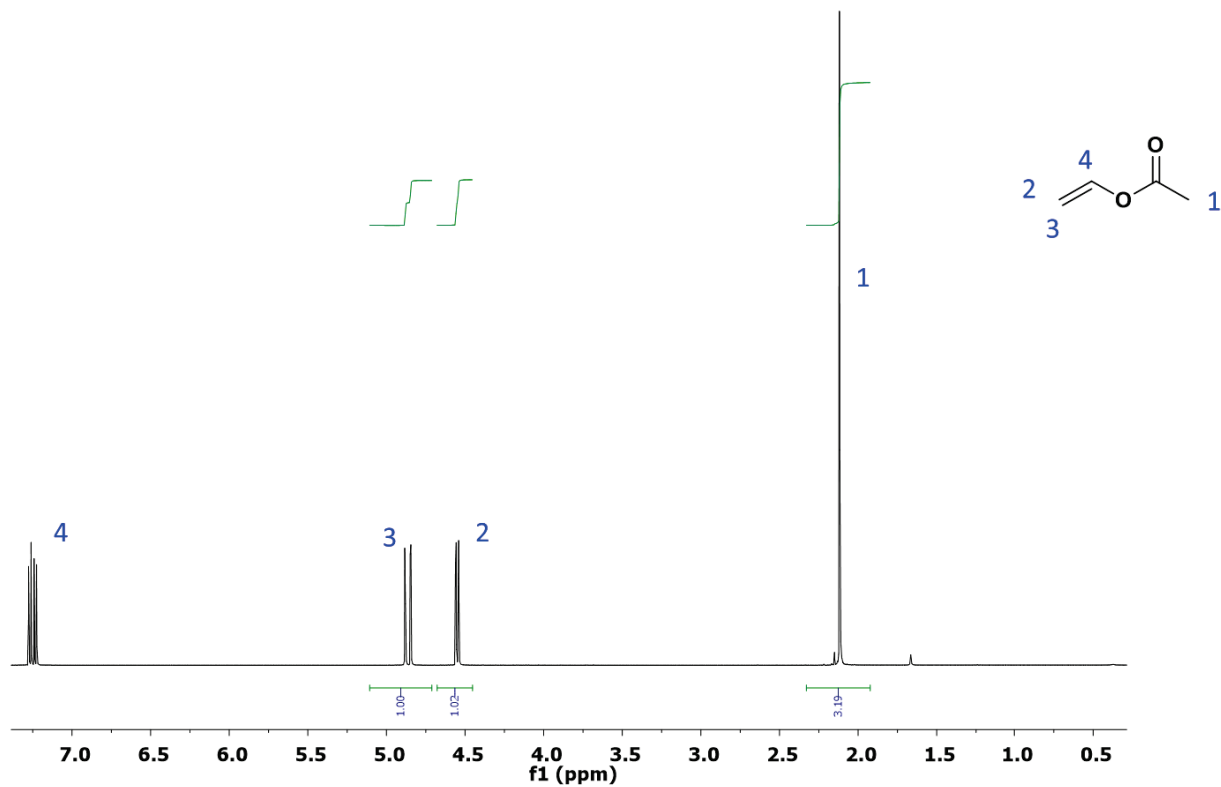
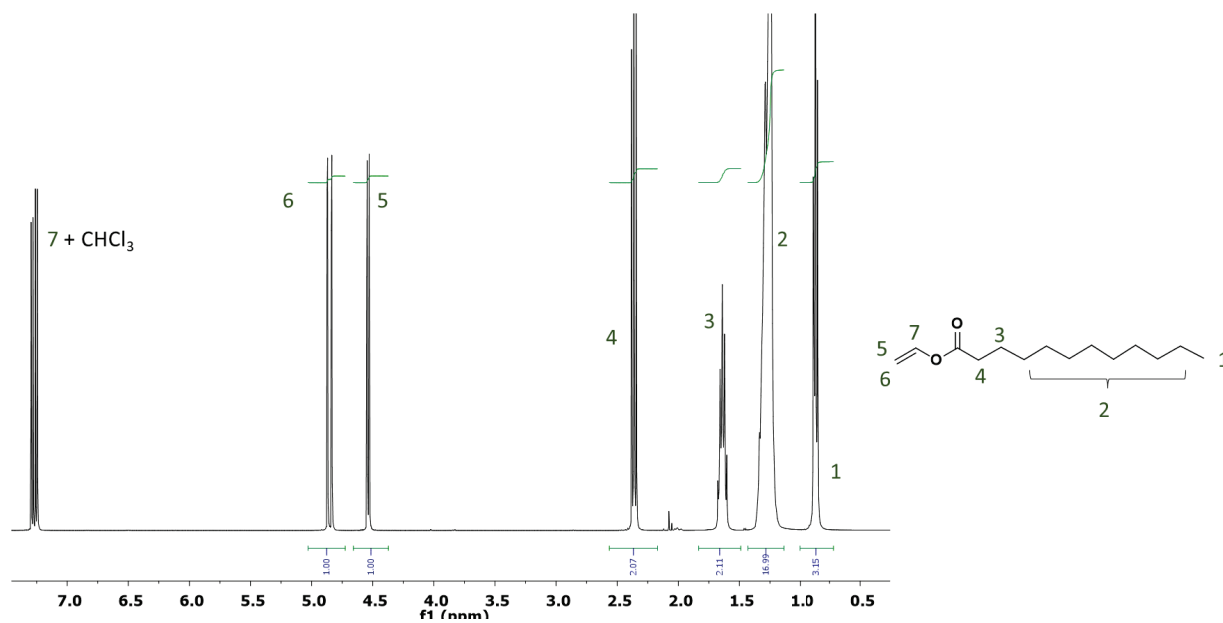


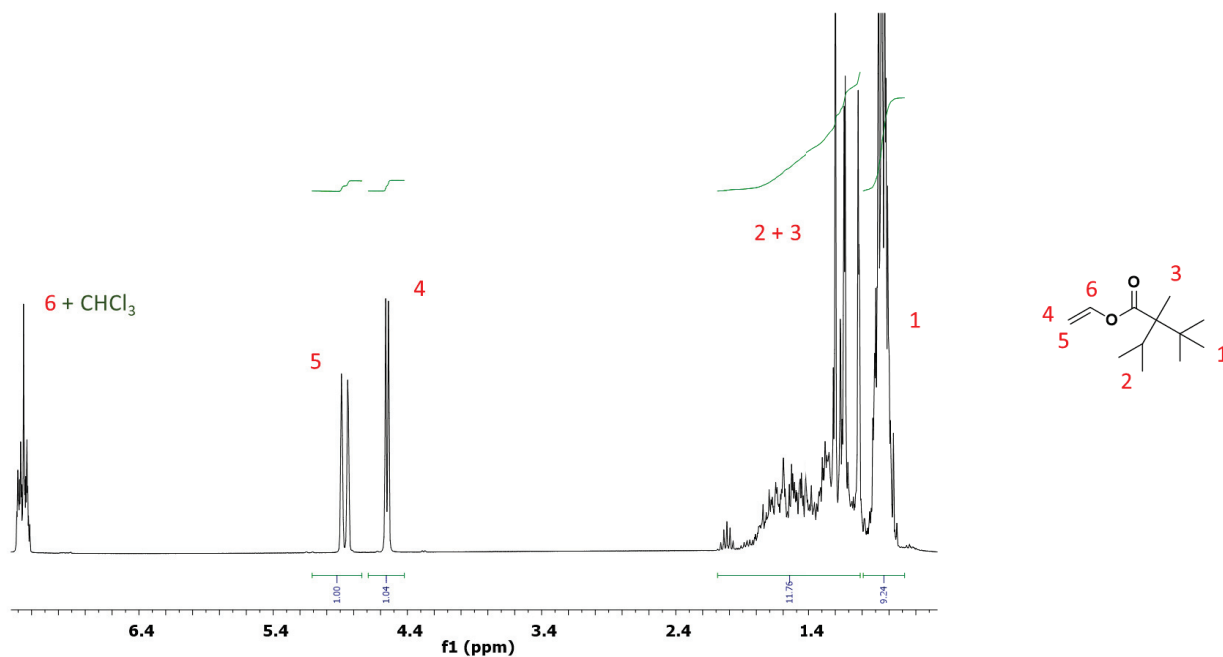
Figure X-1:  $^1\text{H}$  NMR spectrum of VAc in  $\text{CDCl}_3$ , 24 scans, R.T.



## Vinyl laurate (VL)



## Vinyl neodecanoate (Veova)



## **Appendix 2: Calculation of the average number of monomers in the polymer via the $^1\text{H}$ NMR for the kinetic studies**

For each spectrum, letters refer to the integral of the signal corresponding to the proton of a monomer unit inside the polymer and numbers refer to the integrals of the signals corresponding to the protons of the monomer(s). The determination of the average number of monomer units incorporated inside the polymer, the global DP and  $M_n$  during the polymerizations were carried out by the analysis of samplings by  $^1\text{H}$  NMR. The determination of the DP of each monomer (*e.g.*,  $\text{DP}_{\text{VAc}}$ ,  $\text{DP}_{\text{VL}}$  or  $\text{DP}_{\text{VeoVa}}$ ) incorporated inside the polymer during the polymerization was based on equations to isolate the integrals of the protons corresponding to monomer that did not react at the time when the sample was withdrawn from the polymerization media, and the integrals of the protons corresponding to monomer units which were already incorporated to the polymer. To ease the notation, integrals of the signals will be noted I, with subscript letters or number referring to protons from the polymer or from the monomer (see attributions).

For the kinetics studies, molar mass was calculated assuming 100% of the chains are functionalized with the ethoxy Z group and using the integral of this resonance (g) as a reference as the ethoxy R group overlapped with EtAc signal at 4.1 ppm.

## PVAc (Chapter II)

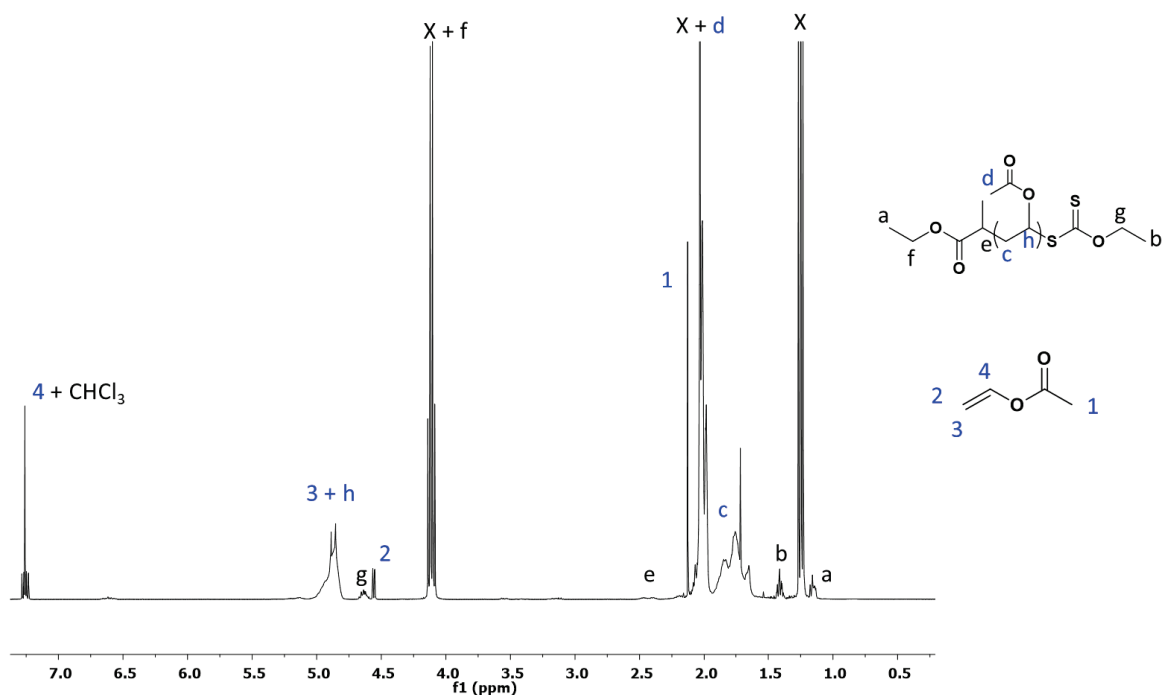


Figure X-4: Determination of the conversion of VAc into PVAc during RAFT/MADIX polymerization by comparing monomer and polymer resonances. R.T., 256 scans, CDCl<sub>3</sub>.

The value of  $I_g$  is set at 2. In that case  $I_{PVAc}$ , which corresponds to the value of the integral of the VAc units incorporated in the polymer, is also  $DP_{VAc}$ .

$$I_{PVAc} = I_{(3+h)} - I_2 \quad (64)$$

$$\%.\text{Conv}(\text{VAc}) = 100 \times \frac{I_{PVAc}}{I_{(3+h)}} \quad (65)$$

### P(VAc-s-VL) (Chapter III)

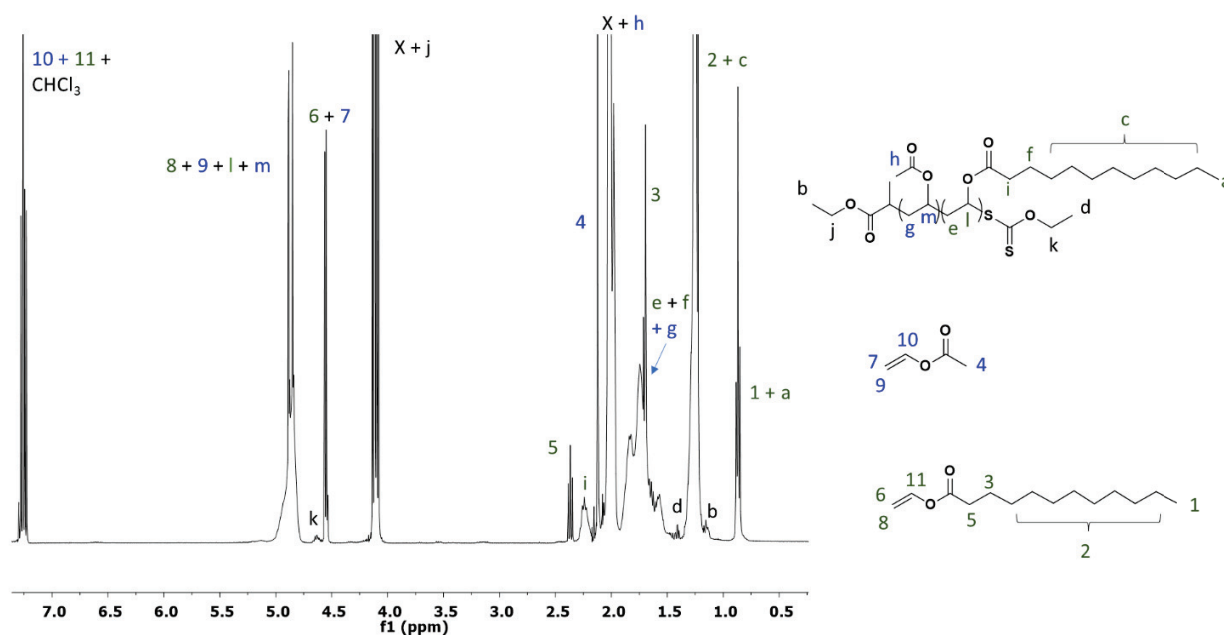


Figure X-5: Determination of the conversion of VAc and VL into P(VAc-s-VL) during RAFT/MADIX polymerization by comparing monomer and polymer resonances. R.T., 256 scans,  $\text{CDCl}_3$ .

The value of  $I_k$  is set at 2. In that case,  $I_{\text{PVL}}$ , which corresponds to the value of the integral of the VL units incorporated in the polymer, and  $I_{\text{PVAc}}$  which is the value of the integral of the VAc units incorporated in the polymer, are also  $DP_{\text{VL}}$  and  $DP_{\text{VAc}}$ , respectively.  $I_{\text{VL}}$  and  $I_{\text{VAc}}$  correspond to the value of the integrals of the VL and VAc units belonging to the monomer.

$$I_{\text{PVL}} = \frac{I_i}{2} \quad (66)$$

$$I_{\text{PVAc}} = I_{(8+9+l+m)} - I_{(6+7)} - I_{\text{PVL}} \quad (67)$$

$$I_{\text{VAc}} = \frac{I_4}{3} \quad (68)$$

$$I_{\text{VL}} = \frac{I_5}{2} \quad (69)$$

$$\%.\text{Conv}(\text{VL}) = \frac{I_{\text{PVL}}}{I_{\text{PVL}} + I_{\text{VL}}} \quad (70)$$

$$\%.\text{Conv}(\text{VAc}) = \frac{I_{\text{PVAc}}}{I_{\text{PVAc}} + I_{\text{VAc}}} \quad (71)$$

### P(VAc-s-VeoVa) (Chapter III)

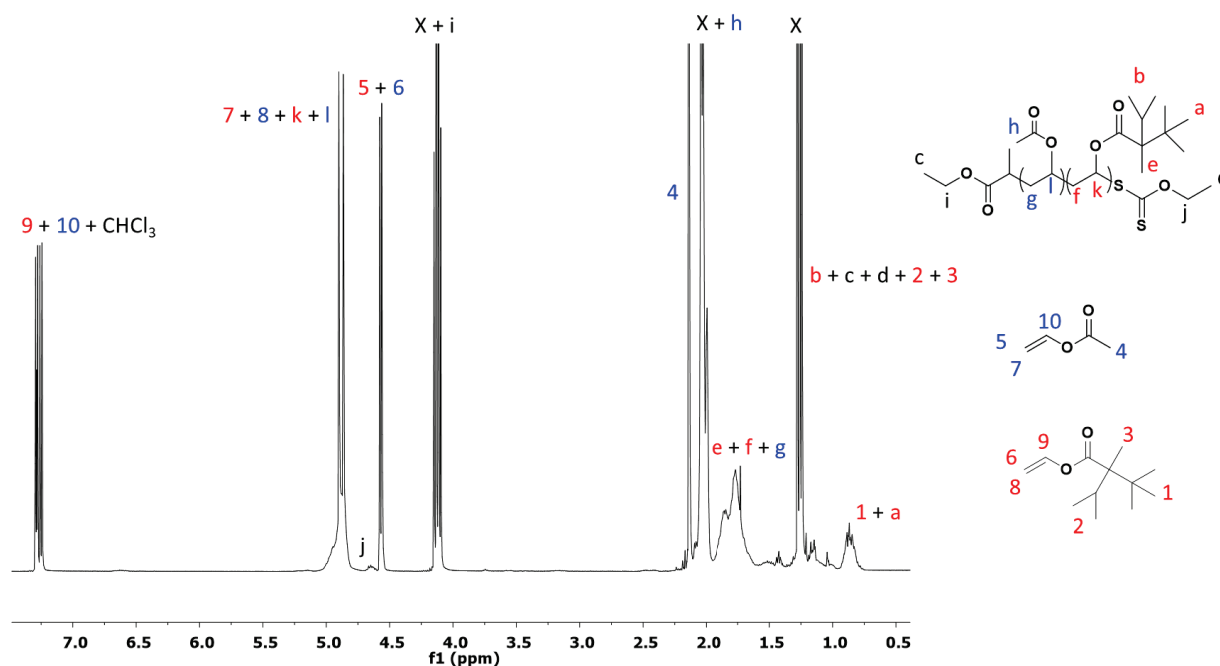


Figure X-6: Determination of the conversion of VAc and VeoVa into P(VAc-s-VeoVa) during RAFT/MADIX polymerization by comparing monomer and polymer resonances. R.T., 256 scans,  $\text{CDCl}_3$ .

The value of  $I_j$  is set at 2. In that case,  $I_{\text{PVeoVa}}$ , which corresponds to the value of the integral of the VeoVa units incorporated in the polymer and  $I_{\text{PVAc}}$  which is the value of the integral of the VAc units incorporated in the polymer, are also  $DP_{\text{VeoVa}}$  and  $DP_{\text{VAc}}$ , respectively.  $I_{\text{VeoVa}}$  and  $I_{\text{VAc}}$  correspond to the value of the integrals of the VeoVa and VAc units belonging to the monomer

$$I_{\text{VAc}} = \frac{I_4}{3} \quad (72)$$

$$I_{\text{VeoVa}} = I_{(5+6)} - I_{\text{VAc}} \quad (73)$$

$$I_{\text{PVeoVa}} = \frac{I_{1+a}}{9} - I_{\text{VeoVa}} \quad (74)$$

$$I_{\text{PVAc}} = I_{(7+8+k+l)} - I_{(5+6)} - I_{\text{PVeoVa}} \quad (75)$$

$$\%.\text{Conv}(\text{VeoVa}) = \frac{I_{\text{PVeoVa}}}{I_{\text{PVeoVa}} + I_{\text{VeoVa}}} \quad \text{and} \quad \%.\text{Conv}(\text{VAc}) = \frac{I_{\text{PVAc}}}{I_{\text{PVAc}} + I_{\text{VAc}}} \quad (76) \text{ and } (77)$$

### PVL (Chapter IV)

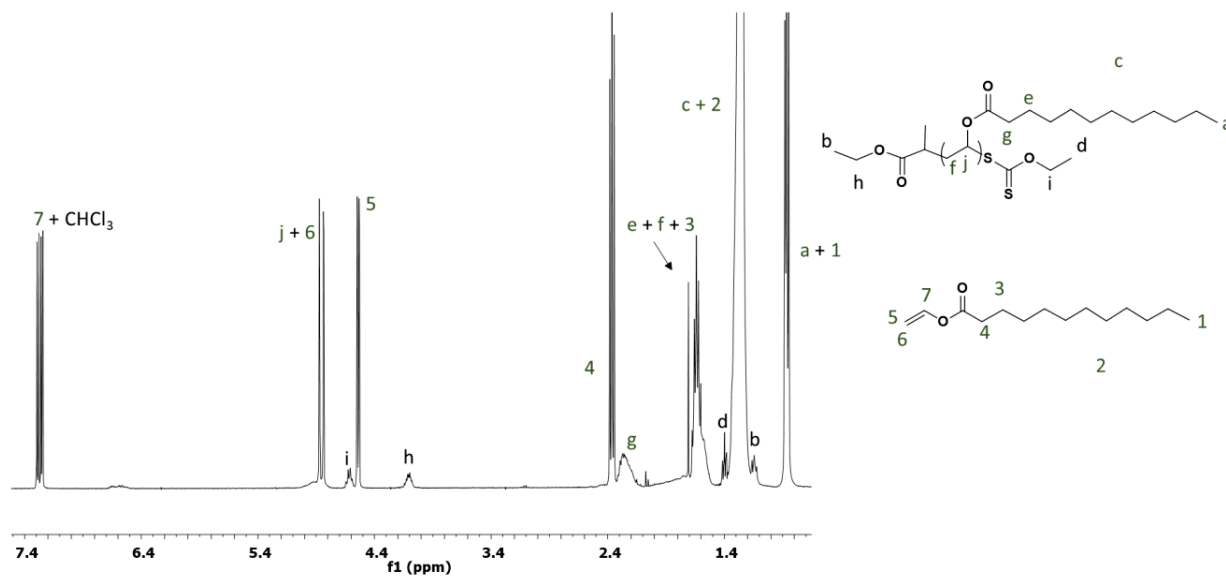


Figure X-7 : Determination of the conversion of VL into PVL during RAFT/MADIX polymerization by comparing monomer and polymer resonances. R.T., 256 scans,  $\text{CDCl}_3$ .

The value of  $I_h$  or  $I_i$  is set at 2. In that case  $I_{\text{PVL}}$ , which corresponds to the value of the integral of the VL units incorporated in the polymer, is also  $\text{DP}_{\text{VL}}$ .

$$I_{\text{PVL}} = I_{(j+6)} - I_5 \quad (78)$$

$$\%.\text{Conv}(\text{VL}) = 100 \times \frac{I_{(j+6)} - I_5}{I_{(j+6)}} \quad (79)$$

## DP1 PVL-*b*-DP2 PVAc (Chapter IV)

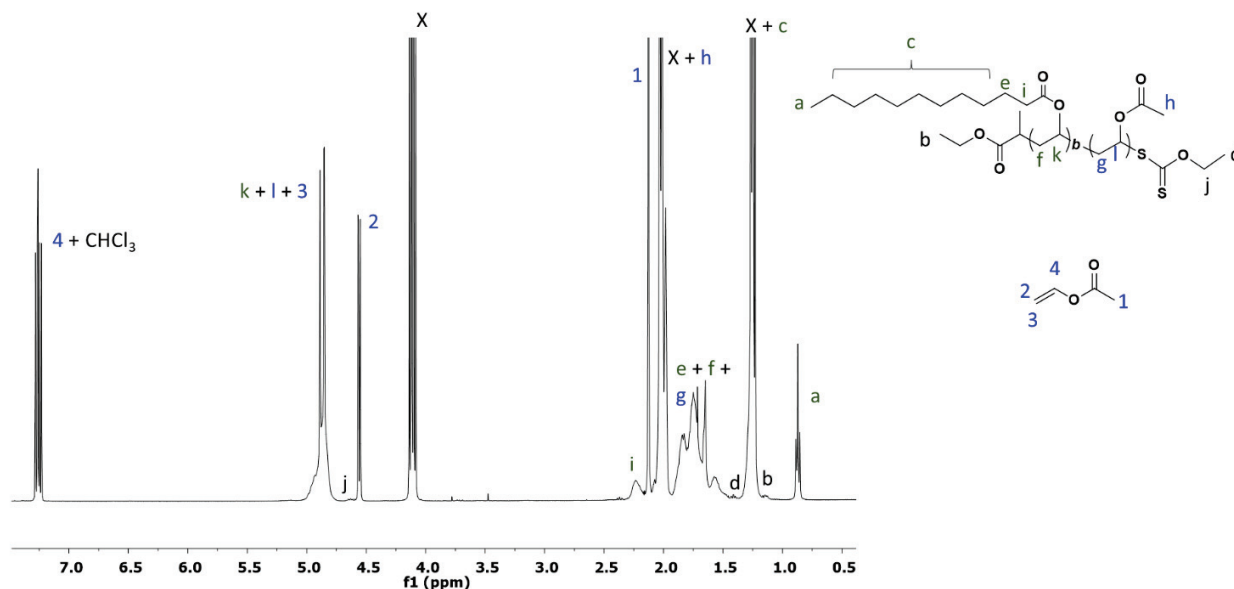


Figure X-8: Determination of the conversion of VAc during the extension of PVL-X by comparing monomer and polymer resonances. R.T., 256 scans,  $\text{CDCl}_3$ .

The value of  $I_j$  is set at 2. In that case  $I_{\text{PVAc}}$ , which corresponds to the value of the integral of the VAc units incorporated in the polymer, is also  $\text{DP}_{\text{VAc}}$ .  $I_k = I_{\text{macroCTA}} = \text{DP}_{\text{VL}} = \text{DP}_1$

$$I_{\text{PVAc}} = \text{DP}_{\text{VAc}} = I_{(k+l+3)} - I_2 - I_{\text{macroCTA}} \quad (80)$$

$$\%.\text{Conv}(\text{VAc}) = \frac{I_{\text{PVAc}}}{I_{\text{PVAc}} + I_2} \quad (81)$$

## PVeoVa (Chapter IV)

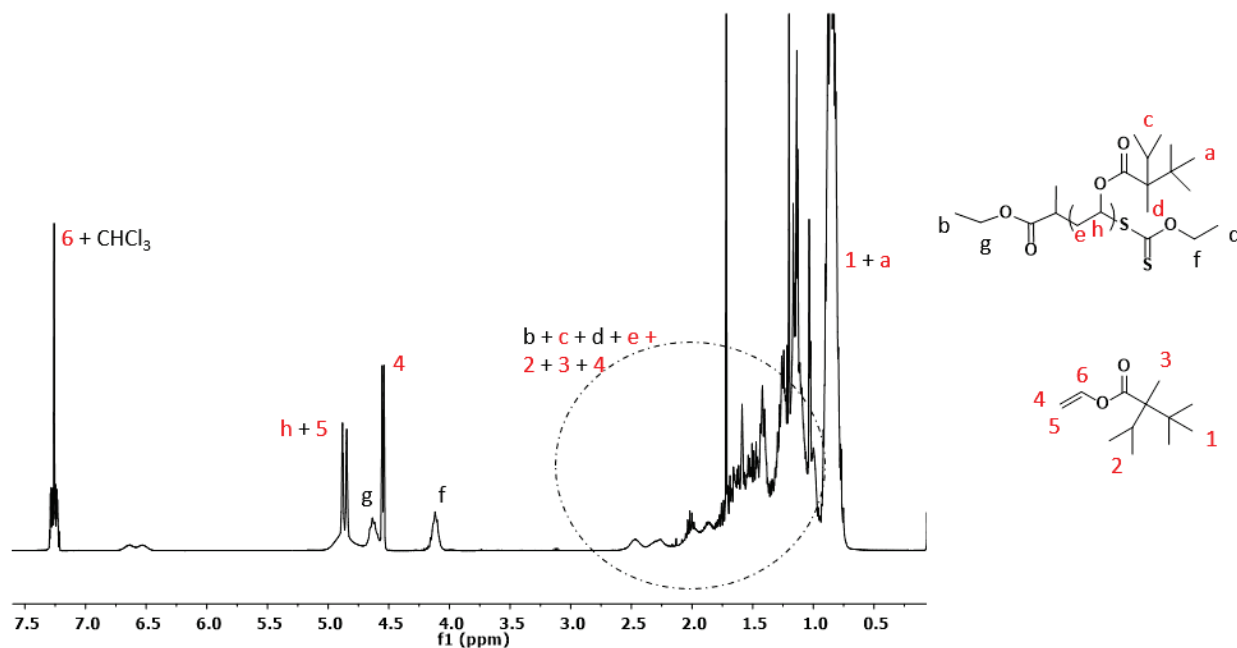


Figure X-9: Determination of the conversion of VeoVa into PVeoVa during RAFT/MADIX polymerization by comparing monomer and polymer resonances. R.T., 256 scans, CDCl<sub>3</sub>.

The value of  $I_f$  or  $I_g$  is set at 2. In that case  $I_{PVeoVa}$ , which corresponds to the value of the integral of the VL units incorporated in the polymer, is also  $DP_{VeoVa}$ .

$$I_{PVeoVa} = I_{(h+5)} - I_4 \quad (82)$$

$$\%Conv(VeoVa) = 100 \times \frac{I_{(h+5)} - I_4}{I_{(h+5)}} \quad (83)$$



## DP1 PveoVa-*b*-DP2 PVAc (Chapter IV)

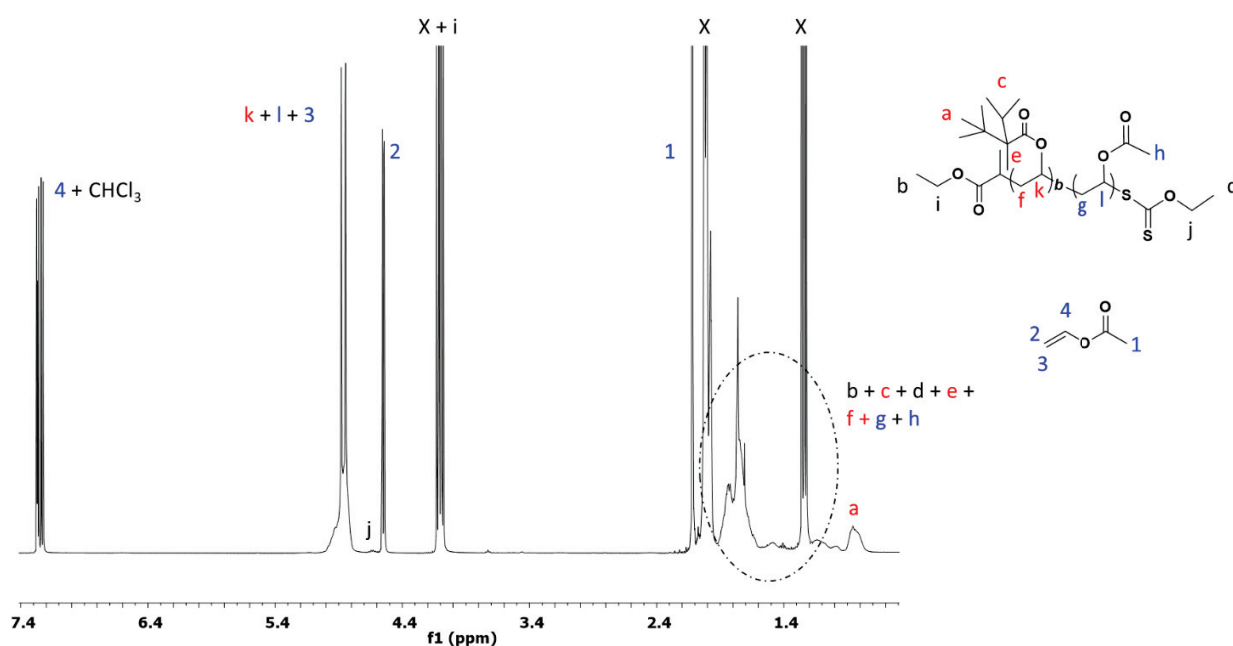


Figure X-10: Determination of the conversion of VAc during the extension of PveoVa-X by comparing monomer and polymer resonances. R.T., 256 scans, CDCl<sub>3</sub>.

The value of  $I_j$  is set at 2. In that case  $I_{PVAc}$ , which corresponds to the value of the integral of the VAc units incorporated in the polymer, is also  $DP_{VAc}$ .  $I_k = I_{macroCTA} = DP_{VeoVa} = DP_1$

$$I_{PVAc} = DP_{VAc} = I_{(k+l+3)} - I_2 - I_{macroCTA} \quad (84)$$

$$\%Conv(VAc) = 100 \times \frac{I_{PVAc}}{I_{PVAc} + I_2} \quad (85)$$

## DP1 PVAc-*b*-DP2 P(VAc-*s*-VL) (Chapter V)

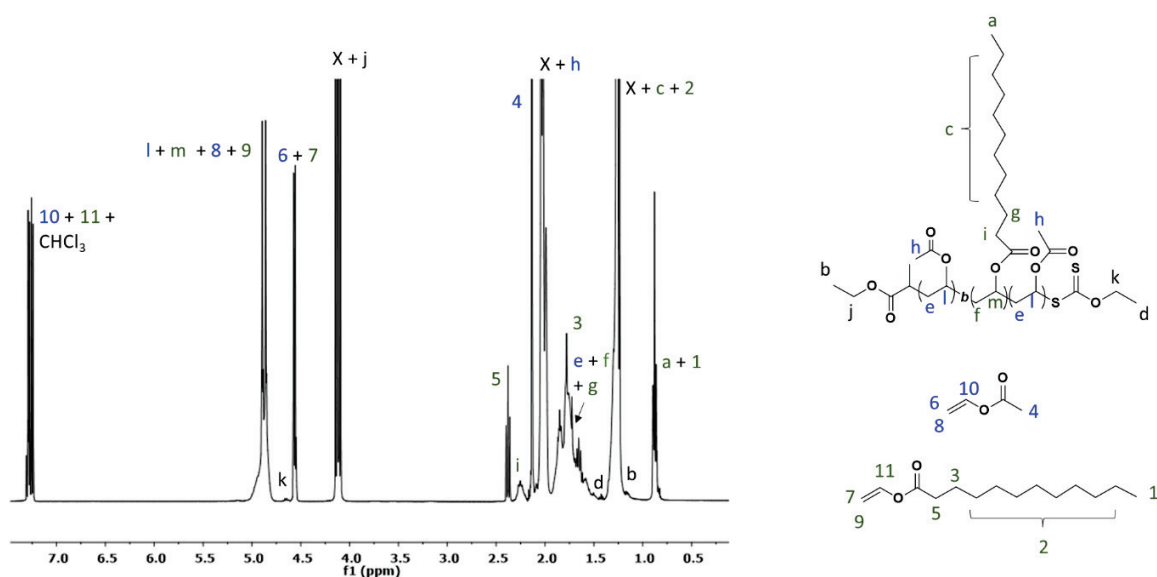


Figure X-11: Determination of the conversion of VAc and VL during the extension of PVAc-*X* into PVAc-*b*-P(VAc-*s*-VL) by comparing monomer and polymer resonances. R.T., 256 scans, CDCl<sub>3</sub>.

The value of  $I_k$  is set at 2. In that case,  $I_{PVL}$ , which corresponds to the value of the integral of the VL units incorporated in the polymer, is also  $DP_{VL}$ .  $I_{VL}$  and  $I_{VAc}$  correspond to the value of the integrals of the VL and VAc units belonging to the monomer.  $I_{macroCTA} = DP_1$ , determined by  $^1H$  NMR before extension.

$$I_{VAc} = \frac{I_4}{3} \quad (86)$$

$$I_{VL} = I_{(6+7)} - I_{VAc} \quad (87)$$

$$I_{PVL} = \frac{I_i}{2} \quad (88)$$

$$I_{PVAc} = I_{(1+m+8+9)} - I_{(6+7)} - I_{PVL} - DP_1 \quad (89)$$

$$\%.Conv(VL) = 100 \times \frac{I_{PVL}}{I_{PVL} + I_{VL}} \quad (90)$$

$$\%.Conv(VAc) = 100 \times \frac{I_{PVAc}}{I_{PVAc} + I_{VAc}} \quad (91)$$

$$\text{Global DP} = \text{DP1} + I_{\text{PVAc}} + I_{\text{PVL}} \quad (92)$$

### DP1 PVAc-*b*-DP2 P(VAc-*s*-VeoVa) (Chapter V)

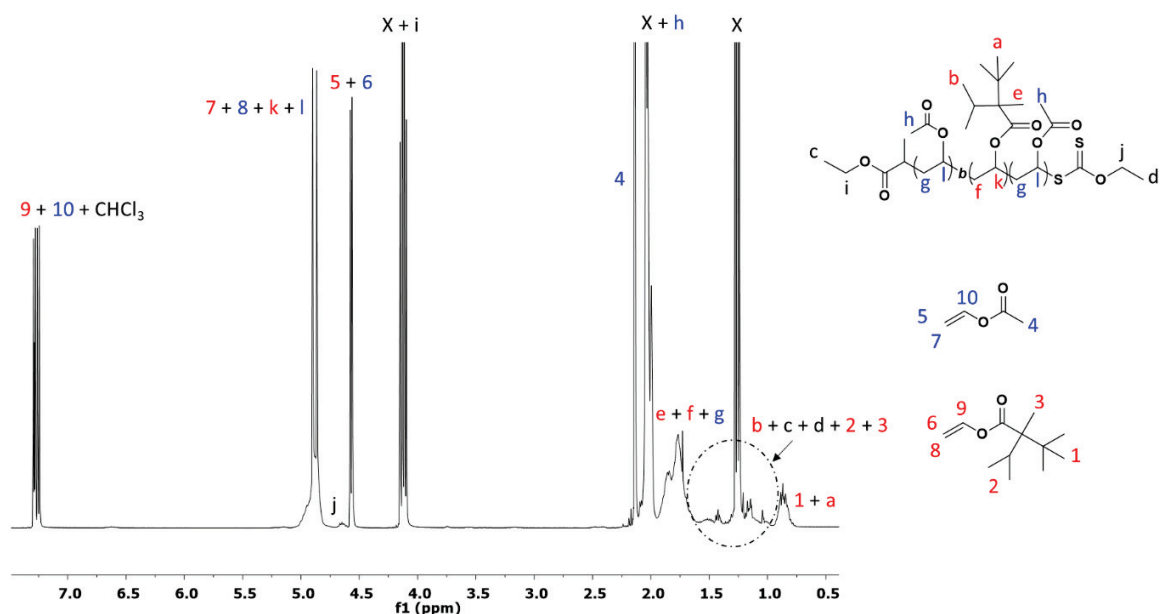


Figure X-12: Determination of the conversion of VAc and VeoVa during the extension of PVAc-*X* into PVAc-*b*-P(VAc-*s*-VeoVa) by comparing monomer and polymer resonances. R.T., 256 scans, CDCl<sub>3</sub>.

The value of  $I_j$  is set at 2. In that case,  $I_{\text{PVeoVa}}$ , which corresponds to the value of the integral of the VeoVa units incorporated in the polymer, is also  $\text{DP}_{\text{VeoVa}}$ .  $I_{\text{VeoVa}}$  and  $I_{\text{VAc}}$  correspond to the value of the integrals of the VeoVa and VAc units belonging to the monomer.  $I_{\text{macroCTA}} = \text{DP1}$ , determined by <sup>1</sup>H NMR before extension.

$$I_{\text{VAc}} = \frac{I_4}{3} \quad (93)$$

$$I_{\text{VeoVa}} = I_{(5+6)} - I_{\text{VAc}} \quad (94)$$

$$I_{\text{PVeoVa}} = \frac{I_{1+a}}{9} - I_{\text{VeoVa}} \quad (95)$$

$$I_{\text{PVAc}} = I_{(7+8+k+l)} - I_{(5+6)} - I_{\text{PVeoVa}} - \text{DP1} \quad (96)$$

$$\%.\text{Conv}(\text{VeovVa}) = 100 \times \frac{I_{\text{PveoVa}}}{I_{\text{PveoVa}} + I_{\text{VeovVa}}} \quad \text{and} \quad \%.\text{Conv}(\text{VAc}) = 100 \times \frac{I_{\text{PVAc}}}{I_{\text{PVAc}} + I_{\text{VAc}}} \quad \text{(97) and (98)}$$

$$\text{Global DP} = \text{DP1} + I_{\text{PVAc}} + I_{\text{PveoVa}} \quad \text{(99)}$$

**Appendix 3: Plot of  $N_p$  as a function of conversion for the emulsion copolymerization of VAc and VeoVa stabilized with 100\_P(VOH<sub>0.88</sub>-S-VAc<sub>0.12</sub>) (Chapter II)**

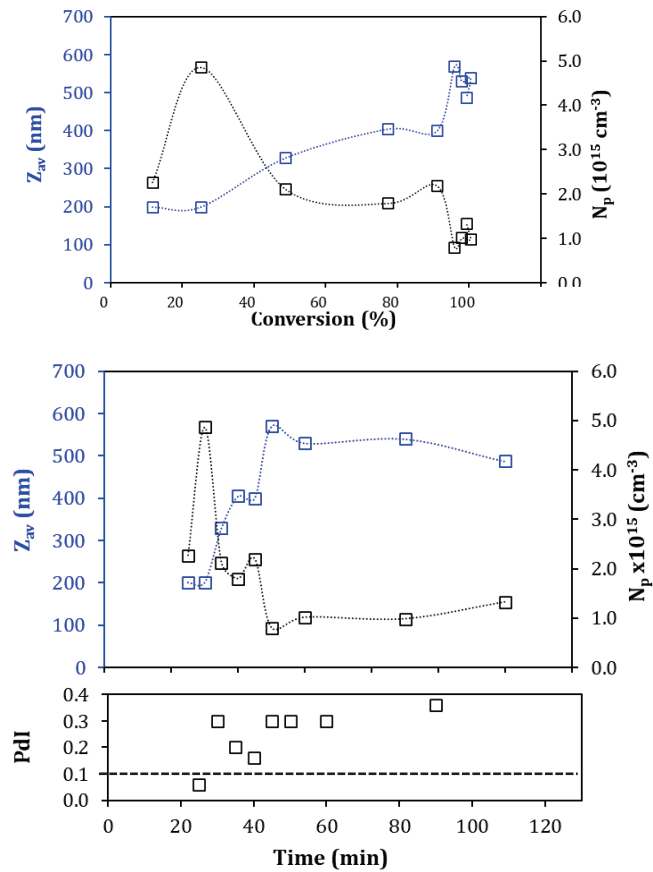


**Figure X-13: Evolution of  $Z_{av}$  and  $N_p$  of the latex obtained with 100\_P(VOH<sub>0.88</sub>-S-VAc<sub>0.12</sub>) as a function of time and conversion and corresponding Pdl.**

**Appendix 4:  $^1\text{H}$  NMR analysis of the dry supernatant of 75\_P(VOH<sub>0.88</sub>-s-VAc<sub>0.12</sub>) to verify that only the stabilizer is present in the supernatant after centrifugation**

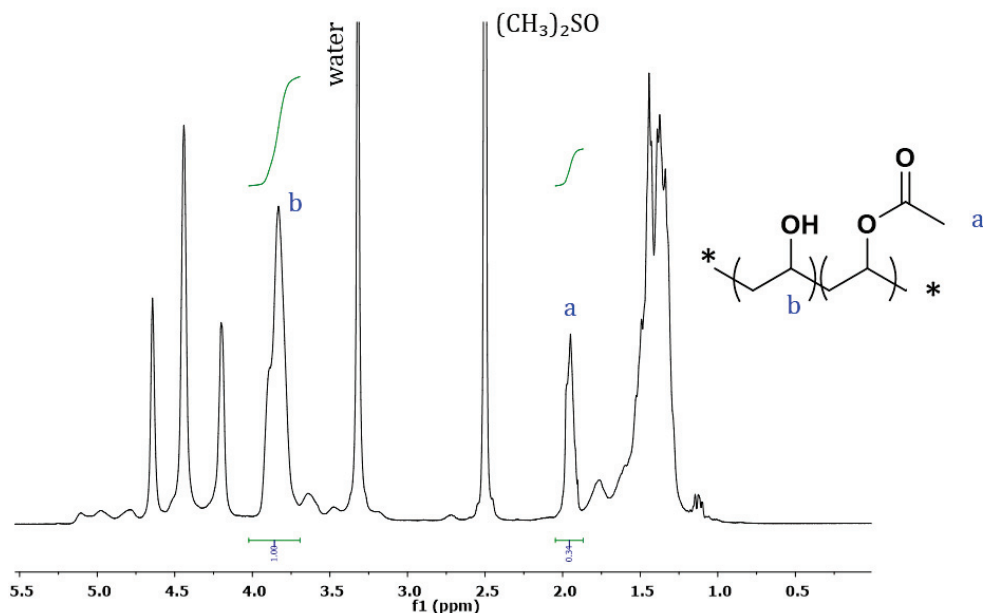


**Figure X-14:  $^1\text{H}$  NMR spectrum of the supernatant of the latex obtained with 75\_P(VOH<sub>0.88</sub>-s-VAc<sub>0.12</sub>) after ultracentrifugation.**

The ratio of the integrals at 3.6 - 4 ppm with the integral at 1.78 - 2 ppm that correspond, respectively, to the methine protons of the VOH units and the methyl protons from the side group of the VAc units, provided a HD of 89%, which corresponds to the HD of the stabilizer (**Chapter II, Section III**). This result indicates that the only VAc and VOH units of the polymer present in the aqueous phase belonged to the stabilizer and not to the soluble fraction of polymer.

## Appendix 5: DLS analysis of the stabilizers in water: volume distributions at 25 °C and intensity distributions at 55 °C for the selected copolymers

Self-assembly properties of the dispersible amphiphilic copolymers were evaluated by DLS. To mimic the emulsion polymerization composition (10 wt.% of stabilizer based on monomers, meaning 2.5 wt.% of stabilizer based on the total volume of the reaction), samples containing deionized water and 2.5 wt.% of each stabilizer candidates were prepared and analyzed by DLS without further dilution.

### 1. Statistical copolymers (Chapter III)

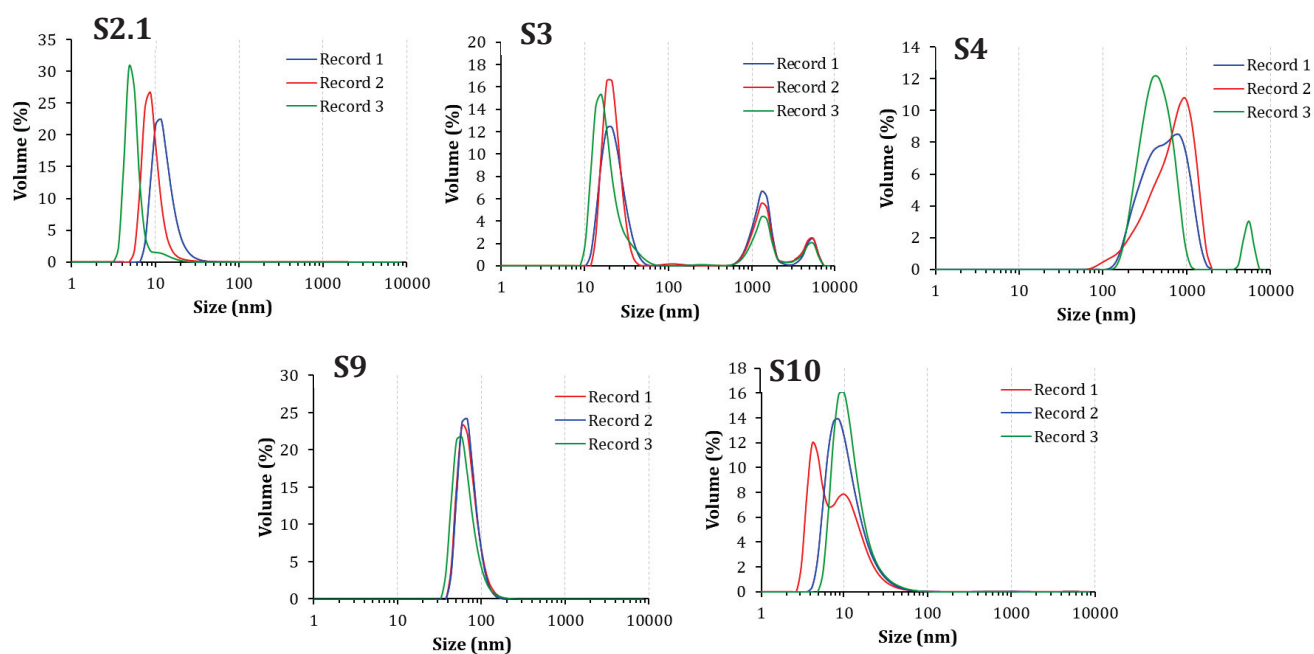


Figure X-15: DLS distribution in volume for the dispersions of the statistical copolymers.

## 2. Block copolymers (Chapter IV)

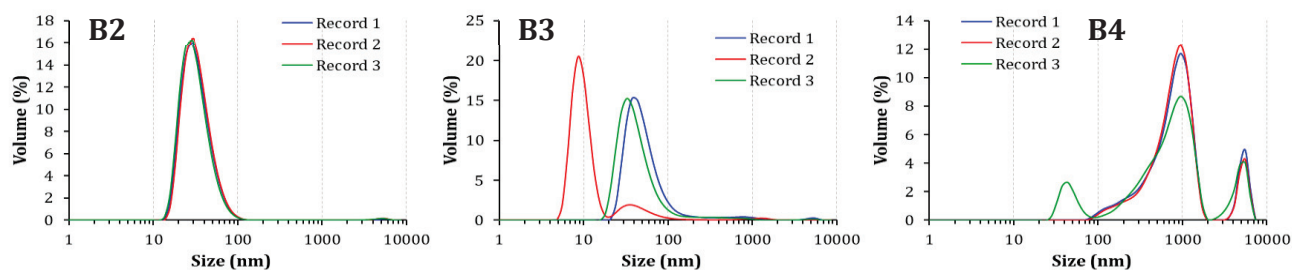


Figure X-16: DLS distribution in volume for the dispersions of the block copolymers.

## 3. Hybrid copolymers (Chapter V)

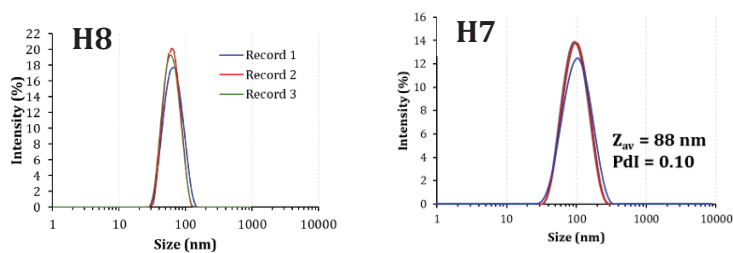


Figure X-17: DLS distribution in intensity for the dispersions of the hybrid copolymers.

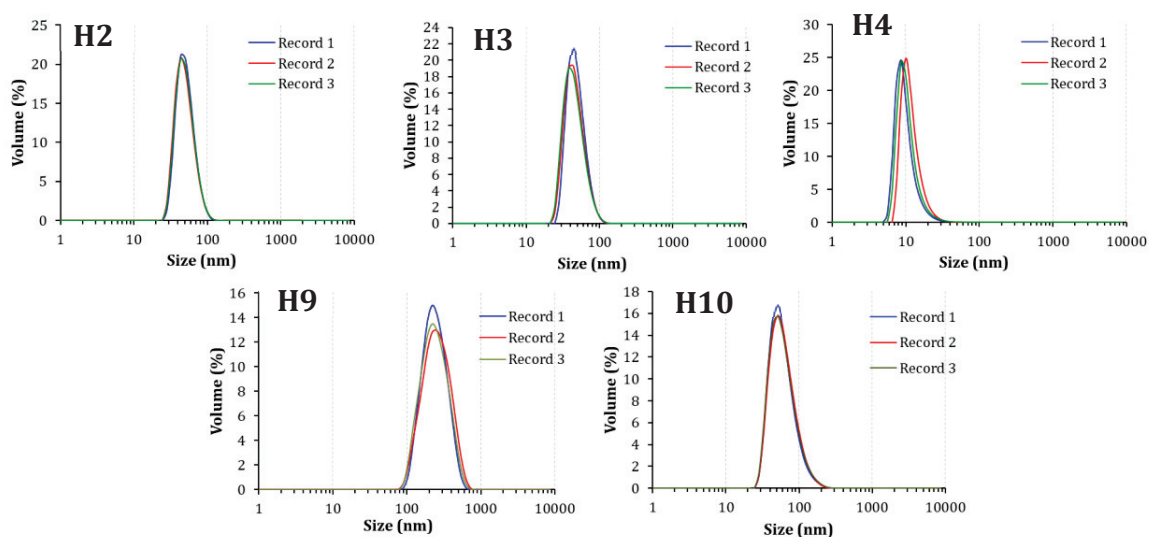
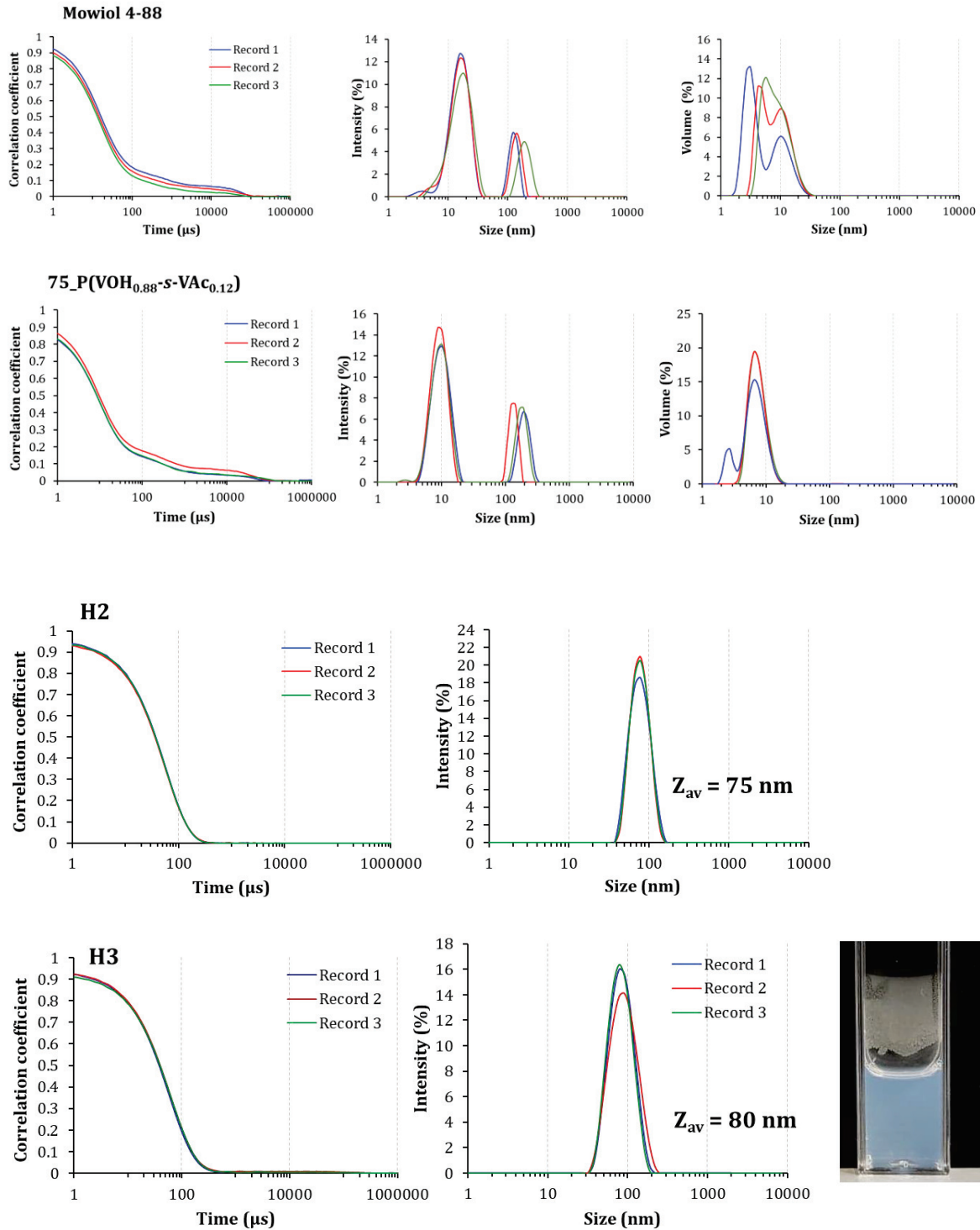


Figure X-18: DLS distribution in volume for the dispersions of the hybrid copolymers.



#### 4. DLS-size distribution in intensity of dispersions at 55 °C (Chapter V)



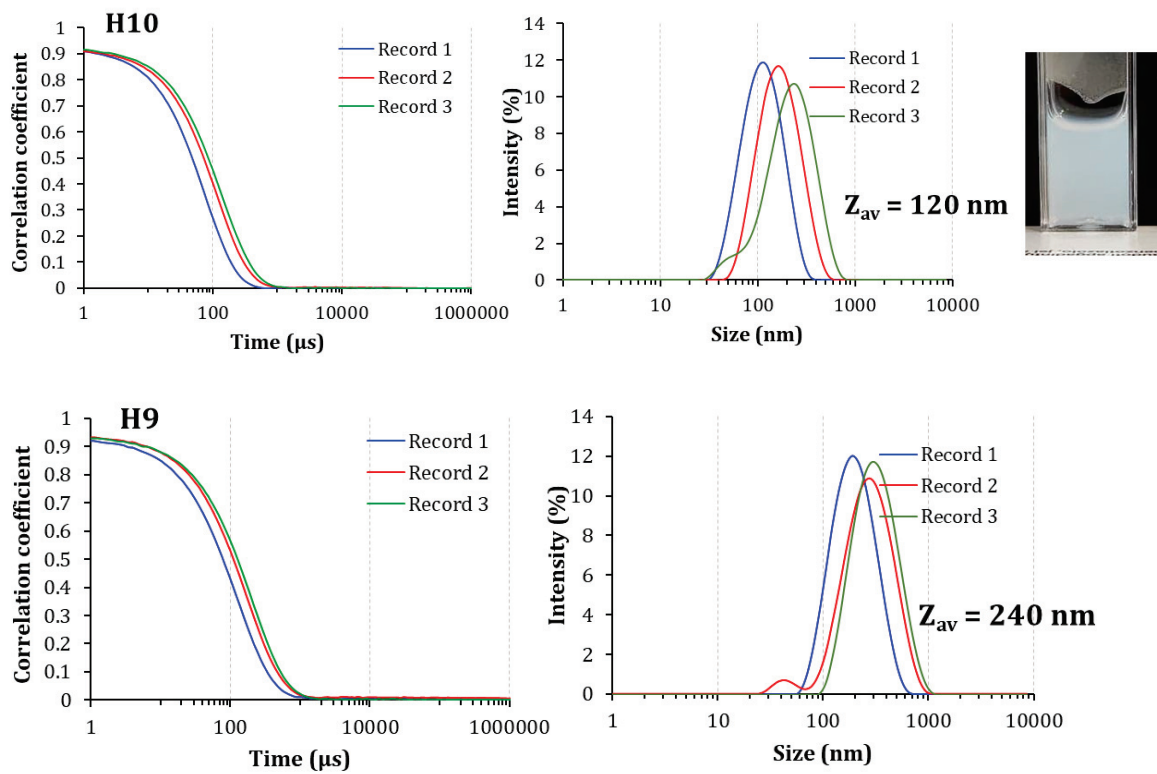


Figure X-19: Correlograms and DLS-size distributions in intensity (and in volume) for the 2.5 wt. % aqueous dispersions hybrid copolymers obtained after thermal treatment for the different copolymers. Measurements were performed at 55 °C.

## Appendix 6: Investigation on the presence of the xanthate moiety after alcoholysis of P(VOH-s-VAc)-*b*-PVeOVA block copolymer

An alternative study from **Chapter IV** was to determine whether the VeoVa units are able to protect the xanthate extremity from hydrolysis. It was already demonstrated in **Chapter II** that the alcoholysis of the xanthate extremity in PVAc-X led to the formation of a thioaldehyde, which was visible in the  $^1\text{H}$  NMR signal at 9.5 - 9.6 ppm. If the PVeOVA block indeed protects the xanthate extremity against hydrolysis, this signal should not be visible in the  $^1\text{H}$  NMR spectrum of the resulting alcoholized P(VOH-s-VAc)-*b*-PVeOVA-X. Therefore, the NMR spectra of **B2** (5\_PVeOVA<sub>0.05</sub>-*b*-95\_P(VOH<sub>0.90</sub>-s-VAc<sub>0.05</sub>)) and **B4** (75\_P(VOH<sub>0.924</sub>-s-VAc<sub>0.016</sub>)-*b*-5\_PVeOVA<sub>0.060</sub>) were compared (**Figure X-20**).

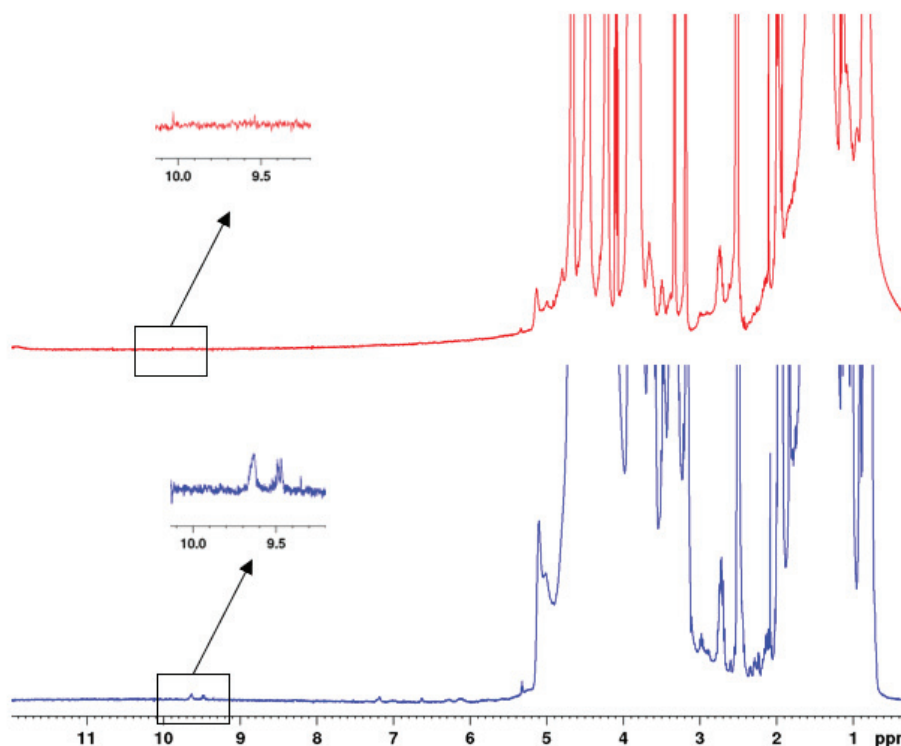
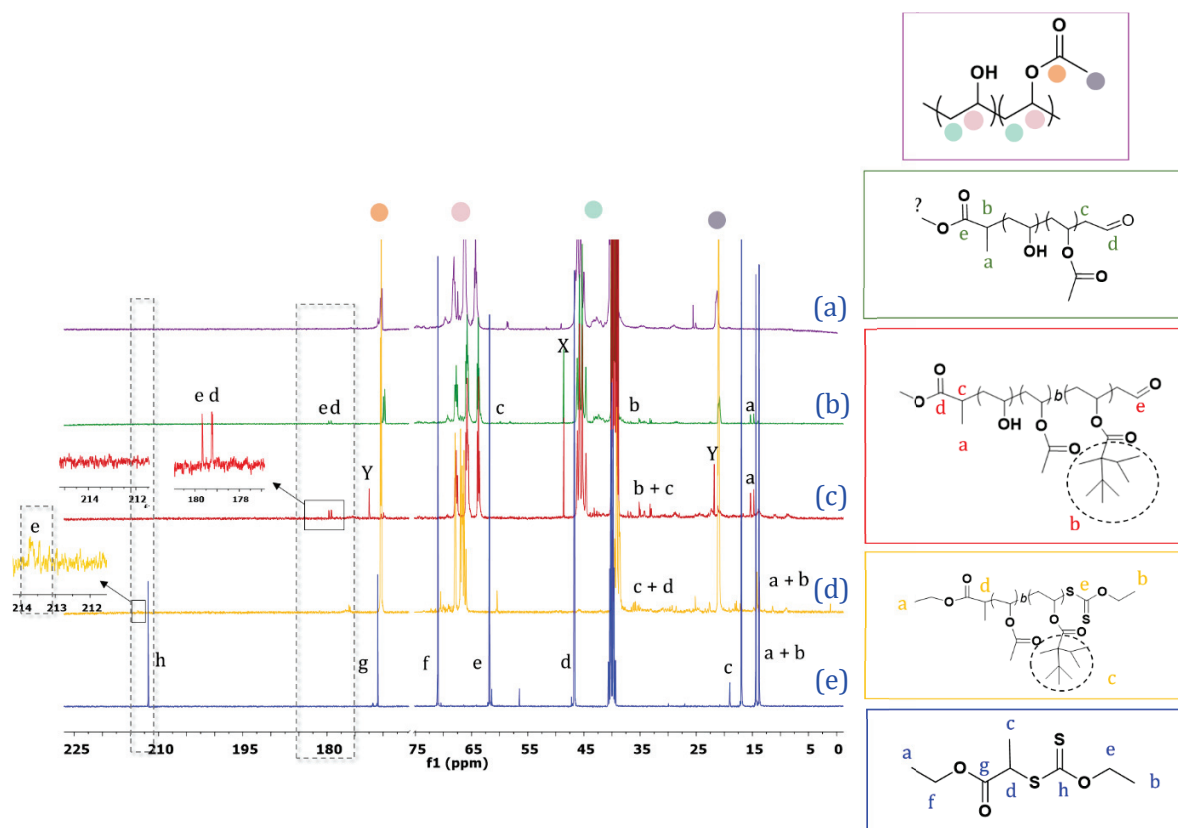


Figure X-20:  $^1\text{H}$  NMR spectrum of 75\_P(VOH<sub>0.924</sub>-s-VAc<sub>0.016</sub>)-*b*-5\_PVeOVA<sub>0.06</sub> (**B4**) (red) and 5\_PVeOVA<sub>0.05</sub>-*b*-95\_P(VOH<sub>0.90</sub>-s-VAc<sub>0.05</sub>) (**B2**) (blue) in DMSO- $d_6$  at R.T.

The NMR spectrum of **B2** shows the presence of the aforementioned thioaldehyde by-product resulting from the alcoholysis of the xanthate moieties, while this signal is not visible in the  $^1\text{H}$  NMR spectrum of **B4**. This result could confirm the hypothesis, but it must be taken with care. The signals from the chain-ends are often weak compared to the signals of the polymer, and can be hidden in the baseline. To crosscheck the information provided by  $^1\text{H}$  NMR, a  $^{13}\text{C}$  NMR analysis was run and the spectrum of **B4** was compared to those of the RAFT agent, Mowiol 4-88 and 75\_P(VOH-s-VAc) (**Figure X-21**).



**Figure X-21:**  $^{13}\text{C}$  NMR spectrum of (a) Mowiol 4-88, (b) 75\_P(VOH<sub>0.88</sub>-S-VAc<sub>0.12</sub>), (c) B4 (d) 75\_PVAc-*b*-5\_PVeoVa and (e) *O*-ethyl-*S*-(1-ethoxycarbonyl)ethyl dithiocarbonate in DMSO-*d*<sub>6</sub>, and the possible chain-end groups related with their hypothesized assignments. X refers to methanol and Y to acid acetic residues.

The main assignments of the polymer backbone are represented by colored stickers and are based on Moritani<sup>[1]</sup> and Budhlall's<sup>[2]</sup> works. The different possible chain-ends are represented on the right of the spectra with different colors, and the hypothesized assignments of the chain-ends are defined by corresponding-colored letters. The assignment of the chain-end signals was not straightforward and must be taken with care as they are just hypotheses. Nevertheless, the signal at 215 ppm, corresponding to the S-C=S carbon of the dithiocarbonate (signal *h* **Figure X-21** (d)) is no longer visible in the  $^{13}\text{C}$  spectrum of **B4** (**Figure X-21**). This could indicate that the xanthate group was not protected by the PVeoVa block during the alcoholysis and would refute the hypothesis. Instead, a signal at 180 ppm was identified in both 75\_P(VOH<sub>0.88</sub>-S-VAc<sub>0.12</sub>) and **B4** (**Figure X-21** (b) and (c), respectively), and could be attributed to the presence of an aldehyde at the end of the chain as already mentioned in **Chapter II** and based on Tong's work.<sup>[3]</sup> Nevertheless, this result is not very conclusive because it was demonstrated that both 75\_P(VOH<sub>0.924</sub>-S-VAc<sub>0.016</sub>) and 75\_P(VOH<sub>0.924</sub>-S-VAc<sub>0.016</sub>)-*b*-5\_PVeoVa<sub>0.060</sub> were present in the polymerization medium after extension of PVAc and alcoholysis of the crude, (**Chapter IV, Section II**), due to the fact that not all the PVAc chains from the first block were chain extended. Therefore, the signal

corresponding to the aldehyde could belong to the chain extremities of 75\_P(VOH<sub>0.924</sub>-S-VAc<sub>0.016</sub>), and the xanthate extremity which would be associated to 75\_P(VOH<sub>0.924</sub>-S-VAc<sub>0.016</sub>)-*b*-5\_PVeoVa<sub>0.060</sub> could be too weak (because in a very low amount compared to the polymer) to be visible.

An alternative study was to synthesize a PVeoVa homopolymer, alcohololyse it and try to further chain extend it with VAc. Unfortunately, none of the RAFT-synthesized PVeoVa were soluble in methanol, which is the alcoholysis solvent.

Another idea was thus to try to chain extend P(VOH-*s*-VAc)-*b*-PVeoVa with VAc. The protocol was adapted from Atanase's<sup>[4]</sup> thesis, where extension of a RAFT-synthesized P(VOH-*s*-VAc) with VAc was investigated after acidic hydrolysis of a PVAc synthesized by RAFT/MADIX polymerization.

- **Experiment 1:**

As an example, 0.5 g of 75\_P(VOH-*s*-VAc)-*b*-5\_PVeoVa (**B4**) was solubilized in 4 mL of DMSO, 2.5 g of VAc (29 mmol) and 0.00113 g of lauroyl peroxide (0.0295 mmol) previously solubilized in 3 mL of DMSO. The reaction was carried out for 4 h at 70 °C.

<sup>1</sup>H NMR in DMSO-*d*<sub>6</sub> was performed to determine the conversion, but after 4 h, no conversion was obtained.

- **Experiment 2:**

Similar reaction, following the same protocol, was performed during 24 h. <sup>1</sup>H NMR analysis was performed on this sample.

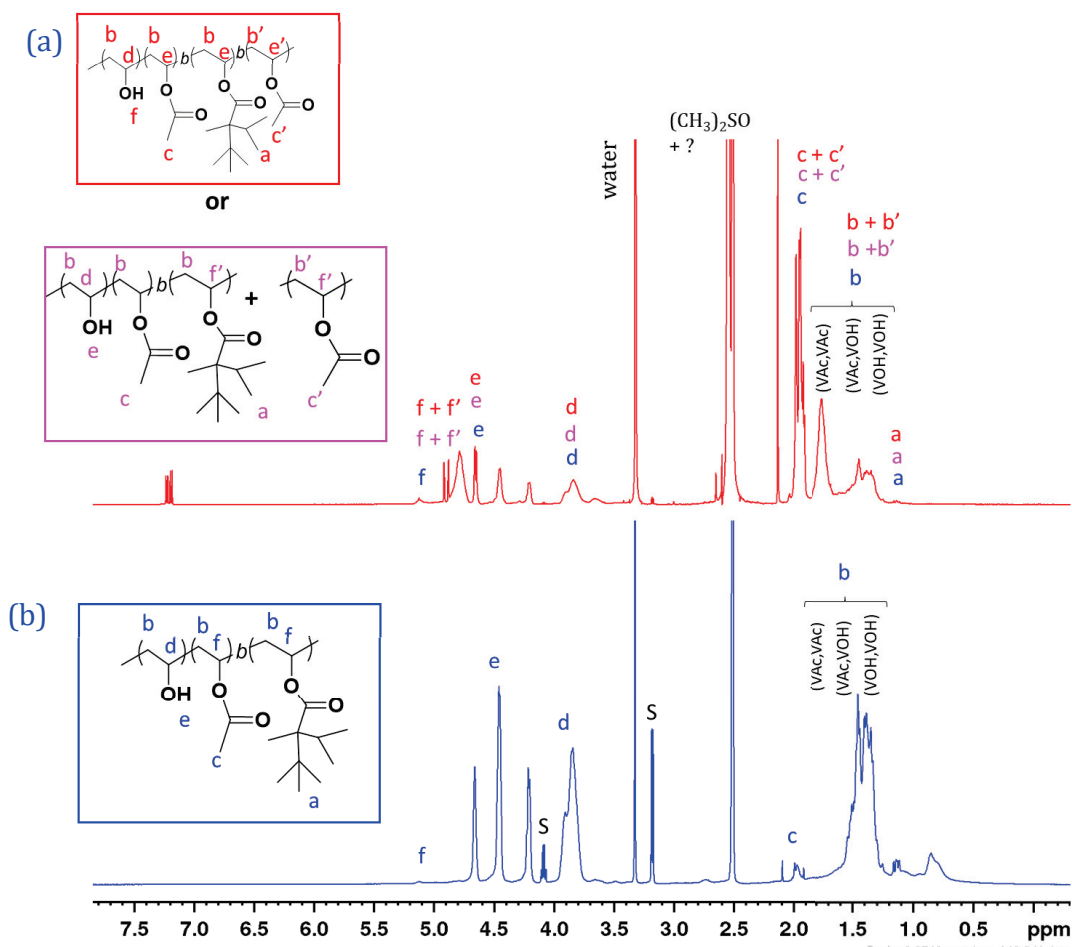


Figure X-22:  $^1\text{H}$  NMR analysis of (a)  $\text{P}(\text{VOH-}s\text{-VAc})\text{-}b\text{-PVeoVa}$  after extension with VAc during 24 h and (b)  $\text{P}(\text{VOH-}s\text{-VAc})\text{-}b\text{-PVeoVa}$  (B4) before extension. R.T., 256 scans,  $\text{DMSO-}d_6$ .

$^1\text{H}$  NMR analysis of the copolymer after 24 h showed that characteristic signals of PVAc were present on the spectrum ( $b'$ ,  $c'$  and  $f'$ ) (Figure X-22 (a)). Nevertheless, it does not attest of the extension of  $\text{P}(\text{VOH-}s\text{-VAc})\text{-}b\text{-PVeoVa}$ . Indeed, it is also possible that homopolymer of PVAc was formed in the presence of the initiator resulting in a mixture of  $\text{P}(\text{VOH-}s\text{-VAc})\text{-}b\text{-PVeoVa}$  and PVAc, as highlighted by the two possible structures.

The polymers before and after extension were thus analyzed by SEC-DMSO.

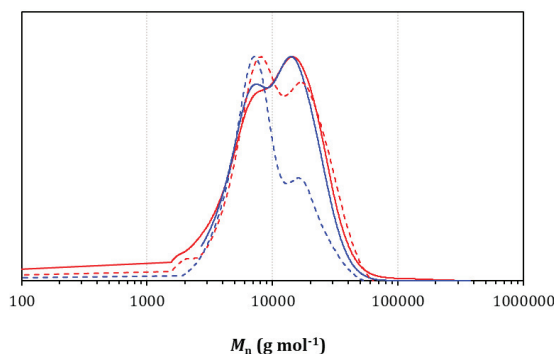


Figure X-23: SEC-DMSO trace of (—) 75\_P(VOH-s-VAc)-b-5\_PVeoVa and (—) the polymer “after extension” with VAc. Full lines represent the RI signal and dashed lines correspond to the UV signal at 280 nm

The SEC traces obtained in DMSO does not provide a clear shift of the molar mass towards higher molar mass, which could indicate that the extension of the block copolymer did not occur, and that either the xanthate moiety has been alcoholized, or that it is not present in a sufficient amount to significantly affect the molar mass of the copolymer. Additionally, a ratio [75\_P(VOH-s-VAc)-b-5\_PVeoVa]:[ACPA] = 5 was used to carry out the experiment, assuming that all the chains of 75\_P(VOH-s-VAc)-b-5\_PVeoVa were functionalized with the xanthate. However, it was proved in **Chapter II** that the chain-end functionality of 75\_P(VOH-s-VAc) before extension was approximately 55%. Thus, half of the chain possibly carry a PVeoVa block, and thus a xanthate moiety (supposing that it has not been hydrolyzed). It is possible that the ratio [75\_P(VOH-s-VAc)-b-5\_PVeoVa]:[ACPA] = 5 was not adapted for RAFT polymerization, and that FRP of VAc occurred instead.

Finally, if the last monomer unit carrying a xanthate is a VeoVa, it was also already proved that fragmentation of the chain was uneasy because of the steric hindrance provided by the monomer, thus limiting the access of another growing chain to the xanthate moiety.

*As a conclusion*, preliminary experiments were carried out to investigate the chain-end function of 75\_P(VOH-s-VAc)-b-5\_PVeoVa, and try to chain extend the block copolymer with VAc, but not enough time was given to these experiments to optimize the parameters, and it did not provide conclusive results so far.

## Appendix 7: Kinetics of VeoVa homopolymerization with targeted DP = 80 and different experimental conditions

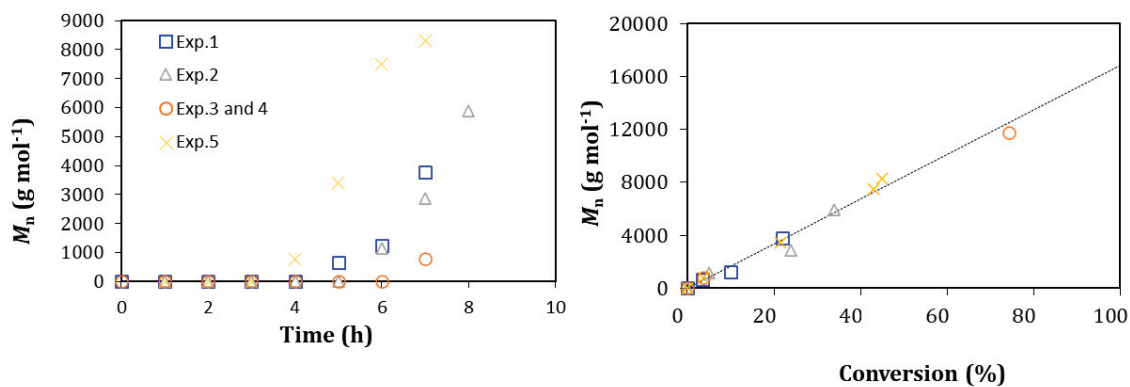


Figure X-24: Evolution of conversion versus time and evolution  $M_n$  (NMR) with conversion of VeoVa during RAFT/MADIX polymerizations using *O*-ethyl-*S*-(1-ethoxycarbonyl)ethyl dithiocarbonate.



## Appendix 8: Main characteristics for the synthesis of two different batches of some copolymers

1. Reproducibility experiments for S2.2 was carried out with the same protocol than for S2.1.

Table X-1: Main characteristics obtained for the synthesis of two different batches of 100\_P(VAc<sub>0.90-S</sub>-VL<sub>0.10</sub>) (S2.1 and S2.2).

Designation	$M_n$ (NMR) (g mol <sup>-1</sup> ) **	$M_n$ (SEC) (g mol <sup>-1</sup> ) **	$\bar{D}$	F <sub>VOH</sub> /F <sub>VeoVa</sub> /F <sub>VAc</sub> after alcoholysis*
S2.1	12 900	15 000	1.4	0.970/0.015/0.015
S2.2	12 500	15 050	1.4	0.966/0.015/0.019

\*  $M_n$  Before alcoholysis

\*\* F is the molar fraction associated to the monomer

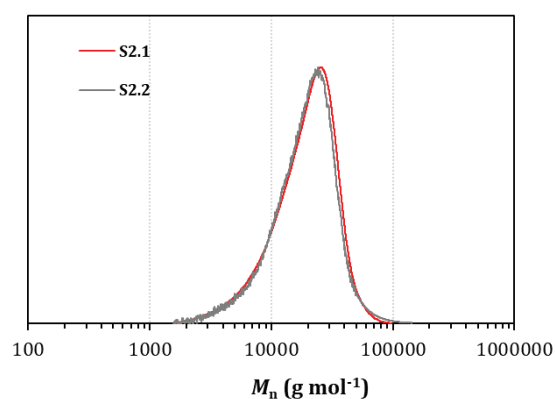


Figure X-25: SEC-THF traces obtained after purification of S2.1 and S2.2.

2. Reproducibility experiments for B2.2 and B4.2 were carried out with the same protocol than for B2 and B4.

**Table X-2: Main characteristics obtained for the synthesis of two different batches of 5\_PVeoVa-*b*-95\_PVAc (B2 and B2.2) and 75\_PVAc-*b*-5\_PVeoVa (B4. and B4.2).**

Designation	$M_n$ (NMR) (g mol <sup>-1</sup> ) *	$M_n$ (SEC) (g mol <sup>-1</sup> ) *	$\bar{D}$	F <sub>VOH</sub> /F <sub>VeOVA</sub> /F <sub>VAc</sub> after alcoholysis**
<b>B2</b>	9820	12 120	1.4	0.90/0.05/0.05
<b>B2.2</b>	16 000	20 000	1.4	0.93/0.05/0.02
<b>B4</b>	7170	8800	1.5	0.924/0.060/0.016
<b>B4.2</b>	8000	9700	1.4	0.918/0.062/0.020

\*  $M_n$  Before alcoholysis

\*\* F is the molar fraction associated to the monomer

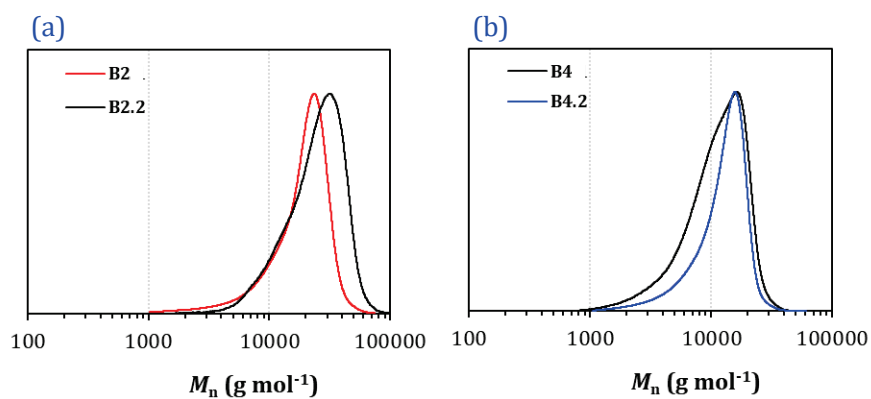


**Figure X-26: SEC-THF traces obtained after purification of (a) B2 and B2.2 and (b) B4 and B4.2.**

## Appendix 9: Alkali resistance of the latexes stabilized by the VeoVa-based block copolymers stored at different pH

The alkali resistance of the latexes stabilized with 100\_P(VOH<sub>0.935</sub>-*s*-VAc<sub>0.015</sub>)-*b*-5\_PVeoVa<sub>0.050</sub> (**B3**) and 75\_P(VOH<sub>0.924</sub>-*s*-VAc<sub>0.016</sub>)-*b*-5\_PVeoVa<sub>0.060</sub> (**B4**) was investigated at different pH: 4, 6, 8, 10 and 12, and compared to the latex obtained with Mowiol 4-88. The pH of the latexes was set *via* a pH-meter and a basic solution of sodium hydroxide (0.1 N) or an acidic solution of hydrochloric acid (0.05 N and 0.1 N). The samples were stored in the fridge over a four-week period, and the pH was measured every week. The results are shown in **Figure X-27**.

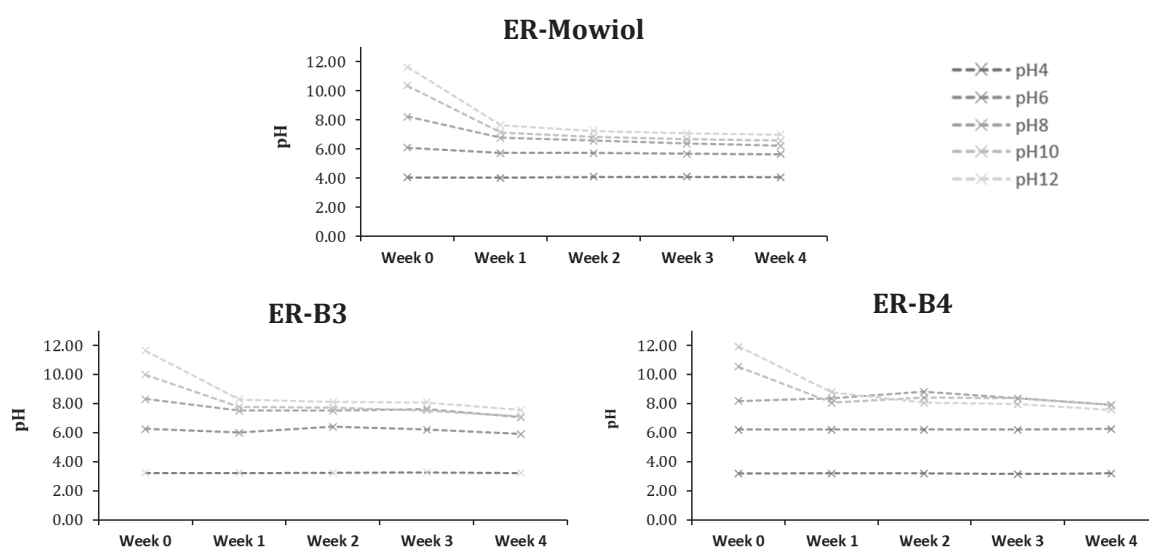
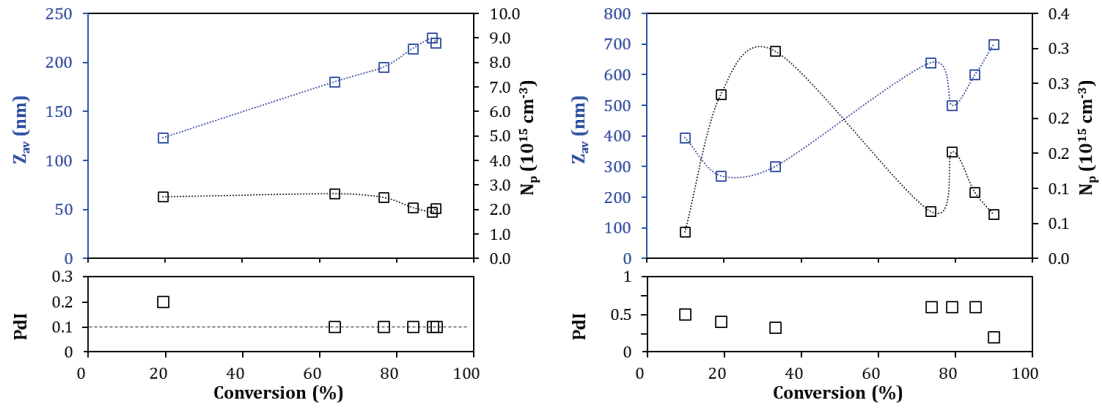


**Figure X-27: Evolution of the pH of the latexes stabilized with 10 wt.% of Mowiol 4-88; B3 and B4. At week 0, the pH was set at 4, 6, 8, 10 and 12 and was then followed each week for four weeks.**

## Appendix 10: Plot of $N_p$ and $Z_{av}$ as a function of conversion for ER-H9 and ER-H10



**Appendix 11: Overlay of the SEC traces of the (co) polymerization carried out in the 150- and 500-mL batch reactors**

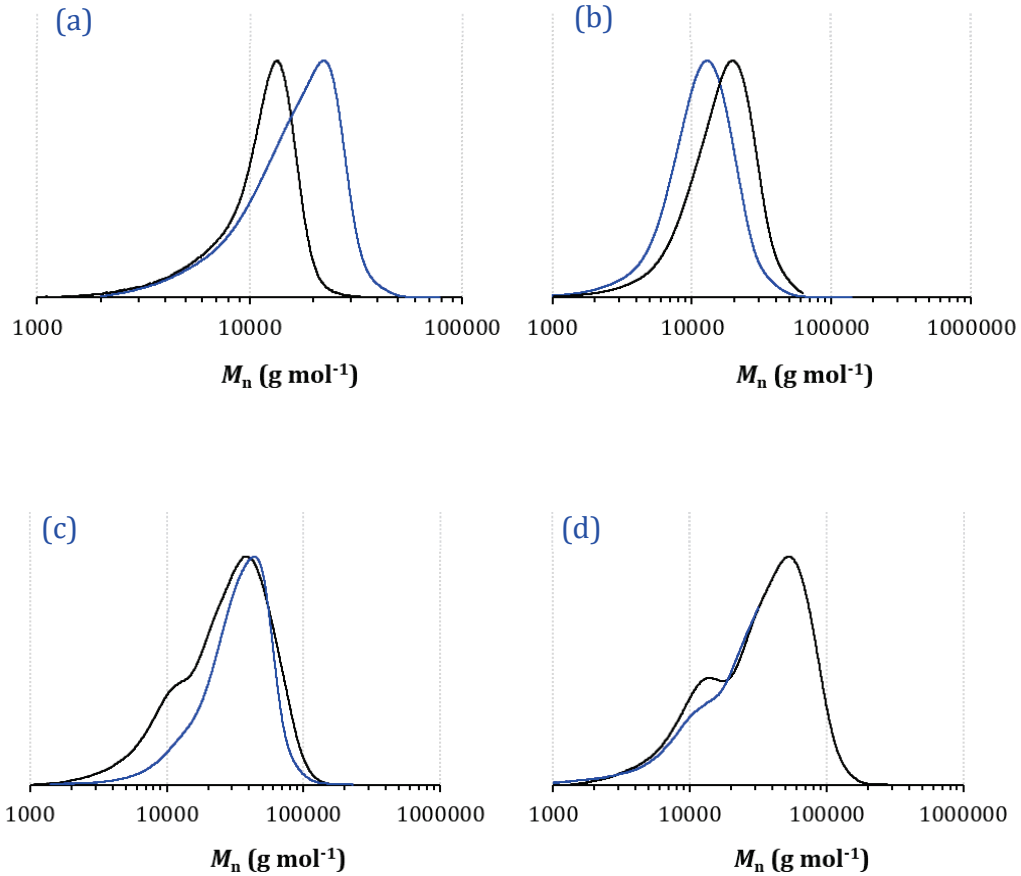


**Figure X-28: Overlay of the SEC-traces of (a) 75\_PVAc; (b) 100\_P(VAc<sub>0.90</sub>-s-VL<sub>0.10</sub>); (c) 75\_PVAc-*b*-100\_P(VAc-*s*-VeoVa)<sub>0.95/0.05</sub> and (d) 75\_PVAc-*b*-100\_P(VAc-*s*-VL)<sub>0.90/0.10</sub> in the 75 mL (black) and 500 mL reactors (blue).**

## Appendix 12: Calculation and determination of suitable parameters for the biodegradability testing

Biodegradability of the stabilizer was determined according to OECD 301F via measurement of oxygen consumption (Manometric Respirometry).

### Carbon Content

The carbon content is calculated from the known elemental composition or determined by elemental analysis of the test substance.

### Theoretical Oxygen Demand (ThOD)

The theoretical oxygen demand (ThOD) may be calculated if the elemental composition is determined. For the compound:



The ThOD, would be:

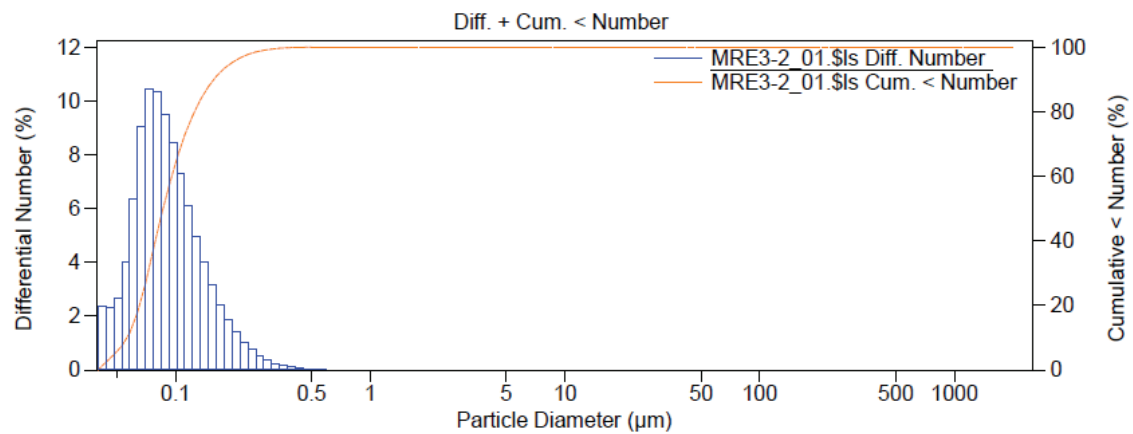
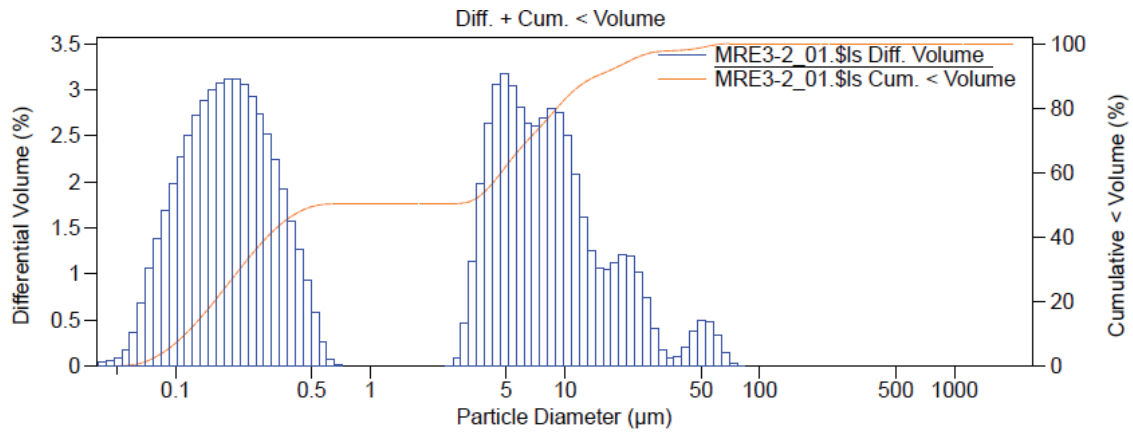
$$ThOD = \frac{16[2c + 1/2(h - cl - 3n) + 3s + 5/2p + 1/2na - o]mg/mg}{M} \quad (100)$$

Where M is the molar mass

The elemental analysis of the stabilizers and the biodegradability measurements were performed by the analytical service at Wacker.

## Appendix 13: Mastersizer analyses of the latexes synthesized at Wacker

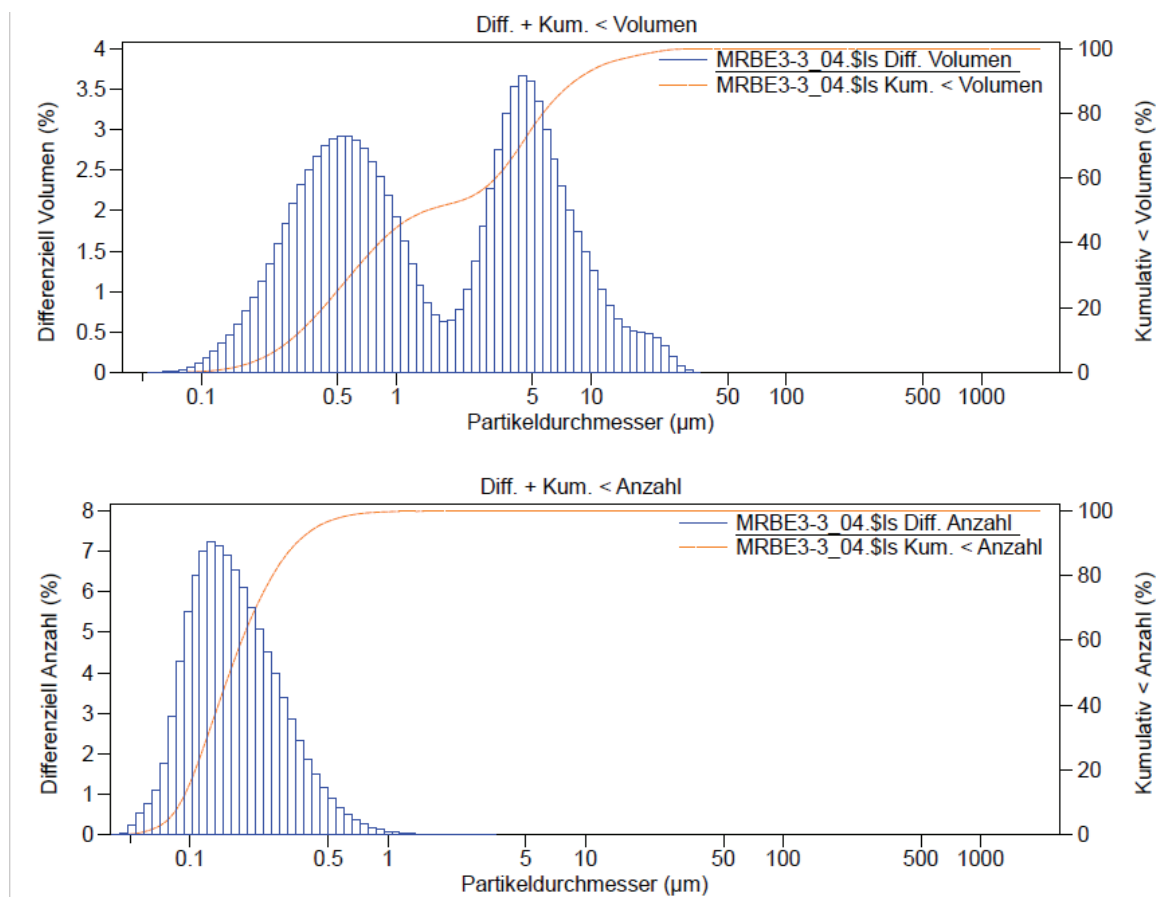
### Latex obtained with 10 wt.% of 75 P(VOH<sub>0.88</sub>-*S*-VAc<sub>0.12</sub>) (L1) (Chapter VI)



Volume Statistics (Arithmetic)		MRE3-2_01.\$\s\$					
Calculations from 0.040 μm to 2000 μm							
Volume:	100%	C.V.:	164%				
Mean:	5.710 μm						
Mode:	4.877 μm						
Specific Surf. Area:	19.37 m <sup>2</sup> /g						
<10%	<25%	<50%	<75%	<100%			
0.112 μm	0.183 μm	0.544 μm	7.689 μm	83.89 μm			
<0.2 μm	<0.4 μm	<0.9 μm	<2 μm	<3 μm	<20 μm	<50 μm	<100 μm
27.9%	46.7%	50.4%	50.4%	50.6%	93.7%	98.7%	100%

Number Statistics (Arithmetic)		MRE3-2_01.\$ls					
Calculations from 0.040 $\mu\text{m}$ to 2000 $\mu\text{m}$							
Number:	100%						
Mean:	0.099 $\mu\text{m}$	C.V.:	51.4%				
Mode:	0.073 $\mu\text{m}$						
Specific Surf. Area:	19.37 $\text{m}^2/\text{g}$						
<10%	<25%	<50%	<75%	<100%			
0.056 $\mu\text{m}$	0.069 $\mu\text{m}$	0.086 $\mu\text{m}$	0.116 $\mu\text{m}$	83.89 $\mu\text{m}$			
<0.2 $\mu\text{m}$	<0.4 $\mu\text{m}$	<0.9 $\mu\text{m}$	<2 $\mu\text{m}$	<3 $\mu\text{m}$	<20 $\mu\text{m}$	<50 $\mu\text{m}$	<100 $\mu\text{m}$
95.6%	99.8%	99.999%	99.999%	99.999%	100%	100%	100%

**Latex obtained with 10 wt.% of 75 P(VOH-s-VAc)-b-100 P(VOH-s-VL-s-VAc)<sub>0.960/0.016/0.024</sub> (L4) (Chapter VI)**





Volumen Statistik (Arithmetisch) MRBE3-3\_04.\$Is

Berechnung von 0.040 µm bis 2000 µm

Volumen: 100%  
 Mittelwert: 3.390 µm C.V.: 124%  
 Maximum: 4.443 µm  
 Spez. Oberfläche: 8.201 m<sup>2</sup>/g

<10%	<25%	<50%	<75%	<100%				
0.287 µm	0.496 µm	1.434 µm	4.913 µm	39.78 µm				
<0.2 µm	<0.4 µm	<0.9 µm	<2 µm	<3 µm	<20 µm	<50 µm	<100 µm	
4.09%	18.5%	42.3%	52.5%	58.2%	98.8%	100%	100%	

Anzahl Statistik (Arithmetisch) MRBE3-3\_04.\$Is

Berechnung von 0.040 µm bis 2000 µm

Anzahl: 100%  
 Mittelwert: 0.196 µm C.V.: 71.9%  
 Maximum: 0.128 µm  
 Spez. Oberfläche: 8.201 m<sup>2</sup>/g

<10%	<25%	<50%	<75%	<100%				
0.089 µm	0.114 µm	0.158 µm	0.235 µm	39.78 µm				
<0.2 µm	<0.4 µm	<0.9 µm	<2 µm	<3 µm	<20 µm	<50 µm	<100 µm	
65.9%	93.5%	99.7%	99.97%	99.98%	100%	100%	100%	

## Appendix 14: List of communications and publications

- **49ème Journées d'Etude des Polymères (JEPO), October 3-8, 2021 (Porquerolles, France)**

*Oral communication:*

Design of amphiphilic copolymers incorporating vinyl alcohol units for the emulsion copolymerization of vinyl acetate and ethylene

M. Raffin, T. Melchin, M. Lansalot, F. D'Agosto

- **Groupe Français d'Etudes et d'Applications des Polymères (GFP), November 15-19, 2021 (Lyon, France)**

*Online poster:*

Design of new macrostabilizers incorporating vinyl alcohol units,  
For the emulsion copolymerization of vinyl acetate and vinyl neodecanoate

M. Raffin, T. Melchin, M. Lansalot, F. D'Agosto

- **37ème édition du Club Emulsion, June, 9 -10, 2022 (Paris, France)**

*Oral communication :*

Synthèse de nouveaux tensioactifs macro moléculaires incorporant des unités alcool  
vinylique,  
pour la (co)polymérisation en émulsion de l'acétate de vinyle

M. Raffin, T. Melchin, M. Lansalot, F. D'Agosto

- **Bordeaux Polymer Conference (BPC), June 13-16, 2022**

**(Bordeaux, France)**

*Oral communication :*

Design of new macrostabilizers incorporating vinyl alcohol units,  
For the emulsion copolymerization of vinyl acetate-based latexes

M. Raffin, T. Melchin, M. Lansalot, F. D'Agosto

- **84<sup>th</sup> Prague Meeting on Macromolecules (84PMM), July 28-28, 2022 (Prague, Czech Republic)**

*Oral communication:*

Design of new macrostabilizers incorporating vinyl alcohol units,  
For the emulsion copolymerization of vinyl acetate-based latexes

M. Raffin, T. Melchin, M. Lansalot, F. D'Agosto

Marie Raffin<sup>a</sup>, Timo Melchin<sup>b</sup>, Muriel Lansalot<sup>a</sup>, Franck D'Agosto<sup>a</sup>

<sup>a</sup> Catalyse, Polymérisation, Procédés et Matériaux (CP2M), CNRS, UMR 5128, Univ Lyon, Université Claude Bernard Lyon 1, CPE Lyon, Villeurbanne, France.

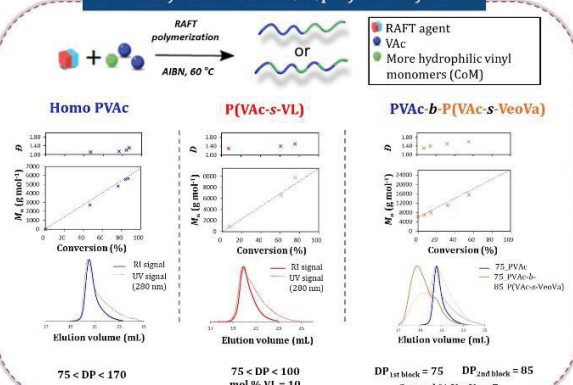
<sup>b</sup> Wacker Chemie AG, Johannes-Hess-Straße 24 84489 Burghausen, Germany

### Introduction

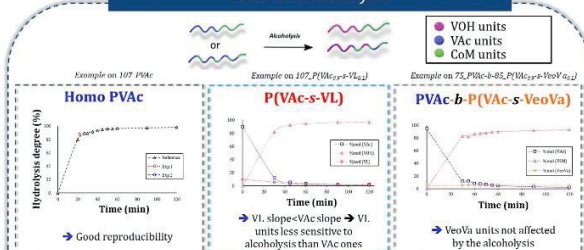
Poly(vinyl alcohol-co-vinyl acetate) (PVOH) copolymers are obtained by partial hydrolysis of poly(vinyl acetate) (PVAc) and are used as stabilizer in emulsion polymerization process. The latexes find applications in various fields such as e.g. adhesives, binders, medical application or paints. [1] Currently, the PVOH chains are not all involved in particle stabilization and free PVOH can be found in the aqueous phase [2]. This can have a negative influence on the final properties of the end product. The aim of the present project is to synthesize alternative amphiphilic copolymers incorporating VOH units, that are able (1) to stabilize latexes with a better involvement of the stabilizer copolymers in particle stabilization.

The synthesis of the targeted copolymers relies on reversible addition-fragmentation chain transfer (RAFT) polymerization, as it allows the formation of well-defined polymer architectures [4]. Therefore, a careful design of amphiphilic copolymers of VAc and vinylic ester comonomers (CoM) was first performed in order to access a range of copolymers structures including block copolymers. CoM are chosen with the aim of identifying hydrolysis conditions that could be selective of the VAc units. They are namely vinyl neodecanoate (VERSA® 10 or VeoVa10) and vinyl laurate (VERSA® 12, or VL). The resulting well-defined amphiphilic copolymers structures are then evaluated as stabilizers in the emulsion copolymerization of VAc and vinyl neodecanoate (VERSA® 10) used as model reaction for the VAE synthesis. The three most promising candidate structures are presented in this poster.

### STEP 1: Synthesis of the (co)polymers by RAFT



### STEP 2: Alcoholysis



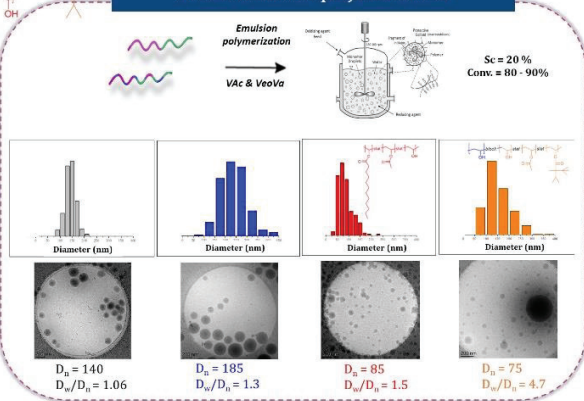
Structure	Range of HD (%)	Solubility at R.T.	Solubility at 70 °C	Solubility after 70 °C, back at R.T.
Homo PVAc	88 - 97	✓	✗	-
P(VAc-s-VL)	90 - 97.5	✗	✗	✓
PVAc-b-P(VAc-s-VeoVa)	80 - 95	✗	✗	✓

### STEP 4: Characterization of the latexes

Structure	Coagulum (wt.%)	Adsorbed & grafted stabilizer	Np (cm <sup>-3</sup> ) x 10 <sup>15</sup>	Surface covered per particle (Å <sup>2</sup> /molecule)
Commercial PVOH	0	45	7.3	750 [4]
PVOH (RAFT)	0	40	1.4	260
	0	87	2.9	408
	1	77	2.24	485

**Principle of the determination of the adsorbed & grafted amount of stabilizer**

### STEP 3: Emulsion polymerization



### Conclusion

During the past three years, many structures of VAc-based copolymers were synthesized, hydrolyzed and evaluated as stabilizer candidates for the emulsion polymerization of VAc and VeoVa. The main issue was the solubility of these copolymers in water, and a special care must be taken during the alcoholysis step to reach an hydrolysis degree which allows for the polymer to become dispersible or soluble in the aqueous phase. Among the different polymers which have been synthesized, three structures were of great interest, as they showed good solubility and allowed for long lasting stabilization of the latex, with enhanced amount of adsorption and grafting onto the particles when compared to the commercial stabilizer.

The next step of this research work is now to evaluate the characteristics of these latexes in the final applications (e.g. paints or adhesive).

[1] Atanase L., Bistac, S.; Riess, G. *Soft Matter*, 2015, 11, 2665-2672.

[2] Carrà, S.; Silepcovich, A.; Canevarolo, A.; Carrà, S. *Polymer (Guildf)*, 2005, 46, 1379-1384.

[3] Perrier, S. *Macromolecules*, 2011, 44, 1455-1461.

[4] Rocha-Botello, G.; Olvera-Guillen, R.; Herrera-Ordóñez, J.; Cruz-Soto M.; Victoria-Valenzuela, D., *Macromolecular reaction engineering*, 2019, 5, 1-9

## **References**

- [1] T. Moritani, Y. Fujiwara, *Macromolecules* **1976**, *10*, 532–535.
- [2] B. M. S. Budhlall, Grafting Reactions in the Emulsion Polymerization of Vinyl Acetate Using Poly(Vinyl Alcohol) as Emulsifier. Ph.D Dissertation, Lehigh University, **1999**.
- [3] Y.-Y. Tong, Y.-Q. Dong, F.-S. Du, Z.-C. Li, *J. Polym. Sci. Part A Polym. Chem.* **2009**, *47*, 1901–1910.
- [4] L.-I. Atanase, Contribution à l'étude Des Complexes Poly(Vinyle Alcool-Vinyle Acétate)/Tensioactifs Anioniques: Caractéristiques Colloïdales Des Nanogels et Extension Au Copolymères à Blocs. Ph.D Dissertation, Université de Haute Alsace - Mulhouse, **2011**.